

Journal of Polymer Science

PART A: GENERAL PAPERS

Volume 1, 1963

Editorial Board: R. M. FUOSS · J. J. HERMANS · H. MARK
H. W. MELVILLE · C. G. OVERBERGER · G. SMETS

N. G. GAYLORD, Book Review Editor

| | | |
|--|---|---|
| Advisory Board: T. ALFREY, JR. <i>Midland, Mich.</i> | P. J. FLORY <i>Pittsburgh, Pa.</i> | A. PETERLIN <i>Durham, N. C.</i> |
| W. O. BAKER <i>Murray Hill, N. J.</i> | J. FURUKAWA <i>Kyoto</i> | C. C. PRICE <i>Philadelphia, Pa.</i> |
| H. BENOIT <i>Strasbourg</i> | G. GEE <i>Manchester</i> | CH. SADRON <i>Strasbourg</i> |
| C. J. BEVINGTON <i>Birmingham</i> | A. KATCHALSKY <i>Rehovoth</i> | G. V. SCHULZ <i>Mainz</i> |
| J. W. BREITENBACH <i>Vienna</i> | A. KELLER <i>Bristol</i> | H. M. SPURLIN <i>Wilmington, Del.</i> |
| A. M. BUECHE <i>Schenectady, N. Y.</i> | G. M. KLINE <i>Washington, D. C.</i> | A. J. STAVERMAN <i>Leiden</i> |
| C. W. BUNN <i>Welwyn Garden City</i> | M. MAGAT <i>Psris</i> | J. K. STILLE <i>Iowa City, Iowa</i> |
| G. M. BURNETT <i>Aberdeen</i> | C. S. MARVEL <i>Tucson, Ariz.</i> | W. H. STOCKMAYER <i>Hanover, N. H.</i> |
| F. S. DAINTON <i>Leeds</i> | G. NATTA <i>Milan</i> | M. SZWARC <i>Syracuse, N. Y.</i> |
| P. DEBYE <i>Ithaca, N. Y.</i> | S. OKAMURA <i>Kyoto</i> | A. V. TOBOLSKY <i>Princeton, N. J.</i> |
| F. EIRICH <i>Brooklyn, N. Y.</i> | | K. UEBERREITER <i>Berlin</i> |

INTERSCIENCE PUBLISHERS

Copyright © 1963, by John Wiley & Sons, Inc.

Statement of ownership, management, and circulation (Act of October 23, 1962: Section 4369, Title 39 United States Code)

1. Date of filing: September 30, 1963
2. Title of Publication: JOURNAL OF POLYMER SCIENCE
3. Frequency of issue: monthly
4. Location of known office of publication: 20th and Northampton Streets, Easton, Pennsylvania, 18042
5. Location of headquarters of general business offices of publisher: 605 Third Avenue, New York 16, New York, 10016
6. The names and addresses of publisher, editor, and managing editor:
Publisher: Eric S. Proskauer, John Wiley & Sons, Inc., 605 Third Avenue, New York 16, New York
Editor: Herman Mark, Polytechnic Institute of Brooklyn, 333 Jay Street, Brooklyn 1, New York
Managing Editor: None

7. Owner: John Wiley & Sons, Inc., 605 Third Avenue, New York 16, New York.
Stockholders owning or holding 1 per cent or more of total amount of John Wiley & Sons, Inc., stock as of September 30, 1963:

Cynthia W. Darby, 23 Farrington St., Newburgh, N. Y.; Maurits Dekker, 511 West 232nd St., Bronx, N. Y.; Rozetta S. Dekker, 511 W. 232nd St., Bronx, N. Y.; Julia W. Gilbert, Box 1191, Carmel, Calif.; Edward P. Hamilton, c/o John Wiley & Sons, Inc., 605 Third Avenue, New York 16, N. Y.; Elizabeth W. Hamilton, c/o John Wiley & Sons, Inc., 605 Third Avenue, New York 16, N. Y.; W. Bradford Wiley and Francis Lobdell, Trustees of Elizabeth W. Hamilton Trust, dated 12/23/52, c/o John Wiley & Sons, Inc., 605 Third Avenue, New York 16, N. Y.; I. M. Kolthoff, University of Minnesota, School of Chemistry, Minneapolis, Minn.; Willy Levinger, 336 Central Park West, New York, N. Y.; R. R. Pennywitt, Box 211, Mantaloking, N. J.; R. C. Runyon, Jr., 130 East End Ave., New York 28, N. Y.; Francis Lobdell and William J. Seawright, Trustees f/b/o Deborah Elizabeth Wiley, u/a dated 6/2/58, c/o John Wiley & Sons, Inc., 605 Third Avenue, New York 16, N. Y.; Kate R. Q. Wiley, 1192 Park Avenue, New York 28, N. Y.; Edward P. Hamilton, Trustee f/b/o Kate R. Q. Wiley, u/a dated 6/6/38, c/o John Wiley & Sons, Inc., 605 Third Avenue, New York 16, N. Y.; Francis Lobdell and William J. Seawright, Trustees f/b/o Peter Booth Wiley, u/a dated 6/2/58, c/o John Wiley & Sons, Inc., 605 Third Avenue, New York 16, N. Y.; K. R. Q. Wiley, E. P. Hamilton, and Cynthia W. Darby, Executors of the will of W. O. Wiley, c/o E. P. Hamilton, 605 Third Avenue, New York 16, N. Y.; Francis Lobdell and William J. Seawright, Trustees f/b/o William Bradford Wiley, 2nd, u/a dated 6/2/58, c/o John Wiley & Sons, Inc., 605 Third Avenue, New York 16, N. Y.; Adele E. Windheim, 8 Dundee Rd., Larchmont, N. Y.; W. Bradford Wiley and E. P. Hamilton, Trustees for Edward P. Hamilton Foundation, u/a dated 12/23/57, c/o John Wiley & Sons, Inc., 605 Third Avenue, New York 16, N. Y.; Powers & Co., P. O. Box 1479, Church St. Station, New York 8, N. Y.; Reing & Co., P. O. Box 491, Church St. Station, New York 8, N. Y.; Eric S. Proskauer & Charles H. Lieb, as Trustees U-A Dated 11/27/62, 220 Central Park South, New York 19, New York.

8. Known bondholders, mortgagees, and other security holders owning or holding 1 per cent or more of total amount of bonds, mortgages, or other securities: None

9. Paragraphs 7 and 8 include, in cases where the stockholder or security holder appears upon the books of the company as trustee or in any other fiduciary relation, the name of the person or corporation for whom such trustee is acting, also the statements in the two paragraphs show the affiant's full knowledge and belief as to the circumstances and conditions under which stockholders and security holders who do not appear upon the books of the company as trustees, hold stock and securities in a capacity other than that of a bona fide owner. Names and addresses of individuals who are stockholders of a corporation which itself is a stockholder or holder of bonds, mortgages or other securities of the publishing corporation have been included in paragraphs 7 and 8 when the interests of such individuals are equivalent to 1 per cent or more of the total amount of the stock or securities of the publishing corporation.

10. This item must be complete for all publications except those which do not carry advertising other than the publishers own and which are named in Sections 132.231, 132.232, and 132.233, Postal Manual (Sections 4355a, 4355b, and 4356 of Title 39, United States Code)

I certify that the statements made by me above are correct and complete:

Eric S. Proskauer
Publisher

CONTENTS

Vol. 1, Issue Nos. 1-12

Journal of Polymer Science *Part A: General Papers*

ISSUE NO. 1, JANUARY

| | |
|---|-----|
| W. R. KRIGBAUM, M. KANEKO, and A. ROIG: Dipole Moments, Stress Relaxation, and Birefringence of Viton Fluoroelastomer. . . | 1 |
| A. V. TOBOLSKY and D. B. HARTLEY: Radical-Anion Polymerization. | 15 |
| HARRY R. ELDEN and MARSHA FELDMAN: A Kinetic Analysis of Swelling of Rat Tail Tendon. | 23 |
| JOHN L. BINDER: The Infrared Spectra and Structures of Polyisoprenes. | 37 |
| JOHN L. BINDER: The Infrared Spectra and Structures of Polybutadienes. | 47 |
| J. BOOR, JR., and J. C. MITCHELL: Kinetics of Crystallization and a Crystal-Crystal Transition in Poly-1-Butene. | 59 |
| K. T. GARTY, T. B. GIBB, JR., and R. A. CLENDINNING: Cocatalysts for the Linear Polymerization of Epoxides by Dibutylzinc | 85 |
| H. W. McCORMICK: Molecular Weight Distribution of Linear Polyethylene by Sedimentation Velocity Analysis. | 103 |
| FUMIO KOBAYASHI and KOICHI MATSUYA: Copolymerization of α -Pyrrolidone and ϵ -Caprolactam. | 111 |
| JORGE HELLER, D. O. TIESZEN, and D. B. PARKINSON: Polymerization of <i>N</i> -Vinylcarbazole with Ziegler-Type Catalyst Systems | 125 |
| N. LAKSHMINARAYANAIAH: Activity Coefficients of Small Ions in Ion-Exchange Resins. | 139 |
| W. KUHN and P. MOSER: The Dielectric Relaxation Time Spectrum and the Corresponding Cole-Cole Diagram for Methylcellulose in Water. | 151 |
| W. COOPER and R. K. SMITH: Melting Transitions in Diene Polymers. | 159 |
| VICTOR E. SHASHOUA: Static Electricity in Polymers. II. Chemical Structure and Antistatic Behavior. | 169 |
| MICHIO KASHIWAGI: Radiation Damage in Oriented Polyamides. . | 189 |
| LEO REICH and S. S. STIVALA: A General Kinetic Scheme for Ziegler-Type Polymerizations. | 203 |
| RICHARD H. WILEY and GERALD L. MAYBERRY: Tracer Techniques for the Determination of Monomer Reactivity Ratios. | |

| | |
|--|-----|
| IV. Copolymerization Characteristics of Some Divinyl Monomers..... | 217 |
| N. T. NOTLEY: Molecular Configuration of Branched Macromolecules..... | 227 |
| V. KALPAGAM and M. RAMAKRISHNA RAO: Effect of Polar and Non-polar Solvents on the Viscosity and the Molecular Weight of Polymer Solutions..... | 233 |
| L. B. TICKNOR: A Thermodynamic Method for the Comparison of the Order Distribution in Cellulose and in Other Polymers.... | 243 |
| P. DEBYE, B. CHU, and D. WOERMANN: Viscosity of Critical Mixtures..... | 249 |
| P. DEBYE, D. WOERMANN, and B. CHU: Critical Opalescence of Polystyrene in Ethylcyclohexane..... | 255 |
| STANLEY MIDDLEMAN: A Theory for Surface Elevation in the Weissenberg Effect..... | 261 |
| ROBERT G. CHARLES: Metal Chelate Polymers Derived from Tetraacetylene..... | 267 |
| ISRAEL S. UNGAR, JOHN F. KIRCHER, WILLIAM B. GAGER, FRANCIS A. SLIEMERS, and ROBERT I. LEININGER: Radiolysis of the Isomeric Poly(butyl Methacrylate)..... | 277 |
| V. S. R. RAO and JOSEPH F. FOSTER: Depolarization of Scattered Light in Solutions of Linear and Branched Polysaccharides | 289 |
| ARTHUR V. TOBOLSKY: Probability Matrices, Chain Dimensions and Statistical Thermodynamics for Semicrystalline Macromolecules | 301 |
| W. BROCK NEELY: Solution Properties of Polysaccharides. IV. Molecular Weight and Aggregate Formation in Methylcellulose Solutions..... | 311 |
| EUGENE C. WINSLOW and JEAN A. MARRIOTT: Effect of Crystallization of the Thermal Stability of Polyvinylphthalic Acid and Its Methyl Ester..... | 321 |
| J. P. KENNEDY, I. KIRSHENBAUM, R. M. THOMAS, and D. C. MURRAY: Fundamental Studies on Cationic Polymerization. II. Mechanism and Theory of Inversion Temperature..... | 331 |
| T. R. CROMPTON and V. W. REID: Unsaturation in High Impact Polystyrene Analytical Studies..... | 347 |
| BERNARD WUNDERLICH and DOUGLAS POLAND: Thermodynamics of Crystalline Linear High Polymers. II. The Influence of Copolymer Units on the Thermodynamic Properties of Polyethylene..... | 357 |
| WILLIAM M. SALTMAN: Separated Aluminum Alkyl-Titanium Tetrachloride Catalysts for Isoprene Polymerization..... | 373 |
| J. F. HARROD: Hydrogen Bonding in Amine-Epoxy Adducts.... | 385 |
| O. REDLICH, A. L. JACOBSON, and W. H. McFADDEN: On the Fractionation of Polypropylene by Coacervation..... | 393 |
| A. ZAMBELLI, J. DIPIETRO, and G. GATTI: The Nature of Active Components in Catalytic Systems Prepared from $TiCl_2$, Mono- | |

| | |
|---|-----|
| alkylaluminum Dihalides, and Electron-Donor Substances, in the Polymerization of Propylene. | 403 |
| LOWELL WESTERMAN: The Molecular Weight Distribution in Polypropylene. | 411 |
| JAMES C. W. CHIEN: Kinetics of Propylene Polymerization Catalyzed by α -Titanium Trichloride-Diethylaluminum Chloride. | 425 |
| MAURICE MORTON, RALPH MILKOVICH, D. B. MCINTYRE, and L. J. BRADLEY: Homogeneous Anionic Polymerization. I. Molecular Weights of Polystyrene Initiated by Sodium Naphthalene | 443 |
| MAURICE MORTON, A. A. REMBAUM, and J. L. HALL: Homogeneous Anionic Polymerization. II. Molecular Weight of Polystyrene Initiated by Lithium Alkyls. | 461 |
| MAURICE MORTON, F. E. BOSTICK, and R. G. CLARKE: Homogeneous Anionic Polymerization. III. Molecular Weight of Polyisoprene Initiated by Butyllithium. | 475 |
| A. V. TOBOLSKY, D. KATZ, and M. TAKAHASHI: Rheology of Polytetrafluoroethylene. | 483 |
| RACHELA TAKSERMAN-KROZER and ANDRZEJ ZIABICKI: Behavior of Polymer Solutions in a Velocity Field with Parallel Gradient. I. Orientation of Rigid Ellipsoids in a Dilute Solution. | 491 |
| RACHELA TAKSERMAN-KROZER and ANDRZEJ ZIABICKI: Behavior of Polymer Solutions in a Velocity Field with Parallel Gradient. II. Viscosity of Dilute Solutions Containing Rigid Ellipsoids. | 507 |
| V. KALPAGAM and M. RAMAKRISHNA RAO: Depolarization Measurements of Polymer Solutions in High Dilutions. Part I. | 517 |
| CHARLES A. KUMINS and JEROME ROTEMAN: Effect of Solid Polymer Interaction on Transition Temperature and Diffusion Coefficients | 527 |
| CHARLES A. KUMINS, JEROME ROTEMAN, and CLIFFORD J. ROLLE: Water Sorption of Titanium Dioxide-Poly(vinyl Acetate-Vinyl Chloride) Copolymer Films. | 541 |
| ALBERT ZILKHA and YAIR AVNY: Polymerization of Acrylonitrile by Electron Transfer Catalysts. | 549 |
| G. H. CRAWFORD, D. E. RICE, and B. F. LANDRUM: Nitroso Fluorocarbon Elastomers. Polymerization Mechanism. | 565 |

ISSUE NO. 2, FEBRUARY

| | |
|--|-----|
| JOHN J. MAURER: Particle Size Distribution in Polymer Solutions. | 577 |
| A. V. TOPCHIEV: Some Aspects of the Production and Study of Semiconducting Polymeric Materials. | 591 |
| A. V. TOPCHIEV and V. P. ALANIYA: Synthesis of Nitroolefins and an Investigation of Their Ability to Polymerize. | 599 |
| SHUN-ISHI OHNISHI, SHUN-ICHI SUGIMOTO, and ISAMU NITTA: Electron Spin Resonance Study of Radiation Oxidation of Polymers. IIIA. Results for Polyethylene and Some General Remarks. | 605 |
| SHUN-ISHI OHNISHI, SHUN-ICHI SUGIMOTO, and ISAMU NITTA: Elec- | |

| | |
|--|-----|
| tron Spin Resonance Study of Radiation Oxidation of Polymers. IIIB. Polypropylene and Poly(Vinyl Chloride)..... | 625 |
| GEORGE ODIAN, MARJORIE SOBEL, ALBERT ROSSI, ROBERT KLEIN, and TERESE ACKER: Radiation-Induced Graft Polymerization of Styrene to Nylon..... | 639 |
| WILLIAM P. BAKER, JR.: Polymerization of Allene by Organometallic Initiation..... | 655 |
| K. J. HERITAGE, J. MANN, and L. ROLDAN-GONZALEZ: Crystallinity and the Structure of Celluloses..... | 671 |
| ARIEL OTTOLENGHI and ALBERT ZILKHA: Termination of the Anionic Polymerization of Acrylonitrile at Low Catalyst Concentrations..... | 687 |
| Z. IZUMI, H. KIUCHI, and M. WATANABE: Copolymerization of Acrylonitrile and <i>p</i> -Sodium Styrene Sulfonate..... | 705 |
| HOWARD W. STARKWEATHER, JR., JOHN F. WHITNEY, and DONALD R. JOHNSON: Crystalline Order in Nylon 66..... | 715 |
| VAHAK M. DER-SARKISSIAN and FREDERICK A. BETTELHEIM: Strain Birefringence of Sodium Hyaluronate Films..... | 725 |
| W. R. MOORE and R. SHUTTLEWORTH: Thermodynamic Properties of Solutions of Cellulose Acetate and Cellulose Nitrate..... | 733 |
| K. R. DUNHAM, J. VANDENBERGHE, J. W. H. FABER, and L. E. CONTOIS: Effect of Side-Chain Structure on Poly- α -Olefin Properties..... | 751 |
| D. C. BASSETT, A. KELLER, and S. MITSUHASHI: New Features in Polymer Crystal Growth from Concentrated Solutions..... | 763 |
| I. KIRSHENBAUM, J. P. KENNEDY, and R. M. THOMAS: Fundamental Studies on Cationic Polymerization. III. Extension of Mechanism Studies to Homogeneous Systems..... | 789 |
| P. DAVIS and B. E. TABOR: Kinetic Study of the Crosslinking of Gelatin by Formaldehyde and Glyoxal..... | 799 |
| M. C. BOURNE, C. O. CHICHESTER, and C. STERLING: Diffusion Constants of a Maltosaccharide Series..... | 817 |
| J. R. SOULEN and M. S. SILVERMAN: Polymerization of Phosphonitrilic Chloride Trimer at High Pressures and Temperatures... | 823 |
| Book Reviews | |
| Polyamino Acids, Polypeptides and Proteins. MARK A. STRAHMANN, ed. Reviewed by H. MORAWETZ..... | 831 |
| Direct Analysis of Diffraction by Matter. R. HOSEMANN and A. N. BAGCHI. Reviewed by H. S. KAUFMAN..... | 831 |
| Erratum | |
| J. J. SHIPMAN and M. A. GOLUB: Infrared Study of the Reaction of Polyisoprene and Polybutadiene With Sulfur by the Use of Deuterated Polymers (article in <i>J. Polymer Sci.</i> , 58 , 1063-1082, 1962)..... | 832 |

ISSUE No. 3, MARCH

| | |
|---|------|
| G. V. D. TIERS and F. A. BOVEY: Polymer NMR Spectroscopy. VII. The Stereochemical Configuration of Polytrifluoro-chloroethylene..... | 833 |
| F. A. BOVEY: Polymer NMR Spectroscopy. VIII. The Influence of the pH of the Polymerization Medium on the Stereochemical Configuration of Polymethacrylic Acid..... | 843 |
| F. A. BOVEY and G. V. D. TIERS: Polymer NMR Spectroscopy. IX. Polyacrylamide and Polymethacrylamide in Aqueous Solution..... | 849 |
| JOSEPH PELLON and W. G. CARPENTER: Polyamides Containing Phosphorus. I. Preparation and Properties..... | 863 |
| TILAK GUHA and SANTI R. PALIT: Study of the Rate of Heterogeneous Polymerization of Methyl Acrylate in Aqueous Solution..... | 877 |
| HARRIS J. BIXLER, ALAN S. MICHAELS, and MORRIS SALAME: Gas Transmission in Irradiated Polyethylene..... | 895 |
| V. KALPAGAM and M. RAMAKRISHNA RAO: Depolarization Measurements of Polymer Solutions at High Dilutions. Part II.... | 921 |
| W. R. MOORE and R. J. FORT: Viscosities of Dilute Solutions of Polymethyl Methacrylate..... | 929 |
| C. WIPPLER et R. GAUTRON: Étude de l'Influence du Tetrahydrofurane sur la Radioreticulation du Chlorure de Polyvinyle.... | 943 |
| IRVING ROSEN, G. H. MCCAIN, A. L. ENDREY, and C. L. STURM: Syndiotactic Polyvinyl Formate and Derived Polyvinyl Alcohol | 951 |
| GIANALVISE CARAZZOLO and MARIO MAMMI: Crystal Structure of a New Form of Polyoxymethylene..... | 965 |
| R. VAN LEEPUT and R. STEIN: Experimental Data on Dilute Polymer Solutions. I. Hydrodynamic Properties and Statistical Coil Dimensions of Poly(<i>n</i> -Butyl Methacrylate)..... | 985 |
| J. P. BERRY: Fracture Processes in Polymeric Materials. IV. Dependence of the Fracture Surface Energy on Temperature and Molecular Structure..... | 993 |
| YOSHIO TOMIMATSU and K. J. PALMER: Light-Scattering Studies on Sugar Beet Arabans..... | 1005 |
| J. SCANLAN and D. K. THOMAS: Crosslinking of Natural Rubber by Dicumyl Peroxide in the Presence of Oxidation Inhibitors.. | 1015 |
| C. E. BROCKWAY and K. B. MOSER: Grafting of Poly(methyl Methacrylate) to Granular Corn Starch..... | 1025 |
| R. J. MORRIS, JR. and H. E. PERSINGER: Molecular Weight Distribution in Polypropylene Glycol 2025..... | 1041 |
| YONEHO TABATA, HIROSHI SHIBANO, HIROSHI SOBUE, and KIYOSHI HARA: Radiation-Induced Cationic Polymerization of Ethylene..... | 1049 |
| DONALD C. VOGELSONG: Crystal Structure Studies on the Polymorphic Forms of Nylons 6 and 8 and Other Even Nylons.... | 1055 |

- NOBORU TOKITA and W. R. KRIGBAUM: Calculation of the Displacement Distance for a Three-Choice Cubic Lattice Chain.. 1069
- ROBERT B. FOX, LAWRENCE G. ISAACS, and SUZANNE STOKES: Photolytic Degradation of Poly(methyl Methacrylate)..... 1079

Book Review

- Advances in Spectroscopy. Vol. II. H. W. THOMPSON, ed.
Reviewed by R. P. BAUMAN..... 1087

Erratum

- G. S. LEVINSON: Molecular Orbital Calculation of Monomer Reactivity Ratios (article in *J. Polymer Sci.*, **60**, 43-54, 1962) 1088

ISSUE NO. 4, APRIL

- L. UTRACKI and ROBERT SIMHA: Corresponding State Relations for the Viscosity of Moderately Concentrated Polymer Solutions 1089
- MACHIO IWASAKI: On the Helical Structure of Polytetrafluoroethylene..... 1099
- NAN SHIEH CHU and CHARLES C. PRICE: Polyethers. XI. Polymerization of *dl*-Propylene Oxide with Optically Active Catalyst Systems..... 1105
- MIKIKO SHIMA and AKIRA KOTERA: Copolymerization Characteristics of Methyl Acrylate and Methyl Methacrylate. I. Study of Copolymerization Kinetics by a Deuterium Tracer Method..... 1115
- JOHN L. LANG, W. A. PAVELICH, and H. D. CLAREY: Homopolymerization of Maleic Anhydride. I. Preparation of the Polymer..... 1123
- R. D. BURKHART and N. L. ZUTTY: Copolymerization Studies. III. Reactivity Ratios of Model Ethylene Copolymerizations and Their Use in *Q-e* Calculations..... 1137
- PAUL W. MORGAN and STEPHANIE L. KWOLEK: Interfacial Polycondensation. XIII. Viscosity-Molecular Weight Relationship and Some Molecular Characteristics of 6-10 Polyamide.. 1147
- ROLAND E. FLORIN and LEO A. WALL: Electron Spin Resonance of Gamma-Irradiated Cellulose..... 1163
- DAVID W. MCCALL and ERNEST W. ANDERSON: Molecular Motion in Polyethylene. III..... 1175
- K. C. ELLIS and J. O. WARWICKER: Crystallite Orientation in Regenerated Cellulose Filaments. I. Measurement of Orientation by X-Ray Methods..... 1185
- E. W. MERRILL, H. S. MICKLEY, A. RAM, and W. H. STOCKMAYER: The Second Newtonian Viscosity Number..... 1201
- HOWARD C. HAAS, HELEN HUSEK, and LLOYD D. TAYLOR: On the Ultraviolet Absorption Spectrum of Polyvinyl Alcohol... 1215

| | |
|--|------|
| G. SMETS and W. VAN HUMBEECK: Reaction Kinetics and Tacticity of Macromolecules. II. Acrylic Acid Copolymers. . . . | 1227 |
| W. A. HEWETT and F. E. WEIR: Dynamic Properties of Homopolymers and Copolymers of 4-Methyl-1-Pentene. | 1239 |
| BERNHARD WUNDERLICH: The Effect of Pressure on the Crystallization of Polyethylene from Dilute Solution. | 1245 |
| R. Y.-M. HUANG, B. IMMERGUT, E. H. IMMERGUT, and W. H. RAPSON: Grafting Vinyl Polymers onto Cellulose by High Energy Radiation. I. High Energy Radiation-Induced Graft Copolymerization of Styrene onto Cellulose. | 1257 |
| P. G. SCHMIDT: Polyethylene Terephthalate Structural Studies. | 1271 |
| CATHERINE S. HSIA CHEN: Polymerization Induced by Ionizing Radiation at Low Temperatures. III. The Effect of Electron Density on the Polymerization of Substituted Styrenes. | 1293 |
| CHAS. W. WILSON, III: NMR Study of Molecular Chain Structure of Polyvinylidene Fluoride. | 1305 |
| A. M. NORTH and G. A. REED: Diffusion-Controlled Polymerization of Some Alkyl Methacrylates. | 1311 |
| NAOYA YODA: Syntheses of Polyanhydrides. XII. Crystalline and High Melting Polyamidepolyanhydride of Methylenebis(<i>p</i> -carboxyphenyl)amide. | 1323 |
| J. R. HUNTSBERGER: The Locus of Adhesive Failure. | 1339 |
| G. R. COTTEN and W. SACKS: Oxidative Crosslinking of Polyethylene by Ultraviolet Light. | 1345 |
| FERENC TÜDÖS, IMRE KENDE, and MÁRIA AZORI: Inhibition Kinetics of the Polymerization of Styrene. II. Investigations on the Effect of <i>s</i> -Trinitrobenzene. | 1353 |
| FERENC TÜDÖS, IMRE KENDE, and MÁRIA AZORI: Inhibition Kinetics of Polymerization of Styrene. III. Investigations on the Effect of Substituted Trinitrobenzenes. | 1369 |
| P. DE SANTIS, E. GIGLIO, A. M. LIQUORI, and A. RIPAMONTI: Stability of Helical Conformations of Simple Linear Polymers. | 1383 |
| K. HAYASHI, T. YONEZAWA, S. OKAMURA, and K. FUKUI: Molecular Orbital Theory of Reactivity in Radical Polymerization. Part III. | 1405 |
| EDMUND A. DiMARZIO and JULIAN H. GIBBS: Molecular Interpretation of Glass Temperature Depression by Plasticizers. | 1417 |
| V. K. KULSHRESTHA: Studies on Biocolloids and Polyelectrolytes—The Plant—Gums Viscosity of Azrehtic Acid. | 1429 |
| C. G. OVERBERGER and S. NOZAKURA: Copolymerization of Styrene and Styrene Derivative with an Aluminum Alkyl-Titanium Trichloride Catalyst. | 1439 |
| BACON KE: Differential Analysis of High Polymers. VI. Comments on Some Material and Experimental Factors. | 1453 |
| D. B. ANDERSON, G. M. BURNETT, and A. C. GOWAN: Some Novel Effects in Solution Polymerization. | 1465 |

Book Review

- Makromolekulare Stoffe. Part I, Vol. XIV, Methoden der Organischen Chemie (Houben-Weyl), E. MÜLLER, Ed. Reviewed by NORBERT M. BIKALES..... 1471

Errata

- A. P. FIRSOR, B. N. KASHPROV, YU. V. KISSIN, and N. M. CHIRKOV: The Dependence of the Stereospecific Action of the Complex Catalyst $\alpha\text{-TiCl}_3\text{-Me}(\text{C}_2\text{H}_5)_n$ during the Polymerization of α -Olefins on the Metal in the Metalloorganic Compound (article in *J. Polymer Sci.*, **62**, S104-S105, 1962)..... 1472
- A. V. TOBOLSKY, D. KATZ, and M. TAKAHASHI: Rheology of Polytetrafluoroethylene (article in *J. Polymer Sci.*, **A1**, 483-489, 1963)..... 1472
- MASATAMI TAKEDA and KAZUYOSHI IIMURA: Studies on the Configuration and Conformation of Vinyl-Type Polymers. II. Temperature Dependence of the Infrared Spectrum of Polyvinyl Chloride in Solution and Stereoregularity (article in *J. Polymer Sci.*, **57**, 383-393, 1962)..... 1472
- B. ROSEN: Some Mechanical Aspects of the Swelling and Shrinking of Polymeric Solids. Part I. External and Internal Restraints (article in *J. Polymer Sci.*, **58**, 821-837, 1962)..... 1472

ISSUE NO. 5, MAY

- W. D. TAYLOR and A. E. WOODWARD: Preparation and Properties of Copolymers of Maleic Anhydride and 2,2-Dimethylaminoethyl Methacrylate..... 1473
- R. G. SABA, J. A. SAUER, and A. E. WOODWARD: Dynamic Shear Behavior of Poly(γ -benzyl L-Glutamate), Poly(D,L-Propylene Oxide), and Poly(ethyl Vinyl Ether)..... 1483
- J. MERCIER and G. SMETS: Copolymerization. I. Structure of Polyacrylic Anhydride..... 1491
- FUMIO OOSAWA: Thermodynamic Properties of Rodlike Polyelectrolyte Solutions in the Presence of Salts..... 1501
- W. COOPER, F. R. JOHNSTON, and G. VAUGHAN: Stereoregularity in Polyvinyl Alcohols and Esters..... 1509
- R. E. FLORIN, L. A. WALL, and D. W. BROWN: Electron Spin Resonance Spectra and Aged, γ -Irradiated Polystyrenes..... 1521
- HERWARD VOGEL and C. S. MARVEL: Polybenzimidazoles. II..... 1531
- TOSHIYUKI SHONO and C. S. MARVEL: Polymers Derived from Unsaturated Esters of Hydronopoxyalkanols..... 1543
- T. HUFF and ELI PERRY: Reaction of Polymeric Radicals with Organometallic Compounds..... 1553
- GIAN ALVISÉ CARAZZOLO: Structure of the Normal Crystal Form of Polyoxymethylene..... 1573

| | |
|--|------|
| ORIN C. HANSEN, JR., THOMAS L. FABRY, LEON MARKER, and ORVILLE J. SWEETING: Apparatus for Measuring the Dynamic Tensile Modulus of Thin Polymeric Films..... | 1585 |
| M. BERGER: Steric Structures in Copolymerization..... | 1601 |
| J. DROUGAS, A. TIMNICK, and R. L. GUILÉ: High Frequency Titrations of Polydicarboxylic Acid Copolymers: Polyitaconic Acid- <i>Co</i> -Styrene and Polymaleic Acid- <i>Co</i> -Styrene..... | 1609 |
| D. E. KLINE: Nuclear Radiation Effects in Polytetrafluoroethylene..... | 1621 |
| HIKARU SEKIGUCHI: Mécanisme réactionnel de la Polymérisation alcaline des Lactames..... | 1627 |
| DOV KATZ: Polymerization and Copolymerization of 1- and 9-Vinylanthracenes and 9-Vinylphenanthrene..... | 1635 |
| ISAAC D. RUBIN: Isomorphism in Polycarbonates. Copolymers of Hydroquinone and Substituted Hydroquinones..... | 1645 |
| A. R. SHULTZ, P. I. ROTH, and J. M. BERGE: Radiation Degradation of Polymethacrylates. Dose Rate and Medium Effects.. | 1651 |
| J. H. GOLDEN and E. A. HAZELL: Degradation of a Polycarbonate by Ionizing Radiation..... | 1671 |
| K. H. BASSETT, C. Y. LIANG, and R. H. MARCHESSAULT: The Infrared Spectrum of Crystalline Polysaccharides. IX. The Near Infrared Spectrum of Cellulose..... | 1687 |
| R. D. GLAUZ: Transient Analysis of a Vibrating Reed..... | 1693 |
| R. W. WARFIELD and M. C. PETREE: Thermodynamic Properties of Polymethyl Methacrylate and Methyl Methacrylate..... | 1701 |
| DAVID W. MCCALL, DEAN C. DOUGLASS, and ERNEST W. ANDERSON: Self-Diffusion and Nuclear Relaxation in Polyisobutylene..... | 1709 |
| M. O. DE LA CUESTA and F. W. BILLMEYER, JR.: The Molecular Structure of Polyethylene. XII. Intrinsic Viscosities of Polyethylene Solutions..... | 1721 |
| MAURICE MORTON, E. E. BOSTICK, R. A. LIVIGNI, and L. J. FETTERS: Homogeneous Anionic Polymerization. IV. Kinetics of Butadiene and Isoprene Polymerization with Butyllithium.. | 1735 |
| F. M. BROWER and H. W. McCORMICK: Narrow Molecular Weight Distribution Polystyrene..... | 1749 |
| ROBERT TOGGENBURGER and STANLEY J. GILL: Anisotropic Properties of Strained Viscoelastic Fluids. III. Birefringence of Polystyrene Solutions..... | 1765 |
| R. TOGGENBURGER, K. BECK, and S. J. GILL: Theoretical Calculations of Stress Relaxation in Concentrated Solutions..... | 1779 |
| C. C. HSIAO and T. S. WU: Orientation and Strength of Branched Polymer Systems..... | 1789 |
| A. KISHIMOTO and Y. ENDA: Diffusion of Benzene in Polyacrylates | 1799 |
| ALBERT ZILKHA, SAMUEL BARZAKAY, and ARIEL OTTOLENGHI: Effect of Solvents on the Anionic Polymerization of Styrene by Phenyllithium..... | 1813 |

| | |
|---|------|
| JAMES C. W. CHIEN: Olefin Polymerizations and Polyolefin Molecular Weight Distribution..... | 1839 |
|---|------|

ISSUE NO. 6, JUNE

| | |
|---|------|
| A. A. MILLER: The Reference Point for Liquid Relaxation Processes. I. Melt Viscosity of Polystyrene..... | 1857 |
| A. A. MILLER: The Reference Point for Liquid Relaxation Processes. II. Melt Viscosity of Polyisobutylene..... | 1865 |
| R. ST. JOHN MANLEY: Growth and Morphology of Single Crystals of Cellulose Triacetate..... | 1875 |
| R. ST. JOHN MANLEY: Hydrolysis of Cellulose Triacetate Crystals | 1893 |
| P. GIORDANO ORSINI, B. MARCHESI, and L. MAZZARELLA: Morphology of Polyethylene Single Crystals..... | 1901 |
| P. JÄGER and E. S. WAIGHT: Solid State Polymerization of Methacrylamide and <i>N</i> -Arylmethacrylamides..... | 1909 |
| M. G. BALDWIN and SAMUEL F. REED: Polymerization Studies on Allylic Compounds. I..... | 1919 |
| DAVID E. BURGE and DOUGLAS B. BRUSS: Preparation and Properties of Some Poly- α -Methylstyrenes..... | 1927 |
| K. IWASAKI, H. FUKUTANI, and S. NAKANO: Polymerization of Vinyl Ethers with Magnesium Compounds. I. Catalytic Reactivity of Magnesium Halides..... | 1937 |
| C. A. J. HOEVE and M. K. O'BRIEN: Specific Diluent Effects on Polymer Chain Dimensions..... | 1947 |
| ADA L. JACOBSON: The Temperature Dependence of Magnesium Chloride Interaction with Polyacrylic Acid..... | 1955 |
| ATANAZY BORYNIEC and BOGUMIŁ ŁASZKIEWICZ: Bulk Copolymerization of Methyl Methacrylate with Phenylchlorophosphine..... | 1963 |
| HIROYOSHI KAMOGAWA and HAROLD G. CASSIDY: Electron Exchange Polymers. XIX. Copolymerization Behavior of Vinylhydroquinone Dibenzoate..... | 1971 |
| GEORGE S. PARKS and HELENE P. MOSHER: Enthalpy and Free Energy Changes in Some Simple Polymerization Processes.... | 1979 |
| W. R. MOORE and R. SHUTTLEWORTH: Thermodynamic Properties of Solutions of Cellulose Triacetate..... | 1985 |
| LAWRENCE E. NIELSEN and FRED D. STOCKTON: Theory of the Modulus of Crystalline Polymers..... | 1995 |
| CHARLES R. MCINTOSH, WILLIAM D. STEPHENS, and CURTIS O. TAYLOR: Changes in the Stereospecificity of a Ziegler Catalyst Used in the Polymerization of Butadiene..... | 2003 |
| MASAKAZU INOUE: Nucleating Effect on the Kinetics of Crystallization and the Spherulites of Nylon 6..... | 2013 |
| C. G. OVERBERGER and KAZUO MIYAMICHI: Copolymerization of Styrene and Aliphatic Olefins..... | 2021 |
| F. RYBNÍKÁŘ: Mechanism of Secondary Crystallization in Polymers..... | 2031 |

| | |
|--|------|
| HIROSHI SOBUE and KENKICHI MURAKAMI: Maximum Relaxation Time on Polymers in the Vicinity of Critical Molecular Weight | 2039 |
| RYONG-JOON ROE and WILLIAM R. KRIGBAUM: A Thermodynamic Study of Viton Elastomer | 2049 |
| D. A. FREY, MASAKI HASEGAWA, and C. S. MARVEL: Preparation and Aromatization of Poly-1,3-Cyclohexadiene. II | 2057 |
| TOSHIYUKI SHONO and C. S. MARVEL: Preparation and Polymerization of Vinyl 12-hydroxystearate | 2067 |
| A. RUDIN and J. S. MACKIE: Some Anomalous Brittleness Temperatures of Polyethylene | 2075 |
| E. TURSKA and S. POŁOWIŃSKI: Examination of Kinetics of Graft Copolymerization on Preirradiated Polymethyl Methacrylate | 2085 |
| A. KATCHALSKY and Z. ALEXANDROWICZ: On the Additivity of Osmotic Properties of Polyelectrolyte-Salt Solutions | 2093 |
| KEIITI SISIDO, NOBUO KUSANO, RYŌZI NOYORI, YŌKO NOZAKI, MASATOSI SIMOSAKA, and HITOSI NOZAKI: Polycondensation of Xylylene Dibromides by Transition Metals in Water Suspension | 2101 |
| H. FISCHER, K.-H. HELLWEGE, und P. NEUDÖRFL: Elektronenspinresonanz-Untersuchungen an Peroxydradikalen in bestrahltem Polypropylen | 2109 |
| J. F. JACKSON: Crystallinity in Ethylene-Propylene Copolymers | 2119 |
| S. SUGAI and A. E. WOODWARD: Counterion Binding in Partially Neutralized Copolymers of Crotonic Acid and Vinyl Alcohol | 2127 |
| TSUNEO YOSHINO and YASUO MANABE: Photosensitivity of Dry-Heated Polyacrylonitrile | 2135 |
| R. SALOVEY and ROSENZWEIG: Radiation Dosimetry in Polyethylene with Silicon Solar Cells | 2145 |
| R. SALOVEY and F. R. DAMMONT: Irradiation of Polyethylene Oxide and Polypropylene | 2155 |
| G. S. WICH and N. BRODOWAY: Relative Radioactivity Ratios for Two New 2-Chloro-1,3-Butadiene Systems | 2163 |
| M. BAER: Anionic Block Polymerization. I. Block Polymerization of Styrene on Polystyrene | 2171 |
| JOAN BOND and D. B. ROBSON: The Role of Metal Chelates in Polymerization Initiation. I. Chromous Chelates | 2179 |
| JOAN BOND and D. B. ROBSON: The Role of Metal Chelates in Polymerization Initiation. II. Cupric Chelates | 2185 |
| E. F. T. WHITE and M. J. ZISSELL: Polymerization of Acrylonitrile in Dimethylsulfoxide | 2189 |
| AKIHIRO ABE and MURRAY GOODMAN: Optical Rotatory Properties of Polyaldehydes | 2193 |
| H. A. POHL, C. G. GOGOS, and C. CAPPAS: Resistivity Studies on Polymer Semiconductors | 2207 |
| A. J. HAVLIK, J. MOACANIN, and I. OTTERNESS: Ebulliometric and Endgroup Molecular Weights of Polyoxypropylene and Polyoxyethylene Glycols | 2213 |

| | |
|---|------|
| MORTON LITT: Poly(4-methyl Pentene): X-Ray Measurement of Crystalline Density and Observation of a Structural Anomaly | 2219 |
| R. BACSKAI and S. J. LAPPORTE: The Chemical Structure of Polyisobutylene Obtained by Ziegler Catalysis | 2225 |
| N. L. ZUTTY: Copolymerization Studies. IV. Transannular Copolymerization of Bicyclo[2.2.1]hepta-2,5-diene | 2231 |

Book Reviews

| | |
|---|------|
| Radiation Chemistry of Polymeric Systems High Polymers, A. CHAPIRO, Ed. Reviewed by G. ADLER | 2237 |
| Introduction to Polymer Chemistry. J. K. STILLE. Reviewed by ROBERT W. LENZ | 2237 |
| Soviet Research on Organo-Silicon Chemistry, 1959, Parts I and II, Consultants Bureau. Reviewed by EUGENE G. ROCHOW | 2238 |
| Unsolved Problems in Polymer Science, FRANK R. MAYO, Ed. Reviewed by C. G. OVERBERGER and E. H. IMMERGUT | 2239 |

Erratum

| | |
|--|------|
| R. MEREDITH and BAY-SUNG HSU: Dynamic Bending Properties of Fibers: Effect of Temperature on Nylon 66 Terylene, Orlon, and Viscose Rayon (article in <i>J. Polymer Sci.</i> , 61 , 271-292, 1962) | 2240 |
|--|------|

ISSUE NO. 7, JULY

| | |
|---|------|
| J. R. HUNTSBERGER: Adhesion. II Relationships between Viscoelasticity, Interfacial Equilibrium, and the Temperature Dependence of Adhesion | 2241 |
| B. R. LOY: Electron Spin Resonance of Polypropylene | 2251 |
| G. M. BRISTOW: The Mastication of Elastomers. Part III. The Solution Properties of Masticated Synthetic <i>cis</i> -Polyisoprene | 2261 |
| CHEVES WALLING and DENNIS D. TANNER: Organic Reactions under High Pressure. IX. The Effect of Pressure on the Stereochemistry of Methyl Methacrylate Polymerization | 2271 |
| G. FILIPOVICH: Nuclear Magnetic Resonance in Solid Polypyrrolidone | 2279 |
| N. L. ZUTTY and F. J. WELCH: Synthesis of Vinyl Polymers Containing α -Substituted γ -Butyrolactone Groups in their Backbones | 2289 |
| W. R. EDWARDS and N. F. CHAMBERLAIN: Carbonium Ion Rearrangement in the Cationic Polymerization of Branched Alpha Olefins | 2299 |
| KWEI-PING SHEN KWEI: Graft Copolymers of Polyacrylic Acid with Desoxyribonucleic Acid (DNA) | 2309 |
| PAUL G. SCHMIDT: Polypropylene Structure | 2317 |
| MARIAN KRYSZEWSKI and MARTA SKORKO: Interactions of Low Molecular Weight Compounds with Solid Polymers | 2327 |

| | |
|---|------|
| S. YAMADA, W. PRINS, and J. J. HERMANS: Determination of Number-Average Molecular Weights by Elastoosmometry | 2335 |
| HAROLD SCHONHORN: Generalized Approach to Adhesion Via the Interfacial Deposition of Amphiphatic Molecules. I. Adhesion of Polyethylene to Aluminum | 2343 |
| ROBERT A. MENDELSON: Elution Fractionation of Crystalline Polypropylene | 2361 |
| K. IWASAKI, H. FUKUTANI, Y. TSUCHIDA, and S. NAKANO: Polymerization of Vinyl Ether with Magnesium Compounds. II. Catalytic Reactivity of Magnesium Compounds Other than Halides | 2371 |
| EUGENE C. WINSLOW and NANCY E. GERSHMAN: Phthalocyanine-Crosslinked Polyvinylphthalic Acid | 2383 |
| P. DEBYE, B. CHU, and H. KAUFMANN: Molecular Configuration of Polystyrene in Benzene | 2387 |
| NOBUHIRO KUWAHARA: On the Polymer-Solvent Interaction in Polymer Solutions | 2395 |
| YUTAKA SAKURADA: Polymerization of α -Methylstyrene with $\text{Al}(\text{C}_2\text{H}_5)_3$ - TiCl_4 Catalyst | 2407 |
| G. J. K. ACRES and F. L. DALTON: Synthesis of Styrene-Methyl Methacrylate Nonrandom Copolymers in Emulsion Systems with Cobalt-60 Gamma Radiation | 2419 |
| D. B. BRUSS and F. H. STROSS: A Comparison of Dynamic Methods for Osmotic Pressure Measurements | 2439 |
| JACK B. CARMICHAEL and JACK B. KINSINGER: Unrestricted Rotation in Polymers with Discrete Rotational States | 2459 |
| A. D. KETLEY and J. D. MOYER: Competing Side Reactions in the Polymerization of α -Olefins by Ziegler-Natta Catalysts | 2467 |
| RACHELA TAKSERMAN-KROZER: Behavior of Polymer Solutions in the Velocity Field with Parallel Gradient. III. Molecular Orientation in Dilute Solutions Containing Flexible Chain Macromolecules | 2477 |
| RACHELA TAKSERMAN-KROZER: Behavior of Polymer Solutions in the Velocity Field with Parallel Gradient. IV. Viscosity of Dilute Solutions Containing Flexible Chain Macromolecules | 2487 |
| Book Reviews | |
| Physik der Kunststoffe, WERNER HOLZMULLER and KURT ALTENBERG, Editors. Reviewed by MAURICE L. HUGGINS | 2495 |
| Advances in Petroleum Chemistry and Refining, Vol. IV, JOHN J. MCKETTA, JR., Editor. Reviewed by HERBERT N. FRIEDLANDER | 2495 |

| | |
|--|------|
| RAFFAELE SHIBA and F. R. EIRICH: Viscoelastic Behavior of Plasticized Polyvinyl Chloride at Large Deformations. I. Stress Relaxation | 2497 |
|--|------|

| | |
|---|------|
| RAFFAELE SABIA and F. R. EIRICH: Viscoelastic Behavior of Plasticized Polyvinyl Chloride at Large Deformations. II. Creep | 2511 |
| TOD W. CAMPBELL and RICHARD N. McDONALD: Polymeric Derivatives of 3,3-Bis(aminomethyl)-Oxetane and of Exoxysuccinyl Chloride..... | 2525 |
| S. M. MILLER, M. W. SPINDLER, and R. L. VALE: Use of Dimaleimides as Accelerators for the Radiation-Induced Vulcanization of Hydrocarbon Polymers. Part II. Synthetic Rubbers and Saturated Polymers..... | 2537 |
| W. G. LLOYD: The Influence of Transition Metal Salts in Polyglycol Autoxidations..... | 2551 |
| R. M. BARRER, J. A. BARRIE, and M. G. ROGERS: Heterogeneous Membranes: Diffusion in Filled Rubber..... | 2565 |
| WAYNE E. SMITH and RALPH G. ZELMER: An Interpretation of Ethylene Polymerization with Alkyl-Promoted Transition-Metal Catalysts..... | 2587 |
| J. SCHMORAK and M. LEWIN: The Chemical and Physicochemical Properties of Wheat Starch Mildly Oxidized with Alkaline Sodium Hypochlorite..... | 2601 |
| S. KRIMM, V. L. FOLT, J. J. SHIPMAN, and A. R. BERENS: Infrared Spectra and Assignments for Polyvinyl Chloride and Deuterated Analogs..... | 2621 |
| SAMUEL H. MARON and THOMAS T. CHIU: Study of Entanglement of Polymers in Solution by Viscosity Measurements. II. Polymethyl Methacrylate in Various Solvents..... | 2651 |
| G. J. HOWARD: Turbidimetric Titration of Nylon 66..... | 2667 |
| MAURICE MORTON and WILLIAM E. GIBBS: The Emulsion Polymerization of 2,3-Dimethylbutadiene-1,3..... | 2679 |
| MASAKAZU INOUE: Studies on Crystallization of High Polymers by Differential Thermal Analysis..... | 2697 |
| F. H. OWENS and F. E. ZIMMERMAN: Photochlorination of Poly(methyl Methacrylate) in Aqueous Suspension..... | 2711 |
| C. M. HUGGINS, L. E. ST. PIERRE, and A. M. BUCHE: Further NMR Studies of Polydimethylsiloxanes: Effects of Radiation-Induced Crosslinking..... | 2731 |
| C. V. STEPHENSON and W. S. WILCOX: Ultraviolet Irradiation of Plastics. IV. Further Studies of Environmental Effects on Films and Fibers..... | 2741 |
| ISSUE NO. 9, SEPTEMBER | |
| RAYMOND L. ARNETT, MELVIN E. SMITH, and BARRY O. BUELL: An Improved Ebullioscope for High Polymers..... | 2753 |
| R. CHIANG: Crystallization and Melting Behavior of Polyacrylonitrile..... | 2765 |
| R. BACSKAI: Polymerization of Alicyclic Epoxides with Aluminum Alkyl Catalysts..... | 2777 |
| SHIRO YAKASHIMA: Effect of Ions on the Dielectric Dispersion of Ovalbumin Solution..... | 2791 |

| | |
|--|------|
| S. E. CHAPPELL, J. A. SAUER, and A. E. WOODWARD: Effects of High Energy Irradiation on Polypropylene..... | 2805 |
| RICHARD H. WILEY and BURNS DAVIS: Tracer Techniques for the Determination of Monomer Reactivity Ratios. IV. Monomer Reactivity Ratios for Styrene-Isoprene Copolymerization..... | 2819 |
| JERRY N. KORAL and EDWIN M. SMOLIN: The Preparation and Polymerization of Suberaldehyde..... | 2831 |
| N. K. J. SYMONS: Growth of Single Crystal of Polytetrafluoroethylene from the Melt..... | 2843 |
| J. F. RUDD and E. F. GURNEE: The Effect of Molecular Weight Distribution on the Optical Properties of Polystyrene in the Transition Region..... | 2857 |
| J. E. GUILLET: Long-Chain Branching Frequency in Polyethylene..... | 2863 |
| F. H. CHOWDHURY and S. M. NEALE: Acid Behavior of Carboxylic Derivatives of Cellulose. Part I. Carboxymethylcellulose.. | 2881 |
| F. H. CHOWDHURY and S. M. NEALE: Acid Behavior of Carboxylic Derivatives of Cellulose. Part II. Oxycellulose..... | 2893 |
| HAZIME KUSUMOTO and H. S. GUTOWSKY: Proton Magnetic Resonance in Natural Rubber: Comparison with Dielectric Measurements..... | 2905 |
| SAKUJI IKEDA, AKIO YAMAMOTO, and HIROSHI TANAKA: Stereoregulated Polydeuteroethylene I. Polymers of <i>trans</i> -1,2-Dideuteroethylene and <i>cis</i> -1,2-Dideuteroethylene by a Ziegler Catalyst..... | 2925 |
| BERND REICHEL, C. S. MARVEL, and R. Z. GREENLEY: Transannular Polymerization of 1,5-Cyclooctadiene..... | 2935 |
| M. BERGER and D. J. BUCKLEY: Structure Effects and Related Polymer Properties in Polybutadiene. I. Preparation and Characterization..... | 2945 |
| NIICHIRO TOKURA, MINORU MATSUDA, and YASUO OGAWA: Polymerization in Liquid Sulfur Dioxide. Part XIII. Polymerization of Styrene Derivatives in Liquid Sulfur Dioxide..... | 2965 |
| T. K. KWEI: Swelling of Highly Crosslinked Network Structure.. | 2977 |
| ALAIN GUYOT et JEAN-CLAUDE DANIEL: Etude de la Polymérisation des Oléfines catalysée par les Oxydes métalliques. I. Méthodes expérimentales d'Etude cinétique; Résultats préliminaires sur la Polymérisation du Propylène par le Système catalytique Phillips..... | 2989 |

ISSUE No. 10, OCTOBER

| | |
|--|------|
| G. J. K. ACRES and F. L. DALTON: On Co ⁶⁰ Gamma-Ray-Initiated Emulsion Polymerization..... | 3009 |
| A. PACKTER: Conductivity and Viscosity Measurements on Sodium Polyacrylates of Different Molecular Weights..... | 3021 |
| HIROYUKI TADOKORO, SHUNSUKE MURAHASHI, REIZÔ YAMADERA, and TEI-ICHI KAMEI: Infrared Absorption Spectra of Polyacrylonitrile and Deuterated Polyacrylonitriles..... | 3029 |

| | |
|--|------|
| MAURICE MORTON and IRJA PIIRMA: The Branching Reaction. III. Polymeric Transfer Constants of Vinyl Acetate with Styrene and Methyl Methacrylate. | 3043 |
| STEFAN CZARNECKI and MARIAN KRYSZEWSKI: Some Applications of Afterglow Studies of Luminescent Compounds in Solid Polymers. | 3067 |
| M. G. SHARMA and T. W. HAAS: Some Viscoelastic Studies on Penton | 3079 |
| M. H. WALTERS: Fibrous Structure in Stretched Crystalline Elastomers. | 3091 |
| J. O. WARWICKER: The Diffusion of Chrysophenine G into Viscose Sheet. | 3105 |
| G. M. BOWER and L. W. FROST: Aromatic Polyimides. | 3135 |
| NAOYA OGATA: Resonance Effect of Amide Group on the Polymerizability of Lactam Derivatives. III. Polymerization of Many-Membered Lactams Ring. | 3151 |
| JOSEPH D. LOCONTI and JOHN W. CAHILL: Zone-Refining Fractionation of Polymers. | 3163 |
| A. M. KOTLIAR: Evaluation of Molecular Weight Averages Resulting from Random Crosslinking and Chain Scission Processes for Wide Schulz-Zimm Distributions. | 3175 |
| BERNARD D. COLEMAN and THOMAS G. FOX: General Theory of Stationary Random Sequences with Applications to the Tacticity of Polymers. | 3183 |
| Z. ZLÁMAL and A. KAZDA: Donor-Acceptor Interaction in Cationic Polymerization. V. Influence of Some Alcohols of the Molecular Weight of Polyisobutylene in Polymerization Catalyzed by Aluminum Trichloride. | 3199 |
| M. G. BALDWIN: Primary Radical Termination in Methyl Methacrylate Polymerization. | 3209 |
| PAUL EHRLICH and JOHN J. KURPEN: Phase Equilibria of Polymer-Solvent Systems at High Pressures Near Their Critical Loci: Polyethylene with <i>n</i> -Alkanes. | 3217 |
| Z. ALEXANDROWICZ and A. KATCHALSKY: Colligative Properties of Polyelectrolyte Solutions in Excess of Salt. | 3231 |
| W. DEWINTER, C. S. MARVEL, and AZIZ ABDUL-KARIM: Polydiacrylylmethane. | 3261 |

ISSUE NO. 11, NOVEMBER

| | |
|--|------|
| P. BATAILLE and D. PATTERSON: An Application of the Prigogine Solution Theory to Intrinsic Viscosities in Polyisobutylene- <i>n</i> -Alkane Systems. | 3265 |
| S. NAKANO, K. IWASAKI, and H. FUKUTANI: Stereospecific Polymerization of Vinyl Alkyl Ethers. | 3277 |
| MITIO INOKUTI and MALCOLM DOLE: Interpretation of the Intrinsic Viscosity of Polymers Undergoing Simultaneous Degradation and Crosslinking. | 3289 |

| | |
|---|------|
| HIROSHI INAGAKI, SYUJI KAWAI, and ATSUSHI NAKAZAWA: Application of the Archibald Ultracentrifugal Method for the Study of Dilute Polymer Solutions. II. Examination of Two Solution Systems near the Flory Temperature. | 3303 |
| FRANK J. LIMBERT and ERIC BAER: Kinetics of Nucleation and Growth of Spherulites in Homopolymers. | 3317 |
| J. GREYSON and A. A. LEVI: Calorimetric Measurements of the Heat of Sorption of Water Vapor on Dry Swollen Cellulose. | 3333 |
| K. I. BEYNON: Monomers Containing Phosphorus. Part I. Copolymerization of Phosphonates with <i>n</i> -Lauryl Methacrylate. | 3343 |
| K. I. BEYNON: Monomers Containing Phosphorus. Part II. Copolymerization of Diallyl Phenyl Phosphine Oxide with <i>n</i> -Lauryl Methacrylate. | 3357 |
| YŪJI SHIOJI, SHUN-ICHI OHNISHI, and ISAMU NITTA: ESR Study of Irradiated Acrylic Acid and Reaction of the Produced Radical | 3373 |
| R. JOSEPHS and J. FEITELSON: Interactions of Polyelectrolytes. A Turbidimetric Method for the Estimation of Ionized Polymers | 3385 |
| GERT F. BAUMANN and SAMUEL STEINGISER: Rheological Measurements on Polycarbonate. | 3395 |
| RUTH R. BENERITO, RALPH J. BERNI, JOHN B. MCKELVEY, and BEVERLY G. BURGIS: Study of the Base-Catalyzed Cellulose — <i>d,l</i> -Butadiene Diepoxide Reaction. | 3407 |
| MASAKAZU INOUE: Properties of Melt-Blends of Crystalline High Polymers. Fusion and Crystallization Behaviors. | 3427 |
| H. F. MARK and N. OGATA: Copolymerization of Aldehydes. | 3439 |
| LOUIS E. MATTISON, MARTHA S. PHIPPS, LILLIAN ALFRED, SALLY TAYLOR, JOHN THOMPSON, and BARRY SAUL: Coordination Compounds of <i>p</i> -Nitrobenzeneazotyrosine. | 3449 |
| A. T. DiBENEDETTO: Molecular Properties of Amorphous High Polymers. I. A Cell Theory for Amorphous High Polymers | 3459 |
| A. T. DiBENEDETTO: Molecular Properties of Amorphous High Polymers. II. An Interpretation of Gaseous Diffusion Through Polymers. | 3477 |
| W. L. HAWKINS and MRS. M. A. WORTHINGTON: Synergistic Antioxidant Combinations. Carbon Black Substitutes. | 3489 |
| W. L. HAWKINS and MRS. H. SAUTTER: Synergistic Antioxidant Combinations. Mechanism of Stabilization with Organo-Sulfur Compounds. | 3499 |
| J. W. WOOD and PETER T. MORA: Preparation and Biological Application of Highly Substituted Cationic Derivatives of Polysaccharides. | 3511 |
| Book Reviews | |
| Analytical Chemistry of Polymers, Vol. XII, Part II., G. M. KLINE, Ed., Reviewed by H. S. KAUFMAN. | 3519 |
| Physical Properties of Polymers, F. BUECHE, and Mechanical Properties of Polymers, L. E. NIELSEN. Reviewed by R. S. STEIN. | 3519 |

ISSUE No. 12, DECEMBER

| | |
|--|------|
| Editorial | 3251 |
| HAROLD SCHONHORN: Generalized Approach to Adhesion Via the Interfacial Deposition of Amphipathic Molecules. II. Adhesion of Polyethylene to Aluminum | 3523 |
| HISASHI UEDA, ZENICHIRO KURI, and SHOJI SHIDA: Electron Spin Resonance Studies of the Reaction of Gases with the Radicals Formed in Irradiated Polytetrafluoroethylene | 3537 |
| M. KHAIRY, S. MORSI, and CLARENCE STERLING: Crystallization in Starch: The Role of Ions in the Lyotropic Series | 3547 |
| JOSEPH PELLON: Polyamides Containing Phosphorus. II. Structural Effects on Softening and Glass Transition Temperatures | 3561 |
| G. NATTA, G. CRESPI, and U. FLISI: Thermodynamic Interpretations of the Elastic Properties of Rubbers Obtained from Ethylene-Propylene Copolymers | 3569 |
| BERNHARD WUNDERLICH, PETER SULLIVAN, TAMIO ARAKAWA, A. B. DICYAN, and J. F. FLOOD: Thermodynamics of Crystalline Linear High Polymers. III. Thermal Breakdown of the Crystalline Lattice of Polyethylene | 3581 |
| THOR L. SMITH: Ultimate Tensile Properties of Elastomers. I. Characterization by a Time and Temperature Independent Failure Envelope | 3597 |
| WILLIAM J. BURKE and HAROLD P. HIGGINBOTTOM: Nitrosation of Linear Phenol-Formaldehyde Polymers | 3617 |
| H. R. ALLCOCK and R. L. KUGEL: Ionic Polymerization of Diphenylvinylphosphine Oxide | 3627 |
| ARIEL OTTOLENGHI, SAMUEL BARZAKAY, and ALBERT ZILKHA: Anionic Polymerization of Acrylonitrile by Various Catalysts | 3643 |
| ROBERT H. HORROCKS and EUGENE C. WINSLOW: Oxine-Formaldehyde Polymers and Their Metallic Chelates | 3655 |
| Book Review | |
| Makromolekulare Stoffe, Part II, Vol. XIV, Methoden der Organischen Chemie (Houben-Weyl), E MÜLLER, Ed. Reviewed by NORBERT M. BIKALES | 3665 |
| Errata | |
| O. C. HANSEN, T. L. FABRY, L. MARKER, and O. J. SWEETING: Apparatus for Measuring the Dynamic Modulus of Thin Polymer Films (article in <i>J. Polymer Sci.</i> , A1 , 1585-1600, 1963) | 3666 |
| M. WALES and S. J. REHFELD: Molecular Weight Distribution by Velocity Ultracentrifugation (article in <i>J. Polymer Sci.</i> , 62 , 179-196, 1962) | 3666 |
| Author Index Volume 1 | 3667 |
| Subject Index Volume 1 | 3678 |

Dipole Moment, Stress Relaxation, and Birefringence of Viton Fluoroelastomer

W. R. KRIGBAUM, M. KANEKO,* and A. ROIG,† *Department of Chemistry, Duke University, Durham, North Carolina*

Introduction

This investigation was undertaken with the initial objective of determining whether the dielectric constant of a network polymer varies significantly during deformation. We hoped that the root mean square dipole moment might provide a means to study the change in the average rotational angle about the chain bonds accompanying elongation of a macroscopic sample. Viton appeared to be suitable for this study, since the dipole moment is large enough to permit the measurement of relatively small changes. However, the interpretation of these results was complicated by a slow relaxation process, which led us to investigate the dependence of the relaxation of stress and birefringence upon temperature and elongation.

Dipole Moment

The sample, a cast sheet of Viton A approximately 0.5 mm. in thickness and lightly crosslinked by gamma radiation, was very kindly furnished by the Elastomer Chemical Department of E. I. du Pont de Nemours and Co. Dielectric constant measurements were performed by use of a conventional capacitance bridge and a General Radio precision condenser. The plates of the test condenser were kept in contact with the surface of the sample by a screw adjustment. A plot of dielectric constant versus separation exhibited a marked discontinuity when contact was made with the sample. The distance of separation could be accurately measured through use of an auxiliary air condenser whose plates moved in unison with those of the test condenser. An air thermostat maintained the test condenser at $35.00 \pm 0.05^\circ\text{C}$. during the measurements.

The capacity of the condenser containing the unstrained sample was first measured as a function of frequency to locate the dispersion region. The results obtained are presented in Figure 1. Data were then obtained at several frequencies in the vicinity of 200 cycles/sec. and 100 kcycles/sec. for the sample at various elongations. These respective frequencies were chosen to lie well below, or above, the dispersion region. The dielectric

* Present address: Department of Polymer Physics, Hokkaido University, Sapporo, Japan.

† Present address: Institute of Physical Chemistry, C.S.L.C., Madrid, Spain.

constants observed for the sample under strain were markedly time dependent. Figure 2 illustrates the variation with time of ϵ_s (low frequency) and ϵ_∞ (high frequency) obtained at two relative elongations, α . The dielectric constant decreases sharply as stress is applied, and then gradually increases as stress relaxation proceeds. However, the limiting values of ϵ_s and ϵ_∞ at long times appear to decrease monotonely with increasing elongation. Values of $(\epsilon_s - \epsilon_\infty)$ extrapolated back to zero time decrease approximately linearly with α , as illustrated by the open circles in Figure 3. Our primary interest concerns the variation with elongation of the ϵ_s and ϵ_∞ values corresponding to very long times. Unfortunately, the duration of our measurements was only sufficient to permit this extrapolation to be performed for the two lowest α values. These

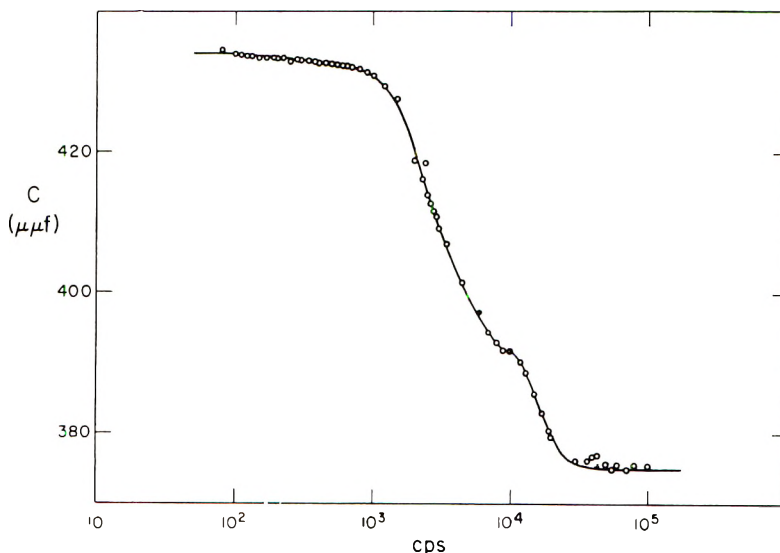


Fig. 1. Capacity measured at 35°C. for the test condenser and Viton sample at various frequencies.

$(\epsilon_s - \epsilon_\infty)$ differences, represented by the filled circles in Figure 3, also exhibit a decrease with elongation.

The root mean square group dipole moment may be evaluated from these data in two different ways. The Onsager equation is:¹

$$\mu^2 = (9kT/4\pi N)(M/\rho)[(\epsilon_s - \epsilon_\infty)(2\epsilon_s + \epsilon_\infty)/\epsilon_s(\epsilon_\infty + 2)^2] \quad (1)$$

where N is Avogadro's number, M the molecular weight, and ρ the density, 1.794 g./cc. for our example. Objections^{2,3} have been raised concerning the assumption that ϵ_∞ can be measured at frequencies as low as 10^5 cycles/sec. For water, Collic, Hasted, and Ritson⁴ obtained $\epsilon_\infty = 5.5$ at 2.4×10^{10} cycles/sec., whereas the square of the refractive index n^2 , is lower by a factor of three, 1.79. The situation is nearly the same for

Viton, since $\epsilon_\infty = 5.98$ at 2×10^5 cycles/sec. and $n^2 = 1.882$. It therefore appears that ϵ_∞ in eq. (1) should be replaced by n^2 .

A more recent treatment has been given by Harris and Alder.² If short-range interactions are neglected, their result may be written as:

$$m^2 = (3kT/4\pi N)(M/\rho)[(\epsilon_s - n^2)(2\epsilon_s + 1)/\epsilon_s(n^2 + 2)] \quad (2)$$

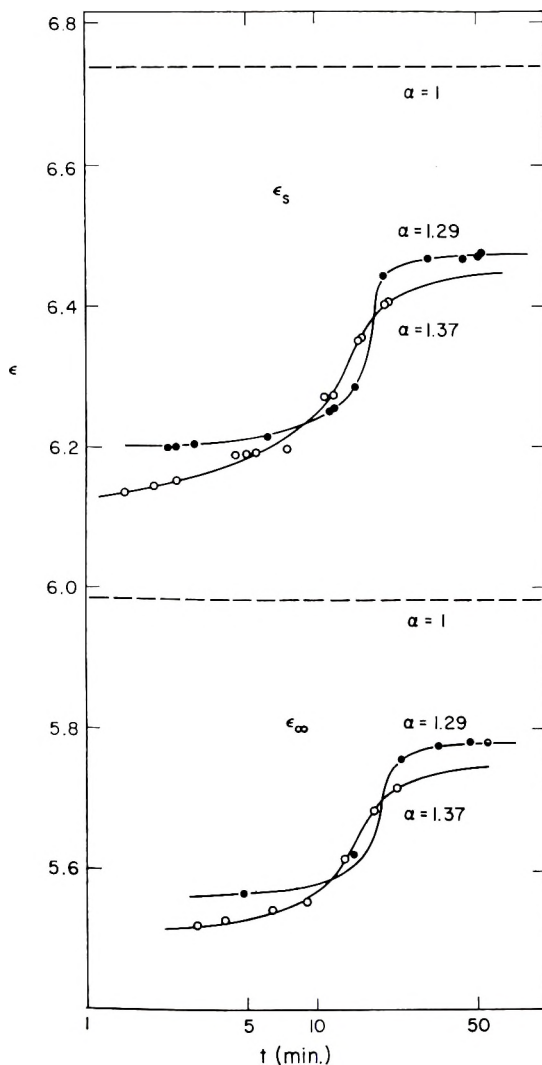


Fig. 2. Dielectric constant at 200 cycles/sec. and 100 kcycles/sec. (ϵ_s and ϵ_∞ , respectively) shown as a function of time for two elongations.

The effect of the surrounding medium may then be taken into account through use of the Onsager relation:

$$m = \mu[(n^2 + 2)/3] [(2\epsilon_s + 1)/(2\epsilon_s + n^2)] \quad (3)$$

These relations yield $\mu = 1.89$ D. for a $C_5F_8H_2$ unit, which decreases instantaneously to 1.79 D. upon elongation to $\alpha = 1.3$, and increases to 1.85 D. after relaxation. Somewhat larger moments are obtained by using the modified form of the Onsager equation discussed above.

We believe the variation with α , although small, is outside the experimental error. Undoubtedly, considerably larger variations would have been obtained if limiting values of the dielectric constant at long times could have been obtained for the higher elongations. It therefore appears that the dielectric constant, or average group moment, can be used to investigate the molecular events which accompany both deformation and stress relaxation in appropriately chosen polymer network systems. The

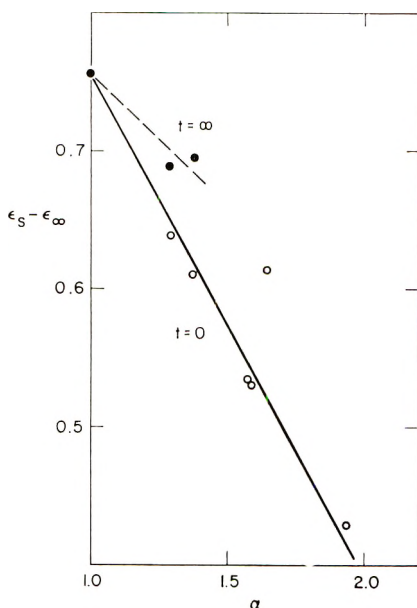


Fig. 3. The variation with elongation of $(\epsilon_s - \epsilon_\infty)$: (O) at zero time; (●) after long times.

work of Müller and Huff⁵ should be mentioned in this regard. They observed the dielectric loss peak for vulcanized natural rubber to shift along the temperature axis with elongation.

Stress Relaxation and Birefringence

We next turn to a more detailed examination of the relaxation process in Viton. The thermostatted stress balance used for these measurements was similar to that described by Stein and Tobolsky.⁶ The lower clamp swings on a pivot, and a reversible motor and spring coupling automatically adjust the stress so as to maintain the sample length constant to within 0.5 mm. The two clamps may be moved apart simultaneously by turning a rod threaded clockwise from the center to one end, and counterclock-

wise toward the other end. With this arrangement the central portion of the sample, where the birefringence was measured, remains stationary. The polarizer and Wallaston prism used for these measurements gave only the absolute magnitude of the birefringence; however, $(n_1 - n_2)$ was found to be positive for Viton by comparison with polyethylene, which is known to be positively birefringent.

Figure 4 illustrates the time dependence of the stress τ on the strained cross section and the birefringence, $(n_1 - n_2)$, as measured at a constant

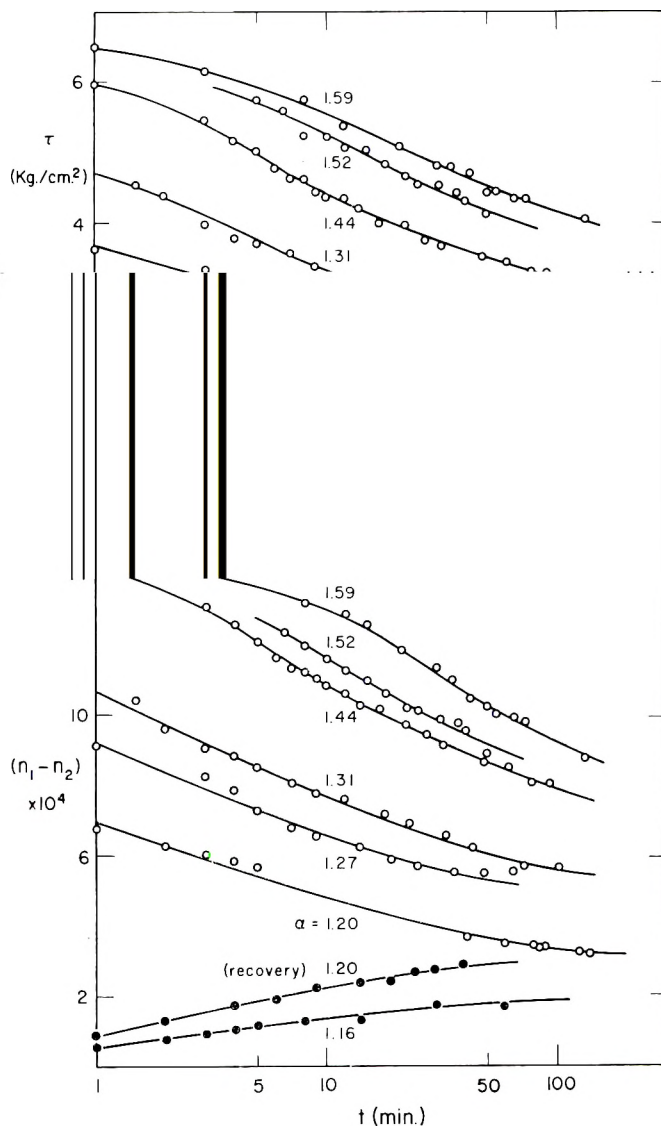


Fig. 4. The stress and birefringence measured at 28°C. for various elongations during stress relaxation and recovery.

temperature, 28°C., for various elongations. The filled circles represent stress and birefringence data measured during recovery. The latter were obtained by holding the sample at constant elongation, for example $\alpha = 1.44$, for several hours, and then quickly reducing the elongation to $\alpha = 1.20$.

We should first ascertain whether Viton exhibits linear viscoelastic behavior. If stress and strain are linearly related, plotting $\tau/(\alpha - 1)$ should reduce the data shown in the upper portion of Figure 4 to single curves for relaxation and recovery. On the other hand, from the statistical treatment of Gaussian networks one obtains for the equilibrium stress upon elongation:

$$\tau = \nu kT (\alpha^2 - 1/\alpha) \quad (4)$$

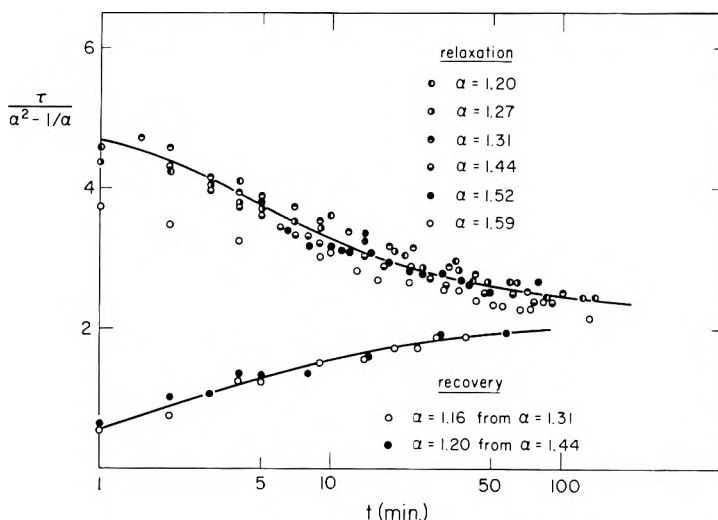


Fig. 5. Values of $\tau/(\alpha^2 - 1/\alpha)$ observed for different elongations during relaxation and recovery at 28°C.

where ν is the number of effective chains in the network. If a similar relationship is assumed for the time dependent stress, a plot of $\tau/(\alpha^2 - 1/\alpha)$ is indicated. As Ferry⁷ has pointed out, the difference between $1/(\alpha - 1)$ and $3/(\alpha^2 - 1/\alpha)$ is rather small for α values up to 1.5. Most of our data falls within this range, so that it does not provide a test between these alternatives. The stress relaxation data appear plotted as $\tau/(\alpha^2 - 1/\alpha)$ versus log time in Figure 5. With the exception of the highest elongation, $\alpha = 1.59$, the strain dependence of the relaxation and recovery data appear to be reasonably well represented in this manner.

We next turn to the relationship between birefringence and stress. For a network of Gaussian chains the birefringence, $(n_1 - n_2)$ is given by:⁸

$$n_1 - n_2 = (2\pi/4.5)[(\bar{n}^2 + 2)^2/\bar{n}]\nu(\delta_1 - \delta_2)(\alpha^2 - 1/\alpha) \quad (5)$$

where \bar{n} is the mean refractive index and $(\delta_1 - \delta_2)$ is the anisotropy of an

equivalent statistical link of the chain. From eq. (4) and (5) one obtains a statement of Brewster's law relating birefringence and stress:

$$n_1 - n_2 = C\tau \quad (6)$$

where the stress-optical coefficient, C , is given by:

$$C = (2\pi/45kT)[(\bar{n}^2 + 2)^2/\bar{n}](\delta_1 - \delta_2) \quad (7)$$

Figure 6 represents a test of eq. (6). These isothermal data indicate that Viton obeys Brewster's law, both during relaxation and recovery. From the slope of the line in Figure 6, $C = 2.35 \times 10^{-4}$ cm.²/kg. at 28°C. Taking

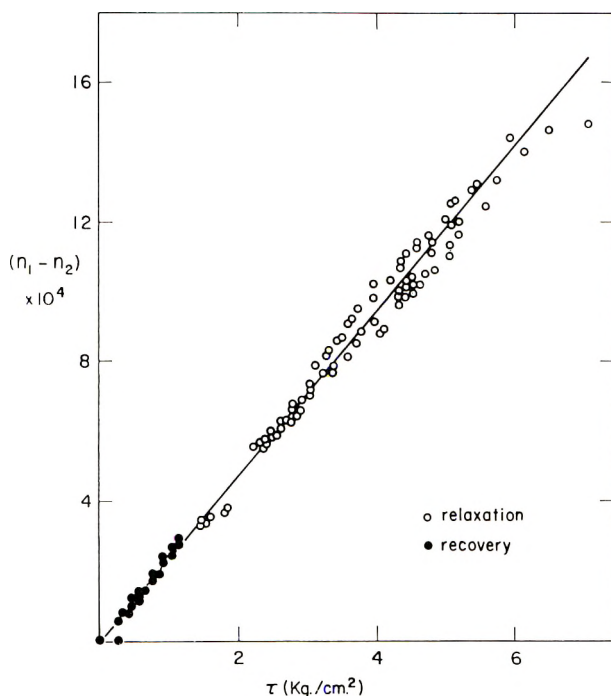


Fig. 6. Birefringence vs. stress during relaxation and recovery for various elongations at 28°C.

for the mean refractive index $\bar{n} = 1.372$, we obtain for the anisotropy of a statistical link, $(\delta_1 - \delta_2)$, 65×10^{-25} cm.³. Unfortunately, we do not have the polarizability values for the C—F bond, hence the anisotropy of a repeating unit can not be calculated.

Stress relaxation and birefringence measurements were also performed for a fixed elongation, $\alpha = 1.23$, as a function of temperature. The stresses reduced to a common temperature, 30°C., through multiplication by the factor $303/T(^{\circ}\text{K.})$, are designated τ' . These data appear plotted as a function of time in Figure 7. It is now well known that, for amorphous polymers at any rate, stress relaxation data at different temperatures T

may be combined to form a master curve by shifting horizontally along the scale of time, t :

$$\tau'_T(t) = \tau'_{T_0}(t/a_T)$$

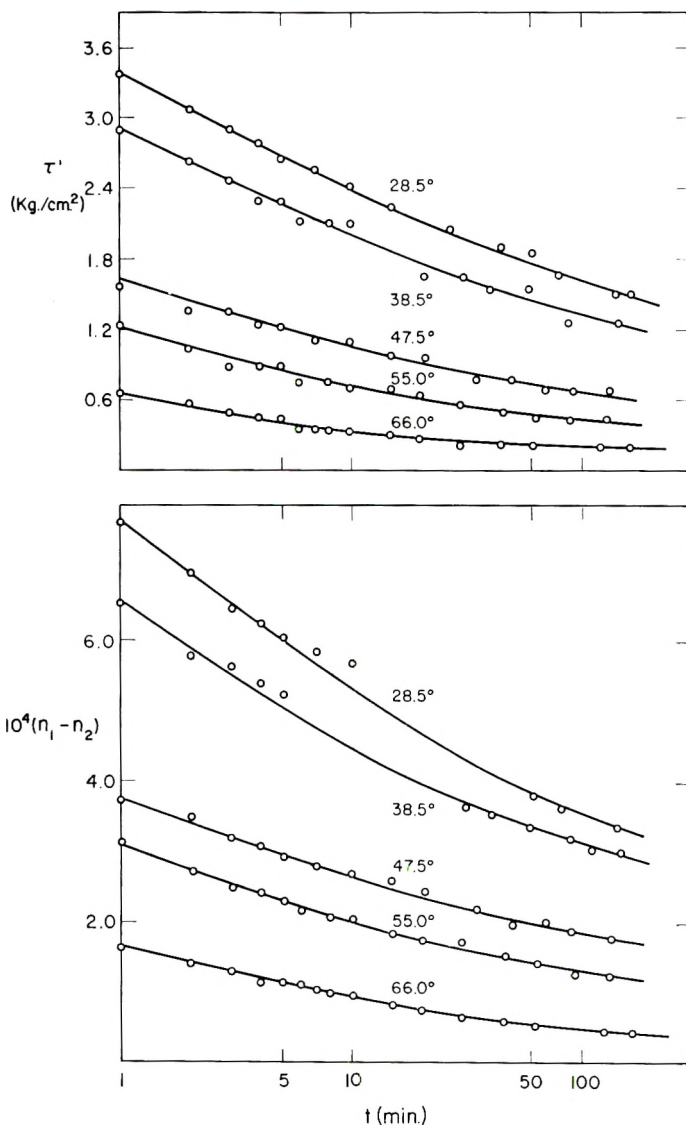


Fig. 7. Stress and birefringence measured at various temperatures for relaxation at constant elongation, $\sigma = 1.23$.

where a_T is a temperature-dependent shift factor. This time-temperature superposition principle has been applied to dielectric measurements for some years.⁹ Its application to mechanical relaxation was first suggested by Leaderman,¹⁰ and has since been verified by the extensive stress relaxa-

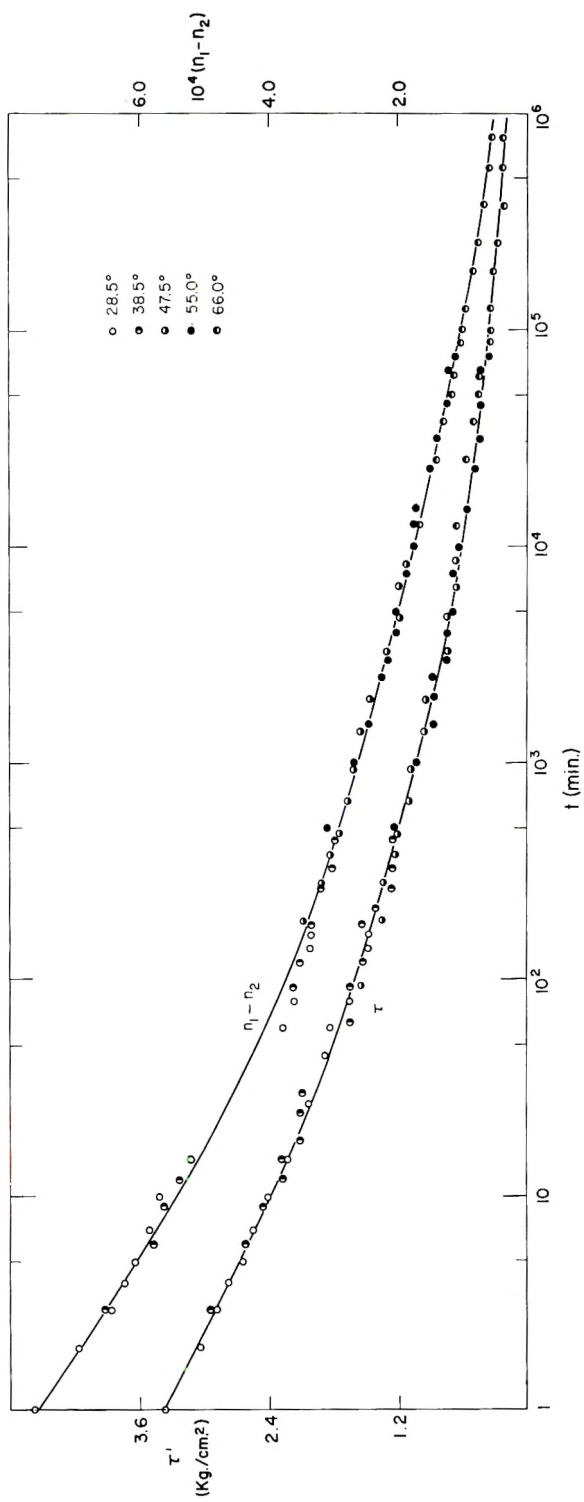


Fig. 8. Master curves for stress reduced at 30°C. and birefringence for $\alpha = 1.23$.

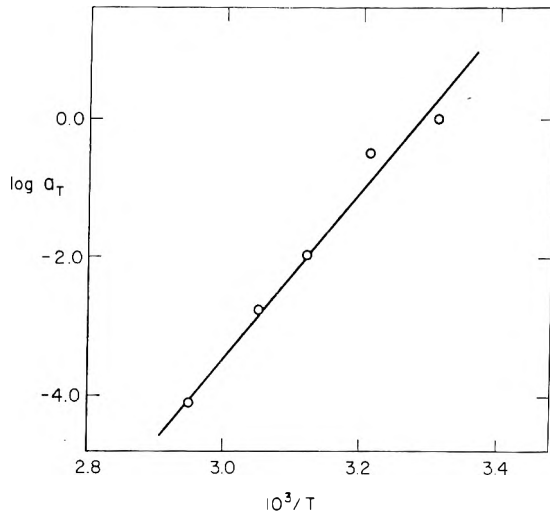


Fig. 9. Shift factors, a_T , used to construct the two master curves appearing in Fig. 8.

tion measurements of Tobolsky et al.,¹¹ and by the dynamic mechanical measurements of Ferry and co-workers.¹² The lower curve of Figure 8 is the master stress curve for Viton at 30°C. and $\alpha = 1.23$. The data covering a temperature range of approximately 40°C. are superposed with fair success. The required shift factors, a_T , appear plotted against the reciprocal of temperature in Figure 9. The apparent activation energy as determined from the slope of this line is 56 kcal./mole. An alternative representation using a simplified form of the WLF equation:

$$\log a_T = -8.86 (T - T_s)/(101.6 + T - T_s) \quad (8)$$

yields $T_s = 336 \pm 5^\circ\text{C}$. Both ΔH_a and T_s seem surprisingly high for an elastomeric material. These values probably reflect the strong dipole-dipole interactions between neighboring units along the chain. The portion of the relaxation time spectrum obtainable from these data appears in Figure 10.

The time-temperature superposition principle may also be applied to

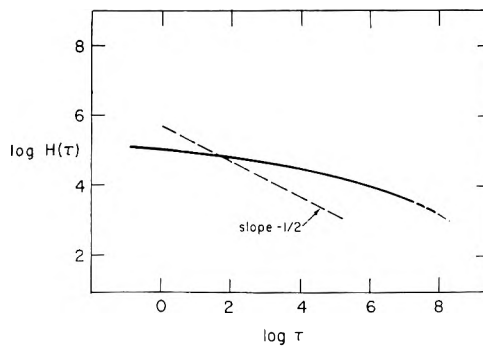


Fig. 10. Part of the spectrum of relaxation times for Viton.

the birefringence data shown in Figure 7. The master birefringence curve in Figure 8 was obtained using the *same* shift factors, a_T , required for the master stress curve. This means that the temperature dependence of the relaxation times for stress and birefringence are experimentally indistinguishable.

Information concerning the temperature dependence of the equilibrium birefringence appears in Figure 11. For these measurements the sample was maintained under constant elongation, $\alpha = 1.23$, at the highest temperature, 67°C ., for several hours. After the birefringence no longer changed significantly with time, measurements were performed at successively lower temperatures. We observe that $(n_1 - n_2)$ is approximately constant in the interval 30 to 67°C . According to eq. (5), this indicates that the anisotropy (and hence the size) of the statistical chain link is independent of temperature. Reference to eq. (7) shows that the stress-

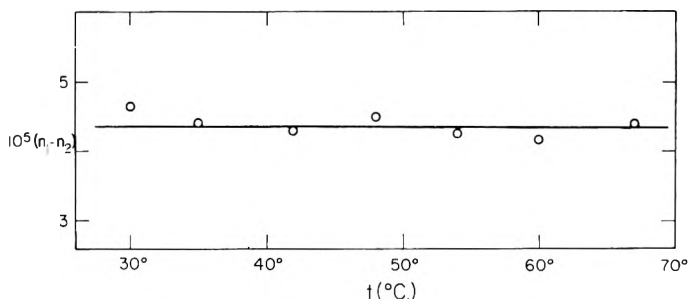


Fig. 11. Equilibrium birefringence measured at various temperatures for a fixed elongation, $\alpha = 1.23$.

optical coefficient should, therefore, be inversely proportional to the temperature, or $(n_1 - n_2)/\tau'$ should be a constant. However, this is not the case for Viton. Average values of $10^2 CT$ calculated from the relaxation data increase from 7.0 at 30°C . to 8.8 at 70°C .

Stein and Tobolsky have examined the relationship between birefringence and stress for a number of polymers.¹¹ For example, Stein, Holmes, and Tobolsky¹³ report that the $(n_1 - n_2)T/\tau$ ratio for polyisobutylene is independent of time, temperature, and elongation. Closer examination reveals, however, that this constancy is only approximate. In fact, the CT products deduced from their data at 0.1 hr. appear to increase regularly over the temperature range -35 to 50°C ., thus resembling our results in this respect.

This departure from Gaussian behavior may be due to nonequilibrium effects, or to an energy contribution to the equilibrium retractive force. Our data do not permit a choice between these alternatives.

Conclusions

Viton has a rather high group dipole moment, which results in a high apparent activation energy and a relatively slow relaxation process at

room temperature. In spite of this, Viton behaves mechanically as a thermorheologically simple material. It exhibits linear viscoelastic behavior up to relatively high elongations, and the time-temperature superposition principle yields master stress and birefringence curves from a single set of shift factors. For a fixed temperature the (birefringence/stress) ratio is a constant, independent of elongation, for both relaxation and recovery.

The dielectric constant also varies during relaxation, but its behavior does not parallel those of the stress and birefringence. As entanglements are removed during relaxation, both the effective number of network chains and their average deformation decrease. Stress and birefringence are affected by both of these factors, whereas only the latter influences the dielectric constant. Hence, a different relaxation behavior in these two cases is not unexpected. It might be possible to obtain a better understanding of relaxation by utilizing this difference to separate the variation with time of these two factors, the effective number of network chains, and their deformation.

W. R. Krigbaum wishes to express his gratitude to the Alfred P. Sloan Foundation for a Research Fellowship.

References

1. Onsager, L., *J. Am. Chem. Soc.*, **58**, 1486 (1936).
2. Harris, F. E., and B. J. Alder, *J. Chem. Phys.*, **21**, 1031 (1953).
3. Birshstein, T. M., L. L. Burshtein, and O. B. Ptitsyn, *Soviet Phys.-Tech. Phys.*, **4**, 810 (1960).
4. Collie, C. H., J. B. Hasted, and D. M. Ritson, *Proc. Phys. Soc. (London)*, **60**, 145 (1948).
5. Müller, F. H., and K. Huff, *Rubber Chem. and Technol.*, **32**, 1027 (1959).
6. Stein, R. S., and A. V. Tobolsky, *Textile Research J.*, **18**, 302 (1948).
7. Ferry, J. D., *Viscoelastic Properties of Polymers*, Wiley, New York, 1961, pp. 109-11.
8. For a derivation and discussion see L. R. G. Treloar, *The Physics of Rubber Elasticity*, Oxford Univ. Press, London, 1958, Chap. 10.
9. Wagner, K. H., *Elektrotech. Z.*, **36**, 135, 163 (1915).
10. Leaderman, H., *Elastic and Creep Properties of Filamentous Materials and Other High Polymers*, The Textile Foundation, Washington, 1943.
11. A summary appears in A. V. Tobolsky, *Properties and Structure of Polymers*, Wiley, New York, 1960, Chap. 4.
12. Ferry, J. D., *op. cit.*, Chap. II.
13. Stein, R. S., F. H. Holmes, and A. V. Tobolsky, *J. Polymer Sci.*, **14**, 443 (1954).

Synopsis

The dielectric constant of a crosslinked sheet of Viton was measured at two frequencies, 200 cycles/sec. and 100 kcycles/sec., for various elongations. The difference ($\epsilon_s - \epsilon_\infty$) decreased sharply when the sample was strained and then increased slowly during stress relaxation. Relaxation was slow at the temperature of these measurements (35°C.), so that we were only able to estimate the behavior at long time for the lowest elongations. Even under these conditions it was possible to demonstrate that the ($\epsilon_s - \epsilon_\infty$) values corresponding to long times decrease with elongation. The root mean square dipole moments for a $C_2F_3H_2$ group are estimated from these data by both a modi-

fied form of the Onsager relation and the more recent treatment of Harris and Alder. Stress relaxation and birefringence measurements were performed with elongation and temperature as variables. Viton exhibits linear viscoelastic behavior up to an elongation α of 1.5. The isothermal data indicate a linear relationship between birefringence and stress, both during stress relaxation and recovery. The stress-optical coefficient, C , is 2.35×10^{-4} cm.²/kg. at 28°C. Master curves could be constructed from both the reduced stress and birefringence data at different temperatures for the *same* shift factors, a_T . The apparent activation energy is 56 kcal./mole and the characteristic temperature in the simplified WLF equation is $T_s = 336 \pm 5^\circ\text{C}$. The birefringence as measured under essentially equilibrium conditions at $\alpha = 1.23$ was independent of temperature in the range 30–70°C.; however, the CT product measured during relaxation increased from 7×10^{-2} to 8.8×10^{-2} in the same temperature interval. The data were insufficient to determine whether this departure from Gaussian behavior arose from the time dependence or represented an equilibrium effect.

Résumé

On a mesuré la constante diélectrique d'une feuille pontée de Viton à deux fréquences, 200 cycles/sec. et 100 cycles/sec., pour différentes elongations. La différence ($\epsilon_s - \epsilon_\infty$), décroît rapidement lorsque l'échantillon est étiré, et croît alors lentement au cours du relâchement de la tension. Le relâchement était lent à la température de ces mesures, 35°, de telle sorte que nous n'étions capable d'estimer le comportement qu'après une longue période pour les elongations les plus faibles. Même dans de telles conditions il a été possible de démontrer que les valeurs ($\epsilon_s - \epsilon_\infty$) correspondant à ces longues périodes décroissent en fonction de l'elongation. On a estimé le moment dipolaire *rms* pour un groupe $\text{C}_3\text{F}_3\text{H}_3$ à partir de ces données basées à la fois sur une forme modifiée de l'équation d'Onsager et sur le traitement le plus récent d'Harris et Alder. On a effectué des mesures de relâchement de tension et de biréfringence avec l'elongation et la température comme variables. Le Viton présente un comportement viscoélastique linéaire par rapport à une elongation, α , de 1.5. Les résultats obtenus dans des conditions isothermiques montre une relation linéaire entre la biréfringence et la tension, à la fois pendant le relâchement de la tension et vice-versa. Le coefficient tensiooptique, C , est 2.35×10^{-4} cm.²/kg. à 28°. On pouvait tracer des courbes modèles à la fois à partir des données de tension réduite et de la biréfringence à différentes températures, en employant un facteur de déplacement, a_T identique. L'énergie d'activation apparente est de 56 Kcal./mole et la température caractéristique dans l'équation WLF simplifiée est $T_s = 336 \pm 5^\circ$. La biréfringence telle qu'on l'a mesurée dans des conditions d'équilibre à $\alpha = 1.23$, est indépendante de la température dans l'intervalle de 30° à 70°; cependant, le produit CT mesuré pendant le relâchement augmente de 7×10^{-2} jusqu'à 8.8×10^{-2} dans le même intervalle de T . Les résultats sont suffisants pour déterminer si cette déviation au comportement de Gauss s'est produit en fonction du temps ou s'il représente un effet de l'équilibre.

Zusammenfassung

Die Dielektrizitätskonstante eines vernetzten Viton-filmes wurde bei zwei Frequenzen, 200 Hz und 100 kHz für verschiedene Dehnung gemessen. Die Differenz, ($\epsilon_s - \epsilon_\infty$), nahm bei der Verformung der Probe scharf ab und anschliessend bei der Spannungsrelaxation langsam zu. Die Relaxation war bei der Versuchstemperatur, 35°, langsam, so dass für die niedrigsten Dehnungen nur das Verhalten nach langer Dauer bestimmt werden konnte. Auch unter diesen Bedingungen konnte gezeigt werden, dass die langen Versuchsdauern entsprechenden ($\epsilon_s - \epsilon_\infty$)-Werte mit der Dehnung abnahmen. Das rms-Dipolmoment der $\text{C}_3\text{F}_3\text{H}_3$ -Gruppe wird aus den Versuchsdaten nach einer modifizierten Form der Onsagergleichung und der neueren Behandlung von Harris und Alder bestimmt. Spannungsrelaxations- und Doppelbrechungsmessungen wurden bei variiertem Elongation und Temperatur durchgeführt. Viton zeigt bis zu einer Elonga-

tion, α , von 1,5 lineares viskoelastisches Verhalten. Die isothermen Daten ergeben eine lineare Beziehung zwischen Doppelbrechung und Spannung, sowohl während Spannungsrelaxation als auch Rückbildung. Der spannungsoptische Koeffizient, C , beträgt bei 28° $2,35 \times 10^{-4}$ cm.²/kg. Gemeinsame Kurven konnten aus den reduzierten Spannungs- und Doppelbrechungsdaten bei verschiedener Temperatur mit den gleichen Verschiebungsfaktoren, a_T , erhalten werden. Die scheinbare Aktivierungsenergie beträgt 56 kcal./Mol und die charakteristische Temperatur in der vereinfachten WLF-Gleichung $T_s = 336 \pm 5^\circ$. Die im wesentlichen unter Gleichgewichtsbedingungen bei $\alpha = 1,23$ gemessene Doppelbrechung war im Bereich von 30° – 70° temperaturunabhängig; das während der Relaxation gemessene Produkt CT nahm jedoch im gleichen Temperaturintervall von 7×10^{-2} auf $8,8 \times 10^{-2}$ zu. Die Daten reichten nicht aus, um zu entscheiden, ob diese Abweichung vom Gausschen Verhalten von der Zeitabhängigkeit verursacht wird oder einen Gleichgewichtseffekt vorstellt.

Received September 13, 1961

Radical-Anion Polymerization

A. V. TOBOLSKY and D. B. HARTLEY, *Frick Chemical Laboratories,
Princeton University, Princeton, New Jersey*

In a recent series of papers¹⁻³ on the copolymerization of methyl methacrylate and styrene by a lithium suspension in a variety of different solvents, O'Driscoll, Boudreau, and Tobolsky found that copolymers were produced which contained considerable styrene. On the basis of the fact that purely anionic copolymerization of these monomers incorporates less than 1% styrene in the polymer, while purely radical copolymerization gives a 50-50% copolymer,⁴ they were led to postulate a polymeric species able to grow simultaneously by a radical and an anionic mechanism.²

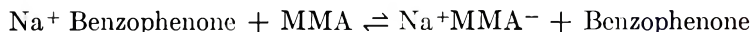
Anionic free radicals of the type used by Szwarc⁵ initiate certain vinyl monomers by electron transfer (or by bond formation, as demonstrated recently in these laboratories^{6,7}) to give radical-ion species of the same nature as those presumed to be produced by metallic lithium.⁸ In view of this observation it was considered that copolymerization of styrene and methyl methacrylate monomers in the presence of an aromatic hydrocarbon radical-ion as initiator might also lead through radical growth to a significant amount of styrene in the copolymer. The present paper examines this possibility and the polymerization by a lithium catalyst from a theoretical basis.

The kinetic analyses of the two cases are obviously quite different. On the one hand, most anionic free radicals transfer instantaneously and completely to methyl methacrylate monomer, while in the polymerization by lithium, catalyst is present in excess throughout the reaction, allowing a steady-state concentration of radicals to be maintained. We shall consider the former case first.

Instantaneous and Complete Electron Transfer Initiation by a Radical-Ion

Not all initiators of the radical-ion type initiate by electron transfer to monomer.^{6,7} Of those that do some transfer more completely than others, depending on the relative electron affinities of monomer and generator molecules and their concentrations. Thus, for example, 10^{-2} - $10^{-1}M$ sodium naphthalene transfers virtually completely to molar methyl methacrylate, while on the other hand only a small fraction of $10^{-1}M$ sodium benzophenone converts molar methyl methacrylate to its radical-ion:

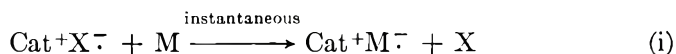




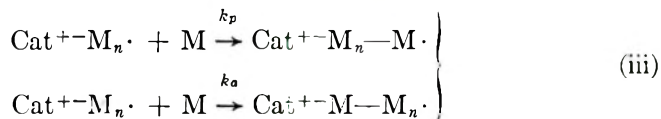
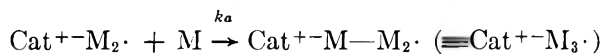
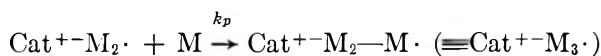
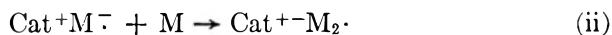
For our immediate purposes we shall be concerned with the reactions of the first type, where electron transfer from initiator is practically complete.

Let $\text{Cat}^+ \text{X}^-$ represent the initiator (X is referred to as the "generator" of the initiator), M the monomer, and $\text{Cat}^+ \text{M}^-$ the true radical-ion first formed, where Cat^+ denotes the cation. Addition of the second (or further) monomer units to $\text{Cat}^+ \text{M}^-$ causes the radical to lose its conjugation with the anionic center. Let us indicate these new polymeric species by $\text{Cat}^+ \text{---M}_n \cdot$. Polymerization takes place according to the following scheme:

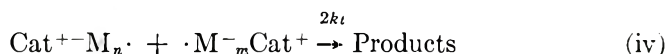
Initiation:



Propagation:



Termination:



There is of course no difference between the polymers $\text{Cat}^+ \text{---M}_n \text{---M} \cdot$ and $\text{Cat}^+ \text{---M---M}_n \cdot$. They have been written this way in order to emphasize the two mechanisms, viz. radical and ionic, by means of which polymer $\text{Cat}^+ \text{---M}_{n+1}$ can be produced from $\text{Cat}^+ \text{---M}_n \cdot$.

Whether termination is by disproportionation or coupling is irrelevant to the kinetic treatment so long as we can say it is a bimolecular process with rate constant $2k_t$.

The present situation is analogous to a polymerization photoinitiated instantaneously to give a known number of radical species which start propagation.⁹ In the present instance radical-ion fragments are produced in quantity equal to the number of initiating molecules added.

We propose to neglect the small contribution of step (ii) to propagation, and also any termination involving the species $\text{Cat}^+ \text{M}^-$. Let the initiator concentration be c_0 and let c^* be the concentration of growing radical ends at time t .

The rate of decay of the radicals is expressed as

$$dc^*/dt = -2k_t c^{*2}$$

which integrates to

$$1/c^* = 2k_t t + (1/c_0)$$

i.e.,

$$c^*(t) = c_0/(1 + 2k_t c_0 t) \quad (1)$$

The rate of radical polymerization is given by

$$R_r = dP_r/dt = k_p c^* m_t$$

where m_t is the concentration of monomer at time t . If we assume that monomer is in excess, so that $m_t = m_0 = \text{constant}$, we have by eq. (1)

$$dP_r/dt = k_p m_0 c_0 / (1 + 2k_t t c_0)$$

This gives

$$P_r = k_p m_0 c_0 \int dt / (1 + 2k_t t c_0)$$

and

$$P_r = (k_p m_0 / 2k_t) \ln (1 + 2k_t t c_0) \quad (2)$$

which represents the concentration of polymer which has grown on the radical ends after a time t . Here, the term concentration of polymer refers to milliliters of monomer polymerized by the indicated mechanism(s) (P_r, P_a, P_t).

In the absence of ionic termination the number of growing anionic centers must always equal c_0 . The rate of anionic polymerization is therefore

$$dP_a/dt = k_a m_0 c_0$$

giving

$$P_a = k_a c_0 m_0 t \quad (3)$$

if m_0 is constant. Hence the total concentration of polymer after a time t becomes simply

$$P_t = P_r + P_a = [(k_p/2k_t) \ln (1 + 2k_t t c_0) + k_a c_0 t] m_0 \quad (4)$$

The rate constants for the radical¹⁰ and anionic¹¹ polymerization of styrene at 20°C. are obtained from the literature as

$$k_p = 35.3 \text{ l. mole}^{-1} \text{ sec.}^{-1}$$

$$k_t = 2.18 \times 10^7 \text{ l. mole}^{-1} \text{ sec.}^{-1}$$

$$k_a = 0.052 \text{ l. mole}^{-1} \text{ sec.}^{-1}$$

Here, k_p and k_t have been obtained by extrapolation of data at 30 and 60°C. to 20°C. The above value of k_a refers to ionic propagation with a lithium counterion in benzene and is assumed to be unchanged in magnitude by the simultaneous radical growth. Other alkali metal cations give rise to enhanced k_a 's. The absence of any styrene in the product from copolymerization with methyl methacrylate initiated by a suspension of sodium, even

in solvents of low solvating power, is considered to be due to the decrease in the ratio k_p/k_a rather than to any fundamental difference in mechanism between polymerizations with lithium and sodium catalysts.

Putting the quoted values in eq. (4), and setting c_0 equal to a reasonable value of 0.1 mole/l., we predict that after 10 sec. the proportion of styrene which has polymerized on the radical ends amounts to less than 0.01% of total polymerization. Theoretically this proportion will decrease with increasing time. Hence for practical purposes no radical polymerization will be observed in these circumstances.

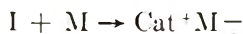
Exceptionally high concentrations of initiator would in principle make the degree of radical polymerization more competitive with the anionic propagation. However, the further the initiator concentration is increased, the less likely will it be that electron transfer to monomer is complete, which is a necessary condition for the above kinetic scheme to hold. The problem then reduces to that of polymerization in the presence of excess initiator in concentration governed by the equilibrium constants for the initial electron transfer step and electron transfer with growing polymers.

Our conclusion must therefore be that styrene will not polymerize significantly on radical ends when the initiating step of electron transfer is instantaneous and complete. It is to be noted however that eq. (2) would allow radical polymerization to go to completion after an extended period of time, but under present conditions the rate of radical polymerization cannot be complete with the simultaneous ionic reaction.

Radical-Anionic Polymerization under Steady-State Conditions

When excess of a suspension of lithium metal is used to initiate polymerization a steady state concentration of radical anions may be assumed to be set up. Similar steady-state conditions could presumably also be obtained by continuously feeding in anionic free radicals at a controlled rate (analogously to continuous photoinitiation⁹) or by having them present in excess. The kinetic scheme below has been developed to include these methods of initiation.

The initiation is to be represented generally as



having constant rate R_i . The remaining reactions taking place are those represented by steps (ii) – (iv) in the scheme given above.

In the steady state of radicals we have

$$R_i = 2k_t c^{*2}$$

i.e.,

$$c^* = (R_i/2k_t)^{1/2} \quad (5)$$

where c^* is the steady-state concentration of ion radicals Cat^+M^- .

Again treating the radical growth as a separate problem to the ionic growth, and making similar assumptions, we have for the rate of radical polymerization

$$dP_r/dt = k_p c^* m_0$$

which yields, by eq. (5)

$$dP_r/dt = k_p (R_i/2k_t)^{1/2} m_0$$

The concentration of monomer converted by radical polymerization is therefore .

$$P_r = k_p (R_i/2k_t)^{1/2} m_0 t \quad (6)$$

if R_i is constant. (If R_i is a function of time, the integrated expressions for P_r and P_a will each show a different dependence on t .)

Since the rate of production of anionic centers is $R_i = 2k_i c^{*2}$ which is constant, a number $R_i t$ of such centers will have accumulated after a time t . The rate of anionic polymerization will thus be

$$dP_a/dt = k_a m_0 R_i t$$

which integrates to

$$P_a = (k_a/2) m_0 R_i t^2 \quad (7)$$

Hence the total concentration of polymer P_t produced by radical-anionic growth is

$$P_t = P_r + P_a = [k_p (R_i/2k_t)^{1/2} t + (k_a/2) R_i t^2] m_0 \quad (8)$$

Equations (6), (7), and (8) are used with initiation rates of 10^{-4} and 10^{-6} moles l.⁻¹ sec.⁻¹ to calculate the proportions of radical growth (P_r/P_t) and of ionic growth (P_a/P_t) in the total polymer concentration P_t present at increasing lengths of time t . The relevant data are presented in Table I. These results refer to styrene polymerization in nonpolar solvents and with a lithium counterion—conditions which most favor a measurable radical growth.

TABLE I

| t , sec. | | P_r/m_0 | P_a/m_0 | P_t/m_0 | 100 (P_r/P_t) |
|-----------------|-----------------|------------------------|-----------------------|------------------------|----------------------|
| $R_i = 10^{-4}$ | $R_i = 10^{-6}$ | | | | |
| 0.1 | 1 | 535×10^{-8} | 2.6×10^{-8} | 537.6×10^{-8} | 99.5 |
| 0.316 | 3.16 | 169×10^{-7} | 2.6×10^{-7} | 171.6×10^{-7} | 98.5 |
| 1 | 10 | 53.5×10^{-6} | 2.6×10^{-6} | 56.1×10^{-6} | 95.4 |
| 3.16 | 31.62 | 16.9×10^{-5} | 2.6×10^{-5} | 19.5×10^{-5} | 86.7 |
| 10 | 100 | 5.35×10^{-4} | 2.6×10^{-4} | 7.95×10^{-4} | 67.3 |
| 31.62 | 316.2 | 1.69×10^{-3} | 2.6×10^{-3} | 4.29×10^{-3} | 39.4 |
| 100 | 1000 | 0.535×10^{-2} | 2.6×10^{-2} | 3.14×10^{-2} | 17.1 |
| 200 | 2000 | 0.107×10^{-1} | 1.04×10^{-1} | 1.15×10^{-1} | 9.9 |

Curves depicting how the contributions of the simultaneous radical and anionic polymerizations change with time are shown in Figure 1 for $R_i = 10^{-6}$ moles l.⁻¹ sec.⁻¹. It is seen that initially propagation is 100%

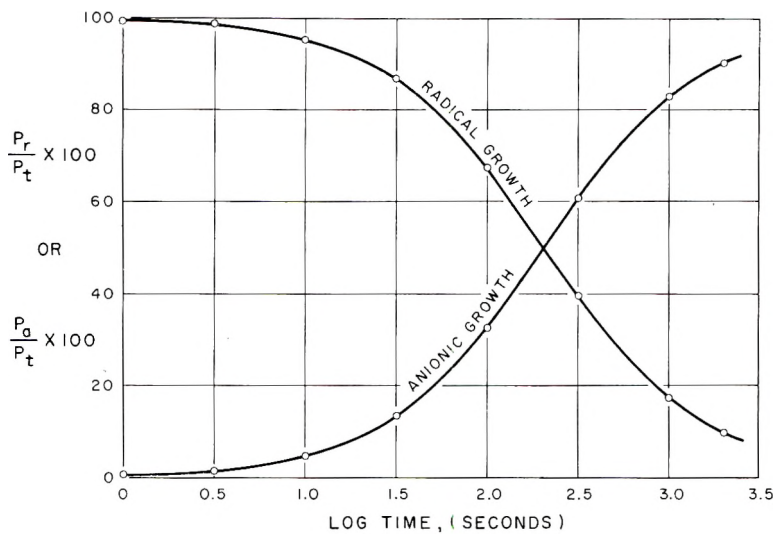


Figure 1.

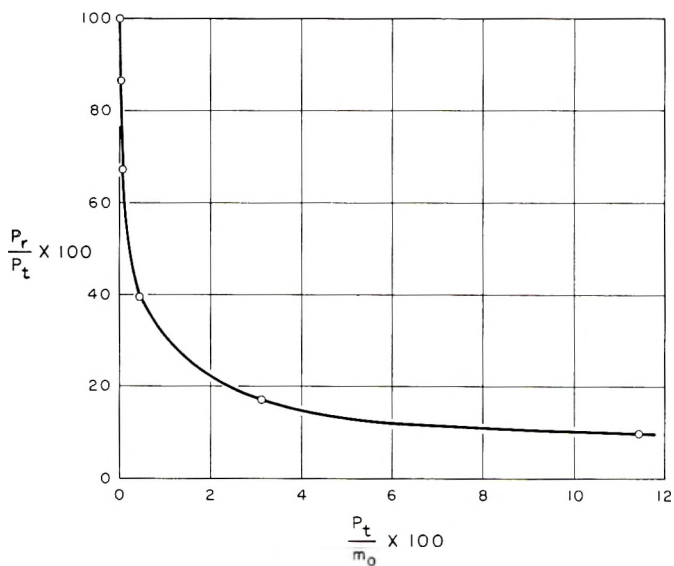


Figure 2.

on the radical, such growth falling off to zero when t gets very large. The rate of decay of this curve obviously depends on R_i .

A further plot based on Table I is shown in Figure 2. This gives the percentage of radical-propagated polymer as a function of conversion.

As the Table I indicates, the curve has the same shape for a given monomer at a fixed concentration and temperature, whatever the constant value of R_i . This fact is made obvious by using eq. (6) and (8) to write

$$P_t = P_r + (k_a k_t / k_p^2 m_0) P_r^2$$

i.e.,

$$P_r / P_t = [1 + (k_a k_t / k_p^2 m_0) P_r]^{-1} \quad (9)$$

The parameters R_t and t have vanished in eq. (9), indicating that for a given monomer a unique ratio P_r / P_t exists for each P_t , independent of the values of R_t and t , though governed, of course, by the initial concentration of monomer (in excess).

The support of the Air Force Office of Scientific Research is deeply appreciated.

References

1. O'Driscoll, K. F., R. J. Boudreau, and A. V. Tobolsky, *J. Polymer Sci.*, **31**, 115 (1958).
2. O'Driscoll, K. F., and A. V. Tobolsky, *J. Polymer Sci.*, **31**, 123 (1958).
3. O'Driscoll, K. F., and A. V. Tobolsky, *J. Polymer Sci.*, **37**, 363 (1959).
4. Walling, C., E. R. Briggs, W. Cummings, and F. R. Mayo, *J. Am. Chem. Soc.*, **72**, 49 (1950).
5. Szwarc, M., *Makromol. Chem.*, **35**, 132 (1960).
6. Tobolsky, A. V., A. Rembaum, and A. Eisenberg, *J. Polymer Sci.*, **45**, 347 (1960).
7. Tobolsky, A. V., and D. B. Hartley, *J. Am. Chem. Soc.*, **84**, 1391 (1962).
8. Szwarc, M., M. Levy, and R. Milkovich, *J. Am. Chem. Soc.*, **78**, 2656 (1956).
9. Bamford, C. H., and M. J. S. Dewar, *Proc. Roy. Soc. (London)*, **A192**, 309 (1948).
10. Flory, P. J., *Principles of Polymer Chemistry*, Cornell Univ. Press, Ithaca, N. Y., 1953.
11. Welch, F. J., *J. Am. Chem. Soc.*, **81**, 1345 (1959).

Synopsis

Two cases of initiation of vinyl polymerization by radical-ions are considered. In the one case the transfer from radical-ion to monomer is instantaneous and virtually complete. Here the relative amount of free radical propagation as compared to anionic propagation is negligibly small. In the second case a continuous feed of radical-ion initiator is considered. Here the relative amount of free radical propagation as compared to anionic propagation may be considerable. Exact expressions are developed for this relative radical versus ionic propagation as a function of conversion. It is suggested that the results of lithium-initiated copolymerization of methyl methacrylate and styrene may be understood in terms of a model similar to the second case of radical-ion initiation considered in this paper.

Résumé

Deux cas d'initiation de polymérisation vinyliques par radicaux-ions sont considérés dans le présent travail. Dans l'un des cas le transfert du radical-ion au monomère est instantané et virtuellement complet. L'importance du processus de propagation radicalaire est négligeable vis-à-vis de la propagation anionique. Dans le second cas où l'alimentation continue en initiateur du type radical-ion est considérée, l'importance de la propagation radicalaire vis-à-vis de la propagation anionique peut être considérable. Des expressions exactes en fonction du degré de conversion sont dérivées pour le rapport des deux types de propagation. Il semble que les résultats de la copolymérisation du méthacrylate de méthyle et du styrène initiée par le lithium, peuvent être interprétés sur la base d'un schéma semblable au second cas d'initiation par radical-ion décrit dans ce travail.

Zusammenfassung

Für den Start der Vinylpolymerisation durch Radikationen werden zwei Möglichkeiten in Betracht gezogen. In dem einen Fall soll die Übertragung vom Radikalion zum Monomeren momentan und praktisch vollständig erfolgen. Der relative Anteil des radikalischen Wachstums ist hier im Vergleich zum anionischen Wachstum vernachlässigbar klein. Im zweiten Fall wird eine kontinuierliche Nachlieferung des Radikalionstarters angenommen. Hier kann der relative Anteil des radikalischen Wachstums in Vergleich zum anionischen Wachstum beträchtlich sein. Für den relativen Anteil des radikalischen gegen das ionische Wachstum als Funktion des Umsatzes werden exakte Ausdrücke entwickelt. Zur Erklärung der Ergebnisse der lithiumgestarteten Copolymerisation von Methylmethacrylat und Styrol wird ein dem zweiten Fall des Radikalionstartes der vorliegenden Mitteilung entsprechendes Modell vorgeschlagen.

Received July 5, 1961

A Kinetic Analysis of Swelling of Rat Tail Tendon*

HARRY R. ELDEN, *Laboratories of Biochemistry,
Howard Hughes Medical Institute, Miami, Florida*

and

MARSHA FELDMAN, *Arthritis Section, Department of Medicine,
University of Miami, Coral Gables, Florida*

Introduction

Intact connective tissues have a great avidity for water, and their mechanical functioning (extension, compression, and shearing) should be expected to depend on degree of hydration.¹ Morphological examination² reveals that connective tissue is a heterogeneous syncytium of collagen fibers surrounded by, or embedded in, a mucopolysaccharide ground substance. Interaction of tendon tissue with water, therefore, is a complicated process.

Collagen fibers in tendon are arranged systematically in a geometrical pattern which may be fundamental for structural integrity. Fitton-Jackson has shown³ that the ordering of fibrils of developing avian tendon approaches a packing fraction of 0.62 which is the theoretical value for hexagonal close packing. Ramachandran⁴ proposed a cylindrical model in which there is a core of 3 + 9 protofibrils. Surrounding the core in concentric rings are core (3 + 9) plus 5 additional units for each ring. Examination of the number of nearest neighbors surrounding each protofibril reveals that hexagonal close packing is not quite realized. Ramachandran pointed out, however, that this slight distortion is a significant feature of his model. The hexagonal packing and cylindrical lattice model are

(dense phase) of these vacuoles. Interfibrillar space then was filled with the water-rich phase (vacuole interior). Histological examination of connective tissue, therefore, shows that a water bridge might exist between collagen fibrils and act as one type of interfibrillar adhesive.

Since rat tail tendons are almost entirely collagenous with but little ground substance,¹⁰ one might possibly measure how water interacts with collagen *in situ* by studying the swelling of this tissue.

Early studies of swelling frequently were restricted to equilibrium conditions. It was established¹¹ that the primary contributor to equilibrium swelling of collagen in acid and basic solutions is the osmotic effect of anions trapped by the Donnan equilibrium. Under these conditions the protein surface acts like a semipermeable membrane to diffusible ions. Swelling in neutral solutions resulted principally from hydration of accessible polar groups, such as are found on the side chains or the amide linkage of polypeptide chains. Mucopolysaccharides present in tendon probably respond similarly to changes in solution pH and water content.

Accepting the importance of equilibrium measurements, what is of concern here is knowledge of how fast water gets into a structure and how rapidly a structure responds to the change in its hydration. From an analysis of these latter two processes, it is hoped that information will be gained pertaining to the mechanisms of connective tissue interaction with water, especially the mechanical phenomena described in the opening paragraph.

This study brings forth experimental data for the uptake of water by rat tail tendons. The application of cylindrical-diffusion theory to data shows that an initial period may be a Fickian process, but that the terminal period does not follow it exactly. An alternate theory is then proposed which describes the entire weight-time data by a single equation.

Methods

Tendons were removed from tails of adult rats (Sprague-Dawley). They were washed in normal saline to remove blood and solubles, rinsed in distilled water, and dried (70% relative humidity at 25°C.). This whole procedure required less than 60 min. to complete. Next, they were weighed to an accuracy of 0.00 mg. and measured to an accuracy of 0.5 mm. for length. The ratio, weight/length, was computed and expressed as g./12 cm. (W_0). It represents a measurement of tendon size because W_0 equals area \times density.

Swelling was achieved by holding a single tendon with a surgical hemostat while it was submerged in a beaker of deionized-distilled water at 26°C. After 10 sec. of immersion, the tendon was blotted dry for 5 sec. with tissue paper, transferred to the weighing pan of a direct-reading analytical balance, and weighed to an accuracy of 0.00 mg. It was returned to the beaker for another 10 sec. This process of intermittent swelling was continued until no further water uptake occurred. A second series of measurements were made where longitudinal stress (a 20-g. weight) was applied to tendons.

Allowing tendons to dry to equilibrium with room air, but no further, was a safeguard against irreversible changes which develop by exhaustive dehydration, a point made by Jordan-Lloyd and Marriott.¹² Continuous measurement of tendons during swelling would require that they be weighed while immersed. This certainly would be easier to do and also would not contain the uncertainty of blotting. At the same time, however, it adds complications due to possible changes in density of the tissue while it swells.¹³ To avoid the complications involved in continuous weighings,

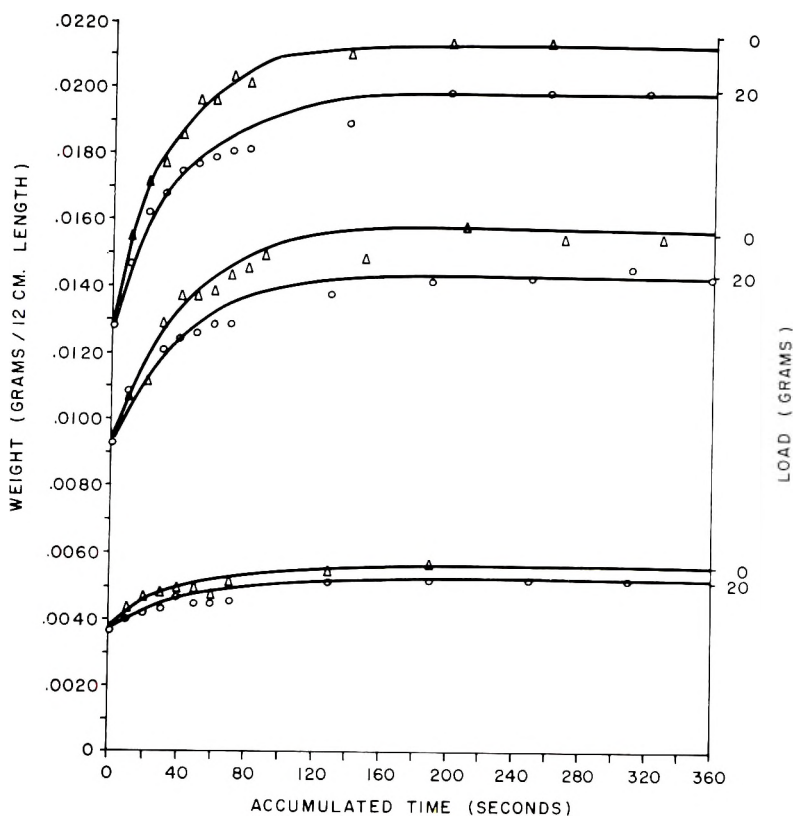


Fig. 1. Typical curves of tendon weight plotted (on the y ordinate) as a function of swelling time (abscissa). The effect of applying a 20-g. weight is shown for three tendons of different size.

it was elected to use the direct weighing technique and carry a possible error due to the blotting.

Results

Kinetic and Equilibrium Data

Rat tail tendons rapidly accumulate water when exposed directly to the liquid phase. It took less than 10 min. for each tendon to reach 95% of its equilibrium weight. When they remained in contact with water for 24 hr.,

small irregular blebs appeared which were separated by tight annular constrictions. Swelling weights measured beyond 15 min., therefore, were discounted from consideration because data obtained during the first quarter hour followed a smooth continuous function, which appeared to reach a fixed value.

Typical swelling curves are shown beginning with Figure 1 for three tendons of different sizes (W_0). Transient-weight (W) is plotted on the y axis as a function of accumulated time of swelling. Application of 20 g. weight to the tendon lowered the extent of water imbibition. The swelling ratio, defined as maximum weight W_∞ divided by the initial weight W_0 , increased linearly with dry size of tendon as shown in Fig. 2. It was also observed that the time required to reach equilibrium (T_∞), which experi-

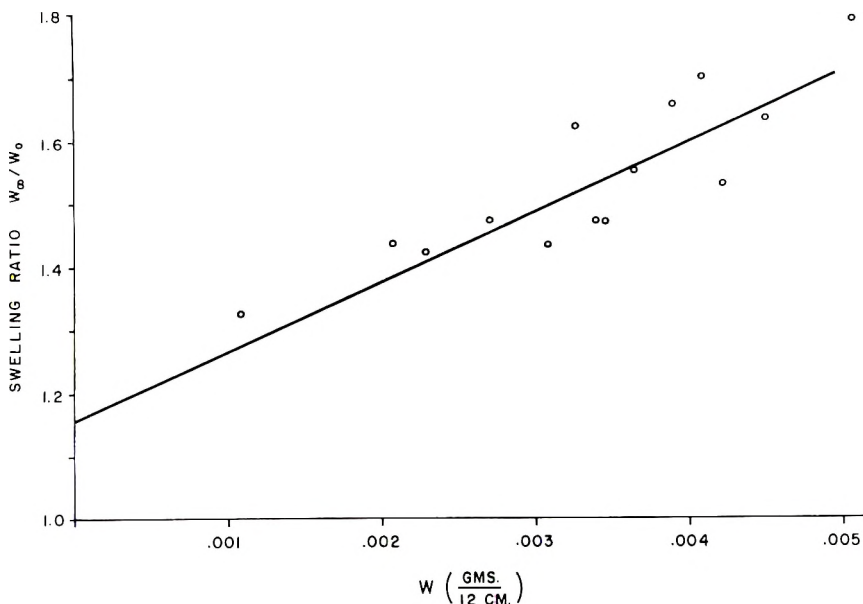


Fig. 2. Swelling ratio plotted as a function of tendon size.

mentally was selected as 98% completion, increased linearly with tendon size W_0 . These data are shown in Figure 3.

Kinetic and equilibrium data illustrated by Figures 1, 2, and 3 are the basic experimental facts descriptive of the swelling system, rat tail tendon-water. These findings will now be analyzed in an attempt to arrive at a rate mechanism for the short-time swelling process.

Diffusion Analysis

For a reasonably good approximation, it may be assumed that tendons are right circular cylinders. The mathematics for penetration of solvent into a cylinder has been worked out by Barrer,¹⁴ and eq. (1) expresses a relationship between quantity of imbibed fluid (Q_t) at time (t), the maximum quantity imbibed (Q_∞), radius r , diffusion coefficient D , and constants a_n

[roots of the Bessel function, $J_0(a, r) = 0$].

$$\frac{Q_t}{Q_\infty} = 1 - \frac{2}{r^2} \sum \frac{1}{\alpha_n^2} \exp \{-D\alpha_n^2 t\} \quad (1)$$

One cannot easily apply eq. (1) but rather uses an acceptable approximation. It is recognized that for a short time after the tendon is placed in contact with water, liquid entry is very close to simple diffusion across a plane. It can be shown that eq. (2) holds very close to the initial part (40%) of eq. (1).

$$\frac{Q_t}{Q_\infty} = \frac{4}{r} \sqrt{\frac{Dt}{\pi}}, \text{ short times} \quad (2)$$

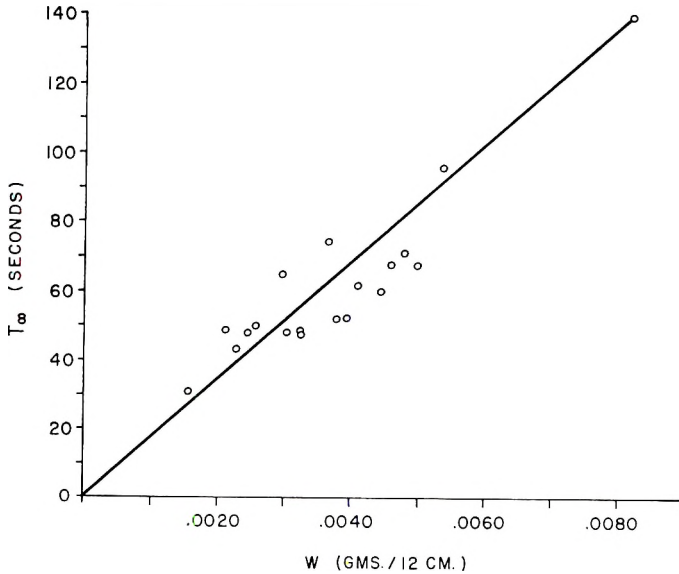


Fig. 3. Time required to reach $0.95Q_\infty$ plotted as a function of tendon size.

When swelling has proceeded for long values of t , however, eq. (1) can be reduced to eq. (3) in the limiting approximation.

$$\text{Log } Q_t \text{ proportional to } D\alpha^2 t, \text{ long times} \quad (3)$$

One can now evaluate diffusion coefficients (D_i , initial, and D_f , final) from data graphed in Figure 1 by using eqs. (2) and (3), respectively. Figure 4 shows a plot of Q_t/Q_∞ versus $t^{1/2}$ for data obtained from initial measurements, and Figure 5 shows a plot of terminal data, $\log Q_t$ versus t . With $r = 0.014$ cm., D_i and D_f were evaluated from the good linear fit of data in Fig. 3, and the limit which data appear to approach in Figure 4. Here D_i was found to be 3.0×10^{-7} cm.²/sec. and D_f was about 1000 times lower.

Evaluation of diffusion coefficients for the tendon-water system yields a mutual diffusion coefficient (D_M), because the comparatively large increase in diameter (more than 50%) results in a mass transfer of tendon into the

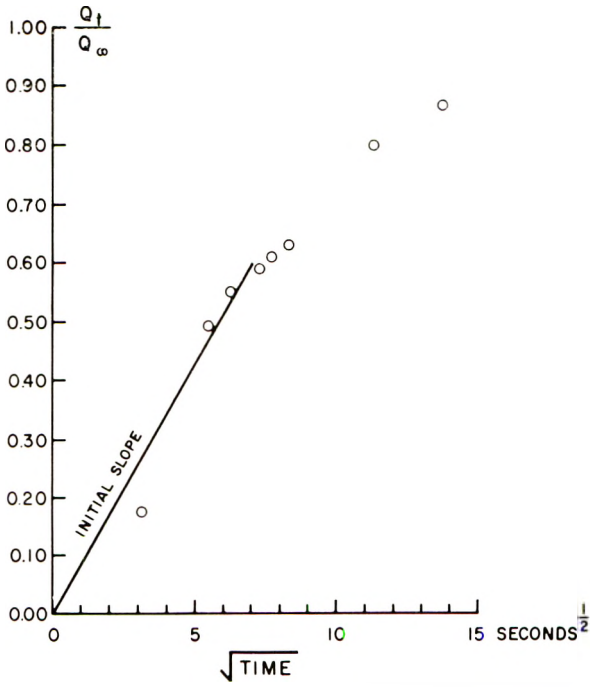


Fig. 4. Plot of initial swelling data showing conformity with Fickian cylindrical-diffusion theory.

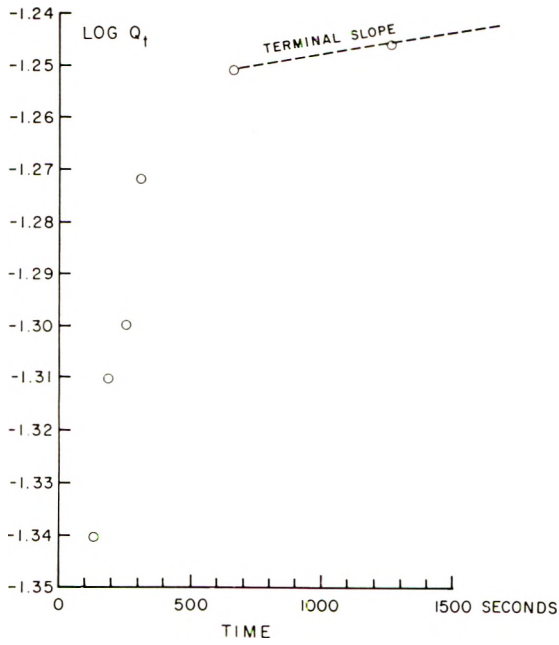


Fig. 5. Plot of terminal data showing approach to linearity as required by limiting form of cylindrical-diffusion theory.

water front. Hartley and Crank¹⁵ have shown that eq. (4) will give a value for an intrinsic diffusion coefficient (D_I) from D_M when the volume fraction (V) is known.

$$D_I = D_M(1 - V)^{-3} \quad (4)$$

Differences between these two coefficients should be greatest at the end of swelling when V is largest, but be negligible at the beginning when V is small. The ratio D_I/D_M was evaluated to be $(3)^3 = 27$ for $V = 1/3$. Correcting for the effect of swelling on diffusion, therefore, does not account for the abnormally large 1000-fold reduction in D as the final stages of swelling were approached.

Extremely low values of D_I , however, do not a priori rule out diffusion as the fundamental mechanism of swelling. Data certainly seemed to approach the limiting function described by eq. (3), but admit an anomalously low diffusion coefficient in the last stages. We can make some interesting deductions if we tentatively accept the diffusion process. To do so, let $Q_t = 0.98Q_\infty$ and express α_1^2 as $2.41^2/r^2$; t becomes T_∞ of Figure 3 and is proportional to $r^2/2.41^2 \times \log 0.98Q_\infty$. Since we have defined the symbol W as weight/length this is proportional to area \times density. Data in Figure 3 show that the time required to achieve 98% of equilibrium swelling is proportional to diameter,² and this is required by the limiting form of cylindrical-diffusion theory.

Proposal of Rate Mechanism for Swelling

Numerous theories and rate mechanisms for swelling were considered in addition to cylindrical diffusion, but only one was found which agreed completely with experimental data. It was accepted that the velocity of swelling, dW/dt , is proportional to the function $(A/W - BW)$. At any time t , then, the term A/W favors imbibition of water whereas BW opposes it. At equilibrium, dW/dt is zero, and $A/B = W_\infty^2$. Equation (5) holds at any finite time, whereas at zero time, $W = W_0(t = 0)$. The constants K_s , A , and B are characteristics of the equation.

$$dW/dt = K_s(A/W - BW) \quad (5)$$

When this is integrated and the limits inserted, eq. (6) is formed and eq. (7) was used to show its agreement with experimental data.

$$W_\infty^2 - W^2 = (W_\infty^2 - W_0^2)e^{-2BK_s t} \quad (6)$$

$$\text{Log}(W_\infty^2 - W^2) = \text{log}(W_\infty^2 - W_0^2) - \frac{2}{2.3} BK_s t \quad (7)$$

Figure 6 shows a good agreement of data with linearity required by eq. (7); the derived expression also conforms all the way to equilibrium. Application of longitudinal stress inhibited the swelling ratio W_∞/W_0 , as can be judged by looking at Figure 1. The velocity of swelling was also influenced, but one cannot determine which rate parameter was singularly influenced, or whether several were affected. Data shown in Figure 6,

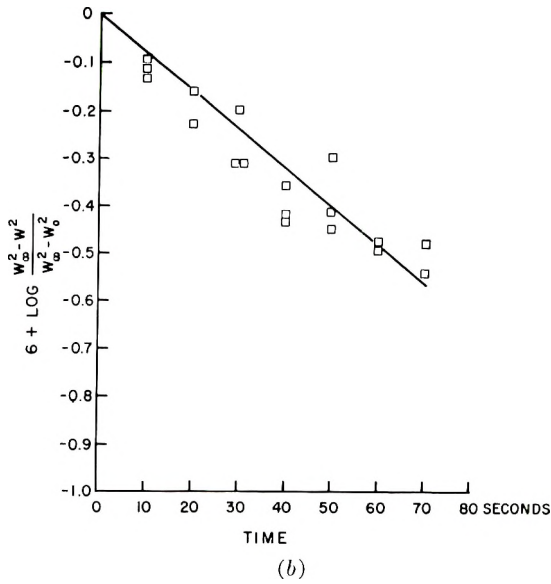
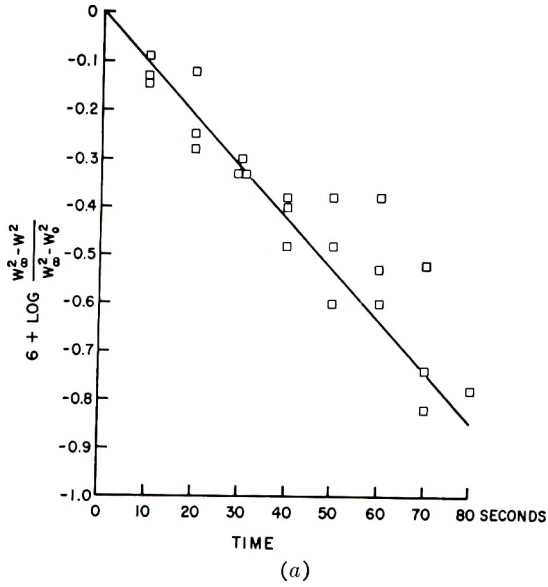


Fig. 6. (a) Linear plot of semilogarithmic function of swelling data for tendons with no load. (b) Linear plot of semilogarithmic function of swelling data for tendons with a 20-g. load.

however, show within limits of reasonable experimental error that eq. (7) was obeyed by loaded and nonloaded tendons swelling in water.

When one considers the initial period of swelling, eq. (6) can be converted to eq. (8) by making the approximation that $e^{-2BK_s t}$ equals $1 - 2BK_s t$ for small times (t).

$$W^2 = W_0^2 + (W_\infty^2 - W_0^2)2BK_s t \quad (8)$$

At this point it is possible to relate the just-derived swelling equation, in its limited form eq. (8), with the approximate solution of the cylindrical-diffusion equation (2). To do this, recall that tendon weight W equals the sum of initial dry-weight W_0 plus the quantity Q_t of water imbibed at time t .

$$W = W_0 + Q_t \quad (9)$$

When eq. (9) is squared, the right-hand side becomes eq. (10). Substitute (2) for Q_t in eq. (10) to obtain eq. (11).

$$W^2 = W_0^2 + 2W_0Q_t + Q_t^2 \quad (10)$$

$$W^2 = W_0^2 + 2W_0Q_\infty \frac{4}{r} \sqrt{\frac{Dt}{\pi}} + Q_\infty^2 \frac{16}{r^2} \frac{Dt}{\pi} \quad (11)$$

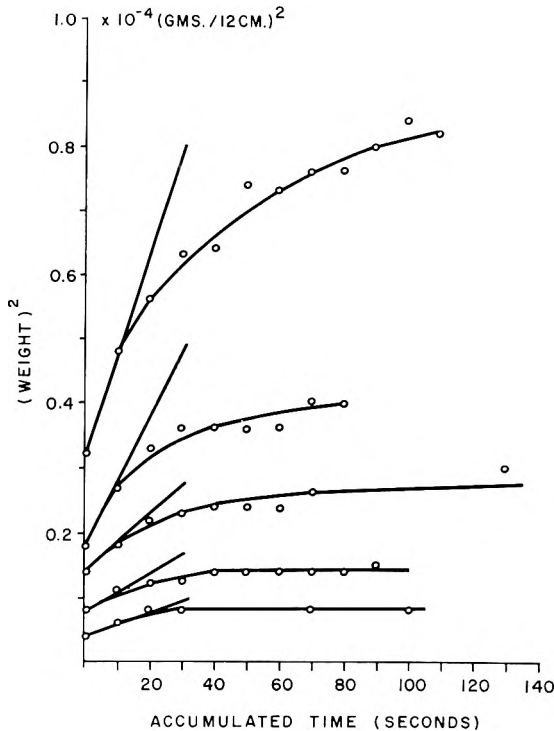


Fig. 7. Plot of short-time data showing the initial tangent from which data depart as swelling proceeds.

When this is rearranged by subtracting the second term of the right-hand side from W^2 , a function is obtained which resembles the linear dependence of W on t in eq. (8). In the limit of $t \rightarrow 0$, at the beginning of the experiment, $t^{1/2}$ tends to zero much faster than t . The initial slope of a plot of W^2 versus t , consequently, would equal the slope of eq. (8). Figure 7 shows the initial slope of a typical set of data. According to eq. (12), then, a relationship is established between the constants of Fickian-diffu-

sion with those of the proposed rate equation for swelling of tendons in water at short times.

$$Q_{\infty}^2 \frac{16 D}{r^2} \frac{D}{\pi} = (W_{\infty}^2 - W_0^2) 2BK_s \quad (12)$$

Discussion

Much valuable information about homogeneous and heterogeneous reaction mechanisms has been obtained by using the kinetic approach. A biological heterocomplex such as connective tissue, even when many of its properties are ideally represented by rat tail tendons, certainly is more difficult to analyze than most physical-chemical systems. Experience shows that a kinetic analysis is greatly expedited by knowing intimate details of structure, composition, and reactivity of various heterogeneities present. Without this information on tissue morphology, the task of elucidating an exact and complete rate mechanism for swelling would be almost hopeless. On the other hand, the probable great dependence of rate processes on structure and heterogeneity, compared to equilibrium methods, may offer a distinct opportunity to ascertain new facts about this important biological system.

Collagen fibrils, even though possibly arising from a soluble monomer, tropocollagen, may not be homogeneous in the solid state. Various chemical solutions have been used to extract a portion of collagen from rat tail tendons, but one always observes some residue. Studies by Tustanovskii et al.¹⁶ have convincingly shown that extractable collagen (procollagen of Orekhovitch) is different from the insoluble residue (collastromin). Procollagen and collastromin acting together as cylindrical sheath and core, respectively, constitute collagen as it might appear in tendon. Sorption of water by procollagen, according to Esipova et al.,¹⁷ is rapid and extensive, whereas collastromin reacts slowly and to a lesser extent. X-ray diffraction patterns of rat tail tendon are sharpened with hydration of the tissue, and regularities of structure appear that are not seen in the dry tissue.

Bolduan and Bear in earlier studies¹⁸ originally contributed knowledge concerning hydration and extension of structure transverse to the collagen fibril axis. Their studies also showed¹⁹ that dry fibrils do not diffract coherently along the longitudinal axis. They proposed that molecular organization comes about when water "welds" individual corrugated protofibrils (15 A. in diameter) into a longitudinally uniform compound protofibril 2000 A. in diameter. Inclusion of water occurs by a succession of steps, and equatorial spacings change accordingly as sites are successively occupied until there are pools of unbound water in between compound protofibrils.

Numerous studies have been reported on heats of hydration of collagen. Kanagy and Cassel²⁰ have shown that integral heats of wetting of collagen are almost twice those of most proteins. Blocking of OH and NH₂ groups had pronounced effects. Deamination, methylation, and acetylation

significantly reduced heats of wetting, and it appeared that blocking or removal of amine groups was especially effective in reducing the heats of hydration. Determination of the infrared dichroic ratio of hydrated and dried kangaroo tendon by Fraser and Macrae²¹ showed that water was also attached to carbonyl oxygen atoms of the peptide amide linkage.

Gustavson¹¹ summarized the general studies on collagen hydration by stating that (a) sorption of water by collagen occurs in a succession of steps, (b) water is bound tightly by amide and polar groups, and (c) while cationic and anionic side chain functional groups have an affinity for water, their role in the hydration of collagen is not important because they are too few in number. It is evident, therefore, that specific chemical and physical interactions do occur between collagen, mucopolysaccharides, and water.

Rat tail tendons are a highly organized form of connective tissue, as pointed out by this brief review, and they possess unique structural and chemical properties both of which can influence intratendon diffusion of water. Asymmetric collagen fibrils are closely packed in a hexagonal pattern, and longitudinal swelling is minimal whereas pronounced radial extension develops when the tissue is hydrated. Looking at its structure from this view, rate of imbibition of water by a tendon might depend upon whether it enters longitudinally or radially. Another factor which must be considered is that of a phenomenon called tangential swelling. This is defined as the amount of opening-up of a radial sector θ degrees aperture associated with radial swelling. It has been shown²² that stresses can develop in a homogeneous cylinder of anisotropic gel because of asymmetric longitudinal, radial, and tangential swelling. Application of experimental data²² by Warburton to a model which he proposed showed that a pressure of 200 atm. existed at the center, while a tangential stress of 50 atm. was created at the surface of a keratin fiber swollen to equilibrium (25°C. and 70% relative humidity). The core stress inhibited further swelling, and could be obviated only after sufficient plastic flow had occurred to relieve the stress. This theoretical study of Warburton gives some qualitative rationale for the *BW* resistance term in the proposed swelling rate equation.

The stressed core and peripheral annulus of swollen gel envisaged by Warburton²² are artifacts which could develop in all asymmetric cylinders. Collastromin and procollagen, however, are specific entities which are core and sheath of a particular collagen fibril. Many of the latter (collastromin + procollagen = collagen) may be in the core region of an equivalent Warburton-model of tendons, while others could be in the swollen annulus. Since Esipova et al.¹⁷ showed a difference in affinity of water for these two substances (procollagen greater than collastromin), it is a further theoretical possibility that each collastromin is a stressed core (inhibiting water infusion), whereas the procollagen sheath is stress relaxed. Since mucopolysaccharide interfibrillar substance also consists of two-phase dry and wet regions, additional complications of asymmetric swelling and stress production are possible. Many important facts undoubtedly remain to be discovered regarding the morphology of tendons.

References

1. Fessler, J. H., *Nature*, **179**, 426 (1957).
2. Maximow, A., and W. Bloom, *A Textbook of Histology*, W. B. Saunders Co., Philadelphia, 1930, p. 72.
3. Fitton-Jackson, S., *Proc. Roy. Soc. (London)*, **B114**, 566 (1956).
4. Ramachandran, G. N., *Arch. Biochem. Biophys.*, **63**, 255 (1956).
5. Gross, J., J. H. Highberger, and F. O. Schmitt, *Proc. Natl. Acad. Sci.*, **40**, 679 (1954).
6. Rich, A., and F. H. C. Crick, *Nature*, **176**, 915 (1955).
7. Bondareff, W., *Gerontologia*, **1**, 222 (1957).
8. Joseph, N. R., M. B. Engel, and H. R. Catchpole, *Biochem. Biophys. Acta*, **8**, 575 (1952).
9. Engel, M. B., N. R. Joseph, and J. H. Catchpole, *A.M.A. Arch. Pathol.*, **58**, 26 (1954).
10. Kao, K.-Y., D. M. Hilker, and T. H. McGavack, *Proc. Soc. Exptl. Biol. Med.*, **104**, 359 (1960).
11. Gustavson, K. H., *The Chemistry and Reactivity of Collagen*, Academic Press, New York, 1956.
12. Jordan-Lloyd, D., and R. Marriott, *Proc. Roy. Soc. (London)*, **B118**, 439 (1935).
13. Theis, E. R., and H. A. Neville, *Ind. Eng. Chem.*, **21**, 377 (1929).
14. Barrer, R. M., *Diffusion in and through Solids*, Cambridge Univ. Press, New York, 1941, ch. 1.
15. Hartley, R. M., and J. Crank, *Trans. Faraday Soc.*, **45**, 801 (1949).
16. Tustanovskii, A. A., A. L. Saider, I. Banga, and G. W. Orlovskaja, *Gerontologia*, **4**, 198 (1960).
17. Esipova, N. G., N. S. Andreena, and T. V. Gatovakaia, *Biophysics*, **3**, 505 (1958).
18. Bolduan, O. E. A., and R. S. Bear, *J. Polymer Sci.*, **6**, 271 (1951).
19. Bolduan, O. E. A., and R. S. Bear, *J. Polymer Sci.*, **5**, 159 (1950).
20. Kanagy, J. R., and J. M. Cassel, *J. Am. Leather Chem. Assoc.*, **52**, 248 (1957).
21. Fraser, R. E. B., and T. P. Macrae, *Nature*, **183**, 179 (1959).
22. Warburton, F. L., *Trans. Faraday Soc.*, 151 (1946).

Synopsis

Interaction of water with connective tissue is an important biophysical process. The chemical and physical morphology of tendons is a complex syncytium of collagen (procollagen + collastromin), mucopolysaccharide (aqueous phase + dense phase), and water (free and bound). It is proposed that a kinetic analysis of swelling of tendons might add new facts concerning the properties of the above tissue system. The present study shows that although diffusion may be the transport basis for swelling, there exists an anomalous dependence of diffusion on time of swelling. It is proposed that the velocity of swelling (dW/dt) is equal to a term $K_s(A/W - BW)$, the latter embodying a specific rate constant K_s , a driving factor A , and a retardation factor B which relates transitory tendon weight W to the initial weight W_0 , the equilibrium weight W_∞ , and

L'interaction de l'eau avec le tissu conjonctif est un processus biophysique important. La morphologie chimique et physique des tendons est un complexe de collagène (procollagène + collastromine) mucopolysaccharide, (phase aqueuse + phase dense), et eau (libre et liée). Une analyse cinétique du gonflement des tendons pourrait ajouter de

nouveaux éléments concernant les propriétés du système de tissus décrit ci-dessus. Cette étude montre que, bien que la diffusion puisse être la base de transport du gonflement, il existe une dépendance anormale de la diffusion en fonction de la durée du gonflement. La vitesse de gonflement (dW/dt) est égale à un terme $K_s (A/W - BW)$, le dernier renfermant une constante de vitesse spécifique K_s , un facteur d'avancement A , et un facteur de retardement B qui relie le poids transitoire du tendon W au poids initial W_0 , le poids à l'équilibre W_∞ et la température t . Cette équation intégrée donne une expression du travail qui concorde d'une façon satisfaisante avec les résultats expérimentaux. En plus cela est étayé par les théories du gonflement des gels anisotropiques. Les résultats mis en diagramme sous la forme de $\log (W^2 - W^2_0)/(W^2_\infty - W^2_0)$ vs. t respectent parfaitement la linéarité requise par l'équation de vitesse ci-dessus. L'étirement longitudinal diminue le rapport du gonflement W_∞/W_0 , mais augmente la vitesse avec laquelle l'équilibre est atteint.

Zusammenfassung

Die Wechselwirkung zwischen Wasser und dem Bindegewebe ist ein wichtiger biophysikalischer Prozess. Die chemische und physikalische Morphologie der Sehnen ist ein komplexes Syncytium von Collagen (Procollagen + Collatromin), Mucopolysaccharid (wässrige Phase + dichte Phase) und Wasser (frei und gebunden). Eine kinetische Analyse der Quellung von Sehnen wird zur Gewinnung eines neuen Tatsachenmaterials betreffend die Eigenschaften des obengenannten Gewebesystems vorgeschlagen. Die vorliegende Untersuchung zeigt, dass, obgleich die Diffusion möglicherweise die Transportgrundlage für die Quellung bildet, eine anomale Abhängigkeit der Diffusion von der Quellungsdauer besteht. Es wird angenommen, dass die Quellungsgeschwindigkeit (dW/dt) einem Term $K_s (A/W - BW)$ gleichgesetzt werden kann, welcher eine spezifische Geschwindigkeitskonstante K_s , einen Antriebsfaktor A und einen Verzögerungsfaktor B enthält; das jeweilige Sehnengewicht W wird dadurch zum Anfangsgewicht W_0 , zum Gleichgewichtsgewicht W_∞ und zur Zeit t in Beziehung gesetzt. Die Integration dieser Gleichung liefert einen Ausdruck, der befriedigend mit experimentellen Daten übereinstimmt. Sie wird ferner durch die Theorie der Quellung anisotroper Gele gestützt. Beim Auftragen als $\log (W^2_\infty - W^2)/(W^2_\infty - W^2_0)$ gegen t zeigten die Daten eine gute Übereinstimmung mit den von der oben angegebenen Geschwindigkeitsgleichung geforderten Linearität. Longitudinalspannung setzte das Quellungsverhältnis W_∞/W_0 herab, beschleunigte jedoch die Gleichgewichtseinstellung.

Received July 3, 1961

The Infrared Spectra and Structures of Polyisoprenes*

JOHN L. BINDER, *Chemical and Physical Research Laboratories,
The Firestone Tire and Rubber Company, Akron, Ohio*

Introduction

In connection with the preparation and development of lithium and other polyisoprenes¹ containing large amounts of *cis*-1,4 addition, over 2000 polyisoprenes have been examined for microstructure. As a consequence of these studies some conclusions have been drawn regarding the origins of bands in the spectra of Hevea and balata which supplement and extend earlier work by Sutherland and Jones² and Saunders and Smith.³ These are reported here.

Experimental

The polarization spectra of polyisoprenes, given in Figure 1, were obtained with a Beckman IR4 spectrophotometer. A polarizer, made with 6 sheets of silver chloride, was placed in the light beam between the source

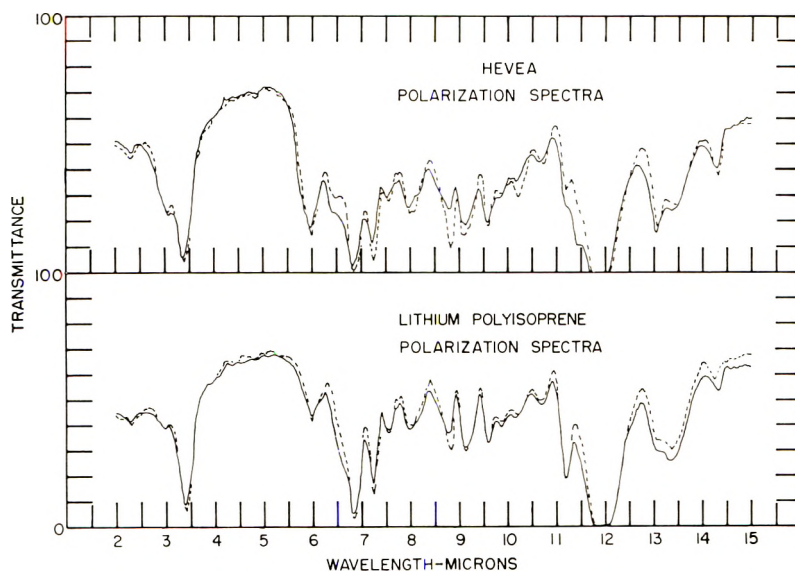


Fig. 1. Polarization spectra of Hevea and lithium polyisoprene at liquid nitrogen temperature. Dotted curve parallel to direction of stretch; solid curve perpendicular.

* Presented at the Symposium on Molecular Structure and Spectroscopy at The Ohio State University, June, 1961.

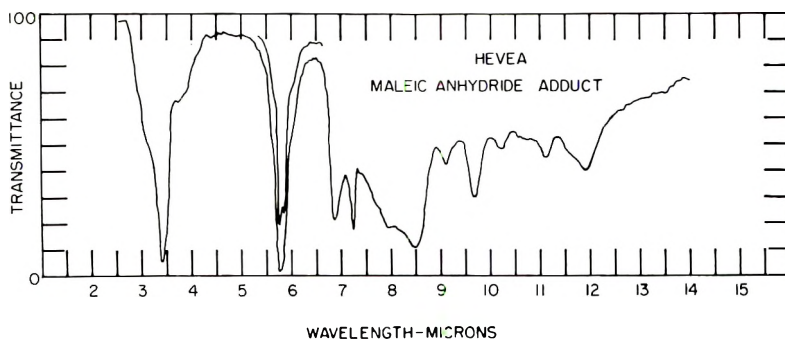


Fig. 2. Infrared spectrum of maleic anhydride adduct of Hevea.

and the focusing mirror so that both the reference and sample beams were equally polarized. In this way a 100% line could be obtained which was flat to $\pm 2\%$ and often $\pm 1\%$. This was not the case when two polarizers were used, one in the sample beam and one in the reference beam. The samples were cured in very thin sheets using only cumyl peroxide. Sections of these were stretched and clamped in aluminum frames which could be fastened to a stud in a low temperature cell. The stud was the termination of a liquid nitrogen well and the cooling of the sample was accomplished by conduction. The low temperature cell could be evacuated and was fitted with rock salt windows. The stretched samples were cooled, in the

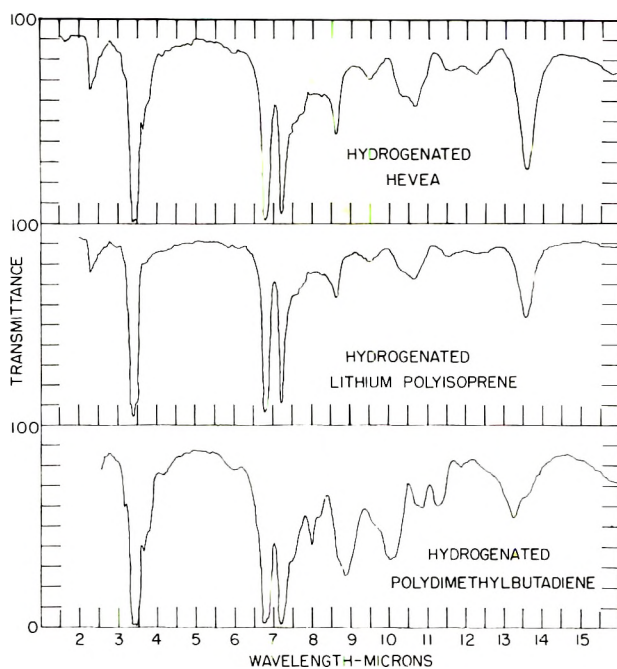


Fig. 3. Infrared spectra of hydrogenated polyisoprenes and polydimethylbutadiene.

frames, to about -25°C . for several days and were kept on Dry Ice while transferring them to the low temperature cell. For spectra at liquid nitrogen temperatures the sample was cooled, at this temperature, for at least $\frac{1}{2}$ hr. before recording the spectra. The plane of polarization was changed by rotating the polarizer.

The maleic anhydride adducts were made by T. B. Talcott using toluene solutions of the polymers and maleic anhydride. The reaction was carried out in a sealed glass tube. The spectra of the purified adducts were recorded with a Beckman IR4 using films of the materials. One is shown in Figure 2.

The hydrogenations were done by A. Fono using Raney nickel catalyst. Toluene solutions of the polymers were used. The amount of hydrogenation varied with different samples. Spectra of films of the purified polymers were recorded with a Beckman IR4. These are shown in Figure 3.

The noise, evident in these figures especially on strong bands, is human "noise" resulting from tracing the spectra with a drawing pen.

Discussion

Saunders and Smith³ discussed the spectra of Hevea and balata in considerable detail and Sutherland and Jones² discussed the origins of certain bands. Their conclusions are summarized in Table I. The purpose here is to discuss new information which sheds some light on the origins of some of the bands in the spectra of Hevea and synthetic polyisoprenes.

A comparison of the spectra of Hevea and balata shows that, in carbon disulfide solutions, many bands in the spectrum of balata are shifted toward shorter wavelengths than their counterparts in the spectrum of Hevea. Thus, for example, the maximum of the $11.9\text{-}\mu$ band is at 837.5 cm.^{-1} in Hevea and at $8\pm 3.0\text{ cm.}^{-1}$ in balata and the 1130-cm.^{-1} band in Hevea is at 1152 cm.^{-1} in balata. It was observed that the 764- and 742 cm.^{-1} bands showed the same behavior being at 764 and 742 cm.^{-1} in Hevea and at 766 and 745 cm.^{-1} in balata. This raised the question of whether these bands are connected with some vibration of the $-\text{C}(\text{CH}_3)=\text{CH}-$ group. A direct correlation was found between the intensity of the 742-cm.^{-1} band and the percent net *cis*-1,4 ($\text{cis-1,4}\%$ \times total found percent), obtained from the microstructure determination, for various high *cis*-1,4-polyisoprenes. The polarization spectra of Hevea and lithium polyisoprene (94% *cis*-1,4) show that these bands are perpendicularly polarized with respect to the direction of stretch and hence are due to a group which is oriented to some extent. The spectrum of hydrogenated Hevea shows that these bands have been replaced by one strong band at about 735 cm.^{-1} which is, most likely, due to the $(\text{CH}_2)_3$ groups formed in the hydrogenation. The spectrum of the maleic anhydride adduct of Hevea does not have these bands either. Maleic anhydride reacts at the carbon double bond so that the disappearance of the bands in the spectrum of the maleic anhydride adduct indicates the removal of the double bonded car-

TABLE I
 Bands in Spectra of Polyisoprenes

| μ | Band cm. ⁻¹ | Saunders and Smith ^a | Sutherland and Jones ^b | Binder |
|-------|---------------------------|--|--|---|
| 3.25 | 3077 | | | =CH stretch of C(CH ₃)=CH ₂ |
| 3.33 | 3000 | | | =CH stretch of C(CH ₃)=CH— |
| 3.42 | 2924 | | | CH ₃ stretch asymmetrical |
| 3.44 | 2907 | | | CH ₂ in phase stretch |
| 3.46 | 2890 | | | CH ₃ stretch symmetrical |
| 3.53 | 2833 | | | CH ₂ out-of-phase stretch |
| 3.68 | 2717 | | | |
| 6.01 | 1665 | C=C | | C=C of C(CH ₃)=CH— |
| 6.10 | 1645 | | | C=C of CH ₂ =C(CH ₃)— |
| 6.90 | 1450 | CH ₃ antisymmetrical | | |
| 7.25 | 1380 | CH ₃ symmetrical | CH ₃ symmetrical | |
| 7.35 | 1361 | CH ₂ wag | CH in-plane def. ^c | |
| 7.55 | 1325 | | | =CH of <i>trans</i> -C(CH ₃)=CH |
| 7.60 | 1315 | CH ₂ twist | | =CH of <i>cis</i> -C(CH ₃)=CH |
| 7.73 | 1294 | C—H in-plane bend | | |
| 8.03 | 1245 | CH ₂ twist | | |
| 8.25 | 1212 | | | |
| 8.68 | 1152 | | | C—CH ₃ of <i>trans</i> -C(CH ₃)=CH |
| 8.85 | 1130 | CH ₂ wag | CH ₃ in plane def. ^c | C—CH ₃ of <i>cis</i> -C(CH ₃)=CH |
| 9.15 | 1105 | C—CH ₂ stretch | | |
| 9.62 | 1040 | CH ₃ rock | | |
| 9.87 | 1013 | C—CH ₂ stretch | | |
| 10.20 | 980 | C—CH ₃ stretch | | |
| 10.74 | 931 | | | |
| 11.24 | 890 | CH ₃ wag | | CH of CH ₂ =C(CH ₃) |
| 11.49 | 870 | CH ₃ wag out of plane | | Crystallinity band |
| 11.90 | 840 | CH ₂ -CH ₂ stretch | | CH out of plane of <i>cis</i> - C(CH ₃)=CH |
| 11.83 | 845 | CH wag out of plane | CH out of plane | CH out of plane of <i>trans</i> - C(CH ₃)=CH |
| 13.12 | 762 | CH ₂ rock | | C(CH ₃)=CH |
| 13.48 | 742 | | | |

^a See ref. 3. ^b See ref. 2. ^c Def. means deformation.

bon. The spectrum of an essentially all 3,4-polyisoprene, shown in Figure 4, does not have these bands either and in this polymer all of the double bonds are in isopropenyl groups CH₂=C(CH₃)—.

While the evidence points to the origins of the 764- (13.1 μ) and 742-cm.⁻¹ (13.5 μ) bands being in the —C(CH₃)=CH— group we do not know what particular kind of vibration is involved. The assignment of Saunders and Smith, in Table I, to a CH₂ rocking seems improbable.

The band at about 12 μ is now generally recognized to be due to the CH out-of-plane vibration of the C(CH₃)=CH— group in both Hevea and balata spectra. Smith and Saunders assigned the other band in this region,

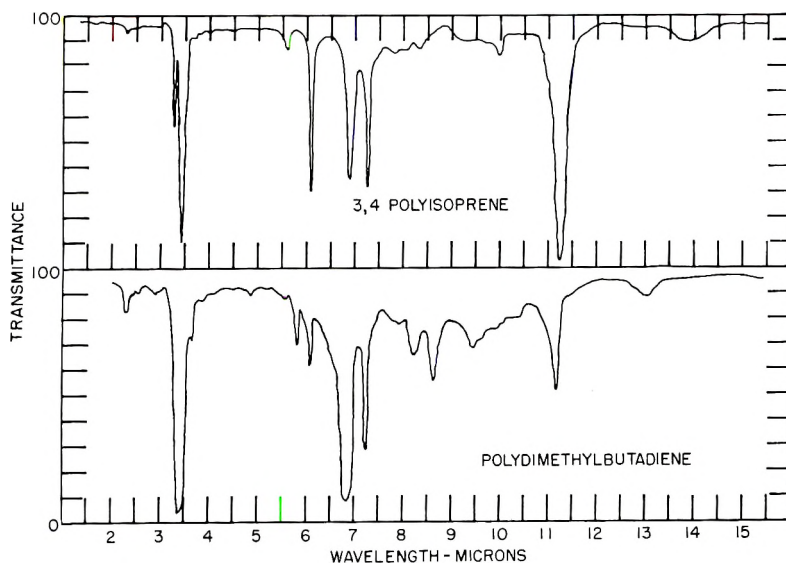


Fig. 4. Infrared spectra of all 3,4-polyisoprene and polydimethylbutadiene.

at 890 cm.^{-1} ($11.25\ \mu$), to a CH_3 wagging vibration. Binder and Ransaw⁴ assigned it to an isopropenyl, $\text{CH}_2=\text{C}(\text{CH}_3)-$ group for the following reasons. If there is an isopropenyl group in Hevea then, besides this 890 cm.^{-1} band, there should be one due to the $\text{C}=\text{C}$ group near 1645 cm.^{-1} and another near 3077 cm.^{-1} due to the CH stretch. Figure 5 shows the in-

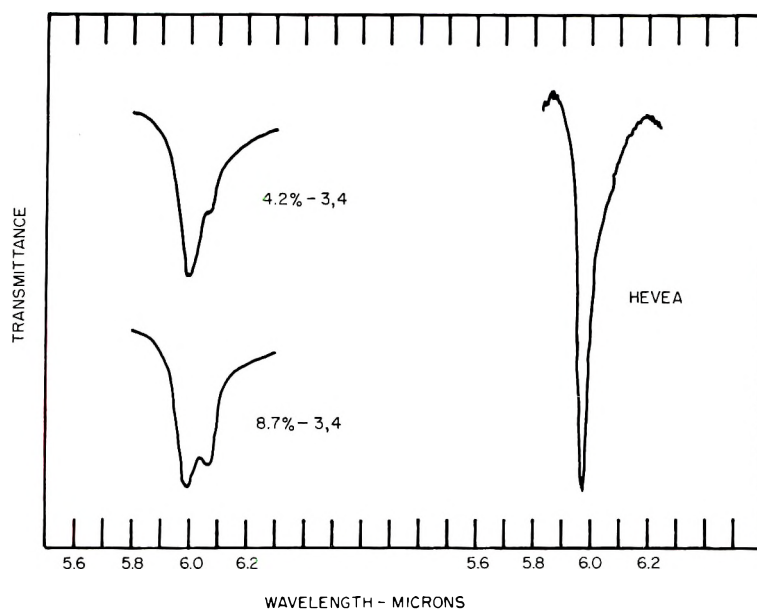


Fig. 5. Infrared spectra of Hevea and synthetic polyisoprenes in the $6\text{-}\mu$ region.

frared spectra of Hevea and two synthetic polyisoprenes containing different amounts of 3,4 addition (isopropenyl groups), in the $6\ \mu$ region. The spectrum of Hevea was recorded with a Beckman IR3 at The Ohio State University so that there is no doubt that the shoulder on the long-wave side of the $6\ \mu$ band is real. The Hevea was deproteinized, purified, and not degraded. The synthetic polyisoprenes were pure and the spectra were obtained with an IR2 by point-by-point measuring. It is evident that the intensity of the $6.1\ \mu$ band increases as the amount of isopropenyl group increases. The magnitude of the change in intensity with the change in amount of isopropenyl groups is such that if Hevea contains only about 2% isopropenyl the $6.1\ \mu$ band would be weak and appear as a shoulder. This is observed.

The absorption at $3077\ \text{cm.}^{-1}$ due to the $=\text{CH}$ stretch vibration of the $\text{CH}_2=\text{C}(\text{CH}_3)$ appears in the IR3 spectrum of Hevea and also in IR4 spectrum of the synthetic polyisoprene. The intensity of this band increases with increasing amount of isopropenyl. The absorption in the Hevea spectrum, although only a slight shoulder on the other strong CH bands, appears at the same place and is real. Therefore it is concluded that it is also due to the $=\text{CH}$ stretch of the $\text{CH}_2=\text{C}(\text{CH}_3)$ group.

The polarization spectra show some dichroism of the 890-cm.^{-1} band and it disappears in the hydrogenated spectra. These facts reinforce the assignment of the 890-cm.^{-1} band to the isopropenyl group and thus it is due to a hydrogen out-of-plane vibration rather than a CH_3 wag.

Golub⁵ has reported the isomerization of Hevea and it might appear from his spectra that the intensity of the 890-cm.^{-1} band decreased as the *cis*-1,4 decreased. This experiment was repeated with purified, deproteinized Hevea, in the manner described by Golub, but the amounts of *cis*-1,4, *trans*-1,4, and 3,4-(isopropenyl) were determined by our analytical method.⁴ In this experiment the *cis*-1,4 decreased to about 32% but the 3,4 actually increased, as was plainly evident from the spectrum, to about 6%. It should be pointed out that the $10.4\ \mu$ band in the Hevea spectrum also increased somewhat in intensity in the spectrum of the isomerized product. Thus the isomerization experiment of Golub does not invalidate the assignment of the 890-cm.^{-1} band to isopropenyl, $\text{CH}_2=\text{C}(\text{CH}_3)-$.

The 1130-cm.^{-1} band in the spectrum of Hevea has been assigned by Saunders and Smith³ to a CH_2 wagging vibration but Sutherland and Jones,² on much the same evidence, suggest that it could be due to a CH_3 in-plane deformation. Our analytical results of synthetic polyisoprenes show, however, that the intensity of this band does change with the amount of *cis*-1,4 addition, or *cis*- $\text{C}(\text{CH}_3)=\text{CH}-$, as does the 1152.5-cm.^{-1} band in the spectrum of balata with the amount of *trans*-1,4 addition. In synthetic polyisoprenes the number of CH_2 groups should be constant regardless of the kind of $-\text{C}(\text{CH}_3)=\text{CH}-$ groups (*cis* or *trans*) so that the intensity of this band should be constant, if due to CH_2 , regardless of the amount of *cis*- or *trans*- $\text{C}(\text{CH}_3)=\text{CH}$. Hence, more in agreement with Sutherland's assignment, it appears that this band is due to a $\text{C}-\text{CH}_3$ vibration of the

cis-C(CH₃)=CH— group. This conclusion is confirmed by the hydrogenation spectrum and the maleic anhydride adduct spectrum. In both, the 1130-cm.⁻¹ band has disappeared as it should if it is connected with a C=C group.

A comparison of the polarization spectra of Hevea and lithium polymer, in Figure 1, confirm some remarks of Sutherland and Jones² about the effect of crystallinity on the intensity of the 1130-cm.⁻¹ (8.85 μ) band in the polarization spectra of Hevea. The lithium polyisoprene contained 94% *cis*-1,4 addition, according to our analysis, and was found, by x-rays, to crystallize less readily than Hevea. It seems unlikely the small difference in *cis*-1,4 would produce the difference in the amount of polarization shown.

As a general rule, infrared vibration bands are symmetrical, at least when resolved with most present-day instruments. From the shapes of the 1130- and 1152-cm.⁻¹ bands it is evident that there must be another band lying between them. Stronger evidence of this band is found in the spectra of emulsion or sodium or potassium-catalyzed polyisoprenes. In these spectra the band appears to be near 1143 cm.⁻¹ It is this band which interferes with determinations of the amounts of *cis*-1,4 and *trans*-1,4 additions in these types of polyisoprenes, using intensities measured at 1130 and 1152 cm.⁻¹, respectively. Its origin is not known.

The bands at about 1315 cm.⁻¹ in the spectrum of Hevea and at 1325 cm.⁻¹ in balata, also appear to be connected with the —C(CH₃)=CH— group. Golub⁵ has pointed out that the 1325-cm.⁻¹ band increases in intensity and the 1315-cm.⁻¹ band decreases during the isomerization of Hevea. His conclusions are supported by our results from synthetic polyisoprenes, which also indicate that about 10% *trans*-C(CH₃)=CH is required for the 1325-cm.⁻¹ band to definitely appear in the spectrum. Again this conclusion is confirmed by the spectra of hydrogenated Hevea (Fig. 3) and of the maleic anhydride adduct (Fig. 2), which show that these bands have disappeared. The polarization spectrum shows that this band is scarcely polarized.

These two bands, 1315 and 1325 cm.⁻¹, are probably due to a =C—H vibration of the C(CH₃)=CH— group in Hevea and balata, respectively, for several reasons. Bands due to the C(CH₃) part of the group are assigned. Bands at 1310 and 1320 cm.⁻¹ appear in polybutadiene spectra and are connected with the *cis*- and *trans*-CH=CH—, as is shown in another place.⁶ In the spectrum of polydimethylbutadiene (see Fig. 4) there is a band at about 1152 cm.⁻¹ but none near 1325 cm.⁻¹ These bands are not present in the spectrum of hydrogenated polydimethylbutadiene (see Fig. 3). This polymer is known, by x-rays, to be *trans*-C(CH₃)=C(CH₃)— and a band at 1152 cm.⁻¹ would be expected, on the basis of the balata assignment. Since there is no CH present in this group a band at 1325 cm.⁻¹ would not be expected and is not found.

Concerning the origins of the remaining bands in the spectrum of Hevea or balata only a few observations can be offered. It will be noted that the band near 1360 cm.⁻¹ is weaker in our spectrum than it is in the spectra of

Sutherland and Jones² and Saunders and Smith's.³ This is in better agreement with the intensity of this band in polybutadiene spectra. On this account it seems more likely to be due to CH_2 , as Saunders and Smith give it, than CII. The 870 cm.^{-1} given by Saunders and Smith for Hevea is certainly due to crystallinity rather than CH_3 wag, as is a band near 820 cm.^{-1} . There are analogous bands in the crystalline balata spectrum at about 862 and 800 cm.^{-1} . Nothing definite can be said here about the origins of the bands in the $9\text{--}11\text{-}\mu$ region.

These conclusions are listed in Table I. Many of the assignments in this table attributed to Saunders and Smith are taken from their table although the frequencies given here do not exactly agree with theirs. Where no assignment is made in the last column it may be assumed that the assignments of Saunders and Smith are accepted.

In a paper⁷ on deuterated polyisoprene the assignment of the 840 cm.^{-1} is discussed and the assignment made here confirmed. None of the other bands is discussed. Estimates of the band positions cannot be made from the published spectra accurately enough to permit any conclusions to be drawn here. The spectra of carotenoid pigments given by Lunde and Zechmeister⁸ show many of the *cis*- $\text{C}(\text{CH}_3)=\text{CH}$ and *trans*- $\text{C}(\text{CH}_3)=\text{CH}$ bands given here if allowance is made for the effects of conjugation. This is also true of the spectra of isoprenoid polyenes published by Oroshnik and Mebane.⁹

Conclusions

It is shown that bands at 764 , 742 , 1130 , and 1315 cm.^{-1} are connected with vibrations of the *cis*- $\text{C}(\text{CH}_3)=\text{CH}$ - group. Of these the 1130 cm.^{-1} band appears to be due to a vibration of the CH_3 or $\text{C}(\text{CH}_3)$ in this group while the 1315 cm.^{-1} band is connected with a C-H vibration of this group.

Bands at 766 , 745 , 1152 , and 1325 cm.^{-1} are due to vibrations of the *trans*- $\text{C}(\text{CH}_3)=\text{CH}$ - group. Of these the 1152 cm.^{-1} is due to a vibration of the CH_3 or $\text{C}(\text{CH}_3)$ in this group and the 1325 cm.^{-1} band due to a CH vibration of this group.

The 1152 cm.^{-1} band appears in the spectrum of polydimethylbutadiene and is due to a $\text{C}(\text{CH}_3)$ vibration of the *trans*- $\text{C}(\text{CH}_3)=\text{C}(\text{CH}_3)$ group.

Thanks are due Mr. H. C. Ransaw and Mr. G. E. Harris who made the measurements and recorded many of the spectra used here. The author is indebted to Mr. T. B. Talcott for making the maleic anhydride adducts and to Dr. A. Fono for the hydrogenated samples. He is also indebted to Drs. E. J. Devlin, J. E. Field, J. J. Shipman, W. C. Sears, and D. C. Smith for their helpful suggestions and criticisms. The interest of Dr. F. W. Stavely and Mr. E. T. Handley is greatly appreciated.

References

1. Stavely, F. W., et al., *Ind. Eng. Chem.*, **48**, 778 (1956); Horne, S. E., et al., *Ind. Eng. Chem.*, **48**, 784 (1956).
2. Sutherland, G. B. B. M., and A. V. Jones, *Discussions Faraday Soc.*, **9**, 281 (1950).
3. Saunders, R. A., and D. C. Smith, *J. Appl. Phys.*, **20**, 953 (1949).

4. Binder, J. L., and H. C. Ransaw, *Anal. Chem.*, **29**, 503 (1957).
5. Golub, M. A., *J. Polymer Sci.*, **36**, 523 (1959).
6. Binder, J. L., "Analysis of Polybutadienes," to be published.
7. Semon, W. L., and D. Craig, *Rubber & Plastics Age*, **40**, 140 (1959).
8. Lunde, K., and L. Zechmeister, *J. Am. Chem. Soc.*, **77**, 1647 (1955).
9. Oroshnik, W., and A. D. Mebane, *J. Am. Chem. Soc.*, **76**, 5719 (1954).

Synopsis

Evidence is offered which confirms, and in some cases, changes previously suggested assignments of bands in the spectra of Hevea and balata. In particular it is shown that bands at 764 (13.1 μ) and 742 cm^{-1} (13.5 μ) are probably connected with vibrations of the *cis*- or *trans*-C(CH₃)=CH— group, a band at 1130 cm^{-1} (8.85 μ) is due to a C—CH₃ vibration of the *cis*-C(CH₃)=CH group, a band at 1155 cm^{-1} (8.68 μ) is due to the C—CH₃ vibration of the *trans*-C(CH₃)=CH group. Likewise the bands at 1315 (7.60 μ) and 1325 cm^{-1} (7.55 μ) are probably due to a CH vibration of the *cis*- and *trans*-C(CH₃)=CH groups, respectively. The 1130- cm^{-1} band and the 1155- cm^{-1} band are found in the spectra of polydimethylbutadiene and thus are probably group frequencies. The 1315 and 1325- cm^{-1} bands (shifted) are also found in polybutadiene and polypiperylene spectra and thus are probably group frequencies also. It is also shown that the 890-, 1645-, and 3077- cm^{-1} bands are best explained by the presence of an isopropenyl, CH₂=C(CH₃)— group. These assignments are based on a study of the polarization spectra, the spectra of maleic anhydride adducts and hydrogenated polyisoprenes, and on microstructure determinations.

Résumé

Des preuves sont données qui confirment, et dans certains cas changent, l'attribution antérieure de bandes d'absorption dans les spectres d'absorption infra-rouge de l'Hévéa et du balata. En particulier il est démontré que les bandes à 764 (13.1 μ) et à 742 cm^{-1} (13.5 μ) sont probablement en relation avec les vibrations du groupe —C(CH₃)=CH— *cis* ou *trans*, que la bande à 1130 cm^{-1} (8.85 μ) est due à la vibration C—CH₃ du groupe —C(CH₃)=CH *cis*, et que la bande à 1155 cm^{-1} (8.68 μ) est due à la vibration C—CH₃ du groupe —C(CH₃)=CH *trans*. Similairement les bandes à 1315 cm^{-1} (7.60 μ) et 1325 cm^{-1} (7.55 μ) sont dues probablement à une vibration CH des groupes —C(CH₃)=CH respectivement *cis* et *trans*. Les bandes 1130 et 1155 cm^{-1} sont présentes également dans le spectre du polydiméthylbutadiène et sont probablement des fréquences de groupe. Les bandes 1315 et 1325 cm^{-1} sont aussi repérées dans les spectres du polybutadiène et du polypipérylène et sont aussi probablement des fréquences de groupe. Il est démontré également que les bandes à 890, 1645 et 3077 cm^{-1} sont justifiées par la présence du groupe isopropényle CH₂C(CH₃)=Ces attributions sont basées sur une étude de spectres de polarisation, de spectres de polyisoprènes hydrogénés et de produits d'addition à l'anhydride maléique et sur des déterminations de microstructures.

Zusammenfassung

Es werden Ergebnisse mitgeteilt, welche die früher angenommene Bandenzuordnung in des Spektren von Hevea und Balata bestätigen, und in einigen Fällen verändern. Im einzelnen wird gezeigt, dass Banden bei 764 (13,1 μ) und 742 cm^{-1} (13,5 μ) wahrscheinlich mit Schwingungen der *cis*- oder *trans*-C(CH₃)=CH-Gruppe zusammenhängen; eine Bande bei 1130 cm^{-1} (8,85 μ) wird durch eine C—CH₃-Schwingung der *cis*-C(CH₃)=CH Gruppe verursacht und eine Bande bei 1155 cm^{-1} (8,68 μ) durch die C—CH₃-Schwingung der *trans*-C(CH₃)=CH Gruppe. Ebenso werden die Banden bei 1315 cm^{-1} (7,60 μ) und 1325 cm^{-1} (7,55 μ) wahrscheinlich durch eine CH-Schwingung der *cis*- bzw. *trans*-C(CH₃)=CH Gruppen verursacht. Die 1130 cm^{-1} und 1155 cm^{-1} -Bande werden in den Spektren von Polydimethylbutadien

gefunden und sind daher wahrscheinlich Gruppenfrequenzen. Die 1315 cm.^{-1} und 1325 cm.^{-1} -Bande (verschoben) werden auch in den Spektren von Polybutadien und Polypiperylen gefunden und sind daher wahrscheinlich auch Gruppenfrequenzen. Es wird gezeigt, dass die 890 cm.^{-1} , 1645 cm.^{-1} und 3077 cm.^{-1} -Bande am besten durch die Anwesenheit einer Isopropenylgruppe, $\text{CH}_2=\text{C}(\text{CH}_3)-$, erklärt werden. Diese Zuordnung beruht auf einer Untersuchung der Polarisationspektren, der Spektren von Maleinsäureanhydridaddukten und hydrierten Polyisoprenen und auf Mikrostrukturbestimmungen.

Received September 28, 1961

The Infrared Spectra and Structures of Polybutadienes*

JOHN L. BINDER, *Chemical and Physical Research Laboratories,
The Firestone Tire and Rubber Company, Akron, Ohio*

Introduction

Until a few years ago, our knowledge of the infrared spectra of polybutadienes was based largely on the spectra of emulsion, sodium, potassium, or alfin polybutadienes. Many of the bands in the spectra were explained on the basis of correlations deduced from olefin spectra although the position of the *cis*-CH=CH band in the polymer spectra was uncertain. With the discovery of methods of making polybutadienes containing large amounts of *cis*-CH=CH—, *trans*-CH=CH— or CH₂=CH₂—,¹ it became possible to re-evaluate polybutadiene spectra. As a result of determining the microstructures of about 2000 such polymers, some conclusions have been reached regarding the origin of some bands in polybutadiene spectra. These are reported here.

Experimental

Polarization spectra of polybutadienes were obtained with a Beckman IR4 spectrophotometer in the same way as described for polyisoprene.² The samples of high *cis*-1,4-polybutadiene were cured in thin sheets using only cumyl peroxide. Films which could be stretched to orient the polymer and thin enough so that all bands showed some transmission (10%) could not be obtained. Polarization spectra of two different polybutadienes, containing different amounts of *trans*-1,4, obtained at the temperature of liquid nitrogen, are shown in Figure 1.

The infrared spectra of hydrogenated polybutadienes and polypiperylene, prepared by A. Fono, were recorded using films of the materials. These are shown in Figure 2. The band at about 9.5 μ in the Ziegler and lithium polybutadienes is due to catalyst. The spectra of maleic anhydride adducts of polybutadiene, prepared by T. B. Talcott, are shown in Figure 3.

Assignments of bands in polybutadiene spectra are given in Table I. The bases of the assignments are given in the discussion.

* Presented at the Symposium on Molecular Structure and Spectroscopy, The Ohio State University, June 1961.

TABLE I
 Bands in Polybutadiene Spectra

| | Band cm. ⁻¹ | Origin |
|----------------------|------------------------|---|
| 3.25 ^a | 3077 | CH stretch of CH ₂ =CH |
| 3.32 ^a | 3012 | CH stretch of <i>cis</i> -CH=CH |
| 3.45 ^a | 2900 | CH stretch of CH ₂ |
| 3.40 | 2841 | CH stretch of CH ₂ |
| 5.4 ^a | 1850 | Overtone of CH ₂ =CH |
| 6.05 ^a | 1660 | C=C stretch of <i>cis</i> -CH=CH |
| 6.10 ^a | 1640 | C=C stretch of CH ₂ =CH |
| 6.8-6.9 ^a | 1470 | CH ₂ def. ^c |
| 7.05 ^a | 1418 | CH in plane def. ^c of CH ₂ =CH |
| 7.10 ^a | 1408 | CH in plane def. ^c of <i>cis</i> -CH=CH |
| 7.38 | 1355 | CH of <i>trans</i> -CH=CH; also in 1, 2A, S, I ^b |
| 7.55 | 1325 | In 1,2 A,S,I ^b |
| 7.63 | 1311 | CH of <i>cis</i> -CH=CH |
| 7.65 | 1307 | In 1,2 A,S,I ^b |
| 7.75 | 1290 | In 1,2 A,S,I ^b |
| 8.1 | 1235 | In all spectra |
| 8.3 | 1205 | In 1,2 I ^b |
| 8.8 | 1136 | In 1,2 S ^b |
| 9.0 | 1111 | In 1,2 I ^b |
| 9.25 | 1081 | In emulsion and <i>cis</i> - and <i>trans</i> -CH=CH |
| 9.3 | 1075 | In 1,2 I,S ^b |
| 9.5 | 1053 | High <i>trans</i> -1,4 (crystallinity) |
| 10.0 | 1000 | High <i>cis</i> -1,4 |
| 10.05 ^a | 995 | CH out of plane of CH ₂ =CH |
| 10.34 ^a | 967 | CH out of plane of <i>trans</i> -CH=CH |
| 10.98 ^a | 910 | CH ₂ out of plane of CH ₂ =CH |
| 11.4 | 877 | In 1,2 I ^b |
| 11.7 | 855 | In 1,2 S ^b |
| 12.4 | 806 | In 1,2 I ^b |
| 12.5 | 800 | In some high <i>cis</i> -1,4 |
| 12.9 | 775 | Crystallinity band of high <i>trans</i> -1,4 |
| 12.7 | 787 | In 1,2 S ^b |
| 13.5 | 740 | <i>cis</i> -CH=CH, 1,2 A,S ^b |
| 14.1 | 709 | 1,2 I ^b |
| 14.4 | 695 | 1,2 I ^b |
| 14.8 | 675 | 1,2 A, I ^b |
| 15.0 | 667 | 1,2 S ^b |

^a These assignments established by olefin spectra.

^b Here 1,2 A,S,I, means atactic, syndiotactic, and isotactic polybutadiene. Syndiotactic and isotactic bands taken from Natta's spectra.

^c Def. means deformation.

Discussion

With the preparation of very high *cis*-1,4 or *trans*-1,4 or 1,2 polybutadienes it is now recognized, as shown for example by Natta,¹ that the spectrum can change markedly depending upon the amounts of these various types of addition. However most of the bands listed in Table I appear in the spectra of emulsion polybutadienes and these are considered first.

The assignments of those bands marked by a superscript a are derived from olefin spectra (see Bellamy^{3a}; or Jones^{3b}) and have been confirmed for polybutadiene spectra by the preparation of high *cis*-1,4 high *trans*-1,4 or high 1,2-polybutadienes.

The other assignments given in Table I are based on work in connection with the determination of the microstructures of polybutadienes which is reported in another place.⁴ It is there shown, by isomerization experiments, that the 1355-cm.^{-1} ($7.38\ \mu$) band is due to *trans*-CH=CH, the 1311-cm.^{-1} ($7.63\ \mu$) band due to *cis*-CH=CH as is a band at 740-cm.^{-1} ($13.5\ \mu$). These experiments were done with high *cis*-1,4-polybutadienes and the assignments are supported by the spectra of the maleic anhydride adducts (Fig. 3), the hydrogenated polybutadiene spectra (Fig. 2) and also the

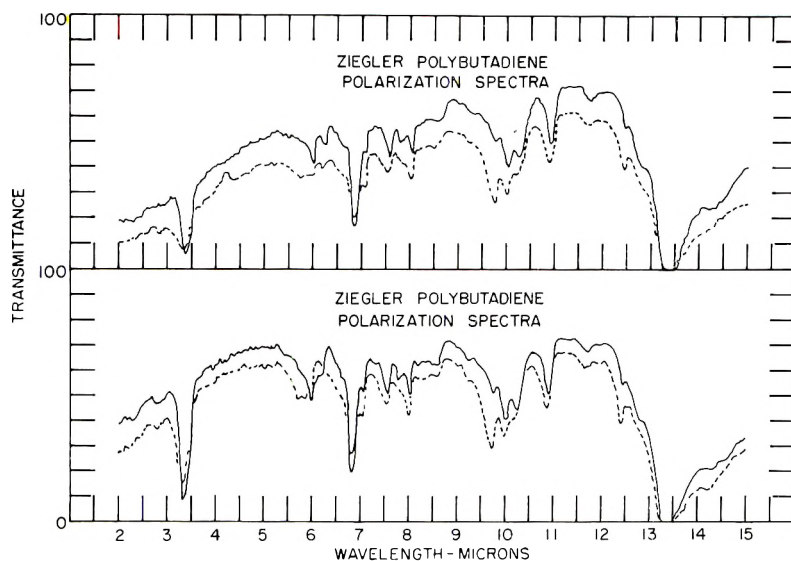


Fig. 1. Polarization spectra of high *cis*-1,4-polybutadienes at liquid nitrogen temperature. Solid curve polarization perpendicular to direction of stretch; dotted curve polarization parallel.

polarization spectra (Fig. 1). The spectrum of the hydrogenated emulsion polymer has bands at about 1370-cm.^{-1} ($7.3\ \mu$) and 1361-cm.^{-1} ($7.35\ \mu$) and 1316-cm.^{-1} ($7.6\ \mu$) also [in addition to the CH_3 band at 1375-cm.^{-1} ($7.25\ \mu$)] but these are similar to those found in polyethylene spectra and, as the spectrum shows, there is considerable polyethylene in this polymer. The 1355-cm.^{-1} ($7.38\ \mu$) and 1311-cm.^{-1} ($7.63\ \mu$) bands have disappeared in the spectra of the maleic anhydride adducts which is to be expected if the addition takes place at the double bond, as it does in Hevea.

It is somewhat surprising that the intensity of the 740-cm.^{-1} band has not changed more if this long-wave absorption is due only to *cis*-CH=CH. It is also to be noted that the long-wave bands have not disappeared in the spectrum of the maleic anhydride adduct of an emulsion polybutadiene and

that the *trans*-1,4 band at 967 cm.^{-1} is still strong. A band is found at about 1310 cm.^{-1} in the spectrum of a thick film of *trans* polybutadiene which apparently is not due to *cis*-CH=CH.

There are several features of the polarization spectrum of the high *cis*-1,4-polybutadiene (Fig. 1) which are of interest and perhaps of some significance. One of these is that, especially compared with the polarization spectrum of Hevea, none of the bands connected with the C=C group are

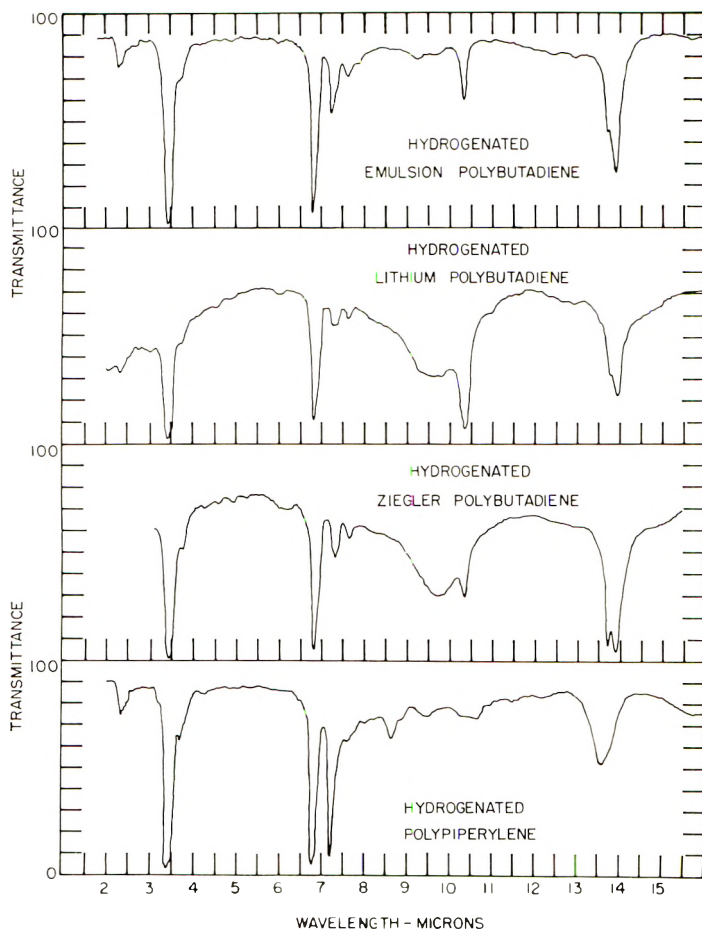


Fig. 2. Infrared spectra of hydrogenated polybutadienes.

strongly polarized. There is some polarization in the parallel direction, as would be expected, and some of the difference may be due to the smaller degree of crystallinity. It might be suspected that the parallel spectrum is only shifted downward (to lower transmission) from the perpendicular spectrum due to recording differences. However the 100% line for both spectra coincided within about 1% throughout the spectrum, except beyond $14\ \mu$ where the difference sometimes amounted to about 10%. Thus

the band intensities for the two spectra can be compared. As a matter of fact, if the differences were due simply to a recording shift in the spectra, the C=C band at $6\ \mu$ would be perpendicularly polarized. This is hardly to be expected.

Another point of interest in the polarization spectra is the shift in the positions of some bands. For example, in these polymers, the strong band is generally at $740\ \text{cm.}^{-1}$ ($13.5\ \mu$) but here it is evident that the maximum must be near $752\ \text{cm.}^{-1}$ ($13.3\ \mu$). Likewise the positions of the 1311 -, 967 -, and 910-cm.^{-1} bands have shifted toward shorter wavelengths, especially in the parallel polarized spectrum. Since other bands have not shifted from their usual positions these shifts are apparently real, not due to shifting of the chart paper. A similar shift in Hevea spectra is discussed by Sutherland and Jones² and attributed to crystallization. We do not know if this shift is due to the crystallization of the polymer, low temperature, or the presence of two components with different orientations in the band.

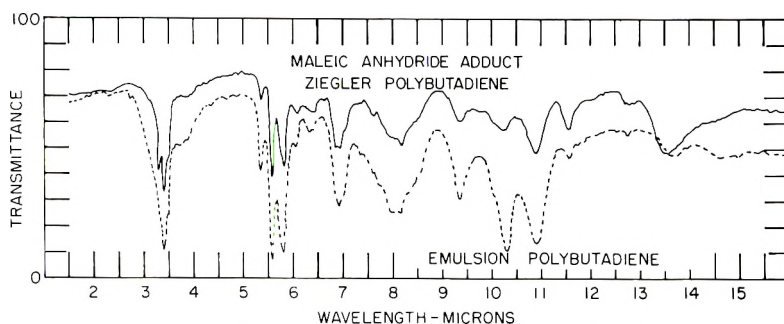


Fig. 3. Infrared spectra of maleic anhydride adducts of high *cis*-1,4-polybutadiene (solid curve) and emulsion polybutadiene (dotted curve).

The last possibility, in view of other work,⁴ is to be expected in the 13 – $15\text{-}\mu$ region. The shift in the *trans*-CH=CH band at $967\ \text{cm.}^{-1}$ may explain the fact that in spectra of emulsion polybutadienes the 967-cm.^{-1} band has a half-bandwidth of about $9\ \text{cm.}^{-1}$ (in our spectra) whereas in the high *trans* and isomerized polybutadienes the half-bandwidth appears to be about $12\ \text{cm.}^{-1}$. This, and other spectral evidence, raises the question as to whether there is more than one kind (with respect to environment) of *trans*-CH=CH groups in some polybutadienes.

A third point of interest in the polarization spectrum of the high *cis* polymer is the apparent intensity of the *trans*-CH=CH band at $967\ \text{cm.}^{-1}$. From the parallel polarized spectrum, which is similar to the ordinary room temperature spectrum, it might be concluded that the *trans*-CH=CH is a very weak band since it appears as a shoulder. However, as the perpendicularly polarized spectrum shows, the *trans*-CH=CH is not very weak; it appears as it ordinarily does because of adjacent bands which evidently are parallel polarized and which arise from *cis*-CH=CH.⁴ This is of impor-

tance in determining the amount of *trans*-1,4 addition in a polybutadiene, by a base line method.

If the spectra in Figure 4 are considered in the order, *trans*-1,4, 1,2, emulsion and *cis*-1,4 the spectrum of the *cis*-1,4 is surprising. By combining the *trans*-1,4 and the 1,2 in about a 70/20 ratio and knowing something about correlations for *cis*-CH=CH, most of the bands in the spectrum of the emulsion polybutadiene can be assigned or explained. Such is not the case

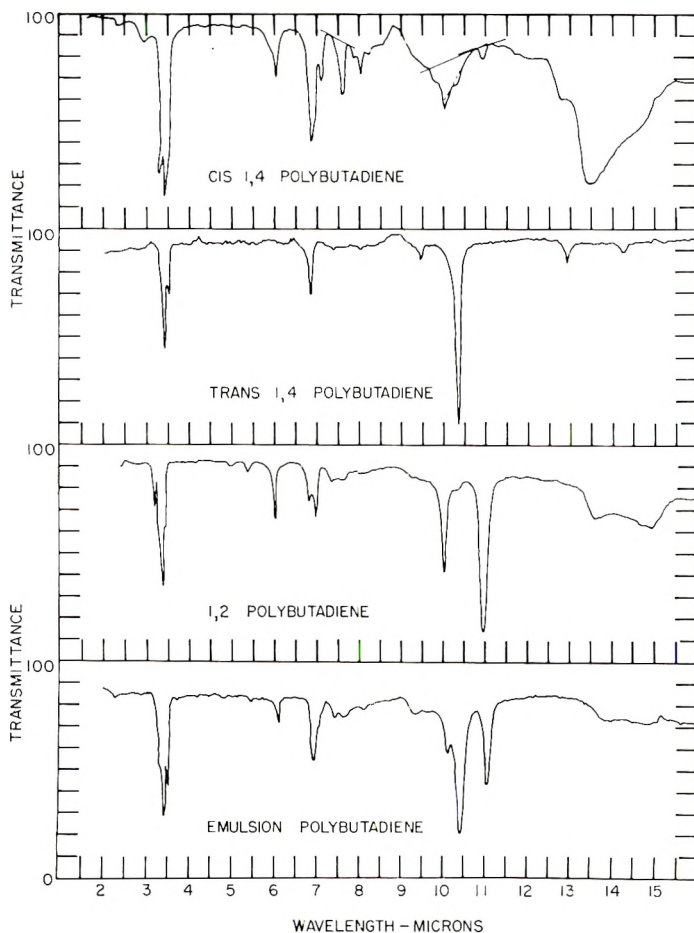


Fig. 4. Infrared spectra of various kinds of polybutadienes.

with the spectrum of the *cis*-1,4 polymer. While a band in the long-wave region, perhaps 740 cm^{-1} , due to *cis*-CH=CH is to be expected the large amount of absorption in this region and the bands near $12\text{ }\mu$ and $10\text{ }\mu$ are unexpected.

The origins of these additional bands in the spectrum of the *cis*-1,4-polybutadiene, in Figure 4, which is similar to many which have been published, are unknown. It seems unlikely that differences in symmetry

of *cis*-1,4- and *trans*-1,4-polybutadienes can account for all of the additional bands in the *cis*-1,4 spectrum, particularly in the long-wave region. They cannot be due to the crystallinity of the polymers since these spectra are either of amorphous (by x-ray) polymers or of solutions. *trans*-1,4-Polybutadiene does have crystallinity bands at 1053, 972, and 1250 cm^{-1} . A very likely possibility is that, during the polymerization with catalysts which cause large amounts of *cis*-1,4 addition, other substances or structures are formed. For example, the spectrum of a heptane-alcohol extract of these high *cis*-1,4-polybutadienes nearly always contains bands

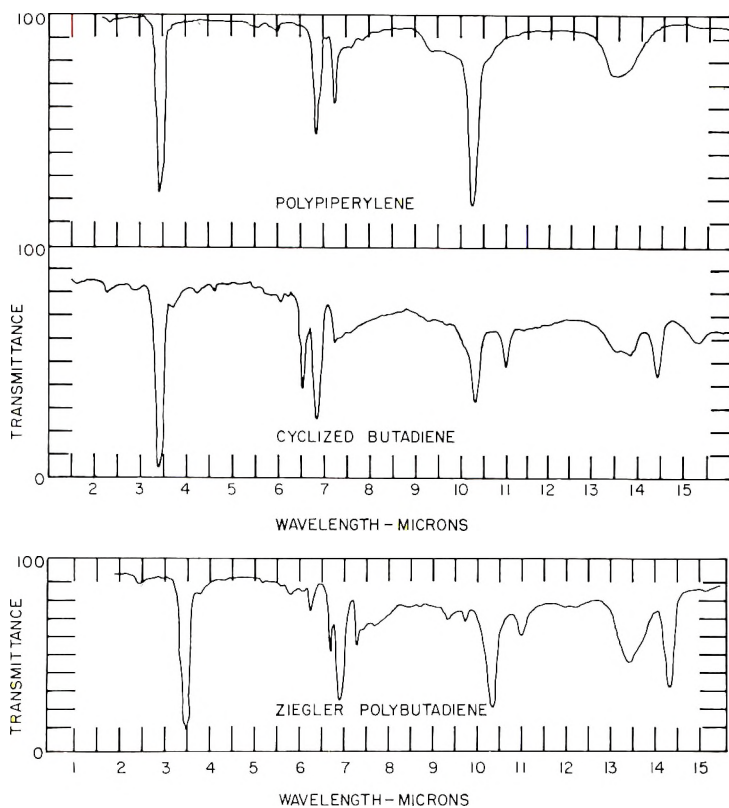


Fig. 5. Infrared spectra of polypiperylene and polymers of butadiene.

near 1500 and 1600 cm^{-1} , as well as in the long-wave region (12.5–15 μ), which are indicative of aromatic compounds. An example of such a spectrum is shown in Figure 5 although this is a spectrum of the whole polymer. This was a purified polymer and did not contain antioxidant. Even in some emulsion polymers a band is often found near 700 cm^{-1} which may be aromatic. Considering that some of the products formed during the preparation of the Ziegler-type catalyst are aluminum halides, the reactivity of butadiene with Friedel-Craft catalysts and the fact that benzene is used as a solvent, it would not be surprising, in view of published work,⁵

if other reactions occurred in these systems during the polymerization of butadiene besides regular 1,4 addition of the monomer. Figure 5 also shows the spectrum of a substance made from butadiene with aluminum triiodide which analyzes C_4H_6 and has an ICI unsaturation of 35%. This substance is much more soluble in carbon disulfide than even a low molecular weight polymer is, and the specific absorbances of the bands in this spectrum are much smaller than they are in the usual polymer spectrum. It is suspected that it is cyclized butadiene but we have no proof. Similar substances have also been made from dimethylbutadiene with other catalysts.

Another possibility for the appearance of extra bands in the spectra of these high *cis*-1,4-polybutadiene spectra is that they arise from the configuration of the *cis* polymer being different from that of the *trans*. Some support for this possibility is afforded by the differences in the spectra of isotactic and syndiotactic 1,2-polybutadienes which are not apparently due to crystallinity, as is discussed below.

A comparison of the spectrum of the 1,2-polybutadiene in Figure 4, which is atactic, with the spectra of the isotactic and syndiotactic polybutadienes given by Natta¹ shows many differences. The bands of interest here are given in Table II, although they are also listed in Table I. The wavelengths of the bands taken from Natta's spectra may be in error by as much as 0.04 μ .

TABLE II
1,2-Polybutadiene Bands (Wavelengths in microns)

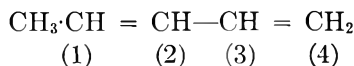
| Atactic | Isotactic | Syndiotactic |
|---------|-----------|--------------|
| 7.38 | 7.42 | 7.43 |
| 7.55 | 7.57 | 7.50 |
| 7.66 | 7.68 | 7.64 |
| 7.85 | 7.77 | 7.72 |
| 8.02 | | |
| 8.13 | 8.13 | 8.22 |
| | 8.37 | |
| | 8.60 | 8.80 |
| | 9.03 | |
| 9.25 | 9.38 | 9.34 |
| 9.52 | 9.53 | 9.57 |
| 10.28 | 10.35 | 10.25 |
| | 10.60 | |
| | 11.42 | |
| | 11.90 | 11.70 |
| 12.5 | 12.4 | 12.65 |
| 13.0 | | |
| 13.6 | 13.6 | 13.5 |
| | 14.1 | |
| | 14.4 | |
| 14.8 | 14.8 | 14.7 |
| | | 15.05 |

The point of interest here is that some of the bands in the isotactic and syndiotactic polymer spectra probably are the same group frequency but shifted because of differences in configuration as has been observed in the spectra of Hevea and balata. From Table II it is evident that there are many bands which are common to all three spectra and thus probably have the same origins. Although we do not have spectra of amorphous, isotactic and syndiotactic 1,2-polybutadienes it is suspected that one of the bands in the 8-9- μ region, perhaps 8.6 or 8.8 μ , is due to crystallinity. In the atactic polymer spectrum the bands at 8.02, 13.0, and 10.28 μ are probably due to some *trans*-CH=CH but the bands at 10.35 μ in the isotactic spectrum and at 10.25 μ in the syndiotactic spectrum are probably due to some other structure common to both. The shift may be due to differences in configuration (i.e., change of symmetry). The bands at 11.9 and 11.7 μ are another pair which probably arise from the same structure and are shifted due to differences in configuration. The same statement very likely applies to the two strong bands at 14.4 and 15.05 μ . In view of the above, the appearance of two strong bands at 13.6 and 14.8 μ in the atactic polymer spectrum would be expected since the atactic polymer can be considered to be a random mixture of isotactic and syndiotactic units. The 14.4- μ band shifts to 13.6 μ and the 15- μ band to 14.8 μ .

The presence of these two bands at these wavelengths in the 1,2 polymer spectrum is of importance in the determination of the microstructures of polybutadienes, especially if there is much 1,2 addition. The atactic polymer reported here had no *cis*-1,4 addition, based on the fact that all of the polymer in a solution could be accounted for with our *trans*-1,4 and 1,2 absorptivities and the absorbances of the resolved *trans*-CH=CH band at 10.28 μ and the 1,2 band at 10.98 μ . Thus the 13.6- μ band does arise from 1,2 addition structures. Consequently, if *cis*-1,4 addition is determined by measuring absorbances at 13.5-13.7 μ the 1,2 correction can become large. These spectra of 1,2-polybutadienes probably explain some of the differences, pointed out by Binder,⁶ in the long-wave spectra of polybutadienes made with sodium and potassium catalysts.

Summing up this discussion of the bands in various polybutadiene spectra it seems clear that all of them do not arise from the different structural units. The spectrum of the all *trans*-1,4-polybutadiene is the simplest followed by the atactic 1,2, the emulsion, the high *cis*-1,4 and finally the isotactic and syndiotactic 1,2-polybutadienes. It seems fairly certain that the long-wave (13-15 μ) spectra of emulsion polybutadienes probably contain more bands than are resolved in the spectra and since crystallinity is eliminated, these bands (omitting the side vinyl bands) probably arise from other structures which are not present in the *trans*-1,4 polymer. In the case of the high *cis*-1,4-polybutadienes it has been shown that there are many additional bands⁴ and, as has been pointed out, some of these very likely arise from other structures or substances. The case for the 1,2-polybutadienes (atactic, isotactic, and syndiotactic) is uncertain because we do not know how many of the extra bands are due to the various configurations or crystallinity.

The 1355-cm.⁻¹ (7.38 μ) band due to *trans*-CH=CH, and the 1311-cm.⁻¹ (7.63 μ) band, due to *cis*-CH=CH also appear in the spectrum of polypiperylene shown in Figure 5. This is to be expected since these structures are formed by 1,4 addition of piperylene. Perhaps the long-wave spectrum of polypiperylene is indicative of how the long-wave spectrum of a *cis*-polybutadiene should appear. Actually, near 13.5 μ , there are two bands which can be at least partially resolved. One of these is probably due to *cis*-CH=CH— and the other is due to *cis*-CH₃—CH=CH— which is formed by 3,4 addition



The spectra of Hevea and balata also have bands at 1325 cm.⁻¹ (7.55 μ), due to *trans*-C(CH₃) = CH and at 1315 (7.60 μ) due to *cis*-C(CH₃) = CH. The similarity of the bands in the polybutadiene and polyisoprene spectra is additional support for assigning these bands in polyisoprene spectra to a =CH vibration of the C(CH₃=CH) group.

As nearly as can be decided from the published spectra, the very interesting work of Golub and Shipman⁷ on the spectra of deuterated polybutadienes seems to confirm some of these assignments but raises questions about other conclusions regarding *cis*-1,4-polybutadienes. For example, the 1311-cm.⁻¹ (7.6 μ) band appears in the spectrum of the *cis*-polybutadiene-2-*d*₁, (—CH₂·CD = CH—CH₂) but not in that of the polybutadiene-2:3-*d*₂ (—CH·CD = CD·CH₂—) or the polybutadiene-*d*₆. The latter two do have bands near where the =C—D band should be however. It is the long-wave spectra that offer difficulties. The polymer was prepared in the same manner as the *cis*-polybutadiene used here however so that some of the possible explanations for the long-wave absorption may still apply. As their spectra show the 740-cm.⁻¹ band shifts to lower frequencies, as is to be expected, and the shift increases with increasing deuteration. It is only in the *d*₆-polybutadiene however that the broad absorption in the 740-cm.⁻¹ region is placed by a reasonably sharp band near 17 μ . We have no explanation for the changing shape of this absorption.

Conclusions

In polybutadiene spectra there are bands due to *cis*-CH=CH at 1311 and 740 cm.⁻¹ and to *trans*-CH=CH at 1355 cm.⁻¹ as well as at 967 cm.⁻¹.

It is shown that high *cis*-1,4 spectra contain bands that cannot be assigned to the expected structures and that they may be due to additional structures, in high *cis*-1,4-polybutadienes, or to changes in the configuration of the polymers or both.

The long-wave spectrum of atactic 1,2-polybutadiene appears to be a mixture of the bands found in the spectra of isotactic and syndiotactic polybutadienes but shifted to shorter wavelengths.

A theoretical study of the spectra of polybutadienes, particularly 1,2,

would be interesting to assess the correctness of some of the assignments made here.

Thanks are due Mr. H. C. Ransaw and Mr. G. E. Harris who made many of the measurements and recorded many of the spectra used here. The author is indebted to Mr. T. B. Talcott for making the maleic anhydride adducts and to Dr. A. Fono for the hydrogenated polybutadienes. The comments and suggestions of Drs. J. E. Field, E. J. Devlin, J. J. Shipman, W. C. Sears, and D. C. Smith regarding this work are greatly appreciated as well as is the interest of Dr. F. W. Stavely and Mr. E. T. Handley.

Addendum

Since this was written it has been found, due to a refinement of our IR4 absorptivity for the side vinyl band at 910 cm^{-1} , that the particular 1,2 polymer used here had 4-5% *cis* 1,4 addition. However other high 1,2 polybutadienes have been prepared which do not have any *cis* 1,4, by our measurements. In the spectra of these polymers the $13.7\text{-}\mu$ band is not as strong as shown here but there is a band at this wavelength.

References

1. Natta, G., Fifteenth Annual Technical Conference of the Society of Plastic Engineers, New York, Jan. 1959.
2. Binder, J. L., *J. Polymer Sci.*, **A1**, 37 (1963).
3. (a) Bellamy, L. J., *Infrared Spectra of Complex Molecules*, 2nd ed., Wiley, New York, 1958; (b) L. N. Jones and C. Sandorfly, *Technique of Organic Chemistry*, Vol. 19, *Inter-science*, New York-London, 1956, ch. IV.
4. Binder, J. L., to be published.
5. Russell, G. A., *J. Am. Chem. Soc.*, **81**, 4834 (1959); G. I. Fray and R. Robinson, *J. Am. Chem. Soc.*, **83**, 249 (1961).
6. Binder, J. L., *Anal. Chem.*, **26**, 1877 (1954).
7. Golub, M. A., and J. J. Shipman, *Spectrochim. Acta*, **16**, 1165 (1960).

Synopsis

Assignments are suggested for many bands in the spectra of various kinds of polybutadienes which either confirm those deduced from olefin spectra or are new. In particular the band at 1355 cm^{-1} ($7.38\text{ }\mu$) is probably due to *trans*-CH=CH, that at 1311 cm^{-1} ($7.63\text{ }\mu$) is due to *cis*-CH=CH as is a band at 740 cm^{-1} ($13.5\text{ }\mu$). These assignments are based on the study of polarization spectra, of the spectra of hydrogenated polybutadienes and maleic anhydride adducts of polybutadienes and on isomerization experiments of *cis*-1,4-polybutadienes: Evidence is offered which indicates that presently known high *cis*-1,4-polybutadienes are not simply butadiene polymerized by *cis*-1,4 addition and that probably other structures are present in the polymer. It is shown that the 1355- and 1311-cm^{-1} bands appear in the spectra of polypiperlylenes and polyisoprenes (shifted somewhat in the latter spectra) and consequently are due to a CH vibration of the *trans*- or *cis*-CH=CH group. Thus they are group frequencies.

Résumé

On suggère des attributions à plusieurs bandes d'absorption dans les spectres de différents polybutadiènes; elles confirment celles déduites de spectres d'oléfinés ou sont entièrement nouvelles. Eh particulier, la bande à 1355 cm^{-1} ($7.38\text{ }\mu$) est probablement due à un CH=CH-*trans*, celle à 1311 cm^{-1} ($7.63\text{ }\mu$) au CH=CH-*cis*, comme celle à 740 cm^{-1} ($13.5\text{ }\mu$). Ces attributions sont basées sur l'étude de spectres de polarisation, de spectres de polybutadiènes hydrogénés et de produits d'addition de polybutadiènes à

l'anhydride maléique, et d'expériences d'isomérisation de *cis* 1,4-polybutadiènes. Il est prouvé que des polybutadiènes-1,4 à haute teneur en isomère-*cis*, ne sont pas simplement du butadiène polymérisé par addition 1,4-*cis*, mais que d'autres structures sont probablement présentes dans ce polymère. Les bandes à 1355 et 1311 cm^{-1} apparaissent également dans les spectres de polypipérylène et de polyisoprènes (légèrement déplacées dans ce dernier cas) et sont dues par conséquent à une vibration CH du groupe $\text{CH}=\text{CH}$ —*cis* ou *trans*. Elles sont donc des fréquences de groupe.

Zusammenfassung

Es werden Zuordnungen für viele Banden in den Spektren verschiedener Arten von Polybutadien angegeben, die entweder die von Olefinspektren abgeleiteten bestätigen oder neu sind. Im einzelnen wird die Bande bei 1355 cm^{-1} (7,38 μ) wahrscheinlich durch die *trans* $\text{CH}=\text{CH}$ —Gruppe verursacht, die bei 1311 cm^{-1} (7,63 μ) und eine Bande bei 740 cm^{-1} (13,5 μ) durch die *cis* $\text{CH}=\text{CH}$ —Gruppe. Diese Zuordnung beruht auf einer Untersuchung der Polarisationspektren, der Spektren von hydriertem Polybutadien und Maleinsäureanhydridaddukten von Polybutadien und auf Isomerisationsversuchen an *cis*-1,4-Polybutadien. Es spricht vieles dafür, dass die gegenwärtig bekannten 1,4-Polybutadiene mit hohem *cis*-Gehalt nicht einfach durch *cis*-1,4-Additionpolymerisierte Butadiene sind und dass wahrscheinlich andere Strukturen im Polymeren vorkommen. Es wird gezeigt, dass die 1355 cm^{-1} und 1311 cm^{-1} Bande in den Spektren von Polypiperylen und Polyisopren (im letzteren etwas verschoben) auftreten und daher durch eine CH—Schwingung der *trans*- oder *cis* $\text{CH}=\text{CH}$ —Gruppe verursacht werden. Daher sind sie Gruppenfrequenzen.

Received September 23, 1961

Kinetics of Crystallization and a Crystal-Crystal Transition in Poly-1-Butene

J. BOOR, JR. and J. C. MITCHELL, *Shell Development Company, Emeryville, California*

INTRODUCTION

In their comprehensive studies of crystalline properties of polyolefins using x-ray, infrared, and density methods, Natta and his co-workers¹⁻⁷ have established that poly-1-butene exhibits dimorphism.* On crystallizing from the melt or from solution this polymer first assumes a crystalline structure which is unstable and gradually transforms into a second form. They have chosen to call the first form "modification 2" and the second "modification 1." We will use this notation in the present paper.

Modification 2 is characterized by a helical chain structure of four-fold symmetry with an identity period of 6.8 Å. A similar helix is a stable chain conformation in 1-olefin polymers whose pendant groups are bulkier than the ethyl groups of poly-1-butene, e.g., 3-methyl-1-butene. Modification 1, in contrast, is characterized by a helical chain structure of three-fold symmetry with an identity period of 6.5 Å, similar to that found in polypropylene, where the pendant groups are smaller. Natta and co-workers⁴ have demonstrated the relation between helical conformation and side chain bulk by showing that the four-fold helix is stable in poly-1-butene which has been chlorinated to enlarge the side chain.

The kinetics of the transformation of modification 2 into modification 1 have not yet been discussed in detail. Natta and his co-workers have indicated that the transformation is slow but can be greatly accelerated by application of stretching or high pressures. In particular, it has been stated that the transformation is essentially complete after a few seconds at 100 atm.⁶

While early references gave melting points in the range of 120-128°C.,^{2,9,10} a value of 136°C. was later reported.¹¹ Although Natta has stated that it is impossible to measure the melting point of modification 2 because it transforms into modification 1 before melting,¹ the data of the

* After the preparation of this manuscript a publication entitled "Cristallinita e polimorfismo del poli-alfa-butene" by R. Zannetti, P. Manaresi, and G. C. Buzzoni has appeared [*Chim. e ind. (Milan)*, **43**, 735 (1961)]. The relationship of this work with ours is not known at this time.

L. M. Welch and his co-workers have also discussed the dimorphism of poly-1-butene at a local American Chemical Society meeting, but the details of this work have not yet appeared in the literature.⁸

present paper would lead one to suspect that the earlier reported melting points probably pertain to modification 2 while the latter one refers to modification 1.

In this paper, we shall discuss in some detail the phase relationships in this polymer and the kinetics of the transformations melt to modification 2 and modification 2 to modification 1. Also, we shall note briefly the changes in some physical properties accompanying the latter transformation.

EXPERIMENTAL

Materials

The poly-1-butene samples used in these investigations had intrinsic viscosities (measured in decalin at 150°C.) of 2.5–3.0 dl./g. They attained densities of at least 0.91 g./ml. if the film specimens were maintained at least 150 hr. at 25°C. after molding. For the values 1.058 and 1.154 ml./g. for the specific volumes of pure crystalline and amorphous poly-1-butene, respectively, additivity of the specific volumes of the two phases being assumed, the density 0.91 g./ml. corresponds to a crystallinity of 57%. This value is close to that (60%) reported by Natta, Corradini, and Bassi for samples they used in x-ray investigations.⁶

The polymer was stabilized against oxidation immediately after isolation from the reaction mixture.

Differential Thermal Analysis

Differential thermograms were obtained by the usual techniques of differential thermal analysis using an apparatus constructed by Dr. F. E. Weir of this laboratory. It consisted of an aluminum block in which both the polymer and the reference material could be heated at any specific rate. Thermocouple readings were calibrated at 0 and 150°C. In the region of the phase transitions, the heating rate was 6°C./min. and the cooling rate was 2°C./min.

Spectroscopy

A Beckman IR4 infrared recording spectrophotometer was used for the infrared investigations. The scanning speed control was set at 0.5, corresponding to a rate of 0.75 μ /min. The absorptions of various bands were studied both as a function of temperature and as a function of time at constant temperature. To obtain the time dependence at room temperature, films were compression-molded (170°C., 20,000 psi), cooled rapidly in air, and scanned repeatedly commencing 25 min. after attainment of room temperature. Where changes in absorption of various bands were desired as a function of temperature, the molded film was inserted between two sodium chloride plates which were then placed in an insulated box in which their temperatures were controlled to $\pm 1-2^\circ\text{C}$. in the region 30–200°C. A thermocouple placed next to the plates was used to record the film temperature. In the region of appearance and disappearance of the charac-

teristic bands the heating and cooling rates were approximately 1–2°C./min. The absorptions at 10.81 and 11.03 μ were corrected by subtracting background intensities determined in the following way. A linear baseline was constructed tangent to the transmission maxima near 10.5 and 11.5 μ . The intersections with this baseline of lines drawn vertically from the absorption maxima were taken as the background intensities at the absorption maxima.

Dilatometry

Measurements of volume changes as a function of temperature and as a function of time at constant temperature were carried out in J-shaped glass dilatometers. The bulbs were attached to the capillary tubing by spherical ground glass joints held together by the appropriate clamps. This construction allowed easy insertion of the samples without the necessity of glassblowing operations. In the early work instruments with a bulb of 15 mm. i.d., a length of 70 mm., and a capillary i.d. of 1.61 mm. were used. These bulbs, partially filled with a glass plug, had a volume of about 9 ml. and called for a sample of about 2.5 g. The extremely rapid rate of the crystallization from the melt required the use of smaller dilatometers to reduce the thermal equilibration time. The smaller instruments were used in all of the kinetics experiments performed below 100°C. These had bulb dimensions of 5 mm. i.d. \times 45 mm. length (about 1 ml. volume) and a capillary of 0.61 mm. i.d. The sample weights used in these small dilatometers were generally of the order of 0.4 g.

The samples were introduced in the form of small chips cut from a molded sheet. The dilatometers were evacuated to about 1 μ Hg pressure and filled with mercury. Prior to the kinetic determinations the loaded dilatometers were given a preheating treatment to minimize the effects of previous thermal and mechanical history. After 15 min. at 170°C. the dilatometers were cooled in the course of another 15 min. to 140°C. and then rapidly transferred to the experimental bath. The precooling to 140°C. was an additional measure to reduce the thermal equilibration period.

Temperature control of better than $\pm 0.01^\circ\text{C}$. was provided over the range of -20 to 80°C . by an Industrial Calibration Bath Model 1082c (Hallikainen Instruments, Berkeley, Calif.) loaded with an ethylene glycol–water mixture. For higher temperature studies a small silicone oil bath controlled by a Thermotrol proportional controller (Hallikainen Instruments, Berkeley, Calif.) provided temperatures constant to $\pm 0.005^\circ\text{C}$.

Optical Melting Points

Optical melting points were taken as the temperatures of disappearance of the last trace of birefringence (associated with the melting of the last crystalline regions) as the sample was heated on a Koefer hot stage (A. H. Thomas, Philadelphia, Pa.) on a polarizing microscope. The thermal history of each specimen prior to the heating is given in the text of the paper. These measurements were supervised by Dr. J. H. Badley of this laboratory.

Densities

Densities at 25°C. were determined for us by E. E. Seibert of these laboratories using the density-gradient technique, ASTM Designation D1505, with minor modification. Ethanol and water were used to construct the density gradient column. Density as a function of column height was established using a set of short cylindrical glass floats with densities in the range 0.86 to 0.93 g./ml. in increments of about 0.01 g./ml. The polymer to be tested was compression-molded into a thin film (170°C., 20,000 psi for 1 min. after first preheating the polymer at 170°C. for 3 min. under atmospheric pressure). Repeatability within 0.001 g./ml. was shown for several specimens examined in a common gradient.

Torsional Damping

An apparatus which will be described in detail elsewhere¹² was used to determine damping values in the temperature range -47 to 40°C. The damping was characterized by the loss tangent, which was calculated from the relation $\tan \delta = (1/n\pi) \ln (t_n/t_0)$, where t_n and t_0 are the times required in the initial and n th oscillations, respectively, for rotation through a fixed small angle about the rest orientation.

Torsion Modulus

Torsion modulus values were determined by known techniques which have been recently reviewed.¹³ An adaptation of the apparatus for these laboratories was made by Drs. P. F. Russel and F. E. Weir.

Offset Yield Points

The stress-strain diagram of poly-1-butene shows no abrupt yield point but only a region of smooth, gradual curvature toward the strain axis. The evaluation of materials showing such behavior requires a method such as that described in ASTM D638-58T. According to this method the offset yield point is the stress at which the stress-strain curve departs from linearity by a specified strain (the offset). We have chosen an offset of 5% elongation for these experiments. Test bars were compression-molded at 170°C. and 1500 psi from previously milled polymer in an electrically heated press. The compression molding procedure consisted of: (a) preheating of the polymer for 5 min. at the above temperature, (b) pressure application for 3 min., and (c) cooling 5 min. under pressure to 100°C.

After removal from the press the specimens were maintained at room temperature for varying times before performing the stress-strain measurements with an Instron tensile tester. The test bars were extended at a crosshead rate of 0.2 in./min.

RESULTS AND DISCUSSION

A. General Studies of Phase Relations

Various experimental methods used in these laboratories have confirmed Natta's findings that poly-1-butene exists in two crystalline modifications.

X-ray diffraction diagrams taken by A. E. Smith of these laboratories have shown that the crystalline modifications that we will describe are those previously reported by Natta and his co-workers.⁶

Differential thermograms shown in Figure 1 reveal two distinct phase changes. Curve *I* shows the thermogram of a sample which has been heated within 10 min. to 2 hr. after it underwent crystallization from the melt (Curve *IV*). Only one peak (at 113°C.) which we associate with the melting of modification 2 is obtained under these conditions. Because of

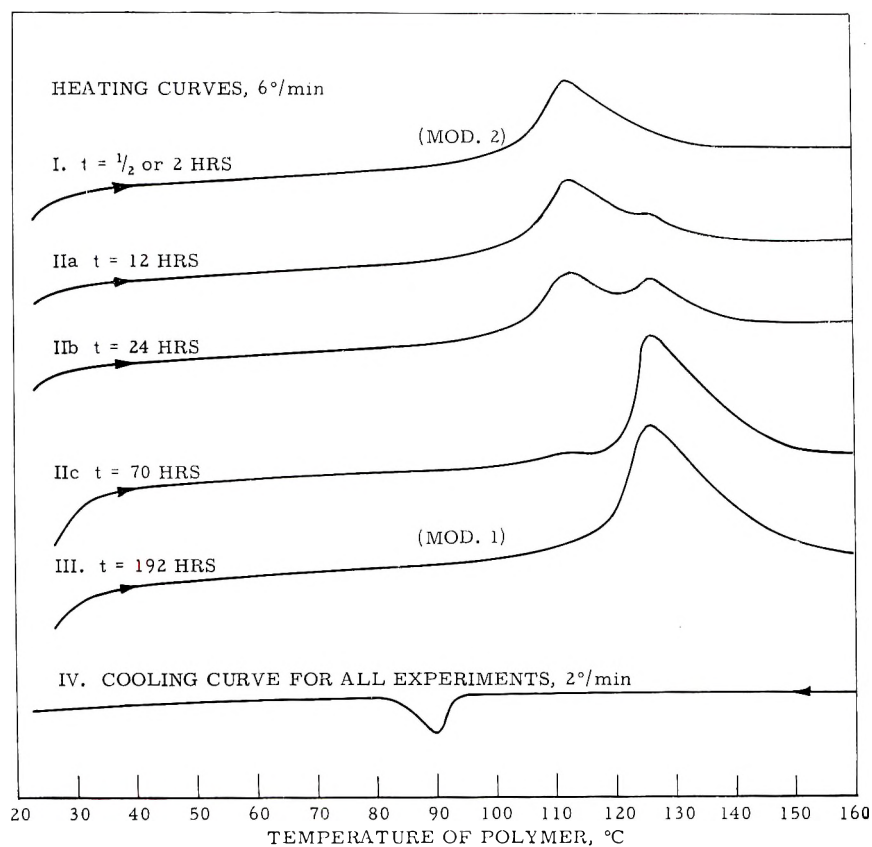


Fig. 1. Differential thermograms taken at various times t after melt was cooled to room temperature.

the nature of the differential thermal analysis method such peak maxima are not numerically identified with melting points such as would be obtained from dilatometric or optical methods. The latter methods measure the final disappearance of crystallinity. In contrast, the differential thermogram peaks are associated with a state of balance between the absorption of heat by the fusion of the crystalline regions and the transfer of heat in the apparatus. The temperatures at which these peaks occur, however, can be used to identify qualitatively the regions of phase transitions. Curves *IIa*, *IIb*, and *IIc* show two peaks in the case of a sample which has been allowed

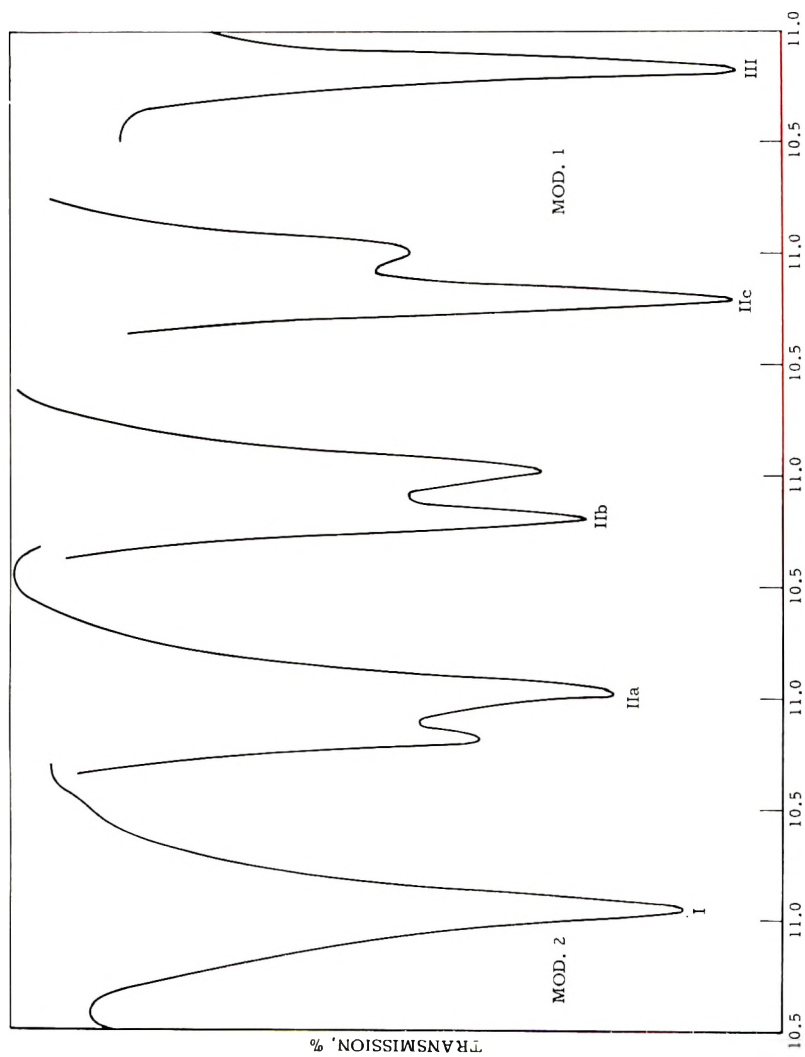


Fig. 2. Infrared spectra showing modifications 1 and 2.

to stand at room temperature for 12, 24, and 72 hr., respectively after cooling from a melt. As in Curve *I*, the first peak occurs at 113°C. (modification 2), and the second peak, occurring at about 124°C., is presumed to be associated with modification 1. The increase in area under the peak corresponding to modification 1 with a simultaneous decrease in area under the peak corresponding to modification 2 suggests that these areas are proportional to the content of each modification in the sample, but the proportionality constant is not known. Curve *III* shows only one peak in the case of a sample which has been allowed to stand at room temperature for 192 hr. after cooling from the melt. This peak corresponds to the stable modification 1. Curve *IV* represents the only type of a cooling thermogram which we have been able to observe in these experiments; it represents a single crystallization process involving only the formation of modification 2 as is evident from Curves *I* through *IV*.

Similar phenomena are seen in the spectroscopic investigations (Fig. 2). Natta and co-workers⁷ have already shown the infrared spectra of poly-1-butene corresponding to the two modifications. From these spectra it can be seen that the bands at 10.81, 11.73, and 12.25 μ are associated with modification 1 and the 11.03 μ band is associated with modification 2. We find that upon cooling a melt (at 2°C./min.) the 11.03 μ band appears quickly at a temperature of about 95°C. (Curve *I*, Fig. 2). If, after the sample was held at 95°C. for about 20 min. to allow the near complete formation of modification 2, it was again heated at a rate of 2°C./min., the 11.03 μ band disappeared at about 126°C. On the other hand, if the sample was cooled to and held at room temperature, a gradual transformation to the stable modification 1 occurred. Figure 2 shows the partial and complete transformation of modification 2 into modification 1 (Curves *Ia*, *Ib*, *Ic*, and *III*, Fig. 2). If the sample was allowed to stand at room temperature for over a week such that only the stable modification 1 was observed, the 11.03 μ band being absent, heating resulted in the disappearance of the 10.81 μ band at about 136°C. During this heating process the 11.03 μ band did not appear, indicating that modification 1 does not revert back to modification 2 before melting.

Dilatometric curves reflecting changes in specific volume of a poly-1-butene sample on heating and cooling are shown in Figure 3. Following heating to 160°C., the sample was cooled at approximately 2°C./min. (In this experiment the sample was in the form of pellets compressed from powder. The curve obtained during the initial heating of these pellets showed an anomalous large contraction presumed to be due to the collapse of a spongy structure as the onset of melting softened the polymer. It is assumed that the pellets had an open cell structure which allowed the escape of air when the dilatometer was evacuated but from which the mercury, subsequently added, was excluded by capillary depression.) The cooling curve (Curve *IV*, Fig. 3) shows the contraction accompanying the crystallization of the supercooled melt to form modification 2. The contraction started at about 95°C. and was complete at about 80°C. Curve *I*, obtained on heating the sample within a few minutes after the cooling experi-

ments, shows the expansion accompanying the melting of the modification 2 crystallinity which was just formed upon cooling. At a heating rate of 1°C./min. , the curve intersects Curve *IV* in the melt region at 125°C. This temperature can therefore be taken as the melting point of modification 2 under these heating conditions. This value is in agreement with the melting point obtained for modification 2 in the infrared investigation,

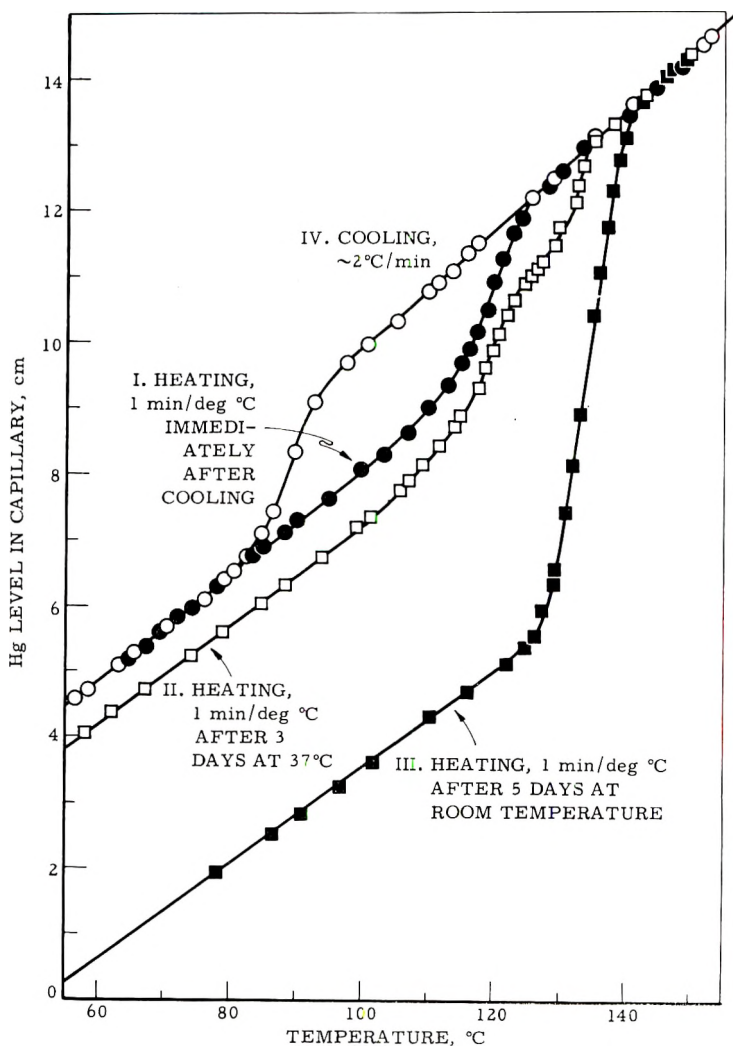


Fig. 3. Dilatometric heating and cooling curves.

i.e., 126°C. On cooling again, a curve *IV* was obtained. The sample was allowed to stand 3 days at 37°C. and was heated again at $1^{\circ}\text{C./per min.}$ The curve thus obtained (curve *II*), commencing at a lower specific volume, shows a break at 125°C. corresponding to the completion of melting of modification 2, but then continues to rise and meets the amorphous level only at 135°C. This is taken to indicate that some modification 1 had

formed during the 3 days at 37°C. Curve *III*, which shows only melting of modification 1 (at 140°C.) was obtained on heating the sample at 1°C./min. after allowing it to stand for 5 days at room temperature. (This is in agreement with the 136°C. melting point obtained spectroscopically, i.e., the temperature at which the infrared 10.81 μ band disappeared.) That no break can be seen at 125°C. indicates that modification 1 was formed during the 5-day interval at the expense of modification 2. Also the curves show that the formation of modification 1 is accompanied by a much greater contraction than takes place during the formation of modification 2. Torsional damping experiments to be described in a subsequent section show that there is only a small change in the fraction of amorphous material in the sample during the transformation of modification 2 to modification 1. The large contraction observed is due therefore to large differences in the density of the two crystalline forms. As in the infrared investigations, we were not able to observe the transformation of modification 1 to modification 2 in these dilatometric measurements.

Optically determined melting points are in good agreement with those determined in the infrared and dilatometric investigations (Table I).

TABLE I
Effect of Temperature on Optical Melting Points^a

| Temperature <i>T</i> , °C. | Melting point, °C. |
|-------------------------------|-----------------------|
| 100 | 122 |
| 90 | 120 |
| 80 | 118 |
| 70 | 118 |
| 60 | 117 |
| 25 | 134 |
| 25 | 136 |
| 0 | 135 |
| -20 | 136 |

^a Conditions: melt polymer at 160°C., then maintain at *T* for 48 hr. before observing melting points.

If poly-1-butene samples were melted (at 160°C.) and maintained for 48 hr. at various temperatures in the range -20 to 100°C. and subsequently heated, melting points in two distinct ranges were observed. Those samples kept at 60°C. or above had melting points in the 117-122°C. range, while samples kept at -20 to 25°C. had melting points of 134-136°C. We associate the lower temperatures with the melting of modification 2 and the higher temperatures with the melting of modification 1.* Since only a small amount of the more stable modification would be necessary to measure a higher melting point, we surmise that at high temperatures no substantial amount of modification 1 was formed. The gradual lowering of melting point of modification 2 in going from 100 to 60°C. is typical of

* We have found optical melting points of 140-142°C. for some of our more crystalline poly-1-butene preparations.

polymeric systems. It arises from lowering of perfection of crystalline structures as crystallization temperatures are lowered.

The fact that we have not been able to observe the transformation of modification 1 to modification 2, coupled with our finding of a higher melting point for modification 1 than for modification 2, is evidence that this is a monotropic as opposed to an enantiotropic type of dimorphism, i.e., that modification 2 is unstable with respect to modification 1 at all

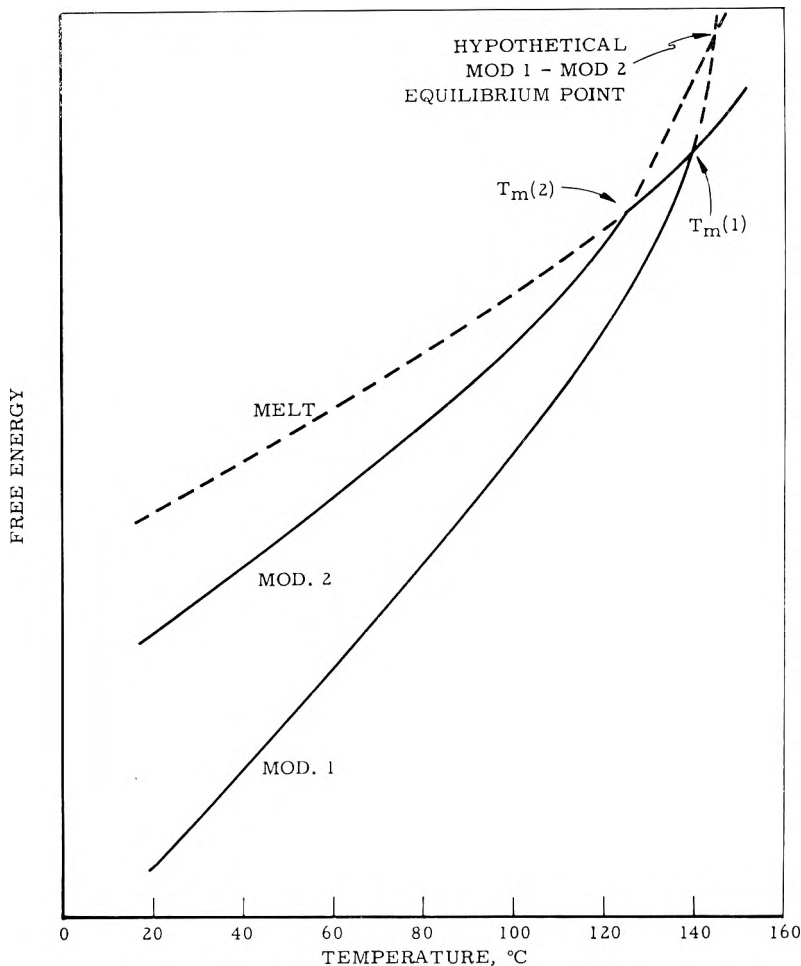


Fig. 4. Assumed free energy diagram for poly-1-butene.

accessible temperatures.¹⁴ Such a situation arises when the equilibration between the two crystalline modifications would take place above the melting point of either form. A free energy relationship which could lead to the observed behavior is illustrated in Figure 4. Hypothetical curves have been drawn for the free energy of the three possible phases as functions of temperature. Their intersections are based on transition points (equilibrium temperatures between the phases being represented by the inter-

secting curves). The lower curve represents, of course, the most stable phase at a given temperature. It is thus seen that the modification 1 must be the most stable form from 25°C. (and lower as is indicated by the kinetic data given below) up to at least 140°C.

B. Isothermal Studies of the Individual Phase Transitions

1. Crystallization of Modification 2 from the Melt

We have observed qualitatively the rapid formation of modification 2 from the melt at about 95°C. in several ways: (a) the appearance of spherulites, (b) the formation of a crystallization peak in a differential thermogram (see Fig. 1, Curve IV), (c) the complete formation of the infrared 11.03 μ band within 12 min., and (d) the dilatometrically measured volume contraction. We have chosen the dilatometric technique for an investigation of the kinetics of crystallization from the melt of the unstable modification 2 at a series of temperatures.

In Figure 5 we have plotted the quotient $(h_{\infty} - h_t)/(h_{\infty} - h_0)$, which is numerically equal to $(V_{\infty} - V_t)/(V_{\infty} - V_0)$, against time on a logarithmic scale. This quotient can be looked upon as the fraction of the transformation remaining to be completed; the h are dilatometer capillary levels, the V are specific volumes and the subscripts ∞ and 0 refer to final and initial levels, respectively, of the variables in each experiment. h_t and V_t are the current values of these variables. h_0 values were obtained from the initial flat portions of the curves if these were sufficiently well defined. Otherwise h_0 was estimated by an extrapolation of the amorphous part of the volume-temperature curve in the dilatometer being used or by adding an assumed contraction value $(h_{\infty} - h_0)$ to the final level, h_{∞} . h_{∞} values were estimated as the asymptotes of the final portions of the experimental curves.

The curves at 62, 90, and 95°C. were determined in the small dilatometers (see Experimental) to reduce the time for thermal equilibration.

The solid curves drawn in Figure 5 represent the Avrami equation:^{15,16}

$$(V_{\infty} - V_t)/(V_{\infty} - V_0) = e^{-kt^n}$$

with n equal to 4, the value which would hold for an idealized crystallization where nuclei appear at a constant rate throughout the process and the crystalline centers thus formed grow at equal rates in three dimensions. The dotted curves follow the experimental deviations from the Avrami equation. The initial deviations can generally be blamed on incomplete thermal equilibration of the dilatometer and contents with the bath. Deviations of the type shown after 50% of the process has been completed are commonly observed in polymer crystallization. These are usually attributed to steric hindrances or entanglements which are slow to relax out and which increase in number as the growing crystalline centers impinge upon one another toward the end of the transformation. The curve obtained at 110°C. may be in poor agreement with the $n = 4$ Avrami isotherm, but the data are inadequate to define the shape of the curve with sufficient precision.

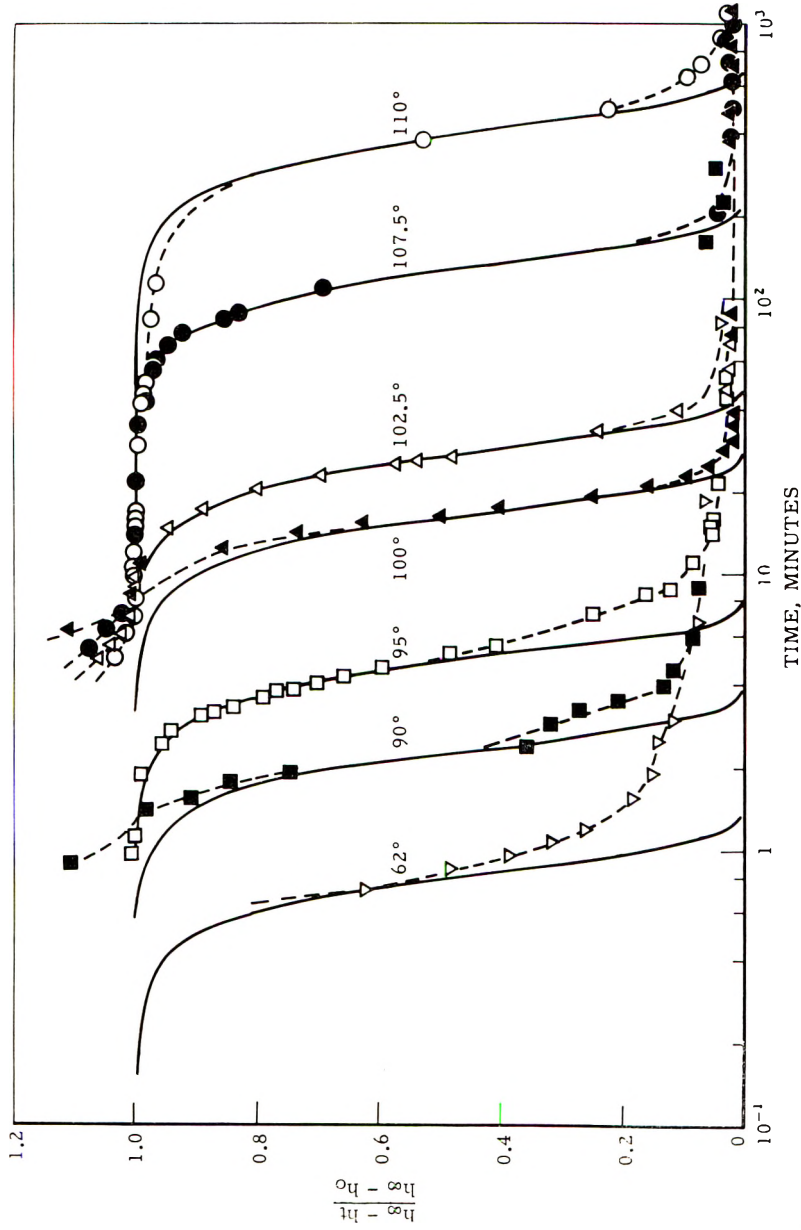


Fig. 5. Dilatometric curves showing the formation of modification 2 from the melt at various temperatures. The ordinate represents the fraction of the transformation remaining to be completed.

TABLE II
Crystallization of Modification 2 From the Melt

| Temperature, °C. | Halftime, min. | Contraction, ml./100 g. |
|-------------------|----------------|-------------------------|
| 110.0 | 380 | 2.48 |
| 107.5 | 132 | 2.22 |
| 102.5 | 26 | 1.85 |
| 100.0 | 15.9 | 1.71 |
| 95.0 ^a | 5.0 | 2.48 |
| 90.0 ^a | 2.2 | (2.48 assumed) |
| 62.0 ^a | <0.8 | (2.48 assumed) |

^a Small dilatometers used here

Times for completion of half of the transformation (halftimes) and extents of contraction observed in these experiments are presented in Table II.

In Figure 6 the halftimes are plotted logarithmically against temperature. The crystallization rate shows the high negative temperature coefficient typical for polymers at temperatures not too far below their melting points.

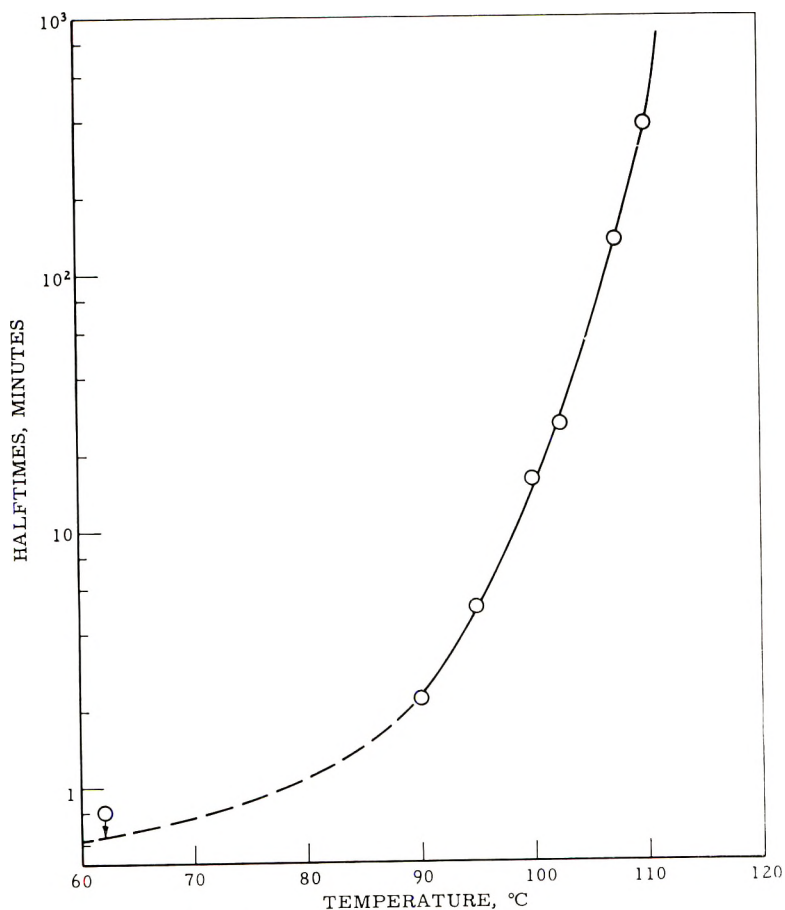


Fig. 6. Modification 2 crystallization halftimes vs. temperature.

It should be noted that the crystallization process becomes extremely rapid below 100°C.

Extent of Crystallization. Examination of Table II shows that the extent of contraction and hence the extent of crystallization has not been constant in these experiments. The cause of this fluctuation is not clear. The first four entries in the table seem to form a series showing decreasing contraction with decreasing temperature. This series, however, is broken by the finding at 95°C. The series does not indicate a gradual deterioration of the particular sample used as the experiments were performed in the

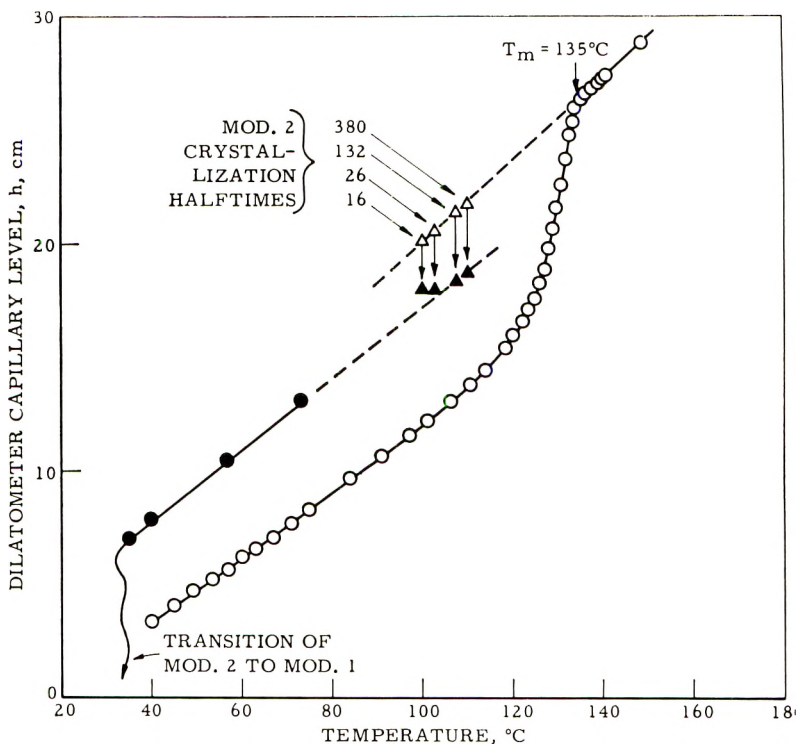


Fig. 7. Relationship of crystallization kinetics endpoints to heating and cooling curves: (●) cooling, 3 min./°C.; (○) heating following transition of modification 2 to modification 1, 1 min./°C.; (Δ) modification 2 crystallization h_c ; (\blacktriangle) modification 2 crystallization h_m .

order 110, 100, 102.5, 107.5°C. Furthermore, a repeat of the 100°C. experiment after completion of the series yielded data coinciding exactly with that of the previous 100°C. experiment. The apparent low extents of contraction observed at 100°C. and 102–105°C. may be associated with the relatively high ratio of thermal equilibration time in the large dilatometer to the low crystallization time at these temperatures.

Danusso, Moraglio, and Natta¹¹ have given the specific volume of amorphous poly-1-butene as 1.154 (density 0.866) at 30°C. and report a linear expansion behavior with slope ($\partial V/\partial t$) 9.0×10^{-4} ml./g. deg. Using these

values it can be calculated that a contraction of 2.50 ml./100 g. at 105°C. corresponds to 2.04% contraction.

In Figure 7 the initial and final volume levels recorded in the isothermal kinetics experiments are plotted along with the curves obtained on cooling the dilatometer from melt temperatures to near room temperature, allowing the transformation of modification 2 to modification 1 to take place, then heating to melt the modification 1 crystallinity thus formed. It can be seen that with the initial kinetics points on the extrapolation of the melt portion of the curve, the final levels come close to an extension of the portion of the cooling curve taken after modification 2 crystallization had occurred.

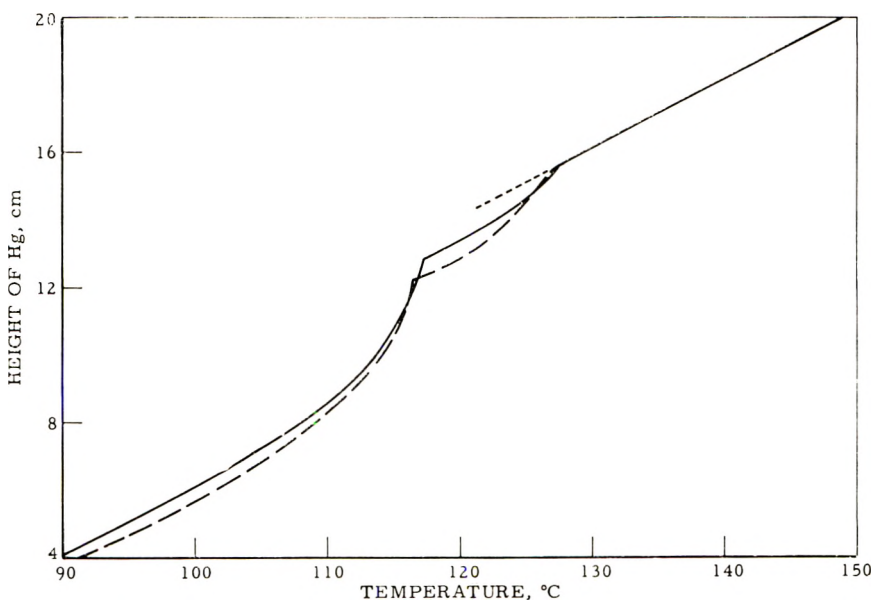


Fig. 8. Dilatometric heating curves following isothermal contractions of quenched samples: (—) expt. A; (---) expt. B (see Table III).

Attempts to "Bypass" the Modification 2 Crystallization by Quenching.

With sufficiently rapid cooling it should be possible to obtain amorphous poly-1-butene at room temperature or lower. By quickly heating such an amorphous sample to some relatively low crystallization temperature it would be possible to study the modification 2 crystallization in the region where viscosity effects would lead to slow rates. Furthermore, it would be of interest to see if modification 1 could be obtained directly from the amorphous polymer without passing through modification 2. Our present attempts to accomplish such a quenching were unsuccessful, but they revealed some interesting aspects of both the modification 2 crystallization and the transition of modification 2 to modification 1.

A 0.4-g. specimen in the small size dilatometer was cooled suddenly by rapid transfer from a bath at 140°C. to baths at -20 or -30°C. The drop of the mercury column in the capillary was essentially complete within

about 10 sec., showing that the low temperature region was rapidly attained. After 2 or 3 min. at low temperature the dilatometer was placed in the crystallization bath at intermediate temperatures. Slow contractions were observed, too slow to permit continuing the experiment to the conclusion of contraction. The constant temperature experiments were terminated by heating at 1°C./min. to determine by the melting behavior which type of crystallinity had been developed. The results so obtained are shown in Table III and Figure 8.

TABLE III
Crystallization Behavior of Rapidly Cooled Poly-1-butene

| Expt. | Crystallization kinetics | | | | Melting behavior on heating at 1°C./min. | | | |
|-------|--------------------------|--------------------------|--|--------------|---|--|--------------------------|--|
| | Quench temp., °C. | Crystn. temp., °C. | Contraction observed at crystn. temp., ml./100 g. | | First T_m , °C. | Ex- pan- sion, ml./ 100 g. | Second T_m , °C. | Ex- pan- sion, ml./ 100 g. |
| | | | 1300 min. | 4000 min. | | | | |
| A | -20 | +62 | 1.15 | — | 117 | 2.2 | 127 | 0.9 |
| B | -30 | +85.5 | 0.48 | 0.71 | 117 | 2.3 | 127 | 0.4 |

The expansions on melting take place over a range of temperature. The numerical estimation of the extent of expansion requires rather arbitrary extrapolation of the melting curves. Values so obtained are relatively crude and must be used only qualitatively.

The melting behavior shows the presence of both crystalline modifications. The somewhat low melting point observed here for modification 2 would be expected because the low crystallization temperatures should lead to imperfect ordering. The low melting point found for the small amounts of modification 1 may result from the small size of the regions of the new phase at this early stage of the transition. The expansion and contraction values indicate that most of the modification 2 crystallinity had been developed by the time the quench temperatures were reached (i.e., within a few seconds). The subsequent slow contractions observed at the crystallization temperatures were due for the most part to the transformation of modification 2 to modification 1. Superimposed on this there was probably some additional contraction due to the completion and perfection of the modification 2 crystallinity.

It would seem from this work that powerful quenching techniques would be necessary to obtain amorphous poly-1-butene at low temperatures. If the sample is not of sufficiently low cross-sectional area, the heat generated by the extremely rapid crystallization process may make rapid cooling especially difficult. In any case, we can conclude that in the subsequent dilatometric studies of the transformation of modification 2 to modification 1 the formation of modification 2 is complete within a few minutes at all the experimental temperatures used.

2. The Transformation of Modification 2 to Modification 1

The kinetics of the transformation of modification 2 to modification 1 were first studied at room temperature by following the time dependence of the appearance of the infrared absorption band at $10.81\ \mu$ (characteristic of modification 1), the disappearance of the band at $11.03\ \mu$ (characteristic of modification 2) and by the change in density as measured in the density

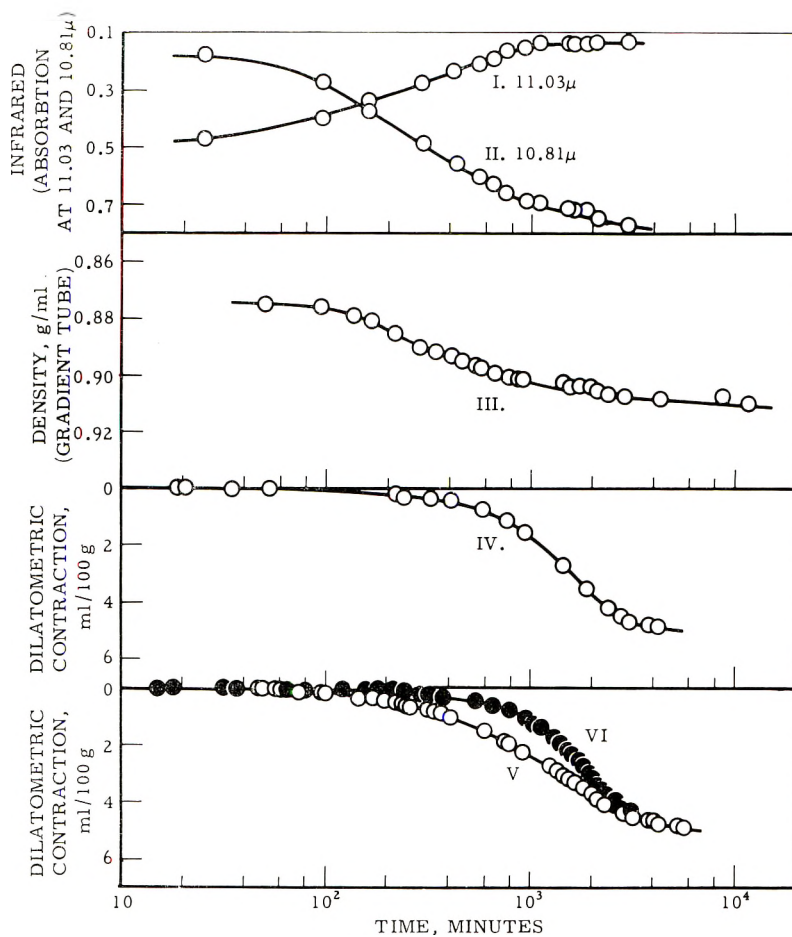


Fig. 9. Infrared, density gradient tube, and dilatometric measurements showing transformation of modification 2 to modification 1.

gradient column. Curves *I*, *II*, and *III* in Figure 9 show the data obtained by these methods. The three curves show essential agreement as to shape. The halftimes corresponding to the two spectral changes are in agreement, 250 min. being obtained for each band. In the density gradient experiment the halftime was about 380 min. In view of the following discussion better agreement than this would not be expected.

In contrast, dilatometric studies of this transition showed disagreement in both shape and halftime, the latter being about five times higher. Curve

IV of Figure 9 shows the results of a dilatometric experiment performed on the same sample at room temperature. The halftime found here is about 1600 min. Orientation effects have been shown to be responsible for the observed discrepancies.

Orientation Effects. In the dilatometric experiments the samples have been fused in the dilatometers at 170°C. to erase thermal and mechanical history before commencing kinetic measurements. The spectroscopic and density gradient experiments, on the other hand, were performed on thinly-pressed films which have not been subjected to such a preheating treatment. Examination through crossed polaroids has shown that films of the type used here are often highly oriented. It would appear, then, that orientation can result in an acceleration of the transformation of modification 2 to modification 1. Such an effect would not be completely unexpected in view of the acceleration of the transition rate in elongation reported by Natta.⁶ To check this point, a thinly pressed film was studied dilatometrically immediately after molding. The resulting data are shown in curve *V*, Figure 9. It can be seen that orientation has led to kinetic behavior approaching that observed in the spectroscopic and density gradient experiments. The results of these latter experiments have not been closely duplicated because the molding pressure in preparing the film for the dilatometric experiment was not as great as that attained in the other experiments, leading to a thick film having lower orientation. (The molding pressure decreases as the amount of sample used in the experiment increases. The dilatometric experiment called for more sample.) Following the kinetic run of curve *V*, the film specimen was fused in the dilatometer and the experiment was repeated. As expected, the transformation observed (curve *VI*) was of the type expected for unoriented material.

That the observed kinetic changes were not due to molding pressure alone was demonstrated by an experiment where bars molded at 20,000 psi and 170°C. were studied dilatometrically with and without preheating. In this case there was no significant change in the transformation kinetics. It appears then that the amount of orientation necessary to accelerate the transformation requires either more extreme dimensional changes in the molding or rapid cooling to "lock in" the orientation, or both. It can readily be seen that film pressing should satisfy these conditions.

In pressing films considerable variation in the resulting amount of orientation would be expected. Thus, as mentioned above, the slight discrepancy between halftimes in the density gradient and spectroscopic experiments would certainly be expected.

Temperature Dependence. Dilatometry was chosen for an investigation of the temperature dependence of the transition because of the ease of eliminating thermal and mechanical history and because of the finer temperature control available when this technique is used. As the transition was expected to be extremely slow at many temperatures, no attempt was made in these experiments to approach the endpoints of the transformations. Although, for this reason the kinetics curves cannot be compared on the basis of actual halftime values obtained for each experiment, they

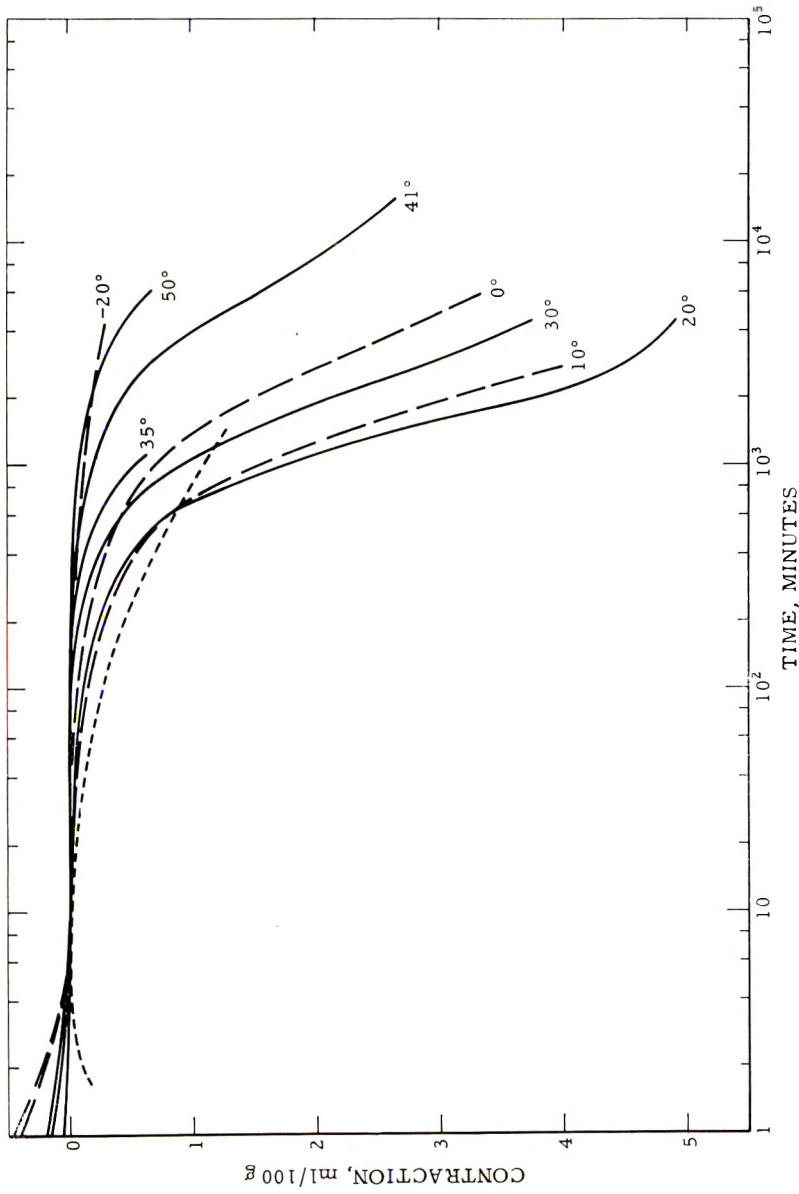


Fig. 10. Isothermal contraction accompanying the transformation of modification 2 to modification 1 at various temperatures: (—) $T >$ temperature of maximum rate; (---) $T <$ temperature of maximum rate; (-·-) $T = 62^\circ\text{C}$. following rapid cooling to -20°C .

can be characterized with sufficient precision for the present purposes by the times required for the attainment of certain standard contraction levels.

The standard contraction levels for time comparisons were chosen arbitrarily as $1/8$, $1/4$, and $1/2$ of the contraction observed in a preliminary experiment in which the progress of the transition was followed for 35 days. In this experiment it was observed that no true end value of contraction was obtained, rather a protracted small contraction took place after the large changes of the early part of the experiment. Such behavior is similar to that attributed to "secondary crystallization" in studies of crystallization from the melt.¹⁷ The "final" contraction estimate for this experiment was 6.56 ml./100 g. (corresponding to 5.7% contraction). Our standard contraction levels were thus chosen as 0.87, 1.64, and 3.28 ml./100 g.

Contraction curves at various temperatures are shown in Figure 10. These curves show a gradual change in shape with temperature indicating a gradual change in the nature of the transition in addition to the obvious change in rate. The time required for attainment of the three contraction levels in these experiments are given in Table IV. In Figure 11 the attainment times for the 0.82 ml./100 g. contraction level are plotted against temperature. From this curve and the tabular data it is seen that the transition rate goes through a pronounced maximum in the neighborhood of 15–20°C.

TABLE IV
Transformation of Modification 2 to Modification 1

| Temperature, °C. | Time to attainment of standard contraction levels, min. | | |
|-------------------|---|---------------------|---------------------|
| | 0.82 ml./100g. | 1.64 ml./100g. | 3.28 ml./100g. |
| -20 | 24,000 ^a | — | — |
| 0 | 1,120 | 2,170 | 5,500 |
| +10 | 580 | 1,020 | 2,090 |
| 20 | 615 | 1,010 | 1,750 |
| 30 | 900 | 1,530 | 3,340 |
| 35 | 1,290 | 2,150 ^a | — |
| 41 | 3,200 | 6,300 | 50,000 ^a |
| 50 | 6,800 | 12,000 ^a | — |
| 62 | 17,000 ^a | — | — |
| 62 ^b | 410 | 2,200 ^a | — |
| 85.5 ^b | 6,500 ^a | — | — |

^a Values estimated by extrapolation.

^b After quenching.

Behavior of this type is commonly reported in crystallization from the melt and has been analyzed in terms of the following ideas: (1) phase transformation is initiated by a nucleation process; (2) at moderate degrees of supercooling the nucleation step is slow and limits the rate of phase change; (3) there is a critical size for nucleus stability which decreases with

decreasing temperature leading to greater ease of nucleation as temperature is lowered and hence to a negative temperature coefficient for the overall rate process; and (4) if the temperature is sufficiently lowered, the slowness of the transport step across the phase boundary required for growth of the new phase becomes rate controlling leading to a temperature of maximum

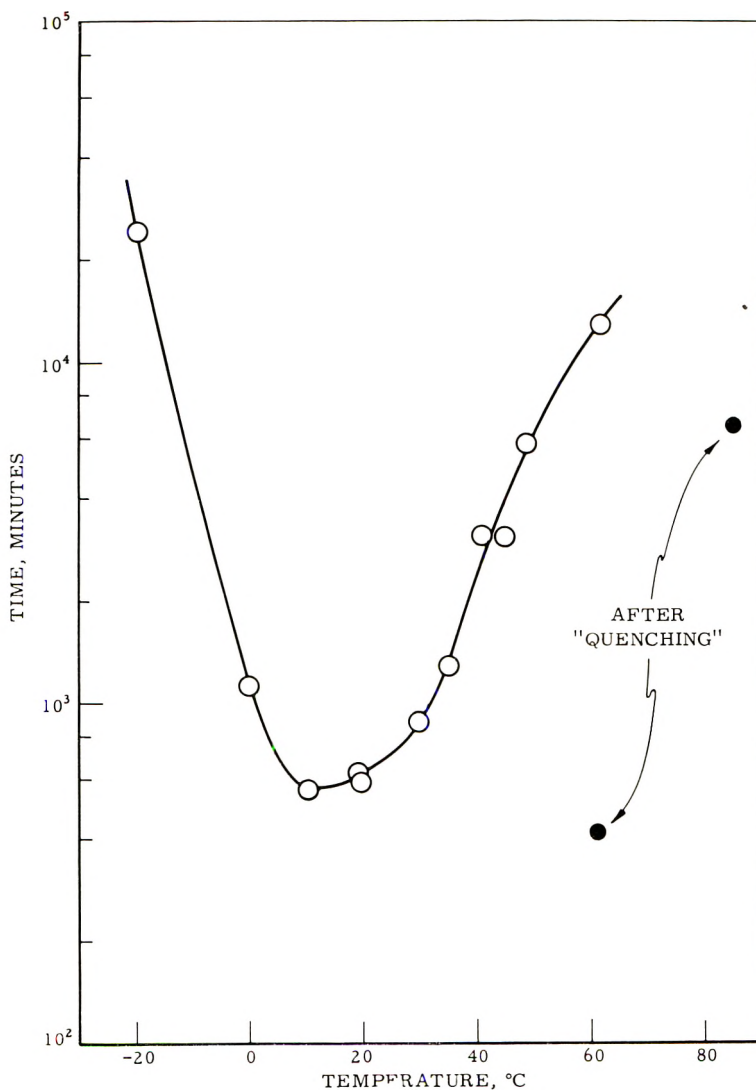


Fig. 11. Time to attain 0.82 ml./100 g. contraction as a function of temperature.

rate below which the temperature coefficient is positive. While we have not seen these concepts applied to a solid-solid transition in polymers, reference to the original development of these ideas (which were first applied to low molecular weight materials) shows them to be just as applicable to solid-solid transitions as they are to crystallization from the melt.¹⁵ For

specific applications of these concepts to the study of solid-solid transformations in low molecular weight materials the reader is referred to the works of deBoer, Burgers, and Groen.^{19,20}

In the present studies then, it would seem that above 15–20°C. the transformation becomes increasingly difficult as the temperature is raised because an increasing critical size for nucleus stability makes the formation of centers of modification 1 crystallinity increasingly improbable. Below this temperature the transformation becomes increasingly retarded as the energy required to bring about the necessary chain motions becomes less and less available.

“Prenucleation” by Quenching. Also shown in Table IV and Figure 11 are kinetic results of the two experiments discussed above under “Attempts to Bypass the Modification 2 Crystallization by Quenching.” It can be seen that precooling to –20 or –30°C. greatly reduces the time required for the attainment of low levels of contraction at 62 and 85.5°C. Passing the sample through the low temperature region has probably resulted in the formation of nuclei of modification 1. Most of the contraction observed at 62 and 85.5°C. was probably due to the growth of these centers, as the nucleation process is extremely slow at 62 and 85.5°C. The contraction curve obtained at 62°C. is shown as a dotted line in Figure 8. The curve obtained at 85.5°C. is similar and has been omitted for the sake of clarity. The peculiar shape of these curves suggests that whatever transformation accelerating mechanism is operating here, it loses effectiveness as the phase change progresses.

Amorphous Content During the Transformation. Torsional Damping Experiments. Torsional damping experiments have been used to determine whether or not the amorphous content remains constant during the transformation of modification 2 to modification 1. While x-ray diffraction techniques should, in principle, provide a more straightforward approach to this problem, the orientation techniques required to obtain adequate x-ray data pertinent to the unstable crystallinity leads to a rapid transformation to the stable form.

In Figure 12 the loss tangent ($\tan \delta$) is plotted against temperature for a poly-1-butene sample before and after the transformation. Curve *A* was taken immediately after the molded sample had been held at 100°C. for 2 hr. to allow essentially complete development of the unstable crystalline phase without any attendant transformation to the stable form. Curve *B* was taken after the sample had been maintained at room temperature for 6 days.

We have attempted to relate these curves to the amorphous content in the following manner. The intensity of the damping peak should increase monotonically with the amount of amorphous poly-1-butene in the sample. According to an empirical relationship between the maximum loss tangent ($\tan \delta_{\max}$) and the amorphous content developed in this laboratory,^{12,21} the change observed here ($\tan \delta_{\max}$ going from 0.278 to 0.183) corresponds to a difference of the order of 5% in the amorphous content. On completing the transformation, the density observed (0.91) corresponds to an amor-

phous content of 43%. Therefore, prior to the transformation the amorphous content is approximately 48%. From this figure, the observed density value of 0.875 for a sample after the formation of the modification 2 and before any transition to modification 1 has taken place, and the value

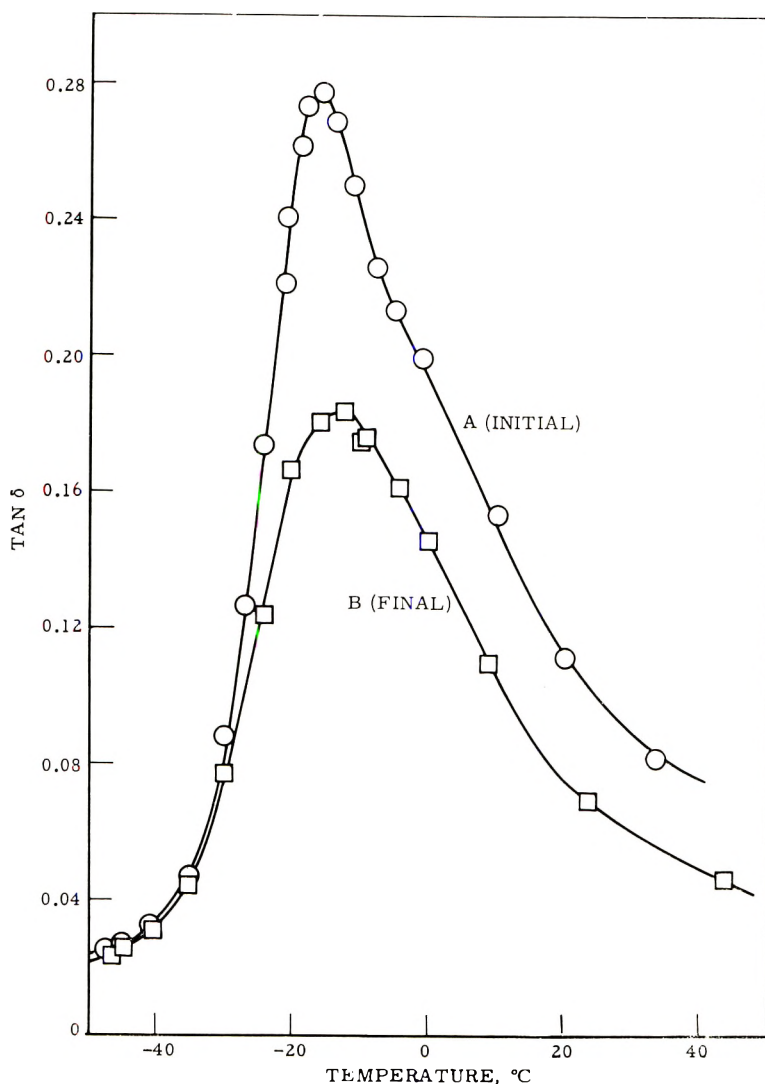


Fig. 12. Torsional damping curves of poly-1-butene before and after transformation of modification 2 to modification 1.

(0.870) for the density of the amorphous polymer,¹¹ a density of 0.88 can be calculated for the pure unstable crystalline phase. The density of modification 2 is thus seen to be close to that of the amorphous phase.

Changes in Mechanical Properties. We have observed pronounced changes in appearance and physical behavior accompanying the crystalline

transformation in poly-1-butene; specimens become increasingly turbid, more rigid, and exhibit higher strength. The mechanical changes taking place at room temperature were studied quantitatively in measurements of torsion moduli and offset yield points. These quantities increased by factors of 2 and 3 respectively, as the transformation took place (Fig. 13).

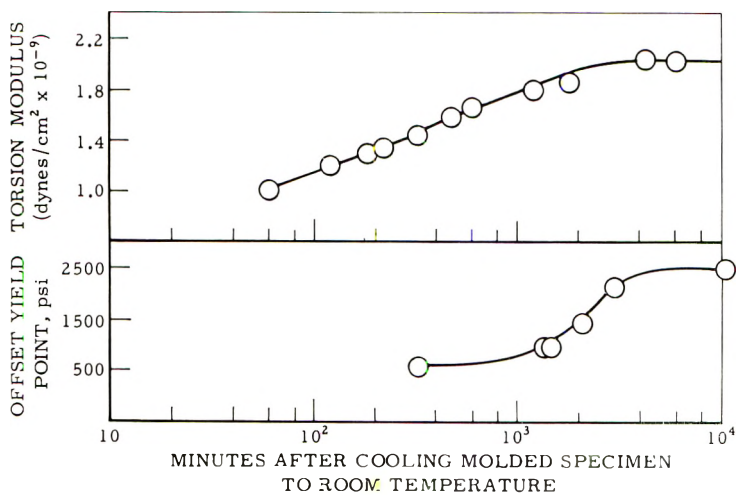


Fig. 13. Changes in mechanical properties during the transformation of modification 2 to modification 1.

The observed changes may result from any of the following factors: the decrease in amorphous content accompanying the transition, a change in the spatial distribution of the amorphous phase, or the changes taking place in the mechanical properties of the crystalline regions themselves. We are not presently able to assess the relative importance of the above factors.

We would like to acknowledge the invaluable advice of our numerous colleagues, especially E. A. Youngman, D. J. Meier, E. C. Shokal, F. E. Weir, and J. H. Badley. Also the indispensable assistance in carrying out the experimental work by Miss M. Ogle, D. W. Penhale, and R. J. Patten is greatly appreciated.

References

1. Natta, G., P. Corradini, and I. W. Bassi, *Atti acad. nazl. Lince, Rend. Classe sci. fis. mat. e nat.* [8], **19**, 404 (1955).
2. Natta, G., et al., *J. Am. Chem. Soc.*, **77**, 1908 (1955).
3. Natta, G., P. Corradini, and I. W. Bassi, *Makromol. Chem.*, **21**, 240 (1956).
4. Natta, G., *Experientia Suppl.*, **7**, 21 (1957).
5. Natta, G., and P. Corradini, *Nuovo Cimento Suppl.*, **15**, 9 (1960).
6. Natta, G., P. Corradini, and I. W. Bassi, *Nuovo Cimento Suppl.*, **15**, 52 (1960).
7. Natta, G., *Makromol. Chem.*, **35**, 94 (1960).
8. Welch, L. M., et al., paper presented at local meeting of Am. Chem. Soc., Baton Rouge, La., December 1959.
9. Natta, G., *Atti acad. nazl. Lincei, Rend. Classe sci. fis. mat. e nat.*, **20**, 560 (1956).
10. Reding, F. P., *J. Polymer Sci.*, **21**, 547 (1956).

11. Danusso, F., G. Moraglio, and G. Natta, *Ind. plastiques modernes (Paris)*, **10**, 40 (1958).
12. Weir, F. E., paper presented at SPE Retech. Meet. Phila., April 1962.
13. Karas, G. C., and B. Warburton, *Brit. Plastics*, **34**, 189 (1961).
14. Moore, W. J., *Physical Chemistry*, 2nd Ed., Prentice-Hall, New York, 1955, p. 111.
15. Avrami, M., *J. Chem. Phys.*, **7**, 1103 (1939); *ibid.*, **8**, 212 (1940).
16. Mandelkern, L., in *Growth and Perfection of Crystals*, R. H. Doremus, B. N. Roberts, and D. Turnbull, Eds., Wiley, New York, 1958, p. 467.
17. See, for example, J. Majer, *Cecl. Czechoslov. Chem. Commun.*, **23**, 2454 (1960); H. G. Zachman, and H. A. Stuart, *Makromol. Chem.*, **41**, 131 (1960).
18. See, for example, D. Turnbull, and J. C. Fisher, *J. Chem. Phys.*, **17**, 71 (1949).
19. DeBoer, J. H., *Discussions Faraday Soc.*, **23**, 171 (1957).
20. Burger, W. G., and L. J. Groen, *Discussions Faraday Soc.*, **23**, 183 (1957).
21. Bauer, R. S., and F. E. Weir, this laboratory, private communication.

Synopsis

The formation and melting of the two crystalline modifications of poly-1-butene have been studied by the techniques of differential thermal analysis, infrared spectroscopy, dilatometry, and polarizing microscopy. On cooling the melt, modification 2 ($T_m = 120\text{--}126^\circ\text{C.}$) appears within minutes. This form is unstable and gradually transforms to modification 1 ($T_m = 135\text{--}142^\circ\text{C.}$). A density change of over 4% accompanies this latter transformation. As torsional damping experiments have shown the amorphous content to decrease by only about 5%, the stable modification must be much more dense than the unstable form. The kinetics of the crystallization of modification 2 from the melt were studied primarily dilatometrically at several temperatures. The data generally followed the Avrami equation with n equal to 4. This crystallization shows a high negative temperature coefficient ($T_{1/2} = 380$ min. at 110°C. and 2 min. at 90°C.) and becomes too rapid to measure by this technique at lower temperatures. The kinetics of the transformation of modification 2 to modification 1 were followed in infrared spectral, density gradient tube, and dilatometric studies. At room temperature, halftimes ranging from 250 to 1600 min. were observed, depending on the mechanical and thermal history of the sample. The observed discrepancies have been shown to be due, at least in part, to orientation effects. In dilatometric studies of the temperature dependence, the transition rate showed a pronounced maximum in the region of 15°C. Large increases in the torsional modulus and offset yield point of the specimen were observed to accompany the transition.

Résumé

On a étudié la formation et la fusion des deux variétés cristallines du poly-1-butène par les techniques de l'analyse thermique différentielle, par spectroscopie infra-rouge, par dilatométrie et au moyen du microscope polarisant. Par refroidissement de la masse fondue, on obtient la variété 2 ($T_m = 120\text{--}126^\circ\text{C.}$) en l'espace de quelques minutes. Cette forme est instable et se transforme graduellement en la variété 1 ($T_m = 135\text{--}142^\circ\text{C.}$). Un changement de densité d'environ 4% accompagne cette dernière transformation. Comme cela a été montré par des expériences de torsion, la partie amorphe diminue d'environ 5% seulement, la variété stable devant être beaucoup plus dense que la forme instable. On a étudié la cinétique de cristallisation de la variété 2 à partir de la substance fondue, par dilatométrie à plusieurs températures. Les résultats suivent généralement l'équation d'Avrami où n est égal à 4. Cette cristallisation indique un coefficient de température fortement négatif ($T_{1/2} = 380$ min. à 110°C. et 2 min. à 90°C.) et devient trop rapide pour effectuer les mesures par cette technique, à de plus faibles températures. On suit la cinétique de la transformation de la forme 2 en forme 1 par spectroscopie infra-rouge, par la méthode au gradient de densité, et par des études dilatométriques. A température de chambre, on observe des demi-périodes de 250 à 1600 min., dépendant du traitement mécanique et thermique de l'échantillon. On a

montré que les contradictions observées sont dues au moins en partie à des effets d'orientation. Dans les études dilatométriques concernant la dépendance de la température, la vitesse de transition indique un maximum prononcé dans la région de 15°C. En même temps que la transition, on observe de grandes augmentations dans le module de torsion et le degré de rendement de l'échantillon.

Zusammenfassung

Bildung und Schmelzen der beiden kristallinen Poly-1-butenmodifikationen wurde mittels Differentialthermoanalyse, Infrarotspektroskopie, Dilatometrie und Polarisationsmikroskopie untersucht. Beim Kühlen der Schmelze erscheint Modifikation 2 ($T_m = 120-126^\circ\text{C.}$) innerhalb von Minuten. Diese Form ist instabil und wandelt sich nach und nach in Modifikation 1 ($T_m = 135-142^\circ\text{C.}$) um. Diese Umwandlung wird von einer Dichte-änderung von über 4% begleitet. Da Torsionsdämpfungsmessungen zeigten, dass der Gehalt an amorphem Material nur um etwa 5% abnimmt, muss die stabile Modifikation eine sehr viel höhere Dichte besitzen als die instabile. Die Kinetik der Kristallisation von Modifikation 2 aus der Schmelze wurde zunächst dilatometrisch bei einigen Temperaturen untersucht. Die Ergebnisse befolgten im allgemeinen die Avramigleichung mit n gleich 4. Die Kristallisation besitzt einen hohen, negativen Temperaturkoeffizienten ($T_{1/2} = 380$ min. bei 110°C. und 2 min bei 90°C.) und wird bei niedrigeren Temperaturen zu rasch, um nach dieser Methode gemessen werden zu können. Die Kinetik der Umwandlung von Modifikation 2 zu Modifikation 1 wurde infrarotspektroskopisch, in einem Dichtegradientenrohr und dilatometrisch untersucht. Bei Raumtemperatur wurden in Abhängigkeit von der mechanischen und thermischen Vorgeschichte der Probe Halbwertszeiten von 250 bis 1600 min. beobachtet. Die beobachteten Unstimmigkeiten liessen sich wenigstens zum Teil auf Orientierungseffekte zurückführen. Bei der dilatometrischen Untersuchung der Temperaturabhängigkeit ergab sich im Gebiete von 15°C. ein ausgeprägtes Maximum für die Umwandlungsgeschwindigkeit. Die Umwandlung war von einer starken Zunahme des Torsionsmoduls und der Fließgrenze der Probe begleitet.

Received August 28, 1961

Cocatalysts for the Linear Polymerization of Epoxides by Dibutylzinc*

K. T. GARTY, T. B. GIBB, JR., and R. A. CLENDINNING,
*Research Department, Union Carbide Plastics Company,
Bound Brook, New Jersey*

INTRODUCTION

Although the use of organometallic compounds for the stereospecific polymerization of epoxides has received an increasing amount of attention in the recent literature, relatively little attention has been paid to epoxides other than ethylene and propylene oxides. In addition, very little work has appeared concerning the use of various cocatalysts with dibutylzinc for the polymerization of ethylene oxide, propylene oxide, epichlorohydrin, and phenyl glycidyl ether. The major part of this study has been devoted to phenyl glycidyl ether.

Our results on ethylene and propylene oxide are in substantial agreement with those of Furukawa and his co-workers who recently reported the polymerization of propylene oxide by diethylzinc in the presence of several cocatalysts.^{1,2} Noshay and Price³ have reported the polymerization of phenyl glycidyl ether by an aluminum isopropoxide-zinc chloride catalyst or by triethylaluminum, but these catalysts require long reaction times to produce relatively low yields of crystalline, high molecular weight product. In a recent publication, Vandenberg⁴ mentions the use of an aluminum alkyl-water catalyst to produce a nearly quantitative conversion of phenyl glycidyl ether to high molecular weight, crystalline polymer. In the present study results similar to Vandenberg's were obtained by using dibutylzinc with a variety of cocatalysts, among which water and acetone were found to be most effective.

EXPERIMENTAL

Monomer Purification

Phenyl Glycidyl Ether. Phenyl glycidyl ether (Shell Chemical Corporation) was distilled under reduced pressure through a 4 ft. by 1.2 in. diameter column packed with glass helices. The first 10% of the distillate was discarded as was the last 5% of the distillation residue. The center cut

* Paper presented at the 141st National Meeting of American Chemical Society, Washington, D. C., March 1962.

boiled at 141°C. at 30 mm. The most reliable method for determining monomer purity was found to be a gas chromatographic survey for high and low boiling components. Monomer was judged to be pure when chromatography on a 2-m. polyester column at 175°C. and on an Apiezon L column at 260°C. disclosed the absence of all peaks other than the major one. In addition, the monomer had a hydrolyzable chlorine content of less than 0.01% and a water content of less than $6.5 \times 10^{-3}\%$.

Propylene Oxide. Propylene oxide (Union Carbide Chemicals Company) was dried statically and stored over Linde 4A Molecular Sieves. Monomer treated in this manner was found to have a water content of 76 ppm by a modified Karl Fischer titration and to be 99.9% propylene oxide by gas-phase chromatography.

Ethylene Oxide. Ethylene oxide (Matheson Coleman and Bell Co.) was passed through a column of potassium hydroxide pellets, a column of calcium sulfate, and finally condensed and stored at 5°C. over Linde 4A Molecular Sieves.

Solvent Purification

Toluene. Reagent-grade toluene (Matheson Coleman and Bell) was refluxed over sodium for at least 24 hr. and, after insuring the presence of metallic sodium, was distilled in a nitrogen atmosphere through a short Vigreux column. It was stored in a glass stoppered bottle under a nitrogen atmosphere.

Heptane and Cyclohexane. Matheson Coleman and Bell reagent-grade heptane and cyclohexane were purified in a manner similar to that of toluene.

Catalyst Preparation

Dibutylzinc was prepared by either the reaction of anhydrous zinc bromide with butylmagnesium bromide^{5a} or by the reaction of a mixture of butyl bromide and butyl iodide with a zinc-copper couple.^{5b} After two distillations (b.p. 80°C. at 14 mm.) it was diluted with toluene to a concentration of approximately 0.15 g. Bu₂Zn/ml. Samples were analyzed by titration of total zinc.

Cocatalyst Purification

Methanol and *n*-butanol were purified by reaction with magnesium metal.⁶ Ethanol, isopropanol, and *tert*-butanol were purified by reaction with the appropriate sodium alkoxide and ϵ -caprolactone. One liter of commercial absolute ethanol was treated with 7 g. metallic sodium followed by 20 g. of ϵ -caprolactone. The mixture was maintained at reflux for 10-12 hr. and the ethanol distilled through a 35-cm. vacuum-jacketed Vigreux column. In the case of isopropanol and *tert*-butanol, mechanical stirring had to be used during the reflux and distillation to minimize bumping. This procedure offers several advantages over the conventional

sodium ester method. The ester is very high boiling and also the alcohol derived from the ester is nonvolatile since it is in the form of a sodium salt of a carboxylic acid. Hence the one ester can be used to dry different alcohols.

Acetone was purified by refluxing over potassium permanganate, drying over magnesium sulfate, and fractional distillation under a nitrogen atmosphere. It was then statically dried over Linde 4A Molecular Sieves.

Phenol was fractionally distilled under nitrogen and a small center cut taken.

Butyraldehyde was purified by drying over magnesium sulfate and fractionally distilling under nitrogen.

The remainder of the cocatalysts listed in Table X were dried and distilled under nitrogen.

Polymerization Technique

Phenyl Glycidyl Ether (PGE). Polymerization studies were carried out in glass tubes that were sealed under nitrogen and then rotated in a circulating air oven at 90°C. for 24 hr. The order of addition of materials to the tube was not fixed but was generally PGE, cocatalyst, if any, diluent, catalyst. Occasionally PGE-diluent solutions were premixed and added to the tube followed by cocatalyst and catalyst. All additions to the tube were carried out with nitrogen flushed syringes. The very small amounts of cocatalyst required were measured by microliter syringes. Except as noted otherwise in the tables, 10 g. of PGE and 15 g. of toluene were used in each tube.

Poly(Phenyl Glycidyl Ether)(PPGE). PPGE was isolated by removing the product from the tube with the aid of acetone, chopping in a Waring Blendor with 200 ml. of toluene to obtain a finely divided swollen product, precipitating in 3 liters of ethanol, filtering and washing with ethanol, and drying in a vacuum oven for at least 15 hr. at 40–60°C. and 10–20 mm. Hg. Reduced viscosity determinations were carried out in *p*-chlorophenol (0.05 g./25 ml.) containing 2% α -pinene at 47°C. Since PPGE was insoluble in nearly all common solvents, it was necessary to heat the polymer and solvent to 140°C. for at least 30 min. to obtain solution. The polymer was shown to be crystalline by x-ray diffraction and had a crystalline m.p. of 204°C., as determined on a Leitz microscope heating stage.

Propylene Oxide (PO). The general procedure for preparing poly(propylene oxide) (PPO) was the same as that for PPGE. Except as otherwise noted in the Tables, 5.8 g. of PO and 13.5 g. of toluene were used in each tube, and the tubes were heated at 50°C. for 24 hr.

PPO was recovered by transferring the contents of the tube with the aid of acetone to a tared evaporating dish. Volatile materials were removed on a steam bath and finally by drying in a vacuum oven at 40°C. for 16–20 hr. Reduced viscosity determinations were carried out in benzene solution (0.05 g./25 ml.) at 25°C.

Ethylene Oxide (EO). The general technique for preparing poly-

(ethylene oxide) (PEO) was the same as that described above except that pressure bottles were used and the polymerization carried out at room temperature for 24 hr.

PEO was recovered by dissolving the polymer in a methanol-toluene mixture, precipitating in 4 liters of heptane, filtering, and drying at 40°C. for 16-20 hr. at 10-20 mm. Reduced viscosity determinations were carried out in methylene chloride solution (0.05 g./25 ml.) at 25°C.

Epichlorohydrin. The polymerization was carried out in the same manner as described for PGE. When no precipitate was observed on pouring into ethanol, the solutions were evaporated under reduced pressure to give the oils described in Table XV.

RESULTS

Phenyl Glycidyl Ether

The results obtained by adding various amounts of water to a mixture of 10 g. of PGE, 15 g. toluene, and 1.5% dibutylzinc (based on monomer weight) are summarized in Table I.

TABLE I
Water as a Cocatalyst in the Polymerization of PGE^a

| H ₂ O, moles/ mole Bu ₂ Zn | Conversion, % | Reduced viscosity |
|---|------------------|----------------------|
| 0 | 1.5 | 4.5 |
| 0.25 | 19.9 | 6.4 |
| 0.5 | 65.5 | 10. |
| 0.75 | 95.4 | 11. ^b |
| 1.0 | 97.0 | 10.2 |
| 1.25 | 3.1 | 0.7 |
| 1.5 | 0.7 | — |
| 2.4 | 0 | — |

^a Conditions: 24 hr. at 90°C., 0.15 g. Bu₂Zn, 10 g. PGE, 15 g. toluene.

^b Sample not completely dissolved.

With the first sample, no water was added and a negligible amount of alcohol-insoluble polymer was obtained. In another series of experiments, the dibutylzinc concentration was varied from 0.5 to 4.0% with no cocatalyst added. In all cases, less than 2.5% of alcohol-insoluble polymer was obtained. These data confirm published results on the polymerization of propylene oxide with diethylzinc^{1,2} and point up the fact that dibutylzinc alone is a poor catalyst for the polymerization of epoxides.

In the succeeding experiments of Table I, the conversion increases with the water concentration until a maximum is reached at 1 mole of water/mole of dibutylzinc. As the water concentration increases past 1 mole, the conversion drops off very rapidly.

In order to determine the effect of catalyst concentration on conversion and reduced viscosity of the resulting polymer, various concentrations of a

1:1 molar mixture of water and dibutylzinc were added to 10 g. of PGE and 15 g. of toluene. The results are shown in Table II.

TABLE II
Effect of Catalyst Concentration in the Polymerization of PGE^a

| Bu ₂ Zn, % | Conversion, % | Reduced viscosity |
|-----------------------|---------------|-------------------|
| 0.5 | 17.2 | — |
| 1.0 | 30.0 | 12 |
| 1.5 ^b | 0.7 | — |
| 1.5 | 39.9 | 14 |
| 1.75 | 49 | 14 |
| 2.3 | 52 | 11 |
| 3.3 | 61 | 10 |
| 4.0 | 64 | 13 |
| 5.0 | 66 | 14 |

^a Conditions: 1 mole H₂O/mole Bu₂Zn, 4 hr. at 90°C., 10 g. PGE, 15 g. toluene.

^b Control: no H₂O added.

As might be expected, increasing the catalyst concentration results in a more rapid polymerization, but the most surprising part of the data obtained is the negligible effect that varying catalyst concentration has on reduced viscosity. In consideration of the fact that poly(phenyl glycidyl ether) is so difficult to dissolve, the values obtained on these reduced viscosity determinations are essentially the same and indicate that varying catalyst concentration cannot be used to control reduced viscosity.

In Table III the effect of three primary alcohols on the dibutyl zinc-catalyzed polymerization of phenyl glycidyl ether is shown.

Several interesting conclusions can be drawn from the data in Table III. It is obvious from the conversion figures that none of the primary alcohols at any concentration is as good a cocatalyst as water in the polymerization of PGE. The maximum conversion is obtained at between 1.0 and 1.5

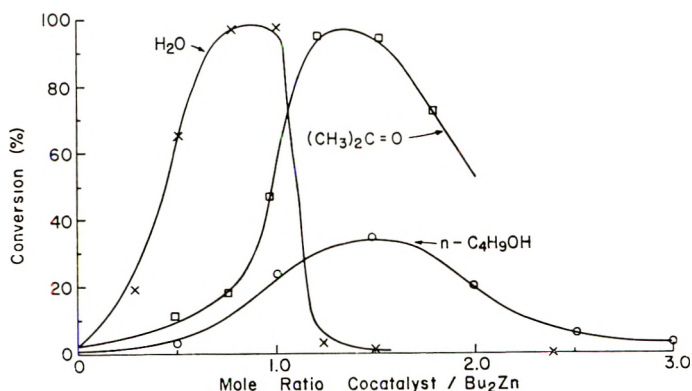


Fig. 1. Conversion vs. ratio of various catalysts in polymerization of 40% PGE in toluene with 1.5% Bu₂Zn, 24 hr. at 90°C.: (×) H₂O; (□) acetone; (○) *n*-butanol.

TABLE III
Primary Alcohols as Cocatalysts in the Polymerization of PGE^a

| MeOH, moles/mole Bu ₂ Zn | Methanol | | | Ethanol | | | <i>n</i> -Butanol | | |
|---|------------------|----------------------|---|------------------|----------------------|---|-------------------|----------------------|--|
| | Conversion, % | Reduced viscosity | EtOH, moles/mole Bu ₂ Zn | Conversion, % | Reduced viscosity | BuOH, moles/mole Bu ₂ Zn | Conversion, % | Reduced viscosity | |
| 0 | 4.0 | — | 0 | 1.5 | — | 0 | 1.3 | — | |
| 1.0 | 14.6 | 11.4 | 0.5 | 2.6 | — | 0.5 | 1.1 | — | |
| 1.25 | 36.0 | 5.8 | 1.0 | 25.0 | 6.1 | 1.0 | 22.3 | 7.3 | |
| 1.50 | 34.3 | 2.8 | 1.5 | 24.9 | 2.0 | 1.5 | 33.3 | 9.1 | |
| 1.75 | 16.7 | 0.8 | 2.0 | 6.0 | — | 2.0 | 19.9 | 1.0 | |
| 2.0 | 21.4 | 0.8 | 2.5 | 1.5 | — | 2.5 | 4.5 | — | |
| | | | 3.0 | 0.5 | — | 3.0 | 2.8 | — | |
| | | | 4.0 | 0.5 | — | 4.0 | 1.0 | — | |

^a Conditions: 10 g. PGE, 15 g. toluene, 0.15 g. Bu₂Zn, 24 hr. at 90°C.

moles of alcohol/mole of dibutylzinc. In each case the maximum appears to be spread over a wider concentration range than was true in the case of water. This is shown for *n*-butanol in Figure 1. Furthermore, the reduced viscosities determined on the samples showing maximum conversions appear to be somewhat lower than in the case of water as a cocatalyst.

In Tables IV and V the effect of isopropanol and tertiary butanol as cocatalyst is shown.

TABLE IV
Isopropanol as a Cocatalyst in the Polymerization of PGE^a

| <i>i</i> -PrOH, moles/ mole Bu ₂ Zn | Conversion, % |
|---|------------------|
| 0 | 0.7 |
| 0.5 | 0.8 |
| 1.0 | 8.2 |
| 1.5 | 0.6 |
| 2.0 | 0.1 |
| 2.5 | 0.1 |
| 3.0 | 0.1 |

TABLE V
tert-Butanol as a Cocatalyst in the Polymerization of PGE^a

| <i>t</i> -BuOH, moles/ mole Bu ₂ Zn | Conversion, % |
|---|------------------|
| 0 | 1.1 |
| 0.5 | 2.0 |
| 1.0 | 2.8 |
| 1.5 | 0.3 |
| 2.0 | 0.2 |
| 2.5 | 0.2 |
| 3.0 | 0.2 |

^a Conditions: 10 g. PGE, 15 g. toluene, 0.15 g. Bu₂Zn, 24 hr. at 90°C.

In the case of isopropanol the maximum conversion was obtained at about 1 mole/mole of dibutylzinc. With *tert*-butanol there appears to be a slight maximum at 1 mole, but this is not at all certain. When conversions obtained with the primary alcohols of Table III are compared with those with isopropanol and *tert*-butanol, it can be seen that the primary alcohols are far more effective cocatalysts. The maximum conversion decreases as one goes from a primary alcohol to isopropanol to *tert*-butanol. If steric considerations are taken into account, this observation is exactly what would be predicted on the basis of the size of the alkyl group of the alcohol.

The effect of catalyst concentration on conversion and polymer molecular weight is shown in Table VI where various concentrations of a 1.75:1 molar mixture of *n*-butanol to dibutylzinc were added to 10 g. of PGE and 24 g. of heptane.

As expected, increasing the catalyst concentration results in a more rapid

TABLE VI
Effect of Various Concentrations of a 1.75:1 Molar Mixture of
n-Butanol and Dibutylzinc^a

| Bu ₂ Zn, % | Conversion, % | Reduced viscosity |
|-----------------------|---------------|-------------------|
| 1.0 | 23.8 | 16 |
| 1.5 | 39.1 | 16 |
| 2.0 | 42.4 | 17 |
| 3.0 | 56.3 | 16 |
| 5.0 | 65.8 | 16 |

^a Conditions: 10 g. PGE, 24 g. heptane, 24 hr. at 90°C.

polymerization and exerts a negligible effect on polymer reduced viscosity as was also found to be the case with water cocatalyst. When these results are compared with those in Table III where *n*-butanol was used as a cocatalyst, it is apparent that the choice and concentration of diluent has an effect on polymer reduced viscosity. When compared with the results in Table II where water was used as a cocatalyst, the same tendency is shown, though to a lesser degree.

The evaluation of acetone as a cocatalyst for the polymerization of PGE is shown in Table VII.

TABLE VII
Acetone as a Cocatalyst in the Polymerization of PGE^a

| Acetone, moles/ mole Bu ₂ Zn | Conversion, % | Reduced viscosity |
|--|---------------|-------------------|
| 0 | 1.0 | — |
| 0.5 | 10.8 | 6.6 |
| 0.75 | 17.8 | 7.8 |
| 0.9 | 45.8 | 9.7 |
| 1.25 | 95.7 | 10.0 |
| 1.5 | 94.9 | 8.4 |
| 1.75 | 72.1 | 4.6 |

^a Conditions: 10 g. PGE, 15 g. toluene, 0.15 g. Bu₂Zn, 24 hr. at 90°C.

As can be seen in Table VII, maximum conversions are obtained when 1.25–1.5 moles acetone per mole dibutylzinc are employed. In addition, acetone is a better cocatalyst than a primary alcohol (i.e., higher conversions are obtained), and is equal to water in this respect. These results are surprising, since it was anticipated that any reaction product between acetone and dibutylzinc would be sterically similar to the reaction product of isopropanol and dibutylzinc, and therefore the results of acetone as a cocatalyst would be similar to those obtained with isopropanol.

The evaluation of phenol as a cocatalyst is shown in Table VIII.

As can be seen in Table VIII, the maximum conversion is obtained at about 1.25 moles phenol/mole of dibutylzinc. The conversions, however, when compared to those obtained with water, *n*-butanol, or acetone, indi-

cate that phenol is a poor cocatalyst for the dibutylzinc-catalyzed polymerization of phenyl glycidyl ether.

The evaluation of *n*-butyraldehyde as a cocatalyst is shown in Table IX.

From Table IX it is evident that, in the concentrations studied, butyraldehyde is a poor cocatalyst for the polymerization of PGE. These results are particularly surprising in view of the fact that acetone has been

TABLE VIII
Phenol as a Cocatalyst in the Polymerization of PGE^a

| Phenol, moles/ mole Bu ₂ Zn | Conversion, % |
|---|---------------|
| 0 | 0.5 |
| 0.5 | 0.5 |
| 0.75 | 1.5 |
| 0.9 | 4.4 |
| 1.25 | 7.0 |
| 1.5 | 3.1 |
| 1.75 | 2.8 |

^a Conditions: 10 g. PGE, 15 g. toluene, 0.15 g. Bu₂Zn, 24 hr. at 90°C.

shown to be an excellent cocatalyst. The use of cyclohexane as a solvent in this experiment cannot contribute to this effect, since results obtained with other cocatalysts and cyclohexane as a solvent were substantially the same as those with toluene as a solvent.

The remainder of the compounds tested as cocatalysts are listed in Table X.

TABLE IX
Butyraldehyde as a Cocatalyst in the Polymerization of PGE^a

| C ₄ H ₈ O, moles/mole Bu ₂ Zn | Conversion, % |
|--|---------------|
| 0 | 1.4 |
| 0.5 | 1.8 |
| 0.75 | 1.5 |
| 1.0 | 1.6 |
| 1.25 | 1.8 |
| 1.50 | 2.9 |

^a Conditions: 10 g. PGE, 15 g. cyclohexane, 0.15 g. Bu₂Zn, 24 hr. at 90°C.

It can be seen from Table X that of all the compounds tested, dry air is the most effective, conversions with this cocatalyst approaching those obtained with water and acetone. The remainder of the compounds tested show either a slight positive effect or an inhibitory effect. The case of pyridine is unusual in that it appears to be more effective at very low concentration than at somewhat higher concentration.

TABLE X
 Miscellaneous Compounds as Cocatalysts for the Polymerization of PGE^a

| Compound | Compound, moles/mole Bu ₂ Zn | Polymerization time, hr. | Conversion, % | Reduced viscosity |
|-------------------------------|---|--------------------------|---------------|-------------------|
| Acetic acid | 1 | 24 | 0 | — |
| Ethyl acetate | 1 | 24 | 0.05 | — |
| Diethylamine | 1 | 24 | 4.3 | 24 |
| Dibutylsulfide | 1 | 24 | 19.9 | 7.9 |
| Cyclohexene | 1 | 16 | 3.3 | 5.9 |
| Cyclohexene | 1 | 88 | 18.2 | 4.9 |
| Thiophene | 1 | 16 | 2.6 | 4.0 |
| Thiophene | 1 | 88 | 14.4 | 9.2 |
| 1-Chloro-3-phenoxyisopropanol | 1 | 16 | 5.2 | 0.5 |
| 1-Chloro-3-phenoxyisopropanol | 1 | 88 | 18.4 | 0.5 |
| Pyridine | 0.02 | 24 | 13 | 4.9 |
| Pyridine | 0.02 | 120 | 62 | 9.0 |
| Pyridine | 0.33 | 24 | 3.8 | 7.6 |
| Pyridine | 0.33 | 120 | 24 | 16 |
| Dry air | ^b | 24 | 16.4 | 4.3 |
| Dry air | ^b | 120 | 51 | 12 |
| Dry air | ^c | 24 | 77 | 3.4 |
| Dry air | ^c | 120 | 99 | 6.0 |
| Dry CO ₂ | ^d | 24 | 0.1 | — |
| Dry CO ₂ | ^d | 120 | 0.9 | — |

^a Conditions: 10 g. PGE, 15 g. toluene, 0.15 gm. Bu₂Zn, 90°C.

^b Dry air bubbled through the monomer-catalyst solution for 10 sec.

^c Dry air bubbled through the monomer-catalyst solution for 10 min.

^d Dry CO₂ bubbled through the monomer-catalyst solution for 5 min.

Propylene Oxide

The results obtained with propylene oxide, while not nearly as complete as those obtained with phenyl glycidyl ether offer confirming evidence of the trends reported above and also confirm data in the literature.^{1,2}

The ineffectiveness of dibutylzinc alone as a polymerization catalyst for propylene oxide is shown by the low conversions recorded in Table XI.

 TABLE XI
 Polymerization of Propylene Oxide by Dibutylzinc^a

| Bu ₂ Zn, % | Conversion, % |
|-----------------------|---------------|
| 0.5 | 1.7 |
| 1.0 | 2.3 |
| 1.5 | 2.2 |
| 3.0 | 3.6 |
| 5.0 | 4.1 |

^a Conditions: 5.8 g. PO, 6.5 g. toluene, 24 hr. at 50°C.

The results in Table XII indicate the effect of various concentrations of water added as a cocatalyst.

TABLE XII
Water as a Cocatalyst in the Polymerization of PO^a

| H ₂ O, moles/mole Bu ₂ Zn | Conversion, % | Reduced viscosity |
|---|------------------|----------------------|
| 0 | 1.4 | — |
| 0.5 | 11.1 | 2.5 |
| 0.75 | 23.2 | — |
| 0.90 | 70.5 | 7.2 |
| 1.0 | 82.5 | 8.3 |
| 1.25 | 62.0 | 0.8 |
| 1.5 | 4.6 | — |
| 1.75 | 5.0 | — |
| 2.0 | 3.3 | — |

^a Conditions: 5.8 g. PO, 13.5 g. toluene, 1.5 g. Bu₂Zn, 24 hr. at 50°C.

These results are comparable to those obtained with phenyl glycidyl ether and water (Table I). The maximum conversion is obtained at 1.0 moles of water/mole of dibutylzinc, and on either side of the maximum the conversion drops off quite rapidly. The dependence of reduced viscosity is also the same as was noted in the case of phenyl glycidyl ether.

The effect of various concentrations of a 0.9:1.0 molar ratio of water to dibutylzinc is shown in Table XIII.

TABLE XIII
Effect of Various Concentrations of a Water-Dibutylzinc Catalyst
System on the Polymerization of PO^a

| Bu ₂ Zn, % | Conversion, % |
|-----------------------|---------------|
| 0.5 | 21 |
| 1.0 | 58 |
| 1.5 | 85 |
| 3.0 | 99 |

^a Conditions: 5.8 g. PO, 6.5 g. toluene, 0.9 moles H₂O/mole Bu₂Zn, 16 hr. at 50°C.

Ethylene Oxide

Results obtained with ethylene oxide are similar to those cited above for propylene oxide and are shown in Table XIV. A somewhat higher catalyst concentration (3%) was used in these experiments.

Again, as was noted with propylene oxide and phenyl glycidyl ether, the conversion goes through a maximum. The fact that the maximum occurs at 0.9 moles of water per mole of dibutylzinc rather than 1 mole per mole of dibutylzinc as was found with propylene oxide and phenyl glycidyl ether probably reflects the greater difficulty in obtaining and storing pure ethylene oxide. The reduced viscosity also goes through a maximum at maximum conversion as was noted with phenyl glycidyl ether and propylene oxide.

TABLE XIV
 Water as a Cocatalyst in the Polymerization of Ethylene Oxide^a

| H ₂ O, moles/mole Bu ₂ Zn | Conversion, % | Reduced viscosity |
|---|------------------|----------------------|
| 0 | 2 | 1.0 |
| 0.5 | 12 | 5.5 |
| 0.75 | 75 | 3.9 |
| 0.9 | 97 | 9.8 |
| 1.0 | 89 | 7.3 |

^a Conditions: 10 g. EO, 23 g. toluene, 0.30 g. Bu₂Zn, 24 hr. at 25°C.

Epichlorohydrin

Attempts to polymerize epichlorohydrin with dibutylzinc alone and the dibutylzinc–water system and the dibutylzinc–*n*-butanol system are shown in Table XV.

 TABLE XV
 Dibutylzinc-Catalyzed Polymerization of Epichlorohydrin^a

| Cocatalyst | Cocatalyst, moles/mole Bu ₂ Zn | Conversion, % | Appearance |
|------------------|---|------------------|------------|
| None | — | 1.9 | Oil |
| <i>n</i> -BuOH | 1.5 | 8.1 | Oil |
| H ₂ O | 0.75 | 8.7 | Oil |

^a Conditions: 10 g. epichlorohydrin, 15 g. toluene, 0.15 g. Bu₂Zn, 24 hr. at 90°C.

Although a slight cocatalytic effect is observed here, the failure to obtain high molecular weight polymer is thought to be due to side reactions between the catalyst and the reactive chlorine in the monomer.

Catalyst–Cocatalyst Reaction Products

A brief study was made of the reaction products resulting from the interaction of dibutylzinc with various cocatalysts such as water, methanol, and acetone in the absence of epoxide monomer. The cocatalyst was added to a toluene solution of dibutylzinc under an argon atmosphere. Samples were withdrawn from the vapor space above the liquid and analyzed by vapor-phase chromatography. Infrared spectra were obtained on the liquid. The vapor-phase chromatography experiments indicated that, in all cases, butane was the major gaseous product and that butene was present in lower concentrations. Also present, but in very low concentration were carbon dioxide, ethylene, and ethane. The most important feature of the infrared spectra of the liquid phase was the absence of hydroxyl, which was particularly surprising in the case of water. These data tend to confirm more quantitative experiments recently published.²

DISCUSSION

Water is by far the most effective promoter for organozinc compounds that has been found in the present investigation. The catalyst system, water-dialkylzinc, has been investigated over a wide range of ratios and concentrations. When used in a ratio of one mole of water to one mole of dialkylzinc, the resulting system has consistently given the highest conversions of epoxide monomers to linear polyethers of any of the catalyst systems studied. As indicated in Figure 1 with phenyl glycidyl ether monomer, the maximum conversion was obtained with one mole of water per mole of dibutylzinc. When the ratio of water to dibutylzinc was increased beyond this point, conversion decreased rapidly so that virtually no polymer was obtained at a ratio of two moles of water to one of dibutylzinc. Figure 2 shows the effect of concentration of a 1:1 water-dibutylzinc mixture on per cent conversion. At a concentration of 5% catalyst, based

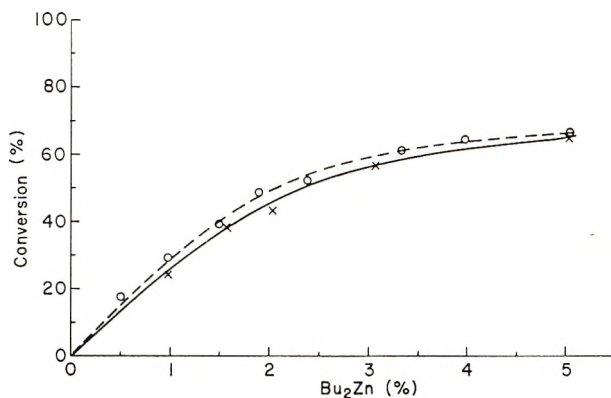


Fig. 2. Conversion vs. % Bu₂Zn: (---) 1:1 water; Bu₂Zn, 4 hr. at 90°C.; (—) 1.75:1 *n*-butanol; Bu₂Zn, 24 hr. at 90°C.

on the weight of monomer, a conversion of 65% polymer was obtained in 4 hr. at 90°C. Surprisingly, it was found that polymer reduced viscosity is not appreciably changed by varying catalyst concentration from 1 to 5%.

Conversions obtained with acetone cocatalyst were almost as high as those obtained with water. The most important differences in behavior are that acetone gives a maximum rate at about 1.25:1 molar ratio as compared to 1:1 molar ratio for water, and that at higher ratios (1.5:1 and 1.75:1) conversion and reduced viscosity drop off gradually whereas with water at these ratios both conversion and reduced viscosity drop off sharply. Comparative conversions are shown in Figure 1.

When primary aliphatic alcohols were used as cocatalysts, the maximum conversion occurred at a cocatalyst : catalyst ratio of about 1.25:1–1.5:1. If one plots cocatalyst : catalyst ratio versus conversion as shown in Figure 1, the curve obtained with *n*-butanol cocatalyst more closely resembles that obtained using acetone than it does that using water cocatalyst. When

various primary alcohols were used as cocatalysts, the differences in behavior exhibited by methanol, ethanol, and *n*-butanol were about that anticipated for the experimental error. When conversions obtained with a primary alcohol cocatalyst are compared with conversions obtained with water cocatalyst at various concentrations, it can be seen from Figure 2 that the conversions obtained with water are approximately six times that obtained with primary alcohol cocatalyst. As shown in Figure 3 when primary, secondary, and tertiary alcohols were used as cocatalysts, there was a steric effect and conversions with secondary and tertiary alcohols were lower by a factor of at least 5 than those obtained with primary alcohols.

A number of other compounds were tested qualitatively in order to determine what general types of compounds can act as cocatalysts for the dibutylzinc-catalyzed polymerization of phenyl glycidyl ether. Oxygen, which was introduced in the form of dry air, appears to be almost as

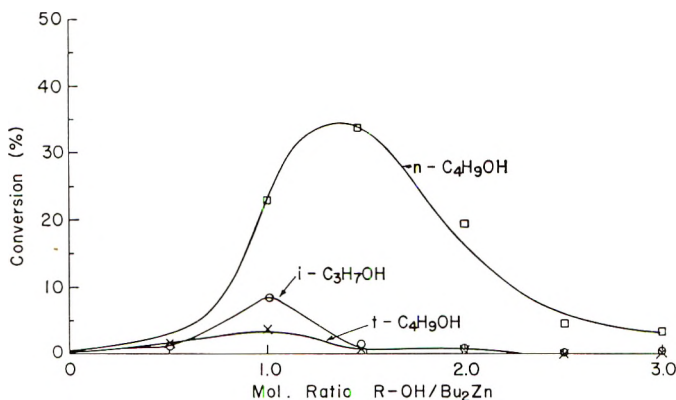


Fig. 3. Conversion vs. mole ratio ROH/Bu₂Zn in polymerization of 40% PGE in toluene with 1.5% Bu₂Zn, 24 hr. at 90°C.: (×) *tert*-butanol; (○) isopropanol; (□) *n*-butanol.

effective as water or acetone. Phenol and butyraldehyde were found to be relatively inactive, being comparable to tertiary butanol. Compounds that showed a slight positive effect include pyridine, diethylamine, and dibutyl sulfide. Thiophene and cyclohexene gave no effect. Acetic acid, ethyl acetate, and carbon dioxide appeared to have a negative effect, since very little or no polymer was isolated from these experiments.

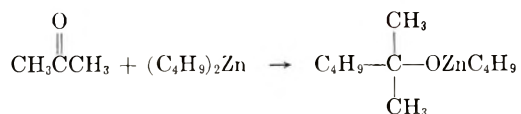
Three other epoxides, ethylene oxide, propylene oxide, and epichlorohydrin were also studied, although in not as great detail. Water had the same general effect when used as a cocatalyst with ethylene oxide and propylene oxide as was described in the case of phenyl glycidyl ether, i.e., water gave a maximum polymerization rate at a cocatalyst:catalyst ratio of about 1:1. Epichlorohydrin, on the other hand, gave no high molecular weight polymer with either water or *n*-butanol. Since it has been reported that epichlorohydrin will polymerize to high molecular weight polymer with a ferric chloride-propylene oxide complex,^{7,8} it is believed that this difference in

behavior is due to side reactions occurring between the active catalyst and the reactive chlorine of the monomer.

Confirmation of most of the general trends described above has been found in the current literature.^{1,2} Sakata, Furukawa, and co-workers, for example, have recently reported a study of the products formed in the reaction between diethylzinc and water. They postulate that the active catalyst is a polymer containing (ZnO) units ending in alkyl groups. When oxygen is present, alkoxide endgroups may also be formed.⁹ It is also reported that alkylzincs will not polymerize epoxides in the absence of cocatalysts. Our conclusions on the conversions induced by water and alcohols, the general stoichiometry of these reactions, and also the indication that oxygen is an effective cocatalyst have been confirmed.

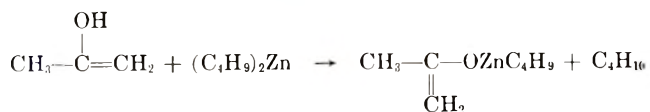
In the case of the alcohol cocatalysts, it can be seen that the steric requirements of the reaction product between the dialkylzinc and the alcohol is important in the polymerization mechanism. This is shown by the decrease in conversion as the alcohol is changed from *n*-butanol to isopropanol to tertiary butanol. Although we have not investigated the more sterically hindered catalyst-cocatalyst species with oxirane derivatives bearing a wide variety of substituents, it seems probable that steric requirements of this species would be more rigid in conjunction with the more highly hindered monomers. It is obvious that a considerable amount of work remains to be done in this field before the exact nature of the catalyst species and its reaction in the polymerization process can be determined.

One particularly puzzling aspect of the present work is the co-catalytic activity of acetone which is far superior to that of the primary alcohols and nearly as good as that of water. If addition to the carbonyl group is assumed, a tertiary alkoxide would be formed which presumably would resemble *tert*-butanol in cocatalytic reactivity:



In addition, this type of reaction does not account for the production of butane in the chromatography experiments nor for the general conception that dialkylzincs do not add to carbonyl groups in a manner analogous to Grignard reagents. Furthermore, reaction with *n*-butyraldehyde would lead to a secondary alkoxide, which would indicate that *n*-butyraldehyde should be a more active catalyst than acetone.

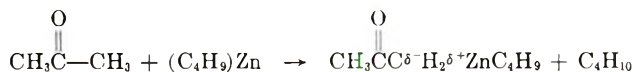
Reaction of the enol form of acetone would lead to an alkoxide which should resemble isopropanol in activity:



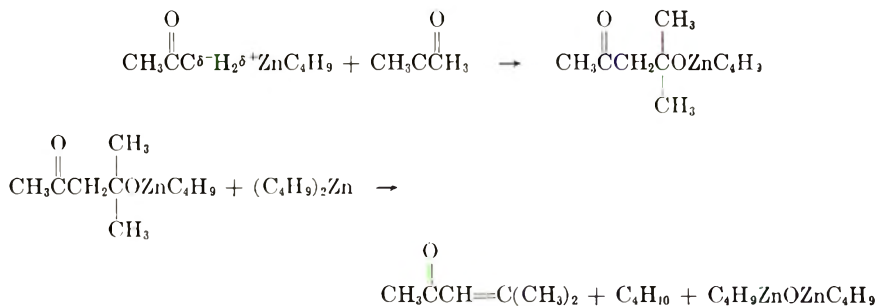
based on general steric considerations. Although the presence of the double

bond would alter the system electronically, it is felt that the magnitude of this effect would not be enough to account for the large difference in reactivity between acetone and isopropanol.

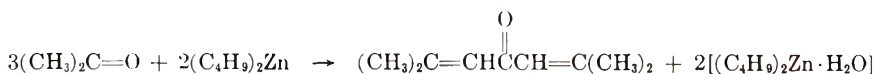
Rejection of the two hypotheses above leads to the possibility of reaction of dibutylzinc at the α -carbon atom to give butane and a zinc-carbon bond which, because of the carbonyl group, may be somewhat polarized:



It is difficult to see why this species would exhibit catalytic activity approximating that of water unless the carbonyl oxygen can coordinate to another zinc atom in such a way as to facilitate approach of the epoxide. In addition, with this mechanism, the difference in reactivity between butyraldehyde and acetone must be explained by the difference in acidities of the α -hydrogen atoms. One further reaction possibility of this species is the aldol reaction, which can give rise to water which may be acting as the cocatalyst:

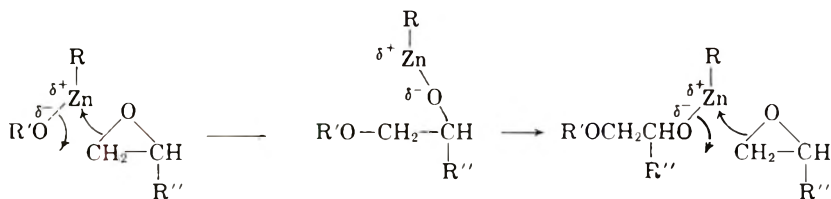


This reaction may continue with the alkyl zinc reacting with the remaining ketonic methyl group to give isophorone and the reaction products of water and dibutylzinc.¹⁰ The stoichiometry of the overall reaction would be:



where the product in brackets would be the same as that derived from the reaction of one mole of dibutylzinc with one mole of water, as discussed earlier. The optimum acetone:dibutylzinc ratio has been found to be 1.25:1; this would provide the same active catalyst that is obtained from water and dialkylzinc at a 0.84:1 ratio which is reasonably close to the 1:1 ratio observed.

Since the active catalysts studied may all be explained on the basis of intermediates having as a general structure $\text{R}(\text{ZnO})_n\text{R}'$, where R is alkyl or alkoxide, R' is alkyl, and n is 1 or higher, it is postulated that, in the general case, polymerization proceeds by the following mechanism:



The authors wish to thank Professor E. J. Corey for many helpful and stimulating discussions. They are also indebted to Miss O. M. Garty of these laboratories for the gas chromatographic analyses and the infrared spectra and to Mr. P. J. Capitano for assistance in conducting some of the experiments.

References

1. Furukawa, J., T. Tsuruta, R. Sakata, T. Saegusa, and A. Kawasaki, *Makromol. Chem.*, **32**, 90 (1959).
2. Sakata, R., T. Tsuruta, T. Saegusa, and J. Furukawa, *Makromol. Chem.*, **40**, 64 (1960).
3. Noshay, A., and C. C. Price, *J. Polymer Sci.*, **34**, 165 (1959).
4. Vandenberg, E. J., *J. Polymer Sci.*, **47**, 486 (1960).
5. *Organic Syntheses*, Coll. Vol. II, Wiley, New York, 1943, (a) p. 187, ref. 7; (b) *ibid.*, p. 184.
6. Vogel, A. I., *A Textbook of Practical Organic Chemistry*, 3rd ed., Longmans, Green, New York, 1956, p. 167.
7. Ishida, S., and S. Murahashi, *J. Polymer Sci.*, **40**, 571 (1959).
8. Baggett, J. M., and M. E. Pruitt, U. S. Pat. 2,871,219 (January 27, 1959).
9. Abraham, M. H., *J. Chem. Soc.*, **1960**, 4130.
10. Coates, C. E., *Organo-Metallic Compounds*, 2nd ed., Wiley, New York, 1960, p. 66.

Synopsis

A study of the nature and quantity of materials that will react with dibutylzinc to act as cocatalysts for the polymerization of phenyl glycidyl ether has led to the finding of several very effective catalyst systems. These cocatalysts may be grouped in the following classifications: (1) highly effective: water and acetone; (2) effective: methanol, ethanol, *n*-butanol, and oxygen; (3) slightly effective: isopropanol, *tert*-butanol, diethylamine, *n*-butylaldehyde, and phenol; and (4) inhibitors: acetic acid, ethyl acetate, and carbon dioxide. The poly(phenyl glycidyl ether) produced by these catalysts is a high melting (204°C.), high molecular weight crystalline polymer which is insoluble in most common organic solvents. Ethylene oxide and propylene oxide have also been polymerized by the dibutylzinc-water system to high molecular weight polymers in high yield. Epichlorohydrin, on the other hand, gave only low molecular weight oils in low yields, probably due to reaction of the catalyst species with the reactive chlorine of the monomer.

Résumé

Une étude de la nature et de la quantité de matériaux qui peuvent réagir avec le zincdibutyle pour jouer le rôle de cocatalyseur pour la polymérisation de l'éther phényl-glycidique a conduit à la découverte de plusieurs systèmes catalyseurs très efficaces. Les cocatalyseurs peuvent être groupés d'après la classification suivante: (1) efficacité élevée: eau et acétone; (2) efficacité: méthanol, éthanol, *n*-butanol, et oxygène; (3) légèrement efficace: isopropanol, butanol tertiaire, diéthylamine, *n*-butylaldéhyde et phénol; (4) inhibiteurs: acide acétique, acétate d'éthyle et anhydride carbonique. Le polyphényl-glycidyl-éther, produit par les catalyseurs, à un point de fusion élevé (240°C.)

et est un polymère cristallin de haut poids moléculaire qui est insoluble dans la plupart des solvants organiques ordinaires. L'oxyde d'éthylène et l'oxyde de propylène ont aussi été polymérisés par le système eau-zinc dibutyle pour fournir des polymères de poids moléculaires élevés avec un rendement élevé. L'épichlorohydrine, d'autre part, donne seulement des huiles de poids moléculaires faibles avec de faibles rendements, probablement à cause de la réaction du catalyseur avec le chlore actif du monomère.

Zusammenfassung

Eine Untersuchung der Natur und Menge der Stoffe, die mit Dibutylzink reagieren und dadurch als Cokatalysatoren für die Polymerisation von Phenylglycidyläther wirken, hat zu der Auffindung einiger sehr wirksamer Katalysatorsysteme geführt. Diese Cokatalysatoren können in folgender Weise in Gruppen eingeteilt werden: (1) Hochgradig wirksam: Wasser und Aceton; (2) Wirksam: Methanol, Äthanol, *n*-Butanol und Sauerstoff; (3) Schwach wirksam: Isopropanol, *tert*-Butanol, Diäthylamin, *n*-Butyraldehyd und Phenol; (4) Inhibitoren: Essigsäure, Äthylacetat und Kohlendioxyd. Der mit diesen Katalysatoren erzeugte Poly(phenylglycidyläther) ist ein hochschmelzendes (204°C.), hochmolekulares, kristallines Polymeres, das in den meisten, üblichen organischen Lösungsmitteln unlöslich ist. Äthylenoxyd und Propylenoxyd wurden mit dem Dibutylzink-Wassersystem ebenfalls in hoher Ausbeute zu hochmolekularen Polymeren polymerisiert. Andererseits gab Epichlorhydrin nur niedermolekulare Öle in geringer Ausbeute, was wahrscheinlich auf eine Reaktion des Katalysators mit dem reaktionsfähigen Chlor des Monomeren zurückzuführen ist.

Received September 9, 1961

Revised November 24, 1961

Molecular Weight Distribution of Linear Polyethylene by Sedimentation Velocity Analysis

H. W. McCORMICK, *Physical Research Laboratory,
The Dow Chemical Company, Midland, Michigan*

Introduction

Several reports¹⁻⁷ have been given describing the determination of the molecular weight distribution of polyethylene principally employing methods of fractionation based on the solubility properties of polymer molecules; however, techniques based on the sedimentation properties of polymer molecules have received very little attention largely due to the need for rather specialized equipment. The successful application of sedimentation velocity techniques in determining the molecular weight distribution of polystyrene^{8,9} and poly- α -methylstyrene¹⁰ along with the availability of a high temperature chamber for the Spinco model E ultracentrifuge has led to increased interest in sedimentation studies on polyethylene. The present work will report the use of sedimentation velocity experiments to determine the molecular weight distribution of linear polyethylene and show the comparison of results obtained by this method with those obtained by solution precipitation fractionation.

Experimental

Materials

Fractions of linear polyethylene and polymethylene obtained by the solution precipitation fractionation of, respectively, a typical high density polyethylene and a polymethylene made by the copper-catalyzed decomposition of diazomethane were furnished by L. H. Tung of The Dow Chemical Co. Inherent viscosities of these samples also furnished by L. H. Tung were measured in Tetralin at 130°C.

Sedimentation Velocity

A Spinco model E ultracentrifuge adapted with a high temperature chamber was employed for the sedimentation velocity experiments. Runs were made at 110°C. in α -bromonaphthalene at polymer concentrations between 0.1 and 0.6 g./100 ml. All runs were made at a rotational speed of 52,640 rpm, the top allowable speed at this temperature. Schlieren patterns produced by the Philpot-Svensson optical system were photographi-

cally recorded at known time intervals with the boundary curves being measured by tracing enlarged projections on graph paper.

Results and Discussion

Molecular weight distributions can be obtained by analysis of the progressive spreading of the sedimentation boundary taking place during sedimentation velocity experiments. It has been shown that separation of the polymer molecules in this sedimenting boundary can best be achieved in a θ -solvent.⁸ Good molecular separation can also be obtained in better

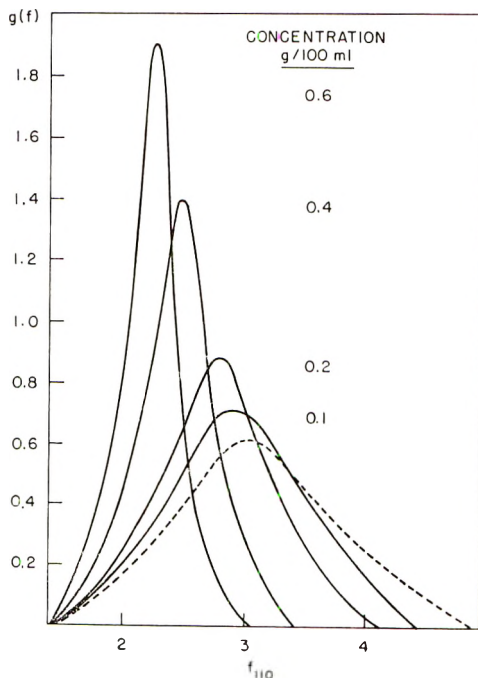


Fig. 1. Apparent distributions of flotation constants for high density polyethylene (E15) at increasing concentrations in α -bromonaphthalene. The broken line represents the curve obtained by the analytical extrapolation of the 0.2 g./100 ml. curve to zero concentration.

solvents at much lower concentrations; however, there exists a practical concentration limit below which the sedimentation boundary can no longer be detected by the schlieren optical system. Success of the sedimentation velocity method, therefore, depends to a large extent upon the solvent employed. The choice of solvent becomes somewhat of a problem for polyethylene, for one is forced to use a solvent having a θ -temperature below the operational temperature since the crystalline melting point of polyethylene is above the top operational temperature, 120°C., for the ultracentrifuge. For the present study the solvent, α -bromonaphthalene, was employed because of its advantageous density and refractive index along

with its moderately poor solubility characteristics. Results from this study might well be improved by the use of a θ -solvent above the crystalline melting point when and if the operational range of the ultracentrifuge is extended to higher temperatures.

Owing to the high density of α -bromonaphthalene the ultracentrifugation of polyethylene in this solvent leads to a flotation process. Refractive index gradient curves recorded during this flotation process are converted to distributions of flotation constants according to the method of Signer and Gross.¹¹ Effects of diffusion are eliminated by graphical extrapolation to infinite time according to the method of Williams and Baldwin.¹² The concentration dependence of flotation, which is rather great in this case owing to the use of a moderately good solvent as shown in Figure 1, is corrected for by an analytical extrapolation to zero concentration according

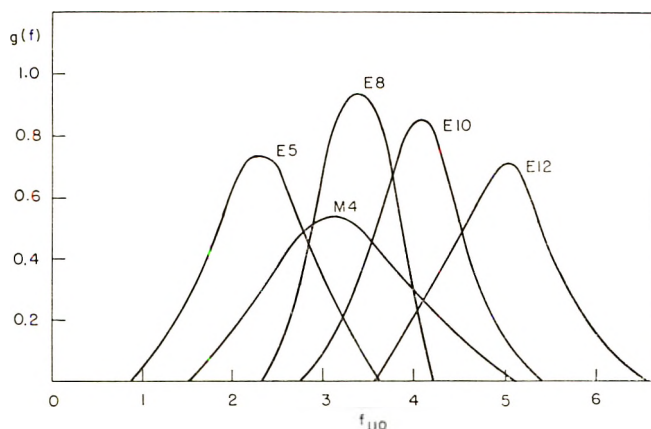


Fig. 2. Distributions of flotation constants for four fractions of high density polyethylene (E) and one fraction of polymethylene (M).

to the method of Baldwin.¹³ Application of this method requires knowledge of the dependence of the flotation constant on concentration which for this system at low concentrations is found to be well represented by $f = f_0 (1 - 0.15 f_0 c)$ where c is the concentration in g./100 ml. and f the flotation constant in Svedberg units. Corrected distributions of flotation constants have been determined for 16 fractions of high density polyethylene and 4 fractions of polymethylene with representative curves shown in Figure 2.

Conversion of the flotation curves to molecular weight distribution curves requires the relationship between the flotation constant and molecular weight which has been obtained by relating the weight-average molecular weight of these fractions to the corresponding average flotation constant. The weight-average molecular weights obtained from viscosity according to the relationship of Tung¹⁴

$$[\eta] = 4.60 \times 10^{-4} \bar{M}_w^{0.725} \quad (1)$$

TABLE I
Molecular Parameters Obtained from Viscosity and Flotation Measurements

| Sample | η^a | \bar{M}_w^b | \bar{M}_n | \bar{f}_{110} | \bar{M}_w^c | \bar{M}_n^c | \bar{M}_w/\bar{M}_n^c |
|---------------------------|----------|---------------------|---------------------|-----------------|---------------|---------------|-------------------------|
| High Density Polyethylene | | | | | | | |
| E1 | 0.17 | 3,500 | | 1.33 | 3,800 | 1,600 | 2.37 |
| E2 | 0.25 | 5,800 | 3,540 ^d | 1.46 | 5,000 | 2,100 | 2.38 |
| E3 | 0.32 | 8,460 | 7,660 ^d | 1.82 | 9,400 | 4,300 | 2.08 |
| E4 | 0.35 | 9,400 | | 1.65 | 7,200 | 3,700 | 1.95 |
| E5 | 0.65 | 22,300 | | 2.41 | 22,100 | 13,600 | 1.62 |
| E6 | 0.95 | 37,400 | | 2.84 | 35,700 | 27,000 | 1.32 |
| E7 | 1.14 | 47,800 | | 3.11 | 45,700 | 38,000 | 1.20 |
| E8 | 1.35 | 61,000 | | 3.39 | 58,000 | 53,500 | 1.08 |
| E9 | 1.58 | 75,300 | | 3.66 | 73,500 | 66,000 | 1.11 |
| E10 | 1.82 | 91,300 | | 4.10 | 103,000 | 94,000 | 1.09 |
| E11 | 2.60 | 150,000 | | 4.58 | 142,000 | 129,000 | 1.10 |
| E12 | 3.08 | 189,000 | | 5.07 | 183,000 | 165,000 | 1.10 |
| E13 | 4.01 | 274,000 | | 5.48 | 245,000 | 145,000 | 1.69 |
| E14 ^f | | 34,000 ^e | 28,800 ^e | 2.84 | 35,000 | 23,500 | 1.48 |
| E15 ^f | | 49,000 ^e | 41,500 ^e | 3.22 | 50,000 | 36,500 | 1.37 |
| E16 ^f | | 73,000 ^e | 50,300 ^e | 3.72 | 78,000 | 48,000 | 1.62 |
| E17 ^e | | | | | 58,000 | 6,400 | 9.06 |
| Polymethylene | | | | | | | |
| M1 | 0.21 | 4,700 | 3,750 ^d | 1.42 | 4,600 | 1,700 | 2.70 |
| M2 | 0.47 | 14,200 | | 2.03 | 13,400 | 6,500 | 2.08 |
| M3 | 0.64 | 21,800 | | 2.39 | 21,200 | 11,800 | 1.79 |
| M4 | 1.25 | 55,000 | | 3.35 | 58,000 | 36,000 | 1.61 |

^a Inherent viscosity (for polyethylene its value is essentially that of intrinsic viscosity) in Tetralin at 130°C.

^b Determined from viscosity.

^c Determined from molecular weight distribution curves obtained by solution precipitation fractionation by Tung.

^d Determined by ebulliometry.

^e Determined from molecular weight distribution curves obtained by sedimentation velocity analysis.

^f Crude fractionation.

^g Mixture of high and low molecular weight fractions.

are listed in Table I along with the corresponding average flotation constants determined by the relationship¹⁵

$$\bar{f} = \left[\int_0^\infty f^{1/a} g(f) df \right]^{1/a} \quad (2)$$

where a is given by

$$f = KM^a \quad (3)$$

The value for a of $1/3$ for use in eq. (2) was determined from a log-log plot of the flotation constant at the peak maximum against the weight-average molecular weight. A log-log plot of the average flotation constant against the weight-average molecular weight shown in Figure 3 leads to the following relationship:

$$f = 7.74 \times 10^{-2} M^{0.344} \quad (4)$$

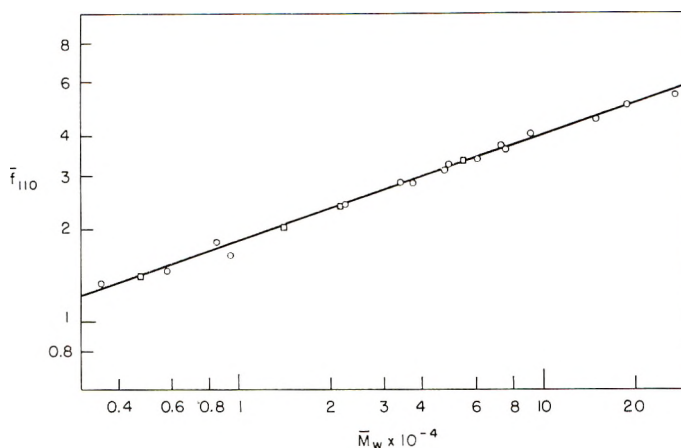


Fig. 3. A log-log plot of the average flotation constant and the weight-average molecular weight for several fractions of high density polyethylene (O) and polymethylene (\square).

It should be noted that the polymethylene and high density polyethylene samples follow the same relationship. By use of this equation the distribution of flotation constants can be converted directly to a molecular weight distribution merely by a change of variables. Figure 4 gives such molecular weight distribution curves which correspond to the distribution of flotation constants shown in Figure 2. Weight-average and number-average molecular weights calculated from the molecular weight distribution curves by proper summation processes are listed in Table I along with the \bar{M}_w/\bar{M}_n ratio. This heterogeneity index shows that the polyethylene fractions in the molecular weight range from 30,000 to 200,000 have a

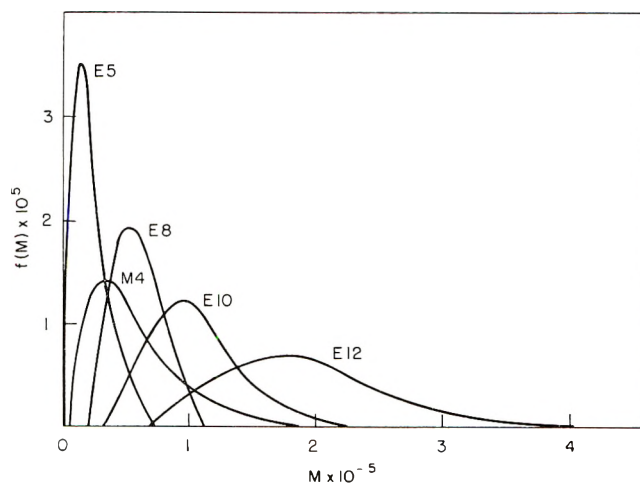


Fig. 4. Molecular weight distributions of four fractions of high density polyethylene (E) and one fraction of polymethylene (M).

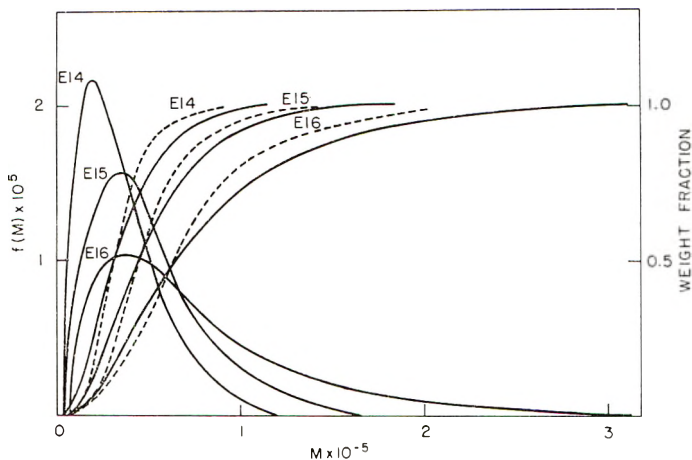


Fig. 5. Differential and integral molecular weight distributions for three crude fractions of high density polyethylene. The solid curves were obtained by sedimentation velocity analysis and the broken curves were obtained by Tung using solution precipitation fractionation.

fairly narrow molecular weight distribution while the others fall off considerably.

In view of the fact that a Θ -solvent was not employed as evidenced by the low value of the exponent in eq. (4) the flotation of polymer molecules in this system is less sensitive to molecular weight and the accuracy cannot be as great as could be expected for an ideal Θ -solvent. In order to gain some idea of the accuracy involved it seemed desirable to compare the results obtained by sedimentation techniques with those obtained by solu-

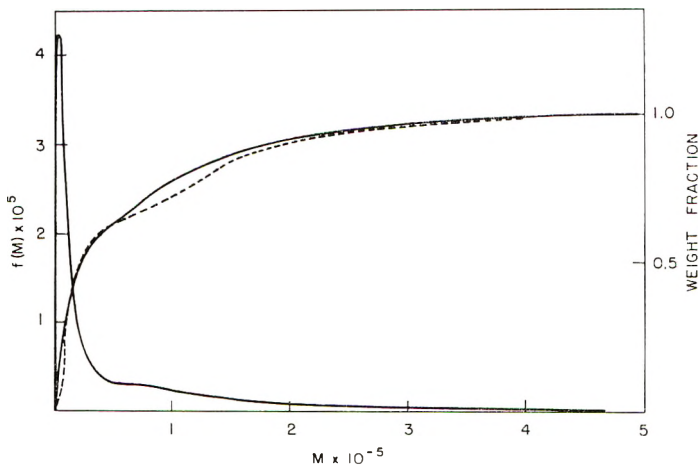


Fig. 6. Differential and integral molecular weight distributions for a synthetic mixture of two fractions of high density polyethylene. The solid curves were obtained by sedimentation velocity analysis and the broken curve was obtained by Tung using solution precipitation fractionation.

tion fractionation techniques. Figure 5 gives the differential and integral molecular weight distribution curves obtained by the present sedimentation method along with the integral molecular weight distribution curves obtained by Tung who employed solution precipitation fractionation methods for three crude fractions of high density polyethylene. The agreement is fairly good with both methods showing the same molecular weight for 50% material; however, in general the sedimentation technique exhibits a somewhat broader molecular weight distribution than for the fractionation technique. A more severe test is shown in Figure 6 which gives a similar comparison of the molecular weight distribution curves obtained for a synthetic mixture of a high and a low molecular weight fraction of high density polyethylene.

This study has demonstrated the applicability of sedimentation techniques for measuring the molecular weight distribution of linear polyethylene when employing a non- θ -solvent at elevated temperatures as evidenced by the rather good resolution of the extremely broad distribution synthetic mixture (E17). It should be pointed out that sedimentation does not depend simply upon molecular weight but also upon the radius of gyration which is effected by branching in the polymer molecules; therefore, before attempting to apply the present method to branched polyethylene it will be necessary to make a thorough investigation into the effect of branching on the sedimentation properties.

The author wishes to thank Mr. F. W. Kristal for carrying out the centrifugal experiments.

References

1. Tung, L. H., *J. Polymer Sci.*, **24**, 333 (1957).
2. Wesslau, H., *Makromol. Chem.*, **20**, 111 (1956).
3. Nicholas, L., *Compt. rend.*, **242**, 2720 (1956).
4. Francis, P. S., R. S. Cooke, Jr., and J. H. Elliott, *J. Polymer Sci.*, **31**, 453 (1958).
5. Henry, P. M., *J. Polymer Sci.*, **36**, 3 (1959).
6. Kenyon, A. S., and I. O. Salyer, *J. Polymer Sci.*, **43**, 427 (1960).
7. Guillet, J. E., R. L. Combs, D. F. Slonaker, and H. W. Coover, *J. Polymer Sci.*, **47**, 307 (1960).
8. McCormick, H. W., *J. Polymer Sci.*, **36**, 341 (1959).
9. Cantow, H. J., *Makromol. Chem.*, **30**, 169 (1959).
10. McCormick, H. W., *J. Polymer Sci.*, **41**, 327 (1959).
11. Signer, R., and H. Gross, *Helv. Chim. Acta*, **17**, 726 (1934).
12. Williams, J. W., and R. L. Baldwin, *J. Am. Chem. Soc.*, **74**, 1542 (1952).
13. Baldwin, R. L., *J. Am. Chem. Soc.*, **76**, 402 (1954).
14. Tung, L. H., *J. Polymer Sci.*, **36**, 287 (1959).
15. Baldwin, R. L., and K. E. van Holde, *Fortschr. Hochpolym.-Forsch.*, **1**, 451 (1960).

Synopsis

The molecular weight distribution of high density polyethylene and polymethylene has been measured by analysis of sedimentation velocity experiments carried out at high temperatures. The solvent, α -bromonaphthalene, produced less sensitivity of flotation to molecular weight than could be expected for a highly desirable but presently impossible

Θ -solvent. The molecular weight distributions obtained by this method are compared with those obtained by solution precipitation fractionation procedures.

Résumé

La répartition des poids moléculaires du polyéthylène et du polyméthylène de haute densité a été mesurée par l'analyse de la vitesse de sédimentation à températures élevées. Le solvant (α -bromonaphtalène) provoque moins de flotation en ce qui concerne le poids moléculaire, que ce qu'on aurait pu prévoir normalement pour un solvant Θ hautement souhaitable mais actuellement non-disponible. Les répartitions des poids moléculaires obtenues par cette méthode sont comparées à celles obtenues par la méthode de précipitation fractionnée.

Zusammenfassung

Die Molekulargewichtsverteilung von Polyäthylen hoher Dichte und Polymethylen wurde durch Auswertung von Sedimentationsgeschwindigkeitsversuchen bei hoher Temperatur bestimmt. Das Lösungsmittel, α -Bromnaphthalin, zeigt eine geringere Flotationsempfindlichkeit für das Molekulargewicht als für ein zwar wünschenswertes aber gegenwärtig nicht vorhandenes Θ -Lösungsmittel erwartet werden könnte. Die nach dieser Methode erhaltenen Molekulargewichtsverteilungen werden mit solchen verglichen, die durch ein Lösungs-Fällungsfraktionierungsverfahren erhalten wurden.

Received October 6, 1961

Copolymerization of α -Pyrrolidone and ϵ -Caprolactam

FUMIO KOBAYASHI and KOICHI MATSUYA, *Nippon Rayon Co., Ltd.,
Research Institute, Uji, Kyoto, Japan*

INTRODUCTION

The alkaline polymerization of ϵ -caprolactam has been extensively studied,¹⁻⁵ and Ney and others^{6,7} reported the polymerization of α -pyrrolidone in the presence of an alkaline catalyst. The copolymerization of these monomers seems possible because of their similarities in chemical constitutions and polymerization conditions. The purpose of this study is to find the optimal conditions for the copolymerization and to obtain some information on the polymerization mechanism and the properties of prepared copolymers.

EXPERIMENTAL

The α -pyrrolidone (PY) used was commercial material, distilled, recrystallized from acetone, redistilled, and dried under reduced pressure over P_2O_5 , m.p. 26-27°C.

ϵ -Caprolactam (CL) was commercial material, treated in the same way as α -pyrrolidone, m.p. 69-70°C.

N-Acetyl- α -pyrrolidone and *N*-acetyl- ϵ -caprolactam were prepared by acetylation of α -pyrrolidone and ϵ -caprolactam, respectively, with acetic anhydride, distilled before use; b.p. *N*-acetyl- α -pyrrolidone 118°C./20 mm., b.p. *N*-acetyl- ϵ -caprolactam 102°C./11 mm.

Acetyl compounds have been found effective in alkaline polymerization of lactams.⁸ Particularly, the copolymerization of ϵ -caprolactam and α -pyrrolidone succeeded in the presence of acetyl compounds. In order to eliminate the effect caused by the differences in compositions of acetyl compounds, acetyl compounds were added in the same mole ratio as that of monomeric lactams.

Polymerization

A mixture of lactams and alkali metal was mixed in a glass cylinder equipped with a capillary, an inlet tube with a stop cock, and an outlet. The mixture was heated for 2 hr. at 50°C. and then an additional 2 hr. at 70°C. under 10 mm. Hg pressure. After the reaction of sodium and lactams had gone to completion, the acetyl compounds were added through the inlet at 50°C. The reactants were heated at 90, 110, or 130°C. The

resulting product was extracted with carbon tetrachloride for 8 hr. The unextracted residue was dissolved into 96% H_2SO_4 and the solution viscosity was measured at 30°C.

Infrared Absorption Measurements

It was difficult to determine the composition of the polymer produced by the usual methods of chemical analysis because of the similar chemical composition of both lactams.

The nitrogen content, for example, is 16.46 wt.-% for poly- α -pyrrolidone and 12.38 wt.-% poly- ϵ -caprolactam, and an unavoidable experimental error in determining the nitrogen content, even if it is very minor, would give a large effect on evaluation of the polymer composition.

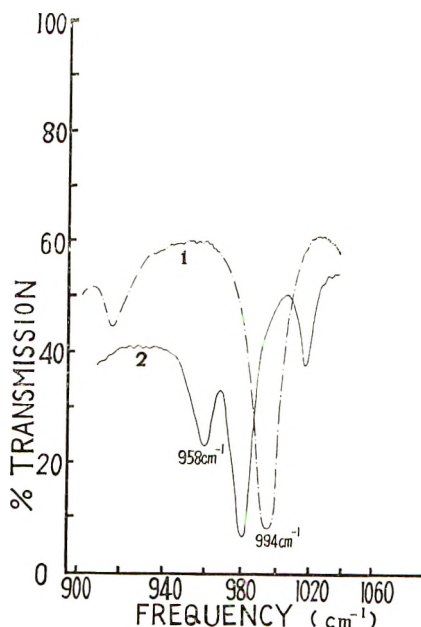


Fig. 1. Infrared absorption characteristics of (1) α -pyrrolidone; (2) ϵ -caprolactam.

To avoid these difficulties, infrared absorption measurement was adopted to obtain the polymer composition. After the carbon tetrachloride had been evaporated from the extracts, the infrared spectra of the residues were measured to determine the mole ratio of two monomers, which served as a measure of the polymer composition. The chromatographic analysis showed that the residue consisted of α -pyrrolidone and ϵ -caprolactam. The infrared spectra of the two lactams showed remarkable differences in the range between 915–1010 cm^{-1} (Fig. 1). The absorptions in this range seem to be those of ring deformations which vary according to the number of carbon atoms in the cycloalkanes (cyclopentane 890–980 cm^{-1} and cyclohexane 950–1055 cm^{-1}).⁹

The spectra were recorded with a Perkin-Elmer model 13 double-beam spectrophotometer equipped with a sodium chloride prism. As characteristic absorptions, the one at 958 cm.^{-1} for caprolactam and another at 994 cm.^{-1} for pyrrolidone were chosen.

On the assumptions that Lambert-Beer's law is applicable to this case the following equation is obtained:

$$D_{958}/D_{994} = KC_{CL}/C_{PY}$$

where D_{958} and D_{994} are optical densities at 958 cm.^{-1} and 994 cm.^{-1} , respectively, C_{CL} and C_{PY} are concentrations of each monomer, and K is a constant. By mixing two monomers in variable ratios this linear relationship was found to be valid, and K was determined as 0.501 as shown in Figure 2.

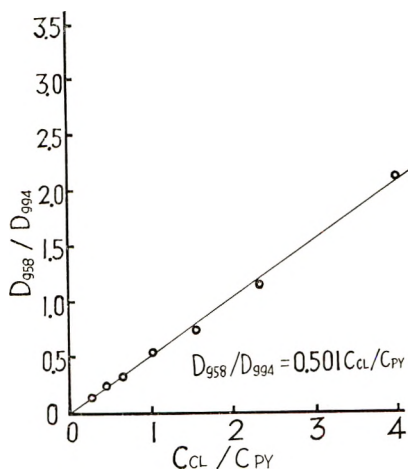


Fig. 2. Optical density ratio vs. ratio of monomers in mixture.

RESULTS

A mixture of 5 g. of caprolactam and 5 g. of pyrrolidone was polymerized under variable conditions. Figure 3 shows the variation of conversion and solution viscosity with the change in the amount of sodium, and Figure 4 shows the variation with change in the amount of acetyl compounds. In all cases, acetyl compounds were added at 50°C . and the mixture was heated for 4 hr. at 110°C . From Figures 3 and 4 it was found that a large quantity of catalyst was necessary to obtain a good yield. Even when a smaller amount of catalyst was employed, viscosities of the produced polymers were low. In most of the experiments 8.4 mole-% of sodium and 3.1 mole-% of acetyl compounds were used.

Changes in conversion and viscosity with time at different temperatures are shown in Figures 5 and 6, respectively. Relatively good yields and high viscosities are obtained at high temperatures but, as will be stated

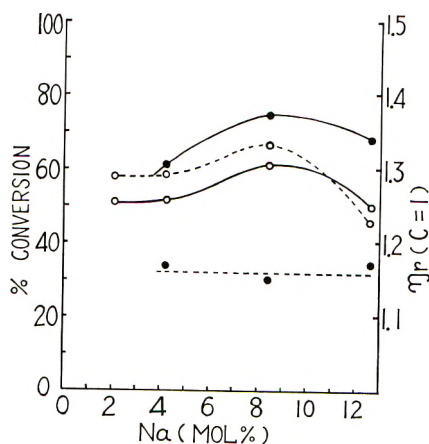


Fig. 3. Effect of sodium concentration on (—) conversion of monomer to polymer and (---) solution viscosity η_{rel} at various levels of *N*-acetyl- α -pyrrolidone: (O) 3.1 mole-%; (●) 6.2 mole-%.

below, they are mostly due to the increase of the caprolactam content in copolymers.

The changes in conversions and viscosities with monomer ratio in the starting materials are shown in Figure 7, together with the change in melting point of the polymer, which was measured by the capillary tube method. The conversions and viscosities show complicated behavior while the melting point curve shows a characteristic V shape. The decrease in melting points is thought to be evidence for the fact that the obtained polymers are not blends of the homopolymers but contain copolymers of two lactams. In order to eliminate the effect of molecular weight on melting points of copolymers, the melting points of the polymers of similar vis-

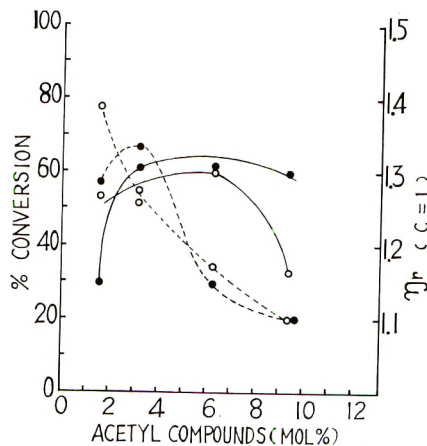


Fig. 4. Effect of concentration of acetyl compounds on (—) conversion of monomer to polymer and (---) solution viscosity at various levels of sodium: (O) 4.2 mole-%; (●) 8.4 mole-%.

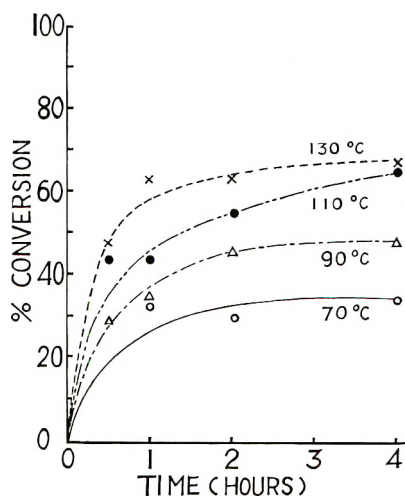


Fig. 5. Copolymerization at various temperatures. α -Pyrrolidone, 5 g.; ϵ -caprolactam, 5 g.; sodium, 8.4 mole-%; acetyl compounds, 3.1 mole-%.

cosities ($\eta_{relc=1.0} = 1.29-1.31$) were measured. Figure 8 shows the result which gives the evidence of the copolymerization.

In addition to this fact, the copolymer shows good solubility in alcohol as is shown in Table I. In this case also copolymers of similar viscosities were chosen ($\eta_{relc=1.0} = 1.39-1.40$). The amount of residue insoluble in ethanol is minimum when the polymer composition is 1:1. The fourth column in Table I shows the amount of polymer reprecipitated from ethanol after cooling. The value in parentheses in the fifth column is the solution viscosity of reprecipitated polymer. It is evident that good

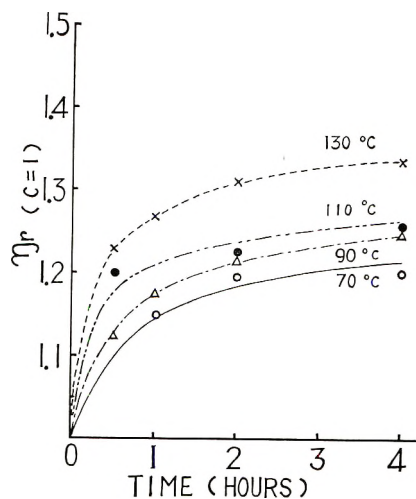


Fig. 6. $\eta_{rel} (c = 1.0)$ vs. time at various temperatures. α -Pyrrolidone, 5 g.; ϵ -caprolactam, 5 g.; sodium, 8.4 mole-% acetyl compounds, 3.1 mole-%.

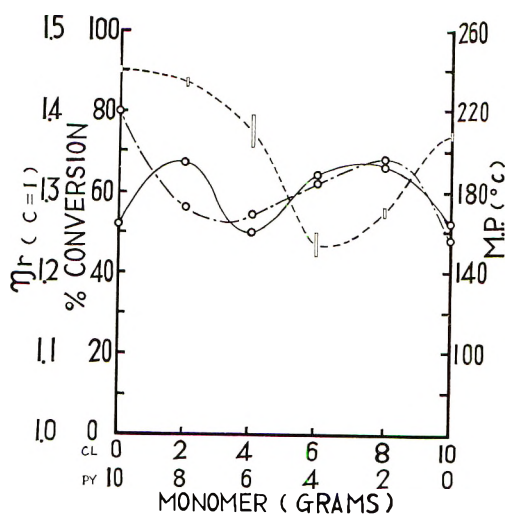


Fig. 7. Effect of monomer ratio in starting mixture on: (—) conversion; (---) solution viscosity; (· · ·) melting point of copolymer.

solubility is not a result of the low molecular weight, but it is one of the properties of copolymers.

The composition was followed by means of this infrared absorption analysis on polymerization at 90°C. The cases of monomer ratios (in weight) of 8:2, 5:5, and 2:8 are shown in Figures 9, 10, and 11, respectively. It is shown that pyrrolidone polymerizes at the early stage of reaction and in the pyrrolidone-rich system it slightly decomposes on prolonged heating. On the other hand, caprolactam comes into the polymer at a steady rate. The differences in polymerization behaviors of two lactams is more prominent at high temperature. The dotted lines in Figure 10 show the behavior at 130°C. Comparison between the change at 90°C. and that at 130°C. shows that the increase in conversion is due mainly to the increase of caprolactam component in polymer.

TABLE I
Solubility of Copolymers in Ethanol

| Polymer composition | | Residue not extracted by hot ethanol, wt.-% | Reprecipitate after cooling, wt.-% | Solution viscosity η_{rel} at $c = 1.0$ |
|---------------------|---------------------|---|------------------------------------|--|
| Caprolactam, mole-% | Pyrrolidone, mole-% | | | |
| 100 | 0 | 92 | — | 1.44 |
| 80 | 20 | 88 | 2 | 1.40 |
| 49 | 51 | 40 | 31 | 1.38 |
| | | | | (1.44) |
| 16 | 84 | 87 | 3 | 1.38 |
| 0 | 100 | 92 | — | 1.40 |

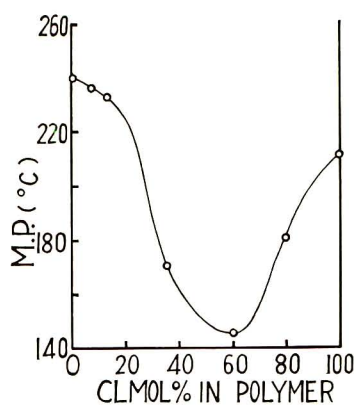


Fig. 8. Melting points of copolymers having similar solution viscosities at $c = 1.0$ ($\eta_{rel} = 1.29-1.31$) as a function of CL content of the copolymer.

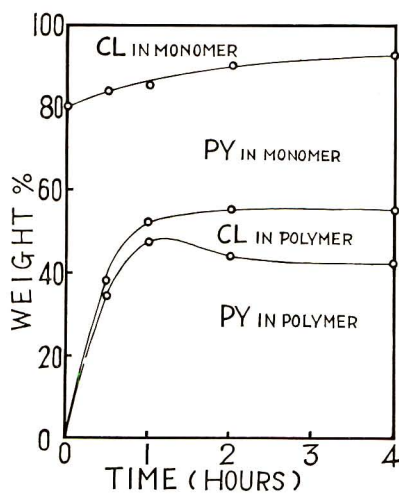


Fig. 9. Polymer composition vs. time α -Pyrrolidone, 8 g.; ϵ -caprolactam, 2 g.; 90°C.

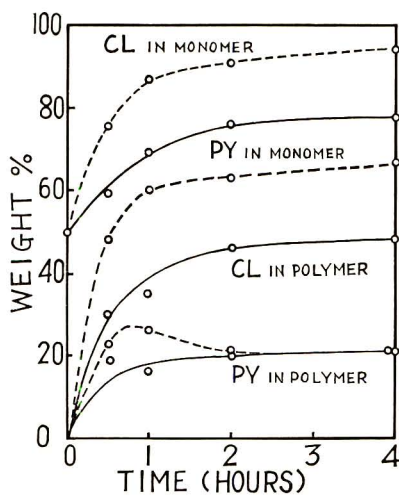


Fig. 10. Polymer composition vs. time for copolymerization at: (—) 90°C.; (---) 130°C. α -Pyrrolidone, 5 g.; ϵ -caprolactam, 5 g.

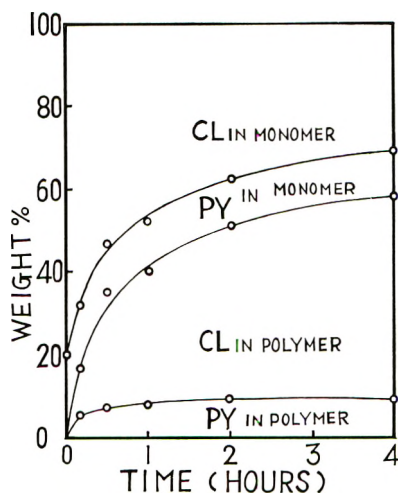


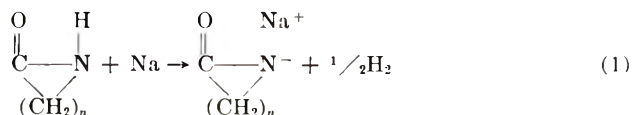
Fig. 11. Polymer composition vs. time. α -Pyrrolidone, 2 g.; ϵ -caprolactam, 8 g.; 90°C.

DISCUSSION

The mechanism of alkaline polymerization of lactams has been discussed by many authors,^{1-5,8,10} and the reaction is considered to consist of the following five reactions: (1) formation of alkali-metal salt; (2) initiation; (3) propagation; (4) termination; (5) degradation.

Formation of Alkali-Metal Salt

The lactams react with alkali metal to form their alkali salt accompanied with generation of hydrogen.

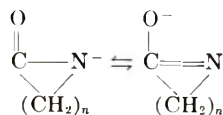


This reaction seems to proceed at a rapid rate when the product has a lower energy and there is maximum delocalization of the negative charge. The following reaction proves this assumption:¹¹



In other words, the compounds with stronger "acidities" react with alkali metal more rapidly than the weaker ones.

In lactams the following resonance will decide their acidities in the same way as in carboxylic acids:



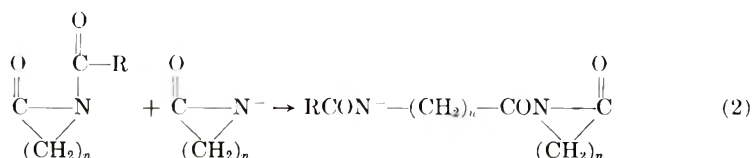
Caprolactam, having two more methylene groups which have an $-I_s$ effect, may be a weaker acid than pyrrolidone.

In reality, pyrrolidone reacts with sodium with much greater speed than

caprolactam. When sodium is made to react with pyrrolidone at 70°C. the reaction is complete in a few minutes, while it takes several hours to reach completion with caprolactam.

Initiation

The following scheme is presumed:¹⁰



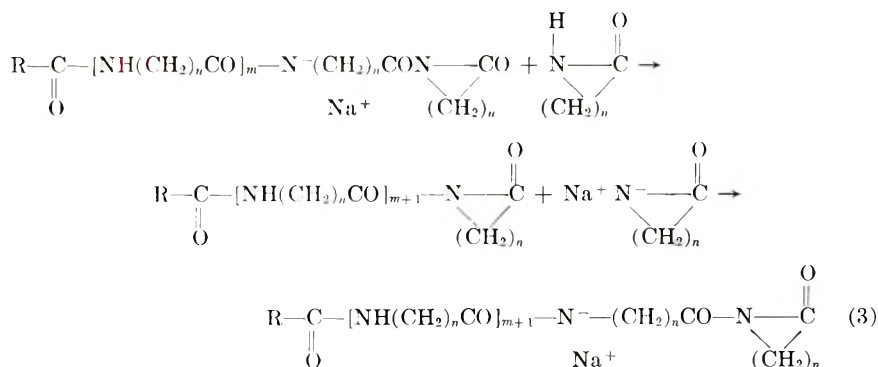
It is found that the polymerization of pyrrolidone alone produces polymers of a comparatively higher degree of polymerization with low yield. This means that the number of chain molecules is few. The increase in the number of chains with increase in caprolactam content can be observed at the pyrrolidone-rich range in Figure 7. Rough estimation shows that in caprolactam polymerization the chain number is about 80% of added acetyl compounds while in pyrrolidone system it is about 40%.

The reverse reaction of reaction (2) may exist, and the stability of the pyrrolidone anion will promote this reverse reaction to decrease the number of chains in the polymerization system.

Propagation

It is interesting to know that pyrrolidone, which has the smallest strain among lactams and would not polymerize in the hydrolytic system, shows a remarkably rapid reaction rate in alkaline polymerization.

The generally admitted propagation scheme is as follows:¹⁰

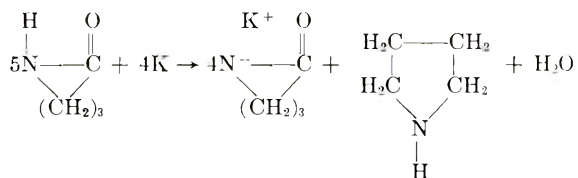


This means that lactam does not enter into the polymer chain directly but does after the formation of its sodium salt. This assumption is suitable to explain the observed results. In the first step in reaction (3), most of the sodium salt formed may be that of pyrrolidone because of the simplicity of the formation of pyrrolidone salt. This would lead to the rela-

tively more rapid polymerization of pyrrolidone compared to caprolactam in the copolymerizing system.

Termination

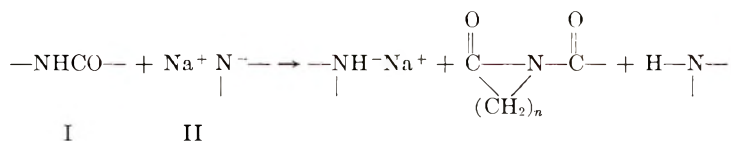
The mechanism of termination in the absence of water is not clear. Wichterle⁵ suggested the formation of acidic compounds and liberation of water through the condensation of two imide groups. Murahashi et al. found that water was liberated by the reaction between pyrrolidone and potassium:¹²



These acidic groups and water will destroy the active base. However, the termination seems not to be so prominent at low temperature. The steady change of caprolactam into copolymer would support this fact.

Degradation

There are two degradation reactions involved: one is the depropagation which is observed especially in pyrrolidone-rich systems, and the other is the chain scission at the amide group by the attack of the anion.



The anion II may be either a monomeric anion or an anion in chain molecules. Clear evidence cannot be obtained at this stage of investigation whether the depropagation in the middle part of the chain will occur or not, but from the observed phenomena it is concluded that the stability of pyrrolidone promotes the depropagation as well as the propagation, and the equilibrium state is completed at the early stage of reaction while caprolactam increases its change slowly.

Apparent Monomer Reactivity Ratios and the Structure of Produced Polymer

The alkaline polymerization of lactam is not the same as addition polymerization, for the former includes the transfer of sodium ion and shows rather slow polymerization rate. It is therefore improper to discuss the monomer reactivity ratio. Moreover it is experimentally difficult to obtain a precise composition of the polymer with a small conversion because of the trivial change in infrared spectra.

In spite of these difficulties it seems to be significant to obtain approximate values of apparent monomer reactivity ratios. These values were determined at a conversion of 10–15% by the Finemann-Ross method as shown in Figure 12. From the obtained values ($r_1 = 5.0$, $r_2 = 0.75$) it is obvious that the produced polymers are block copolymers.

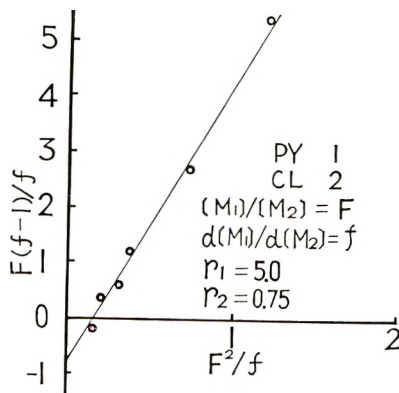


Fig. 12. Apparent monomer reactivity ratio at 10–15% conversion at 90°C.

The authors gratefully acknowledge many helpful discussions with Mr. M. Ishibashi and Mr. S. Ohashi of our institute during this investigation. They also wish to thank Mr. N. Suyama for much of the experimental work.

References

- Griehl, W., *Faserforsch. u. Textiltech.*, **7**, 207 (1956).
- Saunders, J., *J. Polymer Sci.*, **30**, 479 (1958).
- Kralicek, J., and J. Sebenda, *J. Polymer Sci.*, **30**, 493 (1958).
- Yumoto, H., and N. Ogata, *Bull. Chem. Soc. Japan*, **31**, 907, 913 (1958).
- Wichterle, O., *Makromol. Chem.*, **35**, 174 (1960).
- Ney, W. O., Jr., W. R. Nummy, and C. E. Barnes, U. S. pats., 2,638,463, May 12, 1953.
- Ney, W. O., Jr., and M. Crowther, U. S. Pat. 2,739,959, March 27, 1956.
- Griehl, W., and S. Schaaf, *Makromol. Chem.*, **32**, 170 (1959).
- Bellamy, L. J., *The Infra-Red Spectra of Complex Molecules*, 2nd ed., Methuen, London, 1958, p. 29.
- Yoda, N., and A. Miyake, *J. Polymer Sci.*, **43**, 117 (1960).
- Coates, C. E., *Organo-Metallic Compounds*, 2nd ed., Methuen, London, 1960, p. 25.
- Murahashi, S., H. Yuki, and T. Suzuki, *Ann. Repts. Inst. Fiber Research (Osaka)*, No. 11, 50 (1958).

Synopsis

Copolymerization of α -pyrrolidone and ϵ -caprolactam has been carried out in the presence of sodium and acetyl compounds. A large amount of both catalysts is necessary to obtain a comparatively good yield. Infrared absorption measurement was adopted to obtain the polymer composition. The compositions of unreacting monomer were determined by equation: $D_{958}/D_{994} = 0.501(C_{\epsilon}C_{PY})$, where D_{958} and D_{994} are optical

densities at 958 and 994 cm^{-1} , which are characteristic absorptions of ϵ -caprolactam and α -pyrrolidone, respectively, and C_{cl} and C_{py} are concentrations of monomers in weight. The polymer composition was calculated from this composition of residual monomers. The polymerization was followed by this analysis and it was found that the α -pyrrolidone polymerized at the early stage of reaction while ϵ -caprolactam reacts with a steady rate. Higher temperature made this phenomenon distinguishable and the degradation of α -pyrrolidone was observed. The optimum temperature for polymerization was 90–110°C. The stability of α -pyrrolidone anion explains these phenomena, as this anion promotes alkaline-salt formation and degradation and reduces the chain numbers. The prepared copolymers have low melting points and good solubilities which vary according to composition. The melting point of the copolymer whose composition is 1 mole caprolactam:1 mole pyrrolidone is as low as 140°C. and this polymer shows good solubility in ethanol. Apparent monomer reactivity ratios indicate that the copolymers formed are block copolymers.

Résumé

On a effectué la copolymérisation de la α -pyrrolidone et de la ϵ -caprolactame en présence de sodium et de composés acétylés. Une grande quantité de chacun des catalyseurs est nécessaire pour l'obtention de rendements comparablement satisfaisants. On a eu recours aux mesures d'absorption infra-rouge pour déterminer la composition de polymère. Les compositions des monomères, qui n'ont pas réagi, sont déterminées à l'aide de l'équation ci-dessous, $D_{958}/D_{994} = 0,501(C_{cl}/C_{py})$, dans laquelle D_{958} et D_{994} sont des densités optiques à 958 et 994 cm^{-1} fréquences d'absorptions caractéristiques du ϵ -caprolactame et de la α -pyrrolidone, C_{cl} et C_{py} étant les concentrations des monomères en poids. La composition du polymère est calculée à partir de cette composition des monomères résiduels. On suit la polymérisation grâce à cette analyse et l'on trouve que la α -pyrrolidone polymérise à un stade préliminaire de la réaction tandis que la caprolactame réagit à une vitesse constante. L'élévation de la température rend ce phénomène discernable et permet d'observer la dégradation de la pyrrolidone. La température optimum de polymérisation est située entre 90 et 110°C. Ces phénomènes sont interprétés par la stabilité de l'anion issu de la pyrrolidone qui provoque la formation de sel alcalin, la dégradation et la réduction du nombre de chaînes. Les copolymères préparés ont des points de fusion peu élevés et de bonnes solubilités variant suivant la composition. Le point de fusion de copolymères de composition 1-1 est situé à 140°C. et ce polymère est bien soluble dans l'éthanol. Les rapports de réactivité apparents et les points de fusion des sphérolites formés prouvent l'existence de copolymères à bloc.

Zusammenfassung

Copolymerisation von α -Pyrrolidon und ϵ -Caprolactam wurde in Gegenwart von Natrium und Acetylverbindungen durchgeführt. Eine grosse Menge beider Katalysatoren ist notwendig, um eine verhältnismässig gute Ausbeute zu erhalten. Zur Bestimmung der Polymerzusammensetzung wurden Infrarotabsorptionsmessungen verwendet. Die Zusammensetzung des nicht umgesetzten Monomeren wurde nach folgender Gleichung bestimmt: $D_{958}/D_{994} = 0,501 C_{cl}/C_{py}$ wo D_{958} und D_{994} die optische Dichte bei 958 und 994 cm^{-1} , den charakteristischen Absorptionen von ϵ -Caprolactam und α -Pyrrolidon, und C_{cl} und C_{py} die Gewichtskonzentrationen der Monomeren sind. Die Polymerzusammensetzung wurde aus der Zusammensetzung des Monomerrückstandes berechnet. Die Polymerisation wurde mittels dieser Analyse verfolgt und es wurde gefunden, dass α -Pyrrolidon im Anfangsstadium der Reaktion polymerisiert, während ϵ -Caprolactam mit stationärer Geschwindigkeit reagiert. Diese Phänomen trat bei höherer Temperatur hervor, wo auch der Abbau von α -Pyrrolidon beobachtet wurde. Die optimale Polymerisationstemperatur lag zwischen 90–110°C. Diese Erscheinung wird durch die Stabilität des α -Pyrrolidonanions erklärt. Es fördert die Bildung von Alkalisalzen und den Abbau und deduziert die Kettenzahl. Die dargestellten Copolymeren besitzen einen niedrigen

Schmelzpunkt und eine gute, ihrer Zusammensetzung entsprechende Löslichkeit. Der Schmelzpunkt des Copolymeren mit der Zusammensetzung 1 Mol Caprolactam zu 1 Mol Pyrrolidon erreicht den tiefen Wert von 140°C.; dieses Polymere zeigt eine gute Löslichkeit in Äthanol. Scheinbare Monomerreaktivitätsverhältnisse und die Schmelzpunkte der gebildeten Sphärolithe sprechen für die Existenz von Blockcopolymeren.

Received June 7, 1961

Revised October 16, 1961

Polymerization of *N*-Vinylcarbazole with Ziegler-Type Catalyst Systems*

JORGE HELLER, D. O. TIESZEN, and D. B. PARKINSON.
Stanford Research Institute, Menlo Park, California

INTRODUCTION

The polymerization of *N*-vinylcarbazole with free-radical¹ or cationic² catalysts is well known. The purpose of this paper is to describe the polymerization of *N*-vinylcarbazole with Ziegler-type catalyst systems and to examine the resulting polymers with regard to stereoregularity and crystalline structure. The catalysts used in this study were the $\text{TiCl}_4\text{-AlR}_3$, $\text{TiCl}_3\text{-AlR}_3$, and $\text{TiCl}_4\text{-}n\text{-BuLi}$ systems.

While this work was in progress it was learned that Solomon, Dimonie, and Ambrus have carried out a similar study with the $\text{TiCl}_4\text{-}n\text{-BuLi}$ system and have reported the isotactic polymerization of *N*-vinylcarbazole to a highly crystalline polymer.³ However, in our hands the $\text{TiCl}_4\text{-}n\text{-BuLi}$ or any of the other Ziegler-type catalyst systems gave rise only to reactions leading to polymers showing none of the usual indications of crystallinity or stereoregularity.

RESULTS AND DISCUSSION

$\text{TiCl}_4\text{-AlR}_3$ System

The $\text{TiCl}_4\text{-AlR}_3$ system was found to be a very active catalyst for the polymerization of *N*-vinylcarbazole, and, with the exception of experiments carried out at very low temperatures, quantitative conversions were invariably attained. Some pertinent experimental data are summarized in Table I. However, since these data also show that TiCl_4 alone is a very efficient catalyst, it is likely that in experiments in which a low Al/Ti ratio is used the major part of the catalytic activity of the $\text{TiCl}_4\text{-Al}(i\text{-Bu})_3$ system is due to unreduced TiCl_4 .

Figure 1 shows the effect of the Al/Ti ratio on the per cent conversion of *N*-vinylcarbazole to polymer observed after 30 min. reaction time at 30°C. for both the $\text{TiCl}_4\text{-Al}(i\text{-Bu})_3$ and the $\text{TiCl}_4\text{-AlEt}_3$ systems. These results show that with the $\text{TiCl}_4\text{-Al}(i\text{-Bu})_3$ system the reaction rate is diminished by an excess of aluminum alkyl, whereas with the $\text{TiCl}_4\text{-AlEt}_3$

* This work was sponsored by International Business Machines Corporation, San Jose, California.

TABLE I
 Polymerization of *N*-Vinylcarbazole with TiCl_4 , TiCl_3 , and Ziegler-Type Catalyst Systems in Toluene

| Catalyst | Ratio $\text{AlR}_3/\text{TiCl}_n$ | Ratio $\text{TiCl}_n/\text{monomer}$ | Temp., °C. | Reaction time, hr. | Yield, % | Reduced viscosity ^a |
|--|------------------------------------|--------------------------------------|------------|--------------------|----------|--------------------------------|
| TiCl_4 | — | 0.0086 | 0 | 3 | 100 | 0.46 |
| TiCl_4 | — | 0.0086 | -76 | 3 | 100 | 0.55 |
| $\text{TiCl}_4\text{-Al}(i\text{-Bu})_3$ | 3 | 0.0086 | 0 | 3 | 100 | 0.43 |
| $\text{TiCl}_4\text{-Al}(i\text{-Bu})_3$ | 3 | 0.0086 | -76 | 3 | 16 | 0.62 |
| TiCl_3 | — | 0.025 | 80 | 2.75 | 98 | 0.21 |
| TiCl_3 | — | 0.048 | 0 | 1 | 93 | — |
| TiCl_3 | — | 0.048 | -76 | 2 | 19 | 0.47 |
| $\text{TiCl}_3\text{-Al}(i\text{-Bu})_3$ | 1 | 0.025 | 80 | 5 | 50 | 0.17 |
| $\text{TiCl}_3\text{-Al}(i\text{-Bu})_3$ | 1 | 0.025 | 0 | 19 | 21 | 0.23 |
| $\text{TiCl}_3\text{-Al}(i\text{-Bu})_3$ | 1 | 0.028 | -76 | 16 | 8 | 0.38 |

^a At 30°C. in toluene (0.1 g./100 ml.).

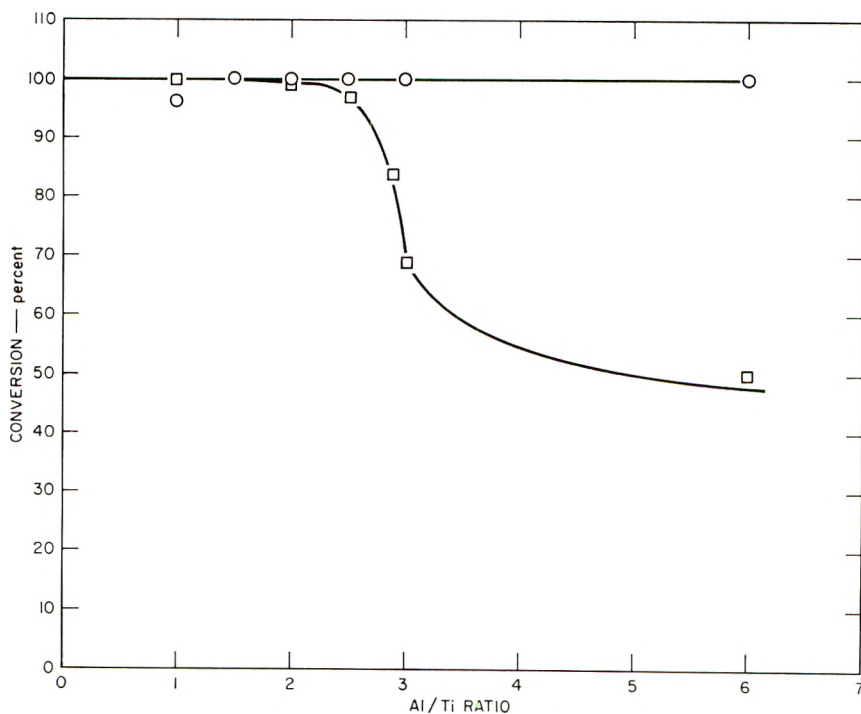


Fig. 1. Polymerization of *N*-vinylcarbazole with the monomer absent during catalyst component interaction for the $\text{TiCl}_4\text{-AlR}_3$ system in toluene at 30°C. for 30 min.: (O) $\text{TiCl}_4\text{-AlEt}_3$; (□) $\text{TiCl}_4\text{-Al}(i\text{-Bu})_3$. Monomer concentration = 0.155 mole/l.; molar ratio of $\text{TiCl}_4/\text{monomer}$ = 0.098.

system the rate remains high even at an Al/Ti ratio of 6:1. The decrease in rate with the $\text{TiCl}_4\text{-Al}(i\text{-Bu})_3$ system which occurs at an Al/Ti ratio of approximately 3:1 most likely indicates that at this particular ratio the surface of the precipitated reduced titanium halide is completely modified by adsorbed $\text{Al}(i\text{-Bu})_3$, thus decreasing the titanium halide-*N*-vinylcarbazole interaction. The drop in rate observed at this particular Al/Ti ratio is in agreement with the work of Orzechowski,⁴ who found a maximum in efficiency at a ratio of 2.8:1 in the polymerization of ethylene with the $\text{TiCl}_4\text{-Al}(i\text{-Bu})_3$ system.

The observation that with the $\text{TiCl}_4\text{-AlEt}_3$ system no decrease in rate is observed in the range of Al/Ti ratios investigated could be attributed to either the smaller bulk of an ethyl group compared with that of an isobutyl group, or to the fact that AlEt_3 usually produces a more finely divided precipitate from TiCl_4 and thus provides a larger area where a titanium halide-*N*-vinylcarbazole interaction can take place.

$\text{TiCl}_3\text{-AlR}_3$ System

In Table I are shown some of the experimental conditions used in the polymerization of *N*-vinylcarbazole with TiCl_3 alone and with the $\text{TiCl}_3\text{-Al}(i\text{-Bu})_3$ system. It is interesting to note that even though TiCl_3 is a considerably weaker Lewis acid than TiCl_4 , it nevertheless exhibits considerable catalytic activity in the polymerization of *N*-vinylcarbazole. Thus, as shown in Figure 2, quantitative conversion to polymer in less than

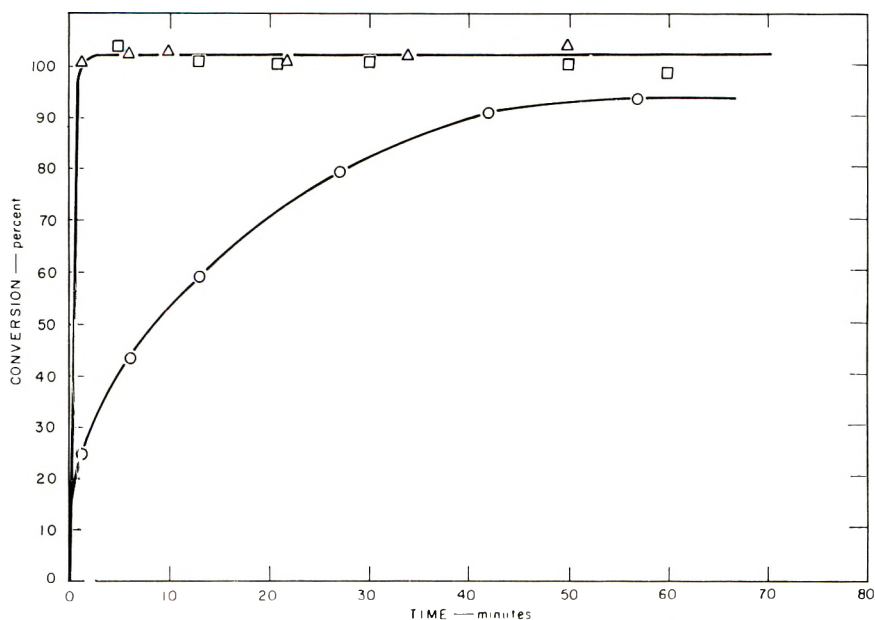


Fig. 2. Effect of temperature on the rate of polymerization of *N*-vinylcarbazole with TiCl_3 in toluene at (□) 75°C.; (△) 45°C.; (○) 0°C. Monomer concentration = 0.2 mole/l.; molar ratio of TiCl_3 /monomer = 0.048.

1 min. is observed at 45°C. and higher temperatures, and even at 0°C. the reaction is 20% complete in 1 min.

The rates of polymerization of *N*-vinylcarbazole with the $\text{TiCl}_3\text{-Al}(i\text{-Bu})_3$ system at various Al/Ti ratios obtained by allowing the catalyst components to react in the presence of monomer are shown in Figure 3. These rates show, particularly at low Al/Ti ratios, a rapid initial reaction followed by an only very gradual increase in per cent conversion with time. This rapid initial reaction is most likely a cationic polymerization brought about by the interaction of *N*-vinylcarbazole and TiCl_3 which can take place before all the $\text{Al}(i\text{-Bu})_3$ has reacted with the TiCl_3 . Since at low Al/Ti ratios the solution contains a large excess of *N*-vinylcarbazole

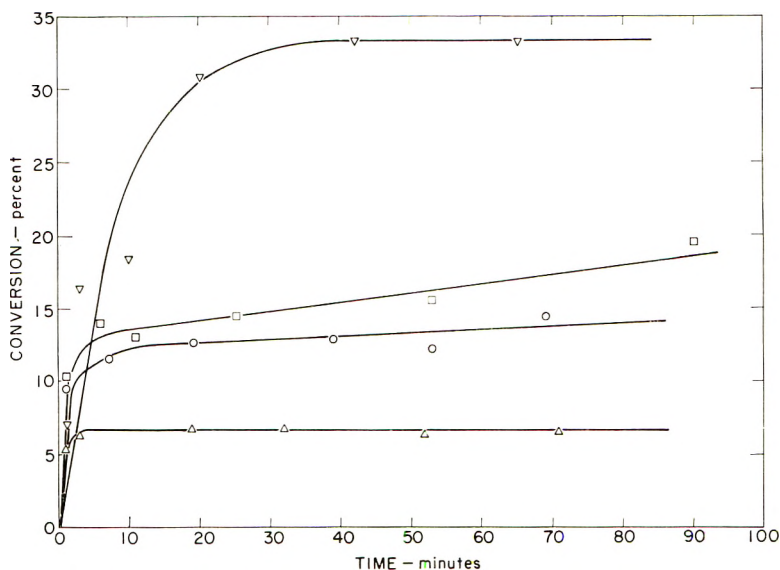


Fig. 3. Effect of Al/Ti ratio on the rate of polymerization of *N*-vinylcarbazole with the monomer present during catalyst component interaction in the $\text{TiCl}_3\text{-Al}(i\text{-Bu})_3$ system in toluene at 75°C.: (▽) Al/Ti = 0.75; (□) Al/Ti = 1; (○) Al/Ti = 2; (△) Al/Ti = 4. Monomer concentration = 0.2 mole/l.; molar ratio of TiCl_3 /monomer = 0.052.

relative to $\text{Al}(i\text{-Bu})_3$, the probability of a $\text{TiCl}_3\text{-N}$ -vinylcarbazole interaction is greater than at high Al/Ti ratios where this probability is decreased. Thus, as shown in Figure 3, the rapid initial reaction becomes less pronounced as the Al/Ti ratio is increased.

The existence of this initial cationic polymerization can be further demonstrated by comparing the rate of polymerization of *N*-vinylcarbazole with a premixed catalyst system to that obtained by allowing the catalyst components to react in the presence of monomer. These rates are shown in Figure 4. It will be noted that, with the premixed catalyst system having an Al/Ti ratio of 1:1, the rapid initial reaction has been markedly reduced and that after a short reaction time both polymerizations proceed

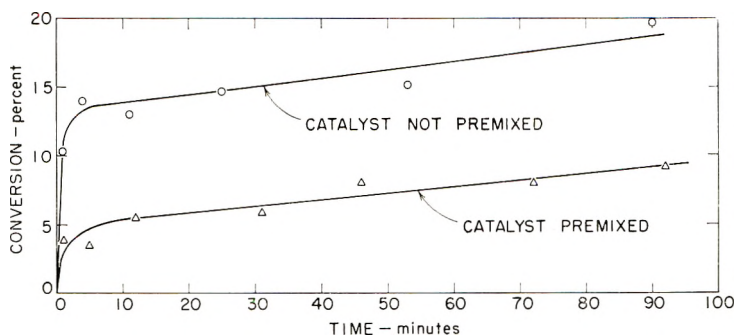


Fig. 4. Effect of premixing the catalyst before addition of monomer on the polymerization rate of *N*-vinylcarbazole for the $\text{Al}(i\text{-Bu})_3\text{-TiCl}_3$ system in toluene at 75°C . Monomer concentration = 0.2 moles/l.; molar ratio of $\text{TiCl}_3/\text{monomer}$ = 0.052; Al/Ti = 1.

at virtually identical rates. This indicates that a complex having an Al/Ti ratio of 1:1 exhibits very little of the cationic character of free TiCl_3 when allowed to form in the absence of monomer. When formed in the presence of monomer some polymerization due to free TiCl_3 takes place before the reaction between TiCl_3 and $\text{Al}(i\text{-Bu})_3$ is complete. However, even though the complex is formed in the presence of monomer, ultimately

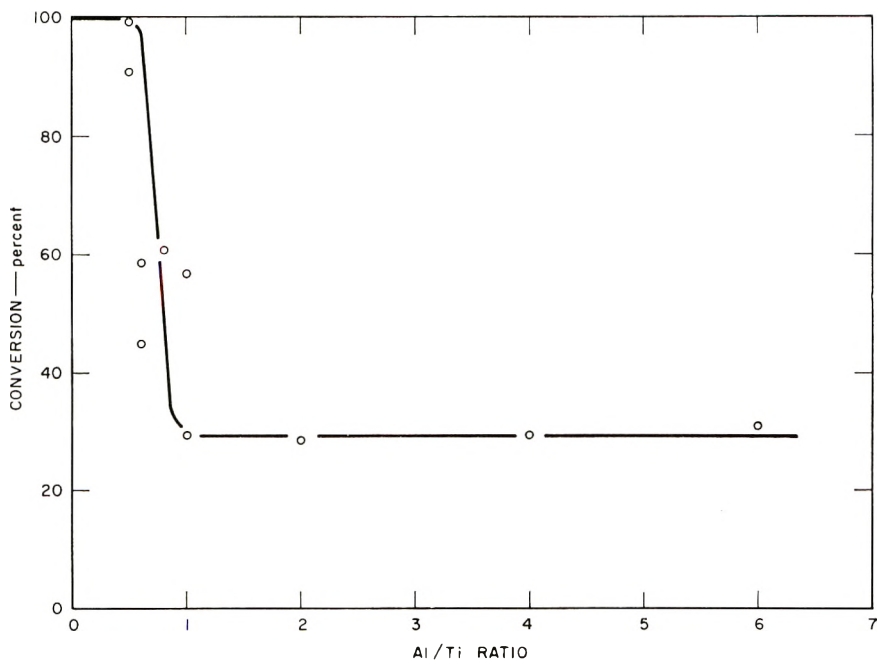


Fig. 5. Polymerization of *N*-vinylcarbazole with monomer absent during catalyst component interaction for the $\text{TiCl}_3\text{-Al}(i\text{-Bu})_3$ system in toluene at 30°C . for 60 min. Monomer concentration = 0.17 mole/l.; molar ratio of $\text{TiCl}_3/\text{monomer}$ = 0.096.

there results the same complex as that formed in the absence of monomer, as evidenced by the nearly identical polymerization rates.

Since the competing reaction between *N*-vinylcarbazole and TiCl_3 can be eliminated by forming the catalyst complex prior to the introduction of monomer, it was of interest to investigate the per cent conversion at a fixed reaction time as a function of the Al/Ti ratio under these conditions. The results are shown in Figure 5. As in the case of the TiCl_4 -Al(*i*-Bu) $_3$ system, a rather sharp drop in conversion is observed at a certain Al/Ti ratio, which indicates that at that particular ratio the surface of the TiCl_3 is completely modified by the metal alkyl. Because of the solid nature of TiCl_3 and the subsequent dependence on the particle fineness which determines the available surface, the reproducibility with this system was poor. However, the data indicate that the drop in rate occurs at an Al/Ti ratio of approximately 0.8:1. It is also interesting to note that after the surface has been completely modified by the metal alkyl, the conversion is no longer dependent on the Al/Ti ratio. This again indicates that catalysis by complexes having an Al/Ti ratio greater than one is not due to free TiCl_3 if the catalyst components are mixed in the absence of monomer.

TiCl_4 -*n*-BuLi System

A study of the polymerization of *N*-vinylcarbazole with the TiCl_4 -*n*-BuLi system has shown that the Li/Ti ratio of the catalyst mixture has a very profound influence on the polymerization rate. This is seen in Figure 6. The sudden drop in conversion with this system is considerably more pronounced than the drops in conversion observed with the TiCl_4 -Al(*i*-Bu) $_3$ or the TiCl_3 -Al(*i*-Bu) $_3$ systems. Because of this sudden change in conversion which suggests an abrupt change in the nature of the catalytic species, the average valence state of Ti was investigated as a function of the Li/Ti ratio. The results are presented in Figure 7 as per cent reduction versus the Li/Ti ratio.

It is apparent that little reduction takes place at Li/Ti ratios of less than 1:1. The fact that quantitative conversion to polymer at high rates is observed at these low Li/Ti ratios indicates that the unreduced TiCl_4 is not appreciably complexed and retains its Lewis acidity. On the other hand, even though again very little reduction takes place, at Li/Ti ratios of 4:1 and higher, the unreduced TiCl_4 must now be complexed so that it no longer retains its Lewis acidity, since essentially no polymerization of *N*-vinylcarbazole is observed. The observation that at higher Li/Ti ratios most of the titanium is in the tetravalent state is in agreement with the work of Friedlander and Oita⁵ and that of Jones, Martius, and Thorne.⁶

The interpretation of the data obtained with Li/Ti ratios in the range of 1:1 to 4:1 is somewhat more difficult. Since the formation of Ziegler-type catalysts is probably a surface reaction and since such catalysts are known to involve transition metal halides in reduced valence states,⁷ the increase in per cent reduction as the Li/Ti ratio is increased indicates

that an increasingly larger portion of the surface is converted to organo-metallic species of the Ziegler type. The abrupt decrease in the rate of polymerization of *N*-vinylcarbazole between Li/Ti ratios of 1.5:1 and 1.8:1 indicates that at these ratios the surface is completely converted to Ziegler-type catalytic species which prevent the rapid TiCl_4 -catalyzed cationic polymerization.

These findings are in accord with the work of Friedlander and Oita,⁵ who found that when ethylene is polymerized with the TiCl_4 -*n*-BuLi system prepared in the absence of monomer, a maximum in conversion takes place at a Li/Ti ratio of 1.5:1, with virtually no polymerization

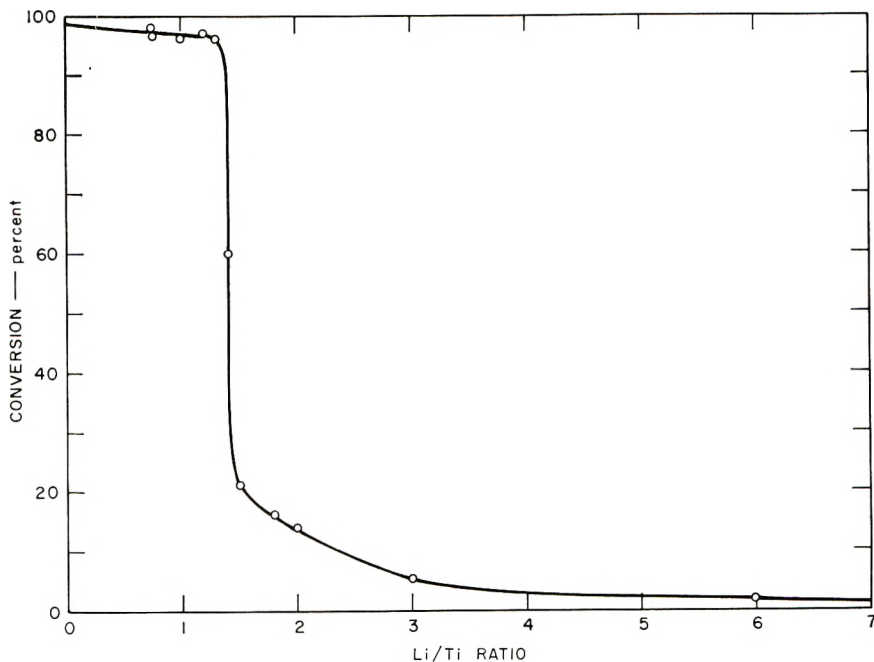


Fig. 6. Polymerization of *N*-vinylcarbazole with the monomer absent during catalyst component interaction for the TiCl_4 -*n*-BuLi system in petroleum ether at 30°C. for 30 min. Monomer concentration = 0.155 mole/l.; molar ratio of TiCl_4 /monomer = 0.098.

taking place above or below this ratio. Since ethylene will not polymerize with TiCl_4 alone, these data indicate that, at a Li/Ti ratio of 1.5:1, sufficient concentration of a Ziegler-type complex is present to catalyze the polymerization efficiently. The abrupt decrease in yield of poly-*N*-vinylcarbazole observed at precisely this ratio is thus in agreement with the observations of Friedlander and Oita and shows that a Ziegler-type complex formed from *n*-BuLi and TiCl_4 is a very inefficient catalyst for the polymerization of *N*-vinylcarbazole. Frankel, Rabani, and Zilkha⁸ have also studied the polymerization of ethylene with the *n*-BuLi- TiCl_4 system mixed in the absence of ethylene and have found a maximum in

conversion at a Li/Ti ratio of 2.1:1. This optimum ratio differs from that observed by Friedlander and Oita, and could be due to the differences in experimental technique, since Frankel, Rabani, and Zilkha used ethylene under 40–50 psi pressure while Friedlander and Oita used ethylene under atmospheric pressure.

The abrupt decrease in conversion shown in Figure 6 which takes place at a Li/Ti ratio of approximately 1.5:1 does not correspond exactly to the maximum in per cent reduction which takes place at a Li/Ti ratio of 2:1. This can be attributed to the fact that at a Li/Ti ratio of 1.5:1

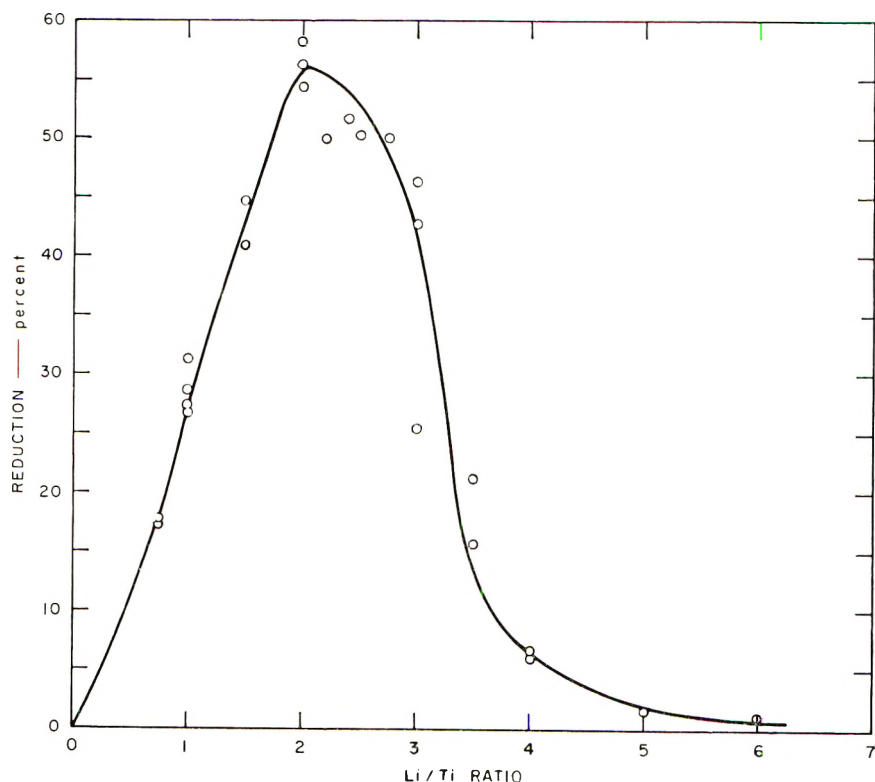


Fig. 7. Reduction of Ti^{+4} vs. the Li/Ti ratio.

the surface is already completely converted to organometallic species of the Ziegler types, and any further increase in concentration of these species, which seems to reach a maximum at a Li/Ti ratio of 2:1, has no noticeable effect on the polymerization of *N*-vinylcarbazole. It should be noted, however, that the maximum in conversion of ethylene under the experimental conditions used by Frankel, Rabani, and Zilkha corresponds almost exactly to the maximum in reduction shown in Figure 7.

As the Li/Ti ratio is further increased beyond 2:1, the amount of Ti in lower valence states rapidly decreases to zero. Since at these higher ratios virtually no polymerization of ethylene or of *N*-vinylcarbazole

is observed, a different reaction scheme must now be invoked. It is likely that a complex between TiCl_4 and *n*-BuLi forms which is somehow stabilized by the excess of unreacted *n*-BuLi present in solution.⁵

Crystallinity and Stereoregularity

The x-ray diffraction pattern of the polymers as prepared showed only amorphous halos. The lack of a crystalline diffraction pattern need not, however, be interpreted as a lack of stereoregularity but could mean that the stereoregular polymer has not crystallized under the polymerization conditions. Attempts to induce crystallization by conventional treatment with borderline solvents, or by various annealment treatments have so far failed, as is evidenced by the absence of any sharp diffraction lines in the x-ray diffraction patterns of polymers thus treated.

Since many crystalline polymers also show the presence of birefringent spherulites when allowed to cool slowly from the melt, a number of samples of poly-*N*-vinylcarbazole were examined by this technique. No spherulitic structures could be discerned, indicating a lack of polymer crystallinity.

These findings are in conflict with the work of Solomon, Dimonie, and Ambrus³ who reported that they detected crystallinity in polymers prepared from *N*-vinylcarbazole by TiCl_4 -*n*-BuLi catalysis, both by x-ray diffraction measurements and by the formation of spherulitic structures when the polymer was allowed to cool from the melt. Because of this discrepancy, our polymers were examined further by infrared spectroscopy and by high resolution nuclear magnetic resonance.

In many polymers crystallization is accompanied by changes in the infrared spectrum, as evidenced by band splitting and a deepening of certain other bands. Careful work with polystyrene⁹ has shown that differences in the infrared spectrum persist even after the polymer is melted and can thus be attributed to a steric regularity of the side-group along the helical chain axis. A study of the infrared spectrum of polypropylene^{10,11} has also shown the existence of bands characteristic of isotactic structures. Therefore, a study of the infrared spectra of the many polymers prepared during this study was carried out. The results of this study indicated that only atactic, noncrystalline materials were prepared.

Similarly, nuclear magnetic resonance can yield information as to crystallinity and stereochemical arrangement of the polymer side groups. For example, Slichter and McCall¹² calculated the per cent crystallinity of partially crystalline polyethylene by using the broad absorption band of the solid polymer as a measure of the amorphous portion, and the narrow band, partially superimposed on the broad band, as a measure of the crystalline regions. However, this method does not appear to be applicable to all polymers, since Miller and Rauhut¹³ failed to observe a band splitting in crystalline poly (*tert*-butyl acrylate). Differences in nuclear magnetic

resonance spectra directly attributable to the various configurations within the polymer chain, aside from the question of crystallinity, have been demonstrated by Bovey and Tiers¹⁴ in their solution NMR study of poly(methyl methacrylate) prepared by free radical and anionic catalysis.

The NMR spectrum of poly-*N*-vinylcarbazole measured in deuteriochloroform is shown in Figure 8. It is of interest that temperature had virtually no effect on the spectral resolution. Examination of the NMR spectra of many *N*-vinylcarbazole polymers prepared with a variety of different Ziegler-type catalyst systems did not show any differences which could be attributed to crystallinity or differences in steric arrangement.

Since no differences between samples prepared by free radical or cationic catalysis and those prepared by stereospecific Ziegler-type catalysts could be detected by any of the means discussed previously, it is probable that

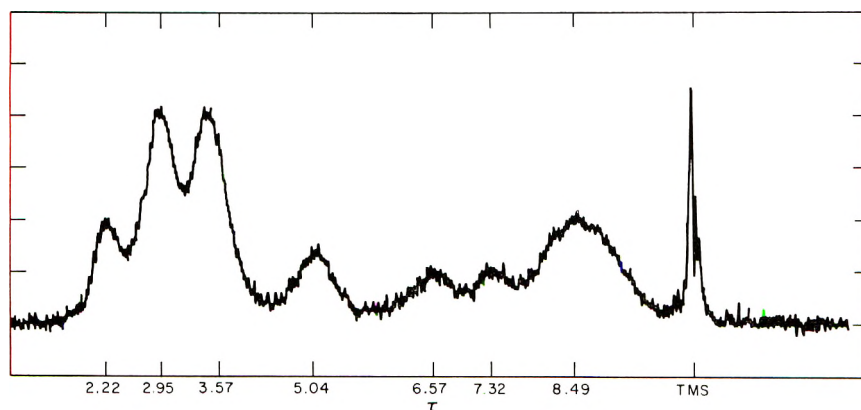


Fig. 8. Nuclear magnetic resonance spectrum of poly-*N*-vinylcarbazole prepared with Ziegler-type catalyst systems.

only noncrystalline, atactic polymers have been prepared. However, an examination of molecular models shows that, because of the large bulk of the carbazole ring system, in poly-*N*-vinylcarbazole these groups are crowded so close together that differences arising from various different steric arrangements may be too small to be readily detectable. Furthermore, Natta, Danusso, and Sianesi¹⁵ have shown that the crystallizability of polymers is related to the size and steric characteristics of the side group and that polymers with large side groups cannot be crystallized, even though they can be shown to have a regular, isotactic structure. Our inability to crystallize poly-*N*-vinylcarbazole could thus be due to either the large bulk of the carbazole side group, or to the nonstereospecific nature of the polymerization, and, therefore, it is not possible to say at this point whether a stereoregulated polymerization had actually been achieved.

EXPERIMENTAL

Materials

All solvents (Baker, analyzed reagents, or Phillips, pure grade) were refluxed and distilled from sodium. They were then stored over fresh sodium wire in 4-liter standard-taper bottles from which they could be dispensed by means of nitrogen pressure.

N-Vinylcarbazole (Badische Anilin u. Soda Fabrik) was recrystallized from absolute methanol to a sharp melting point of 64°C. and stored under refrigeration.

Titanium tetrachloride (Anderson Chemical Co.) was used without further purification as a 1*M* solution in petroleum ether. Aluminum alkyls (Texas Alkyls Inc.) were used as 20% solutions in toluene. *n*-BuLi (Anderson Chemical Company) was obtained as a 1*M* solution in heptane-hexane and the active *n*-BuLi concentration was determined by the double titration method.¹⁶ Titanium trichloride (Stauffer Chemical Co.) was heated at 200°C./0.1 mm for 8 hr. to remove residual TiCl₄ (0.3% by analysis). The TiCl₃ was then used as a 1*M* dispersion in toluene.

Polymerizations

The following represents a typical run.

In a 500-ml. four-necked flask, equipped with a reflux condenser, mechanical stirrer, nitrogen inlet, and thermometer was placed 10 g. (0.052 mole) of *N*-vinylcarbazole and 250 ml. of toluene. Moisture was rigorously excluded by flaming the entire apparatus prior to the introduction of monomer, and oxygen was excluded by maintaining a blanket of purified nitrogen over the solution. To this stirred solution was added by means of hypodermic syringes 2.5 mmoles of Al(*i*-Bu)₃ and 2.5 mmoles of TiCl₃, in that order. At the termination of the reaction, 10–25 ml. of methanol was added to destroy the catalyst, and the entire reaction mixture was added to a large excess of methanol. The polymer was isolated by vacuum filtration, washed with fresh methanol in a Waring Blendor and dried in a vacuum oven at 50–60°C. for 24 hr.

In experiments with inverse addition of catalyst the procedure was essentially identical to that described above except that the catalyst, diluted with a small amount of solvent, was first introduced into the flask and allowed to interact for 10 min. Then the monomer solution was added from a pressure-equalized dropping funnel, and the flow was so adjusted that the addition was complete in 5 min.

Kinetic Measurements

Kinetic measurements were made by a gravimetric technique. For this purpose the reaction vessel was modified with a fifth neck which was equipped with a 10-ml. pipet. By means of nitrogen pressure, part of the reaction mixture could be forced into the pipet and then emptied

by way of a three-way stopcock into an Erlenmeyer flask containing 100 ml. of methanol. In this manner the reaction was not disturbed by the sampling technique.

Polymer Characterizations

X-ray diffractions were obtained with a powder camera in a Norelco x-ray diffraction apparatus by use of standard techniques. The infrared spectra were determined with a Beckman IR-4 spectrophotometer on KBr pellets or films cast from CS₂ on salt plates.

Nuclear magnetic resonance spectra were determined with the Varian V-4302A high resolution spectrometer equipped with superstabilizer, spinner, and fixed frequency units for 60 Mcycles/sec. The 10% deuteriochloroform solutions containing 1% tetramethylsilane (TMS) were sealed under vacuum in 5-mm. o.d. Pyrex tubes. The samples could be heated by means of a heated probe.

A Bausch and Lomb polarizing microscope using cross-polarized light was used in the investigation of spherulitic structure. The microscope was equipped with an electrically heated hot stage arranged so that the sample being viewed could be heated in an inert atmosphere. The effective magnification used was 86 diameters.

Determination of Per Cent Reduction of Ti⁺⁴

The ordinary method for the determination of reduced titanium is not capable of distinguishing between Ti⁺² and Ti⁺³ since during the acid hydrolysis step any Ti⁺² is rapidly oxidized to Ti⁺³,¹⁷ i.e.,



However, from a determination of Ti⁺³ it is possible to determine how much residual Ti⁺⁴ remains in the system.

The *n*-BuLi and TiCl₄ at the desired ratio were added to 35 ml. of petroleum ether under a nitrogen blanket and allowed to interact for 5 min. with frequent shaking. The mixture was then hydrolyzed with water and the layers separated in a separatory funnel. Sufficient water to bring the volume to 35 ml. was then added and the solution was titrated with a standard Fe⁺³ solution, NH₄SCN being used as indicator.¹⁸

We wish to acknowledge the help of Mr. W. A. Wilson and Mrs. Marijane Hoover in carrying out some of the experimental work.

References

1. Danidge, H., *J. Appl. Chem.*, **9**, 241 (1959).
2. Schildknecht, C. E., A. O. Zoss, and F. Grosser, *Ind. Eng. Chem.*, **41**, 2891 (1949).
3. Solomon, O. F., M. Dimonie, and K. Ambroz, *Rev. Chim. (Bucharest)*, **11**, 520 (1960); O. F. Solomon, M. Dimonie, K. Ambroz, and M. Tomescu, *J. Polymer Sci.*, **52**, 205 (1961).
4. Orzechowski, A., *J. Polymer Sci.*, **34**, 65 (1959).
5. Friedlander, H. N., and K. Oita, *Ind. Eng. Chem.*, **49**, 1885 (1957).
6. Jones, M. H., U. Martius, and M. P. Thorne, *Can. J. Chem.*, **38**, 2303 (1960).

7. Gaylord, N. G., and H. F. Mark. *Linear and Stereoregular Addition Polymers*, Interscience, New York—London, 1959, Chap. 7.
8. Frankel, M., J. Rabani, and A. Zilkha, *J. Polymer Sci.*, **28**, 387 (1958).
9. Takeda, M., K. Iimura, A. Yamada, and Y. Imamura, *Bull. Chem. Soc. Japan*, **33**, 1219 (1960).
10. Liang, C. Y., and F. G. Pearson, *J. Mol. Spectroscopy*, **5**, 290 (1960).
11. Liang, C. Y., M. R. Lytton, and C. J. Boone, *J. Polymer Sci.*, **47**, 139 (1960).
12. Slichter, W. P., and D. W. McCall, *J. Polymer Sci.*, **25**, 230 (1957).
13. Miller, M. L., and C. E. Rauhut, *J. Polymer Sci.*, **38**, 63 (1959).
14. Bovey, F. A., and G. V. D. Tiers, *J. Polymer Sci.*, **44**, 173 (1960).
15. Natta, G., F. Danusso, and D. Sianesi, *Makromol. Chem.*, **28**, 253 (1958).
16. Gilman, H., and A. H. Haubein, *J. Am. Chem. Soc.*, **66**, 1515 (1944).
17. Patscheke, G., and W. Schaller, *Z. anorg. Chem.*, **235**, 257 (1938).
18. Herman, D. F., and W. K. Nelson, *J. Am. Chem. Soc.*, **75**, 3882 (1953).

Synopsis

The polymerization of *N*-vinylcarbazole with the $\text{TiCl}_4\text{-Al}(i\text{-Bu})_3$, $\text{TiCl}_4\text{-AlEt}_3$, $\text{TiCl}_3\text{-Al}(i\text{-Bu})_3$, and the $\text{TiCl}_4\text{-}n\text{-BuLi}$ systems was studied. It was found that *N*-vinylcarbazole undergoes a very facile cationic polymerization with TiCl_4 , or TiCl_3 , and that catalyst complexes which contain a low metal alkyl/transition metal halide ratio promote a very rapid cationic polymerization. When the catalyst components are mixed in the presence of monomer, considerable cationic polymerization due to the transition metal halide alone takes place before the reaction between the titanium halide and metal alkyl is complete. Experiments with catalyst components mixed in the absence of monomer have shown that the rate of the reaction is markedly dependent on the ratio of the catalyst components and that each system studied had a characteristic ratio at which the catalytic activity suffered a marked drop. With $\text{TiCl}_3\text{-Al}(i\text{-Bu})_3$ this drop occurred at an Al/Ti ratio of 0.8, with $\text{TiCl}_4\text{-Al}(i\text{-Bu})_3$ at an Al/Ti ratio of 3, and with $\text{TiCl}_4\text{-}n\text{-BuLi}$ at a Li/Ti ratio of 1.5. This was interpreted as indicating that at these ratios the surface of the titanium halide becomes completely modified by the metal alkyl so that no *N*-vinylcarbazole-titanium halide interaction could take place. The per cent reduction of TiCl_4 to lower valence states was studied with the $n\text{-BuLi-TiCl}_4$ system as a function of the Li/Ti ratio and it was found that the maximum per cent reduction takes place at a Li/Ti ratio of 2. The per cent reduction rapidly decreased to zero at higher Li/Ti ratios. The polymers of *N*-vinylcarbazole formed with Ziegler-type catalyst systems were examined by x-ray diffraction, by their appearance under a polarizing microscope, by infrared spectroscopy, and by nuclear magnetic resonance. These measurements indicated that only amorphous, atactic polymers were formed.

Résumé

La polymérisation du *N*-vinylcarbazole avec les systèmes $\text{TiCl}_4\text{-Al}(i\text{-Bu})_3$, $\text{TiCl}_4\text{-AlEt}_3$, $\text{TiCl}_3\text{-Al}(i\text{-Bu})_3$, et $\text{TiCl}_4\text{-}n\text{-BuLi}$ a été étudiée. On a établi que le *N*-vinylcarbazole subit très aisément une polymérisation cationique avec TiCl_4 , ou TiCl_3 , et que les catalyseurs complexes contenant un rapport peu élevé alcoyle métal/halogénure d'un métal de transition favorisent une polymérisation cationique très rapide. Quand les constituants du catalyseur sont mélangés en présence du monomère, une polymérisation cationique considérable due à l'halogénure du métal de transition seul a lieu avant que la réaction entre l'halogénure de titane et l'organométallique ne soit complète. Des expériences avec les constituants du catalyseur mélangés en absence du monomère ont montré que la vitesse de réaction dépend de façon très nette du rapport des constituants du catalyseur et que chaque système étudié possède un rapport caractéristique pour lequel l'activité catalytique subit une diminution marquée. Avec $\text{TiCl}_3\text{-Al}(i\text{-Bu})_3$, cette diminution se présente pour un rapport Al/Ti de 0.8, avec $\text{TiCl}_4\text{-Al}(i\text{-Bu})_3$ pour un rapport Al/Ti de 3, et avec $\text{TiCl}_4\text{-}n\text{-BuLi}$ pour un rapport Li/Ti de 1.5. Ceci a été

interprété comme indication qu'à ces rapports la surface de l'halogénure de titane se modifie complètement par l'organométallique de sorte qu'aucune interaction entre l'halogénure de titane et le *N*-vinylcarbazole ne peut avoir lieu. Le pourcentage de réduction de TiCl_4 en dérivés de valence inférieure a été étudié au moyen du système $n\text{-BuLi-TiCl}_4$ en fonction du rapport Li/Ti et il a été établi que le pourcentage maximum de réduction a lieu pour un rapport Li/Ti égal à 2. Le pourcentage de réduction décroît rapidement vers une valeur nulle pour des rapports plus élevés Li/Ti. Les polymères de *N*-vinylcarbazole obtenus au moyen des systèmes catalyseurs du type Ziegler ont été examinés par diffraction des rayons-X, par étude au microscope polarisant, par spectroscopie infrarouge, et par résonance magnétique nucléaire. Ces mesures ont indiqué qu'il n'y avait formation que de polymères amorphes atactiques.

Zusammenfassung

Die Polymerisation von *N*-Vinylcarbazol mit $\text{TiCl}_4\text{-Al}(i\text{-Bu})_3$, $\text{TiCl}_4\text{-AlEt}_3$, $\text{TiCl}_3\text{-Al}(i\text{-Bu})_3$ und mit den $\text{TiCl}_4\text{-}n\text{-BuLi}$ -Systemen wurde untersucht. Es wurde gefunden, dass *N*-Vinylcarbazol mit TiCl_4 oder TiCl_3 sehr leicht kationisch polymerisiert und dass Katalysatorkomplexe, die ein niedriges Verhältnis von Metallalkyl zu Übergangsmetallhalid besitzen, eine sehr rasche kationische Polymerisation bewirken. Werden die Katalysatorkomponenten in Gegenwart des Monomeren gemischt, so tritt eine beträchtliche kationische Polymerisation durch das Übergangsmetallhalid allein auf, bevor die Reaktion zwischen dem Titanhalid und dem Metallalkyl vollständig abgelaufen ist. Experimente mit Katalysatoren, deren Komponenten in Abwesenheit vom Monomeren gemischt worden waren, zeigten, dass die Reaktionsgeschwindigkeit merklich vom Verhältnis der Katalysatorkomponenten abhängt und dass jedes untersuchte System ein charakteristisches Verhältnis besitzt, bei dem die katalytische Aktivität eine merkliche Abnahme zeigt. Mit $\text{TiCl}_3\text{-Al}(i\text{-Bu})_3$ trat diese Abnahme bei einem Al/Ti-Verhältnis von 0,8 auf, mit $\text{TiCl}_4\text{-Al}(i\text{-Bu})_3$ bei einem Al/Ti-Verhältnis von 3 und mit $\text{TiCl}_4\text{-}n\text{-BuLi}$ bei einem Li/Ti-Verhältnis von 1,5. Dies wurde durch die Annahme gedeutet, dass bei diesen Verhältnissen die Oberfläche des Titanhalids durch das Metallalkyl eine vollständige Modifikation erfährt, so dass keine Wechselwirkung mehr zwischen *N*-Vinylcarbazol und dem Titanhalid stattfinden kann. Die prozentuelle Reduktion von TiCl_4 zu niedrigeren Wertigkeitsstufen wurde an dem $n\text{-BuLi-TiCl}_4$ -System als Funktion des Li/Ti-Verhältnisses untersucht und es wurde gefunden, dass die maximale prozentuelle Reduktion bei einem Li/Ti-Verhältnis von 2 auftritt. Die prozentuelle Reduktion nahm bei höherem Li/Ti-Verhältnis rasch bis zu Null ab. Die mit Katalysatorsystemen des Zieglerstyps hergestellten *N*-Vinylcarbazolpolymeren wurden mittels Röntgenbeugung, Polarisationsmikroskop, Infrarotspektroskopie und magnetischer Kernresonanz untersucht. Diese Messungen zeigten, dass nur amorphe, ataktische Polymere gebildet wurden.

Received August 7, 1961

Revised October 16, 1961

Activity Coefficients of Small Ions in Ion-Exchange Resins

N. LAKSHMINARAYANAI AH,* *Department of Chemistry, Central College, Bangalore, India*

I. INTRODUCTION

Ion-exchange resins consist of crosslinked, three-dimensional networks of polymer chains to which are chemically attached a number of anionic groups in the case of cation-exchange resins and of cationic groups in the case of anion-exchange resins. In contact with an electrolyte solution an exchange of ions between the resin and the solution phases takes place. The Donnan equilibrium set up at the interface governs the distribution of solute, and the osmotic forces determine the distribution of water between the two phases. The activity of the mobile ions in the two phases is given by the Donnan relation:

$$RT \ln \bar{a}_i/a_i = Z_i F(\psi - \bar{\psi}) + (P - \bar{P})V_i \quad (1)$$

Where a_i and \bar{a}_i are single-ion activities of the species i in the resin and in the external solution, respectively (barred terms refer to the external solution phase), $(\psi - \bar{\psi})$ is the Donnan potential difference, Z_i the valency, F the Faraday, $(P - \bar{P}) = \pi$ is the difference between the swelling pressure in the resin and the hydrostatic pressure in the outside solution, and V_i is the partial molal volume of i .

Evaluation of the electrical potential $(\psi - \bar{\psi})$ depends on the assignment of values for single-ion activity coefficients for the ions in the resin phase and in the solution. Values of $\bar{\gamma}_i$ can be computed by the usual formulae for dilute external solutions. No such calculation is possible for values of γ_i in the resin phase. The theory of membrane potentials proposed simultaneously by Teorell¹ and by Meyer and Sievers² assumes γ_i to be unity. The implications of this assumption have been discussed in a recent paper by Hills et al.³

For any electrolyte ij in contact with an ionic membrane the condition for equilibrium is $\mu_{ij} = \bar{\mu}_{ij}$; the electrical potential terms in eq. (1) disappear, giving the relation

$$\ln \bar{a}_{ij}/a_{ij} = \pi V_{ij}/RT \quad (2)$$

* Present address: Department of Pharmacology, School of Medicine, University of Pennsylvania, Philadelphia, Pennsylvania.

If the electrolyte ij dissociates into ν_i and ν_j ions and it is remembered that

$$\gamma_{\pm} = (\gamma_i^{\nu_i} \gamma_j^{\nu_j})^{1/\nu}$$

where

$$\nu = \nu_i + \nu_j$$

eq. (2) becomes

$$\ln \bar{m}_i^{\nu_i} \bar{m}_j^{\nu_j} \bar{\gamma}_{\pm}^{\nu} / m_i^{\nu_i} m_j^{\nu_j} \gamma_{\pm}^{\nu} = \pi V_{ij} / RT$$

which on rearrangement, yields

$$\gamma_{\pm}^{\nu} e^{\pi V_{ij} / RT} = \bar{m}_i^{\nu_i} \bar{m}_j^{\nu_j} \bar{\gamma}_{\pm}^{\nu} / m_i^{\nu_i} m_j^{\nu_j} \quad (3)$$

The left-hand side of eq. (3) can be evaluated, as the parameters in the numerator are accurately known and the parameters in the denominator can be determined by a complete analysis of the composition of the resin phase. Some experimental work has been done on this problem of activity coefficients in the resin phase by use of ion-exchange granules^{4,5} and membranes.^{3,6} The external solution used has been of the uni-univalent type in most cases. In this work analysis of the resin phase has been carried out for a rodlike crosslinked phenol sulfonate resin in equilibrium with aqueous solutions of NaCl, NaBr, Na₂CO₃, and sodium citrate, Na₃C₆H₅O₇.

II. EXPERIMENTAL

Resin

Phenol was sulfonated at 60°C. and on cooling brown crystals of phenol-sulfonic acid were obtained. A known weight of this (2 parts) was mixed with calculated quantities of 38% solution of formaldehyde (1 part) and water (0.68 part). The solution thus obtained was transferred into clean and dry glass tubes (15 to 20 cm. long, bore diameter about 4 mm.) sealed at one end. After filling the tubes with the liquid the other ends were also sealed. They were immersed and heated in a water bath at 85°C. for 6 hr. and left overnight for cooling. The glass tubes were broken and the brown and tough resin rods obtained were washed with conductivity water. Repeated washing over a period of three days was required to remove the last traces of formaldehyde. These rods were agitated with 1N HCl and washed free of acid with conductivity water in which they were preserved.

Electrolyte Solutions

AR grade chemicals (BDH) were used, but the sodium citrate was of ordinary grade.

Standard solutions of NaCl, NaBr, Na₂CO₃, and Na₃C₆H₅O₇ in the range 0.001–3.0N were prepared in conductivity water and in all cases their normality was checked by titration against standard reagents. In the case of Na₃C₆H₅O₇, however, as there was doubt about the quantity of

water of crystallization, the standard solutions were prepared in the following manner. At 30°C. a nearly saturated solution of sodium citrate was prepared. Exactly 2 ml. of this was sent down a cation-exchange column in H⁺ form and the citric acid in the effluent was titrated against standard alkali with phenolphthalein as the indicator.⁷ From this standard solution, all the other dilute solutions were prepared.

Equilibration of Resin Rods

The resin in H⁺ form was converted into the Na⁺ form by treating it with the required strong solution. Duplicate pieces of resin, nearly 5 cm. in length were put in Pyrex test tubes of 50 ml. capacity which were filled with 30 ml. of the standard solution. The mouths of the test tubes were closed with tight fitting rubber bungs, and the tubes were fixed in a shaking machine which was run for nearly 24 hr. with frequent changings of the electrolyte solutions.

Density of Resin Rods

The pieces of resin equilibrated in various solutions were dried between the folds of a filter paper (Whatman No. 1). Immediately each piece was transferred into a previously weighed tube fitted with an air-tight stopper and weighed. The volume of the piece was determined by transferring it into a 5-ml. microburet containing petroleum ether. The rise in the level of ether was noted on a cathetometer. As the diameter of the bore of the buret was known accurately, the volume of the resin and hence its density could be calculated for the duplicates.

Water Content of the Resin Rods

The Na⁺ form of the resin in equilibrium with the standard solution was dried and weighed as described above. It was dried to constant weight in an air oven at 110°C. Duplicates were always used.

Analytical Estimations

Sorption of the chloride and the bromide by the resin and its exchange capacity were determined as follows.

The pieces of resin were weighed after surface drying as above. Each piece was transferred into a Pyrex test tube containing exactly 25 ml. 0.1*N* HNO₃. The tubes were closed and fixed in the shaking machine which was run for 24 hr. The liquid in each of the tubes was transferred into separate vessels. The pieces of resin were washed a number of times with conductivity water by agitating them in the shaking machine. The washings were transferred into the respective vessels containing the liquid collected in the previous treatment. The liquid in each vessel was analyzed for its acid and halide content by titrating against 0.05*N* carbonate-free NaOH and 0.05*N* AgNO₃ in the usual way.

Rods equilibrated in Na₂CO₃ solutions after surface drying and weighing

were repeatedly washed with conductivity water and the washings were collected in separate vessels and titrated against standard acid, screened methyl orange being used as the indicator. This gave the uptake of CO_3^{-2} anion by the resin. The same resin pieces were next subjected to HNO_3 treatment for their capacity determinations.

In the case of sodium citrate solutions, the resin rods were washed with conductivity water and the washings were sent down a cation exchange column in H^+ form. The citric acid in the effluent was titrated against standard alkali. This gave the amount of citrate ion uptake by the resin. The capacities of the rods were determined as above.

III. RESULTS AND DISCUSSION

The density data for the resin in equilibrium with various standard solutions are given in Table I. The density values for each system rise with increase in the concentration of the external solution. This is due to

TABLE I
Density of the Resin in Na^+ Form in Equilibrium with Electrolyte Solutions

| Concn. of solution, equiv/l. | Density of resin, g./ml. | | | |
|------------------------------|--------------------------|-------|--------------------------|---|
| | NaCl | NaBr | Na_2CO_3 | $\text{Na}_3\text{C}_6\text{H}_5\text{O}_7$ |
| 0.001 | 1.161 | 1.162 | 1.161 | 1.161 |
| 0.01 | 1.161 | 1.164 | 1.161 | 1.161 |
| 0.10 | 1.161 | 1.163 | 1.161 | 1.161 |
| 0.50 | 1.171 | 1.184 | 1.175 | 1.175 |
| 1.00 | 1.186 | 1.190 | 1.190 | 1.187 |
| 2.00 | 1.201 | 1.231 | 1.213 | 1.215 |
| 3.00 | 1.236 | 1.257 | 1.234 | 1.244 |

two factors: (1) the progressive loss in the selectivity of the resin and the consequent increase in the sorption of the electrolyte and (2) the decrease in the water content and the attendant slight decrease in the volume of the resin as the external concentration is increased.

The water content (expressed as the weight of water per gram of wet resin), and total molality of Na^+ (moles per kilogram of water in the resin), and total molality of Cl^- , Br^- , CO_3^{-2} , and $\text{C}_6\text{H}_5\text{O}_7^{-3}$ (also as moles per kilogram of water in the resin) in the resin phase are shown in Table II as functions of the molality of the external solution \bar{m} . The corresponding mean molal activity coefficients $\bar{\gamma}_{\pm}$ for the various electrolytes are also included in Table II. $\bar{\gamma}_{\pm}$ values at 30°C . are available for aqueous solutions of NaCl and NaBr⁸ as also the values for Na_2CO_3 .⁹ In all these cases $\bar{\gamma}_{\pm}$ values for dilute solutions have been calculated using the equation¹⁰

$$\log f_{\pm} = - \frac{A|Z_1Z_2|\sqrt{I}}{1 + Ba\sqrt{I}} + bI \quad (4)$$

where $a = 4.0$ A., and $B = 0.055$ l/mole, and the other terms have their usual significance.

$\bar{\gamma}_{\pm}$ values are not available for sodium citrate solutions. The only guide in this case is the Davies equation:¹¹

$$\log f_{\pm} = -\frac{A|Z_1Z_2|\sqrt{I}}{1+\sqrt{I}} + 0.1|Z_1Z_2|I \quad (5)$$

which has been used in the calculation of activity coefficients shown in Table II.

TABLE II

Equilibrium Water Content w , Molality m_+ and m_- , and the Activity Coefficient Term $\bar{\gamma}_{\pm} e^{\pi v/\nu RT}$ in the Resin Phase as Functions of the Activity of the External Solution

| Equilibrating solution | \bar{m} | $\bar{\gamma}_{\pm}$ | Water content w , g. water/g. wet resin | m_+ | m_- | $\bar{\gamma}_{\pm} e^{\pi v/\nu RT}$ |
|------------------------|-----------|----------------------|---|-------|--------|---------------------------------------|
| Sodium chloride | 0.001004 | 0.965 | 0.638 | 1.264 | 0.004 | 0.014 |
| | 0.01004 | 0.902 | 0.631 | 1.309 | 0.008 | 0.088 |
| | 0.1006 | 0.777 | 0.630 | 1.388 | 0.033 | 0.367 |
| | 0.5064 | 0.679 | 0.610 | 1.626 | 0.247 | 0.542 |
| | 1.024 | 0.658 | 0.600 | 1.940 | 0.595 | 0.627 |
| | 2.090 | 0.677 | 0.575 | 2.598 | 1.235 | 0.790 |
| | 3.210 | 0.735 | 0.558 | 3.510 | 2.138 | 0.861 |
| Sodium bromide | 0.001004 | 0.966 | 0.646 | 1.247 | 0.003 | 0.017 |
| | 0.01004 | 0.910 | 0.644 | 1.280 | 0.006 | 0.103 |
| | 0.1007 | 0.781 | 0.636 | 1.367 | 0.024 | 0.435 |
| | 0.5084 | 0.692 | 0.629 | 1.541 | 0.204 | 0.628 |
| | 1.031 | 0.688 | 0.596 | 1.789 | 0.437 | 0.802 |
| | 2.119 | 0.750 | 0.566 | 2.384 | 1.001 | 1.029 |
| | 3.277 | 0.860 | 0.545 | 3.007 | 1.603 | 1.283 |
| Sodium carbonate | 0.000502 | 0.915 | 0.680 | 1.184 | 0.002 | 0.005 |
| | 0.00502 | 0.780 | 0.672 | 1.228 | 0.004 | 0.034 |
| | 0.0502 | 0.543 | 0.670 | 1.304 | 0.016 | 0.145 |
| | 0.2511 | 0.386 | 0.669 | 1.519 | 0.131 | 0.230 |
| | 0.503 | 0.326 | 0.651 | 1.801 | 0.281 | 2.268 |
| | 1.010 | 0.276 | 0.610 | 2.496 | 0.606 | 0.284 |
| | 1.529 | 0.240 | 0.607 | 3.068 | 0.904 | 0.285 |
| Sodium citrate | 0.000335 | 0.860 | 0.670 | 1.199 | 0.0004 | 0.004 |
| | 0.00335 | 0.652 | 0.635 | 1.294 | 0.0007 | 0.025 |
| | 0.0335 | 0.381 | 0.625 | 1.376 | 0.003 | 0.095 |
| | 0.1693 | 0.332 | 0.612 | 1.531 | 0.052 | 0.195 |
| | 0.3427 | 0.482 | 0.605 | 1.742 | 0.136 | 0.409 |
| | 0.7079 | 1.401 | 0.566 | 2.466 | 0.361 | 1.483 |
| | 1.100 | 4.660 | 0.546 | 3.204 | 0.600 | 5.546 |

The mean molal activity coefficients $\bar{\gamma}_{\pm}$ of small ions of NaCl, NaBr, Na₂CO₃, and Na₃C₆H₅O₇ absorbed by the resin calculated according to eq. (3) are also shown in the last column of Table II and in Figures 1-4. These

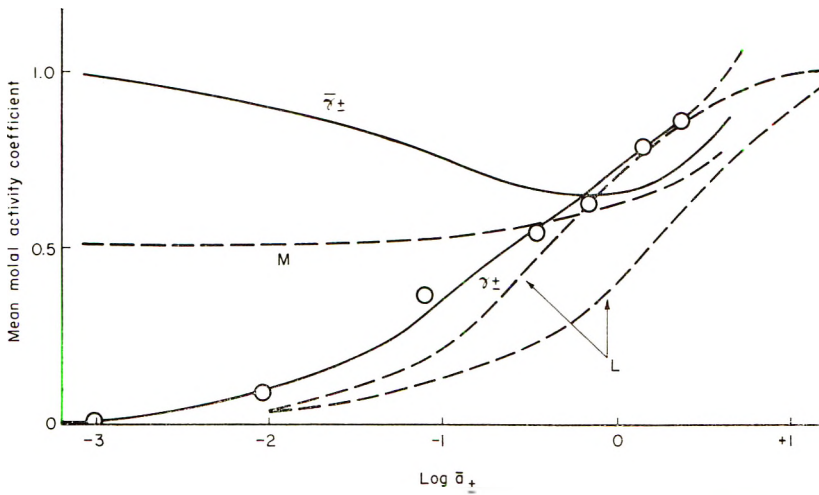


Fig. 1. Calculated and observed activity coefficients of small ions of NaCl in the resin. (L denotes the limits of γ_{\pm} predicted by the theory of Lazare et al.;¹² M denotes limits by the theory of Mackie and Meares.⁶)

γ_{\pm} values derived by analyzing the resin phase include the term $e^{\pi v/\nu RT}$. It has been shown by Mackie and Meares⁶ that the contribution of this term to γ_{\pm} values is negligible. Although these values of γ_{\pm} are determined unambiguously by experiment it is prohibitively difficult to calculate them from first principles. However two theoretical attempts have been made to calculate them. Mackie and Meares⁶ have applied the theory of Katchalsky developed for solutions of uncrosslinked polyelectrolytes to

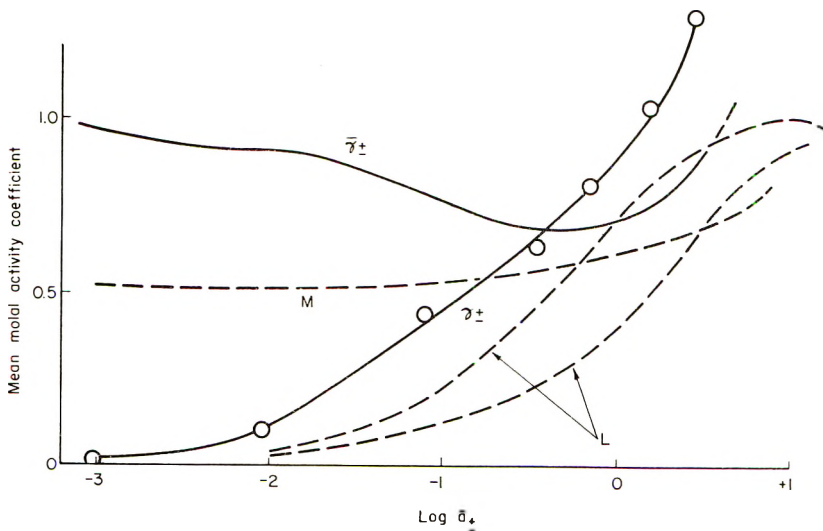


Fig. 2. Calculated and observed activity coefficients of small ions of NaBr in the resin (L and M as in Fig. 1).

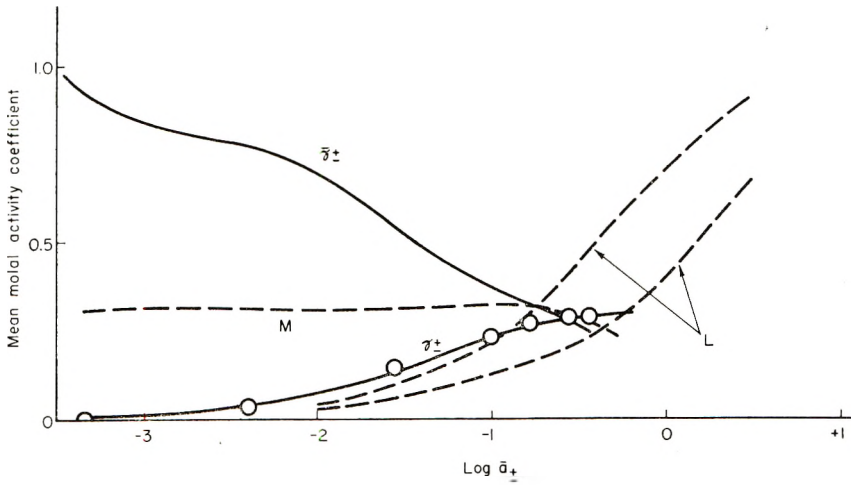


Fig. 3. Calculated and observed activity coefficients of small ions of Na_2CO_3 in the resin (L and M as in Fig. 1).

ion-exchange systems to calculate the activity coefficients of small ions γ_{\pm} in the resin phase. The following expression has been used to calculate them:

$$\ln f_i/f_i^{\circ} = -3Z_{\rho}^2 Z_i^2 e^2 / DKT \sum n_i Z_i^2 (kh_0^2 + 6h_0\alpha) \quad (6)$$

Here f_i/f_i° is the ratio between the internal molar activity coefficient of small ions and that in an aqueous solution of the same ionic concentration, D the

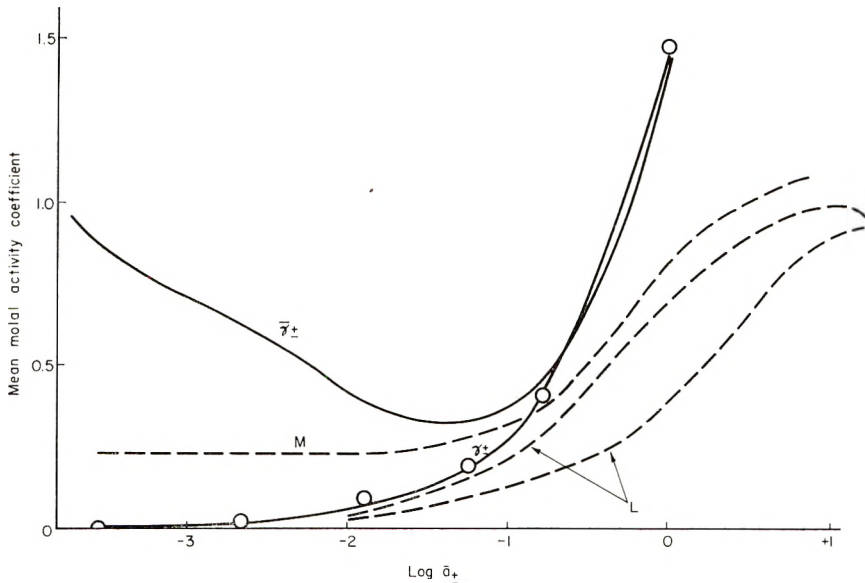


Fig. 4. Calculated and observed activity coefficients of small ions of $\text{Na}_2\text{C}_6\text{H}_6\text{O}_7$ in the resin (L and M as in Fig. 1).

dielectric constant, K the Boltzmann constant, T the absolute temperature, e the electronic charge, Z_p the mean number of fixed charges between network junction points, Z_i the valency, and n_i the number of small ions of type i associated with each polymer chain between junction points. k is the Debye reciprocal length for the internal aqueous phase and is given by

$$k^2 = 4\pi e^2 N \sum c_i Z_i^2 / 1000 DKT$$

where N is the Avogadro's number and c_i the molar concentration of small ions of type i . h_0 is the distance between network junction points in the reference state and is given by

$$h_0^2 = Zsb^2$$

where Z is the number of monomer units between junction points, b the hydrodynamical length of the monomer and s the number of monomer units in each statistical chain element. α is the ratio of the distance between junction points in the actual charged network to h_0 .

The difficulty in applying eq. (6) is to assign reasonable values to the various parameters appearing in the equation. As the resin used in this work is chemically similar to Zeo-Karb 315, the following values taken from the paper of Mackie and Meares are used: $\alpha = 1.66$, $Z = 250$, $Z_p = Z/4.5$, $s = 2$, and $b = 5 \text{ \AA}$.

Activity coefficients have been calculated on the basis of these values, and their variation as a function of external activity is shown in Figures 1-4.

The other theory developed by Lazare, Sundheim, and Gregor¹² is based on Overbeek's concept of charge distribution in an ion-exchange resin. The mathematical treatment is highly complex, and computation involved is difficult and tedious. No attempt therefore is made to calculate the activity coefficients in the resin phase by this method. However their results considered to be of general applicability are taken directly from their paper and are also shown in Figures 1-4.

Hills, Jacobs, and Lakshminarayanaiah⁸ have found that the range of values of mean molal activity coefficients of KOH in 10% crosslinked polymethacrylate (PMA) membranes determined by experiment deviate considerably from the values derived by the theory of Mackie and Meares but agree remarkably with the values predicted by the theory of Lazare et al. No such agreement is found in the present study, however. The observed values deviate from the predictions of both the theories, even though the qualitative nature of variation is in accordance with the theory of Lazare et al. In the region of external concentration $\sim 1 \text{ } \bar{m}$ there is some agreement between experimental values and the values derived by the two theories although it is not observed by the small ions of NaBr and Na₃C₆H₅O₇. The cause of divergence of γ_{\pm} values of sodium citrate may be due to uncertainties inherent in the use of the Davies equation to calculate $\bar{\gamma}_{\pm}$ values.

The difference in the behavior of small ions noticed in case of PMA

resin and phenol sulfonate (PSA) resin can be attributed possibly to the difference in the fixed charge capacity of the resins. PMA resins have a high capacity $\sim 3m$ whereas PSA resins have only $\sim 1.2m$, and thus the former binds more counterions than the latter and the absorption of nebenions in the two cases is almost the same. This is reflected according to eq. (3) in γ_{\pm} values being lower in PMA resins than what they are in PSA resins at corresponding external concentrations. With the other Uni-

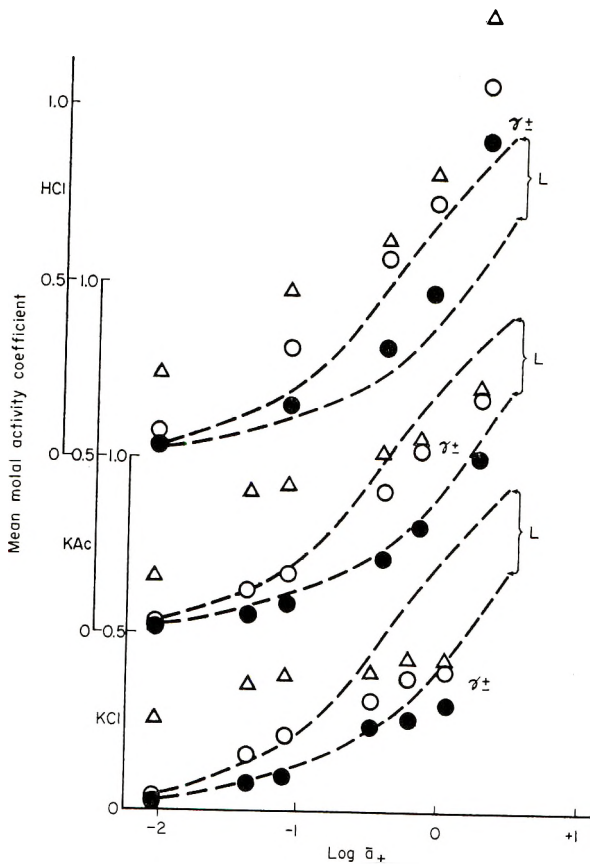


Fig. 5. Calculated and observed activity coefficients of KCl, KAc, and HCl in (Δ) 2%; (\circ) 10%, and (\bullet) 26% crosslinked PSS resins (L as in Fig. 1).

divalent and uni-trivalent electrolytes (see Figs. 3 and 4) the agreement seems to be good with Na_2CO_3 but not quite so with $\text{Na}_3\text{C}_6\text{H}_5\text{O}_7$. Unfortunately no such work for polyvalent electrolytes exists for PMA resins. Nevertheless it can be readily stated that the theory of Lazare et al. is successful in predicting γ_{\pm} values for small ions in high exchange capacity resins but fails in case of resins of low capacity except in the region of external concentration $\sim 1\bar{m}$ where the small ions tend to acquire the chief characteristics of their behavior in aqueous solutions. This can be noticed

in the γ_{\pm} values of ions in the resin phase at external concentrations exceeding $1m$ tending towards values normally observed in aqueous solutions. To facilitate comparison, $\bar{\gamma}_{\pm}$ values in aqueous solutions are also shown in Figures 1-4.

Confirmation of the observations made above is available in the work of Gregor and Gottlieb⁵ concerned with the absorption of various electrolytes by differently crosslinked divinylbenzene (DVB) polystyrenesulfonic acid (PSS) resins. Their experimental results connected with the sorption of KCl, KAc, and HCl electrolytes by PSS resins containing 2, 10, and 26% DVB are shown in Figure 5. γ_{\pm} values in 10 and 26% crosslinked systems satisfy the predictions of the theory of Lazare et al., although the HCl behavior in 10% resin is a bit abnormal. The values with 2% resin deviate considerably from the theoretical values, and, intriguingly enough, the γ_{\pm} values in the neighborhood of the external concentration $\sim 1m$ are within the limits set by the theory. The exchange capacities of these 2, 10, and 26% crosslinked PSS resins are $\sim 1.3m$, $\sim 7m$, and $9-12m$, respectively, and thus substantiate the remarks made above regarding the applicability of the theory of Lazare et al.

References

1. Teorell, T., *Proc. Soc. Exptl. Biol., N. Y.*, **33**, 282 (1935); T. Teorell, *Proc. Natl. Acad. Sci., U. S.*, **21**, 152 (1935).
2. Meyer, K. H., and J. F. Sievers, *Heiv. Chim. Acta*, **19**, 649, 665, 987 (1936).
3. Hills, G. J., P. W. M. Jacobs, and N. Lakshminarayanaiah, *Proc. Roy. Soc. (London)*, **A262**, 257 (1961).
4. Davies, C. W., and G. D. Yeoman, *Trans. Faraday Soc.*, **49**, 968 (1953).
5. Gregor, H. P., and M. H. Gottlieb, *J. Am. Chem. Soc.*, **75**, 3539 (1953).
6. Mackie, J. S., and P. Meares, *Proc. Roy. Soc. (London)*, **A232**, 485 (1955).
7. Scott, M. M., *Standard Methods of Chemical Analysis*, Vol. II, Van Nostrand, New York, (1939) 5th Ed., p. 2253.
8. Harned, H. S., and B. B. Owen, *The Physical Chemistry of Electrolyte Solutions*, Reinhold, New York (1943), pp. 557, 559.
9. Taylor, C. E., *J. Phys. Chem.*, **59**, 653 (1955).
10. Robinson, R. A., and R. H. Stokes, *Electrolyte Solutions*, Butterworths, London, 2nd Ed., 1959, p. 231.
11. Davies, C. W., *J. Chem. Soc.*, **1938**, 2093.
12. Lazare, L., B. R. Sundheim, and H. P. Gregor, *J. Phys. Chem.*, **60**, 641 (1956).

Synopsis

Crosslinked phenol sulfonic acid resins in the form of rods have been prepared. Anion uptake by these resins in equilibrium with aqueous solutions of NaCl, NaBr, Na_2CO_3 , and $\text{Na}_2\text{C}_6\text{H}_5\text{O}_7$ at 30°C . in the concentration range 0.001-3.0N, their density, water content, and exchange capacity have been determined. From these data, activity coefficients of small ions in the resin phase have been calculated and compared with the values derived by the existing theories of Mackie and Meares, and Lazare et al. The agreement between the observed and calculated values is not satisfactory.

Résumé

On a préparé des résines pontées d'acide phénol sulfonique sous forme de harres. On a déterminé la fixation d'anions par ces résines en équilibre avec des solutions aqueuses

de NaCl, NaBr, Na₂CO₃, et Na₃C₆H₅O₇ à 30°C. dans des domaines de concentration de 0.001 à 3.0*N*, ainsi que leur densité, teneur en eau et capacité d'échange. De ces données on a calculé les coefficients d'activité de petits ions dans la phase polymérique et on les a comparés avec les valeurs dérivées par les théories connues de Mackie, Meares, et Lazare et al. L'accord entre les valeurs observées et calculées n'est pas satisfaisant.

Zusammenfassung

Vernetzte Phenolsulfonsäureharze wurden in Stäbchenform hergestellt. Die Anionenaufnahme dieser Harze im Gleichgewicht mit wässrigen Lösungen von NaCl, NaBr, Na₂CO₃, und Na₃C₆H₅O₇ bei 30°C. im Konzentrationsbereich von 0,001 bis 3,0*N*, ihre Dichte, Wassergehalt und Austauscherkapazität wurden bestimmt. Aus diesen Daten wurden die Aktivitätskoeffizienten kleiner Ionen in der Harzphase berechnet und mit den aus den bekannten Theorien von Mackie und Meares, sowie Lazare und anderen erhaltenen Werten verglichen. Die Übereinstimmung der beobachteten und berechneten Werte ist nicht befriedigend.

Received October 19, 1961

The Dielectric Relaxation Time Spectrum and the Corresponding Cole-Cole Diagram for Methylcellulose in Water

W. KUHN and P. MOSER, *Institute of Physical Chemistry of the University of Basle, Switzerland*

1. RELAXATION TIME SPECTRUM

It is known that the dielectric behavior of a substance (pure substance or solution) may be described by its relaxation time spectrum. With this description, if $\mu_{t=0}$ is the dipole moment of the fully or partially oriented system at time zero, the dipole moment μ_t at time t will be

$$\mu_t = \mu_{t=0} \int_0^{\infty} M(\tau) e^{-t/\tau} d\tau \quad (1)$$

where $M(\tau)$ is normalized in such a way that

$$\int_0^{\infty} M(\tau) d\tau = 1 \quad (2)$$

is the distribution function of the relaxation time spectrum and $M(\tau)d\tau$ is the relative partial dielectric moment which decays to the e th part of the initial value in a time τ .

It is possible, if the dielectric relaxation time spectrum, i.e., $M(\tau)$ is known, to answer any question with respect to the dielectric behavior of the substance or the solution. It is then possible to indicate in particular the real part (ϵ') and the imaginary part ϵ'' of the dielectric constant in the case of a pure substance [or the real part $d\epsilon'/dc$ and the imaginary part $d\epsilon''/dc$ of the dielectric increment in the case of a solution; see eqs. (10) and (11) below].

2. COLE-COLE DIAGRAM

Another way of representing the dielectric behavior is realized by use of the Cole-Cole-Diagram.¹

a. Pure Substance with One Relaxation Time

In the case of a substance having only one dielectric relaxation time τ , the complex dielectric constant $\hat{\epsilon}$ would be²

$$\hat{\epsilon} = \epsilon_{\infty} + [(\epsilon_s - \epsilon_{\infty}) / (1 + \omega^2 \tau^2)] (1 - i\omega\tau) \quad (3)$$

where $\omega = 2\pi\nu$, ν being the frequency of the alternating electric field em-

ployed for the measurement of $\hat{\epsilon}$, and ϵ_∞ the dielectric constant for $\omega \gg \tau$. ϵ_s is the static dielectric constant (dielectric constant for $\omega = 0$).

The real part ϵ' and the imaginary part ϵ'' of the dielectric constant will, if $\hat{\epsilon}$ is given by eq. (3), be

$$\epsilon' = \epsilon_\infty + [(\epsilon_s - \epsilon_\infty)/(1 + \omega^2\tau^2)] \quad (4)$$

and

$$\epsilon'' = (\epsilon_s - \epsilon_\infty)[\omega\tau/(1 + \omega^2\tau^2)] \quad (5)$$

The interesting feature of the use of the Cole-Cole diagram i.e., when ϵ'' is plotted as the ordinate versus ϵ' as the abscissa, is the observation that the curve is found to be a half circle with radius $(\epsilon_s - \epsilon_\infty)/2$ whose center is on the abscissa at the point $(\epsilon_s + \epsilon_\infty)/2$, the intersection of the half circle with the abscissa being at $\epsilon' = \epsilon_\infty$ and $\epsilon' = \epsilon_s$.

b. Solution of Solute with One Relaxation Time

In the case of a dilute solution where ϵ and ϵ_0 are the dielectric constants of the solution and the solvent, respectively, we have

$$\epsilon = \epsilon_0 + (\partial\epsilon/\partial c)c \quad (6)$$

where $\partial\epsilon/\partial c$ is the dielectric increment. In a frequency region far from the relaxation frequencies of the solvent and near the relaxation frequency of the solute we have then, in close analogy to eqs. (4) and (5)

$$\frac{\partial\epsilon'}{\partial c} = \frac{\partial\epsilon_\infty}{\partial c} + \frac{(\partial\epsilon_s/\partial c) - (\partial\epsilon_\infty/\partial c)}{1 + \omega^2\tau^2} \quad (7)$$

and

$$\partial\epsilon''/\partial c = [(\partial\epsilon_s/\partial c) - (\partial\epsilon_\infty/\partial c)] [\omega\tau/(1 + \omega^2\tau^2)] \quad (8)$$

from which it follows that the points $\partial\epsilon''/\partial c$ plotted on the ordinate versus $\partial\epsilon'/\partial c$ as the abscissa will be found to describe a Cole-Cole half circle whose center is at the abscissa value of $1/2[(\partial\epsilon_s/\partial c) + (\partial\epsilon_\infty/\partial c)]$, as shown in Figure 1 (curve 1) for the special case $\partial\epsilon_\infty/\partial c = 0$ and $\partial\epsilon_s/\partial c = 1$.

c. Case with a Number of Relaxation Times

In the case of liquids, solids, high polymers, and high polymer solutions, the experimental plots of ϵ'' versus ϵ' have been shown in many cases to form a half circle whose center is not on the abscissa; the height of the curve was found to be smaller in those cases where a number of different relaxation times instead of one single relaxation time was to be expected. Cole and Cole have shown empirically that the values of ϵ'' versus ϵ' also in many of these cases form a half circle whose center is however below the abscissa as shown in Figure 1 (curve 2). The angle β (Fig. 1) formed by the two vectors from the center (below the abscissa) to the intersection of the Cole-Cole circle with the abscissa has often been used as a scale for the width of the dielectric relaxation time spectrum.^{3,4}

Cases of solid high polymers have, moreover, been observed⁵⁻⁷ in which

the experimental points of ϵ'' versus ϵ' deviate from a Cole-Cole circle, and it has been proposed⁵ that this deviation be interpreted by an overlap of a so-called α - and β -absorption.

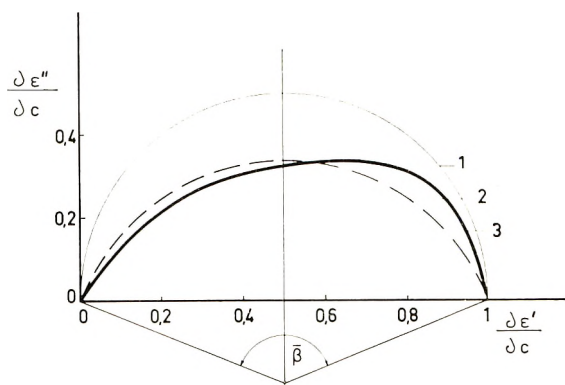


Fig. 1. Cole-Cole diagram [$\partial\epsilon''/\partial c$ vs. $\partial\epsilon'/\partial c$] with $\partial\epsilon_s/\partial c = 1$ and $\partial\epsilon_\infty/\partial c = 0$: (1) semicircular shape for substances or solutions with one relaxation time; (2) circular shape with center of circle below the abscissa for substances with a broad but symmetrical relaxation time spectrum; (3) Cole-Cole diagram of methylcellulose in water on the basis of the experimentally determined relaxation time spectrum (see Fig. 2).

3. EXPERIMENTAL AND THEORETICAL DETERMINATION OF THE DIELECTRIC RELAXATION TIME SPECTRUM OF METHYLCELLULOSE IN WATER

From measurements of the frequency dependence of the dielectric increment produced by methylcellulose in water, it has recently been possible to determine the dielectric relaxation time spectrum of the methylcellulose macromolecule in water.^{8,9} It was found, furthermore, that this relaxation time spectrum was in good agreement with the spectrum calculated a few years ago by W. Kuhn,¹⁰ when using for the parameters occurring in the theoretical formula values obtained from measurements of viscosity and birefringence of flow. As a fair knowledge of the dielectric relaxation time spectrum $M(\tau)$ is thus provided (see Fig. 2); and as $\partial\epsilon'/\partial c$ and $\partial\epsilon''/\partial c$ can be deduced from this, it is interesting to find the corresponding statements in terms of the Cole-Cole diagram.¹¹

It has been shown^{8,10} that the dielectric relaxation time spectrum in dilute solution of a flexible filament containing electrical dipole moments fixed partly parallel and partly perpendicular to the flexible chain axis, is fully determined by three parameters:¹² the orientation relaxation time, the change of shape resistance from the embedding medium, and the activation energy for change of molecular shape.

a. Orientation Relaxation Time

The first parameter is the orientation relaxation time τ_{or} characteristic for the *rigid* statistical coil. This constant can be calculated from the

statistical coil dimensions, which again can be obtained from viscosity measurements in the limit of small velocity gradients. Thus for methylcellulose of a degree of polymerization $P = 890$, we have $\tau_{or} = 0.78 \times 10^{-4}$ sec.

b. Change of Shape Resistance from Embedding Medium

Changes of the resultant dipole moment of the macromolecule can, in addition, be produced by changes of the coil shape. Even if the coil were infinitely flexible, a change of the shape would require some time due to the viscous resistance of the embedding medium. A parameter characteristic for this is the time ϑ_{Ah} , which a statistical chain element of length

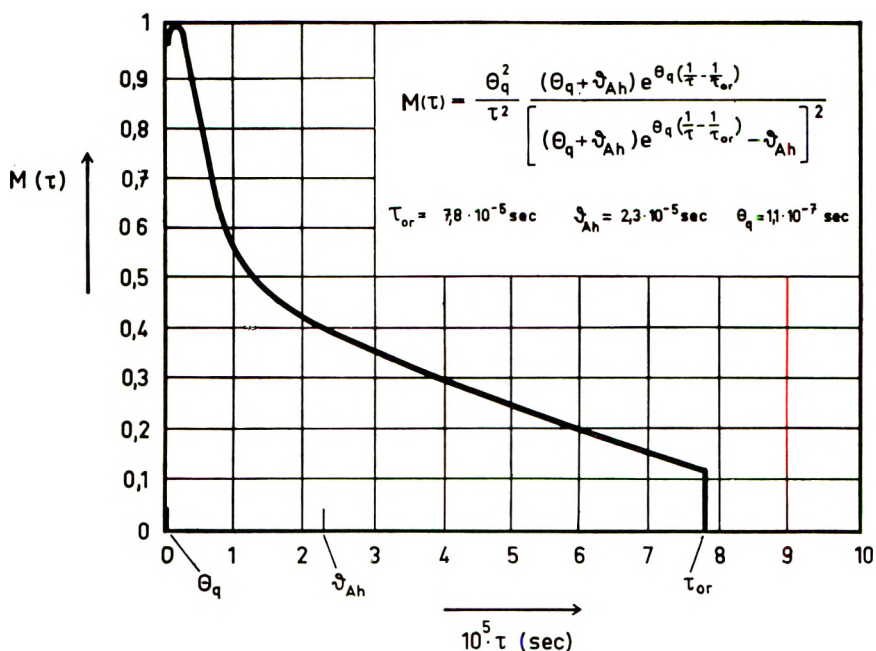


Fig. 2. Relaxation time spectrum of methylcellulose of degree of polymerization $P = 890$ in water, 20°C ., calculated from eq. (9) for $\tau_{or} = 7.8 \times 10^{-5}$ sec., $\vartheta_{Ah} = 2.3 \times 10^{-5}$ sec., $\theta_q = 1.1 \times 10^{-7}$ sec.

A requires for a displacement by the distance $h\sqrt{2}$ (where h is the end-to-end distance of the statistical coil) by diffusion in the embedding medium of viscosity η . ϑ_{Ah} , too, can be predicted if the length A of the statistical chain element and the statistical coil dimension h have been determined, again from viscosity measurements. For an aqueous solution of methylcellulose with $P = 890$, we thus have $\vartheta_{Ah} = 2.3 \times 10^{-5}$ sec.

c. Activation Energy for Change of Molecular Shape

The third parameter, θ_q , will be due to the chain molecule in solution being neither absolutely rigid nor perfectly flexible. An energy of activation q

will be necessary if one part of the molecular chain has to be rotated through a chain bond as an axis from one position of minimum potential energy to a neighboring position of minimum potential energy. If q is known, e.g., if $q = 6700$ cal./mole, the average time θ_q can be indicated which is necessary for the rotation through an angle of about 115° of a group near the chain end around an axis of limited rotation.

In the case of methylcellulose in water, we put $q = 6700$ cal./mole (while an earlier estimate,¹³ based on viscosity and birefringence of flow at high values of the flow gradient, where a mechanical deformation of the statistical coil shape occurs, gave 7600 cal./mole). With this value of q we obtain for methylcellulose $\theta_q = 1.1 \times 10^{-7}$ sec.

In our case, the orientation of the dipole moment occurs simultaneously by rotation of the statistical coil as a whole and by a change of shape of the coil, the resistance for the latter change being due both to the viscosity of the embedding medium and to the internal chain activation energy q . The dielectric relaxation spectrum is therefore in total determined by the three parameters τ_{or} , ϑ_{Ah} , and θ_q ; the formula for $M(\tau)$ is:¹⁰

$$M(\tau) = \frac{\theta_q^2}{\tau^2} \frac{(\theta_q + \vartheta_{Ah}) \exp \left\{ \theta_q \left(\frac{1}{\tau} - \frac{1}{\tau_{or}} \right) \right\}}{\left[(\theta_q + \vartheta_{Ah}) \exp \left\{ \theta_q \left(\frac{1}{\tau} - \frac{1}{\tau_{or}} \right) \right\} - \vartheta_{Ah} \right]^2} \quad (9)$$

It is, by the way, easy to show that $M(\tau)$ fulfills the condition (2).

In those cases in which the dipole moments of some groups in the molecule, instead of being fixed, have a mobility of their own relative to the chain axis, the relaxation times corresponding to the independent orientation of such mobile groups will be found in addition to the relaxation time spectrum described by eq. (9). It has been shown⁹ that the dielectric relaxation time spectrum of methylcellulose does not contain high frequency components of this kind. This is proved by the fact that *all* high frequency components disappear from the spectrum when loose aggregation of the macromolecules takes place in the solution.⁸ It is, however, emphasized that high frequency components corresponding to an independent orientation of mobile dipole groups may accede to eq. (9) and may even be dominant in particular cases. Thus eq. (9) takes account of the phenomena due to dipole moments rigidly fixed to a flexible chain.

Introducing in eq. (9) the values valid for methylcellulose with $P = 890$ in water at 20°C ., i.e. $\tau_{or} = 0.78 \times 10^{-4}$ sec., $\vartheta_{Ah} = 2.3 \times 10^{-5}$ sec., and $\theta_q = 1.1 \times 10^{-7}$ sec. gives for $M(\tau)$ the curve shown in Figure 2.

The values of $d\epsilon'/dc$ (the real part) and of $d\epsilon''/dc$ (the imaginary part) of the dielectric increment for the frequency $\omega/2\pi$ [see eqs. (7) and (8)] are immediately obtained, if $M(\tau)$ is known, from eqs. (10) and (11):

$$\partial\epsilon'/\partial c = \partial\epsilon_\infty/\partial c + [(\partial\epsilon_s/\partial c) - (\partial\epsilon_\infty/\partial c)] \cdot \int_0^\infty M(\tau) d\tau / (1 + \omega^2\tau^2) \quad (10)$$

$$\partial\epsilon''/\partial c = [(\partial\epsilon_s/\partial c) - (\partial\epsilon_\infty/\partial c)] \int_0^\infty \omega\tau M(\tau) d\tau / (1 + \omega^2\tau^2) \quad (11)$$

Curve 2 in Figure 3 shows the real part of the dielectric increment, calculated from eq. (10) using the measured $\partial\epsilon_s/\partial c$ and $\partial\epsilon_\infty/\partial c$ values and the $M(\tau)$ values obtained from eq. (9) with the values mentioned for τ_{or} , ϑ_{ah} , and θ_σ , while curve 1 in Figure 3 shows the observed values of the dielectric increment. The agreement of curves 1 and 2 in Figure 3 demonstrates the validity, in a good approximation, of the actual dielectric relaxation time spectrum of methylcellulose according to eq. (9) and Figure 2.

4. COLE-COLE DIAGRAM OF METHYLCELLULOSE IN WATER

Introducing the values of $M(\tau)$ from eq. (9) (or Fig. 2) into eq. (11) gives the imaginary part of the dielectric increment, which can be plotted in a Cole-Cole diagram as ordinate versus the $\partial\epsilon'/\partial c$ - values obtained from eq. (10) and represented in Figure 3. The result is shown in Fig. 1 curve 3, where, for reason of simplicity, we set $\partial\epsilon_s/\partial c = 1$ and $\partial\epsilon_\infty/\partial c = 0$.

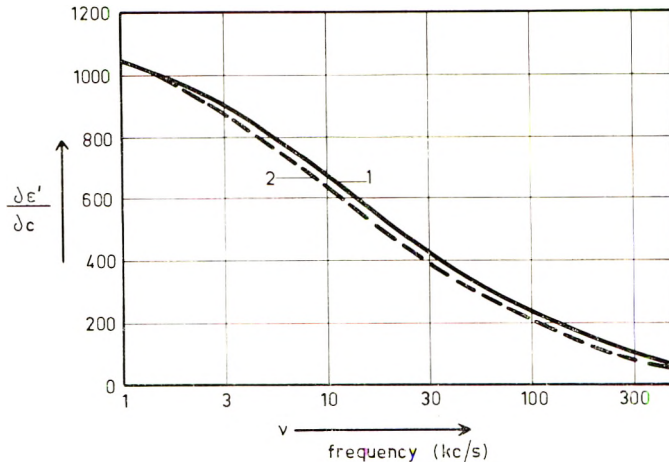


Fig. 3. Experimental and calculated dielectric increment of methylcellulose of degree of polymerization $P = 890$ in water at 20°C .: (1) experimental; (2) calculated from eq. (10) for $M(\tau)$ given by eq. (9) or Fig. 2.

(This simplification has no effect on the shape of the curve.) It is seen that the Cole-Cole diagram corresponding to the dilute aqueous solution of methylcellulose is remarkably unsymmetrical. It is by no means represented by a circle or part of a circle with center somewhere on or underneath the abscissa.

It follows from this analysis that, if $M(\tau)$ is determined, it is always possible to draw a Cole-Cole diagram, but that this diagram does not necessarily in general have the shape of a circle or part of a circle. Deviations from the shape of a circle are possible, even in the case of simple substances in solution, if their dielectric relaxation time spectrum is (as

in the example Fig. 2) unsymmetrically distributed over widely different values of τ .

References

1. Cole, K. S., and R. H. Cole, *J. Chem. Phys.*, **9**, 341 (1941).
2. Böttcher, C. J. F., *Theory of Electric Polarisation*, Elsevier, Amsterdam, 1952.
3. Ishida, Y., M. Yoshino, M. Takayanagi, and F. Irie, *J. Appl. Polymer Sci.*, **1**, 227 (1959).
4. Ishida, Y., Y. Takada, and M. Takayanagi, *Kolloid-Z.*, **168**, 121 (1960).
5. Ishida, Y., *Kolloid-Z.*, **174**, 124 (1961).
6. Ishida, Y., and K. Yamafuji, *Kolloid-Z.*, **177**, 97 (1961).
7. Higasi, K., K. Bergmann, and C. P. Smyth, *J. Phys. Chem.*, **64**, 880 (1960).
8. Kuhn, W., P. Moser, and H. Majer, *Helv. Chim. Acta*, **44**, 770 (1961).
9. Kuhn, W., and P. Moser, *Z. Elektrochem.*, **65**, 649 (1961).
10. Kuhn, W., *Helv. Chim. Acta*, **33**, 2057 (1950).
11. The treatment of this particular question has been suggested through a discussion remark by K. Bergmann on the occasion of a lecture of W. Kuhn at the Tagung der deutschen Bunsengesellschaft, in Karlsruhe, Germany, May 13, 1961; ref. 9.
12. Cf. other statements by J. G. Kirkwood and R. M. Fuoss, *J. Chem. Phys.*, **9**, 329 (1941); *J. Am. Chem. Soc.*, **53**, 385 (1941); L. K. H. van Beek and J. J. Hermans, *J. Polymer Sci.*, **23**, 211 (1957); L. de Brouckère and R. Van Nechel, *Bull. soc. chim. Belg.*, **61**, 261 (1952); L. de Brouckère and L. K. H. van Beek, *Rec. trav. chim.*, **75**, 355 (1957).
13. Kuhn, W., and H. Kuhn, *Helv. Chim. Acta*, **29**, 609 (1946).

Synopsis

From a measurement of the dielectric increment of methylcellulose in water, including the frequency dependence of this increment, the dielectric relaxation time spectrum has been determined and represented quantitatively by a formula containing three parameters τ_{or} , δ_{AA} , and θ_q , each of which can be obtained from earlier published viscosity and birefringence of flow data. On the basis of this relaxation time spectrum, the Cole-Cole diagram of the aqueous solution of methylcellulose can be drawn. It is found that this diagram is dissymmetrical, i.e., different in shape from a circle or part of a circle; the circular form of the Cole-Cole diagram is thus not a general phenomenon, even if it is realized in many cases.

Résumé

La mesure expérimentale de l'incrément diélectrique et de sa dépendance vis-à-vis de la fréquence, a permis de déterminer pour une solution aqueuse de méthylcellulose le spectre de la relaxation diélectrique de cette substance. La distribution des intensités pour les diverses régions de ce spectre a été représentée d'une façon quantitative par une formule établie il y a quelques années et dans laquelle figurent trois paramètres τ_{or} , δ_{AA} , et θ_q qu'il est possible de déterminer un à un en employant des résultats obtenus antérieurement par la viscosité et la biréfringence d'écoulement des solutions. La connaissance du spectre de relaxation diélectrique permet d'établir le diagramme Cole-Cole de la méthylcellulose dans l'eau. On trouve que ce diagramme est fortement dissymétrique, c.à.d. que la courbe diffère de la forme demicirculaire qui a été trouvée pour un certain nombre de substances. La forme circulaire du diagramme Cole-Cole ne représente donc pas une régularité universelle.

Zusammenfassung

Die Messung des dielektrischen Inkrementes und dessen Frequenzabhängigkeit an wässrigen Lösungen von Methylcellulose ermöglichte eine Bestimmung des dielektri-

sehen Relaxationszeitspektrums dieser Substanz. Das Spektrum erstreckt sich über einen Frequenzbereich von etwa 10^{-7} bis 10^{-4} sec und kann durch eine vor einigen Jahren abgeleitete Formel quantitativ wiedergegeben werden; der Verlauf des Relaxationszeitspektrums wird hiernach durch drei Parameter, τ_{or} , ϑ_{Ah} und θ_q , bestimmt, wobei jeder dieser drei Parameter auf Grund früher veröffentlichter Messungen der Viskosität und der Strömungsdoppelbrechung von Methylcelluloselösungen berechnet werden kann. Die Kenntnis des dielektrischen Relaxationszeitspektrums gestattet seinerseits die Aufstellung des Cole-Cole-Diagramms. Die Auswertung ergibt einen stark unsymmetrischen Verlauf der Cole-Cole-Kurve, d.h. eine starke Abweichung der Kurve von der Kreisgestalt. Der in vielen Fällen gefundene kreisförmige Verlauf der Cole-Cole-Kurve entspricht daher keiner allgemein gültigen Gesetzmässigkeit.

Received October 11, 1961

Melting Transitions in Diene Polymers

W. COOPER and R. K. SMITH, *Central Research Division, Dunlop Research Centre, Birmingham, England*

INTRODUCTION

The melting behaviors of gutta-percha¹ and rubber² have been extensively studied. Melting points depend on the conditions under which crystallization has occurred and on the rate of heating. As interconversion of less to more stable crystallites can occur during melting, it follows that equilibrium melting points are obtained only with very slow heating rates.^{3,4} These changes have normally been measured in dilatometers. In this work differential thermal analysis (DTA), which has been employed for the detection and measurement of thermal transitions in hydrocarbon polymers,^{5,6} has been employed. It is not suited for the measurement of equilibrium melting points, but is convenient for studying detail in the melting curves.

EXPERIMENTAL

Apparatus

Two types of apparatus were employed in this work. In the first of these the cells were in the form of thin copper tubes (2 in. \times $\frac{3}{8}$ in.) suspended in air in a well-lagged, electrically heated, metal block. The sample size was approximately 2 g. The other, more robust and suited for manipulating tough materials such as rubber or balata, was a cylindrical copper block (3 in. \times $2\frac{1}{4}$ in.), with two $\frac{3}{4}$ -in. diameter holes for sample and reference material; the size of sample was 10 g. Screwed brass caps, fitted with guides held the thermistors; thermocouples were inserted in the center of the sample and in the block for the temperature records. The metal block was fitted with cast phenolic feet, detachable lifting handles, wound with a flexible heating tape, and well insulated by wrapping in glass cloth. The assembly was placed in a large Dewar vessel, with a lid of foamed polystyrene. The reference material, polybutadiene prepared in the presence of butyl lithium catalyst, showed no evidence of thermal transitions over the temperature range employed. The apparatus in which the cells were isolated was of greater sensitivity in spite of the smaller sample size. The differential temperature observed for any transition, after allowing for the difference in sample size was greater by a factor of 10. Thermograms of diene polymers were identical from both sets of apparatus,

and since the measuring system employed had ample sensitivity, the more robust apparatus was preferred. Heating rates of 0.01–0.3°C./min. were generally employed. For measurement of the differential temperatures, matched thermistors, Type F22 for temperatures of –50 to +20°C. and Type F23 for temperatures from 20 to 80°C. (Standard Telephone and Electric Ltd.) were used. The bridge circuit used is shown in Figure 1. The output from the bridge was recorded on a 1-mv. Xactrol recorder (Ether Ltd.).

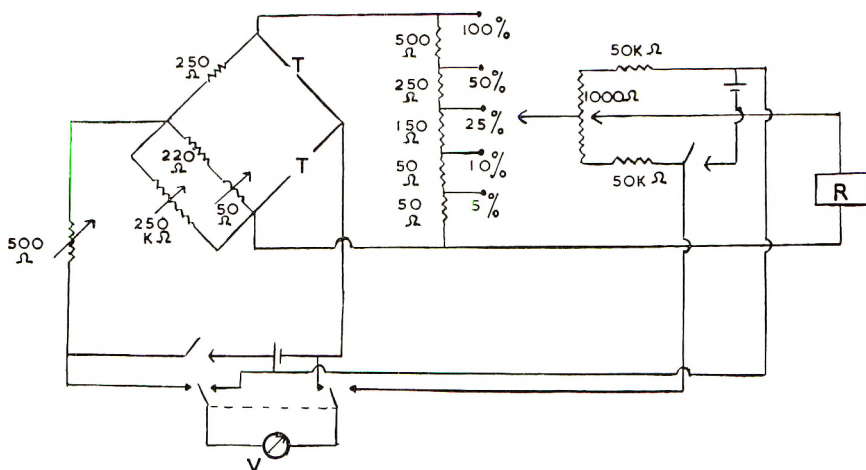


Fig. 1. Bridge circuit. (*R*) recorder; (*V*) voltmeter; (*T*) thermistor.

A separate record was made of the change of temperature in the center of the sample. Except at a transition this was found to be identical, within the precision of the measurements, with that of the reference material and about 0.5°C. lower than that of the metal block.

Calibration

The most convenient method of calibration was to reduce the resistance of one arm of the bridge by placing a resistor in parallel with the thermistor and observing the response of the recorder.

The off-balance current in the circuit *g* is given by

$$g = \frac{(PX - QR)ET}{[GT + (P + R)(Q + X)] [BT + (P + Q)(R + X)]} \quad (1)$$

where *P*, *Q*, *X*, and *R* are the resistances of the arms of the bridge, *G* is the resistance of the recorder, *E* the potential of the battery and *B* its internal resistance, and $T = P + Q + R + X$. In the present case $X = Q = 250\Omega$; *R* is the thermistor resistance; the resistance of parallel circuit of thermistor and resistor $P = R - \Delta$; $B = 1\Omega$; $E = 1.5\text{ v}$. The resistor chosen was of a high value ($10^5\Omega$) so as to disturb the current flowing in the thermistors as little as possible. It was confirmed by separate measurements that little or

no error was introduced if the value of the resistor was above $10^4\Omega$. Measurements were made at several temperatures from -20 to $+12^\circ\text{C}$., the thermistor resistance changing from 800 to 2400Ω over this interval. From eq. (1) the value of Δ for a reading of 1 mv. on the recorder can be calculated. It is shown as the continuous line in Figure 2; the circles represent the experimental points. At -18°C . the change in thermistor resistance is $30\Omega/^\circ\text{C}$. and at $+12^\circ\text{C}$., $7\Omega/^\circ\text{C}$. Thus over the whole range the sensitivity remains substantially constant at $0.11^\circ\text{C}/\text{mv}$. The maximum sensitivity is, assuming 1% accuracy, 0.001°C . while, with minimum sensitivity (5%) a maximum temperature differential of 2.2°C . can be measured. This range was ample for most purposes, since the maximum differential temperatures observed with rates of heating up to $0.3^\circ\text{C}/\text{min}$. were in the region of 1.0 and 0.4 degrees, respectively, for the two sets of equipment for *trans*-polyisoprene, which gave the largest temperature differentials.

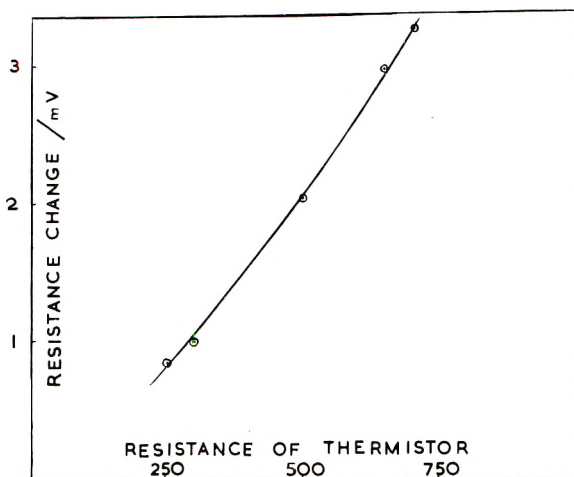


Fig. 2. Calibration curve for bridge.

Peak areas were measured graphically, but often there was difficulty in assessing the temperature range over which melting occurred. With most diene polymers some melting occurs to some extent over a wide range of temperature below the melting point. In the case of balata (Fig. 3) no great error was involved in comparing the relative areas of the peaks, except where they overlapped, but with natural rubber (Fig. 4) the transitions were so gradual that they could not be measured with certainty. In the case of balata a single, well defined peak was obtained on cooling, from which, by comparison with the areas found for standard substances (benzophenone, naphthalene, and *p*-dichlorobenzene) the melting enthalpy was estimated to vary between 7 and 10 cal./g., dependent on the rate of cooling, which presumably influences the degree of crystallinity to some extent.

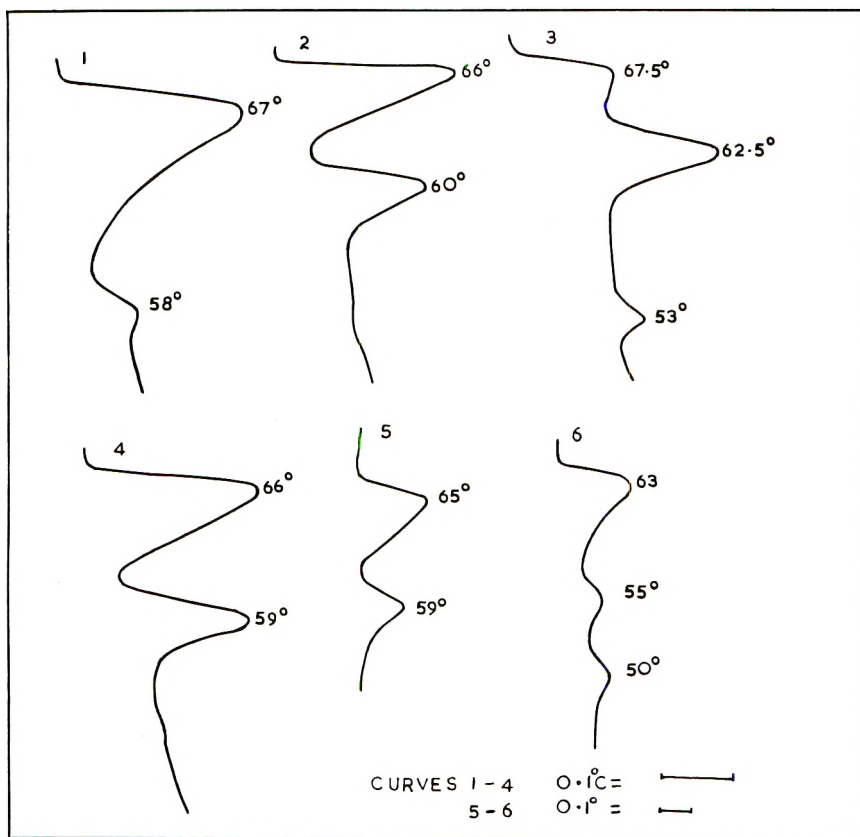


Fig. 3. Differential thermal curves for gutta-percha, balata, and *trans*-polyisoprenes: (1) gutta-percha crystallized at 54°C.; (2) gutta-percha, normal cooling from 75°C.; (3) gutta-percha, cooled rapidly to 50°C.; (4) balata, normal cooling from 74°C.; (5), (6) synthetic *trans*-polyisoprenes.

RESULTS AND DISCUSSION

trans-Polyisoprene

a. Gutta-Percha and Balata. These polymers behave similarly (e.g., Fig. 3, curves 2 and 4), and the major peaks relate to the well known α and β forms. The relative importance of the two forms is dependent both on the temperature at which the sample is melted, and on the subsequent cooling cycle (Fig. 3, curves 1-3). In Figure 5 is shown the influence of the temperature to which a sample of gutta-percha was heated before cooling on the relative areas of the two peaks. It can be seen that the α form predominates unless the sample is heated above 74°C., although in each case the sample appeared to be molten.* Presumably, below the equilibrium temperature of 74°C.⁴ crystal nuclei remain in the melt, from

*The sample was melted in the cell and it was observed that in each case the melting transition as judged by the differential thermogram was complete.

which the α form is obtained on cooling. The cooling cycle is equally important, and in Table I is shown the change in the relative size of the two peaks with different cooling conditions.

Cooling slowly at $50\text{--}54^\circ\text{C}$. resulted mainly in the α form, but a little of

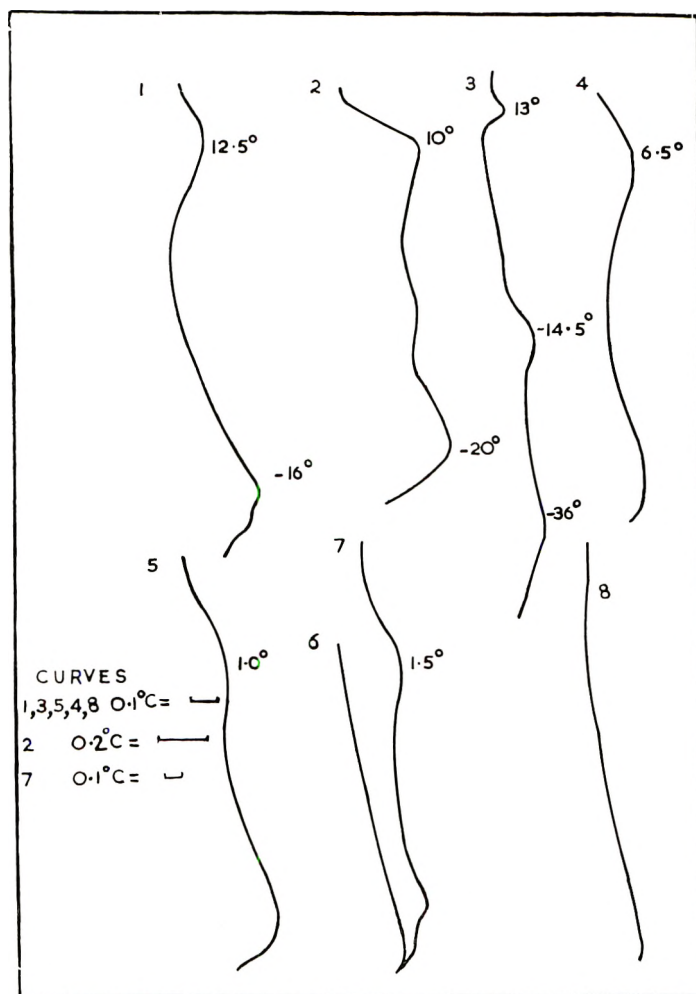


Fig. 4. Differential thermal curves for natural rubber and synthetic *cis*-polyisoprenes: (1) natural rubber, crystallized 16 hr. at -25°C .; (2) natural rubber, stored 6 months at -25°C .; (3) natural rubber, crystallized 45 hr. at -80°C .; (4), (5) *cis*-polyisoprenes (Ziegler catalyst); (6) thermistor drift; (7) *cis*-polyisoprene (Ziegler catalyst); (8) *cis*-polyisoprene (butyllithium catalyst).

the β form was produced whatever the cooling cycle employed. Rapid cooling to below 30°C . froze in mainly the α form, which was the predominant nucleus at the initial temperature of 70° . Not until in the region of 50°C . is the rate of conversion into the β form appreciable. It was found that some α form always resulted, irrespective of the crystallization condi-

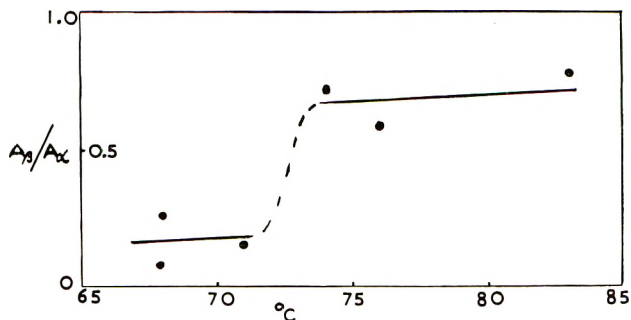


Fig. 5. Influence of temperature of melt on relative proportions of α and β forms of gutta-percha.

TABLE I
Influence on Cooling on Ratio of Isomorphous Forms of Gutta-Percha

| Cooling from 70°C. | A_{β}/A_{α} ^a |
|--------------------|-------------------------------------|
| Rapidly to 0°C. | 0.11 |
| " " 30°C. | 0.14 |
| " " 40°C. | 0.30 |
| " " 50°C. | 1.76 |
| Slowly to 50°C. | 0.05 |
| " " 54°C. | 0.03 |

^a The crystal melting points of the two forms and the total areas under the peaks were, within the accuracy of the experiments, the same.

tions. One possibility is that this had resulted by recrystallization of molten β polymer, evidence for which follows from the influence of heating rate on the size of the β peak (Table II). This change must occur during the melting of the β form, since there is no evidence from the DTA curves of heat liberation between the peaks nor does the aggregate area of the two peaks change greatly with alteration in their relative sizes.

TABLE II
Effect of Heating Rate on Melting of Gutta-Percha

| Heating rate, °C./hr. | Melting point, °C. | | A_{β}/A_{α} |
|--------------------------|--------------------|---------|------------------------|
| | α | β | |
| 0.9 | 68.2 ^a | 60.2 | 0.17 |
| | 66.5 | | |
| 2.5 | 66.2 | 60.0 | 0.34 |
| 6 | 66.0 | 60.0 | 0.54 |
| 10 | 66.0 | 60.0 | 1.30 |
| 15 | 66.0 | 60.0 | 1.48 |

^a Split peak observed in this case.

In some cases, a third peak (Fig. 3, curve 3) was observed. The position of this peak, which was small, was not so well defined and appeared at

temperatures varying from 43 to 53°C. It seems likely that it results from imperfect crystals produced during cooling.

b. Synthetic *trans*-Polyisoprene. These polymers showed, in general, similar behavior to the natural products. A characteristic feature of the thermograms was the appearance of a third melting transition. This occurred at a similar temperature to that observed with gutta-percha and is probably of the same origin. Also like the latter, however, this transition was not observed with all the samples (Fig. 3, curves 5 and 6).

cis-Polyisoprene

a. Natural Rubber. The melting transitions with this polymer, which were crystallized at -25°C ., were much less well defined than in the case of the *trans* isomer (Fig. 4, curve 1). At the heating rate chosen ($0.08^{\circ}\text{C}/\text{min}$.) the melting point is in the region of $+13^{\circ}\text{C}$., the lower peak occurs at -18 to -13°C . Storage of the rubber for a prolonged period at -25°C . made little or no difference to the shape of the curve (Fig. 4, curve 2), but when the sample was brought up from a much lower temperature (-50°C .) (Fig. 4, curve 3), the lower transition is more sharply defined at -14.5°C . and is readily distinguished from one occurring at -36°C .

b. Synthetic Polymers. In Figure 4 (curves 4-7) are shown results for a number of synthetic polyisoprenes; all show less crystallinity than natural rubber, and the polyisoprene of 92% *cis* content (curve 8) shows no transition at all. Owing to the difficulty of quantitative infra-red analysis of high *cis* content polymers, identification of the upper melting transition with *cis* content is not too precise. Nevertheless it can be seen that a correlation exists (Table III).

TABLE III
Relationship between *cis* Content and Melting Point of Polyisoprene

| Catalyst | Content <i>cis</i> 1,4, % | Upper melting transition, °C. ^a |
|------------------|------------------------------|---|
| Lithium | 92 | None |
| Ziegler | 96 | 1 |
| " | 96 | 1.7 |
| " | 97 | 6.5 |
| (Natural rubber) | 98+ | 13.5 |

^a All polymers crystallized at -25°C . for 20 hr.; heating rates $0.08^{\circ}\text{C}/\text{min}$.

The melting point of rubber depends on the rate of heating and on the temperature at which crystallization was carried out. It has been found that the melting point varies from ca. -2°C . to 20°C . as the crystallization temperature is varied from -40°C . to 14°C . The range of temperature over which melting occurs sharpens as the upper melting point increases. (With rubber melting at 0°C . the range is ca. 25 degrees and for rubber melting at 15°C . the range is ca. 10 degrees.) From determinations carried out with extremely slow heating rates the equilibrium melting tem-

perature for unstressed rubber has been shown to be in the vicinity of $+28^{\circ}\text{C}$.³ The values obtained in the present work are, therefore, non-equilibrium. It follows that reproducible results can only be obtained under strictly controlled conditions, and in different samples of polyisoprene the deviations from equilibrium melting points are not necessarily the same. The heating rates employed here were about $0.1^{\circ}\text{C}/\text{min}$., giving rise to melting points somewhat higher than reported in the literature for crystallization at -25°C ., but considerably below the equilibrium value. The heating rate necessary to obtain the latter value has been found to be in the region of $1^{\circ}\text{C}/\text{day}$.³ Such a rate would be quite impracticable with this technique, and it must be concluded that, with polyisoprene at least, ideal conditions cannot be achieved.

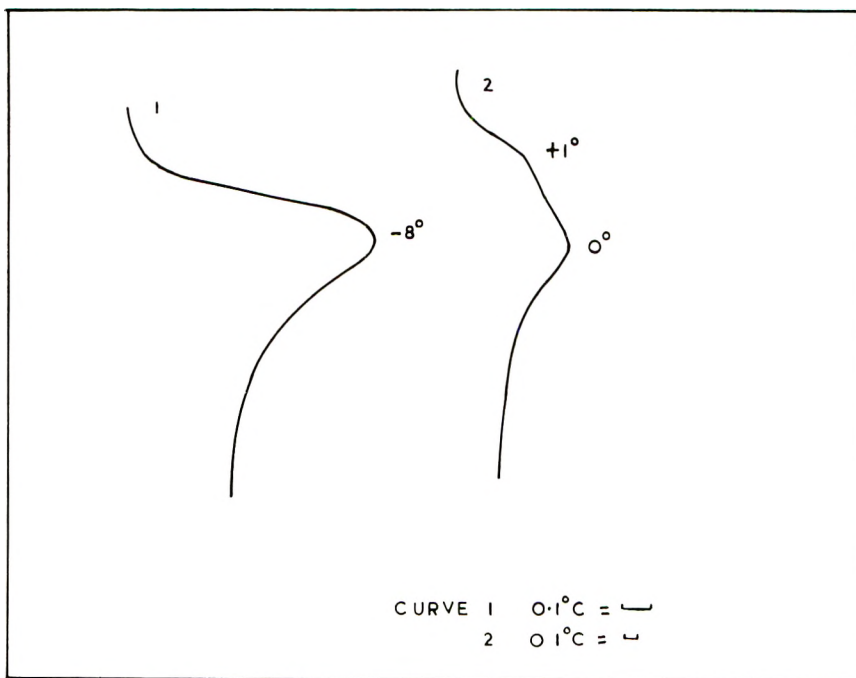


Fig. 6. Differential thermal curves for *cis*-polybutadienes: (1) 93% *cis*-1,4; (2) 98.5% *cis*-1,4.

***cis*-Polybutadiene**

In Figure 6 are shown curves for high *cis*-polybutadiene. All are characterized by a melting transition which occurs over a wide temperature range from about -20°C ., but melting is relatively slow to within $2\text{--}3^{\circ}\text{C}$. from the final melting point. The melting transition depends on the *cis* content (Table IV), as has been shown also from dilatometric measurements.⁷ Under more sensitive conditions fine detail can be seen in the curves. Thus sample 4 gives a broad melting peak (Fig. 6, curve 2), which

TABLE IV
Relationship between *cis* Content and Melting Point of Polybutadiene

| Sample | Catalyst | <i>cis</i> content, % | Transition temperature, °C. |
|--------|--|-----------------------|-----------------------------|
| 1 | TiI ₄ -AlR ₃ | 93 | -8 |
| 2 | TiI ₄ -AlR ₃ | 94 | -6.5 |
| 3 | CoCl ₂ -AlR ₂ Cl | 97 | +0.5 |
| 4 | " | 98.5 | +1.0 |

indicates the presence of crystallites of different melting points. (As this curve was repeated several times and showed no variation it is clearly significant.) The region of partial melting (-20 to -5°C.) also shows small transitions, but these are much less marked than is the case with polyisoprene. The dependence of melting point of polybutadiene on heating rate is also much less marked than it is with polyisoprene. With sample 4 of Table IV a reduction in heating rate from 0.15°C./min. to 0.04°C./min. resulted in an increase in melting point of ca. 2°C.

The authors thank Mr. A. Hiron for assistance with the bridge circuit and the Dunlop Rubber Company Limited for permission to publish this work.

References

1. Dean, J. N., *Trans. Inst. Rubber Ind.*, **8**, 25 (1932); E. A. Hauser, and G. von Susich, *Kautschuk*, 137 (1932).
2. Wood, L. A., *Advances in Colloid Sci.*, **2**, 78 (1946).
3. Roberts, D. E., and L. Mandelkern, *J. Am. Chem. Soc.*, **77**, 781 (1955).
4. Mandelkern, L., F. A. Quinn, Jr., and D. E. Roberts, *J. Am. Chem. Soc.*, **78**, 926 (1956).
5. Ke, B., *J. Polymer Sci.*, **42**, 15 (1960).
6. Ke, B., *J. Polymer Sci.*, **50**, 79 (1961).
7. Natta, G., *Makromol. Chem.*, **35**, 94 (1960); see also G. Kraus, J. N. Short, and V. Thornton, *Rubber and Plastics Age*, **38**, 880 (1957).

Synopsis

The melting transitions of natural rubber, *cis*-polyisoprene, gutta-percha, balata and synthetic *trans*-polyisoprene, and *cis*-polybutadiene have been examined by means of differential thermal analysis. Natural rubber melts over a wide range of temperature giving several transitions, the magnitude and temperature of which depend on the experimental conditions. At heating rates feasible for differential temperature measurements the values observed are markedly below the equilibrium melting points. Natural and synthetic *trans*-polyisoprenes possess similar melting points and extents of crystallinity. The ratio of the peaks associated with the α and the β forms is not only dependent on the rate of cooling and temperature of crystallization, but also on the temperature to which the sample was heated before crystallization. This is thought to be due to the persistence of crystalline nuclei in the polymer melt. Under certain conditions a small melting transition occurs at a lower temperature. Synthetic *cis*-polyisoprenes show melting characteristics similar to those of natural rubber, but the upper transition is lower than that of the natural product and correlates with the *cis* content of the polymer. *cis*-Polybutadienes melt slowly over a wide range of temperature below the characteristic melting transition which is dependent on the *cis* content. The highest melting point observed for a polymer of 98% *cis* content was +1°C.

Résumé

On a examiné par analyse thermique différentielle les transitions de fusion du caoutchouc naturel, du *cis*-polyisoprène, du gutta-percha, du balata du *trans*-polyisoprène synthétique et du *cis*-polybutadiène. La fusion du caoutchouc naturel s'étend sur un large domaine de température et présente plusieurs états de transition. L'importance et la température à laquelle ont lieu ces états de transition dépendent des conditions expérimentales. Avec des vitesses de chauffage acceptables pour effectuer des mesures de température différentielle, les valeurs observées se situent nettement en dessous des points de fusion à l'équilibre. Le polyisoprène naturel et le polyisoprène-*trans* synthétique possèdent des points de fusion similaires ainsi que des degrés de cristallinité identiques. Le rapport des pics associé aux formes α et β dépend non seulement de la vitesse de refroidissement et de la température de cristallisation, mais encoure de la température à laquelle l'échantillon a été chauffé avant la cristallisation. On estime que cela est dû à la conservation du noyau cristallin dans le polymère fondu. Sous certaines conditions, une faible transition de fusion a lieu à plus basse température. Le polyisoprène-*cis* synthétique présente des caractéristiques de fusion semblables au caoutchouc naturel, mais la transition supérieure est plus basse que celle du produit naturel et est à mettre en relation avec la teneur en composé *cis* du polymère. Le polybutadiène-*cis* fond lentement dans un large domaine de température et en-dessous des points caractéristiques de transition qui dépendent de la teneur en isomère-*cis*. Le point de fusion le plus élevé observé pour un polymère renfermant 98% de forme *cis* est $+1^\circ\text{C}$.

Zusammenfassung

Die Schmelzumwandlung von Naturkautschuk, *cis*-Polyisopren, Guttapercha, Balata und synthetischem *trans*-Polyisopren und *cis*-Polybutadien wurde mittels Differentialthermoanalyse untersucht. Naturkautschuk schmilzt über einen grossen Temperaturbereich und zeigt mehrere Umwandlungen, deren Gröss und Temperatur von den Versuchsbedingungen abhängen. Bei Erhitzungsgeschwindigkeiten, welche für die differentielle Messung der Temperatur geeignet sind, liegen die beobachteten Werte merklich unter den Gleichgewichtsschmelzpunkten. Natürliches und synthetisches *trans*-Polyisopren besitzen einen ähnlichen Schmelzpunkt und einen ähnlichen Kristallinitätsgrad. Das Verhältnis der Spitzen für die α - und β -Form ist nicht nur von der Abkühlungsgeschwindigkeit und der Kristallisationstemperatur abhängig, sondern auch von der Temperatur, auf die die Probe vor der Kristallisation erhitzt wurde. Dies wird auf das Bestehenbleiben von Kristallkeimen in der Polymerschmelze zurückgeführt. Unter bestimmten Bedingungen tritt eine kleine Schmelzumwandlung bei einer tieferen Temperatur auf. Synthetisches *cis*-Polyisopren zeigt ähnliche Schmelzcharakteristika wie Naturkautschuk, die obere Umwandlung liegt jedoch tiefer als beim Naturprodukt und steht in Beziehung zum *cis*-Gehalt des Polymeren. *Cis*-Polybutadien schmilzt langsam über einen weiten Temperaturbereich unterhalb der charakteristischen Schmelzumwandlung, welche vom *cis*-Gehalt abhängig ist. Der höchste, für ein Polymeres mit 98% *cis*-Gehalt beobachtete Schmelzpunkt betrug $+1^\circ\text{C}$.

Received October 31, 1961

Static Electricity in Polymers. II. Chemical Structure and Antistatic Behavior

VICTOR E. SHASHOUA,* *Pioneering Research Laboratory, Textile Fibers Department, E. I. du Pont de Nemours & Co., Inc., Wilmington, Delaware*

INTRODUCTION

Previous attempts to correlate the chemical structure of polymers with their tendency to accumulate electrostatic charges were primarily concerned with explaining a given triboelectric series. For example, Sippel¹ noted that certain polymers with carbonyl groups tended to develop positive charges when rubbed against brass, while vinyls and polyesters became negatively charged. More recently Medley² noted that cross-linked ion exchange resins with carboxyl groups acquired negative charges, but resins with quaternary ammonium groups became positively charged when rubbed against neutral surfaces. These observations suggest that there is a relationship between the sign of the electrostatic charge developed and the chemical composition of a polymer.

The first paper³ of this series described an instrument for measurement of the rates of build-up and decay of charges on polymers. It was noted that polymers could be classified into three general types, namely: (1) those from which negative charge decayed slower than positive or "electrostatically negative"; (2) those from which positive charge decayed slower than negative, "electrostatically positive"; and (3) those for which there was no charge preference; i.e., "electrostatically neutral."

In this paper an attempt is made to correlate the chemical structure of polymers with antistatic behavior. A variety of vinyl and condensation polymers containing different functional groups were thus synthesized and tested as coatings on fabrics and films. The rates of dissipation of electrostatic charges from these surfaces were then measured and used to obtain certain generalities about the relationship of antistatic behavior and chemical structure.

EXPERIMENTAL

Source of the Monomers

Most of the monomers were obtained commercially. Some were synthesized according to published methods: *N*-vinyl methylformamide by

* Present address: Applied Physics Section, Engineering Research Laboratory, Experimental Station, E. I. du Pont de Nemours & Co., Wilmington, Delaware.

vinylation of methylformamide with acetylene,⁴ *p*-styrenesulfonamide from styrenesulfonic acid,⁵ and *N*-vinylcaprolactam by vinylation of caprolactam.⁶ *N*-Acrylyl morpholine and its analog were prepared from the acid chloride and excess base.

Freshly distilled acrylylchloride (45 g.) dissolved in 50 ml. of benzene was added in about 1 hr. to 88 g. of an ice-cooled morpholine solution in 200 ml. benzene containing 0.2 g. added sulfur. The mixture was then allowed to stand at room temperature for 1 hr. Next, the precipitated morpholine hydrochloride was filtered off and the filtrate, a benzene solution of the monomer, was fractionated in a spinning band column.

A main fraction (28 g. of a colorless liquid, b.p. 100°C./2 mm.), and a second fraction (11 g. of colorless liquid, b.p. 113°C./2 mm.) in addition to a polymerized pot residue were obtained. Fraction 1 was analyzed by vapor phase chromatography to be 96.8% pure while Fraction 2 was 98.6% pure.

ANAL. Calc. for C₇H₁₁NO₂: C, 59.5%; H, 7.8%; N, 10%. Found: C, 58.2%; H, 7.7%; N, 10.2%.

N-Acrylyl pyrrolidine was synthesized by a similar method in 55% yield. The purified monomer boiled at 90°C./1 mm.

ANAL. Calc. for C₇H₁₁NO: C, 67.2%; H, 8.8%; N, 11.2%. Found: C, 66.9%; H, 8.7%; N, 11.1%.

Synthesis of the Polymers

Table I summarizes the synthesis of the various vinyl polymers used in this work. The interfacial polycondensation⁷ method was used to synthesize poly(piperazine adipamide),⁸ poly(dimethylpiperazine adipamide), and the various polyterephthalamides from primary and secondary diamines.⁹ The addition polymer from piperazine and *N,N'*-methylene bisacrylamide, supplied by N. Field, was prepared according to the method of Hulse.¹⁰ A number of new polymers containing specific functional groups were synthesized as follows.

Synthesis of the *N*-Dimethylurea Adduct of Polymethylolacrylamide.

This polymer containing an *N*-dialkylated urea side chain was synthesized according to the following reaction scheme:

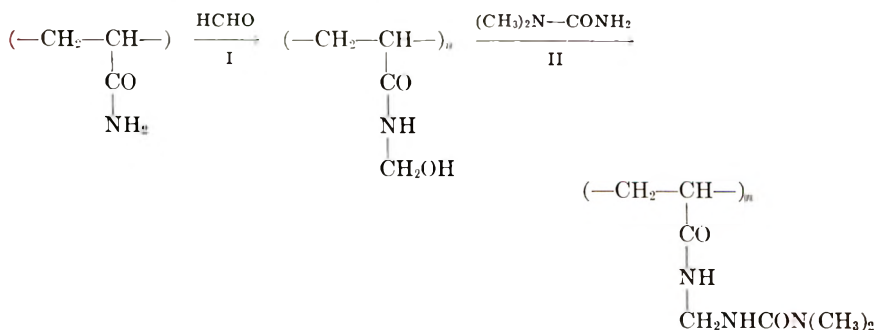


TABLE I
 Synthesis of the Polymers

| Polymer | Monomer Amount | Source | Solvents | Catalysts ^a | Temp., °C. | Time, hr. | Yield, % |
|---------------------------------------|-------------------|--------------------|--|--|---------------|--------------|-----------------|
| Poly(sodium styrenesulfonate) | 50 g. | Dow Chem. Co. | H ₂ O (100 ml.) + <i>tert</i> -Butanol (100 ml.) | A ₁ (0.2 g.) | 80 | 16 | 45 |
| Poly(sodium ethylenesulfonate) | 40 g. | Du Pont Org. Chem. | H ₂ O (100 ml.) + <i>tert</i> -Butanol (100 ml.) | A ₁ (0.2 g.) | 80 | 16 | 80 |
| Poly(dimethylaminoethyl methacrylate) | 20 g. | Du Pont Org. Chem. | <i>tert</i> -Butanol (200 ml.) | A ₁ (0.2 g.) | 80 | 16 | 95 |
| Polystyrenesulfonamide | 50 g. | Du Pont Org. Chem. | <i>tert</i> -Butanol (300 ml.) | B ₁ (0.5 g.) | 80 | 16 | 65 |
| Polydimethylacrylamide | 30 ml. | Monomer-Polymer | H ₂ O (250 ml.) | K ₂ S ₂ O ₈ (0.3 g.) + NaHSO ₃ (0.3 g.) | 40 | 16 | 95 |
| Polydiethylacrylamide | 30 g. | Monomer-Polymer | H ₂ O (250 ml.) | K ₂ S ₂ O ₈ (0.2 g.) + NaHSO ₃ (0.2 g.) | 40 | 16 | 85 ^b |
| Poly- <i>N-tert</i> -butylacrylamide | 10 g. | American Cyanamide | H ₂ O (300 ml.) | NaHSO ₃ (0.2 g.) | 40 | 16 | 95 |
| Poly- <i>N</i> -vinylmethylformamide | 10 g. | Synthesized | H ₂ O (100 ml.) | A ₁ (0.2 g.) | 80 | 16 | 95 |
| Poly(<i>N</i> -acrylyl morpholine) | 20 ml. | Synthesized | H ₂ O (300 ml.) + SLS (2 g.) | K ₂ S ₂ O ₈ (0.2 g.) + NaHSO ₃ (0.2 g.) | 40 | 16 | 80 |
| Poly(<i>N</i> -acrylyl pyrrolidine) | 10 g. | Synthesized | <i>tert</i> -Butanol (100 ml.) | A ₁ (0.2 g.) | 80 | 16 | 90 ^c |
| Poly- <i>N</i> -vinylcaprolactam | 10 g. | Synthesized | H ₂ O (150 ml.) | A ₁ (0.2 g.) | 40 | 16 | 98 |
| Poly(methyl vinyl ketone) | 39 g. | Eastman Org. Chem. | H ₂ O (100 ml.) + EtOH (100 ml.) | 30% H ₂ O ₂ (1 ml.) + T.U. (0.2 g.) | 90 | 4 | 95 |
| Poly- <i>N</i> -vinylimidazole | 10 g. | Synthesized | <i>tert</i> -Butanol (150 ml.) | B (0.2 g.) | 80 | 4 | 98 |

^a A = α,α' -azobis(α,γ -dimethylvaleronitrile); B = α,α' -azobisisobutyronitrile; T.U. = thiourea.

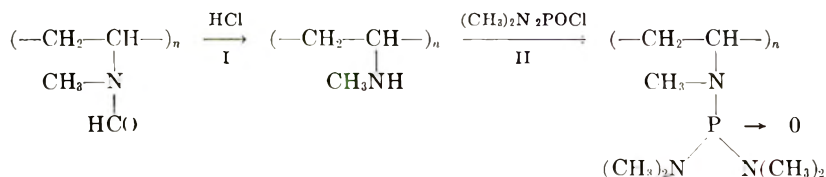
^b $\eta = 0.45$ in dimethylsulfoxide; polymer melt temperature (P.M.T.) = 254°C.

^c $\eta = 0.5$ in H₂O; P.M.T. = 130°C.

In step I, 104 g. of polyacrylamide (Type 75, American Cyanamid Company) was dissolved in three liters of distilled water and stirred with 110 ml. of 1*M* sodium carbonate and 130 ml. of 37% aqueous formaldehyde for a period of 24 hr. at 50°C. The reaction mixture remained a clear, viscous liquid. A small portion of this mixture was then dialyzed to remove the excess formaldehyde and then used in step II of this synthesis.

A 100-ml. portion of the dialyzed solution I was stirred with 5 g. of 1,1-dimethyl urea (Sharples Chemical Corporation), and 1 ml. of *o*-phosphoric acid over a steam bath for 24 hr. The resultant clear viscous solution was dialyzed to remove unreacted monomers. A sample of the dried substance was analyzed for nitrogen and found to contain 18.5%, indicating a 76% conversion in the step II of the synthesis.

Synthesis of Polyvinylpentamethylphosphoramide. This polymer was prepared from poly(vinylmethylformamide) in accordance with the reaction scheme:



Polyvinylmethylformamide (5.4 g.) was dissolved in 190 ml. of distilled water and refluxed for 16 hr. over a steam bath with 11 ml. of concentrated hydrochloric acid. This was then dialyzed against distilled water and passed through an ion exchange column of Amberlite IRA-400 to liberate the polyvinylmethylamine in the step I of the synthesis.

In step II, the product from step I was dried and mixed with a solution of 9.4 g. of tetramethyldiamidophosphoryl chloride¹¹ and 7 g. of triethylamine in 300 ml. of benzene. The mixture was refluxed for 16 hr. and then concentrated by stripping most of the benzene. The product was mixed with water and the remainder of the benzene was azeotropically distilled. The aqueous solution was next dialyzed to remove the salt impurities and then used for coatings. A sample of the solution was dried and analyzed for phosphorus (P analysis found = 10.9%, theoretical = 16.2%, i.e., 66% conversion to the required polymer).

Preparation of Test Samples

All the water-soluble polymers, unless otherwise specified, were first dialyzed for 24 hr. against distilled water to remove ionic impurities and then coated on either Dacron (Du Pont trademark for polyester fiber) or a Mylar (Du Pont trademark for polyester film) film, dried, conditioned at the test humidity for at least 24 hr., and then tested. The water-insoluble polymers were examined as either films or as fabrics. These were washed with a 0.2% sodium lauryl sulfate solution for 30 min. at 80°C. and then boiled three times in distilled water for a period of 15 min. each. The

cleaned samples were then dried in a 120°C. oven and conditioned for at least 24 hr. at the test humidity before measurement.

Charge Decay Measurement

The charge decay measurements were carried out with the static propensity tester as described in the first paper³ of this series. The test samples were either charged electrically or by friction to about +5000 v. and -5000 v. The frictional method was used only when the rate of charging by the electrical method was extremely slow, i.e., for Dacron, nylon, Orlon (Du Pont trademark for acrylic fiber), etc. In most cases, wool was used to rub against the test sample to produce a negatively charged surface. The halfives of charge decay for positive charge and negative charge (i.e., τ_+ and τ_-) were then measured. From these, the value of the root-mean-square halfife of charge decay τ_{RMS} was calculated:

$$\tau_{\text{RMS}} = \sqrt{(\tau_+^2 + \tau_-^2)/2} \quad (1)$$

A determination of τ_{RMS} for at least two relative humidity conditions was then used according to eq. (2) to evaluate the antistatic behavior of the test sample.

$$\tau_{\text{RMS}} = \tau_0 e^{-\alpha RH} \quad (2)$$

where τ_0 is the hypothetical root mean halfife of charge decay at 0% R.H. and α is a constant, and RH denotes relative humidity. A plot of $\log \tau_{\text{RMS}}$ versus humidity in accordance with eq. (3) gave straight lines with slopes and intercepts characteristics of the test polymer.

$$\log \tau_{\text{RMS}} = \log \tau_0 - \alpha RH \quad (3)$$

All the measurements were carried out at 22°C.

RESULTS AND DISCUSSION

The antistatic property of a given substance may be defined as its capacity to dissipate electrostatic charges quickly. In polymers, where the electrical resistance is extremely high, antistatic properties can be assumed to be associated with the nature of the polymer surface. This assumption is well substantiated by the fact that surface coatings¹² of antistatic agents can be used to change the behavior of a given polymer from an undesirable to a satisfactory state of performance. In this investigation, it has been assumed that the chemical structure of a given polymer governs the nature of its surface and, therefore, its antistatic properties. It was further assumed that polar or functional groups present in a polymer have a major influence on antistatic behavior, so that from a study of a series of vinyl polymers with a constant hydrocarbon backbone it was possible to correlate the changes in antistatic properties produced by various functional groups as side chain substituents.

Throughout this study, cotton has been used as the standard for good

TABLE II
Properties of the Standard Polymers

| Expt. no. | Polymer | τ_{RMS}^a | | τ_0 , sec. |
|-----------|------------------------------|-----------------------|--------|-------------------|
| | | Sec. | % R.H. | |
| 1 | Cellophane film | 0.26 | 65 | 140 |
| | | 15 | 20 | |
| 2 | Cotton fabric | 4.24 | 65 | 2.5×10^4 |
| | | 259 | 33 | |
| 3 | Wool fabric | 1.29 | 65 | 3.5×10^4 |
| | | 132 | 35 | |
| 4 | Nylon 66 fabric ^b | 735 | 65 | 1.4×10^6 |
| | | 4.1×10^{4c} | 31 | |
| 5 | Orlon fabric ^d | 5475 | 65 | 1.3×10^4 |
| | | 8140 | 35 | |
| 6 | Dacron fabric ^b | 1.96×10^{4c} | 65 | 2.3×10^5 |
| | | 4.93×10^{4c} | | |

^a Only two of the measured values are reported here. ^b Continuous filament fabric used. ^c Sample charged by friction. ^d Staple filament fabric used.

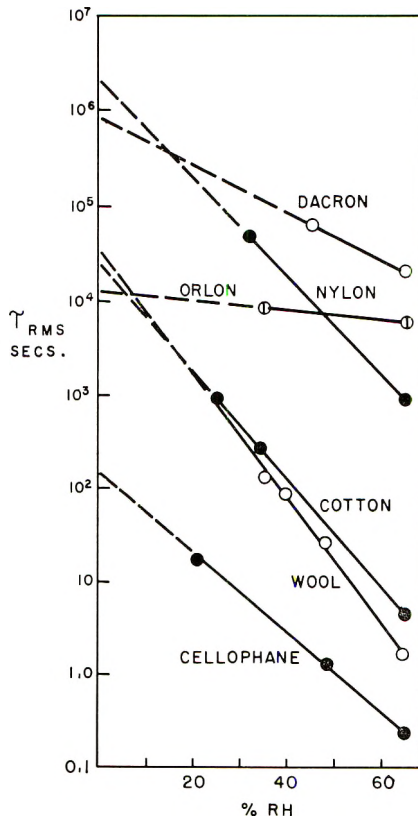


Fig. 1. Charge decay properties for some standard polymers. A plot of $\log \tau_{RMS}$ vs. relative humidity.

antistatic properties. Figure 1 and Table II show a collection of results for a number of common polymers in comparison with cotton. The plots of the $\log \tau_{\text{RMS}}$ in Figure 1 as a function of the per cent relative humidity in accordance with the eq. (3) illustrate the wide range in properties that are observed for various materials.

Hydrophilic Character and Antistatic Behavior

It has been widely believed that the antistatic behavior of a polymer is directly related to its moisture absorption. This generality, however, is not always true. Table III lists the results for a number of highly water-

TABLE III
Moisture Content vs. Antistatic Behavior

| Expt. no. | Polymer | Moisture absorption | τ_{RMS} at 65% R.H., sec. |
|-----------|---|------------------------|---------------------------------------|
| 7 | Polyvinyl alcohol ^a | Water-soluble | 1389 |
| 8 | Poly(<i>N</i> -acrylyl morpholine) ^a | " " | >8000 |
| 9 | Poly(<i>N</i> -acrylyl pyrrolidine) ^a | " " | >8000 |
| 10 | Pip-MBAM ^{a,c} | " " | >8000 |
| 11 | Poly(<i>N,N'</i> -diethylpropylene terephthalamide) ^a | Highly water-sensitive | >8000 |
| 12 | Poly(piperazine adipamide) ^a | " " " | >8000 |
| 13 | Poly(2,5-dimethylpiperazineadipamide) ^b | 50.5% at 98% R.H. | >8000 |
| 14 | Poly(ethylene terephthalamide) ^b | 17% at 98% R.H. | >8000 |
| 15 | Poly(propylene terephthalamide) ^b | 22% at 98% R.H. | >8000 |
| 16 | Nylon 66 ^b | 11.5% at 98% R.H. | 735 |
| | Cotton | 26% at 98% R.H. | 4.24 |

^a Tested as a coating on Dacron polyester fibers. ^b Tested as a fabric. ^c Pip-MBAM=



sensitive polymers with poor antistatic properties. For example, poly(2,5-dimethylpiperazine adipamide) (Expt. 13), which absorbs about 50% water at 78% R.H., i.e., greater than cotton, had such poor properties that there was no noticeable charge decay in 8000 sec. Similar results were obtained for poly(ethylene terephthalamide) and poly(propylene terephthalamide), which have moisture absorption values in the same range as cotton. A most surprising and unexpected result was poor behavior of a group of water-soluble polymers (Expts. 7-10 in Table III). Even polyvinyl alcohol with a half-life of charge decay of 1389 sec. and the addition polymer from piperazine and *N,N'*-methylenebisacrylamide with free tertiary amine groups gave poor antistatic properties at as high humidity conditions as 65% R.H. These results illustrate that a high moisture sensitivity or even water solubility does not necessarily confer good antistatic properties to a given polymer.

Some Observations on Structure-Property Relationships

Tables IV and V summarize the results for a large number of vinyl polymers with various substituent groups. An examination of the charge decay properties shows that such hydrocarbons as polystyrene and polyethylene have extremely poor antistatic properties, whereas certain polymers with *N*-alkylated amide substituents, such as polyvinylpentamethyl-

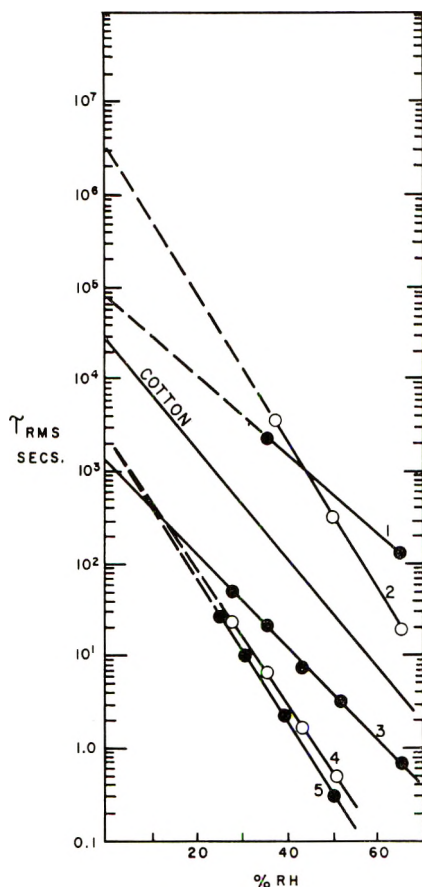


Fig. 2. Charge decay properties of some nonionic polymers: (1) Niatex (unwashed); (2) poly-*N*-vinylmethylformamide; (3) poly-*N*-vinylpentamethylphosphoramidate; (4) $(\text{CH}_2\text{-CHCONHCH}_2\text{NHCONMe}_2)_n$; (5) polydimethylacrylamide. Measurements were obtained with 1% coatings of the polymers on fabrics of Dacron polyester fiber.

phosphoramidate, polyvinylpyrrolidone, and polyvinylmethylformamide, have very good properties; i.e., extremely fast charge decay rates. In Figure 2, the plot of $\log \tau_{\text{RMS}}$ versus the relative humidity in accordance with eq. (2) illustrates how the properties of these substances are comparable to those of cotton through a wide range of humidity conditions. Thus, polyvinylpentamethylphosphoramidate and the poly-*N*-dimethylurea deriva-

TABLE IV
 Charge Decay Results for Various Polymers

| Expt. no. | Polymer ^a | τ_{RMS} at | τ_{RMS} | | τ_0 , sec. |
|--------------|--|------------------------|---------------------|-----------|--------------------|
| | | 65% R.H., sec. | Sec. | % R.H. | |
| 17 | Polyethylene film | >8000 | | | |
| 18 | Polystyrene film | >8000 | | | |
| 19 | Polyvinyl fluoride film | 8.4 | 20 | 20 | 29 |
| 20 | Polyvinyl chloride film | >8000 | | | |
| 21 | Poly(methyl acrylate) film | >8000 | | | |
| 22 | Polyacrylamide | 3.46 | 13 | 40 | 102 |
| 23 | Polydimethylacrylamide | 0.58 | 15.7 | 29 | 2500 |
| 24 | Polydiethylacrylamide | 16.5 | — | | |
| 25 | Poly- <i>tert</i> -butylacrylamide | >8000 | | | |
| 26 | Poly- <i>N</i> -vinylpyrrolidone | 12.5 | 1264 | 42 | 6×10^6 |
| 27 | Poly- <i>N</i> -vinylcaprolactam | 32 | — | | |
| 28 | Poly(<i>N</i> -acrylyl morpholine) | >8000 | | | |
| 29 | Poly(<i>N</i> -acrylyl pyrrolidine) | >8000 | | | |
| 30 | Poly- <i>N</i> -vinylmethylformamide | 45 | 3700 | 30 | 2×10^6 |
| 31 | Polyvinylpentamethylphosphor- amide | 0.23 | 47 | 29 | 1450 |
| 32 | PDMUAM ^d | 0.13 | 26.5 | 36 | 2×10^4 |
| 33 | Niatex (unwashed) ^b | 133.6 | 2544 | 35 | 8×10^4 |
| 34 | Niatex (washed) | 0.21 | — | | |
| 35 | Silicone oil X-527 ^c | 0.33 | — | | |
| 36 | Polystyrenesulfonamide | >8000 | — | | |
| 37 | Poly(vinyl methyl ketone) | >8000 | | | |

^a Unless otherwise specified all measurements were carried out as coating on fabrics of Dacron.

^b Commercial agent (Carbide & Carbon Co.), essentially polyethylene oxide.

^c Commercial product from Linde Air Products Co.

^d See Table VI.

 TABLE V
 Properties of Polyelectrolytes

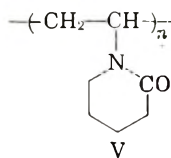
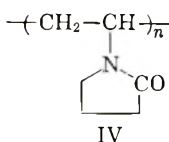
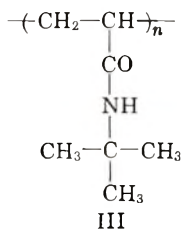
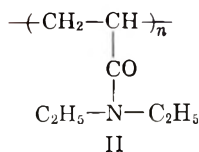
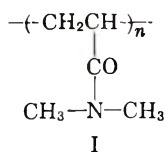
| Expt. no. | Polymer | τ_{RMS} at | τ_{RMS} | | τ_0 , sec. |
|--------------|--|------------------------|---------------------|-----------|--------------------|
| | | 65% R.H., sec. | Sec. | % R.H. | |
| 38 | Poly(acrylic acid) | 1.3 | 500 | 20 | 2800 |
| 39 | Poly(sodium acrylate) | 0.4 | 3 | 20 | 10 |
| 40 | Poly(sodium ethylenesulfonate) | 2.0 | 10 | 30 | 28 |
| 41 | Poly(sodium styrenesulfonate) | 0.3 | 0.4 | 20 | 0.57 |
| 42 | Poly(dimethylaminoethyl methacry- late) | 20 ^a | 2500 | 38 | 23×10^9 |
| 43 | Poly- <i>N</i> -vinylimidazole | 0.19 | 3.57 | 38 | 700 |
| 44 | Polymer 42 + poly(styrenesulfonic acid) (washed 12 times) | 4.03 | 610 | 51 | 6×10^{10} |

^a Measured at 50% R.H.

tive of polymethylolacrylamide have better antistatic properties than cotton, while polyvinylmethylformamide has acceptable properties down to about 40% R.H. Other examples in Tables IV and V indicate how specific functional groups are responsible for the polymer properties.

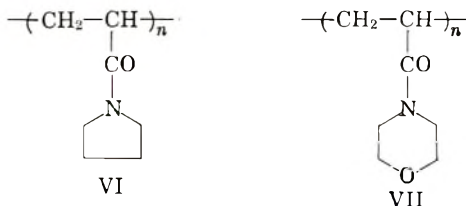
Another interesting observation which may be deduced from the results in Tables III, IV, and V is the marked influence of the position of a functional group in a polymer chain on the charge decay rates. For example, a functional group which gives good antistatic properties as a side chain substituent does not necessarily give the same behavior when incorporated in the main polymer chain. Thus, a tertiary amine group as found in poly(dimethylaminoethyl methacrylate) gives good antistatic properties at high humidities, but when the group is placed in the main polymer chain as in Pip-MBAM (Expt. 10 in Table III) poor results are obtained. In fact, the charge decay from this polymer was so slow that it could not even be measured within a reasonable time scale. What is most surprising about these two polymers is that they are both water-soluble and yet the charge decay half-life at 65% R.H. changes from about 0.2 sec. to >8000 sec. Another example of the side chain substitution effect is provided by *N*-alkylated polyamides. For example, it is found that polydimethylacrylamide and polydiethylacrylamide are good antistatic agents at high relative humidity conditions, whereas in poly(piperazine adipamide) (Expt. 12, III) and poly(*N,N'*-dimethylpropylene terephthalamide) (Expt. 11, III), there is no detectable charge decay in 8000 sec.

In the *N*-alkylated amides, a number of interesting structure-property relationships were observed for the type of *N*-alkyl substituent. Here for a series of water-soluble (with the exception of III below) vinyl polymers, it was noted that good antistatic properties were obtained when the substituent group was small, i.e., methyl or ethyl (polymers I and II). If, however, the *N*-alkyl substituent was a large bulky group such as *tert*-butyl (polymers I and III), then extremely slow charge decay rates were obtained. When the bulky substituent constituted part of a cyclic system



such as in polyvinylcaprolactam or polyvinylpyrrolidone (structures IV and V), then the charge decay rates were in the same range as for cotton and wool.

If the *N*-alkyl substituent formed a cyclic ring which did not contain the carbonyl group of the amide in the ring, then slow charge decay rates were obtained, i.e., poly-*N*-acrylylpyrrolidine (VI) and poly-*N*-acrylylmorpholine (VII).



The case of polymer VII is especially surprising, since the addition of the ether group in the morpholine ring does not appear to improve the charge decay rate.

These results tend to emphasize that it is not as yet possible to generalize about the antistatic behavior of a given functional group. Nevertheless, it can be said from the above examples that the hydrocarbon *N*-alkyl substituent group should not be large enough to shield the polarity of the amide function and it is best to have the carbonyl of the *N*-alkyl amide group fixed in a coplanar configuration with the nitrogen in a ring in order to obtain good antistatic behavior. This may well be connected with the dipolar resonance contribution of the amide group to antistatic behavior.

Properties of Polyelectrolytes

Polyelectrolytes as a group showed the greatest tendency to dissipate electrostatic charges quickly (see Table V). This finding is in keeping with their wide use in antistatic agents. Figure 3 shows a plot of the $\log \tau_{\text{RMS}}$ values versus the per cent relative humidity in accordance with eq. (2). The results show that polyacrylic acid, poly(styrenesulfonic acid), and poly-*N*-vinylimidazole had faster charge decay properties than cotton over the whole relative humidity scale. The best results were given by the sodium salts of the polyacids (see curves 1, 2, and 3 in Fig. 3). In an attempt to study the properties of polyampholytes, a number of fabrics of Dacron were coated with a layer of a polybase followed with a layer of a polyacid to give a polymeric salt coating. Such coatings were stable and could be washed in distilled water without any loss in antistatic properties. However, upon washing in tap water, they became extremely poor in behavior. Experiment 44 in Table V shows the results for this type of double-layer coating with poly(dimethylaminoethyl methacrylate) and poly(styrenesulfonic acid). The results were found to be extremely dependent upon the relative humidity. The properties were satisfactory in comparison with cotton at 65% R.H. but became extremely poor at lower

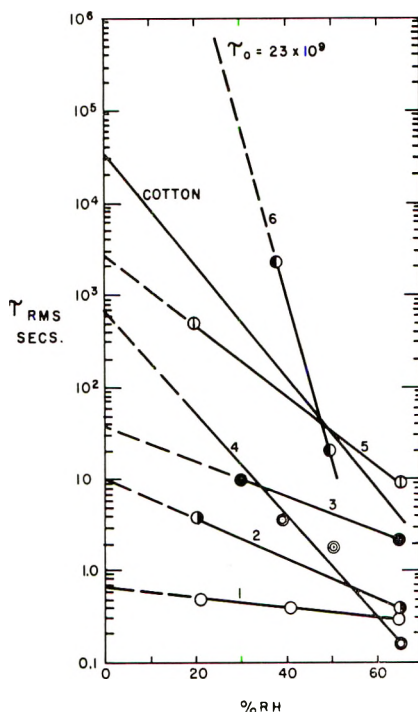


Fig. 3. Charge decay properties of some polyelectrolytes: (1) poly(sodium styrene-sulfonate); (2) poly(sodium acrylate); (3) poly(sodium ethylenesulfonate); (4) poly-*N*-vinylimidazole; (5) poly(acrylic acid); (6) poly(*N*-dimethylaminoethyl methacrylate).

values, and the extrapolated τ_0 values were 6×10^{10} sec. (half-life of charge decay at 0% R.H.).

Charge Selectivity in Polymers

As shown in the first paper³ of the series, most polymers exhibit different rates of charge decay for positive and negative applied potentials. This must be related to the withholding power of a polymer surface for the type of charge applied. In an attempt to study this property, a parameter, the charge selective power σ , was devised to measure the tendency of a substance to behave electrostatically positive or electrostatically negative. The charge selective power is, therefore, a means of assessing the preference of a polymer for positive or negative charges on its surface, whether these charges arise by friction or through an applied potential. It is defined by eq. (3) below:

$$\sigma = (\tau_+ - \tau_-) / \tau_{RMS} \quad (3)$$

where τ_+ and τ_- are the half-lives of charge decay for positive charge and negative charges, respectively, and

$$\tau_{RMS} = \sqrt{(\tau_+)^2 + (\tau_-)^2} / 2$$

Table VI lists values of the charge selective power for polymers at 65% R.H. in order of highest positive through zero to greatest negative. A study of the table immediately shows that σ is not related to the rapidity with which charges are lost from a given polymer so that the antistatic properties of a given polymer are not a consequence of its charge selectivity. A comparison of the order of listing of substances in Table V with published tables of triboelectric series¹³ shows many similarities.

TABLE VI
Charge Selective Power of Polymers at 65% R.H. and 70°F.

| Polymer | τ_{+} , sec. | τ_{-} , sec. | σ |
|---------------------------------------|----------------------|----------------------|----------|
| Poly-N-vinylpyrrolidone | 41.0 | 15.8 | +0.92 |
| Wool | 2.5 | 1.55 | +0.89 |
| Polyvinyl alcohol | 8470 | 3774 | +0.71 |
| Poly(acrylic acid) | 1.5 | 0.96 | +0.66 |
| Mylar film | 9708 | 5153 | +0.58 |
| Nylon 66 | 936 | 720 | +0.56 |
| Polyacrylamide | 4.14 | 2.65 | +0.43 |
| Polydimethylacrylamide | 0.66 | 0.48 | +0.31 |
| PDMUAM ^a | 2.13 | 1.44 | +0.37 |
| Polyvinylmethylformamide ^b | 21.6 | 16.8 | +0.16 |
| Polyvinylpentamethylphosphoramidate | 0.24 | 0.22 | +0.13 |
| Cellophane | 0.30 | 0.30 | 0 |
| Niatex (washed) | 0.21 | 0.21 | 0 |
| Polyacrylonitrile film | 667 | 687 | -0.03 |
| Orlon fabric | 5340 | 5670 | -0.06 |
| Dacron fabric | 19,080 | 20,160 | -0.06 |
| Polyvinyl fluoride ^c | 8.0 | 8.7 | -0.08 |
| Silicone X-527 | 0.32 | 0.36 | -0.12 |
| Cotton | 3.6 | 4.8 | -0.28 |
| Poly-N-vinylimidazole ^b | 0.18 | 0.24 | -0.29 |
| Poly(dimethylaminoethyl methacrylate) | 4.2 | 7.3 | -0.50 |
| Niatex (unwashed) | 73.8 | 174.0 | -0.75 |
| Daktose C ↔ PSSSA ^d | 1.77 | 5.43 | -0.9 |

^a PDMUAM = $\text{-(CH}_2\text{-CHCONHCH}_2\text{NHCONMe}_2\text{)}_n$

^b Measured at 50% R.H.

^c The fast charge decay rates for this polymer were subsequently shown to be due to impurities, such as FeF₃ dissolved in the polymer.

^d Same combination as experiment 44, Table V.

Figure 4 shows a plot of the charge selective power as a function of the root-mean-square half-life of charge decay τ_{RMS} . Such a plot conveniently arranges polymers into electrostatically positive and electrostatically negative groups independent of the rates of charge decay. It also indicates which polymers should have good antistatic behavior; i.e., those with τ_{RMS} values <10 sec. The dotted vertical lines divide the figure into a number of zones indicative of what charge sign a substance will develop upon rubbing with one of a lower charge selective power. Thus, for

example, wool with a charge selective power of $+0.85$ should develop a positive charge when rubbed with nylon 66 with a charge selective power of 0.65 , etc. Here, for the first time, we have a reason for the fact that one can formulate a triboelectric series. It is also evident that one cannot combine a substance of a positive charge selective power with a substance of an equal negative value and expect to get no charge developed upon rubbing, since the rate of decay will then be the determining factor.

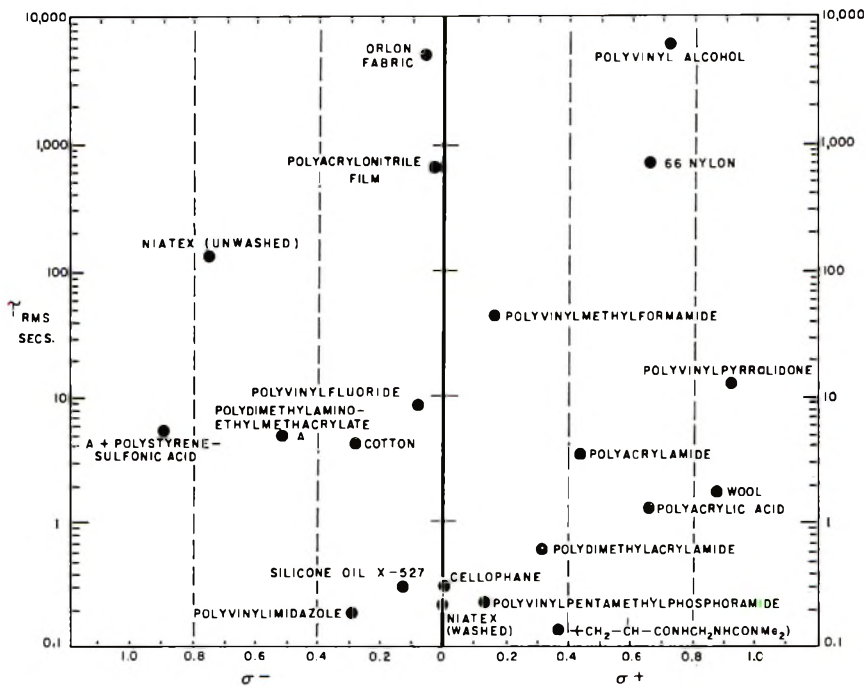


Fig. 4. Charge selective powers (τ_+ and τ_-) of various polymers arranged as a function of their τ_{RMS} values. (The results are for 65% R.H. and 70°F.)

Influence of Impurities

Aside from its charge selective power and the rate of charge decay, the most important factor in determining the antistatic behavior of a given polymer is its tendency to accumulate impurities from its environment. We have already noted³ how wool changes its properties by absorbing impurities. Table VII illustrates the effect of impurities on the observed charge decay rates and the charge selective power results for wool and other polymers. When a piece of wool fabric was washed with distilled water, a τ_{RMS} value of 1.79 sec. at 65% R.H. was obtained. Upon washing with tap water, the τ_+ value changed to 98 sec. This change is believed to be due to the absorption of calcium ions from the water.* Similar

* Additional experiments to illustrate this will be discussed in a paper on the mechanism of charge decay.

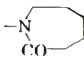
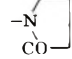
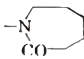
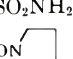
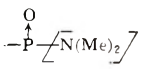
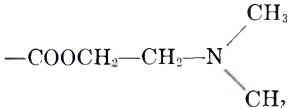
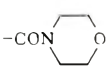
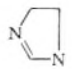
TABLE VII
Influence of Impurities on Charge Selective Power and
Charge Decay Properties

| Expt. no. | Polymer | Treatment | τ_{RMS} (65% R.H.), sec. | σ |
|-----------|----------------------|-------------------------------|--|----------|
| 45 | Wool | Distilled water wash | 1.79 | +0.88 |
| 46 | Wool | Tap water wash | 98 ^a | |
| 47 | Polyacrylamide | Unpurified commercial product | 0.83 | -0.18 |
| 48 | " | Dialyzed one day | 3.46 | +0.43 |
| 49 | " | Dialyzed one week | 68.5 | 0.10 |
| 50 | Polyvinylpyrrolidone | Commercial product | 0.3 | 0 |
| 51 | " | Dialyzed | 36.0 | +0.92 |
| 52 | " | 0.83% coating on Dacron | 4.8 | -0.55 |
| | | 2.79% " " " | 12.3 | +0.50 |
| 53 | " | 30% on nylon 66 | 0.25 | +0.11 |
| 54 | " | 12% on Dacron | 0.23 | -0.11 |
| 55 | Niatex | Unwashed | 133.6 | -0.75 |
| | " | Washed | 0.21 | 0 |

^a This is a τ_+ value.

effects are found for polyacrylamide. Here, a coating of a freshly dissolved commercial sample on Mylar film showed a half-life of 0.83 sec. at 65% R.H. with a negative charge selective power of -0.18. When the sample was dialyzed for one day against distilled water and then coated onto Mylar, the half-life of charge decay changed to 3.46 sec., and the charge selective power became completely reversed to a value of +0.43. Finally, when the sample was dialyzed for a week against distilled water the half-life of charge decay changed to 68.5 sec.; i.e., to a region of poor antistatic

TABLE VIII
Antistatic Behavior of Functional Groups

| Good | Moderate | Poor |
|---|---|--|
| -CONMe ₂ | -CONH ₂ | -Cl |
| -CONEt ₂ | -SO ₃ H | -CN |
| HCONCH ₃ | -COOH | -OH |
| -COONa | -N(CH ₃) ₂ | -COOMe |
| -SO ₃ Na |  | -CONHC(CH ₃) ₃ |
|  | -COOCH ₂ -CH ₂ -N(CH ₃) ₂ | -SO ₂ NH ₂ |
| +OCH ₂ CH ₂ + |  | -CON  |
|  |  | -CON  |
| -CONH-CH ₂ NHCONMe ₂ | | |
|  | | |

behavior. Similar variations were obtained for polyvinylpyrrolidone. In this case a study of the various polyvinylpyrrolidone coatings at different relative humidity values was carried out. Figure 5 illustrates the wide range in properties obtained.

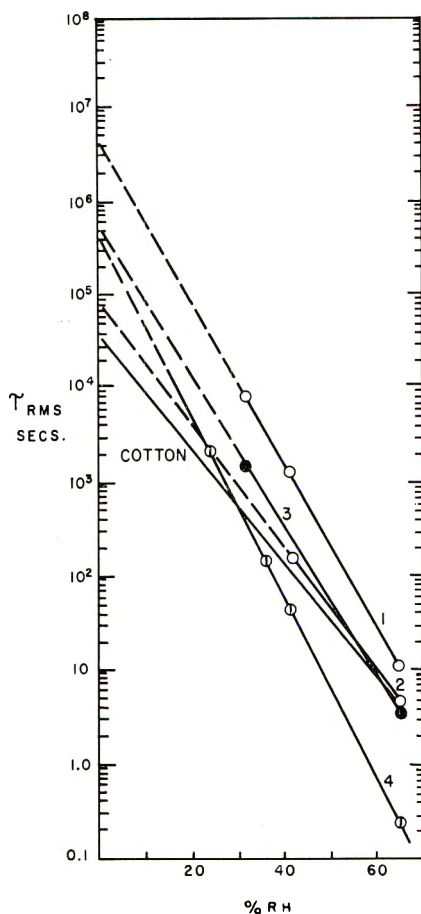


Fig. 5. Influence of impurities on the charge decay properties of poly-*N*-vinylpyrrolidone (PVP) as a function of relative humidity: (1) purified PVP on fabric of Dacron polyester fibers; (2) and (3) PVP coating with impurities on fabric of Dacron polyester fiber; (4) undialyzed PVP on nylon 66 fabric.

CONCLUSIONS

From the above studies one can obtain a number of correlations of anti-static properties of polymers with their chemical constitution. It is found that for a given functional group the fastest charge decay occurs when the groups are present as side chain substituents rather than in the main chain of the polymer. Table VIII shows a classification of functional groups into three types according to their capacity to enhance the rate of charge decay from a vinyl polymer. Here, "good" signifies properties similar to

cotton at all humidities, "moderate" represents acceptable properties at only high humidity conditions, and "poor" is unacceptable.

The charge selective power of a polymer appears to be simply related to its ability to bind ions on its surface. Thus polyanions, such as poly(acrylic acid), poly(styrenesulfonic acid), and wool have a positive charge selective power and are able to bind cations. On the other hand, polybases such as poly(diethylaminoethyl methacrylate) or poly-*N*-vinylimidazole have a negative charge selective power because they tend to absorb anions when in a hydrated state. These considerations make it clear how small quantities of impurities can alter the charge selective power of a given substance. Also, the reason that one can formulate a triboelectric series can be attributed to the fact that in normal use an electrostatically positive surface tends to accumulate impurities which cause it to withhold positive charge more strongly than a negative charge. Thus, both the reproducibility of the charge selective power of a substance and the assignment of a position in a triboelectric series for a given material are largely a measure of the ability of a substance to accumulate impurities from its environment.

The slow decay rate of electrostatic charges from such high water-sensitive and water-soluble polymers as poly(*N*-acryl morpholine) indicates that other factors than the degree of hydration of a surface are responsible for the antistatic properties of the polymers. One can only speculate that antistatic properties of a given polymer are intimately linked with such variables as the degree of dissociation of ionic impurities and the extent of dispersion of complexed ions into the hydrated outer aqueous surface layers.

References

1. Sippel, A., *Textile Praxis*, **8**, No. 12, 1030 (1953).
2. Medley, J. A., *Brit. J. Appl. Phys., Suppl.*, **2**, 28 (1953).
3. Shashoua, V. E., *J. Polymer Sci.*, **33**, 65 (1958).
4. Hanford, W. E., and H. B. Stevenson, U. S. Pat. 2,231,905, to E. I. du Pont & Co. (1941).
5. Wiley, R. H., and C. C. Ketterer, *J. Am. Chem. Soc.*, **76**, 1926 (1954).
6. Shastakovskaya, M. S., et al., *Bull. Acad. Sci. U.S.S.R., Div. Chem. Sci.*, 633 (1952).
7. Wittbecker, E. L., and P. W. Morgan, *J. Polymer Sci.*, **40**, 289 (1959).
8. Beaman, R. G., P. W. Morgan, C. R. Koller, E. L. Wittbecker, and E. E. Magat, *J. Polymer Sci.*, **40**, 329 (1959).
9. Shashoua, V. E., and W. M. Eareckson, *J. Polymer Sci.*, **40**, 343 (1959).
10. Hulse, G. E., U. S. Pat. 2,759,913, to Hercules Powder Company (1956).
11. Dickey, J. B., and H. W. Coover, U. S. Pat. 2,487,859, to Eastman Kodak (1949).
12. Loeb, L. B., *Static Electrification*, Springer-Verlag, Berlin, 1958, p. 210.
13. Hersh, P. S., and D. J. Montgomery, *Textile Research J.*, **25**, 291 (1955).

Synopsis

From studies of the rate of buildup and decay of positive and negative charges on the surfaces of vinyl and condensation polymers, a number of general observations were obtained correlating the polymer chemical structure with antistatic behavior. Polymers with functional groups such as $-\text{COONa}$, $-\text{SO}_3\text{Na}$, $-\text{HCONCH}_3$, $-\text{CONEt}_2$, $-\text{P}-(\text{NMe}_2)_3$, and imidazole were found to have good antistatic properties. These func-

tional groups were more effective in improving the antistatic properties of polymers when they were used as side chain substituents than when they were employed as part of the main polymer chain. A number of highly water-sensitive and water-soluble polymers were found to have extremely poor antistatic properties, indicating that there is no direct correlation of antistatic properties with hydrophilic character. A new parameter, the charge selective power of a substance, was devised to describe the charge polarity preference of a given substance. It is defined by the equation: $\sigma = (\tau_+ - \tau_-) / \tau_{\text{RMS}}$, where τ_+ is the half-life of charge decay for positive charge, τ_- is the half-life of charge decay for negative charge, and τ_{RMS} is the root-mean-square half-life of charge decay. The charge selective power of a substance was found to correlate well with the assignments of substances in the tables of triboelectric series. The effect of impurities on charge decay properties and the charge selective power of polymers was found to be extremely important in influencing antistatic behavior. The synthesis of the following polymers with specific functional groups is described: polyvinylpentamethyl phosphoramidate; the poly-*N*-dimethylurea derivative of polymethylacrylamide; poly(*N*-acrylyl morpholine); poly(*N*-acrylyl pyrrolidine).

Résumé

L'étude de la vitesse d'apparition et de disparition de charges positives et négatives à la surface de polymères vinyliques et de polycondensats a permis de faire un certain nombre d'observations qui relient la structure chimique du polymère au comportement antistatique. On a observé que les polymères porteurs des groupes fonctionnels tels que $-\text{COONa}$, SO_3Na , $-\text{HCONCH}_3$, $-\text{CONEt}_2$, $-\text{P}-(\text{NMe}_2)_3$ et imidazol possèdent de bonnes propriétés antistatiques. Ces groupes fonctionnels améliorent plus efficacement les propriétés antistatiques du polymère lorsqu'ils sont substituants de la chaîne latérale que lorsqu'ils font partie intégrale de la chaîne. Un nombre de polymères hautement sensibles à l'eau et soluble dans l'eau possède des propriétés antistatiques extrêmement faibles, ce qui montre qu'il n'y a pas de relation directe entre les propriétés antistatiques et le caractère hydrophile. Un nouveau paramètre, le pouvoir sélectif de charge, a été imaginé pour décrire la préférence polaire de charge d'une substance donnée. Il est défini par l'équation suivante: $\sigma = \tau_+ - \tau_- / \tau_{\text{RMS}}$, où τ_+ est la moitié du temps de disparition des charges positives, τ_- est la moitié du temps de disparition des charges négatives, τ_{RMS} est la moitié du temps de disparition quadratique moyen d'une charge. On a trouvé une bonne concordance entre le pouvoir sélectif de charge d'une substance et les données des tables des séries triboélectriques de ces substances. L'effet d'impuretés sur les propriétés de disparition de charge et sur le pouvoir sélectif de charge des polymères s'est avéré d'une très grande influence sur le comportement antistatique. On a décrit des polymères suivants qui possèdent des groupes fonctionnels spécifiques: la poly(vinylpentaméthyle phosphoramidate), la poly-*N*-diméthyleurée dérivée de la polyméthylacrylamide, la poly-*N*-acrylylmorphine, la poly-*N*-acrylylpyrrolidine.

Zusammenfassung

Bei der Untersuchung der Geschwindigkeit des Aufbaues und Abklingens positiver und negativer Ladungen auf Vinyl- und Kondensationspolymeroberflächen wurden einige allgemeine Beobachtungen über die Beziehung der chemischen Struktur der Polymeren zum antistatischen Verhalten gemacht. Es zeigte sich, dass Polymere mit funktionellen Gruppen, wie $-\text{COONa}$, $-\text{SO}_3\text{Na}$, $-\text{HCONCH}_3$, $-\text{CONEt}_2$, $-\text{P}-(\text{NMe}_2)_3$ und Imidazol, gute antistatische Eigenschaften besitzen. Diese funktionellen Gruppen haben bei Verwendung als Seitenkettensubstituenten einen grösseren Einfluss auf die Verbesserung der antistatischen Eigenschaften von Polymeren als bei ihrer Benützung als Teil der Hauptkette. Eine Anzahl hochgradig wasserempfindlicher und wasserlöslicher Polymerer hatten extrem geringe antistatische Eigenschaften, was dafür spricht, dass keine direkte Beziehung der antistatischen Eigenschaften zum hydrophilen

Charakter besteht. Zur Beschreibung der bevorzugten Ladungspolarität einer gegebenen Substanz wurde ein neuer Parameter, die Ladungsselektivität der Substanz, angegeben. Sie wird durch folgende Gleichung definiert: $\sigma = \tau_+ - \tau_- / \tau_{RMS}$, wo τ_+ die Halbwertszeit des Ladungsabfalls für eine positive Ladung, τ_- die Halbwertszeit des Ladungsabfalls für eine negative Ladung, und τ_{RMS} die Wurzel aus dem mittleren Quadrat der Halbwertszeit des Ladungsabfalls ist. Die Ladungsselektivität einer Substanz zeigte ausgeprägte Beziehung zur Einordnung der Substanzen in der triboelektrischen Reihe. Der Einfluss von Verunreinigungen auf den Ladungsabfall und auf die Ladungsselektivität von Polymeren war für das antistatische Verhalten von äusserster Wichtigkeit. Die Synthese folgender Polymerer mit spezifischen, funktionellen Gruppen wird beschrieben: Poly(vinylpentamethylphosphoramid); das Poly-*N*-dimethylharnstoffderivat des Polymethylacrylamid; Poly-*N*-acrylmorpholin; Poly-*N*-acrylylpyrrolidin.

Received September 11, 1961

Radiation Damage in Oriented Polyamides

MICHIO KASHIWAGI, *Central Research Laboratories, Toyo Rayon Company, Otsu, Japan*

INTRODUCTION

In recent years many studies¹⁻⁷ have been made of the ESR spectra of free radicals in irradiated polymers. However, for such complicated systems as polymer substances, the spectra are very difficult to interpret because of overlapping lines or a blurring of the spectrum, and few extensive investigations³ have been made. Previous studies on the ESR spectra of polymer radicals have been made on unoriented specimens, and in these anisotropic dipolar interactions produce a broadening of the ESR lines. In oriented specimens, in contrast with this, radicals have well-defined orientations, and magnetic anisotropy yields much useful information on the complete analysis of the spectra. Therefore, the oriented specimens are very suitable for the ESR studies.

In case of organic low molecular weight compounds, investigations on the oriented specimens, i.e., single crystals, have already been made by several workers,⁸⁻¹⁰ and many instructive results have been obtained. In case of polymeric substances, Kiselev et al.¹¹ quite recently have reported an ESR study on oriented polyethylene and polytetrafluoroethylene.

This paper presents results of an ESR study on irradiated polyamides in the form of oriented specimens, which confirms that the predominant radicals of the polyamides are the same type radicals as shown by Burrell¹² in irradiated amides. In addition, this paper discusses briefly the presence of the other kind of radicals.

EXPERIMENTAL

Sample Preparation

Materials used were several kinds of polyamides (nylon 610, nylon 66, nylon 57, and nylon 6) obtained either commercially or by preparation according to the usual method¹³ and polyurea as commercial Urylon,¹⁴ $-\text{[(CH}_2\text{)}_9\text{NHCONH]}_n-$, manufactured by the Toyo Koatsu Industrial Company.

Drawn filaments of these polymers were used in general as uniaxially oriented specimens. In nylon 610 and nylon 66, moreover, biaxially oriented specimens were prepared by rolling the filaments at about 100°C.

Irradiation and ESR Measurements

The oriented specimens, bound in the desired size with parallel arrangement of orientation axes, were evacuated and sealed off at 10^{-4} mm. Hg in a glass tube of 5 mm. diameter and about 100 mm. length. They were irradiated at low temperature ($-78^{\circ}\text{C}.$) by a 1.5-M.e.v. Van de Graaff accelerator at the dose rate of 7.7×10^6 rad/min. to 1×10^8 rad. After irradiation, color centers were removed from the glass by heating one end nearly to annealing temperature. The irradiated specimens were then shaken to the clear end.

The ESR measurements were made with the use of a Japan Electron Optics Laboratory Co., Ltd. JES-1 type spectrometer operating at 9400 Mcycles/sec. The measurements were made at low rf-power levels to avoid saturation effects. The sample tube was mounted into a H_{012} rectangular cavity. It could be rotated from outside the cavity about an axis perpendicular to the magnetic field, and such angles of rotation were read on a scale.

RESULTS AND DISCUSSION

ESR Spectra of Irradiated Uniaxially Oriented Specimens

Figure 1 shows ESR spectra of irradiated polyamides obtained with the magnetic field imposed perpendicularly to filament axes. The spectra are almost the same for each of the polyamides and show six lines, although there are some differences of hyperfine resolutions among the polymers,

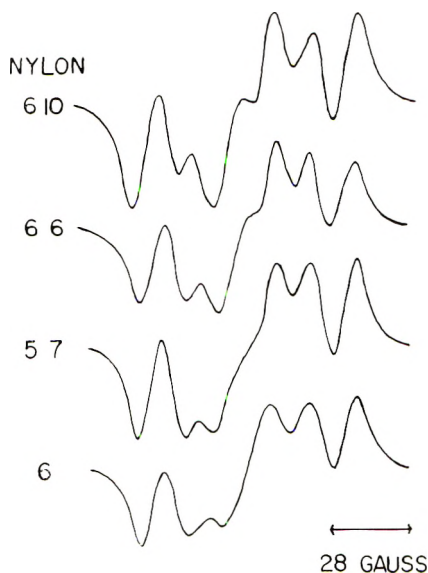


Fig. 1. ESR spectra of uniaxially oriented polyamides (nylon 610, nylon 66, nylon 57, and nylon 6) irradiated to 1×10^8 rad.

especially irradiated nylon 6, which exhibits an apparent five-line spectrum with an incompletely resolved hyperfine structure.

The spectra are variable with various orientations of the filament axes in the magnetic field. For example, Figure 2 shows how the spectrum changes in nylon 610. The feature of the change is that an overall spread of the spectrum increases with decrease of the angle between the filament axis and the magnetic field, and simultaneously a ratio of the central peak to the outside peak increases approximately from 2 to 3. Detailed analysis, as will be discussed later, shows that the spectrum is a triplet (splittings; 28 gauss) with a doublet substructure with intensity ratio of approximately 1:1:2:2:1:1, where the doublet splitting changes from 14 gauss to 26 gauss with the variation of the angle.

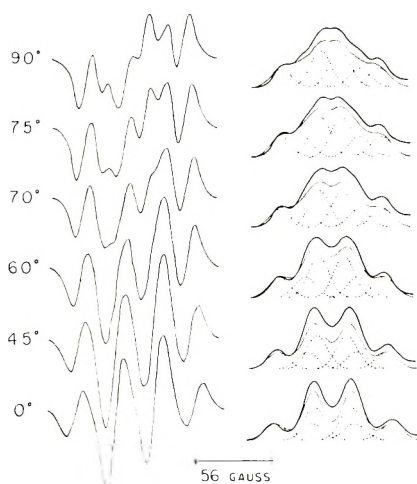


Fig. 2. ESR spectra of uniaxially oriented nylon 610, irradiated to 1×10^8 rad, for various orientations of the specimen in the magnetic field: (left) observed first-derivative curves; (right) their integrated absorption curves. Calculated absorption curves are shown for comparison.

The doublet, dependent on orientation in the magnetic field, arises from the interaction of an unpaired electron with a σ -proton,¹⁰ and the triplet arises from equal couplings of the electron to two π -protons.¹⁵ Therefore, the plausible radical is in the form of $-\dot{\text{C}}\text{HCH}_2-$, which is either (a) $-\text{CONH}\dot{\text{C}}\text{HCH}_2-$ or (b) $-\text{CH}_2\dot{\text{C}}\text{HCONH}-$ in the irradiated polyamide. Whether (a) or (b) is the form, is not determined by the present experiment alone.

Figure 3 shows the change in the spectrum of irradiated polyurea. This resembles that of the irradiated polyamides, giving no essential difference, and then we may well consider the radical in the irradiated polyurea to be of the same type as that in the irradiated polyamide, namely $-\dot{\text{C}}\text{HCH}_2-$. Since the chemical structure of the polyurea is $-\text{[(CH}_2)_9\text{NHCONH]}_n-$, the radical is shown to be $-\text{CH}_2\dot{\text{C}}\text{HNH}-$. This leads to a conclusion that

(a) radicals are trapped in the irradiated polyamide. Our conclusion is consistent with Burrell's on irradiated amides.¹² This conclusion will be again discussed in a later section, in relation to the problem of the hyperfine interaction with the NH group.

As mentioned above, we can elucidate the change of the spectrum by assuming the radical to be $-\dot{C}HCH_2-$, and the change is produced through the variation of the doublet splitting due to the σ -proton anisotropy.

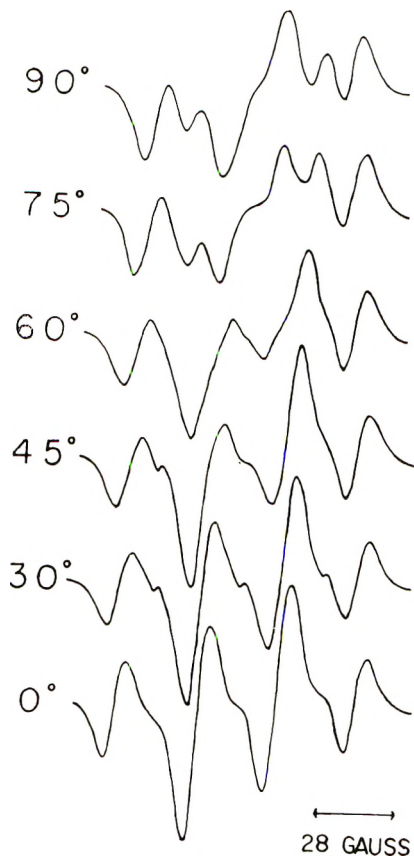


Fig. 3. ESR spectra of uniaxially oriented polyurea, irradiated to 1×10^8 rad for various orientations of the specimen in the magnetic field.

The σ -proton anisotropy has been reported by many workers,^{9,10,16} and it has been treated by McConnell et al.¹⁰ in detail. At the X-band measurements, if a weak doublet caused by the forbidden transition of proton spin is neglected, the doublet splitting D due to the σ -proton is as given in eq. (1).¹⁹

$$D = [(\nu_p - \frac{1}{2}\rho A)^2 \alpha^2 + (\nu_p - \frac{1}{2}\rho B)^2 \beta^2 + (\nu_p - \frac{1}{2}\rho C)^2 \gamma^2]^{1/2} + [(\nu_p + \frac{1}{2}\rho A)^2 \alpha^2 + (\nu_p + \frac{1}{2}\rho B)^2 \beta^2 + (\nu_p + \frac{1}{2}\rho C)^2 \gamma^2]^{1/2} \quad (1)$$

In eq. (1), ν_p is the resonance frequency of the proton in the magnetic field,

and A , B , and C are principal values of a tensor with respect to a , b , and c axes of an orthogonal coordinate system, respectively, where the a axis is along the \dot{C} —H bond, the b axis is along the p -orbital of the radical, and the c axis is the third axis of the orthogonal system. α , β , and γ are direction cosines of the magnetic field to the principal axes. ρ is the spin density on the p -orbital of the radical.

Here, we assume that the uniaxial orientation in the sample is complete, i.e., polymer chains are completely aligned along the filament axis. This assumption is permitted because contributions to ESR on the room temperature measurement come chiefly from the crystalline region, whose orientation is accomplished at the early stage of drawing the unoriented filament.¹⁷ Under this assumption the $\dot{C}H$ radical will be described in terms of the coordinate system of Figure 4. The z axis is along the filament

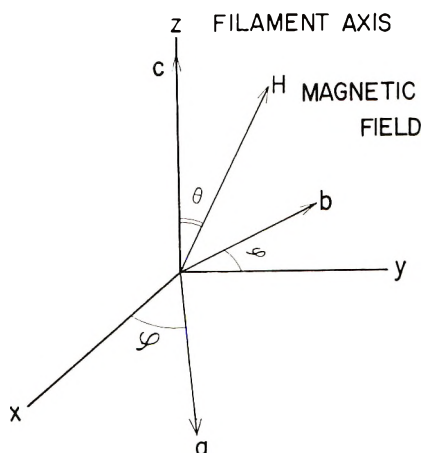


Fig. 4. Coordinate system defining the orientation of a , b , and c axes fixed in the $\dot{C}H$ radical and the magnetic field H in terms of the angles ϕ and θ .

axis. The vectors \mathbf{a} , \mathbf{b} , and \mathbf{c} express the foregoing principal axes. The angle between the x axis (y axis) and the a axis (b axis) is designated as ϕ . The vector H along the magnetic field is in the yz plane and represented by the angle θ from the z axis. The squares of direction cosines α , β , and γ of the vector H to the vectors \mathbf{a} , \mathbf{b} , and \mathbf{c} are given in eq. (2):

$$\begin{aligned}\alpha^2 &= (\sin \phi \sin \theta)^2 \\ \beta^2 &= (\cos \phi \sin \theta)^2 \\ \gamma^2 &= (\cos \theta)^2\end{aligned}\quad (2)$$

In the case of uniaxial orientation, ϕ varies randomly. The average values of α^2 , β^2 , and γ^2 are given as follows;

$$\begin{aligned}\bar{\alpha}^2 &= 1/2 \sin^2 \theta \\ \bar{\beta}^2 &= 1/2 \sin^2 \theta \\ \bar{\gamma}^2 &= \cos^2 \theta\end{aligned}\quad (3)$$

Using eqs. (1) and (3), we obtain eq. (4)

$$D = \left\{ \frac{1}{2} [(\nu_p - \frac{1}{2}\rho A)^2 + (\nu_p - \frac{1}{2}\rho B)^2] \sin^2\theta + (\nu_p - \frac{1}{2}\rho C)^2 \cos^2\theta \right\}^{1/2} \\ + \left\{ \frac{1}{2} [(\nu_p + \frac{1}{2}\rho A)^2 + (\nu_p + \frac{1}{2}\rho B)^2] \sin^2\theta + (\nu_p + \frac{1}{2}\rho C)^2 \cos^2\theta \right\}^{1/2} \quad (4)$$

which describes the doublet splitting D for the orientation where the angle between the filament axis and the magnetic field is θ . Figure 5 shows the

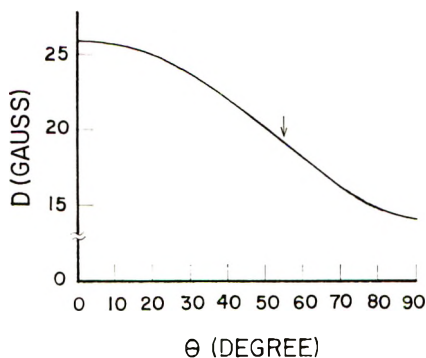


Fig. 5. Doublet splitting D against the angle θ between the filament axis and the magnetic field at $\rho = 0.7$.

doublet splitting D against the angle θ at $\rho = 0.7$, where the values $A = -7.5$ gauss, $B = -24.6$ gauss, $C = -36.8$ gauss, and $\nu_p = 52$ gauss^{10,18} have been used. Now, the doublet splitting of the unoriented specimen, which can be easily calculated, is 19 gauss,¹⁹ and this corresponds to 55° orientation of the oriented specimen as shown in Figure 5. This is found to be the fact, by reference to Figures 2 and 10 (a top spectrum).

The absorption curves calculated by using the values of Figure 5 are described in Figure 2, where each of hyperfine lines is represented by a Gaussian line shape with the half width of 17.5 gauss. These well explain the feature of the observed curves. The discrepancy between the observed and the calculated curves is due to the presence of the other kind of radicals, as will be discussed in a later section. The above line width is quite broad in comparison with those of other polymers.^{2,5} This may arise from the ill-resolved hyperfine interaction of the NH group on the radical $-\text{CON}-\text{H}\dot{\text{C}}\text{HCH}_2-$. This will be also discussed later.

ESR Spectra of Irradiated Biaxially Oriented Specimens

As already discussed under uniaxial orientation, the ESR spectra faithfully reflect the radical orientations in polymer substances as well. The present discussion will be offered to the biaxial orientation under the extreme assumption that contribution to ESR comes only from the crystalline region.

The crystal structures of polyamides have been investigated by many

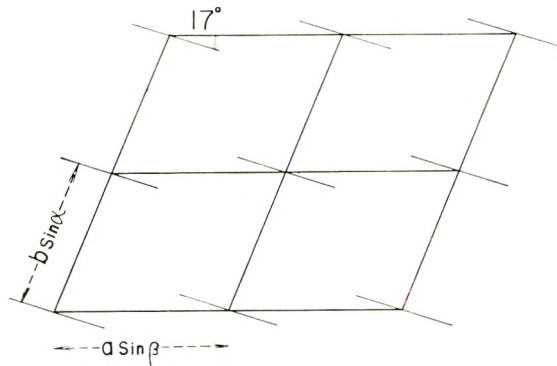


Fig. 6 Projected basal plane of nylon 610 and nylon 66. Four unit cells shown. (Twist angle 17° represents that of nylon 610.)

workers.²⁰⁻²² For nylon 66 and nylon 610 these have been fully treated by Bunn and Garner.²⁰ They have shown that the polymer chains are planar or very nearly so, and the molecules are linked by hydrogen bonds between C=O and NH groups, to form sheets. The unit cell is triclinic, with the c axis parallel to the chain direction and with a c plane parallel to the hydrogen-bonded sheets. Strictly speaking, the molecular sheet does not form a complete plane, but the plane of the polymer chain is twisted out of the ac plane. In nylon 66 and nylon 610, they are twisted toward the shorter diagonal of the projected cell base (for example, the twist angle of nylon 610 is 17°) (Fig. 6).

Biaxial orientation of the crystals can be obtained by pressing or rolling the nylon filaments. In a fully drawn filament rolled in the direction of the filament axis, the c axes of the crystals remain parallel to the filament axis with the ac planes parallel to the rolled plane. Therefore, four different orientations of the unit cell, all of them consistent with the restrictions (one axis common and one plane common), are possible, and the specimen simulates, not a single crystal, but a quadruplet.

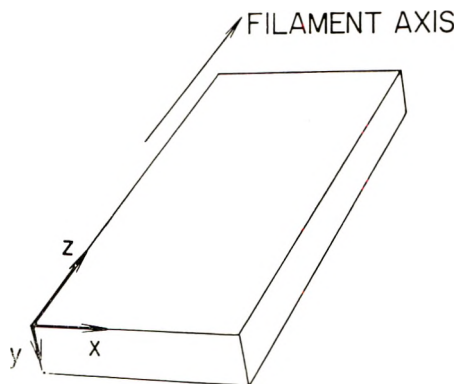


Fig. 7. Coordinate axes employed on the rolled specimen

For convenience we now define a rectangular coordinate system x , y , and z for the rolled specimen (Fig. 7).

In the irradiated specimen, the nodal plane of the p -orbital of the radical is assumed to be in the plane of the polymer chain with the \dot{C} -H bond perpendicular to the chain direction. The result of this is that the c axes fixed in the radicals are parallel to the z axis and the a axes are twisted by an angle $\pm 17^\circ$ from the x axis, where the $+17^\circ$ and the -17° twisted axes are present together in equal amounts.

Figures 8 and 2 show the ESR spectra of nylon 610 obtained with the magnetic field imposed along each of the x , y , and z axes. The spectrum for the x axis shows an apparent triplet with the small splitting of the doublet substructure. On the other hand, the spectrum for the z axis, which is the same as that for 0° orientation in Figure 2, is a quartet with the doublet

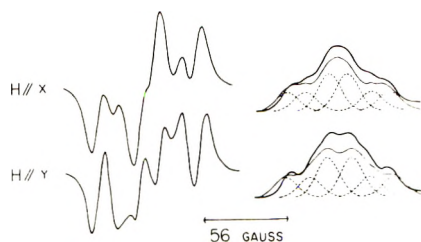


Fig. 8. ESR spectra of biaxially oriented nylon 610, irradiated to 1×10^8 rad, obtained with the magnetic field imposed along each of the x and y axes. (The spectrum for the z axis orientation is the same as that for the 0° orientation in Figure 2.)

splitting comparable to that for the triplet (due to two π -protons). The spectrum for the y axis shows an intermediate of these two.

Using eq. (1) for the doublet splitting and the above information on the structure of the biaxial orientation, we can calculate the splittings D_x , D_y , and D_z for the three axes:

$$\begin{aligned}
 D_x &= \{ [5.2 - \frac{1}{2}(0.7)(7.5)]^2 \cos^2 17^\circ + [5.2 - \frac{1}{2}(0.7)(24.6)]^2 \cos^2 73^\circ \}^{1/2} \\
 &\quad + \{ [5.2 + \frac{1}{2}(0.7)(7.5)]^2 \cos^2 17^\circ + [5.2 + \frac{1}{2}(0.7)(24.6)]^2 \cos^2 73^\circ \}^{1/2} \\
 &\simeq 11 \text{ gauss} \\
 D_y &= \{ [5.2 - \frac{1}{2}(0.7)(7.5)]^2 \cos^2 73^\circ + [5.2 - \frac{1}{2}(0.7)(24.6)]^2 \cos^2 17^\circ \}^{1/2} \\
 &\quad + \{ [5.2 + \frac{1}{2}(0.7)(7.5)]^2 \cos^2 73^\circ + [5.2 + \frac{1}{2}(0.7)(24.6)]^2 \cos^2 17^\circ \}^{1/2} \\
 &\simeq 17 \text{ gauss} \\
 D_z &= (0.7)(36.8) \\
 &\simeq 26 \text{ gauss}
 \end{aligned} \tag{5}$$

where ρ is assumed to be 0.7.

From these values we can derive the calculated absorption curves as done in the uniaxial orientation. These also account for the observed curves, as shown in Figure 8, although there is more discrepancy owing to the incompleteness of the biaxial orientation on the specimen. Thus, the good agreement between the observation and the theory justifies the mentioned as-

sumption, which indicates that, as a matter of course, radiation-induced radicals are trapped mainly in the crystalline region at room temperature.

One interesting point can be seen by the spectrum of a rolled, undrawn (unoriented) filament. In this case, the x orientation gives a clear four-line spectrum similar to that for the 0° orientation in Figure 2. It is caused by the fact that, if an undrawn filament is pressed, the c axes of the crystals become perpendicular to the original filament axis, i.e., the c axes set themselves along the direction of greatest flow during pressing.

Similar results have been observed in nylon 66.

Effects of NH Groups on ESR Spectra

The ESR spectra of the irradiated polyamides do not show the resolved hyperfine structure due to the NH group. The reasons for the lack of the NH hyperfine structure are that the splitting of a triplet due to N-coupling is of the order of 5 gauss with reference to irradiated single crystal of

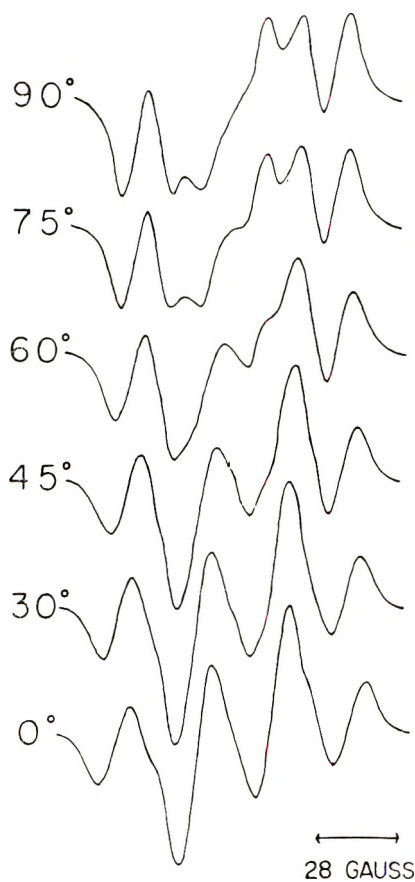


Fig. 9. ESR spectra of uniaxially oriented nylon 57, irradiated to 1×10^8 rad, for various orientations of the specimen in the magnetic field.

glycine,⁹ and such a small splitting would not be observed in polymers, even if the oriented specimen is used. No H-coupling results from the fact that the NH group is approximately in the plane of the molecular chain and the N—H bond does not overlap with the *p*-orbital of the radical.¹⁵

However, this fact is not true in the series of polyamides with odd numbers of CH₂ groups whose crystal structures have been found to be of the γ form.²² In the γ form the amide plane is twisted out of the plane of the CH₂ chain zigzag, and the N—H bond would overlap with the *p*-orbital of the radical. It is expected under these circumstances to observe spectra showing the hyperfine structure due to H-coupling in these polymers.

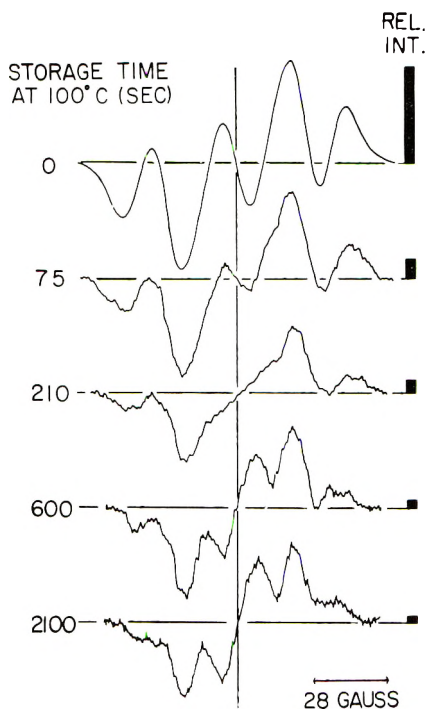


Fig. 10. Change of ESR spectrum of unoriented nylon 610, irradiated to 1×10^8 rad, on storage at 100°C.

However, this objective has not been achieved, as seen in Figure 9. The spectra of irradiated nylon 57 indicates no difference from those of nylon 610 (Fig. 2). The same result has been obtained for the γ form of nylon 6.²³ Since the spectra of polymers are even broader in oriented specimens, the present experiment might be inadequate to discuss the above point. The details should be investigated by using completely oriented specimens such as single crystals.

Although there are some ambiguous points as mentioned above, the ESR spectrum of the irradiated polyamide has six lines with the broad component line presumably due to the ill-resolved hyperfine structure of the NH

group. This leads to the identification of the resonance center as $-\text{CONH}\dot{\text{C}}\text{HCH}_2-$.

Other Kinds of Radicals

The hitherto discussed spectra have been obtained by the ESR measurement immediately after irradiation. These spectra decay and change in hyperfine structure with time. Figure 10 shows the array of spectra of unoriented nylon 610 at various storage periods of 100°C . The shape of the spectrum changes rapidly at first, becoming narrower, until at the end of 600 sec. radical component $-\text{CONH}\dot{\text{C}}\text{HCH}_2-$ has completely disappeared, leaving but a five-line spectrum with an overall spread of about 100 gauss. This spectrum decays very slowly, the amplitude decreasing about 20% during 1500 sec. additional storage at 100°C . Decay of the relative intensity of the resonance signal is shown plotted as a function of storage

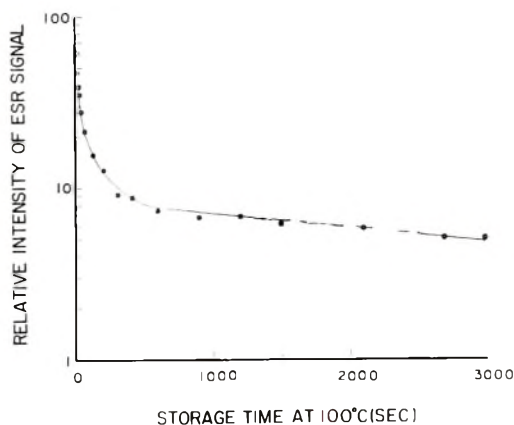


Fig. 11. Decay of the relative intensity of resonance signal at 100°C . in nylon 610 irradiated to 1×10^8 rad.

time at 100°C . in Figure 11. The signal appears to decay at two different rates. The primary component, which disappears during the first part of the 600-sec. storage period is responsible for the radical $-\text{CONH}\dot{\text{C}}\text{HCH}_2-$, while the slowly decaying component is responsible for the other radical giving the five-line spectrum. An extrapolation of the slowly decaying component slope to zero time gives the fraction of the other radical and indicates that about 10% of all of the radicals are involved. This value just accounts for the discrepancy between the observed and the calculated absorption curves.

The array of spectra in Figure 12 shows the changes at various orientations of a uniaxially oriented nylon 610 stored for 600 sec. at 100°C . For parallel orientation of the filament axis to the magnetic field, the spectrum shows five lines with an overall spread of 105 gauss and, for perpendicular orientation, the spectrum similarly has five lines with a smaller spread of 85 gauss. It may be noted that the number of hyperfine lines is unchanged,

and the hyperfine splittings alone change with the rotation of the magnetic field. The five-line spectrum of the irradiated unoriented specimen is very similar to that observed in irradiated solid alcohols²⁴ or in irradiated polyethylene,³ and the similarity suggests that the spectrum might be due to a $-\dot{\text{C}}\text{H}_2 \dots \text{H}_2\dot{\text{C}}-$ biradical resulting from a C—C main chain scission. The suggested radical is consistent with the changes of Figure 12. In this radical an unpaired electron interacts with four equal σ -protons, and the magnitude of the interaction decreases accompanied by the change from the

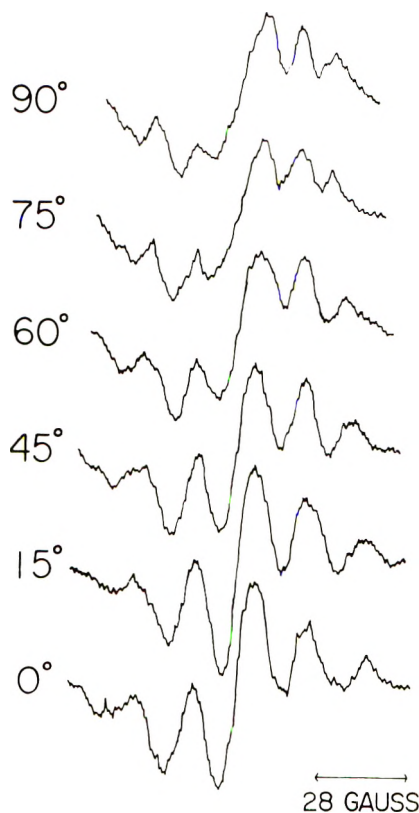


Fig. 12. ESR spectra of uniaxially oriented nylon 610, stored for 600 sec. at 100°C following irradiation to a total dose of 1×10^8 rad, for various orientations of the specimen in the magnetic field.

parallel orientation to the perpendicular one, as already mentioned. However, the amount of the slowly decaying radical is very small, and the observed spectrum is fairly distorted by the noise. There remains a possibility that additional fine structures might have been missed in the observation of the spectrum. This prevents a more detailed analysis and the definite identification of the radical.

Moreover, the present measurements have been made on other polyamides, and similar results have been observed. In nylon 6, for example,

the radical decays more rapidly, and the five-line spectrum is of poorer resolution, as has been shown in the predominant spectrum. This is apparently due to some differences of the physical properties among each polyamide, which are not clearly understood at present.

The author wishes to thank Mr. Y. Shinohara for helpful discussions and invaluable advice.

He is also indebted to Dr. H. Kobayashi and Mr. E. Mukoyama for their kind encouragement in the course of this study.

References

1. Abraham, R. J., and D. H. Whiffen, *Trans. Faraday Soc.*, **54**, 1291 (1958).
2. Abraham, R. J., H. W. Melville, D. W. Ovenall, and D. H. Whiffen, *Trans. Faraday Soc.*, **54**, 1133 (1958).
3. Lawton, E. J., J. S. Balwit, and R. S. Powell, *J. Chem. Phys.*, **33**, 395 (1960); *ibid.*, **33**, 405 (1960).
4. Florin, R. E., L. A. Wall, and D. W. Brown, *Trans. Faraday Soc.*, **56**, 1304 (1960).
5. Libby, D., M. G. Ormerod, and A. Charlesby, *Polymer*, **1**, 212 (1960).
6. Lawton, E. J., and J. S. Balwit, *J. Phys. Chem.*, **65**, 815 (1961).
7. Ohnishi, S., Y. Ikeda, M. Kashiwagi, and I. Nitta, *Polymer*, **2**, 119 (1961).
8. Miyagawa, I., and W. Gordy, *J. Chem. Phys.*, **30**, 1590 (1959).
9. Ghosh, D. K., and D. H. Whiffen, *Molecular Phys.*, **2**, 285 (1959).
10. McConnell, H. M., C. Heller, J. Cole, and R. W. Fessenden, *J. Am. Chem. Soc.*, **82**, 766 (1960).
11. Kiselev, A. G., M. A. Makoulskii, and Yu. S. Lazurkin, *Vysokomolekulyarne Soedineniya*, **2**, 1678 (1960).
12. Burrell, E. J., *J. Am. Chem. Soc.*, **83**, 574 (1961).
13. Coffman, D. D., G. J. Berchet, W. R. Peterson, and E. W. Spanagel, *J. Polymer Sci.*, **2**, 306 (1947).
14. Inaba, Y., and K. Kimoto, *J. Soc. Textile and Cellulose Inds. Japan*, **14**, 798 (1958).
15. Heller, C., and H. M. McConnell, *J. Chem. Phys.*, **32**, 1535 (1960).
16. Miyagawa, I., and W. Gordy, *J. Chem. Phys.*, **32**, 255 (1960).
17. Chappel, F. B., *Polymer*, **1**, 409 (1960).
18. McConnell, H. M., and J. Strathdee, *Molecular Phys.*, **2**, 129 (1959).
19. Kashiwagi, M., *J. Chem. Phys.*, in press.
20. Bunn, C. W., and E. V. Garner, *Proc. Roy. Soc. (London)*, **A189**, 39 (1947).
21. Holmes, D. R., C. W. Bunn, and D. J. Smith, *J. Polymer Sci.*, **17**, 159 (1955).
22. Kinoshita, Y., *Makromol. Chem.*, **33**, 1 (1959); *ibid.*, **33**, 21 (1959).
23. Ide, K., S. Ohnishi, and I. Nitta, *Ann. Rept. Japanese Assoc. Radiation Research on Polymers*, **1**, 195 (1958-1959).
24. Fujimoto, M., and D. J. E. Ingram, *Trans. Faraday Soc.*, **54**, 1302 (1958).

Synopsis

Oriented polyamides were irradiated with 1.5-M.e.v. electrons and the paramagnetic resonance was examined to determine the radical species. The spectrum is composed of two radical species which decay at different rates. The predominant radical has a spectrum with three main lines (intensity ratio; 1:2:1), each split into two. The doublet splitting changes with the rotation of the magnetic field, while the triplet splittings undergo slight change. The spectrum indicates that the radical is of an unpaired electron interacting with one σ -proton and two equal π -protons. In addition, the width of the individual lines is broad (half width = ca. 18 gauss) and it is presumably due to the ill-resolved hyperfine structure of NH group. These confirm that the radical

is $-\text{CONH}\dot{\text{C}}\text{HCH}_2-$ as indicated by the findings of Burrell on irradiated amides. The other radical has a five-line spectrum, which indicates that the radical may be of the type resulting from a $-\text{C}-\text{C}-$ bond scission, although not fully investigated.

Résumé

On a irradié des polyamides orientés avec des électrons de 1,5 Mev. et on les a examinés du point de vue résonance paramagnétique dans le but de déterminer la nature des radicaux. Le spectre se compose de deux espèces radicalaires qui se détruisent à des vitesses différentes. Le radical prédominant possède un spectre à trois lignes principales (rapport d'intensité, 1:2:1) chacune se scindant en deux. La scission du doublet varie avec la rotation du champ magnétique, tandis que les scissions en triplet ne subissent qu'un faible changement. Le spectre montre que le radical provient de l'interaction d'un électron non apparié avec un proton σ et deux protons π égaux. En outre la largeur des lignes individuelles est prononcée (demi largeur, ~ 18 gauss) et est probablement due à la structure hyperfine mal résolue du groupement NH. Ceci confirme que le radical est $-\text{CONH}\dot{\text{C}}\text{HCH}_2-$ ainsi que le proposait Burrell pour les amides irradiés. L'autre radical a un spectre de cinq lignes, ce qui indique que le radical peut être du type résultant d'une scission du lien $-\text{C}-\text{C}-$; ceci toutefois n'a pas été examiné complètement.

Zusammenfassung

Orientierte Polyamide wurden mit 1,5 Mev Elektronen bestrahlt und auf paramagnetische Resonanz zur Bestimmung der Radikalarten untersucht. Das Spektrum entspricht zwei Radikalarten, die mit verschiedener Geschwindigkeit abklingen. Das vorherrschende Radikal besitzt ein Spektrum mit drei Hauptlinien (Intensitätsverhältnis 1:2:1), die jede in zwei Linien gespalten ist. Die Dubbett-Aufspaltung ändert sich mit der Rotation des magnetischen Feldes, während die Triplett-Aufspaltung eine geringe Änderung erfährt. Das Spektrum zeigt, dass das Radikal ein ungepaartes Elektron besitzt, das mit einem σ -Proton und zwei π -Protonen in Wechselwirkung steht. Weiters ist die Breite der einzelnen Linien gross (Halbwertsbreite ≈ 18 Gauss) und hauptsächlich durch die schlechte Auflösung der Hyperfeinstruktur der NH-Gruppe bedingt. Dadurch wird bestätigt, dass es sich um ein $-\text{CONH}\dot{\text{C}}\text{HCH}_2-$ Radikal handelt, wie schon von Burrell an bestrahlten Amiden gefunden wurde. Das andere Radikal besitzt ein Spektrum von fünf Linien, was darauf hinweist, dass es sich um ein Radikal aus der Spaltung einer C-C-Bindung handeln kann; es wurde jedoch nicht vollständig aufgeklärt.

Received October 23, 1961

A General Kinetic Scheme for Ziegler-Type Polymerizations

LEO REICH* and S. S. STIVALA,† *Department of Chemistry and Chemical Engineering, Stevens Institute of Technology, Hoboken, New Jersey*

INTRODUCTION

The aim of this paper is to present a general scheme to explain in a qualitative and quantitative manner various features of Ziegler-type polymerizations, such as (1) the dependence of polymerization rate on monomer concentration, (2) the dependence of rate on aluminum alkyl and metal halide concentrations, (3) the dependence of rate on catalyst ratio, (4) the factors upon which molecular weight is dependent, (5) the effect of temperature on molecular weight, (6) the effect of temperature on polymerization rate, (7) the different activities of different Ziegler catalysts, (8) the stereospecific polymerization aspects, (9) the "hair-like" growth observed to occur from an active site on a catalyst surface, e.g., in the case of polyethylene.¹

It is to be realized that, due to limitation of space, it is not feasible to include all references that would support or contradict the postulations presented in this paper.

BACKGROUND

An early attempt to explain Ziegler-type kinetics was made by Eirich and Mark,² for example, they presented equations which related polymerization rate as a function of strength of monomer adsorption, nature of the catalyst complex, etc. Several systems were subsequently found to conform with their expressions.³ However, many systems could not be explained in the light of their work, e.g., there was no explanation for the maxima obtained for various systems when polymerization rate is plotted against catalyst ratio.

Saltman and co-workers³ also developed theoretical relationships based on the polymerization of isoprene with Ziegler catalysts. However, no elaborate scheme was presented, and their treatment failed to account for second-order kinetics with respect to monomer as obtained for several modified Ziegler systems.⁴⁻⁶ Recently, Saltman⁷ proposed a more detailed mechanism to explain experimental results obtained by Natta^{8,9} for the system, propylene-TiCl₃-Al Et₃. The expressions obtained for polymeri-

* Present address: Plastics Research Laboratory, Picatinny Arsenal, Dover, N. J.

† To whom inquiries should be sent.

zation rate and degree of polymerization were found to be in satisfactory agreement with Natta's results.

Friedlander¹⁰ and co-workers have also presented a kinetic scheme in order to explain the polymerization of ethylene by means of molybdena-alumina catalyst in the presence of hydrogen. Although satisfactory correlations could be obtained, the scheme does not deal directly with Ziegler catalysts and is limited.

POSTULATED REACTIONS

A. Ionic-Coordinated vs. Free Radical Mechanism

Although several authors^{11,12} have ascribed a radical mechanism to Ziegler-type polymerizations, Natta¹³⁻¹⁵ presented strong evidence against this. Thus, he has indicated the unlikelihood of free radical mechanisms by advancing the following: (1) the possibility of producing block copolymers by alternately feeding different monomers, even if polymerization is interrupted; (2) polar effect of substituents in series of vinyl-aromatic monomers which is opposite to that known in radical polymerizations; (3) high percentage of macromolecules to which aluminum is bound when a catalytic system containing aluminum alkyls is used, etc. In this paper, we favor Natta's views.

B. Equilibrium Processes and Initiation

Equilibrium processes have been presented for the adsorption of monomer and aluminum alkyl on a Ziegler catalyst surface. Both alkyl and monomer are adsorbed on the surface and compete for available sites.⁷⁻⁹ Since the monomer is considerably less polar than the metal alkyl, it is less strongly adsorbed and probably so on fewer sites. The concept that active centers are complexes formed by the reduced titanium halide and the aluminum alkyl is supported by various reports.¹⁶ Adsorbed alkyl on the surface is necessary in order for polymerization to occur. Thus, the initiation is postulated as occurring between adsorbed alkyl and neighboring adsorbed or unadsorbed monomer. The number of active sites would be expected to depend on the amount of reduced metal halide present in the system. Most of the alkyl, in one form or another, should remain in solution. This alkyl could then participate in adsorption equilibria and compete for the active catalyst sites with monomer in solution. In the general scheme to be presented later, the monomer has been postulated as being adsorbed on an active dual site, S^*_2 , which can orient the monomer in a unique fashion (resulting in stereoregularity).¹⁰

Recently,¹⁷ it has been indicated that dipolar active centers may be adsorbed on the border of a basal plane of a crystal of $TiCl_3$. This was presumed to represent the major component of the stereo-specific catalyst.

C. Propagation Processes

Natta⁸ postulated that adsorbed monomer is inserted between the metal and alkyl portions of the aluminum alkyl. In this "insertion" hypothesis,

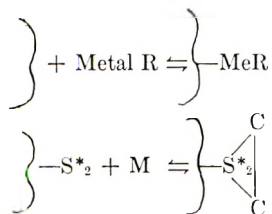
interactions between catalyst components are still occurring. In the heterogeneous media employed, this type of chemical interaction can also vary locally.

The basic assumption in the general scheme proposed is that Ziegler-type polymerizations all involve a similar basic mechanism. However, depending upon the system, some steps will probably predominate over others. It is also assumed that catalyst ratio can play an important role in changing the catalyst surface. However, reactions occurring on the surface are postulated as playing the predominant role in determining the shape of curves obtained in kinetic studies, provided there are no large surface alterations as the catalyst ratio is markedly changed, e.g., the system³ isoprene-TiCl₄-Al(*i*-Bu)₃.

PROPOSED GENERAL KINETIC SCHEME

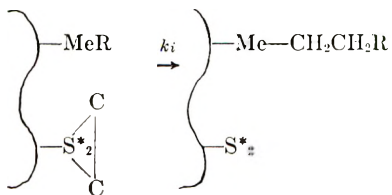
A general kinetic scheme, bringing into account those factors previously discussed, is as follows:

Equilibria:

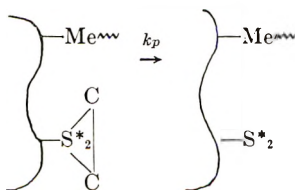


where M is monomer, e.g., C₂H₄

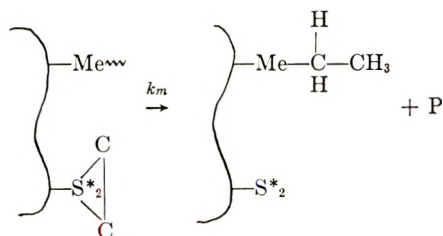
Initiation:



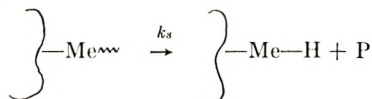
Propagation:



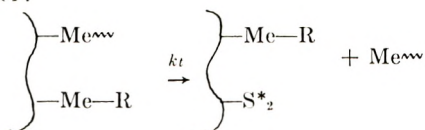
Monomer transfer:



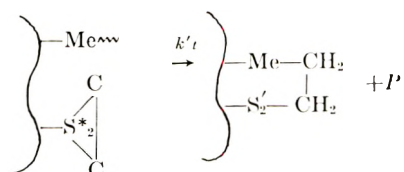
Spontaneous transfer:



Catalyst transfer:



Termination by monomer:



where S'_2 is no longer an active dual site.

Interaction Between Adsorbed Molecules

If we assume high stirring speeds are used (where polymerization rate is not diffusion-controlled), the monomer is ethylene, and the solvent becomes rapidly saturated, we may write for the concentration of ethylene in solution, $[C_2H_4]_s$, assuming Henry's law applies,

$$[C_2H_4]_s = K_s [C_2H_4]_g \quad (1)$$

where K_s is the equilibrium constant at saturation and $[C_2H_4]_g$ is the partial pressure of ethylene in the gas phase. We may then write for the concentration of adsorbed monomer,

$$[C_2H_4]_a = K [C_2H_4]_g C_s \quad (1a)$$

where C_s is the concentration of bare surface sites. Similarly, for the adsorption of alkyl in solution (AlR_3 , AlR_2X , etc.), we may write:

$$[Alk]_a = K' [Alk]_s C_s \quad (2)$$

also:

$$[C_2H_4]_a + [Alk]_a + C_s = L \quad (3)$$

where L is the concentration of active surface sites when the surface is completely bare. From eqs. (1), (2), and (3) we obtain

$$[\text{C}_2\text{H}_4]_a = \frac{KL[\text{C}_2\text{H}_4]_s}{1 + K[\text{C}_2\text{H}_4]_s + K'[\text{Alk}]_s} \quad (4)$$

and

$$[\text{Alk}]_a = \frac{K'L[\text{Alk}]_s}{1 + K[\text{C}_2\text{H}_4]_s + K'[\text{Alk}]_s} \quad (5)$$

From eqs. (4) and (5), the expressions for the fraction of the surface covered by monomer and alkyl are, respectively,

$$\begin{aligned} [\text{C}_2\text{H}_4]'_a &= [\text{C}_2\text{H}_4]_a/L \\ &= \frac{K[\text{C}_2\text{H}_4]_s}{1 + K[\text{C}_2\text{H}_4]_s + K'[\text{Alk}]_s} \end{aligned} \quad (4a)$$

and

$$\begin{aligned} [\text{Alk}]'_a &= [\text{Alk}]_a/L \\ &= \frac{K'[\text{Alk}]_s}{1 + K[\text{C}_2\text{H}_4]_s + K'[\text{Alk}]_s} \end{aligned} \quad (5a)$$

The average number of adsorbed alkyls adjacent to any given adsorbed monomer is equal to $S\theta'$, where S is the maximum number of possible near neighbors and $\theta' = [\text{Alk}]_a/L$. Then, the total number of adsorbed alkyl-monomer pairs becomes

$$\frac{SLKK'[\text{C}_2\text{H}_4]_s[\text{Alk}]_s}{(1 + K[\text{C}_2\text{H}_4]_s + K'[\text{Alk}]_s)^2}$$

Thus, it is seen from the above that if the surface remains uniform during the reaction ($S \approx \text{constant}$), a constant reaction temperature is maintained, and if it is assumed that partition functions and activation energies remain constant, then reaction rate may be expressed in terms of adsorbed monomer and alkyl.

From the proposed scheme, we may write (neglecting the initiation step) for the rate of monomer consumption per unit of active surface sites,

$$-dM/dt = (k_p + k_m) [\text{C}_2\text{H}_4]'_a \sum_n [\text{Polymer}]_a \quad (6)$$

and, assuming steady-state considerations,

$$\sum_n [\text{Polymer}]_a = \frac{k_i[\text{Alk}]'_a [\text{C}_2\text{H}_4]'_a}{k_s + k_t[\text{Alk}]'_a + k'_t[\text{C}_2\text{H}_4]'_a} \quad (7)$$

From eqs. (4a), (5a), (6), and (7), we obtain

$$\begin{aligned} -dM/dt &= \frac{(k_p + k_m)k_i[\text{Alk}]_s K' K^2 [\text{C}_2\text{H}_4]_s^2}{(1 + K[\text{C}_2\text{H}_4]_s + K'[\text{Alk}]_s)^3 \left\{ k_s + \frac{k_t K' [\text{Alk}]_s + k'_t K [\text{C}_2\text{H}_4]_s}{1 + K[\text{C}_2\text{H}_4]_s + K'[\text{Alk}]_s} \right\}} \end{aligned} \quad (8)$$

Equation (8) may be reduced to any number of simpler forms, depending upon which processes in the scheme predominate. Thus, if termination occurs essentially by means of monomer, and adsorbed monomer reacts with adsorbed alkyl on the surface, eq. (8) becomes

$$-dM/dt = \frac{k_i(k_p + k_m)KK'_1 [\text{Alk}]_s [\text{C}_2\text{H}_4]_s}{(1 + K[\text{C}_2\text{H}_4]_s + K'[\text{Alk}]_s)^2} \quad (9)$$

For the case where the concentration of active dual surface sites varies, eq. (9) becomes

$$\text{Rate} = \left\{ \frac{B[\text{Alk}]_s [\text{C}_2\text{H}_4]_s}{(1 + K[\text{C}_2\text{H}_4]_s + K'[\text{Alk}]_s)^2} \right\} f[\text{Ti}] \quad (10)$$

where $B = k_i(k_p + k_m)KK'_1 = \text{constant}$ and $f[\text{Ti}]$ is a function of active dual sites formed, and denotes the titanium halide concentration introduced into the system.¹⁹

By an approach similar to the one above, other expressions may be ob-

TABLE I
Summary of Conditions and Appropriate Rate Equations in Ziegler-Type Polymerizations

| Mechanism number (M.N.) | Predominant termination step | Type of surface reaction | Form of rate equation |
|-------------------------|------------------------------|--|--|
| I | Via monomer | Adsorbed alkyl and adsorbed monomer | $\frac{B[\text{Alk}]_s[\text{M}]_s f[\text{Ti}]}{(1 + K[\text{Alk}]_s + K'[\text{M}]_s)^2}$ |
| II | Via monomer | Adsorbed alkyl and unadsorbed monomer | $\frac{B[\text{Alk}]_s[\text{M}]_s f[\text{Ti}]}{(1 + K[\text{Alk}]_s)}$ |
| III | Via monomer | Adsorbed alkyl and adsorbed monomer but unadsorbed monomer in initiation | $\frac{B[\text{Alk}]_s[\text{M}]_s f[\text{Ti}]}{(1 + K[\text{Alk}]_s + K'[\text{M}]_s)}$ |
| IV | Spontaneous | As in M.N. I | $\frac{B'[\text{Alk}]_s[\text{M}]_s^2 f[\text{Ti}]}{(1 + K[\text{Alk}]_s + K'[\text{M}]_s)^3}$ |
| V | Spontaneous | As in M.N. II | $\frac{B'[\text{Alk}]_s[\text{M}]_s^2 f[\text{Ti}]}{(1 + K[\text{Alk}]_s)^2}$ |
| VI | Spontaneous | As in M.N. III | $\frac{B'[\text{Alk}]_s[\text{M}]_s^2 f[\text{Ti}]}{(1 + K[\text{Alk}]_s + K'[\text{M}]_s)^2}$ |
| VII | Via catalyst | As in M.N. I | $\frac{B''[\text{M}]_s^2 f[\text{Ti}]}{(1 + K[\text{Alk}]_s + K'[\text{M}]_s)^2}$ |
| VIII | Via catalyst | As in M.N. II | $\frac{B''[\text{M}]_s^2 f[\text{Ti}]}{(1 + K[\text{Alk}]_s)}$ |
| IX | Via catalyst | As in M.N. III | $\frac{B''[\text{M}]_s^2 f[\text{Ti}]}{(1 + K[\text{Alk}]_s + K'[\text{M}]_s)}$ |

TABLE II
Rate Data and Appropriate Rate Expressions from Table I for Various Ziegler-Type Systems

| Monomer | Catalyst | Kinetic order with respect to | | | Effect of catalyst ratio (C.R.) on rate | Appropriate equation from Table I | Reference |
|-----------|--|-------------------------------|-------------------|-------------------|---|-----------------------------------|-----------|
| | | Monomer | Alkyl | Ti | | | |
| Ethylene | TiCl ₄ -AlR ₃ | 1 | — | 1 | Maximum produced | M.N. I | 19, 20 |
| Ethylene | LiR | | 0 | | | | |
| | TiCl ₄ - or ZnBu ₂ | 2 | -1 (large C.R.) | 1 | Independent except for large C.R. | M.N. VIII or IX | 4, 5 |
| Ethylene | Ti(OR) ₄ -AlR ₃ | 1 (limited range) | 1 (limited range) | 1 (limited range) | Maximum produced | — | |
| Propylene | TiCl ₃ -AlR ₃ | 1 | 0 | 1 | Independent | M.N. II or III | 8 |
| Propylene | CrCl ₃ -AlR ₃ | 1 | 0 | 1 | Independent | M.N. II or III | 22 |
| 1-Butene | TiCl ₃ -AlR ₃ | 1 | 0 | 1 | Independent | M.N. II or III | 23 |
| 1-Butene | TiCl ₄ -AlR ₃ | 1 | (1) | 1 | Maximum produced | M.N. I | 24 |
| Isoprene | TiCl ₄ -AlR ₃ | 1 | 1 | 1 | Maximum produced | M.N. I | 3 |
| Butadiene | TiCl ₄ -AlR ₃ | 1 (low C.R.) | 1 | 1 | Maximum produced | M.N. I | 6 |
| | | 2 (high C.R.) | | | | M.N. VI | |
| Styrene | TiCl ₃ -AlR ₃ | 1 | 0 | 1 | Independent | M.N. II or III | 25, 26 |
| Styrene | TiCl ₄ -AlR ₃ | 1 | — | 1 | Maximum produced | M.N. I | 25 |

tained for various prevailing conditions. These expressions corresponding to various conditions are summarized in Table I.

Application of Rate Equations from Table I

Various Ziegler-type systems are listed in Table II, including pertinent rate data. The appropriate rate expression for each system has been taken from Table I.

It can be seen from Table II that the system ethylene-Ti(OR)₄-AlR₃ is not analogous to any system listed in Table I. However, it must be noted that other expressions are possible, depending upon the mechanism postulated. Thus, if we assume termination by monomer and monomer adsorption, and if both alkyl and unreacted metal halide (alkoxide) participate in adsorption competition, then the following expression is obtained,

$$\text{Rate} = \frac{B[\text{Alk}]_s[\text{M}]_s[\text{Ti}]}{(1 + K[\text{Alk}]_s + K'[\text{M}]_s + K''[\text{Ti}]_s)^2} \quad (11)$$

This expression conforms to the rate data listed for the above system. For this soluble system, a "cut-off" pressure has been observed which increases with increasing Ti(OR)₄ concentration. A possible explanation would be the competition that Ti(OR)₄ offers the monomer for active surface sites.

From Table II it is further noted that data for several systems may conform to more than one form of rate expression (M.N. II or III). However, we prefer mechanism III, since it is otherwise difficult to explain how monomer could come close to the surface in the propagation and termination steps (monomer is inserted between metal adsorbed on the surface and the carbon from the chain attached to it) without being adsorbed. The monomer, e.g., ethylene, for the initiation step, may be sufficiently reactive to undergo initially a Rideal type of mechanism. (Initially, there would be less steric influences than later on when a polymer chain had formed.) Medvedev and co-workers²⁷ polymerized ethylene using the catalyst system, TiCl₃-AlR₃, in the presence of other monomers (butadiene, isoprene, styrene, and isobutylene). The additives lowered the polymerization rate; however, they did not affect the molecular weight of the polyethylene formed and remained unreacted. This indicated that the propagation step occurred more readily when ethylene was adsorbed on a Ziegler surface prior to entering the growing polymer molecule. Similarly, M.N. IX would be preferred to VIII. In the butadiene-TiCl₄-AlR₃ system, two different reaction orders with respect to monomer concentration were observed as the catalyst ratio was varied. This could be explained by assuming that one mechanism (I) occurred at low catalyst ratio (C.R.) followed by another mechanism (VI) at high C.R. The major difference between the two mechanisms would be whether termination occurred by means of monomer or spontaneously.

It should be mentioned that rate of polymerization may be virtually zero

for low catalyst ratios. This can be explained as follows: At low C.R., active alkyl species may not exist ($\text{AlR}_3 > \text{AlR}_2\text{X} > \text{AlRX}_2 \gg \text{AlX}_3$).²⁴ Thus, $[\text{Alk}]_s$ may be considered to be negligible, therefore, polymerization rate will be very small. It can be seen from Table II that not all of the expressions in Table I can explain the rate data listed. Thus, the rate expression for the system ethylene-Ti(OR)₄-AlR₃ is not analogous to any expression in Table I. However, it may be possible, by assuming other prevailing conditions, to explain the rate data obtained for this system.

Catalyst Ratio and Active Surface

The type of Ziegler catalyst and the catalyst ratio (C.R.), Al/Ti, will affect the percentage of Ti(IV) reduced to Ti(III) (denoted as PRT). This is shown in Table III. In this table, side reactions such as $\text{R}\cdot + \text{TiX}_4 \rightarrow \text{TiX}_3 + \text{RX}$ and the reduction of Ti(IV) to a valence state below Ti(III) have been neglected. The latter may become important for systems involving trialkyl-aluminum.

TABLE III
Effect of Catalyst Ratio on PRT for Various Systems^{28,29}

| Catalyst system | Catalyst ratio (m) | PRT | Alkyl remaining as active species, % | Active alkyl species |
|---------------------------------------|------------------------|---------------|--------------------------------------|---|
| AlRX ₂ + TiX ₄ | <1 | 100 <i>m</i> | 0 | 0 |
| | >1 | 100 | 100 (1-1/ <i>m</i>) | AlRX ₂ |
| AlR ₂ X + TiX ₄ | <1/2 | 200 <i>m</i> | 0 | 0 |
| | >1/2, <1 | 100 | 100 (2-1/ <i>m</i>) | AlRX ₂ |
| | >1 | 100 | 100 | AlRX ₂ , AlR ₂ X |
| AlR ₃ + TiX ₄ | <≈0.4 | ≈250 <i>m</i> | 100 (50) | Al ₂ RX ₆ (AlRX ₂) |
| | >1 | 100 | 100 | AlR ₃ , AlR ₂ X, (AlRX ₂) |

If it is assumed that the formation of active dual surface sites is a function of PRT, which in turn is related to $[\text{Ti}]$,²⁰ then Table III may be used to correlate catalyst ratio (C.R.) with the amount of active dual surface sites formed. For the system, ethylene-TiCl₄-AlR₂Br, there is an indication²⁸ that we may apply the rate expression in the form (cf. M.N. III),

$$\text{Rate} = \frac{B[\text{Alk}]_s[\text{M}]_s}{(1 + K[\text{Alk}]_s + K'[\text{M}]_s)} \quad (12)$$

From Table III, it is noted that for values of $m < 1/2$ there will be no active alkyl species. Thus, rate will be very low. Between m values of $1/2$ to 1, the active alkyl species would be AlRX₂. As m increases from $1/2$ to 1, $[\text{Alk}]_s$ should increase almost linearly with m (or C.R.), the value of $[\text{Ti}]$ being maintained constant. Above $m = 1$, the denominator in the above expression may be expected to become approximately $K[\text{Alk}]_s$, and rate is

now independent of alkyl concentration and C.R. This behavior has been observed for the above system in which R = ethyl. Similarly, for the system $\text{AlRX}_2\text{-TiCl}_4$, it would be expected that for values of $m < 1$, $[\text{Alk}]_s$ would be very small and hence rate should be low. This has been observed for the modified Ziegler catalyst, AmNa-TiCl_4 .²⁸ Above $m = 1$, the overall polymerization rate for ethylene increased almost linearly with C.R.

Some Molecular Weight Expressions from Scheme

As an example of some of the expressions for number-average degree of polymerization which may be obtained from the scheme, let us assume termination by monomer and monomer transfer. Then we may write

$$\begin{aligned}\bar{P} &= \frac{k_p[\text{M}]_a \sum_n [\text{Polymer}]_a}{(k_m + k'_t) [\text{M}]_a \sum_n [\text{Polymer}]_a} \\ &= k_p / (k_m + k'_t)\end{aligned}\quad (13)$$

If we assume termination to occur mainly by catalyst and monomer transfer, we obtain

$$1/\bar{P} = (k_m/k_p) + (k_t[\text{Alk}]/k_p[\text{M}])\quad (14)$$

Expression (13) has been found to hold for many systems. Thus, for isoprene- $\text{TiCl}_4\text{-AlR}_3$, it was found that the intrinsic viscosity increased with conversion up to a certain value, after which it became virtually constant. For the system involving 1-butene, the intrinsic viscosity increased with C.R. up to a certain value and then remained almost constant. Zilkha and co-workers³⁰ polymerized ethylene using TiCl_4 in conjunction with various sodium alkyls and found that the molecular weights of the resulting polyethylene did not vary over a wide range of C.R. Topchiev³¹ also found that intrinsic viscosity did not change appreciably over a wide range of C.R. in the polymerization of 1-butene. Ziegler³² found in the polymerization of ethylene that for a C.R. between 1 to 12, the molecular weights did not vary much.

Although the average degree of polymerization has been found to be nearly constant over a wide range of variable conditions for many systems, the products obtained have been fractionated into various molecular weight fractions. Thus, Ang³³ and others³²⁻³⁷ have found that Ziegler-type polymerizations gave products which could be separated into many fractions. This could be explained as follows. Since \bar{P} involves rate constants [cf. eq. (13)] it is possible that polymerization at different sites on the solid surface may result in different values for the rate constants, thereby leading to broad molecular weight distributions. Expression (14) has also been found to apply for several systems.

Temperature Effects from Scheme

The temperature dependence of polymerization rate can be predicted by applying the proper rate expression in Table I to the system involved. For

example, let us apply the expression involved in M.N.I, viz.,

$$\text{Rate} = B[M]_s[\text{Ti}]/K[\text{Alk}]_s \quad (15)$$

assuming high alkyl concentration or $K[\text{Alk}]_s \gg 1 + K'[\text{M}]_s$. In eq. (15), K is a function of adsorption equilibrium constants and $B \approx f(k_i, k_p, k_t)$. We therefore obtain (varying temperature only),

$$\begin{aligned} \text{Rate} &= A \exp \{[-(E_i + E_p - E_t') + \Delta F_a]\}/RT \\ &= A \exp \{(\Delta F_a - \Delta E)/RT\} \end{aligned} \quad (16)$$

where ΔF_a is the free energy of adsorption and ΔE is the sum of activation energies of the initiation, termination, and propagation steps (E_i , E_t , and E_p , respectively).

As often occurs, when the natural logarithm of rate is plotted against $1/T$, the rate of reaction passes through a maximum value. This is attributed to changes in $(\Delta F_a - \Delta E)$ with changing temperature. As temperature increases, positive and then negative values of $(\Delta F_a - \Delta E)$ may be obtained. This behavior has been observed²⁰ for systems which follow eq. (15), e.g., ethylene-TiCl₄-AlR₃. Topchiev³¹ also found a maximum to occur for the system 1-butene-TiCl₄-Al(Et)₃ when rate was plotted against temperature. Similar results were obtained for other systems,^{38,39} e.g., propylene-CrCl₃-Al(Et)₃. However, if $(\Delta F_a - \Delta E)$ remains constant or nearly so with changing temperature, then a linear relationship would be anticipated, as observed by Natta and others.

SUMMARY AND CONCLUSIONS

A general scheme has been postulated for Ziegler-type polymerizations which can explain either qualitatively or quantitatively the dependence of rate upon monomer, alkyl, and metal halide concentrations, and upon catalyst ratio. Molecular weight and temperature considerations have also been discussed in the light of this scheme.

Dual active sites, upon which monomer molecules may be adsorbed and oriented in a unique manner, have been postulated. This could explain the stereospecific polymerization of α -olefins as well as the different activities that different Ziegler-type catalysts have. With different catalysts, different dual-site activity may result, thereby changing the polymerization characteristics of the system involved. The growth of the polymer chain on an active site can explain the "hair-like" growth observed, as in the case of polyethylene.

References

1. Mark, H., *Progress in Plastics*, Philosophical Library, New York, 1957, p. 2.
2. Eirich, F., and H. F. Mark, *J. Colloid Sci.*, **11**, 748 (1956).
3. Saltman, W. M., W. E. Gibbs, and J. Lal, *J. Am. Chem. Soc.*, **80**, 5615 (1958).
4. McGowan, J. C., and B. M. Ford, *J. Chem. Soc.*, **1958**, 1149.
5. Gilchrist, A., *J. Polymer Sci.*, **34**, 49 (1959).
6. Gaylord, N. G., T. K. Kwei, and H. F. Mark, *J. Polymer Sci.*, **42**, 417 (1960).

7. Saltman, W. M., *J. Polymer Sci.*, **46**, 375 (1960).
8. Natta, G., *J. Polymer Sci.*, **34**, 21 (1959).
9. Natta, G., *Advances in Catalysis*, Vol. 11, Academic Press, New York, 1959, pp. 1-66.
10. Friedlander, H. N., *J. Polymer Sci.*, **38**, 91 (1959).
11. Nenitzescu, C. D., C. Huch, and A. Huch, *Angew. Chem.*, **68**, 438 (1956).
12. Friedlander, H. N. and K. Oita, *Ind. Eng. Chem.*, **49**, 1885 (1957).
13. Natta, G., *J. Polymer Sci.*, **48**, 219 (1960).
14. Natta, G., E. Giachetti, and I. Pasquon, Italian Pat. 594,018 (1958).
15. Natta, G., F. Danusso, and D. Sianesi, *Makromol. Chem.*, **28**, 253 (1958).
16. Gaylord, N. G., and H. F. Mark, *Linear and Stereoregular Addition Polymers*, Interscience, New York-London, 1959, p. 197.
17. Malatesta, A., *J. Polymer Sci.*, **51**, 545 (1961).
18. Huggins, M. L., *J. Polymer Sci.*, **48**, 473 (1960).
19. Feilchenfeld, H., and M. Jeselson, *J. Phys. Chem.*, **63**, 720 (1959).
20. Ludlum, D. B., A. W. Anderson, and C. E. Ashley, *J. Am. Chem. Soc.*, **80**, 1380 (1958).
21. Bawn, C. E. H., and R. Symcox, *J. Polymer Sci.*, **34**, 139 (1959).
22. Gillespie, J. F., and J. W. L. Fordham, *Ind. Eng. Chem.*, **51**, 1365 (1959).
23. Jones, M. H., V. Martins, and M. P. Thorne, *Chem. Eng. News*, **37**, 40 (1959).
24. Medalia, A. I., A. Orzechowski, J. A. Trinchera, and J. P. Morley, *J. Polymer Sci.*, **41**, 241 (1959).
25. Burnett, G. M., and P. J. T. Tait, *Polymer*, **1**, 151 (1960).
26. Natta, G., F. Danusso, and I. Pasquon, *Proceedings of the International Symposium on Macromolecular Chemistry, Sept. 1957 (Prague)*, Pergamon Press, New York, pp. 191-218.
27. Lanovskaya, L. M., et al., *Vysokomolekulyarnye Soedineniya*, **2**, 1391 (1960).
28. Havinga, R., and Y. Y. Tan, *Rec. trav. chim.*, **79**, 56 (1960).
29. Arlman, E. J., and J. R. DeJong, *Rec. trav. chim.*, **79**, 910 (1960).
30. Zilkha, A., et al., *J. Polymer Sci.*, **33**, 141 (1958).
31. Topchiev, A. V., et al., *Doklady Akad. Nauk S.S.S.R.*, **124**, 1255 (1959).
32. *Metal Organic Compounds*, Am. Chem. Soc. Publication, Washington, D. C., 1959, p. 170.
33. Ang, F., *J. Polymer Sci.*, **25**, 126 (1957).
34. Wasslau, H., *Makromol. Chem.*, **20**, 111 (1956).
35. Aries, R. S., and A. P. Sacks, *J. Polymer Sci.*, **21**, 551 (1956).
36. Francis, P. S., et al., *J. Polymer Sci.*, **31**, 453 (1958).
37. Tung, L. H., *J. Polymer Sci.*, **24**, 333 (1957).
38. Berger, N. N., and T. H. Boulbee, *J. Appl. Chem.*, **1959**, 490.
39. Kodama, S., et al., *J. Appl. Polymer Sci.*, **3**, 20 (1960).

Synopsis

A general kinetic scheme is postulated for Ziegler-type polymerizations. The scheme may be used to explain either qualitatively or quantitatively the dependence of rate on monomer, alkyl, and metal halide concentrations, and on catalyst ratio. Molecular weight and temperature considerations are discussed in the light of the general kinetic scheme. Dual active sites, upon which monomer molecules may be adsorbed and oriented in a unique manner and which could explain the stereospecific polymerization of *c*-olefins as well as the activities of Ziegler-type catalysts are also discussed.

Résumé

Un schéma cinétique général est proposé pour les polymérisations du type Ziegler. Ce schéma peut servir à expliquer soit qualitativement soit quantitativement la dépendance de la vitesse en fonction des concentrations en monomère, en halogénure

d'alcoyle et en halogénure métallique, et en fonction du rapport des catalyseurs. Des considérations sur le poids moléculaire et sur la température sont discutées à la lumière du schéma cinétique général. Des sites actifs doubles sur lesquels les molécules de monomères peuvent être adsorbées et orientées d'une même façon sont également discutés. Ceci pourrait expliquer la polymérisation stéréospécifique d' α -oléfines aussi bien que l'activité des catalyseurs du type Ziegler.

Zusammenfassung

Ein allgemeines kinetisches Schema für Polymerisationen vom Ziegler-Typ wird aufgestellt. Das Schema gibt eine qualitative oder quantitative Erklärung der Geschwindigkeitsabhängigkeit von der Monomer-, Alkyl- und Metallhalidkonzentration und vom Katalysatorverhältnis. Molekulargewicht und Temperatureinflüsse werden im Licht des allgemeinen, kinetischen Schemas diskutiert. Weiters wird die Annahme dualer, aktiver Stellen diskutiert, an welchen Monomermoleküle adsorbiert und in spezifischer Weise orientiert werden können und welche die stereospezifische Polymerisation der α -Olefine ebenso wie die Aktivität der Ziegler-Katalysatoren erklären können.

Received September 29, 1961

Tracer Techniques for the Determination of Monomer Reactivity Ratios. IV. Copolymerization Characteristics of Some Divinyl Monomers

RICHARD H. WILEY and GERALD L. MAYBERRY, *Department of Chemistry, College of Arts and Sciences, University of Louisville, Louisville, Kentucky*

It has been shown^{1,2} that the copolymerization characteristics of divinyl monomers can be determined by using radioisotope assay techniques for analysis and that they vary significantly with minor structural changes in the divinyl monomer. The observation that *m*-(but not *p*-) divinylbenzene-styrene copolymerization systems can be analyzed in terms of the usual two-component copolymerization kinetics scheme, the divinyl monomer being used as the equivalent of two moles of a monovinyl monomer, indicates that it should be possible to correlate the copolymerization behavior of other nonconjugated divinyl monomers with their structure and thus identify systems having different, more precisely defined, and more rationally controlled crosslinked structures. To this end we have prepared some additional divinyl monomers and obtained the data necessary to assign monomer reactivity ratios to these materials.

EXPERIMENTAL

Melting points are uncorrected. Carbon-hydrogen analyses were performed by Micro-Tech Laboratories. The biphenyl, diphenylmethane, 1,2-diphenylethane, 1,3-diphenyl-2-propanone, phenylacetic acid, phenyl ether, and phenyl sulfide were used as supplied by Distillation Products division of Eastman Kodak Company. 1,3-Diphenylpropane (b.p. 133°C./2 mm.; n_D^{27} 1.5563; reported^{3,4} 165°C./25 mm.; n_D^{15} 1.5634) was prepared in 93.7% yield by the Wolff-Kishner reduction of 1,3-diphenyl-2-propanone. 1,4-Diphenyl-1,3-butadiene (m.p. 149–153°C.; reported⁶ 149.5–153°C.) was prepared in 31% yield from phenylacetic acid and cinnamaldehyde and reduced with Raney nickel catalyst to 1,4-diphenylbutane (m.p. 49–52°C. from ethanol; reported⁶ 51.5–53°C.; 52°C.).

Diacetyl Compounds

These compounds were prepared as previously described by Friedel-Crafts acetylation of the diphenyl compounds. Most of the acylations were run in carbon bisulfide with excess (6 moles to 2.5 moles of acetyl

chloride to one mole of hydrocarbon) aluminum chloride as catalyst. To avoid cleavage of the starting hydrocarbon, a mixture of hydrocarbon and acetyl chloride in carbon bisulfide was added to the catalyst suspended in carbon bisulfide. The diphenylbutane was acylated by means of the Perrier technique.⁷ 4,4'-Diacetylbiphenyl (m.p. 190–192°C.; reported⁸ 191°C.) was obtained in 37% yield. Bis(4-acetylphenyl)methane (m.p. 92–93°C.; reported⁹ 92.5–93°C.) was obtained in 44% yield. 1,2-Bis-(4-acetylphenyl)ethane (m.p. 164–167°C.; reported⁹ 164–166°C.) was obtained in 72% yield. 1,3-Bis(4-acetylphenyl)propane (m.p. 83–86°C.; reported³ 83–85°C.) was obtained in 76% yield. 1,4-Bis(4-acetylphenyl)butane (m.p. 105–107°C.; reported¹⁰ 109.5–110.2°C.) was obtained in 74.7% yield. Bis(4-acetylphenyl) ether (m.p. 99–101°C.; reported¹¹ 99–101°C.) was obtained in 57% yield, Bis(4-acetylphenyl) sulfide (m.p. 88–90°C.; reported¹² 90–91°C.) was obtained in 53% yield.

The bis(*p*-nitrophenylhydrazone) of bis(4-acetylphenyl) ether was prepared, m.p. 215.5–217°C., from glacial acetic acid.

ANAL. Calc. for C₂₃H₂₄O₆N₆: N, 16.02%. Found: N, 15.91%:

Reduction of the Diacetyl Compounds to Dicarbinols

The diketones were reduced to dicarbinols by the Meerwein-Ponndorf-Verley technique in anhydrous isopropyl alcohol with aluminum isopropoxide (Distillation Products Industries). Except for the diphenylmethane derivative, these compounds have not been completely characterized in the literature.

4,4'-Di(1-hydroxyethyl)biphenyl^{13,14} (m.p. 156–157°C.) was obtained in 70.7% yield. Recrystallization from toluene gave the analytically pure sample, m.p. 159–161°C.

ANAL. Calc. for C₁₆H₁₈O₂: C, 79.31%; H, 7.49%. Found: C, 79.56%; H, 7.70%.

Bis[4-(1-hydroxyethyl)phenyl]methane (m.p. 87–88°C.; reported¹⁵ 85–86°C.) was obtained in 89% yield.

1,2-Bis[4-(1-hydroxyethyl)phenyl]ethane was obtained in 82.4% yield. Recrystallization from toluene gave the analytical sample, m.p. 137–139.5°C.

ANAL. Calc. for C₁₈H₂₂O₂: C, 79.96%; H, 8.20%. Found: C, 79.98%; H, 8.17%.

1,3-Bis[4-(1-hydroxyethyl)phenyl]propane was obtained as an oil which could not be induced to crystallize and could not be distilled without decomposition. It was used without further purification.

1,4-Bis[4-(1-hydroxyethyl)phenyl]butane, m.p. 102.5–105°C., was obtained in 91.6% yield. Recrystallization from toluene gave the analytical sample, m.p. 110–112°C.

ANAL. Calc. for C₂₀H₂₆O₂: C, 80.49%; H, 8.78%. Found: C, 80.57%; H, 8.79%

Bis[4-(1-hydroxyethyl)phenyl] sulfide, m.p. 105–108°C., was obtained in 81% yield. Recrystallization from benzene–cyclohexane gave the analytical sample, m.p. 107–109°C.

ANAL. Calc. for $C_{16}H_{18}O_2S$: C, 70.03%; H, 6.61%. Found: C, 70.13%; H, 6.53%.

Bis[4-(1-hydroxyethyl)phenyl] ether,¹⁶ m.p. 92.5–94.5°C. from benzene–cyclohexane, was obtained in 89% yield.

ANAL. Calc. for $C_{16}H_{18}O_3$: C, 74.39%; H, 7.02%. Found: C, 74.39%; H, 7.00%.

Dehydration of the Carbinols to Divinyl Compounds

The dicarbinols were dehydrated in peroxide-free dioxane over $1/8$ in. alumina (Harshaw) pellets at 300–320°C. and 1–3 mm. pressure in a modification of the previously described technique.^{15,17} The divinyl compounds were collected in an ice-cooled trap, precipitated from the dioxane solution by addition of water and recrystallized three times from methanol, ethanol, or ethanol–water.

4,4'-Divinylbiphenyl (m.p. 152.5°C., reported¹³ 152°C.) was obtained in 46.9% yield on dehydration of 10 g. of carbinol in 60 ml. of dioxane. The melting point is difficult to detect because the compound polymerizes to a solid immediately on melting. The compound also polymerizes on standing under vacuum and did not give acceptable carbon analysis. Addition of bromine gives a product melting at 201°C.

Bis(4-vinylphenyl)methane (m.p. 32°C., reported¹⁵ 32°C.) was obtained in 37.8% yield. The tetrabromo derivative melts at 144–145°C., (reported,¹⁵ 146°C.).

1,2-Bis(4-vinylphenyl)ethane was obtained in 30.4% yield. Recrystallization from ethanol gave the analytical sample, m.p. 95.5–97.5°C.

ANAL. Calc. for $C_{18}H_{18}$: C, 92.26%; H, 7.74%. Found: C, 92.15%; H, 7.71%.

The tetrabromo derivative melts at 193.5–195°C. (from nitromethane).

ANAL. Calc. for $C_{18}H_{18}Br_4$: C, 39.02%; H, 3.27%. Found: C, 39.21%; H, 3.49%.

1,3-Bis(4-vinylphenyl)propane was obtained in 17.1% yield and recrystallized from ethanol–water, m.p. 50.0–51.5°C.

ANAL. Calc. for $C_{19}H_{20}$: C, 91.88%; H, 8.12%. Found: C, 91.76%; H, 8.18%.

1,4-Bis(4-vinylphenyl)butane was obtained in 27.3% yield and recrystallized from ethanol–water, m.p. 60.5–61.8°C.

ANAL. Calc. for $C_{20}H_{22}$: C, 91.55%; H, 8.45%. Found: C, 91.53%; H, 8.51%.

The tetrabromo derivative melts at 146–147.8°C. (from nitromethane).

ANAL. Calc. for $C_{20}H_{22}Br_4$: C, 41.27%; H, 3.81%. Found: C, 41.59%; H, 3.85%.

Bis(4-vinylphenyl) sulfide was obtained in 17.5% yield and recrystallized from methanol-water, m.p. 63.5–65°C.

ANAL. Calc. for $C_{16}H_{14}S$: C, 80.62%; H, 5.92%. Found: C, 80.37%; H, 6.01%.

The tetrabromo derivative melts at 159–160°C. (from cyclohexane).

ANAL. Calc. for $C_{16}H_{14}Br_4S$: C, 34.43%; H, 2.52%. Found: C, 34.26%; H, 2.65%.

Bis(4-vinylphenyl) ether was obtained in 19.7% yield and recrystallized from ethanol-water, m.p. 89–90°C.

ANAL. Calc. for $C_{16}H_{14}O$: C, 86.45%; H, 6.35%. Found: C, 86.26%; H, 6.44%.

The tetrabromo derivative melts at 115.5–116.5°C. (from cyclohexane).

ANAL. Calc. for $C_{16}H_{14}Br_4O$: C, 35.46%; H, 2.60%. Found: C, 35.49%; H, 2.85%.

Copolymerization

Copolymerizations for each pair of monomers were run in three pairs at monomer ratios of approximately 80/20, 50/50, and 20/80 by the techniques previously described.² The solid monomers were weighed into reaction cells which were attached to a vacuum line. The required amount of styrene- β - C^{14} was distilled into the cell. After appropriate weighings to determine the monomer concentrations, 2 ml. of benzene was added to dissolve the divinyl monomer, $0.2 \pm 0.02\%$ of benzoyl peroxide was added, and the cells were sealed under vacuum and polymerized at $61 \pm 0.5^\circ\text{C}$. to 5–10% conversion. The 10% conversion time is usually just prior to the time at which gelation occurs. The copolymerizations were run for 1.25–7.50 hr. and stopped at the point when gelation took place. These times were 1.25–2.25 hr. for the biphenyl, 1.5–6.0 hr. for the methane, 2.5–4.0 hr. for the ethane, 7.5 hr. for the propane, 3–5 hr. for the butane, 6.5–7.0 hr. for the ether, and 1.75–3.0 hr. for the sulfide compounds. The copolymers were isolated as described before,³ but, being crosslinked, could not be redissolved and reprecipitated from solution. They were freed of monomer by swelling with benzene and washing with methanol or methanol-acetone (swelling and washing repeated five times) to dissolve traces of unreacted monomer.

Radioactivity Assay

Radioactivity assay was carried out as described previously² with the ionization chamber-vibrating reed electrometer technique. Data like those given in Table I of the preceding paper² were collected.

Monomer Reactivity Ratios

Monomer reactivity ratios were obtained from the analytical data for the copolymers by graphical analysis. Intersect and Fineman-Ross plots were made and the curves for the latter located by the method of least squares. Data are given in Figures 1–6 and summarized in Table I. The data for 4,4'-divinylbiphenyl gave no intersect.

TABLE I
Monomer Reactivity Ratios in Copolymerization
of Divinyl Monomers (r_2) with Styrene (r_1)

| Divinyl monomer | Intersect solution ^a | | Fineman-Ross plot solution ^b | | $r_1 r_2$ product ^c |
|-------------------------------|---------------------------------|-------|---|-------|--------------------------------|
| | r_1 | r_2 | r_1 | r_2 | |
| Bis(4-vinylphenyl)methane | 1.01 | 0.93 | 1.00 | 0.91 | 0.91 |
| 1,2-Bis(4-vinylphenyl)ethane | 1.05 | 0.87 | 1.06 | 0.87 | 0.92 |
| 1,3-Bis(4-vinylphenyl)propane | 1.11 | 0.89 | 1.13 | 0.90 | 1.02 |
| 1,4-Bis(4-vinylphenyl)butane | 1.13 | 0.78 | 1.12 | 0.78 | 0.87 |
| Bis(4-vinylphenyl) ether | 0.94 | 1.06 | 0.91 | 1.02 | 0.93 |
| Bis(4-vinylphenyl) sulfide | 0.60 | 1.50 | 0.61 | 1.51 | 0.92 |
| Ethyleneglycol dimethacrylate | 0.40 | 0.65 | 0.40 | 0.64 | 0.26 |
| <i>m</i> -Divinylbenzene | 0.65 | 0.60 | 0.65 | 0.60 | 0.39 |

^a Estimated from plot.

^b From slope and intersect of line given by method of least squares.

^c From Fineman-Ross solution.

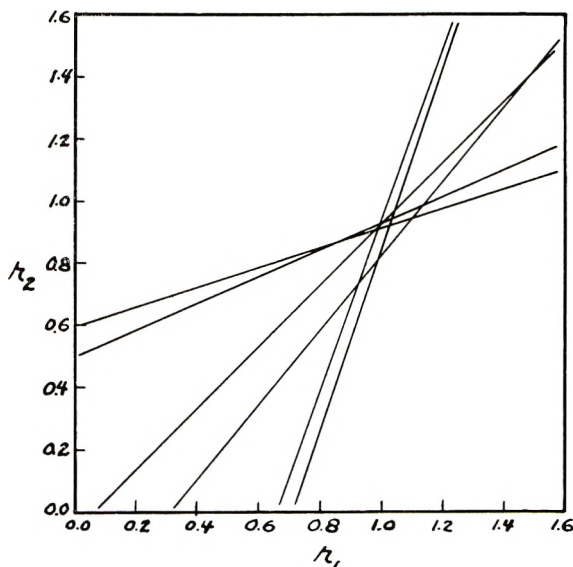


Fig. 1. Graphical solution of the copolymerization equation for the styrene ($r_1 = 1.01$) bis(4-vinylphenyl)methane ($r_2 = 0.93$) copolymerization.

DISCUSSION

The kinetic data for the copolymerization of the series of divinyl monomers available in this study have confirmed our previous observations with other divinyl monomers. The usual treatment of copolymerization kinetics can be used with twice the molecular concentration of divinyl monomer for M_2 and the mole per cent of divinyl monomer in the copolymer for m_2 . With this modification of the equation, intersects are obtained on intersect plots and straight lines are obtained in Fineman-Ross plots for those di-

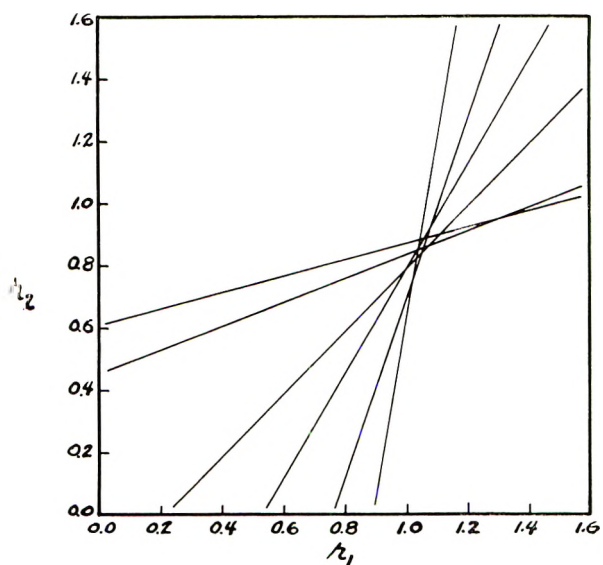


Fig. 2. Graphical solution of the copolymerization equation for the styrene ($r_1 = 1.05$), 1,2-bis(4-vinylphenyl)ethane ($r_2 = 0.87$) copolymerization.

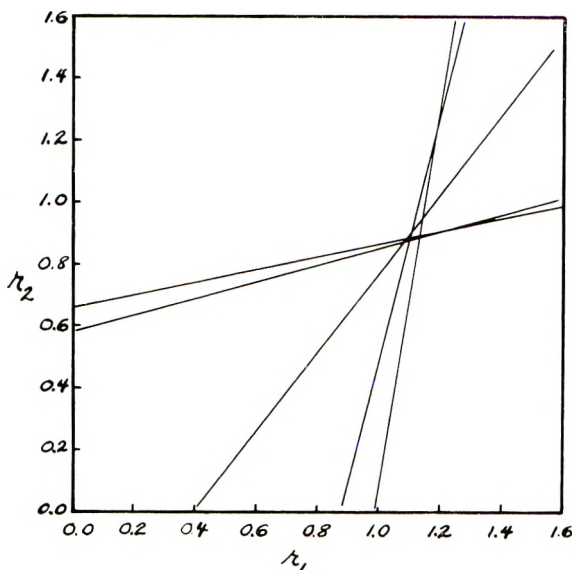


Fig. 3. Graphical solution of the copolymerization equation for the styrene ($r_1 = 1.11$), 1,3-bis(*p*-vinylphenyl)propane ($r_2 = 0.89$) copolymerization.

vinyl monomers in which the two vinyl groups are not conjugated. This group now is known to include, in addition to *m*-divinylbenzene and ethyleneglycol dimethacrylate previously reported,¹ four di(*p*-vinylphenyl)-alkanes, bis(*p*-vinylphenyl) ether, and bis(*p*-vinylphenyl) sulfide. Con-

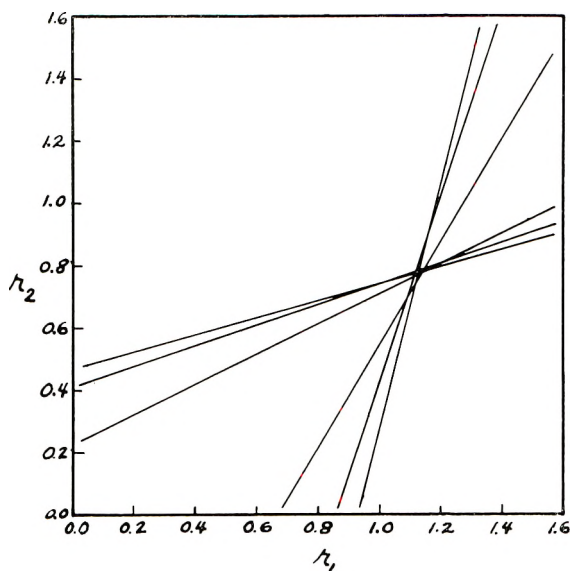


Fig. 4. Graphical solution of the copolymerization equation for the styrene ($r_1 = 1.13$) 1,4-bis(*p*-vinylphenyl)butane ($r_2 = 0.78$) copolymerization.

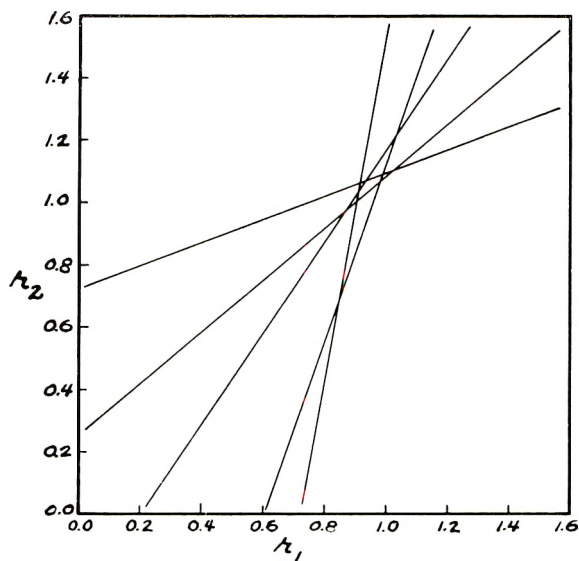


Fig. 5. Graphical solution of the copolymerization equation for the styrene ($r_1 = 0.94$) bis(*p*-vinylphenyl) ether ($r_2 = 1.06$) copolymerization.

jugated divinyl compounds, such as *p*-divinylbenzene and 4,4'-divinylbiphenyl, do not give intersect or Fineman-Ross solutions for the copolymerization equation.

A comparison of the r_2 values thus obtained for nonconjugated divinyl monomers with the r_2 values for the corresponding monovinyl moiety indi-

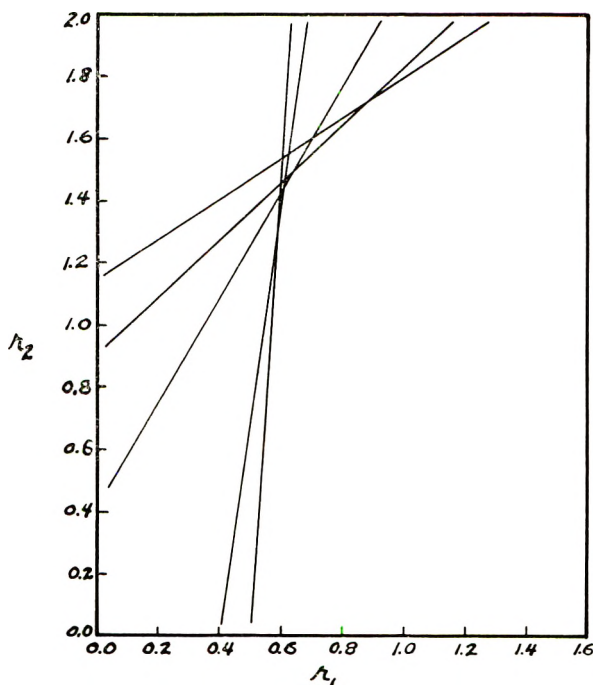


Fig. 6. Graphical solution of the copolymerization equation for the styrene ($r_1 = 1.12$) bis(*p*-vinylphenyl) sulfide ($r_2 = 1.50$) copolymerization.

cates that rather considerable differences can be encountered. With the styrene-ethyleneglycol dimethacrylate system ($r_1 = 0.40$, $r_2 = 0.65$), there was but little deviation from the styrene-methyl methacrylate values ($r_1 = 0.50$; $r_2 = 0.50$). The styrene-bis(*p*-vinylphenyl)alkanes give values of $r_1 = 1.00$ – 1.13 and $r_2 = 0.78$ – 0.91 as compared to values of $r_1 = 0.83$, $r_2 = 0.93$ for the styrene-*p*-methylstyrene pair.² Although the difference is not great it is in the opposite direction in the two different structural types. This may result from an alteration in the chain transfer characteristics of the methyl (CH_3-), diarylmethyl (Ar_2CH_2), and aryl alkyl methyl (ArCH_2R) groups present in the vinylphenyl series of a different kind than is observed in the methacrylic esters. Data for comparisons of the divinyl ether and sulfide with mono vinyl types are not available. The rates of copolymerization but not the monomer reactivity ratios for *p*-vinylidiphenyl oxide and sulfide have been observed.¹⁸ The r_1r_2 products, which are a measure of the degree and kind of alternating tendencies, for the alkanes, ether, and sulfide are in the 0.87–1.02 range. This indicates a fairly random copolymerization for these divinyl monomers and a rather distinct departure from the higher degree of alternating tendency noted for the glycol dimethacrylate ($r_1r_2 = 0.26$) and *m*-divinylbenzene ($r_1r_2 = 0.39$) systems. This has rather profound implications in terms of the structure of the product. Copolymerizations with small quantities of those divinyl monomers for which the alternating tendency is high (r_1r_2 small) will take

place with early exhaustion of the divinyl monomer from the monomer feed. The result will be copolymers with crosslinks, which come from the divinyl monomer, bunched in a nucleus and with long, pendant, linear chains radiating out therefrom. The copolymerizations run with divinyl monomers for which random incorporation is possible ($r_1r_2 = 1$) will have more uniformly distributed crosslinks. Differences in r_1 and r_2 values which result in r_1r_2 products of ca. 1.0 will result in different distributions of crosslinks. It is obvious, however, that factors involved in the copolymerization kinetics of the divinyl monomer will be of great importance in the copolymerization process itself, determining the gross physical nature of a bead for example, and in the utilization of the copolymers wherever molecular structural factors are important.

The data for the series of 4-vinylphenyl alkanes $(\text{CH}_2=\text{CHC}_6\text{H}_4)_2(\text{CH}_2)_n$, where $n = 1, 2, 3$, or 4 show a trend toward higher r_1 and lower r_2 values as the alkane chain is lengthened. The range is not great ($r_1 = 1.00-1.13$ and $r_2 = 0.91-0.78$) and the propane ($n = 3$) derivative appears to be out of order. It is perhaps worth noting that the propane derivatives, and also the ether derivative, also showed different times for onset of gelation. With these two divinyl monomers gelation had not taken place after 7 hr., whereas the other systems gelled usually within 2-3 hr. and never over 5 hr. The copolymerization with the sulfide gelled most rapidly. Since gelation usually occurs at 6-7% conversion of monomers to copolymer, this difference in gelation time can be taken as a measure of the overall rate of copolymerization in these systems. This indicates that the propane and ether derivatives copolymerize more slowly than do other pairs and establishes the desirability of obtaining copolymerization rate data for these systems.

The data now available from these studies establish that it is possible to design and identify copolymerization systems which will give rather gross differences in the structural nature of the crosslinked network. To do so, it is necessary to define divinyl monomers whose characteristics cover the range of possibilities. Much study is needed to be able to state the exact nature of the crosslinking pattern in such copolymers but there can no longer be any question that materials of widely different properties can be made. The significance of such structural changes in terms of the physical and chemical characteristics of exchange beads and membranes establishes the desirability of additional study of this problem.

The authors wish to acknowledge partial support of this research under Contract AT-(40-1)-229 between the University of Louisville and the Atomic Energy Commission.

References

1. Wiley, R. H., and E. E. Sale, *J. Polymer Sci.*, **42**, 491 (1960).
2. Wiley, R. H., and B. Davis, *J. Polymer Sci.*, **46**, 423 (1960).
3. Cram, D. J., and H. Steinberg, *J. Am. Chem. Soc.*, **73**, 5691 (1951).
4. Sirks, J. F., *Rec. trav. chim.*, **62**, 193 (1943).
5. Carson, B. B., *Organic Syntheses*, Coll. Vol. II, Wiley, New York, 1943, p. 229.

6. Kuhn, R., and A. Wintersteiner, *Helv. Chim. Acta*, **11**, 123 (1928).
7. Perrier, G., *Ber.*, **33**, 815 (1900).
8. Silver, S. L., and A. Lowy, *J. Am. Chem. Soc.*, **56**, 2429 (1934).
9. Lutz, R. E., et al., *J. Org. Chem.*, **12**, 617 (1947).
10. Cram, D. J., and N. L. Allinger, *J. Am. Chem. Soc.*, **76**, 726 (1954).
11. Diltthey, W., E. Bach, H. Grutering, and E. Hansdorfer, *J. prakt. Chem.*, **117**, 337 (1927).
12. Diltthey, W., L. Nenhaus, E. Reis, and W. Schommer, *J. prakt. Chem.*, **124**, 110 (1930).
13. Rosenthal, F., U. S. Pat. 2,465,486 (1949).
14. Valyi, I., A. G. Janssen, and H. Mark, *J. Phys. Chem.*, **49**, 461 (1945).
15. Marvel, C. S., and D. W. Hein, *J. Am. Chem. Soc.*, **70**, 1895 (1948).
16. Copp, F. C., Brit. Pat. 651,445 (1953).
17. Mowry, D. T., M. Renoll, and F. Huber, *J. Am. Chem. Soc.*, **68**, 1105 (1946).
18. El'tsova, P. A., M. M. Kotov, O. K. Mineeva, and O. K. Surnina, *Vysokomoleculyarnye Soedineniya*, **1**, 1369 (1959).

Synopsis

A series of divinyl monomers of the formula $(\text{CH}_2=\text{CHC}_6\text{H}_4-)_2\text{X}$ where X is CH_2 , CH_2CH_2 , $\text{CH}_2\text{CH}_2\text{CH}_2$, $\text{CH}_2\text{CH}_2\text{CH}_2\text{CH}_2\text{O}$, and S have been prepared from the carbinols by dehydration and copolymerized with styrene. The kinetic data are consistent with a copolymerization in which the two vinyl groups react independently. The divinyl monomer behaves as two equivalents of a vinyl monomer to give solutions for the copolymerization equation in which r_1 (for styrene) varies from 0.61 to 1.13 and r_2 (for the divinyl compound) varies from 0.78 to 1.51.

Résumé

Une série de monomères divynyliques du type $(\text{CH}_2=\text{CHC}_6\text{H}_4-)_2\text{X}$ où X est CH_2 , CH_2CH_2 , $\text{CH}_2\text{CH}_2\text{CH}_2$, $\text{CH}_2\text{CH}_2\text{CH}_2\text{CH}_2\text{O}$, et S ont été préparés à partir des carbinols par déshydratation et copolymérisés avec du styrène. Les données cinétiques sont en accord avec une copolymérisation dans laquelle les deux groupes vinyliques réagissent indépendamment. Le monomère divynylique se comporte comme deux équivalents de monomère vinylique et donne dans l'équation de copolymérisation des valeurs de r_1 (pour le styrène) variant de 0.61 à 1.13, et des valeurs de r_2 (pour le composé divynylique) variant de 0.78 à 1.51.

Zusammenfassung

Es wurde eine Reihe von Divinylmonomeren der Formel $(\text{CH}_2=\text{CHC}_6\text{H}_4-)_2\text{X}$ wo X für CH_2 , CH_2CH_2 , $\text{CH}_2\text{CH}_2\text{CH}_2$, $\text{CH}_2\text{CH}_2\text{CH}_2\text{CH}_2\text{O}$, und S steht, aus den Carbinolen durch Dehydratisierung hergestellt und mit Styrol copolymerisiert. Die kinetischen Daten entsprechen einer Copolymerisation, bei der die beiden Vinylgruppen unabhängig reagieren. Das Divinylmonomere verhält sich wie zwei Äquivalente eines Vinylmonomeren und gibt für die Copolymerisationsgleichung Lösungen, worin r_1 (für Styrol) von 0,61 bis 1,13 und r_2 (für die Divinylverbindung) von 0,78 bis 1,51 variiert.

Received September 25, 1961

Revised October 23, 1961

Molecular Configuration of Branched Macromolecules

N. T. NOTLEY* *Cornell University, Ithaca, New York*

Free-radical polymerization frequently gives branched polymers for which the molecular configuration has been discussed theoretically.¹ Full control of the chemical nature, chain length, and distribution of branches in one polymer would be very useful for experimental comparison.

The essentially linear character of polystyrene prepared by peroxide initiation has been demonstrated,² so a homobranched polystyrene is required. An interesting possibility of control was to attack a polystyrene chain with peroxide to initiate a definite number of side chains, but the peroxide attack was found to cause degradation.³ Another possibility was to copolymerize styrene with a polyfunctional monomer in which the branching tendency was less vigorous than the primary polymerization, but the difficulties with *p*-isopropenylstyrene have been described elsewhere.⁴

We discuss here the easier experimental problem of obtaining hetero branches of controlled proportion and uniform length, firstly on polystyrene and secondly on cellulose acetate.

EXPERIMENTAL

I. Stearyl and Lauryl Side Chains on Polystyrene

Preparation of Monomers. *p*-Amino- β -phenylethyl alcohol was prepared following the reaction scheme of Ferber⁵ and with subsequent dehydration to *p*-aminostyrene by the method of Sabetay.⁶

| | | |
|------------------------------|---|--|
| β -phenylethyl acetate | HNO ₃ (fuming) → -12°C. | <i>p</i> -nitro- β -phenylethyl acetate (unpurified, yield 86%) |
| HCl/methanol | <i>p</i> -nitro- β -phenylethyl alcohol | (yield 44%, m.p. 60-61°C.) |
| Zn/CaCl ₂ | <i>p</i> -nitro- β -phenylethyl alcohol | (yield 97%, m.p. 107-108°C.) |
| KOH | <i>p</i> -aminostyrene | (yield 73%, b.p. 92-93°C./3 mm., n _D ²⁵ = 1.6218) |

A lauryl monomer was prepared by shaking a solution of 5 g. *p*-aminostyrene and 15 g. lauryl chloride in 200 ml. chloroform. After extracting the amide with ether, washing with water, drying over anhydrous magnesium sulfate and filtration, white crystals were separated and recrystallized from cyclohexane/*n*-hexane to constant melting point (m.p. 108-109°C., yield 90%).

* Present address: Metal Box Co. Ltd., Research Dept., London, England.

The stearyl monomer was similarly obtained from 12 g. stearyl chloride and 3 g. *p*-aminostyrene and recrystallized from cyclohexane (yield 84%, m.p. 111–112°C.).

Commercial styrene was washed twice with 10% caustic soda, dried over calcium chloride, and distilled at atmospheric pressure.

Preparation of Polymers. Styrene was copolymerized with its laurylamide by heating at 9:1 molar ratio for two days at 100°C. in the absence of light or catalyst. The polymer was fractionated by preferential evaporation from butanone/butanol solution. The middle fraction was similarly refractionated and again refractionated before selection of a polymer for solution measurements. Since a heteroatom had been introduced, the extent of chain branching could be determined by nitrogen analysis, which here indicated one lauryl branch for each eight styrene units.

TABLE I

| | Side chains | | |
|---|--|---|--|
| | Stearylamido ($1/15$ styrene units) | Stearylamido ($1/8$ styrene units) | Laurylamido ($1/7$ styrene units) |
| Molecular weight (light scattering) | 1,690,000 | 2,070,000 | 1,800,000 |
| Backbone M.W. (calculated) | 1,420,000 | 1,550,000 | 1,410,000 |
| $[\eta]$ for backbone, dl./g. ^{a,b} (Ref. 7,8) | 2.87 | 2.97 | 2.85 |
| $[\eta]$ (direct experi- ment), dl./g. | 1.91 | 1.90 | 1.68 |
| $[\eta]$ for backbone (derived from experi- ment), dl./g. | 2.28 | 2.53 | 2.15 |
| Radius of gyration for backbone, A. ⁷ | 480 | 507 | 477 |
| Radius of gyration (experimental), A. | 780 | 836 | 670 |

^a Data of Debye and Notley.⁷

^b Data of Notley and Debye.⁸

Polystyrene with stearyl branches was made in a similar way. Copolymerizing in 9:1 molar ratio gave one branch for each 8 styrene units and in 19:1 molar ratio one stearyl branch for each fifteen styrene units.

Solution Measurements. The intrinsic viscosity of the fraction was obtained from measurements of relative viscosity at four concentrations of the polymer in toluene at 25°C. The concentration used in the calculation of Table I is the concentration of backbone polystyrene, which leads to a modified intrinsic viscosity particularly suited to an estimation of the effect of steric factors.

Molecular weight was determined by light-scattering measurements in toluene solution by a procedure which has been described earlier.⁷ Meas-

urements were made over the angular range of 30° to 135° with respect to the incident beam with light of wavelength 4358 Å. From this molecular weight and the known chemistry of the molecule, the weight of the polystyrene backbone was calculated. The intrinsic viscosity for polystyrene of the same molecular weight without pendant groups⁸ is compared with the presently determined value.

Radii of gyration were determined by light-scattering measurements in toluene solution and compared with those which were found for unmodified polystyrene of the same degree of polymerization.⁷

II. Acetate and Hydrogen Succinate Side Chains on Cellulose

All cellulose esters were prepared from a commercial secondary cellulose acetate of intrinsic viscosity 1.55 dl./g. in 92% acetic acid. Degrees of esterification are expressed as the number per cellulose unit, so total esterification would be represented as 3.0. The parent polymer had an acetate substitution of 2.39.

Hydrogen succinate esters were made by base-catalyzed reaction in glacial acetic acid,⁹ precipitated in a sixfold volume of distilled water, and dried in a gentle stream of warm air (45°C). No fractionation was attempted.

Intrinsic viscosities of the mixed esters were obtained from measurements of relative viscosity at three concentrations of polymer in 92% acetic acid at 25°C . (Table II).

TABLE II

| Acetate substitution | $[\eta]$ for cellulose acetate | Steric parameter $([\eta]m)^{1/3}$ | Hydrogen succinate substitution | $[\eta]$ for Cellulose acetate-hydrogen succinate | Steric parameter $([\eta]m)^{1/3}$ |
|----------------------|--------------------------------|------------------------------------|---------------------------------|---|------------------------------------|
| 2.4 | 1.55 | 7.42 | 0.3 | 1.42 | 7.46 |
| | | | 0.5 | 1.45 | 7.69 |
| 1.9 | 1.67 | 7.39 | 0.8 | 1.50 | 7.85 |
| 1.8 | 1.59 | 7.24 | 0.4 | 1.48 | 7.44 |
| | | | 1.1 | 1.56 | 8.16 |
| 1.6 | 1.56 | 7.10 | 0.8 | 1.56 | 7.85 |

Further hydrogen succinate esters were made with lower acetyl degrees of substitution. Saponification to lower acetyl content was made under relatively nondegradative conditions. A 3% solution of the cellulose acetate in 67% aqueous acetic acid catalyzed by 6% sodium acetate was held at 100°C . for a time appropriate to the decrease in acetyl degree of substitution required. Precipitation in ice water was followed by washing for 16 hr. and vacuum drying at 110°C .

DISCUSSION

In Table I measurements on the substituted polystyrenes are compared with corresponding data for linear polystyrenes of the same degree of polymerization, that is, the same chain length as the backbone of the substituted polymers. In both series of measurements, fractionations were made with great care, and it was assumed that the molecular distributions were narrow and perhaps similar. The relatively large radii of gyration found for the substituted polymers might indicate large steric effects associated with the presence of side groups. However, a comparison of intrinsic viscosity values is inconsistent. Now the radius of gyration is a *Z*-average property, the molecular weight is a weight-average property, and the intrinsic viscosity is a somewhat lower average. Thus, the present anomaly could be attributed to difficulties in the molecular weight fractionation of the branched polymer.

Comparison of intrinsic viscosity of a polymer with unknown configuration with the intrinsic viscosity of the corresponding linear polymer of the same weight-average molecular weight is recognized¹⁰ as a very convenient measure of chain branching. The present work suggests that attempts to apply this principle to unfractionated polymers¹¹ are misleading and that very narrow molecular weight fractions are essential.

The necessity for highly efficient fractionation is avoided if a branched polymer is made from the corresponding linear polymer by reactions which are free of degradative and crosslinking possibilities. The succinylation reaction described above has been demonstrated to satisfy these conditions. A mixed (almost) triester analyzed as 2.4 acetate, 0.5 hydrogen succinate was held in typical succinylation conditions for some three times the normal reaction cycle (24 hr.). The triester was recovered, and its analysis and intrinsic viscosity were unchanged at 1.45 dl./g.

According to Manson and Arquette¹² a steric factor can be taken from the Flory viscosity equation.¹³

$$[\eta] = \Phi (\bar{r}^2)^{3/2}/M = \Phi (\bar{r}^2)^{3/2}/Nm$$

A change in the product of intrinsic viscosity and unit molecular weight m can indicate a change in the chain length or a much smaller change in the chain extension r . In view of the direct evidence against degradation during succinylation $([\eta]m)^{1/3}$ is expected to be proportional to the chain extension and to be a useful steric parameter.

In Table II horizontal comparisons, that is comparisons made at constant acetate substitution, are believed to represent constant degree of polymerization. At all levels of acetate substitution, the addition of hydrogen succinate groups increases the steric parameter and so stiffens the cellulosic chain.

Comparisons within the vertical columns of Table II are less rigorous. The decline in values of the steric parameter for cellulose acetates with declining acetate substitution might be explained by some degradation during

the saponification reaction by which they were prepared or it might suggest that acetyl groups stiffen slightly the cellulose chain. Probably both effects contribute to the results.

In Figure 1 all the results are brought together in plotting values of the steric parameter against the degree of hydrogen succinate substitution.

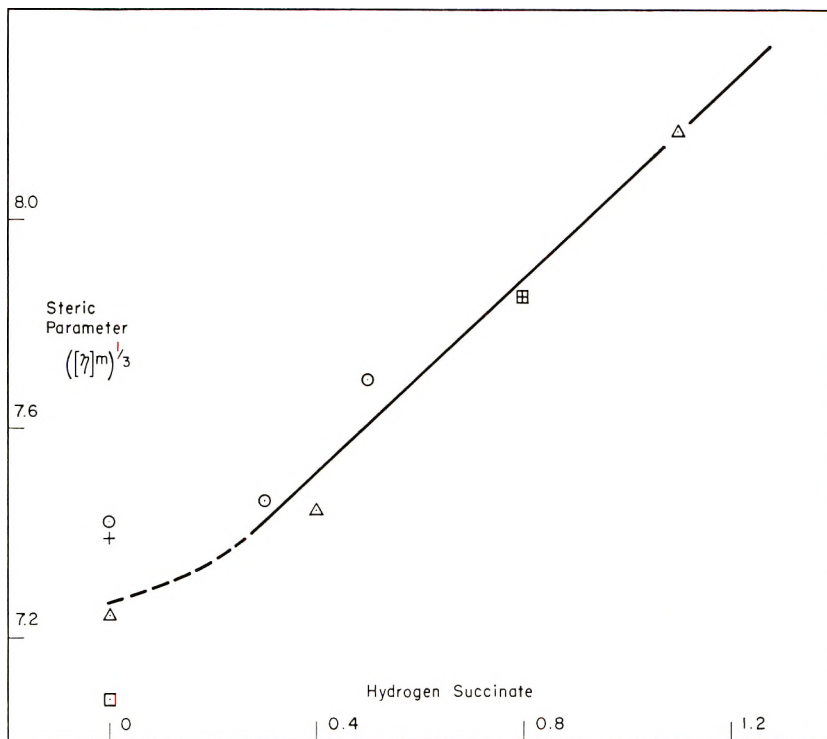


Fig. 1. Short side chains on cellulose acetate for various degrees of acetate substitution: (○) 2.4; (+) 1.9; (△) 1.8; (□) 1.6.

This demonstrates that in the stiffening of the cellulose chain the hydrogen succinate substituent has the dominant effect and the acetate substituent a minor role except when present alone.

The author is indebted to Professor P. J. W. Debye in whose Laboratory the work was begun and to Mrs. P. Dreyfuss for experimental assistance.

References

1. Stockmeyer, W. H., and M. Fixman, *Ann. N. Y. Acad. Sci.*, **57**, 334 (1953).
2. Outer, P., C. I. Carr, and B. H. Zimm, *J. Chem. Phys.*, **18**, 830 (1950).
3. Smets, G., L. Convent, and X. Van der Borgh, *Makromol. Chem.*, **23**, 162 (1957).
4. Dreyfuss, P., and N. T. Notley, *J. Polymer Sci.*, **28**, 611 (1958).
5. Ferber, E., *Ber.*, **628**, 183 (1929).
6. Sabetay, S., T. Mintsou, *Bull. Soc. Chim.*, **45**, 842 (1929).
7. Debye, P. J. W., and N. T. Notley, *J. Polymer Sci.*, **17**, 99 (1955).
8. Notley, N. T., and P. J. W. Debye, *J. Polymer Sci.*, **24**, 275 (1957).

9. Hiatt, G. D., and J. Emerson, U. S. Pat. 2,794,799 (1954).
10. Zimm, B. H., and W. H. Stockmeyer, *J. Chem. Phys.*, **17**, 1301 (1949).
11. Atkins, J. T., and F. W. Billmeyer, *J. Phys. Chem.*, **63**, 1966 (1959).
12. Manson, J. A., and G. J. Arquette, *Makromol. Chem.*, **37**, 187 (1960).
13. Flory, P. J., *Principles of Polymer Chemistry*, Cornell Univ. Press, Ithaca, N. Y., 1953, p. 611.

Synopsis

Macromolecules with very long backbone and a multiplicity of side chains have been prepared. Polystyrene with stearyl-amido and polystyrene with lauryl-amido side chains were obtained by the copolymerization of *p*-vinylstearanilide and of *p*-vinyl-lauranilide with styrene. Polymers were made suitable for configurational studies by repetitive precipitation fractionation. Light-scattering and viscosity studies on dilute solutions indicated however that the effect of side chains on molecular volume was secondary in importance to the effect of variations in fractionation efficiency. Hydrogen succinate side groups on secondary cellulose acetate were obtained by a reaction on the polymer which was demonstrated to be nondegradative. A series of polymers was obtained with the same backbone molecular weight and varying substitution. A steric parameter was derived from viscosity measurements in acetic acid and its dependence on increasing extent of succinylation showed a progressive stiffening of the cellulose chain.

Résumé

On a préparé des macromolécules ayant une très longue chaîne principale et une multiplicité de chaînes latérales. Dans la première partie on a obtenu du polystyrène avec du stéarylamide et du polystyrène avec du laurylamide comme chaîne latérale, par copolymérisation du *p*-vinyl stéaranilide et du *p*-vinyl lauranilide avec du styrène. On a adapté ces polymères pour des études configurationnelles par des précipitations fractionnées répétées. Des études de diffusion de lumière et des viscosités en solution diluée indiquent toutefois que l'effet des chaînes latérales sur le volume moléculaire a une importance secondaire par rapport à l'effet des variations de l'efficacité du fractionnement. Dans la seconde partie on a incorporé des groupes latéraux succinate acide sur le diacétate de cellulose, par une réaction sur le polymère, réaction qui n'entraîne pas de dégradation. On a obtenu une série de polymères ayant une chaîne principale de même poids moléculaire et de substitution variée. On a dégagé un paramètre stérique à partir des mesures de viscosité dans l'acide acétique et sa dépendance sur le degré croissant de succinylation a montré un raidissement progressif de la chaîne de cellulose.

Zusammenfassung

Makromoleküle mit sehr langer Kette und einer Vielfalt von Seitenketten wurden dargestellt. Im 1. Teil wurde Polystyrol mit Stearylamid- und Polystyrol mit Laurylamidseitenketten durch Copolymerisation von *p*-Vinylstearanilid und *p*-Vinyl-lauranilid mit Styrol erhalten. Die Polymeren wurden durch wiederholte Fällungsfractionierung in einen für Konfigurationsuntersuchungen geeigneten Zustand gebracht. Lichtstreuungs- und Viskositätsmessungen an verdünnten Lösungen zeigten jedoch, dass der Einfluss der Seitenketten auf das Molvolumen an Bedeutung hinter dem Einfluss der Fractionierungswirksamkeit zurücktrat. Im 2. Teil wurden Hydrogensuccinatseitengruppen an sekundärem Celluloseacetat durch eine Reaktion mit dem Polymeren erhalten, die ohne Abbau verlief. Es wurde so eine Reihe von Polymeren mit gleicher Kettenlänge und verschiedenem Substitutionsgrad erhalten. Aus Viskositätsmessungen in Essigsäure wurde ein sterischer Parameter erhalten; seine Abhängigkeit vom zunehmenden Succinylierungsgrad liess eine fortschreitende Versteifung der Cellulosekette erkennen.

Received October 23, 1961

Effect of Polar and Nonpolar Solvents on the Viscosity and the Molecular Weight of Polymer Solutions

V. KALPAGAM and M. RAMAKRISHNA RAO, *Department of Inorganic and Physical Chemistry, Indian Institute of Science, Bangalore, India*

INTRODUCTION

The molecular weight of any polymer molecule, whether large or small, is generally independent of the solvents employed or the temperatures at which the measurements are carried out. But recently, there has been considerable experimental evidence to the effect that the variation of molecular weight of a polymer species depends on the nature of the solvents employed and the method of preparation of the samples. It has been observed that the molecular weights of some polymers are higher in a nonpolar solvent than a polar solvent.

Trementozzi¹ observed that aggregation of the molecules takes place in the case of a nonpolar polymer like polystyrene (prepared by the emulsion polymerization technique) in a relatively nonpolar solvent such as toluene but the polymer dissociates upon the addition of polar solvents like dioxane and dimethylacetamide. Doty² et al. observed for a polystyrene fraction a pronounced aggregation in a nonpolar solvent like toluene.

Cleverdon and Smith³ reviewed the discrepancies in the evaluation of $[\eta]$ and M and showed that the Huggin's constant k' for polystyrene in the same solvent may vary substantially according to the source of the polymer.⁴ Bacon⁵ and Morgan⁶ have shown that emulsion polymerizations involving persulfate and an activator are able even to introduce ionic endgroups into the polymer. Sully⁷ has shown that polystyrene prepared in emulsion by means of monothionic acid radicals have sulfonic acid endgroups. Walker and Winkler⁸ found substantial differences in k' between polystyrenes and copolymers of styrene and divinylbenzene.

In the case of the polar polymer polyvinyl chloride, Doty⁹ et al. noticed aggregation taking place in the solvent dioxane which dissociated upon raising the temperature. This phenomenon was explained to be as due to the presence of secondary bond-forming groups of different types in the polymer. Such aggregation phenomena have been reported by Morawetz and Gobran¹⁰ in some copolymers like poly(methyl methacrylate-methacrylic acid) and poly(methyl methacrylate-dimethylaminoethyl methacrylate). Nord¹¹ et al. observed that in the case of the copolymer poly(vinyl alcohol-vinylacetate) aggregation takes place with increase in tem-

perature while a decrease in temperature induces the copolymer to dissociate.

In light of the varying results reported above, the present investigation was taken up to study the effect of polar and nonpolar solvents on poly(vinyl acetate) fractions prepared by the bulk polymerization method. Besides this, the $[\eta]-M_w$ relation has been established for poly(vinyl acetate) in a few solvents.

EXPERIMENTAL

Preparation of the Polymer Fractions

After first subjecting the commercial monomer, vinyl acetate, to vacuum distillation to remove the inhibitor, polymerization was carried out by the bulk method at a constant temperature of $40 \pm 0.25^\circ\text{C}$. at various concentrations of the catalyst benzoyl peroxide to obtain different molecular weight ranges. The conversion was kept well below 20% to obtain linear polymer molecules.¹²

The polymer thus obtained was dissolved in freshly distilled acetone to obtain a 2% solution. Fractionation was carried out by the fractional precipitation method with petroleum ether as the precipitant. The fractions thus obtained were subjected to one or two more fractionations to get better homogeneous fractions.

All the solvents employed were purified by the standard methods. Always the polymer solutions were prepared in freshly distilled solvents. First a stock solution of about 1% concentration was prepared, and then different concentrations were obtained by taking various volumes of this solution and diluting them.

Clarification of the Solutions

The complete removal of dust particles from solvents and solutions for light-scattering experiments is a difficult problem. After a lot of experimentation, the method of filtering successively through two sintered glass filters, the first one to remove the coarse particles and the second one the fine particles, directly into the cell was employed.

Viscosity Measurements

The viscosity measurements for some of the well fractionated samples described above were carried out at $30 \pm 0.05^\circ\text{C}$. in the solvents, ethyl formate, methyl isobutyl ketone, acetonitrile, and dioxane in an Ostwald-Fenske viscometer. The kinetic energy and the rate of shear corrections were not applied as they were found to be negligible.

Light-Scattering Measurements

In the present investigation the Brice-Phoenix Universal light-scattering photometer type 1000-D¹³ has been used. The light source was a high

pressure mercury vapor lamp type AH-3, 85 w. Throughout the course of this investigation the mercury blue line (436 $m\mu$) was employed.

For each polymer fraction the experimental data were taken at five or six different concentrations (0.05–0.3%) and for each concentration at the different angles 0°, 45°, 90°, and 135°. The molecular weight M_w and the interaction constant A_2 for a polymer molecule in solution were determined from Debye's equation.¹⁴ The specific refractive index increment (dn/dc) for the various systems studied was determined by a differential refractometer.¹⁵ The dn/dc values thus obtained for the systems poly-(vinyl acetate) (PVA)–acetonitrile(AN), PVA–ethyl formate (EF), PVA–methyl isobutyl ketone(MIBK) and PVA–dioxane were 0.104, 0.095, 0.068, and 0.028, respectively.

RESULTS AND DISCUSSION

The molecular weights of the PVA fractions in different solvents were obtained from the intercepts of the plots of the reciprocal turbidity versus concentration shown in Figures 1–4 and are given in Table I after applying the correction for the intraparticle interference effect.

TABLE I
Light-Scattering Viscosity Data of Poly(vinyl Acetate) Fractions

| Solvent | Fraction | $M_w \times 10^{-6}$ | $A_2 \times 10^4$ | $R, \text{ \AA}$ | $[\eta]$ |
|------------------------|-----------------|----------------------|-------------------|------------------|----------|
| Ethyl formate | F ₃ | 1.54 | 3.82 | 1000 | 3.38 |
| | F ₅ | 1.06 | 3.68 | 920 | 2.62 |
| | B | 0.517 | 5.48 | 737 | 1.60 |
| Acetonitrile | F | 0.155 | 6.56 | 369 | 0.715 |
| | F ₃ | 1.53 | 3.15 | 941 | 2.85 |
| | F _{4a} | 1.49 | 3.01 | 925 | 2.82 |
| | F _{4c} | 1.34 | 3.91 | 892 | 2.60 |
| Dioxane | F ₅ | 0.97 | 3.00 | 827 | 2.00 |
| | F ₃ | 3.81 | 1.68 | 737 | 2.80 |
| | F _{4a} | 2.77 | 1.33 | 722 | 2.56 |
| Methyl isobutyl ketone | F _{4c} | 2.15 | 1.70 | 706 | — |
| | A | 0.689 | 2.65 | 684 | 1.42 |
| | C | 0.403 | 2.30 | 591 | 1.10 |
| | D | 0.395 | 2.85 | 575 | 1.07 |
| | E | 0.336 | 1.73 | 544 | 0.93 |
| | F | 0.117 | 2.52 | 327 | 0.47 |

It is observed from the table that there is very close agreement in the molecular weights of the fractions F₃, F_{4c}, and F₅ in the solvents ethyl formate and acetonitrile but in the case of dioxane the values are twice as high. This discrepancy, which is far above the experimental error, can be attributed either to the low specific refractive index increment or to another phenomenon, viz., secondary bonding as observed in the case of polystyrene and poly(vinyl chloride). However, consistent results were obtained for the specific refractive index values and the molecular weights

on repeating the experiments. Hence the discrepancy can be attributed to secondary bonding.

Higher molecular weights in dioxane solutions indicate that crosslinkages might be taking place between the chains thereby forming clusters. This

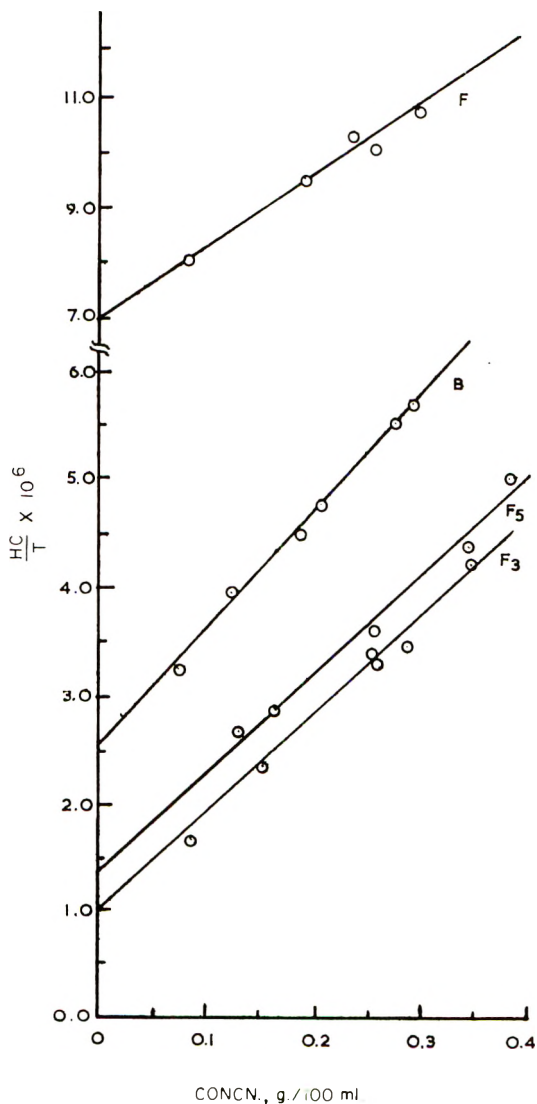


Fig. 1. Relation between reciprocal turbidity and concentration of the PVA-ethyl formate system.

shows that secondary bond formation is facilitated by the relatively nonpolar solvent (dioxane), which also is a poor solvent for this polymer. The same solvent has played an entirely different role of breaking up the clusters in polystyrene-toluene solutions by combining with the specific

groups involved. As all the fractions in this investigation are prepared by the bulk polymerization method, in which there is no possibility of introducing hydrogen bond-forming groups, one can expect dioxane to have a different role in this case. In the case of the other solvents, as they are all polar and good solvents for the polar polymer, PVA solubility has been facilitated and no secondary bonds are formed.

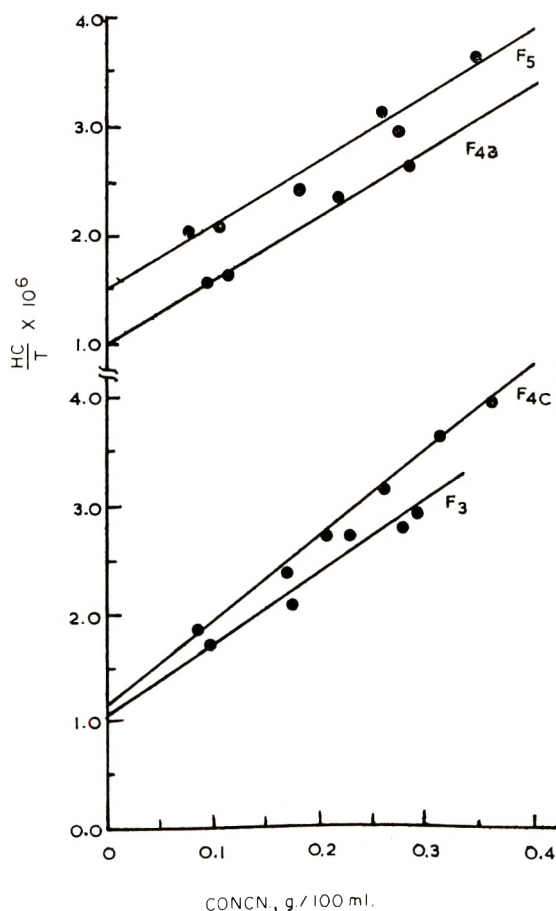


Fig. 2. Relation between reciprocal turbidity and concentration of the PVA-acetonitrile system.

From the intrinsic viscosity values it is seen that the $[\eta]$ values in dioxane are less than those obtained in the other solvents. From the large value of the molecular weights obtained in dioxane, one would naturally expect a deviation in the viscosity values in this solvent. In the viscosity measurements, the size is the largest average parameter which determines the specific viscosity. Hence from this it is evident that the molecules are highly coiled and packed in the cluster so that the viscosity is not affected.

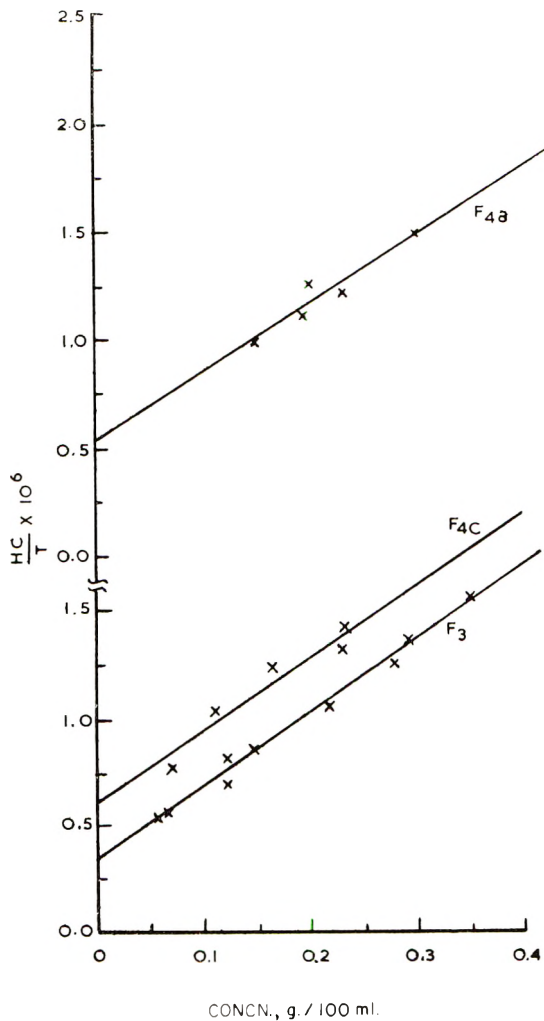


Fig. 3. Relation between reciprocal turbidity and concentration of the PVA-dioxane system.

$[\eta]-M_w$ Relations

The molecular weights obtained for the different fractions of poly-(vinyl acetate) in the solvents ethyl formate, acetonitrile, and methyl isobutyl ketone have been related to the intrinsic viscosity by plotting the relation between $\log [\eta]$ and $\log M_w$ (Fig. 5). The following equations have been obtained for the three systems.

Ethyl formate:

$$[\eta]_{30} = 3.2 \times 10^{-4} M_w^{0.65}$$

Acetonitrile:

$$[\eta]_{30} = 4.15 \times 10^{-4} M_w^{0.62}$$

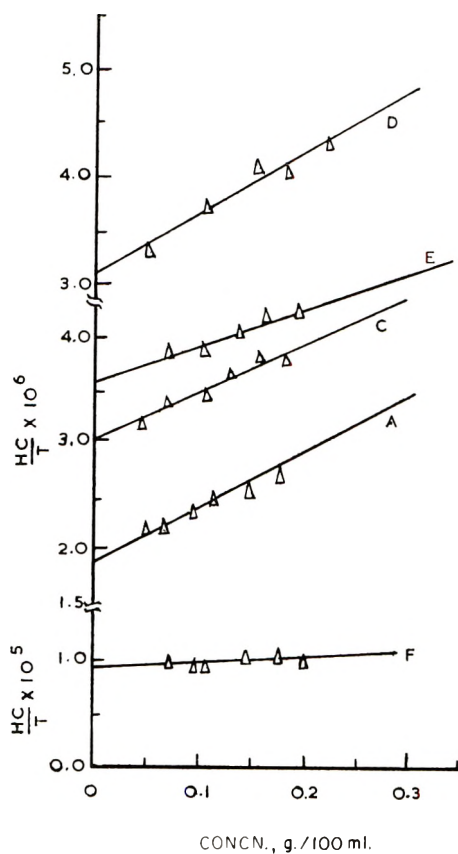


Fig. 4. Relation between reciprocal turbidity and concentration of the PVA-methyl isobutyl ketone system.

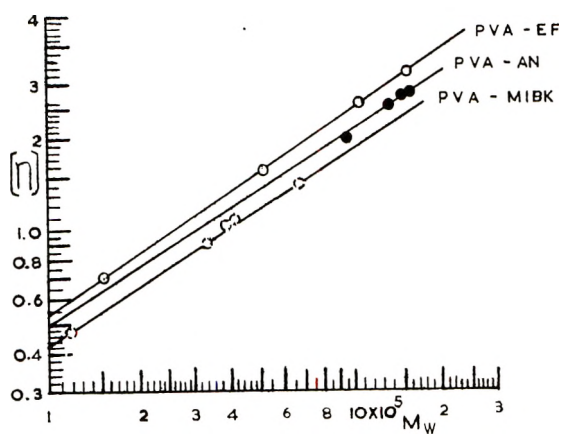


Fig. 5. Relation between $\log [\eta]$ and $\log M_w$ of PVA fractions in ethyl formate (EF), acetonitrile (AN), and methyl isobutyl ketone (MIBK).

Methyl isobutyl ketone:

$$[\eta]_{30} = 4.49 \times 10^{-4} M_w^{0.60}$$

From the values of index of solvent power α it is seen that ethyl formate is a better solvent for PVA than acetonitrile and methyl isobutyl ketone.

Second Virial Coefficient A_2

The values of the second virial coefficient A_2 obtained from the intercept of the plots of HC/τ against C are given in column 4 of Table I. Since A_2 also determines the solvent power, on this basis the solvent power of the solvents employed in this investigation is in the decreasing order of ethyl formate, acetonitrile, methyl isobutyl ketone, and dioxane.

The values of A_2 increase with decreasing molecular weight. This is so in the case of ethyl formate, where the A_2 values increase from 3.82×10^{-4} to 6.56×10^{-4} as the molecular weight decreases from 1.54×10^6 to 0.155×10^6 . In the case of the other solvents, however, where the molecular weight range employed is very narrow, the A_2 values are more or less constant within experimental error.

The Root-Mean-Square End-to-End Distance R

The root-mean-square end-to-end distance R of the polymer chain for the different fractions studied in the various solvents are given in column 5 of Table I. From the table it is seen that the values of R decrease with decreasing molecular weight and are greater in ethyl formate which is a better solvent.

The authors wish to express their grateful thanks to Dr. S. Bhagavantam, Director, Indian Institute of Science and Prof. M. R. A. Rao, Head of the Department of Inorganic and Physical Chemistry for their keen interest and guidance during the course of this investigation.

References

1. Trementozzi, Q. A., *J. Phys. & Colloid Chem.*, **54**, 1227 (1950).
2. Trementozzi, Q. A., R. F. Steiner, and P. Doty, *J. Am. Chem. Soc.*, **74**, 2070 (1952).
3. Cleverdon, D., and P. G. Smith, *J. Polymer Sci.*, **14**, 375 (1954).
4. Cleverdon, D., D. Laker, and P. G. Smith, *J. Appl. Chem.*, **3**, 15 (1953).
5. Bacon, R. G. R., *Trans. Faraday Soc.*, **42**, 141 (1946).
6. Morgan, L. B., *Trans. Faraday Soc.*, **42**, 169 (1946).
7. Sully, B. D., *J. Chem. Soc.*, **1498** (1950).
8. Walker, O. J., and C. A. Winkler, *Can. J. Research*, **28B**, 298 (1950).
9. Doty, P., H. Wagner, and S. Singer, *J. Phys. & Colloid Chem.*, **51**, 32 (1947).
10. Morawetz, H., and R. H. Gobran, *J. Polymer Sci.*, **12**, 133 (1954).
11. Nord, F. F., M. Bier, and S. N. Timasheff, *J. Am. Chem. Soc.*, **73**, 289 (1951).
12. Wheeler, O. L., S. L. Ernest, and R. N. Orozier, *J. Polymer Sci.*, **8**, 409 (1952).
13. Brice, B. R., M. Halwer, and R. Speiser, *J. Opt. Soc. Am.*, **40**, 768 (1950).
14. Debye, P., *J. Appl. Phys.*, **15**, 338 (1944).
15. Brice, B. A., and M. Halwer, *J. Opt. Soc. Am.*, **41**, 1033 (1951).

Synopsis

Light-scattering studies of well fractionated samples of poly(vinyl acetate) were carried out in four solvents, viz., acetonitrile, ethyl formate, methyl isobutyl ketone, and dioxane, in order to investigate the effect of the polar and nonpolar nature of the solvents on the molecular weight and the viscosity of the samples studied. The molecular weights thus obtained are found to be in good agreement in all the solvents except dioxane, in which the values are twice as high. This twofold increase in dioxane has been explained in terms of secondary bonding. The relation between $[\eta]$ and M_w are established for the systems poly(vinyl acetate)-ethyl formate, poly(vinyl acetate)-acetonitrile, and poly(vinyl acetate)-methyl isobutyl ketone. The root-mean-square radii and the second virial coefficients are also determined.

Résumé

Des études de diffusion lumineuse ont été effectuées sur des échantillons bien fractionnés d'acétate de polyvinyle et cela dans quatre solvants, à savoir l'acétonitrile, le formiate d'éthyle, la méthyl-isobutyle cétone et le dioxanne, dans le but d'étudier l'effet de la nature polaire et non-polaire des solvants sur le poids moléculaire et la viscosité des échantillons étudiés. Les poids moléculaires obtenus sont en parfait accord dans tous les solvants excepté dans le cas du dioxanne pour lequel les valeurs sont deux fois plus élevées. Cette double augmentation dans le dioxanne a été expliquée par une liaison secondaire. La relation entre (η) et M_w a été établie pour les systèmes acétate de polyvinyle-formiate d'éthyle; acétate de polyvinyle-acétonitrile et acétate de polyvinyle-méthylisobutyle cétone. On a également déterminé la racine carrée moyenne des rayons et les seconds coefficients viriels.

Zusammenfassung

Eine Lichtstreuungsuntersuchung an gut fraktionierten Polyvinylacetatproben wurde in vier Lösungsmitteln, nämlich Acetonitril, Äthylformiat, Methylisobutylketon und Dioxan, zur Bestimmung des Einflusses der polaren und nichtpolaren Natur der Lösungsmittel auf Molekulargewicht und Viskosität der untersuchten Proben durchgeführt. Die erhaltenen Molekulargewichte waren in allen Lösungsmitteln, mit Ausnahme von Dioxan, in guter Übereinstimmung; in diesem hatten sie den doppelten Wert. Die Zunahme auf das Doppelte in Dioxan wurde durch die Annahme von sekundären Bindungen erklärt. Die Beziehung zwischen $[\eta]$ und M_w wurde für die Systeme Polyvinylacetat-Äthylformiat, Polyvinylacetat-Acetonitril und Polyvinylacetat-Methylisobutylketon ermittelt. Die Wurzel aus dem mittleren Radienquadrat und der zweite Virialkoeffizient wird ebenfalls bestimmt.

Received September 13, 1961

A Thermodynamic Method for the Comparison of the Order Distribution in Cellulose and in Other Polymers*

L. B. TICKNOR, *Research and Development Division, American Viscose Corporation, Marcus Hook, Pennsylvania*

Introduction

The mathematical analysis of the concept of order distribution (sometimes called lateral order distribution) in cellulose was proposed by Coppick¹ in 1945 and first published in the second edition of *Cellulose and Cellulose Derivatives*² in 1954. The concept, as then developed, interpreted the order of a region as the ratio of the number of hydrogen bonds in a certain region to the maximum number if all the molecules were perfectly crystallized. This definition has been criticized on the basis that the hydrogen bonds in cellulose have different strengths and that essentially all of the hydroxyls in cellulose are hydrogen bonded. It may be further criticized in that it would be difficult to apply this definition to polymers not having hydrogen bonds.

The methods of measuring the order distribution in cellulose have been reviewed by Marchessault and Howsmon.³ Basically, these methods involve treating samples of a given cellulose material under conditions that are progressively more severe (greater swelling, for instance). The fraction of the cellulose material that is accessible under each of these conditions is determined and plotted against some parameter related to the severity of the treatment conditions. This parameter is assumed to be a measure of the most highly ordered material that became accessible. The curve so obtained is the summative mass order curve. The order distribution curve is obtained by plotting the slope of the summative curve against the order function.

Previous methods have included (a) sodium hydroxide swelling followed by measurement of the moisture regain of the resulting cellulose,³ (b) hydrolysis of the cellulose followed by determination of the solubility in caustic solutions of various concentrations,⁴ (c) esterification with 90% formic acid at various temperatures.³ These methods are probably the best devised up to the present time, but they all are related to a questionable interpretation of order, and the order function used may not be directly proportional to the order in the polymer.

* Presented at the 140th Meeting of the American Chemical Society, Division of Cellulose, Wood and Fiber Chemistry, Chicago, Illinois, September 3-8, 1961.

New Method of Defining Order

It was recognized some time ago³ that a better definition of order would be in terms of thermodynamic quantities. However, the definition must be amenable to experimental measurement, and, in reality, order is defined by the experimental method. Although the energy, the heat content, or the entropy of the region under consideration might yield useful measures of its order, we will use its free energy. Specifically, order will be defined as the difference between the free energy of a certain small quantity of polymer (of uniform order) in the state in which it exists and the free energy of the same quantity of polymer in a completely amorphous disoriented state, per unit quantity of polymer. For highly ordered material this difference will be large, while for low order material it will be small.

Order, defined in terms of this free energy difference, may be measured by swelling experiments. When a polymer is immersed in a swelling agent, it may be essentially unswollen (e.g., cellulose in hexane), it may be swollen only in the low-order regions (e.g., cellulose in water) or it may be swollen throughout its entire structure (e.g., cellulose in strong caustic). The free energy change for swelling a small element of polymer may be expressed as the sum of the free energy required to melt (bring to the amorphous state) this small element at constant temperature and pressure plus the free energy of mixing this amorphous and crosslinked polymer with swelling agent. The first term is positive, and the second is negative. For elements of low order this sum, the free energy of swelling, will be negative. For elements of high order this sum would be positive, and these highly ordered elements would remain unchanged. Thus, there is a certain degree of order such that all elements of lower order will be swollen, all elements of higher order will be unswollen, but for elements of this particular order the free energy of swelling will be zero.

Now, if the free energy of the swelling agent can be progressively changed, the quantity of polymer swollen can be varied. To do this, the chosen agent should be capable in its pure state of swelling (or dissolving) the entire polymer structure. Its free energy may be reduced by lowering the pressure of the agent when being used in the gaseous state, or by mixing with a nonswelling agent when used in the liquid state. Then the quantity of polymer swollen may be plotted versus the order of the highest order material swollen (the limiting order) to give the summative mass order curve.

The value of the free energy of fusion for the elements of limiting order may be determined as follows. Suppose that a polymer sample is immersed in the vapor of a swelling agent at a pressure less than its normal vapor pressure. The total free energy change upon swelling of any element in the polymer may be estimated as the sum of three free energy changes: (a) the fusion of the element of polymer, ΔG_f , (b) the condensation of the swelling agent to pure liquid, ΔG_{pl} , and (c) the mixing of amorphous (cross-linked) polymer and pure liquid swelling agent, $\Delta G_m + \Delta G_e$. This third

change is made up of two terms. The first, ΔG_m , is the free energy of mixing amorphous polymer and solvent, such as would be given by the Flory-Huggins⁵ expression. The second, ΔG_e , is the free energy of extension of the crosslinked network (the elastic free energy), such as would be given by the Flory-Rehner⁵ or Hermans⁶ theories.

Likewise, in a mixed solvent system the chemical potential of the swelling agent can be changed by varying the concentration. ΔG_{pl} would then be the difference in free energy of the swelling agents in their pure liquid states and in the binary liquid mixture.

The free energy change upon swelling may therefore be expressed as

$$\Delta G_s = \Delta G_f + \Delta G_{pl} + \Delta G_m + \Delta G_e \quad (1)$$

This equation would apply to any element in the polymer. But it is the limiting order, $\Delta G_f'$, the free energy of fusion for those elements of polymer for which ΔG_s is zero, that is needed. Therefore, since the last three terms in eq. (1) may in principle be calculated, the limiting order may be determined. Finally, this free energy change must be related to a unit quantity of polymer which may be taken as a mole of monomer (anhydroglucose) units.

In addition, the quantity of polymer that is swollen must be measurable. It may be possible to do this by esterification, oxidation, deuterium exchange, etc., but a significant change in the polymer should be avoided.

Use of Single-Component Gaseous Swelling Agent

The specific equations for the case wherein the chemical potential (or swelling power) of the swelling agent is varied by changing its vapor pressure will now be developed. It is assumed that n_u moles of monomer units of a certain order are swollen by n_1 moles of swelling agent. The vapor will be taken to be an ideal gas. Therefore,

$$\Delta G_{pl} = n_1 RT \ln P_1/P_0 \quad (2)$$

where n_1 is the number of molecules of swelling agent, P_1 is the vapor pressure used in the experiment, and P_0 is the equilibrium vapor pressure of the swelling agent at the same temperature.

The free energy of mixing may be given by the Flory-Huggins⁶ theory:

$$\Delta G_m = RT(n_1 \ln Z_1 + n_u A Z_u) \quad (3)$$

where Z_1 is the volume fraction of swelling agent, Z_u is the volume fraction of polymer, and A is the interaction parameter. The number of polymer molecules is taken as zero, since it is a crosslinked network.

Finally, since the polymer network is crosslinked (by the crystallites), there will be a free energy term in the swelling due to the extension of the network. This free energy may be given by the Hermans⁶ or Flory-Rehner⁵ theories. We will use the Hermans equation because it is simpler. For isotropic swelling of an amorphous disoriented network Hermans⁶ gives

$$\Delta G_e = (n_u V_u RT/2XV_1)[(3/Z_u^{2/3}) - 3 + 2 \ln Z_u] \quad (4)$$

where V_1 and V_u are the molar volumes of the swelling agent and monomer units in the polymer, respectively, n_u is the number of moles of monomer units in the swollen polymer, and X is the ratio of the average volume of a chain between crosslinks to the volume of a molecule of the liquid swelling agent.

Now, upon combining the various free energy expressions, the free energy of swelling a certain region of polymer is given by

$$\Delta G_s = \Delta G_f + n_1 RT(\ln Z_1 + AZ_u) + \frac{n_u V_u RT}{2XV_1} \left(\frac{3}{Z_u^{2/3}} - 3 + 2 \ln Z_u \right) + n_1 RT(\ln P_{10}/P_1) \quad (5)$$

The free energy of fusion must now be expressed per mole of monomer units. This may be conveniently accomplished by differentiation of ΔG_s with respect to n_u . Differentiation of eq. (5) and setting $\Delta G_s = 0$ gives

$$\frac{\Delta G_f'}{n_u} = \frac{RTV_u}{V_1} \left[Z_1 - AZ_1^2 - \left(\frac{Z_u + 1/2}{X} \right) \left(\frac{1}{Z_u^{2/3}} - 1 \right) - \frac{1}{X} \ln Z_u \right] \quad (6)$$

The right-hand side of this equation is therefore the "order" function.

For the evaluation of eq. (6) it is necessary to know X and Z_1 . The value of X may be known from auxiliary experiments or it may perhaps be estimated. The former is difficult for cellulose and an estimated value may be adequate. The value of Z_1 is determined by differentiation of eq. (5) with respect to n_1 . Such differentiation yields an expression for the difference in the chemical potential of the swelling agent in the gaseous and the swollen polymer phase. At equilibrium swelling, however, this difference is zero; therefore

$$\ln Z_1 + (1 - Z_1) + A(1 - Z_1)^2 + (1/X)(Z_u^{1/3} - Z_u) = \ln P_{10}/P_1 \quad (7)$$

Since $Z_u = 1 - Z_1$ and the values of X , A , P_{10} , and P_1 are known, the value of Z_1 may be calculated. It is assumed that the composition of the swollen phase is uniform throughout.

The equations for a two-component liquid swelling agent may be similarly developed. However, such equations will involve an interaction parameter for the nonswelling component with the polymer, and such parameters would be difficult to determine.

Utility of the Method

The utility of this method will depend on the applicability of the underlying theories. The Flory-Huggins theory is well established, but the determination of the interaction parameters for cellulose is difficult because of its poor solubility. For this same reason it will be difficult to find an adequate swelling agent for cellulose for use in this method; however, ethyl amine and nitrogen dioxide may be suggested.

This application of the theories for the elastic free energy of swelling is questionable for several reasons.

(1) The elastic theories treat only an entropic effect, but when there is a very strong interaction between polymer and swelling agent (as is the case with cellulose), an enthalpic contribution to the elastic free energy may exist.

(2) The elastic theories usually assume a Gaussian distribution of chain lengths between crosslinks and a random configuration for each chain. For cellulose, these assumptions would probably be at least somewhat invalid due to chain stiffness and the short distance between crystallites (the crosslinks).

(3) The functionality is usually taken to be small but for cellulose crystallites the functionality is high. Some preliminary calculations indicate, however, that the elastic contribution to the free energy of swelling may be small compared to the other terms and therefore the above objections may be unimportant. It is also suggested that the value of X in these equations may be taken as 100 for cellulose, since calculations show little difference in the final results between values of 10 and 100.

In view of these considerations it appears that the method will not give an absolute measure of the order distribution in polymers, but it should be adequate for obtaining realistic qualitative comparisons of the order distribution in various samples of the same polymer. It is doubtful that different polymers should be compared except in a rather general way.

This method is published in its present form and without experimental work in hopes that such early publication will encourage its further development and use.

References

1. Coppick, S., private communication.
2. Howsmon, J. A., and W. A. Sisson, in *Cellulose and Cellulose Derivatives*, Part I, E. Ott, H. M. Spurlin and M. W. Grafflin, Eds., Interscience, New York, 1954, Chap. 4B.
3. Marchessault, R. H., and J. A. Howsmon, *Textile Research J.*, **27**, 30 (1957).
4. Maeda, H., *J. Soc. Textile Cellulose Ind., Japan*, **12**, 6 (1956).
5. Flory, P. J., *Principles of Polymer Chemistry*, Cornell Univ. Press, Ithaca, N. Y., 1953, Chap. 13.
6. Hermans, J. J., *Trans. Faraday Soc.*, **43**, 591 (1947).

Synopsis

Previous definitions of order (i.e., lateral order) in cellulose materials have been essentially in terms of the experimental method and order has been interpreted as the extent of hydrogen bonding. These definitions are inadequate. Order is defined herein as the difference in free energy of the element of polymer in its present state and in a completely amorphous state. The free energy of swelling is equated to the conceptual process of fusion of the element of polymer plus mixing the amorphous and crosslinked (by crystallites) polymer with swelling agent as would be given by the Flory-Huggins theory of mixing and the Flory-Rehner or Hermans theories for the swelling of networks. For those elements of polymer for which the free energy of swelling is zero the free energy of fusion (i.e., "order") may be determined. This limiting order of the polymer elements that are swollen may be reduced by lowering the pressure of the swelling agent if it is in the gaseous state or if the swelling agent is a liquid by mixing it with a nonswelling

liquid. Such a variation in the swelling agent gives a variation in the quantity of polymer swollen. The summative mass order (quantity accessible vs. limiting order) and order distribution (slope of summative curve vs. limiting order) plots are made as usual. This method should give realistic qualitative comparisons of the order distribution among various samples of the same polymer, and it should be applicable to other crystalline polymers as well as to cellulose.

Résumé

Des définitions précédentes d'ordre (c.à.d. l'ordre latéral) dans des substances cellulose ont été essentiellement interprétées en fonction de la méthode expérimentale et l'ordre a été considéré comme étant la mesure de la liaison hydrogène. Ces définitions ne sont pas exactes. L'ordre est défini ici comme la différence entre l'énergie libre de l'élément de polymère dans son état présent et celle du même élément dans son état entièrement amorphe. L'énergie libre de gonflement est égal au processus de fusion de l'élément de polymère plus le processus de mélange du polymère amorphe et ponté (par des cristallites) avec un agent de gonflement comme le prévoit la théorie de Flory-Huggins pour les mélanges et les théories de Flory-Rehner ou Hermans pour le gonflement des réseaux. L'énergie libre de fusion (c.à.d. l'ordre) peut être déterminée pour les éléments de polymère pour lesquels l'énergie libre de gonflement est nulle. Cet ordre limite des éléments de polymère qui sont gonflés peut être diminué en abaissant la pression de l'agent de gonflement s'il est à l'état gazeux ou si l'agent de gonflement est un liquide après mélange avec un liquide non gonflant. Une telle variation dans l'agent de gonflement provoque une variation dans la quantité de polymère gonflé. Les graphiques de l'ordre total en bloc (la quantité accessible en fonction de l'ordre limite) et de la distribution d'ordre (la pente de la courbe totale en fonction de l'ordre limite) ont été établis à la façon habituelle. Cette méthode donnerait des comparaisons qualitatives valables de la distribution de l'ordre en fonction de différents échantillons du même polymère et il pourrait être appliqué à d'autres polymères cristallins qu'à la cellulose.

Zusammenfassung

Die früher gegebenen Definitionen für die Ordnung (d.h. seitliche Ordnung) in Cellulosematerialien waren im wesentlichen durch die Versuchsmethode bestimmt und die Ordnung wurde als das Ausmass der Wasserstoffbindung interpretiert. Diese Definitionen sind unzulänglich. Ordnung wird hier als der Unterschied der freien Energie des Polymerbausteins in seinem tatsächlichen Zustand und einem vollständig amorphen Zustand definiert. Die freie Quellungsenergie entspricht einem hypothetischen Schmelzvorgang der Polymerbausteine plus der Mischung des amorphen und vernetzten (durch Kristallite) Polymeren mit Quellungsmedium, wie sie durch die Mischungstheorie von Flory und Huggins und Netzwerkquellungstheorie von Flory und Rehner oder Hermans gegeben wird. Für Polymerbausteine, für welche die freie Quellungsenergie Null ist, kann die freie Schmelzenergie (d.h. "Ordnung") bestimmt werden. Dieser Grenzwert der Ordnung der gequollenen Polymerbausteine kann durch Herabsetzen des Druckes eines gasförmigen Quellungsmediums oder durch Mischung eines flüssigen Quellungsmediums mit einer nicht quellenden Flüssigkeit reduziert werden. Eine solche Änderung des Quellungsmediums liefert eine Variierung der Menge des gequollenen Polymeren. Die summativen Massen-Ordnungs- (angegriffene Menge gegen Ordnungsgrenzwert)- und Ordnungs-Verteilungs- (Neigung der summativen Kurve gegen Ordnungsgrenzwert)-diagramme werden wie üblich angefertigt. Diese Methode sollte einen realistischen, qualitativen Vergleich der Ordnungsverteilung zwischen verschiedenen Proben des gleichen Polymeren ermöglichen und sollte auf andere kristalline Polymere ebenso wie auf Cellulose anwendbar sein.

Received November 3, 1961

Viscosity of Critical Mixtures

P. DEBYE, B. CHU, and D. WOERMANN, *Department of Chemistry, Cornell University, Ithaca, New York*

In the vicinity of the critical point, the concentration fluctuations are large and persist over distances comparable with the wavelength of visible light. For critical mixtures, the persistence length (or correlation length of the local concentration fluctuations manifests itself in the angular dissymmetry of scattered intensity which has been connected with the range of molecular forces.¹ This persistence length can also be determined by measurements of deviations from Rayleigh's law concerning the scattering power in its dependence on the wavelength.² Other physical properties of critical mixtures, such as heat capacity,^{3,4} ultrasonic absorption,⁵ and viscosity,⁶⁻¹⁰ also suggest the existence of a large correlation length of the local concentration fluctuations near the critical temperature. The viscosity, for instance of binary liquid mixtures, shows a strong characteristic temperature dependence as the critical solution temperature is approached. A first attempt at a theory of the viscosity of critical mixtures has recently been made.¹¹ Comparison of this theory with experiments so far is inconclusive.

In this paper, the authors have extended viscosity measurements of critical mixtures to polymer solutions (polystyrene-cyclohexane). An empirical expression for the viscosities of critical binary mixtures as a function of temperature is derived.

Experimental

The polystyrene samples are identical with fractions used in our earlier studies^{2,12} and are characterized by data in Table I. Each sample was purified by precipitating it out of a dilute benzene solution with an excess of methanol.

The viscosities were determined in an Ubbelohde viscometer which was calibrated with aqueous glycerol solutions of known viscosity.¹³ The small correction for kinetic energy could be neglected. Temperature was controlled to $\pm 0.005^\circ\text{C}$. and read on a Beckman thermometer inserted in the bath.

The phase separation temperature T_p of the polystyrene solutions was determined for each concentration in a separate experiment by visual observation.

TABLE I
 Polystyrene in Cyclohexane

| Sample ^a | $\bar{M}_n \times 10^{-3}$ | \bar{M}_w/\bar{M}_n | Half-width, % ^b | $T_p - T_c$ | |
|---------------------|----------------------------|-----------------------|-------------------------------|---------------------------|-------------------------------|
| | | | | Transmission ^c | Light scattering ^d |
| B | 118 | 1.05 | 38 | 0.13 | 0.82 |
| D | 221 | 1.08 | 32 | — | 0.53 |

^a The samples are identified by the same letters as in earlier publications (references (12) and (2)).

^b Calculated from molecular weight distribution curves: half width = $\Delta M \times 100/M_{\max}$, where ΔM is half-width of distribution curve, M_{\max} is the molecular weight corresponding to peak of distribution curve.

^c Data of Debye et al.² (reference (2)).

^d Data of Debye et al.¹²

Results and Discussion

If for a given temperature the relative temperature coefficient of the viscosity is plotted versus concentration, this curve exhibits a pronounced maximum when the temperature approaches the phase separation temperature. This maximum demonstrates the anomalous viscosity effect near the critical point. A maximum of the same type is also shown in Figure 1 for high polymer solutions.

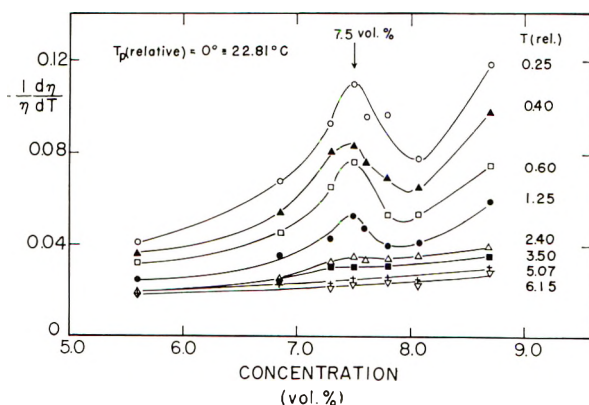


Fig. 1. Plot of the relative decrease of the viscosity per degree, $(1/\eta)(d\eta/dT)$, vs. concentration in volume per cent for polystyrene ($\bar{M}_n = 118,000$) in cyclohexane. Temperature expressed in relative scale in which T_p (relative) = 0 is equivalent to 22.81°C .

Preliminary calculations on binary liquid mixtures showed that if a constant α was subtracted from the coefficient $(1/\eta)(d\eta/dT)$, where η = is viscosity and T is temperature, determined at the critical concentration and different temperature distances from the critical temperature T_c , the product $[(1/\eta)(d\eta/dT) - \alpha]\Delta T$ is constant; thus:

$$[(1/\eta)(d\eta/dT) - \alpha]\Delta T = \beta \quad (1)$$

and

$$\Delta T = T - T_c$$

α and β are constants, and η is in centipoises. Integrating eq. (1) with $(T - T_c)/T_c$ as the integration variable, we get:

$$\log \eta = A(\Delta T/T_c) + B \log (\Delta T/T_c) + C \quad (2)$$

in which A , B , and C are constants. The term $A(\Delta T/T_c)$ represents the normal temperature dependence of viscosity, while the constant C indicates the magnitude of the viscosity. The second term, $B \log (\Delta T/T_c)$, takes into account the anomalous increase of the viscosity with respect to temperature when the critical temperature is approached, and thus may probably be related to the range of molecular forces. The constants A , B , and C can be determined by the method of least squares from measurements of viscosity of solutions as a function of temperature at the critical concentration. Values of the constants A , B , and C for three different systems: water-isobutyric acid,⁷ water-phenol,⁷ and perfluoro-*n*-heptane-isooctane¹⁰ are compiled in the first three rows of Table II. The viscosities for

TABLE II

| System | T_c , °K. ^a | Crit. concn. of first component, vol.-% ₀ | Constants of eq. (2) | | |
|---|-----------------------------|---|----------------------|---------|--------|
| | | | A | B | C |
| Isobutyric acid-water ^b | 298.98 | 38.6 ^c | -2.99 | -0.0466 | 0.284 |
| Phenol-water ^b | 339.15 | 36.1 ^c | -2.20 | -0.0489 | -0.141 |
| Isooctane- <i>n</i> -C ₇ F ₁₆ | 296.88 | 55 | -0.756 | -0.0718 | -0.432 |
| Polystyrene-cyclohexane | | | | | |
| $\bar{M}_n = 118,000$ | 295.59 ^e | 7.5 | -2.55 | -0.0394 | 0.839 |
| $\bar{M}_n = 221,000$ | 298.28 ^e | 6.1 | -1.42 | -0.0531 | 0.852 |

^a The second decimal place is only significant on a relative temperature scale.

^b Data of Friedländer.⁷

^c Concentration in weight-%.

^d Data of Reed and Taylor.¹⁰

^e $T_p - T_c$ is assumed to be 0.40 c. from an average of the results of light scattering¹² and transmission² measurements.

the systems water-isobutyric acid, and water-phenol, were calculated from relative viscosities η_{rel} , defined as $\eta_{rel} = \eta/\eta_{H_2O}^{25^\circ}$. The viscosity of water at 25°C. was taken to be 0.8937 centipoises. Figure 2 shows a plot of $\log \eta$ versus $\Delta T/T_c$ for the system water-isobutyric acid at the critical concentration. The points indicate experimental data. The solid curve was calculated from eq. (2) for the values of the constants A , B , and C given in Table II. The viscosity of critical mixtures as a function of $\Delta T/T_c$ is very well represented by the empirical formula [eq. (2)]. The agreement with experiment is within 0.5% for the systems water-isobutyric acid and perfluoro-*n*-heptane-isooctane for values of $T - T_c$ up to 10°C. For the

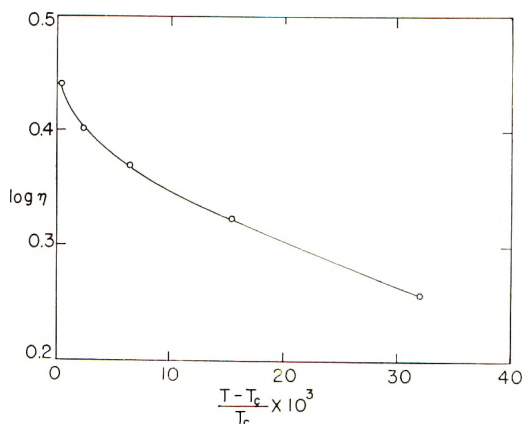


Fig. 2. Plot of logarithm of viscosity vs. $(T - T_c)/T_c$ for the water-isobutyric acid system: (—) calculated; (O) experimental (data of Friedländer⁷).

system water-phenol, there are deviations at small values of ΔT . However, we feel that the difficulties involved in handling this system have made the experimental results less reliable.

Good agreement exists between the critical concentration of binary liquid mixtures determined by viscosity measurements and by visual observation. In this last case the critical concentration and the critical temperature are determined by the maximum in a plot of the phase separation temperature versus concentration.

The visual method, however, is not suitable for finding the critical concentration of high polymer solutions, because the phase separation temperature changes only slightly with concentration, as shown in Figure 3. Moreover, the molecular weight distribution of our polymer samples prevented us from doing our experiments very close to the critical temperature because the fraction of the high molecular weights of the distribution precipitated before we reached the critical temperature. In other words, we can no longer assume $T_c = T_p$ (at the critical concentration) for high polymer solutions. The critical temperature cannot be determined by visual observation and is not exactly defined. Despite the difficulties, the critical

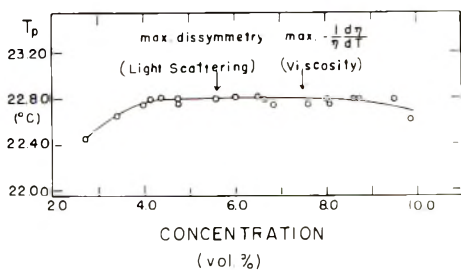


Fig. 3. Plot of phase separation temperature vs. concentration for polystyrene ($M_n = 118,000$) in cyclohexane.

concentration can (also) be determined from measurements of the dissymmetries of scattered intensities, $I_{45^\circ}/I_{135^\circ}$, as a function of concentration at fixed temperatures of a few tenths of a degree above the phase separation temperature.¹² Curves obtained in this manner again exhibit a distinct maximum which defines the critical concentration.

For polystyrene in cyclohexane, the critical concentration ϕ_{2c} determined by viscosity measurements is higher than that determined by light-scattering measurements¹² (for $M_n = 118,000$, ϕ_{2c} (light scattering) = 5.6 vol.-% polystyrene, ϕ_{2c} (viscosity) = 7.5 vol.-%; for $M_n = 221,000$; ϕ_{2c} (light scattering) = 4.6 vol.-% polystyrene; ϕ_{2c} (viscosity) = 6.1 vol.-%). The quotient, ϕ_{2c} (light scattering)/ ϕ_{2c} (viscosity), is 0.75 for both cases. The discrepancy could perhaps be due to the polydispersity of the polystyrene samples.

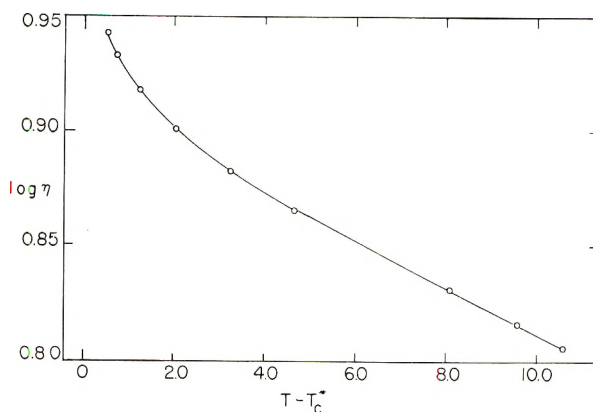


Fig. 4. Plot of logarithm of viscosity vs. $T - T_c^*$ polystyrene ($\bar{M}_n = 118,000$) in cyclohexane ($T_p - T_c^* = 0.4^\circ\text{C}$.): (—) calculated; (O) experimental.

The critical temperature can be expected to coincide with the phase separation temperature in the case of an ideally monodisperse polymer (or in the case of liquids). For our polystyrene samples, $T_p - T_c$ is of the order of 0.4°C . as calculated from light-scattering¹² and transmission² measurements. The constants A , B , and C of eq. (2) were determined on the basis of an assumed value of 0.4°C . for $T_p - T_c^*$. The results are shown in the last two rows of Table II. The curve calculated from the empirical formula agrees with experimental data to within 0.5% for values of $T - T_c^*$ up to more than 10°C . (Fig. 4).

The authors gratefully acknowledge the financial support given by the National Science Foundation, by the Office of Naval Research, and by the Air Force Office of Scientific Research.

References

1. Debye, P., *J. Chem. Phys.*, **31**, 680 (1959).
2. Debye, P., D. Woermann, and B. Chu, *J. Chem. Phys.*, **36**, 851 (1962).

3. Jura, G., D. Fraga, G. Maki, and J. H. Hildebrand, *Proc. Natl. Acad. Sci. U.S.*, **39**, 19 (1953).
4. Fixman, M., private communication.
5. Alfrey, G. F., and W. G. Schneider, *Discussions Faraday Soc.*, No. **15**, 218 (1953).
6. Ostwald, W., *Trans. Faraday Soc.*, **9**, 34 (1913); *ibid.*, **29**, 1002 (1933).
7. Friedländer, J., *Z. physik. Chem.*, **38**, 385 (1901).
8. Semenchenko and Zorina, *Doklady Akad. Nauk. S.S.S.R.*, **73**, 331 (1950); *ibid.*, **80**, 903 (1951).
9. Semenchenko and Skripov, *Zhur. Fiz. Khim.*, **25**, 362 (1951).
10. Reed, T. M., III, and T. E. Taylor, *J. Phys. Chem.*, **63**, 58 (1959).
11. Fixman, M., *J. Chem. Phys.*, **36**, 310 (1962).
12. Debye, P., H. Coll, and D. Woermann, *J. Chem. Phys.*, **33**, 1746 (1960).
13. Sheely, M. L., *Ind. Eng. Chem.*, **24**, 1060 (1932).

Synopsis

Measurements of the viscosity of critical mixtures were extended to high polymer solutions (polystyrene-cyclohexane). An anomaly is found in the temperature coefficient of the viscosity. An empirical expression for the viscosities of critical mixtures as a function of $\Delta T/T_c$, where $\Delta T = T - T_c$, and T_c is the critical temperature, is derived.

Résumé

On a appliqué les mesures de viscosité de mélanges critiques à des solutions de hauts polymères (polystyrène-cyclohexane). On a trouvé une anomalie dans le coefficient de température de la viscosité. On en a déduit une expression empirique pour les viscosités de mélanges critiques en tant que fonction de $\Delta T/T_c$ ($\Delta T = T - T_c$; T_c est la température critique).

Zusammenfassung

Viskositätsmessungen an kritischen Mischungen wurden auf Lösungen von Hochpolymeren (Polystyrol-Cyclohexan) ausgedehnt. Eine Anomalie des Temperaturkoeffizienten der Viskosität wird festgestellt. Eine empirische Beziehung für die Viskosität kritischer Mischungen als Funktion von $\Delta T/T_c$ ($\Delta T = T - T_c$; T_c ist die kritische Temperatur) wird abgeleitet.

Received October 31, 1961

Critical Opalescence of Polystyrene in Ethylcyclohexane

P. DEBYE, D. WOERMANN, and B. CHU, *Department of Chemistry,
Cornell University, Ithaca, New York*

In a recent publication on critical opalescence it was shown that, for a binary liquid mixture of critical concentration, measurements of the angular dependence of scattered intensity at small temperature distances above the critical temperature can be related to the range of molecular forces.¹ This concept has been applied to polymer solutions. The range of molecular forces and the critical temperature of solutions of polystyrene of different molecular weights in cyclohexane have been reported.² It was found that the range of molecular forces l was strikingly small. Thus, we investigated the critical opalescence of polystyrene in ethylcyclohexane in order to see whether the smallness of l is characteristic only of the system polystyrene-cyclohexane.

The scattering formula of solutions of critical concentration at small temperature distances above the critical temperature is stated in a simplified form in eq. (1):

$$I = C(T/T_c)/[(\Delta T/T_c) + (8\pi^2/3)(l^2/\lambda^2)\sin^2(\theta/2)] \quad (1)$$

I is scattered intensity, C is a constant characteristic for the system, T is absolute temperature, T_c is critical temperature, $\Delta T = (T - T_c)$, λ is wavelength of light in the medium, l is interaction range, and θ is scattering angle. Equation (1) is applicable only to polymer solutions of low molecular weight for which no angular dissymmetry of scattered light due to the extension of the polymer coil is observed.

Experimental

A detailed description of the light-scattering apparatus and of the experimental procedures is given elsewhere.²

The polystyrene samples were prepared by anionic polymerization of styrene. (Samples were obtained by courtesy of the Dow Chemical Company, Midland, Michigan.) They are identical with fractions used in our earlier studies and are characterized by data³ in the first four columns in Table I. Each sample was purified by precipitating it out of a dilute benzene solution with an excess of methanol.

Ethylcyclohexane (practical grade) was passed through a column of silica gel and carefully fractionated.

TABLE I
 Polystyrene in Ethylcyclohexane

| Sample ^a | $\bar{M}_n \times 10^{-3}$ | \bar{M}_w/\bar{M}_n | Half-width, % ^b | T_c , °C. ^c | $T_p - T_c$, °C. | $(\phi_2)_{crit} \times 100$, vol.-% | l , Å. |
|---------------------|----------------------------|-----------------------|----------------------------|--------------------------|-------------------|---------------------------------------|----------|
| A | 69 | 1.16 | — | — | — | 8.2 | — |
| B | 118 | 1.05 | 38 | 52.7 ₉ | 0.34 | 6.6 | 28.7 |
| C | 147 | 1.04 | 30 | 54.6 ₆ | 1.11 | 5.85 | 29.8 |
| D | 221 | 1.08 | 32 | 57.3 ₇ | 0.94 | 5.25 | 32.4 |
| F | 522 | 1.09 | — | 62.0 ₂ | 0.93 | 3.60 | 46.6 |

^a The samples are identified by the same letters as in an earlier publication.²

^b Calculated from molecular weight distribution curves. Halfwidth = $\Delta M \times 100/M_{max}$ where ΔM is halfwidth of distribution curve and M_{max} is molecular weight corresponding to peak of distribution curve.

^c The second decimal place is significant only on a relative temperature scale.

The solutions were prepared from weighed amounts of polymer and solvent, and the volume fractions calculated from the respective densities (density of polystyrene: 1.08 g./cc.; density of ethylcyclohexane: 0.789 g./cc.). The temperatures of phase separation T_p were determined in separate experiments by visual observation. After heating the solutions at 80°C. for more than 1 hr., the degradation of polystyrene caused a decrease in T_p . Therefore the solutions for the light-scattering experiments were never heated above 70°C. They were filtered directly into the scattering cell through a thermostated medium (M) glass frit. After the experiment, the concentration was redetermined by weighing small amounts of the solution before and after evaporation of the solvent.

The critical concentrations were determined by measuring the concentration dependence of the dissymmetry ($I^*_{45^\circ}/I^*_{135^\circ}$) at small fixed temperature distances above T_p . The curves so obtained show a distinct maximum at the critical concentration.

Treatment of Data⁴

The measured intensity of scattered light (galvanometer reading in relative units) has to be corrected for the change in the effective scattering volume by multiplying G with $\sin \theta$; $I^* = G \sin \theta$. The scattered intensity I^* has also to be corrected for the attenuation of incident and scattered intensities because of high turbidity of the solution. The correction can be carried out by multiplying I^* with $f(T)$; $I = I^* \times f(T)$ in which $f(T)$ is a function of temperature. However the form of the temperature function $f(T)$ is immaterial for our purpose.

According to eq. (1), the reciprocal of the scattered intensity can be written as:

$$1/I^* = F(T)(T_c/T)[(\Delta T/T_c) + (8\pi^2/3)(l^2/\lambda^2) \sin^2(\theta/2)] \quad (2)$$

with $F(T) = f(T)/C$. A plot of $1/I^*$ versus $\sin^2 \theta/2$ at small temperature distances above T_c should give straight lines. T_c and l^2 can be computed

from the quotients of slopes (B) and intercepts (A) of these straight lines. Consequently, the factor $F(T)$ cancels out.

A plot of the measured $1/I^*$ versus $\sin^2 \theta/2$ is linear between 30° (the lowest angle of observation) and 160° . The curves bend slightly upward at higher angles. It is possible that the curvature can be attributed to higher moments of l . However, the experiments are yet inconclusive.

Determination of T_c . With reference to eq. (2), we can write:

$$A/B = \text{const. } \Delta T$$

Plotting A/B versus T , one finds T_c from intercept and slope of the resulting straight line. $T_c = \text{intercept/slope}$.

Determination of l^2 . We can define a quantity S

$$S = (B/A) \Delta T$$

S and l^2 are related by:

$$l^2 = 3\lambda^2 S / 8\pi^2 T_c$$

Results and Discussion

Results of our findings are compiled in the last four columns of Table I.

Phase separation temperatures, T_p , of the system polystyrene-ethylcyclohexane have previously been reported by Shultz and Flory.⁵ According to the Flory-Huggins theory, the theta temperature of a system can be calculated from the expression:

$$1/T_c = (1/\Theta) \{1 + (1/\psi_1) [(1/X^{1/2}) + (1/2X)]\} \quad (3)$$

x , defined as $v_p M_p / v_s M_s$, is the number of statistical chain segments, where v_p and v_s are the specific volumes of polymer and solvent, respectively, and M_p and M_s are the corresponding molecular weights. ψ_1 is the entropy parameter. A plot of $1/T_c$ against $(1/x^{1/2}) + (1/2x)$ should give a straight line whose reciprocal intercept is the theta temperature. Our data give a theta temperature of 69.8°C . compared with 70.0°C . for the theta temperature reported by Shultz and Flory. (They interpreted the maximum temperature in a plot of T_p versus composition as the critical temperature.)

T_p coincides with T_c for an ideally monodisperse polymer. We found $T_p - T_c$ to be about 0.9°C . If we assume that T_p is the temperature where the highest molecular weight fraction of the sample begins to precipitate, we can expect such a difference between T_p and T_c in view of the molecular weight distribution in our samples. $T_p - T_c$ for the system polystyrene-cyclohexane is smaller (about 0.5°C .). This difference can be explained qualitatively by examining eq. (3). A plot of $1/T_c$ versus $\bar{M}_n^{1/2}$ will be linear for large molecular weights. The slope for the system polystyrene-ethylcyclohexane is larger than that for the system polystyrene-cyclohexane (slope for polystyrene-ethylcyclohexane = 5.27×10^{-2} ; slope for polystyrene-cyclohexane = 4.04×10^{-2}). Furthermore, the system polystyrene-ethylcyclohexane has higher critical temperatures. There-

fore the difference between T_c for the highest and the lowest molecular weight fraction of a polystyrene sample is larger in a solution of ethyl cyclohexane than that in a solution of cyclohexane.

A plot of the reciprocal of the critical concentration, $1/\phi_{2c}$, against $M_n^{1/2}$ is shown in Figure 1. The curve is linear in accordance with the theoretical formula:

$$\phi_{2c} = 1/(1 + x^{1/2}) \quad (4)$$

assuming $x = (\text{constant})M_n$. However, the measured values are roughly twice as big as the values calculated from eq. (4) by use of the theoretical definition of x in eq. (3). Similar observations have been reported in the literature.⁵

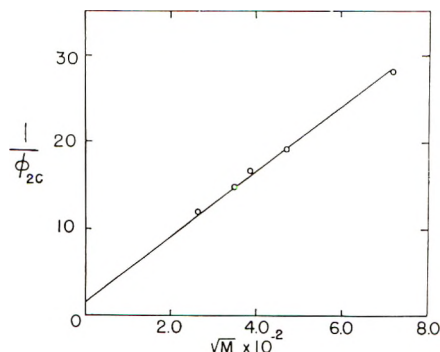


Fig. 1. Plot of reciprocal critical concentration $1/\phi_{2c}$ vs. square root of molecular weight for polystyrene in ethyl-cyclohexane.

The critical concentrations are larger than that of the system polystyrene-cyclohexane because the statistical chain segment as calculated from eq. (3) for a given polystyrene sample is smaller in ethylcyclohexane.

The range of molecular forces l of polystyrene in ethylcyclohexane is strikingly small. It is about 15% larger than the range of molecular forces of the same polystyrene samples in cyclohexane.² l^2 is a linear function of M_n for the molecular weights of polystyrene between 69,000 and 522,000.

References

1. Debye, P., *J. Chem. Phys.*, **31**, 680 (1959).
2. Debye, P., H. Coll, and D. Woermann, *J. Chem. Phys.*, **33**, 1746 (1960).
3. McCormik, J. W., Dow Chemical Company, private communication.
4. Debye, P., B. Chu, and D. Woermann, *J. Chem. Phys.*, **36**, 1803 (1962).
5. Shultz, A. R., and P. J. Flory, *J. Am. Chem. Soc.*, **75**, 3888 (1953).

Synopsis

The range of molecular forces and the critical temperature of polystyrene in ethyl-cyclohexane are calculated from measurements of the angular dependence of critical opalescence. The polystyrene samples have molecular weights ranging from 69,000

to 552,000. The range of molecular forces remains strikingly small and is comparable with values obtained earlier on the system polystyrene-cyclohexane.

Résumé

On calcule la portée des forces moléculaires et la température critique du polystyrène dans l'éthylcyclohexane à partir des mesures de dépendance angulaire de l'opalescence critique. Les échantillons de polystyrène ont des poids moléculaires allant de 69.000 à 552.000. La portée des forces moléculaires reste très faible et est comparable aux valeurs obtenues précédemment pour le système polystyrène-cyclohexane.

Zusammenfassung

Die Reichweite von Molekularkräften und die kritische Temperatur von Polystyrol in Äthylcyclohexan werden aus der Messung der Winkelabhängigkeit der kritischen Opaleszenz berechnet. Die Polystyrolproben besitzen Molekulargewichte im Bereich von 69000 bis 552000. Die Reichweite der Molekularkräfte bleibt auffallend klein und ist mit Werten vergleichbar, die früher für das System Polystyrol-Cyclohexan erhalten wurden.

Received October 3, 1961

A Theory for Surface Elevation in the Weissenberg Effect

STANLEY MIDDLEMAN, *Department of Chemical Engineering,
The University of Rochester, Rochester, New York*

Introduction

Many liquids, when subjected to simple shearing flows, develop normal stresses in the direction of flow and perpendicular to it. These normal stresses manifest themselves in phenomena whose nature depends upon the geometry of flow. Among the class of normal stress phenomena is the Weissenberg effect, which is commonly observed whenever a stirring rod is rotated normal to the free surface of a concentrated polymer solution. The surface is observed to climb the rod, rather than be depressed, as is the case with Newtonian fluids.

Although this phenomenon is well known, few attempts have been made to study the Weissenberg effect quantitatively. It should be of interest, therefore, to examine the equations of motion of a general fluid with a free surface, in which a cylindrical rod is rotating normal to the surface, in order to see whether solutions to the equations, obtained under physically reasonable assumptions, approximate experimentally observed behavior.

Theory

We consider a steady state Couette flow generated by an infinitely long circular cylinder of radius R_0 concentric with an outer cylinder of radius R_1 . The annular space between the cylinders contains a fluid with a horizontal free surface. The inner cylinder rotates about its axis at Ω rev./sec., while the outer cylinder is stationary.

We neglect effects at the boundaries of the fluid, and assume the flow is symmetrical in circles concentric with the annular flow region.

The velocity vector, in cylindrical coordinates, is

$$(\mathbf{v}_r, \mathbf{v}_\theta, \mathbf{v}_z) = (0, v, 0) \quad (1)$$

The stress tensor is

$$\mathbf{T} = \begin{pmatrix} T_{rr} - p & \tau_{r\theta} & \tau_{rz} \\ \tau_{r\theta} & T_{\theta\theta} - p & \tau_{\theta z} \\ \tau_{rz} & \tau_{\theta z} & T_{zz} - p \end{pmatrix} \quad (2)$$

With the above assumptions regarding the symmetry of the flow, the

dynamic equations become

$$\frac{\partial p}{\partial z} = -\rho g \quad (3)$$

$$\frac{d}{dr} (r^2 \tau_{r,\theta}) = 0 \quad (4)$$

and

$$\frac{\partial p}{\partial r} = \rho \frac{v^2}{r} + \left[\frac{T_{\theta\theta}}{r} - \frac{1}{r} \frac{d}{dr} (r T_{rr}) \right] \quad (5)$$

Integrating eqs. (3) and (5), we find

$$p = -\rho g z + F(r) + C \quad (6)$$

where

$$F(r) = \int \left\{ \rho \frac{v^2}{r} + \left[\frac{T_{\theta\theta}}{r} - \frac{1}{r} \frac{d}{dr} (r T_{rr}) \right] \right\} dr \quad (7)$$

The constant of integration, C , is determined by the condition that the volume of liquid in the annulus must remain constant. If the free surface of the liquid, when there is no flow, lies in the plane $z = 0$, then when the equilibrium surface configuration is attained, the volume of fluid above $z = 0$ just balances the decrease in the volume below $z = 0$. (Fig. 1)

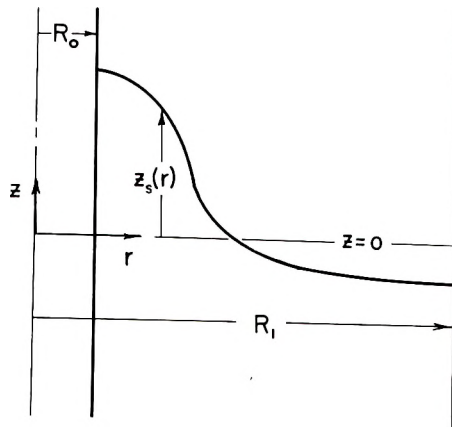


Fig. 1. Surface elevation $Z_s(r)$ of fluid contained between cylinders of radii R_0 and R_1 . The inner cylinder is rotating, while the outer cylinder is stationary.

If we let $z_s(r)$ represent the free surface of the liquid, and let the arbitrary isotropic pressure at the free surface be zero, then the equation for the free surface is, from eq. (6),

$$z_s(r) = [F(r) + C]/\rho g \quad (8)$$

The boundary condition takes the form

$$2\pi \int_{R_0}^{R_1} z_s(r) r dr = 0 \quad (9)$$

Substituting for z_s in this integral, we find

$$C = [2/(R_0^2 - R_1^2)] \int_{R_0}^{R_1} F(r) r dr \quad (10)$$

We can write eq. (8) explicitly as a function of r only if we have explicit expressions for the stress components, from which $F(r)$ [eq. (7)] may be obtained.

In order to write the stress components explicitly we must make assumptions regarding the nature of the fluid.

The shear behavior is assumed to follow a "power law," which takes the form

$$\tau_{r\theta} = M \left[r \frac{d}{dr} \left(\frac{v}{r} \right) \right]^n \quad (11)$$

where M and n are fluid constants. This behavior, with $0 < n < 1$, is observed for many polymer solutions over a range of shear stress of about one decade.¹

We assume

$$T_{\theta\theta} = \kappa T_{rr} \quad (12)$$

Possible choices of κ and experimental evidence for these choices are discussed in detail by Markovitz.²

Finally, we assume

$$T_{rr} = a(\tau_{r\theta})^b \quad (13)$$

where a and b are fluid constants. For many polymer systems eq. (13) is obeyed with $b = 2$ at low shear stress, and $b = 1$ at high shear stress.³

A solution for $z_s(r)$ can now be obtained. With eqs. (11) and (4) the velocity distribution $v(r)$ can be solved for. From $v(r)$, with eq. (11), $\tau_{r\theta}(r)$ can be found, and eqs. (13) and (12) give $T_{rr}(r)$ and $T_{\theta\theta}(r)$. Finally, eq. (7) gives $F(r)$ explicitly, and eq. (10) yields the surface elevation $z_s(r)$.

Following this scheme, we find that the velocity distribution is

$$v(\zeta) = \frac{2\pi\Omega R_0}{1 - s^{-2/n}} \zeta(\zeta^{-2/n} - s^{-2/n}) \quad (14)$$

where $\zeta = r/R_0$ is a dimensionless radial variable and $s = R_1/R_0$. This solution is subject to the boundary conditions

$$v = 2\pi\Omega R_0 \quad r = R_0(\zeta = 1) \quad (15)$$

and

$$v = 0 \quad r = R_1(\zeta = s) \quad (16)$$

The shear stress, after simplification, becomes

$$\tau_{r\theta} = A^{1/b} \zeta^{-2} \quad (17)$$

where

$$A^{1/b} = M [4\pi\Omega/n(1 - s^{-2/n})]^n \quad (18)$$

The normal stresses are

$$T_{rr} = aA\zeta^{-2b} \quad (19)$$

and

$$T_{\theta\theta} = \kappa\Omega A\zeta^{-2b} \quad (20)$$

Finally, we find

$$z_s(\zeta) = \frac{C}{\rho g} - \frac{1}{g} \left(\frac{2\pi\Omega R_0}{1 - s^{-2/n}} \right)^2 \mathcal{C}(\zeta) + \left(\frac{1 - \kappa}{2b} - 1 \right) aA\zeta^{-2b} \quad (21)$$

where

$$\mathcal{C}(\zeta) = \frac{\zeta^{2-4/n}}{4/n - 2} - \frac{\zeta^2}{2s^{4/n}} - \frac{\zeta^{2-2/n}}{s^{2/n}(1 - 1/n)} \quad (22)$$

The constant C could now be obtained from eq. (10), but need not be written out here. The second term on the right-hand side of eq. (21) represents the effect of centrifugal forces generated by the circular flow field. These forces tend to depress the surface in the neighborhood of the rod ($\zeta = 1$).

For a Newtonian fluid, $n = 1$, and $a = 0$, and a separate solution gives

$$z_s(\zeta) = \frac{C}{\rho g} - \frac{1}{g} \left(\frac{2\pi\Omega R_0}{1 - s^{-2}} \right)^2 \left(\frac{1}{2\zeta^2} - \frac{\zeta^2}{2s^4} + \frac{2 \ln \zeta}{s^2} \right) \quad (23)$$

If the fluid is of infinite extent ($s = \infty$), we have, for the Newtonian fluid,

$$z_s(\zeta) = -(1/g)(2\pi\Omega R_0)^2(1/2\zeta^2) \quad (24)$$

For the sake of simplicity we shall take s to be sufficiently large that the fluid is effectively of infinite extent, in which case $\mathcal{C}(\zeta)$ in the neighborhood of the rod, which is the region of interest when we are considering the surface elevation, is given by

$$\mathcal{C}(\zeta) = \frac{\zeta^{2-4/n}}{4/n - 2} \quad (25)$$

Equation (25) is valid for $n = 1$ also.

We rewrite eq. (21) in a form which makes the dependence of z_s on Ω and R_0 explicit, as we shall later discuss the observed effects of these variables:

$$z_s(\zeta) = -(1/g)(2\pi\Omega R_0)^2 \mathcal{C}(\zeta) + A'\Omega^{bn}\zeta^{-2b} \quad (26)$$

where

$$A' = \frac{Aa}{\Omega^{bn}} \left(\frac{1 - \kappa}{2b} - 1 \right) = M^b \left(\frac{4\pi}{n} \right)^{bn} a \left(\frac{1 - \kappa}{2b} - 1 \right) \quad (27)$$

The second term on the right-hand side of eq. (26) represents the effect of normal stresses, and since we observe appreciable surface elevation rather than depression near $\zeta = 1$, we conclude that, for the fluids we wish to consider, the second term is opposite in sign to, and much larger than, the centrifugal term.

Thus we would expect the surface shape to be nearly

$$z_s(\zeta) = A' \Omega^{bn} \zeta^{-2b} \quad (28)$$

and the maximum height of climb of the fluid, $z_s(1)$, to be

$$z_s(1) = A' \Omega^{bn} \quad (29)$$

Comparison with Existing Data

Some data exist in the literature for studies of the Weissenberg effect in solutions of polyisobutylene. For such solutions, typical values of b and n , at conditions usually attained for this type of flow, are $b = 2$ and $n = 0.6$.³

With these values eq. (28) predicts

$$z_s(\zeta) = A' \Omega^{1.2} \zeta^{-4} \quad (30)$$

and eq. (29) predicts

$$z_s(1) = A' \Omega^{1.2} \quad (31)$$

Garner, Nissan, and Walker⁴ observed

$$z_s(\zeta) = A' \Omega^\alpha \zeta^{-4} \quad (32)$$

with α varying from 0.67 to 1.

Ward and Lord⁵ find $z_s(1)$ to be nearly linear ($\alpha = 1$) with Ω at low values of Ω , but to increase more slowly than linearly ($\alpha < 1$) with Ω as Ω is increased. We can see in eq. (26) that the centrifugal term increases as Ω^2 . Thus, as Ω increases, the centrifugal term grows more rapidly than the normal stress term, and, being small but of opposite sign to the normal stress term, it has the effect of decreasing the rate at which $z_s(1)$ increases with Ω .

It is interesting to note that eq. (29) predicts no dependence of the maximum height of climb on R_0 . There appear to be no data available with which to compare this prediction.

Conclusions

The published data are insufficient to allow a more extensive evaluation of the present theory. The limited success of the theory, as outlined here, indicates that it would be worthwhile to present more extensive data and attempt an interpretation based on this theory.

References

1. Brodnyan, J. G., F. H. Gaskins, and W. Philippoff, *Trans. Soc. Rheology*, **1**, 109 (1957).
2. Markovitz, H., *Trans. Soc. Rheology*, **1**, 37 (1957).
3. Middleman, S., Dr. E. Dissertation, The Johns Hopkins University, Baltimore, Md., 1961.
4. Garner, F. H., A. H. Nissan, and J. Walter, *Ind. Eng. Chem.*, **51**, 858 (1959).
5. Ward, A. F. H., and P. Lord, in *Proc. Intern. Congr. Rheol., 2nd Congr. Oxford 1953*, 214 (1954).

Synopsis

A Couette flow generated by a cylinder rotating perpendicular to the free surface of a fluid is considered and the equations of motion are solved to yield an expression for the surface shape in the vicinity of the rod. The fluid model chosen is one for which the shear stress $\tau_{r\theta}$ and the normal stresses T_{rr} and $T_{\theta\theta}$ obey the relations

$$\begin{aligned}\tau_{r\theta} &= M \left[r \frac{d}{dr} \left(\frac{v}{r} \right) \right]^n \\ T_{rr} &= a(\tau_{r\theta})^b \\ T_{\theta\theta} &= \kappa T_{rr}\end{aligned}$$

where M , n , a , b , and κ are constants characteristic of the fluid and v is the flow velocity component in the angular direction. The results are found to be in reasonable agreement with previous experimental observations of the Weissenberg effect.

Résumé

Un écoulement du type Couette engendré par un cylindre tournant perpendiculairement à la surface libre d'un fluide, est considéré et les équations de mouvement sont résolues pour obtenir une expression de la forme de la surface à proximité du piston. Le modèle de fluide choisi est celui pour lequel la force de cisaillement $\tau_{r\theta}$ et les forces normales T_{rr} et $T_{\theta\theta}$ obéissent aux relations:

$$\begin{aligned}\tau_{r\theta} &= M \left[r \frac{d}{dr} \left(\frac{v}{r} \right) \right]^n \\ T_{rr} &= a(\tau_{r\theta})^b \\ T_{\theta\theta} &= \kappa T_{rr}\end{aligned}$$

où M , n , a , b et κ sont des constantes caractéristiques du fluide et v est la composante de la vitesse d'écoulement suivant la direction angulaire. Les résultats sont en bon accord avec les observations expérimentales antérieures de l'effet Weissenberg.

Zusammenfassung

Eine durch einen senkrecht zur freien Oberfläche einer Flüssigkeit rotierenden Zylinder erzeugte Couette-Strömung wird untersucht und die Bewegungsgleichungen werden gelöst, um einen Ausdruck für die Gestalt der Oberfläche in der Umgebung des Stabes zu erhalten. Das gewählte Flüssigkeitsmodell ist von der Art, dass die Scherspannung $\tau_{r\theta}$ und die Normalspannungen T_{rr} und $T_{\theta\theta}$ den Beziehungen

$$\begin{aligned}\tau_{r\theta} &= M \left[r \frac{d}{dr} \left(\frac{v}{r} \right) \right]^n \\ T_{rr} &= a(\tau_{r\theta})^b \\ T_{\theta\theta} &= \kappa T_{rr}\end{aligned}$$

gehörchen, wo M , n , a , b , und κ für die Flüssigkeit charakteristische Konstante sind und v die Komponente der Strömungsgeschwindigkeit in der Winkelrichtung ist. Die Ergebnisse zeigen eine brauchbare Übereinstimmung mit früheren Versuchsergebnissen am Weissenbergeffekt.

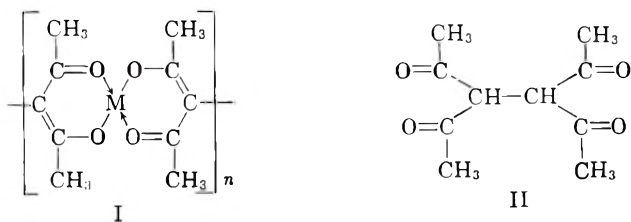
Received October 26, 1961

Metal Chelate Polymers Derived from Tetraacetylethane*

ROBERT G. CHARLES, *Westinghouse Research Laboratories, Pittsburgh, Pennsylvania*

There has been considerable interest in the preparation of metal coordination polymers as possible heat-stable materials. Three recent reviews summarize work in this area.¹⁻³ Much of the work which has been done to date has been concerned with the synthesis of these materials, and little is known concerning the factors which influence their heat stabilities. Very little is also known of the products which result from pyrolysis and of the mechanisms by which pyrolysis takes place.

A previous paper from this laboratory concerned the preparation and pyrolysis of copper chelate polymers derived from tetraacetylethane (TAE, II) which contained the recurring grouping I (where M is Cu).⁴ It was of interest to prepare similar polymers, containing other divalent metal cations, in order to determine the effect of varying the metal upon the



heat stability. Attempts to prepare such polymers by the method previously used⁴ failed to give solid products. We have now found that TAE polymers containing the metals Cu, Ni, Co, Zn, Cd, and Mg can be prepared by first forming the dipotassium salt of II in methanol solution and then allowing this solution to react with an aqueous solution containing a divalent metal acetate.† We report here the properties of the polymers obtained by this technique with emphasis on their pyrolytic characteristics.

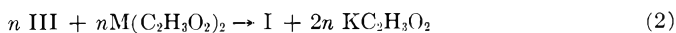
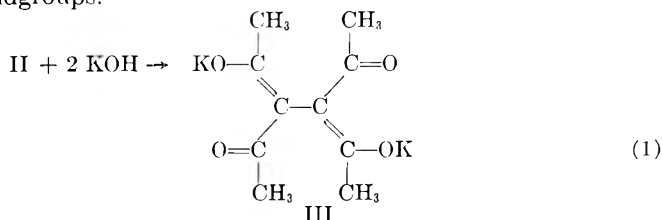
* Presented, in part, at the Inorganic Polymer Symposium, 136th National Meeting of the American Chemical Society, Atlantic City, N. J., September 1959.

† Tetraacetylethane in its dienolic form is a weak dibasic acid. Its potassium salt will be hydrolyzed in a solution containing water to form an equilibrium mixture involving tetraacetylethane, its mono- and dipotassium salts, and KOH.⁵

RESULTS AND DISCUSSION

Preparation and Characterization

The reactions involved in the polymer preparations can be written, in simplified form, as eqs. (1) and (2), where eq. (2) does not take into account the presence of endgroups.



The polymers containing the recurring unit I precipitate from solution as finely divided solids which, except for the Cu polymers, retain water of hydration upon drying in air at room temperature. In most cases the solids contained 90% or more of both the TAE and divalent metal taken for their preparation. The polymers are infusible and are insoluble in water and in the common organic solvents. The infrared spectra of the polymers are all very similar to each other and to the spectrum previously reported⁴ for the copper TAE polymer. The correspondence between the spectra obtained here and that previously obtained⁴ is good evidence for the presence of grouping I in all these materials. An additional absorption peak at about 3350 cm.^{-1} was, however, present in the spectra for the Ni, Co, Zn, Cd, and Mg polymers. This is presumably due to the presence of water of hydration, since the thermogravimetric results (Fig. 2) also show the presence of water for these materials, but not for the CuTAE polymers.

Table I lists analytical data for typical products obtained by adding 2×10^{-3} mole metal acetate to 2×10^{-3} mole III. For one preparation (prep. 1), a ratio of M/III of 0.83 was used. It will be noted that all the polymers except the copper and cadmium ones contain potassium. This is presumably bound in the endgroups IV, since it is not removed by washing. The amount of potassium indicates a relatively low degree of polymerization. Since, however, it is not known what fraction of the endgroups contain potassium (as opposed to other possibilities such as V and VI) one cannot calculate the degree of polymerization from the potassium content with any degree of confidence.

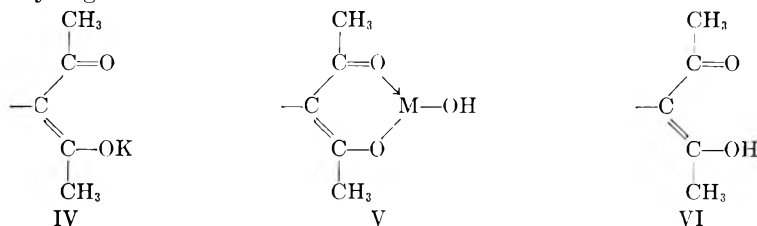


TABLE I
Analysis of Metal TAE Polymers Dried at Room Temperature

| Preparation no. | M | Yield, mg. | Color | K, % | M, % | C ₁₀ H ₁₄ O ₄ , % | Molar Ratios | |
|-----------------|-----------------|------------|-------|------|------|--|-------------------|---|
| | | | | | | | K/M | C ₁₀ H ₁₄ O ₄ /M |
| 1 | Cu ^a | 498 | Green | <0.1 | 21.6 | 79.7 | 0 | 1.18 |
| 2 | Cu ^b | 534 | Green | <0.1 | 24.2 | 74.2 | 0 ^c | 0.98 |
| 3 | Ni | 641 | Green | 2.65 | 17.3 | 60.8 | 0.23 ^d | 1.04 |
| 4 | Co | 613 | Red | 1.72 | 18.4 | 63.9 | 0.14 | 1.03 |
| 5 | Zn | 625 | White | 3.74 | 20.2 | 54.3 | 0.31 ^e | 0.89 |
| 6 | Cd | 629 | White | 0.1 | 34.8 | 57.3 | 0 ^c | 0.93 |
| 7 | Mg | 630 | White | 3.86 | 8.57 | 62.2 | 0.28 | 0.89 |

^a Calculated for (C₁₀H₁₃O₄Cu)₅C₁₀H₁₄O₄: yield, 499 mg.; Cu, 21.2%; C₁₀H₁₄O₄, 79.4%.

^b Calculated for C₁₀H₁₃O₄Cu: yield, 523 mg.; Cu, 24.4%; C₁₀H₁₃O₄, 76.0%.

^c The same value was found for a separate preparation.

^d Found for two other preparations: 0.21, 0.26.

^e Found for a separate preparation: 0.27.

Attempts were made to determine combining ratios, divalent metal/III by means of spectrophotometric titrations. In Figure 1 are given plots of the absorbance of the filtrate versus the ratio divalent metal added/TAE taken for the preparation. The curve for the copper titration gives a sharp break at a ratio of 0.83. This corresponds to a value of $n = 5.0$ in I. (The assumption was made that the endgroups in the polymer precipitated to this point did not contain Cu.) Analyses of the solid precipitated at this ratio of reactants (prep. 1, Table I) are in good agreement with this degree of polymerization. It is interesting that for the CuTAE polymers previously prepared by a different method,⁴ n also was found to be 5. Since the copper preparation 1 (Table I), by the present procedure, did not contain potassium, the endgroups are presumably VI. When a molar ratio Cu/III = 1 was used in the preparation (prep. 2, Table I) a ratio of Cu/TAE = 1.02 was found for the polymer. This could be interpreted

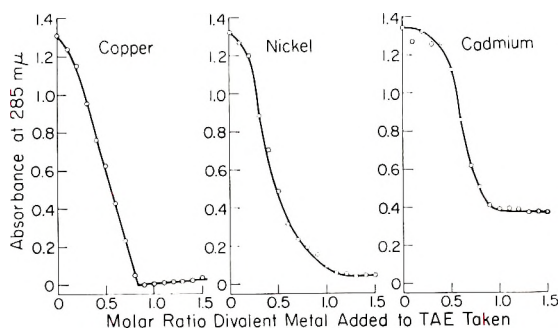


Fig. 1. Spectrophotometric titrations of equivalent amounts of tetraacetyethane and KOH with divalent metal acetates.

as due to an increase in the molecular weight through interaction of endgroups present in the initially precipitated material with additional copper ion. One cannot rule out the possibilities, however, that preparation 2 contains precipitated basic copper salts or that the endgroups VI are partially replaced by V.

The titration curves obtained with nickel and with cadmium acetates (Fig. 1) fall to minimum absorbance values in the vicinity of $M/TAE = 1$. The breaks in the curves are not sufficiently well defined to be of direct value, however, in calculating the average degree of polymerization of the precipitates. The shapes of these curves are probably the result of greater tendencies of the NiTAE and CdTAE chelates to dissociate to the dianion of TAE and the metal cations in solution, as compared with the CuTAE polymers. The curve for CdTAE did not fall to zero absorbance, evidently due to the presence of some low molecular weight, soluble species. Upon standing, additional insoluble polymer gradually separated from solution.

The insoluble cadmium polymer, like the copper preparations 1 and 2, did not contain significant potassium. This may indicate a relatively high molecular weight for this material, or alternatively, that the endgroups are entirely V and VI.

It must be emphasized that the compositions of the materials obtained here (Table I) are determined by the particular set of reaction conditions chosen. It should be possible to change the molecular weight of the polymers and also the nature of the endgroups through suitable alterations in the experimental procedure. Except for CuTAE we have not studied the effect of such changes in reaction conditions.

Heat Stability and Pyrolysis

In Figure 2 thermogravimetric curves are given for the polymers listed in Table I. The curves for the copper polymers are very similar to those obtained previously⁴ for CuTAE chelates prepared by a different method. Initial weight losses, to about 200°C., for the Mg, Ni, Co, Zn, and Cd polymers are due to loss of water of hydration. Weight losses at higher temperatures are due to volatilization of pyrolysis products. The temperature at which pyrolysis first becomes appreciable under these conditions varies from about 225°C. to about 350°C. and is a function of the nature of the bonded metal. The order of decreasing heat stability, as judged by the curves in Figure 2, is $Mg > Ni > Co > Cu > Zn > Cd$. While the principal factor determining this order is undoubtedly the nature of the bonded divalent metal ion, the stabilities of adjacent members of the series are sufficiently similar that the order may be determined in part by such factors as the molecular weight of the polymer and the nature of the endgroups. However it should be noted that the results obtained here (Fig. 2) for CuTAE polymers and also those obtained previously,⁴ indicate that heat stability is relatively insensitive to the synthetic method employed and to the nature of the endgroups.

The heat stabilities of the polymeric materials studied here appear to be of the same general magnitude as those of the structurally analogous metal acetylacetonates.^{4,6,7} Except for the copper chelates,⁴ a closer comparison is probably not justified because of the different experimental methods which have been used in studying the two classes of materials.* The order of decreasing heat stability for the divalent metal acetylacetonates has been determined to be $\text{Ni} > \text{Cu} > \text{Co}$ and $\text{Mg} > \text{Zn}, \text{Cd}$.^{6,7}

It was of interest to compare the heat stabilities of the TAE polymers with that of metal-free TAE.⁴ The Cu, Zn, and CdTAE polymers are

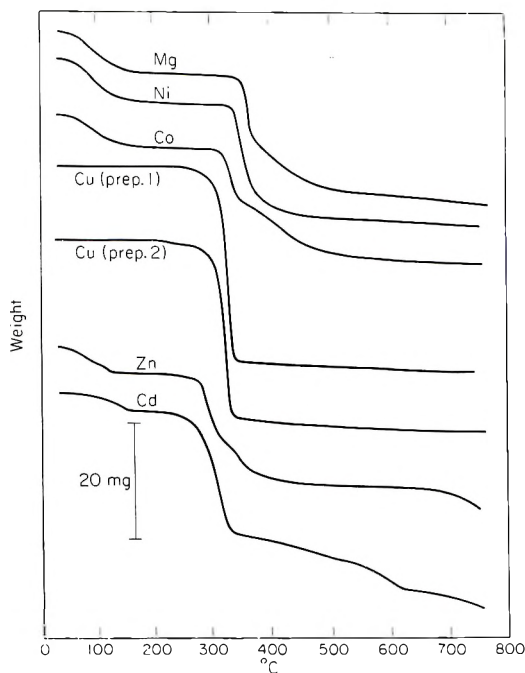


Fig. 2. Weight loss vs. temperature curves for divalent metal tetraacetylene polymers (50 mg. samples) heated in argon at atmospheric pressure.

less heat stable than is TAE, while the Mg, Ni, and CoTAE materials have higher heat stabilities than does TAE.

The nature of the gaseous products of decomposition was determined by means of mass spectrometric analysis. The results are listed in Table II. In each case the products detected were hydrogen, methane, carbon monoxide, carbon dioxide, and acetone. These products are also among those which result from the pyrolysis of the structurally analogous metal acetylacetonates⁷ and, except for acetone, were also found in our earlier work with CuTAE polymers.⁴

* Many of the acetylacetonates are sufficiently volatile to make results obtained with the thermobalance difficult to interpret.

TABLE II
Gaseous Products from the Pyrolysis of Metal Tetraacetylene Polymers at 400°C. in Argon (4 Hr.)

| M | Gas, moles/total g.-atom M | | | | |
|-----------------|----------------------------|-----------------|------|-----------------|---------|
| | H ₂ | CH ₄ | CO | CO ₂ | Acetone |
| Cu ^a | 0.11 | 0.05 | 0.12 | 0.34 | 0.01 |
| Ni | 0.87 | 0.39 | 0.10 | 0.75 | 0.00 |
| Co | 0.97 | 0.18 | 0.13 | 0.75 | 0.02 |
| Zn | 0.25 | 0.14 | 0.09 | 0.23 | 0.13 |
| Cd | 0.03 | 0.05 | 0.01 | 0.34 | 0.09 |
| Mg | 0.04 | 0.13 | 0.09 | 0.57 | 0.34 |

^a Preparation 2, Table I.

The products listed in Table III account for from 12% (Cu) to 62% (Mg) of the weight losses which the anhydrous polymers undergo when heated on the thermobalance to 400°C. (Fig. 2). The remainder of the weight loss is due to less volatile products which cannot be detected by the mass spectrometer under the experimental conditions used here. A major component of the latter fraction from each of the polymers (except MgTAE) was identified as 3,4-diacetyl-2,5-dimethylfuran (VII) by the infrared absorption spectra of the semisolids which condensed on the reaction tube outside the furnace. Each of the spectra also contained a broad absorption peak at about 3400 cm.⁻¹ which we attribute to water formed through dehydration of initially formed TAE to produce VII.⁴ (With the different experimental conditions used previously⁴ water could be measured in the gas phase with the mass spectrometer.) Tetraacetylene itself was not detected by the spectra. The appearance of the spectra, however, suggested that smaller amounts of organic products other than VII were probably also present. The spectrum of the condensate from the MgTAE polymer differed from the other spectra in that little,

TABLE III
Nonvolatile Residues from the Pyrolysis of TAE Polymers in Argon

| Preparation no. | M identified by x-ray diffraction | | Elemental analyses | |
|-----------------|-----------------------------------|---------------------|--------------------|------|
| | 400°C. ^a | 750°C. ^b | C, % | H, % |
| 2 | Cu ^c | Cu ^c | 22.9 | 0.80 |
| 3 | Ni ^c | Ni ^c | 46.5 | 0.82 |
| 4 | Co ^d | Co ^e | 50.3 | 0.92 |
| 5 | ZnO ^e | ZnO ^e | 30.6 | 1.16 |
| 6 | Cd, CdO ^e | — | 90.3 | 2.50 |
| 7 | MgO | MgO ^e | 34.7 | 1.04 |

^a Heated 4 hr. at 400°C. in argon.

^b Heated to 750°C. on the thermobalance in argon (2.1°C./min.).

^c Also weak unidentified lines.

^d Also a strong unidentified pattern not due to hydroxide, oxide, or carbonate.

^e Plus a trace of CdCO₃.

if any, VII appeared to be present. The species responsible for the absorption peaks observed in this case were not identified. Principal absorption peaks were at 3400, 2950, 1705, 1625, 1605, 1437, 1378, 1324, 1281, 1179, 1030, 961, and 837 cm.^{-1} .

Elemental analysis of the dark brown or black nonvolatile residues from pyrolysis showed the presence of carbon and hydrogen in addition to metal (Table III). Except for CdTAE all the divalent metal initially present in the polymers was found in the residues. Cadmium metal is sufficiently volatile at the higher temperatures to partially volatilize from the residue. Analysis of the material which condensed above the furnace showed that 31% of the Cd initially present in the sample had volatilized at 750°C. This did not necessarily represent all the Cd metal formed, since separate thermogravimetric experiments with pure Cd metal showed that Cd began to volatilize appreciably at about 600°C. but had not volatilized completely at 750°C. under our experimental conditions. An x-ray diffraction powder pattern of the organic residue from the pyrolysis of CdTAE at 750°C. did not show the presence of metallic Cd or other crystalline species. This may be due to segregation, since the Cd metal formed melts and flows away from the organic portion of the residue. Any cadmium remaining bonded in the latter must be in an amorphous form.

X-ray powder patterns show that CuTAE, NiTAE, and CoTAE yield the free metals upon pyrolysis, while ZnTAE and MgTAE give the oxides (Table III). At the lower temperatures CdTAE gives a mixture of metal and oxide. A means for estimating the amount of free Ni and Co produced by pyrolysis is provided by the fact that these metals are ferromagnetic. The ferromagnetism of the residues obtained by heating the NiTAE and CoTAE polymers 4 hr. at 400°C. was measured. The results showed that 87% of the Ni content and 60% of the Co content of the respective polymers had been converted to the free metals under the experimental conditions employed. The remainder of the metal may continue to be bonded within metal chelate ring structures as was previously postulated for the CuTAE polymers.⁴

It appears possible to explain the pyrolysis results obtained here by a mechanism similar to that previously suggested for the CuTAE chelates.⁴ This involves, as an initial step, dehydrogenation to form more highly conjugated polymeric species in which the metal chelate ring systems are retained. The hydrogen released during this process may be liberated as the gas, or it may react with remaining starting material to reduce part of the bonded metal to the metallic form, with the concomitant formation of TAE.⁴ The latter dehydrates to form the observed compound VII.⁴ Other observed products (Table II) may then result from the pyrolysis of VII. The formation of the oxides by the less easily reducible metals may also involve the attack of the chelate ring by H_2 with the formation of metal oxide, TAE, and unidentified organic products derived from TAE through the loss of oxygen atoms. The pyrolysis of the MgTAE polymer must proceed by a somewhat different mechanism, since VII is not observed among the products.

EXPERIMENTAL

Polymer Preparation

A 50-ml. portion of methanol was added to 396 mg. (2×10^{-3} mole) of tetraacetylene⁸ in a small flask; 4 ml. of 1.00 *M* aqueous KOH was added by pipet and the mixture was stirred until the TAE had dissolved. To this, 10-ml. of 0.200 *M* aqueous metal acetate solution was then added dropwise from a buret over a period of 1 hr. (For preparation 1, 8.3 ml. was used.) The mixture was stirred continuously during the addition with a magnetic stirrer. The polymer usually started to precipitate after the first few drops of metal acetate solution had been added. Stirring was continued for 1 hr. following the addition of metal acetate. The solid was then filtered off on a sintered glass filter, washed with 100 ml. of methanol in small portions, and air-dried at room temperature for 1 week. The filter cake was broken to a fine powder in a mortar and stored in a tightly capped vial to prevent further changes in hydration.

The moist CoTAE polymer was found to oxidize readily in the air. All operations for this material were therefore carried out in an atmosphere of nitrogen. The dry, hydrated, Co polymer was stable to air.

Analyses

Divalent metal was determined by conventional methods after destruction of the organic portion of the materials with acid. Potassium was determined by flame photometry. Carbon and hydrogen analyses were performed by the Galbraith Laboratories, Knoxville, Tennessee.

The quantity of bound tetraacetylene in the polymers was determined indirectly by determining the amount left in the filtrates from their preparation. A 1.00-ml. aliquot of the filtrate was mixed with 5 ml. of a 0.1*M* solution of acetic acid in 95% ethanol. The resulting solution was diluted to 100 ml. with 95% ethanol, and the absorbance of the solution was measured at 285 $m\mu$. The concentration of TAE could then be calculated from this value and the spectral data of Martin, Fernelius, and Shamma.⁹

Spectrophotometric Titrations

Titration were carried out in the same manner as for the preparations described above. At intervals during the titrations, 0.100 ml. portions of filtrate were withdrawn through a fine sintered glass filter into a micro-syringe. Each aliquot was mixed with 2.5 ml. of 0.1*M* acetic acid in 95% ethanol and the solution made up to 50 ml. with 95% ethanol. The absorbance at 285 $m\mu$ was measured with a Cary model 14 spectrophotometer in 1 cm. quartz cells.

Thermogravimetric Experiments

These were conducted in a stream of argon at atmospheric pressure, as described previously.⁴ The rate of temperature increase was 2.1°C./min.

Gas Evolution Experiments

Samples (100 mg.) of the polymers were dehydrated by heating for 1 hr. at 100°C. in a vacuum oven. Each dehydrated sample was placed in a Pyrex glass reaction tube equipped with standard taper glass joints and a stopcock arrangement. The apparatus was flushed repeatedly with high purity argon and then sealed, by means of the stopcock, at a pressure of 535 mm. Hg. That portion of the tube containing the sample was heated in a constant temperature furnace at 400°C. for 4 hr. Volatile pyrolysis products were free to distill to cooler portions of the tube. After cooling to room temperature the tube was attached to the inlet of the mass spectrometer and the gas phase analyzed.⁷ The mass spectrometer, when used in this way, detects only gaseous products or those having high vapor pressure at room temperature.

Magnetic Susceptibility Measurements

These were made by the Faraday method.¹⁰ The metal contents of the pyrolysis residues were calculated from the saturation magnetic moment values: $\sigma_s = 54.4$ e.m.u./g. and $\sigma_s = 161$ e.m.u./g. for Ni and Co metals respectively.¹¹ The susceptibility of the Co residue was determined as a function of magnetic field and the value extrapolated to infinite field taken for calculation.

The writer is grateful to Mrs. M. A. Dolan and to Miss A. Perrotto for help in the experimental portion of this work. He is indebted to Dr. W. M. Hickam for the mass spectrometer results, to Dr. A. Taylor for the x-ray diffraction analyses, and to Dr. D. E. Cox for the magnetic susceptibility measurements.

References

1. Kenney, C. N., *Chem. & Ind. (London)*, **1960**, 880.
2. Berlin, A. A., and N. G. Matveeva, *Russ. Chem. Revs.*, **29**, 119 (1960) [English translation of *Uspekhi Khim.*, **29**, 277 (1960)].
3. Sowerby, D. B., and L. F. Audrieth, *J. Chem. Educ.*, **37**, 134 (1960).
4. Charles, R. G., *J. Phys. Chem.*, **64**, 1747 (1960).
5. Martin, D. F., and W. C. Fernelius, *J. Am. Chem. Soc.*, **81**, 1509 (1959).
6. Charles, R. G., and M. A. Pawlikowski, *J. Phys. Chem.*, **62**, 440 (1958).
7. Von Hoene, J., R. G. Charles, and W. M. Hickam, *J. Phys. Chem.*, **62**, 1098 (1958).
8. Charles, R. G., *Org. Syntheses*, **39**, 61 (1959).
9. Martin, D. F., W. C. Fernelius, and M. Shamma, *J. Am. Chem. Soc.*, **81**, 130 (1959).
10. Selwood, P. W., *Magnetochemistry*, 2nd Ed., Interscience, New York, 1956, p. 11.
11. Bozorth, R. M., *Ferromagnetism*, Van Nostrand, New York, 1951.

Synopsis

Polymeric materials have been prepared by the reaction of the divalent Cu, Ni, Co, Zn, Cd, and Mg cations with the dipotassium salt of tetraacetylene in methanol-water solutions. The polymers appear to be of low molecular weight and generally contain potassium in the endgroups. The insoluble, infusible, materials decompose on heating in the absence of air to give, among other products, H₂, 3,4-diacetyl-2,5-dimethylfuran, and the free metal or metal oxide. The order of decreasing heat stability is Mg > Ni >

Co > tetraacetylthane > Cu > Zn > Cd. The Cd chelate polymer decomposes appreciably at 225°C., while the Mg polymer, heated under the same conditions, begins to decompose at about 350°C.

Résumé

On a préparé des polymères en faisant réagir les cations divalents Cu, Ni, Co, Zn, Cd et Hg avec le sel dipotassique du tétracétylthane dans un mélange méthanol-eau. Les polymères semblent être de faible poids moléculaire et contiennent généralement du potassium dans les groupes terminaux. Le matériau obtenu, insoluble et infusible se décompose par chauffage en absence d'air pour fournir, parmi d'autres produits, H₂, du 3,4-diacétyl-2,2-diméthylfuran, et le métal libre ou l'oxyde métallique. La diminution de stabilité thermique suit l'ordre suivant: Mg > Ni > Co > tétracétylthane > Cu > Zn > Cd. Le polymère chélaté avec le Cd se décompose d'une façon appréciable vers 225°C tandis que le polymère chélaté avec le Mg, chauffé dans les mêmes conditions commence à se décomposer aux environs de 350°C.

Zusammenfassung

Durch Reaktion der zweiwertigen Kationen, Cu, Ni, Co, Zn, Cd und Mg mit dem Dikaliumsalz von Tetraacetyläthan in Methanol-Wasser-Lösung wurden polymere Stoffe dargestellt. Die Polymeren scheinen niedrigmolekular zu sein und enthalten im allgemeinen Kalium in der Endgruppe. Die unschmelzbaren, unlöslichen Stoffe zersetzen sich beim Erhitzen unter Luftausschluss und liefern unter anderem H₂, 3,4-Diacetyl-2,5-dimethylfuran und das freie Metall oder Metalloxyd. Die Hitzebeständigkeit nimmt in folgender Reihe ab: Mg > Ni > Co > Tetraacetyläthan > Cu > Zn > Cd. Das Cd-Chelatpolymere zersetzt sich bei 225°C merklich, während das Mg-Polymere beim Erhitzen unter gleichen Bedingungen sich bei etwa 350°C zu zersetzen beginnt.

Received September 25, 1961

Revised October 27, 1961

Radiolysis of the Isomeric Poly(butyl Methacrylates)*

ISRAEL S. UNGAR,† JOHN F. KIRCHER, WILLIAM B. GAGER,
FRANCIS A. SLIEMERS, and ROBERT I. LEININGER, *Battelle
Memorial Institute, Columbus, Ohio*

INTRODUCTION

Of the numerous chemical reactions which have been found to be effected by radiation, polymerizations and copolymerizations are perhaps of the greatest interest industrially. The technique of graft and block copolymerization is of particular interest because it offers a new dimension in structural variation of polymers. As a direct result of these different structures, novel and unique properties are obtained. Of the methods which are available, radiation is perhaps most flexible and gives the most precise control of the grafting process.

The present investigation was undertaken to increase our understanding of the first step in the copolymerization process, free-radical site formation. The four butyl methacrylate polymers have been employed in this study.

EXPERIMENTAL

Radiation Source

All irradiations were performed in a Co₆₀ gamma facility. The geometry of the source used in this work yields a dose rate of about 2.0×10^5 rads/hr., as measured with a CO₂-graphite ion chamber. The ion chamber was calibrated with the ferric-ferrous dosimeter, and corrections were made for the difference in electron density between the systems.

Polymer Preparation

All polymers were prepared by irradiation polymerization from purified monomers, as previously described.¹ Following preparation, the polymers were powdered and were deactivated by heating *in vacuo*.

Determination of Polymer-Free Radicals

The polymers were irradiated *in vacuo*, and free-radical concentrations were determined by electron paramagnetic resonance (EPR) measure-

* This work has been supported by the Office of Isotope Development under AEC Contract W-7405-eng-92.

† Present address: Nitrogen Division, Allied Chemical Corporation, Hopewell, Virginia.

ments and calculated both from decreases in number-average molecular weight and from the types and concentrations of major irradiation products formed.

A Varian V-4500 spectrometer (Varian Associates, Palo Alto, California) was used for EPR measurements. Polymer molecular weights were determined with the Menzies-Wright boiling-point-elevation apparatus. A comparison of the M_n values before and after irradiation was used to measure the number of backbone scissions occurring. An estimate of free-radical concentration was obtained by assuming that each backbone scission was accompanied by the formation of one stable free-radical site.

Determination of Products in Irradiated PBMA by Mass Spectrometry and Vapor-Phase Chromatography

Two 5-g. samples of polymer were sealed *in vacuo* in reaction tubes of the type shown in Figure 1 and irradiated to approximately 3×10^7 rads. One sample was analyzed for highly volatile materials, and the other for higher molecular weight constituents.

Results

Samples of poly(*n*-butyl methacrylate) (PnBMA), poly(*sec*-butyl methacrylate) (PsecBMA), poly(isobutyl methacrylate) (PisoBMA), and poly(*tert*-butyl methacrylate) (PterBMA) were irradiated to various dosages and the number of free-radical sites formed was determined by EPR measurements. It was found (Fig. 2) that the efficiency of site formation, expressed as concentration of free-radical sites per monomer unit, is greater for the branched esters than for the normal one.

An interesting feature of the sites versus dose data is that the log-log curve not only deviates from a straight line but passes through a maximum. Further, at high doses ($\sim 5-6 \times 10^7$ rads) the total number of available sites has decreased to a point considerably below the number present after short-term irradiations at the same dose rate. This behavior is indicative of two or more opposing reactions in which long-lived free-radical sites are formed and/or destroyed. A somewhat similar result has been obtained with poly(methyl methacrylate).^{2,3}

One would generally expect the rate of formation of radicals to remain constant at a fixed dose rate and temperature. As the concentration of radicals increases, the rate of their reactions would increase and the rate of increase of radical concentration with dose would be less. Eventually a steady state would be achieved, characteristic of the dose rate and temperature, and the concentration of radicals would not change with further irradiation. The fact that no steady state was obtained, but rather the radical concentration actually decreased with increasing dose indicates either that the radical-initiating reactions have decreased or that some additional radical-terminating reactions have become the controlling factors in the overall mechanism. The latter possibility seems more likely than the former. The nature of the reactions is not at all well understood.

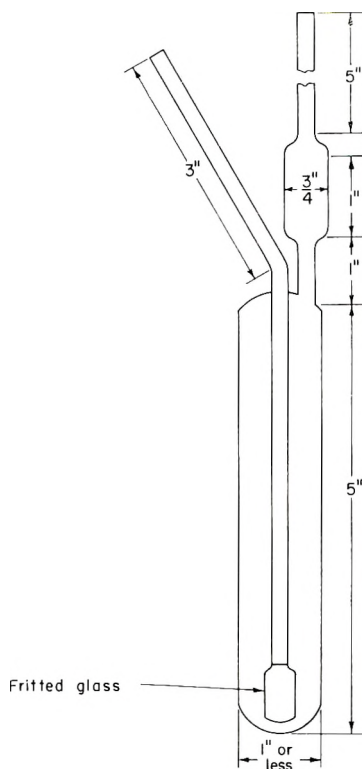


Fig. 1. Pyrex reaction tube.

It may be that irradiation has decreased the molecular weight and, hence, increased radical mobility so that the rate of all radical termination steps is increased. This problem is still under investigation.

For the decay studies (Fig. 3), samples of three of the isomeric polymers were irradiated *in vacuo* to a total dose of 5.5×10^7 rads. This dose was,

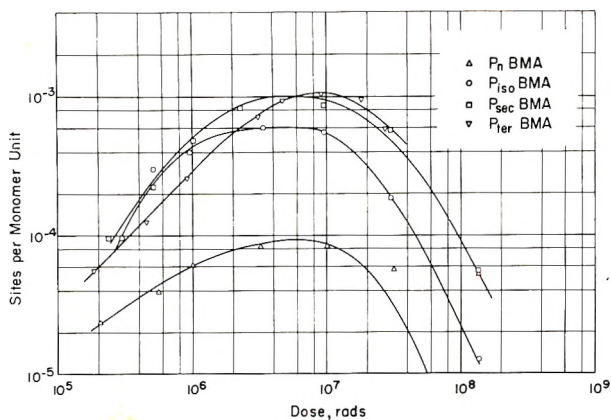


Fig. 2. Sites per monomer unit vs. dose for poly-(butyl methacrylates): (Δ) P_nBMA; (\circ) P_{iso}BMA; (\square) P_{sec}BMA; (∇) P_{ter}BMA.

in each case, considerably in excess of that at which the maximum site concentration was obtained. The polymers were allowed to decay at room temperature. The number of free-radical sites in each sample was determined periodically after irradiation. In all cases, decay was quite rapid at first, but gradually decreased until a nearly constant number of sites remained. This is in qualitative agreement with the work of others.² The level portion of the curve was not obtained for PnBMA. After about 30 hr., the number of sites in the polymer sample had fallen below the level of sensitivity of the EPR spectrometer.

Although the decay data are limited, it is apparent that the slope of the decay curve does not remain constant over a very wide concentration range. The data do not seem to fit any integral-order rate expression, indicating

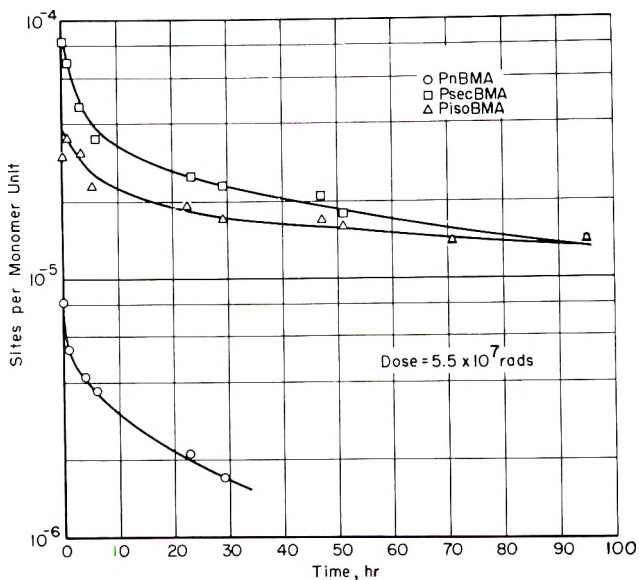


Fig. 3. Free-radical decay curves for poly(butyl methacrylates): (○) PnBMA; (□) Psec BMA; (△) Piso BMA.

that several radical species may be reacting at various rates. It is tentatively concluded that (1) at least two, and probably more, distinct types of free-radical sites are formed during irradiation, and (2) the total number of sites formed is influenced by the structure of the hydrocarbon tail of the ester side chain.

The concentrations of the various products obtained from the irradiation of the butyl methacrylate polymers, expressed as mole per cent of total products, are listed in Table I. The minimum yields of total products found were 193, 239, 290, and 470 μ moles, respectively, for the *n*-butyl, *iso*-butyl, *sec*-butyl, and *tert*-butyl polymers. These product yields may be low for some of the higher molecular weight materials. The high yield of products from the *tert*-butyl polymer compared to that of the other butyl isomers

TABLE I
Products of Irradiated Poly(butyl Methacrylate)^a

| Product | Concentration of product in indicated polymer, mole-% | | | |
|------------------------------|---|---------|---------|---------|
| | PnBMA | PisoBMA | PsecBMA | PterBMA |
| Carbon dioxide | 12.8 | 18.1 | 32.2 | 64.1 |
| Carbon monoxide ^b | 26.7 | 28.4 | 16.5 | 7.1 |
| Hydrogen ^b | 26.1 | 20.0 | 16.5 | 6.5 |
| Methane ^b | 0.7 | 1.3 | 0.5 | 5.4 |
| Ethane | 0.5 | 0.1 | 2.6 | 0.2 |
| Propane | 0.3 | 7.8 | 0.3 | — |
| <i>n</i> -Butane | 16.2 | 0.4 | 10.7 | — |
| Isobutane | — | 8.2 | — | 2.2 |
| Isobutene | — | — | — | 8.2 |
| Methyl formate | — | Trace | 0.1 | 0.1 |
| Ethyl formate | 0.3 | 1.1 | 1.7 | — |
| Propyl formate | 0.1 | 0.2 | 4.6 | — |
| <i>n</i> -Butyl formate | 8.1 | — | Trace | — |
| Isobutyl formate | 1.1 | 9.3 | — | — |
| <i>sec</i> -Butyl formate | 0.3 | 0.5 | 0.6 | — |
| <i>tert</i> -Butyl formate | 0.1 | 0.1 | — | 0.2 |
| <i>n</i> -Butyl alcohol | 3.5 | — | — | — |
| Isobutyl alcohol | 2.5 | 3.4 | — | 5.1 |
| <i>sec</i> -Butyl alcohol | 0.7 | 1.1 | 5.7 | 0.1 |
| <i>tert</i> -Butyl alcohol | — | — | — | 0.8 |

^a Five-gram samples of polymer were irradiated to a dose of 3×10^7 rads.

^b Determined by mass spectrometry.

is believed to be due to a combination of steric and inductive effects which make complete ester removal the predominant radiation-produced scission.

Another point of interest is the formation of a high concentration of isobutene in the case of the *tert*-butyl polymer. Similar results were obtained by Grant and Grassie,⁴ who studied the thermal decomposition of this material. However, they found that the corresponding polyacid was formed with the isobutene. This cannot be the case in the present study, since more CO₂ than isobutene was formed. This is a point of significant difference between the thermal and radiation-induced decomposition of poly(*tert*-butyl methacrylate).

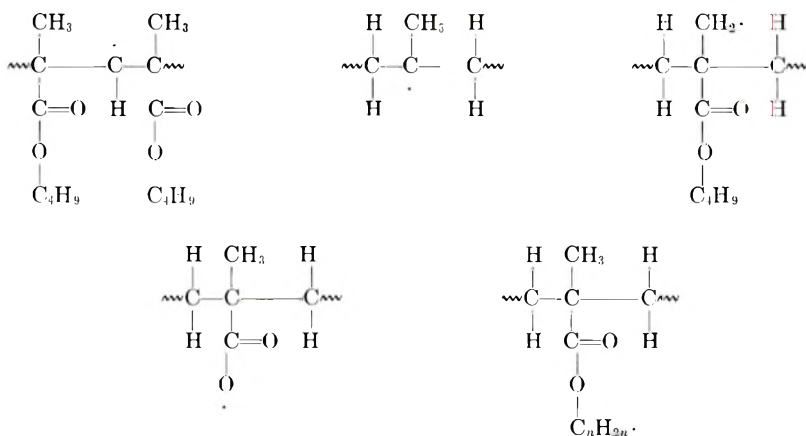
In addition to the EPR and product measurements, the number-average molecular weights of the polymers were determined both before and after irradiation. These results are listed in Table II.

TABLE II
Effect of Irradiation on the Number-Average Molecular Weight of the Poly(butyl Methacrylates)^a

| | PnBMA | PisoBMA | PsecBMA | PterBMA |
|-----------------------------------|-------|---------|---------|---------|
| \bar{M}_n before irradiation | 5960 | 5870 | 6930 | 3580 |
| \bar{M}_n following irradiation | 4170 | 4050 | 5150 | 2665 |

^a A dose of 3.0×10^7 rads was employed.

Analysis of the data of Table I indicates that the most probable free-radical types on the polymer backbone are:



The calculated maximum concentrations of the various backbone free-radical types predicted from the products if no site-destroying or site-

TABLE III
Estimated Concentrations of Various Free Radicals on the Polymer Chain in Irradiated Poly(butyl Methacrylates)^a

| Type of free radical | Concentration, sites per monomer unit $\times 10^3$ | | | |
|---|---|---------|---------|---------|
| | PnBMA | PisoBMA | PsecBMA | PterBMA |
| | 2.7 | 3.9 | 5.3 | 9.6 |
| | 0.3 | — | — | — |
| Formed from abstraction of a hydrogen directly from the polymer backbone, from a methyl group, or from the hydrocarbon tail of the ester group ^d | 4.7 | 5.0 | 5.4 | 3.6 |
| Total | 7.7 | 8.9 | 10.7 | 13.2 |

^a Based on results obtained from gas chromatography and mass spectrometry following irradiation of 5-g. samples of polymer to a dose of 3.0×10^7 rads.

^b Calculated from sum of concentrations of CO, CO₂, and ester.

^c Calculated from concentration difference between hydrocarbon and CO₂.

^d Calculated from sum of the concentrations of hydrocarbon (excluding isobutene in the case of the *tert*-butyl polymer), hydrogen, alcohol, and formate.

rearranging reactions occur, are listed in Table III. It should be pointed out that crosslinking, double-bond formation, recombination, etc., could, and probably do, reduce the concentrations of these radicals. Further, rearrangement reactions may cause changes in the position of the free radical. Moreover, in cases where chain scission accompanies free-radical formation, the position of the free-radical site will not be as shown. Consequently, the types described in Table III represent the molecular arrangement which would be predicted if no rearrangement occurs.

Table IV compares site formation in the four isomeric polymers as measured by EPR, calculated from product analyses, and calculated from molecular weight data. The numbers of sites calculated from the analytical and molecular weight data are considerably greater than those determined by EPR. This is to be expected since many relatively short-lived sites might be predicted from the product analyses but not detected by EPR. From the initial slope of the decay curves, it is apparent that many radicals do not have long lifetimes. It is probable that only those radicals with lifetimes of the order of minutes or longer are measured by EPR.

TABLE IV
Site Formation in Poly(butyl Methacrylates) Irradiated to a Dose of 3.0×10^7 Rads

| Method | Concentration, sites per monomer unit $\times 10^3$ | | | |
|---|---|---------|---------|---------|
| | PnBMA | PisoBMA | PsecBMA | PterBMA |
| Product analysis ^a | 7.7 | 8.9 | 11 | 13.2 |
| By molecular-weight decrease ^b | 10 | 11 | 7.1 | 13.6 |
| Measured by EPR | 0.06 | 0.2 | 0.6 | 0.58 |

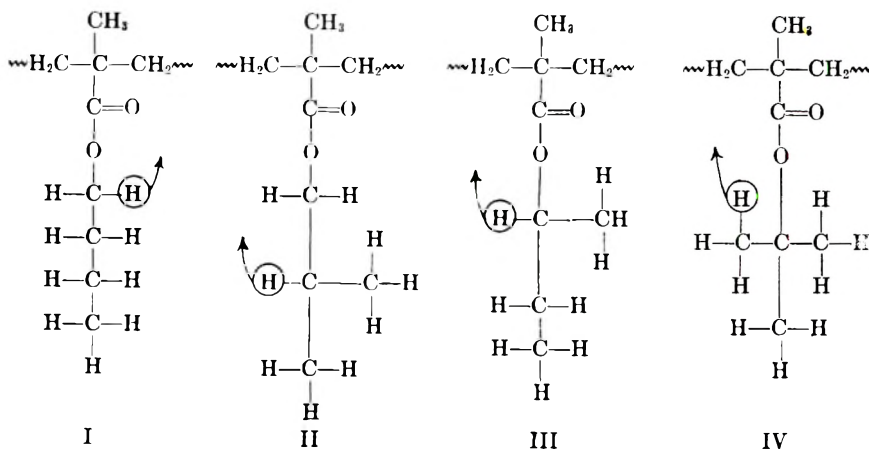
^a Calculated from data presented in Table I.

^b Assuming one stable site per chain scission.

On the basis of the volatile-product data of Table IV, approximately one backbone scission occurs for each free radical that is formed. This represents about one scission per 100 monomer units, or one scission per two to three molecules of polymer at a dose of 3×10^7 rads.

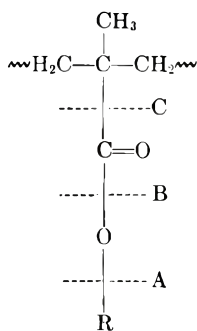
DISCUSSION

Since the number of free-radical sites for a given total dose differs among the four isomers, it is probable that free-radical formation originates on, or is influenced by, the hydrocarbon portion of the ester side chain. The first step may be the removal of a hydrogen from the ester leaving an unpaired electron. Since the ease of removal of hydrogen to form free radicals follows roughly in the ratio of 33:3:1⁵ for tertiary:secondary:primary hydrogen, total site concentration in the butyl methacrylates should increase in the order *tert* < *n* < *iso* = *sec*.

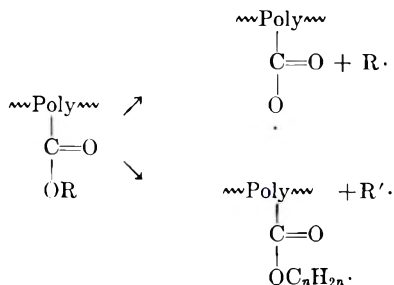


However, the inductive and steric effects produced by the various butyl configurations must also be factors, since more free radicals are formed by the *tert*-butyl than by any of the other polymers and since more are formed by the *sec*-butyl than by the isobutyl polymer. More recent work³ with other methacrylate systems has emphasized the importance of these effects.

Following hydrogen scission, the reaction progresses with breaks occurring at A, B, or C:

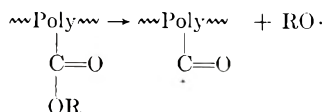


The proportion of each break is a function of polymer structure. Scission at A produces a hydrocarbon radical but does not produce CO or CO₂. It may be a complete hydrocarbon scission in which case only butanes would be formed or it may be a partial hydrocarbon scission, a C₁ to C₃ hydrocarbon being formed.



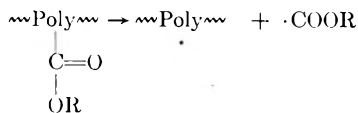
It is very interesting that this type of reaction does not readily occur. In the *n*-butyl polymer there is some evidence for it. There is a slight excess of butane over CO₂. In all other cases, there is more CO₂, even considering CH₄ which might not originate at the ester groups. In the case of the *n*-butyl polymer the poly—COO· or poly—COOC_{*n*}H_{2*n*}· radical picks up a hydrogen or other scavenger specie or crosslinks with another active polymer site.

Scission at B would produce an alkoxy radical:



The presence of the corresponding polymer free radical would be indicated by an excess of alcohol over CO. Scission at B occurs only in combination with scission at C, since the concentration of CO is equal to or greater than the concentration of alcohol for all of the butyl isomers.

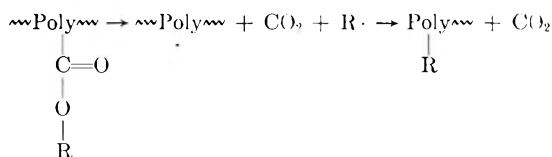
Scission at C produces the polymer radical and a formyl radical:



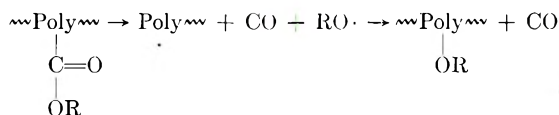
The formyl radical may then decarboxylate, decarbonylate, or react with a hydrogen to form the corresponding formate. The maximum concentration of the polymer free radical is determined by summing up the concentrations of CO, CO₂, and formate. The data indicate that scission at C is the major reaction occurring at the ester group.

Obviously, the formate production is not as simple as the above reaction would seem to indicate. In the case of the *n*-butyl and isobutyl polymers, the corresponding formate is by far the major formate produced (~90%). The *sec*-butyl formate, however, constitutes only about 58% of the formate produced. Therefore, significant formate is produced as a result of other reactions, such as removal of methane or ethane. In the case of the *tert*-butyl polymer, there was no formate among the major products, i.e., scission at C is always accompanied by scission at A or B.

Since more CO₂ is formed than hydrocarbon in all but the case of the *n*-butyl polymer, it is possible that decarboxylation is followed by hydrocarbon recombination with the polymer chain:

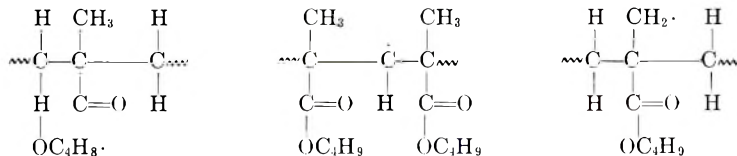


Similarly, where more CO is formed than alcohol, the following recombination reaction may occur:



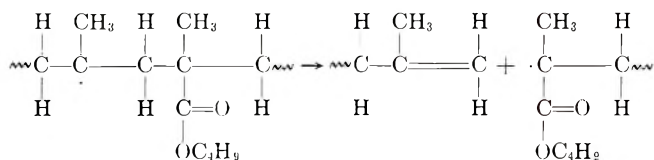
The two recombination reactions have not been considered in estimating concentrations of the various polymer free radicals because the supposition is required that all hydrocarbon and alkoxy free radicals reattach to the polymer chain. This would tend to make the estimate of polymer radical concentrations high.

In addition to scissions at positions A, B, and C, additional polymer free radicals are formed by means of hydrogen scissions from the hydrocarbon tail of the ester, from the methyl group, and directly from the polymer backbone. Some methyl radical backbone scissions may also occur, but the product analyses reveal that little reaction of this type takes place. The polymer free radicals produced by hydrogen scissions are of the type



The maximum total concentration of these free radicals has been estimated from the sum of the concentrations of hydrocarbon (excluding isobutene in the case of the *tert*-butyl polymer), hydrogen, alcohol, and formate. The EPR spectra appear to confirm the supposition that several types of stable free radicals exist.

Backbone scissions, as evidenced by a decrease in molecular weight following irradiation, are probably produced by means of a molecular rearrangement of the type:



Several effects due to the molecular arrangement of the hydrocarbon tail of the ester group are also predictable. These may be summarized as follows. (1) As branching increases, the number of sites increase. This indicates that the additional sites are on the ester or are, at least, influenced by the presence of the particular ester. (2) The rate of formation, as well as the stability of these sites, increases with increased branching. This may be illustrated by a comparison of the ratios of G_{sites} for the branched and unbranched hydrocarbon tails at zero time and at a dose of 3.0×10^7 rads (Table V). The initial free-radical rates of formation were estimated by obtaining yields (G values) at low doses and extrapolating to zero dose. In this low dose range, below about 5×10^5 rads, the G value was essentially independent of dose. (3) Decarboxylation of the ester side chain also

TABLE V

| | G _{site} Ratio | |
|---------|-------------------------|--------------------------|
| | Initial | 3 × 10 ⁷ rads |
| PnBMA | 1 | 1 |
| PisoBMA | ~2.5 | 3.3 |
| PnBMA | ~2.5 | 10 |
| PsecBMA | ~2.5 | 10 |
| PnBMA | ~2.5 | 10 |
| PterBMA | ~2.5 | 10 |
| PnBMA | | |

increases with branching. (4) Amounts of CO₂ greater than hydrocarbon are formed for the branched polymers and amounts of CO equal to or greater than alcohol are formed for the normal, as well as the branched, polymers (Table VI). Consequently, some sites on the backbone which would lead to scission must be terminated before scission through a recombination of hydrocarbon and/or alkoxy radicals with the sites. In the case of the PnBMA, more hydrocarbon is formed than CO₂. Therefore, the hydrocarbon carbon-oxygen bond on the ester is being broken preferentially to the carbonyl carbon-polymer bond. The increase with branching of CO₂ formation relative to hydrocarbon indicates that the probability of this mechanism decreases. (5) A corresponding phenomenon may explain why, in some cases, the molecular weight decrease indicates a larger number of sites than the products formed. Just as the hydrocarbon and alkoxy radicals tend to neutralize the polymer radical before scission, the formyl radical may react with the polymer radical after scission.

SUMMARY

The effect of gamma irradiation on the production of free radicals in the four isomeric poly(butyl methacrylates) has been investigated. The total concentrations of free radicals were determined as a function of dose by

TABLE VI
Comparison of Yields of Major Products in the Poly(butyl Methacrylates)

| | Yield, μmoles | | | | | |
|---------|---------------|-----------------|--------------------------|---------|---------|--------------------|
| | CO | CO ₂ | Hydrocarbon ^a | Formate | Alcohol | Total ^b |
| PnBMA | 51.4 | 24.6 | 32.9 | 19.2 | 10.7 | 193 |
| PisoBMA | 67.8 | 43.1 | 39.4 | 25.9 | 12.7 | 239 |
| PsecBMA | 48.2 | 93.5 | 39.7 | 43.6 | 16.5 | 290 |
| PterBMA | 33.5 | 304.0 | 36.6 | 1.2 | 28.3 | 470 |

^a Refers to saturated hydrocarbon.

^b Includes yields of minor, as well as major products.

EPR. Molecular weight changes and the concentrations of volatile fragments, determined by mass spectrometry and gas chromatography, have also been used to calculate site concentrations. The latter technique has also permitted an estimate of the concentrations of the various types of polymer free radicals. A mechanism of free-radical formation is proposed. Differences in irradiation susceptibility attributable to the configuration of the ester site chain are discussed.

The authors wish to thank R. I. Iden, E. R. Blosser, and R. J. Jakobsen, of Battelle's Analytical Chemistry Division, for the gas-chromatographic, mass-spectrometric, and infrared analyses.

References

1. Ungar, I. S., W. B. Gager, and R. I. Leininger, *J. Polymer Sci.*, **44**, 295 (1960).
2. Ohnishi, W. I., and I. Nitta, *J. Polymer Sci.*, **38**, 451 (1959).
3. Sliemers, F. A., I. S. Ungar, E. Gulbaran, W. B. Gager, J. F. Kircher, and R. I. Leininger, to be published.
4. Grant, D. H., and N. Grassie, *Polymer*, **1**, 445 (1960).
5. Rice, F. O., and K. K. Rice, *The Aliphatic Free Radicals*, Johns Hopkins Press, Baltimore, Md., 1935, p. 100.

Synopsis

A study has been made of the effect of gamma irradiation on the production of free radicals in poly(butyl methacrylates). A mechanism of radiation attack on the polymers is proposed. Free-radical measurements and the determination of the products of irradiation have been used in establishing this mechanism. The effects of configuration of the ester chain on radiation susceptibility are discussed.

Résumé

On a étudié l'effet des rayons γ sur la production de radicaux libres dans les polyméthacrylates de butyle. On propose un mécanisme d'attaque par radiation sur les polymères. Pour établir ce mécanisme, on a utilisé des mesures de radicaux libres et on a déterminé les produits d'irradiation. Les effets de la configuration du chaînon ester latéral sur la sensibilité à l'irradiation ont été discutés.

Zusammenfassung

Der Einfluss von γ -Bestrahlung auf die Erzeugung freier Radikale in Polybutylmethacrylat wurde untersucht. Ein Mechanismus für die Einwirkung der Strahlung auf das Polymere wird angegeben. Die Messung der freien Radikale sowie die Bestimmung der Bestrahlungsprodukte wurde bei der Aufstellung dieses Mechanismus verwendet. Der Einfluss der Konfiguration der Esterseitengruppen auf die Strahlungsempfindlichkeit wird diskutiert.

Received October 30, 1961

Depolarization of Scattered Light in Solutions of Linear and Branched Polysaccharides

V. S. R. RAO and JOSEPH F. FOSTER, *Department of Chemistry, Purdue
University, Lafayette, Indiana*

Though it has been long recognized that measurement of the depolarization of the light scattered from polymer solutions should provide additional information on the polymer conformation, relatively few studies of this type have been reported. The depolarization properties may be defined through three ratios:

$$\begin{aligned}\rho_u &= H_u/V_u = (H_v + H_h)/(V_v + V_h) \\ \rho_v &= H_v/V_v \\ \rho_h &= V_h/H_h\end{aligned}\tag{I}$$

Here H and V denote the intensity of the horizontal and vertical components, respectively, of the light scattered at 90° . The subscripts u , v , and h refer to incident light which is unpolarized, vertically polarized, and horizontally polarized, respectively. Krishnan¹ showed that the depolarization ratios are regular functions of the size and shape of the molecules. A finite value of either ρ_v or ρ_h is an indication of finite size and anisotropy of the scattering particles. Krishnan¹ also related the three ratios through the equation

$$\rho_u = [1 + (1/\rho_h)]/[1 + (1/\rho_v)]\tag{II}$$

which was derived later by Perrin² on a rigorous mathematical basis. This relation has been verified experimentally.^{1,3,4}

Doty⁵ discussed, from a qualitative standpoint, the variation of these ratios and the individual components of the scattered light, for flexible and rigid molecules, with respect to concentration, solvent power and molecular weight. Some measurements of depolarization ratios for unbranched synthetic polymers have been reported.⁶⁻⁸

For flexible chain molecules, the anisotropy as a whole depends on two factors: (1) the intrinsic anisotropy of the statistical elements; (2) the form anisotropy of the structure of the molecule. Thus, coiling of the chains tends to annul the effect of the individual segments. Hence, it should be possible to obtain information about changes in structure and branching of molecules by measuring the ratios of the depolarization of the light scattered.

It was reported by Stacy⁹ that the intrinsic viscosity (in 1*N* KOH) for corn amylopectin and its β -amylase limit dextrin are 1.27 and 1.22 respectively. Their weight-average molecular weights are 80×10^6 and 30×10^6 . The drop in intrinsic viscosity in the formation of limit dextrin is smaller than might be expected on the basis of the large decrease in mass. Stacy and Foster¹⁰ have concluded from flow birefringence data that corn limit dextrin is more compact and isotropic than the parent amylopectin. At first it seems surprising that the molecule, by losing some of the branches, becomes more isotropic. Hence the present work was undertaken primarily to throw more light on the structure of amylose, amylopectin and limit dextrin. Secondly, as no such measurements have been made on branched molecules so far, these measurements have also been extended to dextran fractions in order to test Doty's predictions as regards the variation with concentration and solvent power of the individual components and the depolarization ratios of scattered light.

Experimental

A Brice-Phoenix light-scattering photometer was employed to measure the different components of the scattered light. The operation of the instrument was checked by determining the ρ_u values of water and benzene. The values obtained were 0.09 and 0.45 for water and benzene, respectively. These measurements were carried out with incident light of wavelength 5461 Å. (except for potato amylose solutions, where 4358 Å. light was used) in a cylindrical cell with narrow (4 mm.) slit diaphragm supplied by the makers. All the measurements were carried out at room temperature ($25 \pm 2^\circ\text{C}$).

Two dextran fractions, one corn amylopectin, and one corn β -amylase limit dextrin, one corn amylose, and three potato amylose subfractions were used for this work. The two dextran fractions (APC-48 and APC-49) were supplied by the Northern Utilization Research Branch, U.S.D.A. (NRRL B-512), and the molecular weights (\bar{M}_w) of these fractions are 71,000 and 131×10^6 , respectively. The corn amylopectin and β -amylase limit dextrin are the same samples used by Stacy and Foster¹⁰ and their molecular weights (\bar{M}_w) are 80×10^6 and 33×10^6 , respectively. The corn amylose fraction was prepared by R. L. Smith and its molecular weight is approximately 4.2×10^5 . The potato amylose was isolated from potato starch as described by Killion and Foster,¹¹ and subfractionation of this amylose was carried out in dimethylsulfoxide with absolute ethanol as a nonsolvent.¹² Three of these fractions were taken, designated as A, B, and C, and their molecular weights, determined by light scattering, are 2.4×10^6 , 1.14×10^6 , and 0.27×10^6 , respectively.

Doubly distilled water was used for both light-scattering work and the cleaning of the cells. Potassium hydroxide solution was prepared by dissolving analytical grade KOH in doubly distilled water. All the solutions were clarified by centrifuging at 15,000 rpm in a Servall angle centrifuge

and then filtering directly into the cell through fine Pyrex glass filters under pressure.

Results and Discussion

For each concentration all the components of the light scattered, i.e., H_u , V_u , H_v , V_v , H_h , and V_h , were measured.

The graphs of V_v/C versus C are shown in Figures 1 and 2. The V_v component constitutes practically all the light scattered at 90° . Hence

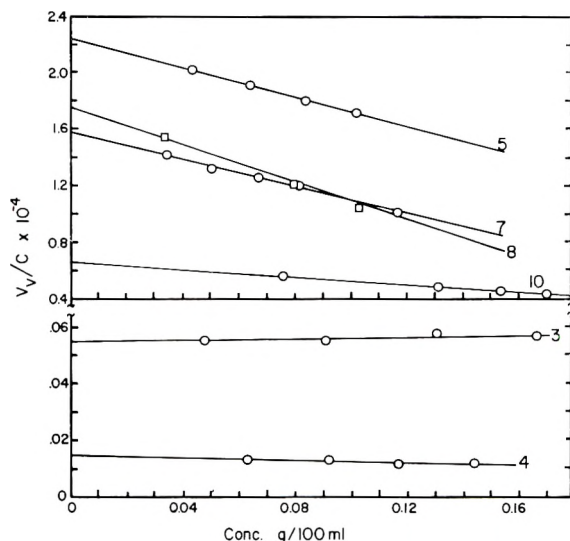


Fig. 1. Plots of V_v/C as a function of concentration: (1) high molecular weight dextran fraction in water; (2) high molecular weight dextran fraction in 0.5N KOH; (3) low molecular weight dextran fraction in water; (4) low molecular weight dextran fraction in 0.5N KOH; (5) corn amylopectin fraction in 0.5N KOH; (6) corn limit dextrin fraction in 0.5N KOH; (7) corn amylose in 0.5N KOH; (8) potato amylose fraction A in 1N KOH; (9) potato amylose fraction B in 1N KOH; (10) potato amylose fraction C in 1N KOH.

the V_v/C versus C curves will be essentially the inverse of HC/τ versus C and should decrease with concentration in a good solvent and should be independent of concentration in an ideal solvent.⁵ For amylose, V_v/C decreases with concentration in KOH, indicating that KOH is a good solvent. This is in agreement with data of Everett and Foster¹² on viscosity and light scattering. In case of amylopectin, V_v/C decreases with concentration, and this parameter remains constant for limit dextrans. For dextran fractions in water, V_v/C increases very little with concentration, showing that water is an indifferent solvent. In KOH both the fractions show decreasing values with increasing concentration, showing this to be a better solvent. (In all the cases the value of V_v at infinite dilution is not corrected for intraparticle interference since we are interested in the variation of this component with concentration.)

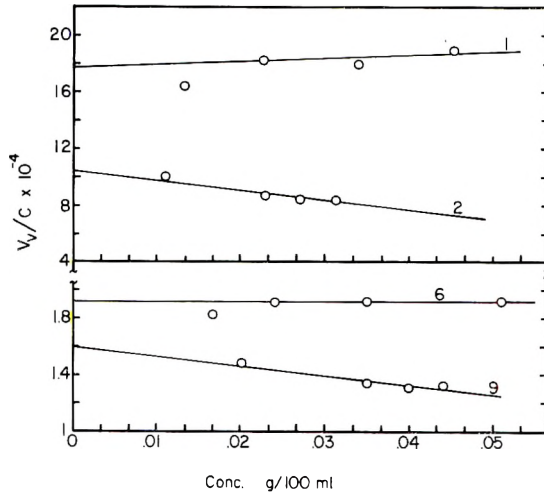


Fig. 2. Plots of V_v/C as a function of concentration. Numbering of curves is the same as in Fig. 1.

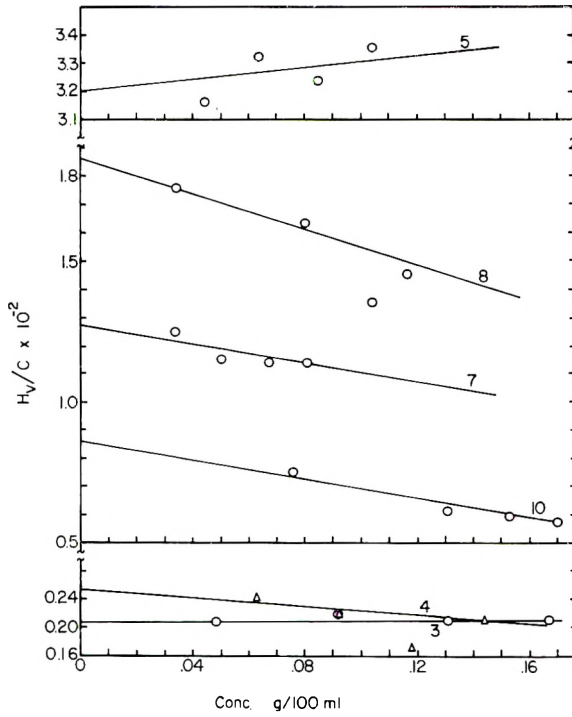


Fig. 3. Plots of H_v/C as a function of concentration. Numbering of curves is the same as in Fig. 1.

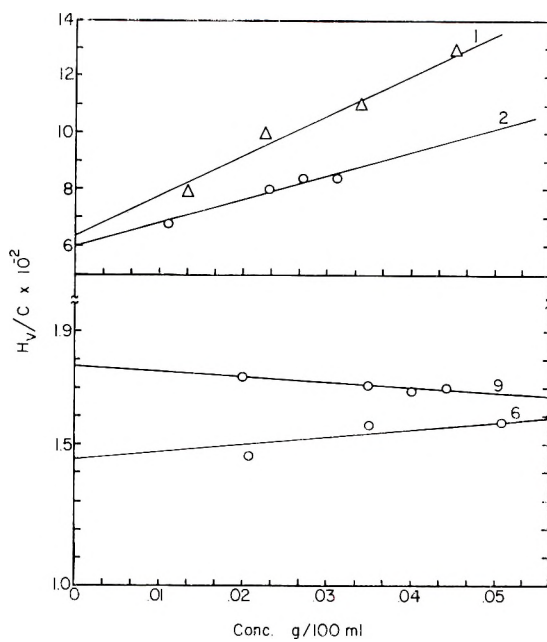


Fig. 4. Plots of H_v/C as a function of concentration. Numbering of curves is the same as in Fig. 1.

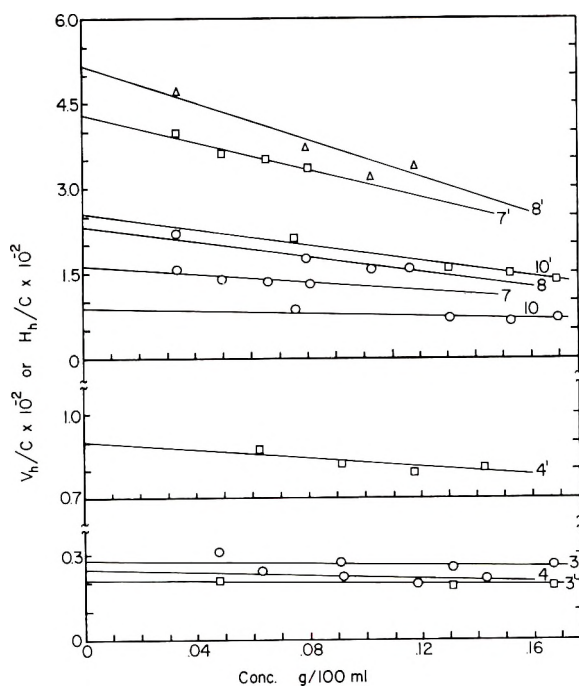


Fig. 5. Plots of H_h/C or V_h/C as a function of concentration. Numbering of curves is the same as in Fig. 1. The primed numbers represent H_h/C vs. C plots.

Graphs of H_v/C versus C are shown in Figures 3 and 4. For corn amylose, potato amylose, and the low molecular weight dextran fraction in aqueous KOH, H_v/C is found to decrease with increasing concentration. For the low molecular weight dextran fraction in water, H_v/C is independent of concentration. The values of H_v/C for amylopectin, limit dextrin, and high molecular weight dextran in KOH and also for high molecular weight dextran in water are seen to increase with concentration. The increase of H_v/C with concentration, observed in several cases, may be attributed to multiple scattering rather than to a change in the anisotropy of the molecules themselves. In an ideal solvent the molecule is unper-

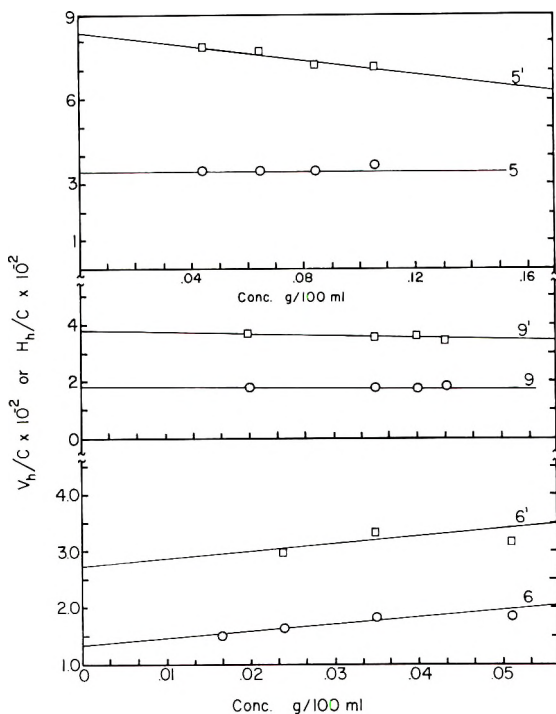


Fig. 6. Plots of H_h/C or V_h/C as a function of concentration. Numbering of curves is the same as in Fig. 1. The primed numbers represent H_h/C vs. C plots.

turbed, hence H_v/C should be independent of concentration, as is observed for the low molecular weight dextran fraction in water. The variations of V_h and H_h components are shown in Figures 5, 6, and 7. These are similar to those for component H_v ; hence their discussion is omitted.

In all the cases the variation of ρ_u with concentration is similar to that of ρ_v ; moreover ρ_u is more complex, because it contains all the four components of the scattered light, hence its discussion is omitted. The graphs of ρ_v versus C are shown in Figure 8.

Doty⁵ has concluded that at infinite dilution ρ_v should reflect essentially the anisotropy of the segments of the polymer. He further predicts, how-

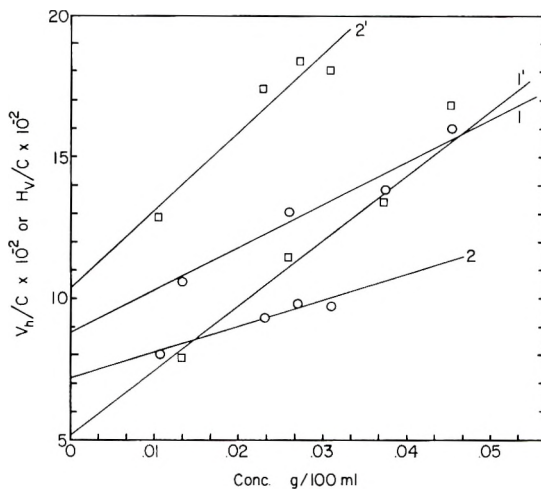


Fig. 7. Plots of H_h/C or V_h/C as a function of concentration. Numbering of curves is the same as in Fig. 1. The primed numbers represent H_h/C vs. C plots.

ever, that ρ_v will decrease with increasing molecular weight, the argument being based on the following reasoning: The V_v component should increase strongly with molecular weight, though less than linearly because of intramolecular interference. The H_v component, on the other hand, should be essentially independent of molecular weight, since this component is expected to depend on the relative locations and orientations of the anisotropic segments which should be essentially uncorrelated for large molecular weight. The H_v component should thus depend on the

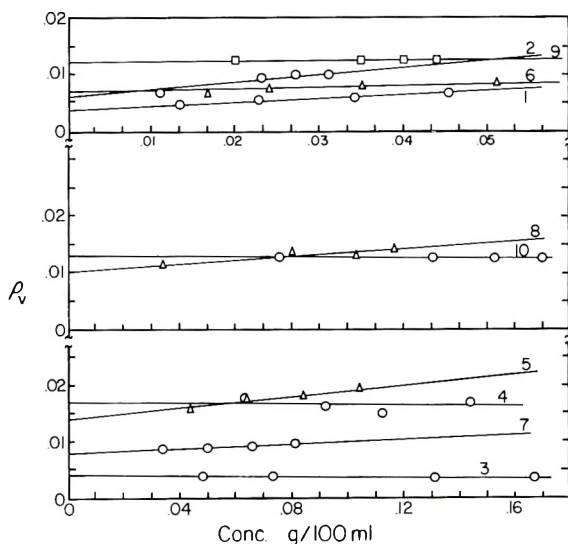


Fig. 8. Plots of ρ_v as a function of concentration. Numbering of curves is the same as in Fig. 1.

total number of segments in solution (the weight concentration) and not on the molecular weight.

Our results are found to be in disagreement with these predictions. Thus the extrapolated value of ρ_v is slightly higher for amylopectin than for limit dextrin (0.014 versus 0.008). This indicates the limit dextrin molecule to be more isotropic than the parent amylopectin. This is in general accord with the conclusion of Stacy and Foster¹⁰ from flow birefringence studies that limit dextrin is more compact. Furthermore, in water both the dextran fractions have the same value of ρ_v within experimental error (0.0038 and 0.0035) in spite of the large (2000-fold) difference in molecular weight. Finally, all of the amylose samples yield similar values of ρ_v (0.009–0.013), in spite of a tenfold variation in molecular weight.

As stated earlier, the intrinsic anisotropy of a coiled polymer molecule may be considered as depending on (1) the intrinsic anisotropy of the segments and (2) the form anisotropy of the molecule. Thus coiling of the chains tends to annul the effect of the individual segments. It is a well known fact that in a poor solvent the molecule coils back on itself, yielding more polymer–polymer contacts, whereas in a good solvent the molecule tends to uncoil, resulting in more polymer–solvent contacts. Hence, the coiling effect will be greater in a poor solvent than in a good solvent, and the total anisotropy of the molecule decreases with decreasing solvent power. The coiling and the uncoiling of a polymer molecule depends upon the interaction between the segments of the polymer and the solvent. The second virial coefficient A_2 , occurring in the light-scattering equation, is a measure of this interaction. As both ρ_v and A_2 depend upon the interaction of the segments and solvent, from comparison of the variation of A_2 with solvent power and M , one can predict the behavior of ρ_v with solvent power and molecular weight. It has already been established that A_2 will have higher values in a good solvent than in a poor solvent. It decreases with increasing molecular weight. This decrease with molecular weight is more pronounced in a good solvent than in a poor solvent. In an ideal solvent A_2 becomes zero, whatever the molecular weight may be. Hence ρ_v should have higher values in a good solvent than in a poor solvent. In the same solvent it should decrease with the increasing molecular weight. This decrease will be more pronounced in a good solvent than in a poor solvent. In an ideal solvent, if the chains are sufficiently long, the molecule coils on itself, the overall anisotropy decreases, and it may thus become independent of the size of the molecule. This can explain the nearly identical values of ρ_v for both the dextran fractions in water. The higher values of ρ_v for dextran fractions in KOH than in water and the higher value of ρ_v for low molecular weight fraction are in agreement with the above predictions. The slight variation of ρ_v with M for potato amylose fractions is also expected.

As pointed out above, the coiling of the chains reduces the anisotropy of the segments of a polymer molecule. In branched molecules, if the side branches are not sufficiently long, the coiling effect for these branches will

TABLE I
Summary of the Depolarization Ratios^a

| Polymer | \bar{M}_w | Solvent | $(\rho_{90})_{C=0}$ | $(\rho_{90})_{C=0}$ | $(\rho_{90, \text{ent}})_{C=0}$ | $(\rho_{90})_{C=0}$ |
|-----------------------------|--------------------|----------|---------------------|---------------------|---------------------------------|---------------------|
| Dextran | 131×10^5 | Water | 0.006 | 0.0035 | 1.2 | 1.44 |
| | " | 0.5N KOH | 0.02 | 0.0065 | 0.52 | 0.59 |
| | 71×10^5 | Water | 0.007 | 0.0038 | 1.11 | ~ |
| | " | 0.5N KOH | 0.067 | 0.0165 | 0.32 | 0.28 |
| Amylopectin | 80×10^6 | 0.5N KOH | 0.051 | 0.014 | 0.37 | 0.39 |
| Limit dextrin | 33×10^6 | 0.5N KOH | 0.021 | 0.008 | 0.60 | 0.64 |
| Amylose | 4×10^6 | 0.5N KOH | 0.036 | 0.008 | 0.28 | 0.30 |
| Potato amylose ^b | | | | | | |
| Fraction A | 2.4×10^6 | 1N KOH | 0.035 | 0.01 | 0.39 | 0.43 |
| Fraction B | 1.14×10^6 | 1N KOH | 0.048 | 0.012 | 0.33 | 0.38 |
| Fraction C | 0.27×10^6 | 1N KOH | 0.058 | 0.013 | 0.28 | 0.35 |

^a All the values are the limiting values at $C = 0$.

^b Incident light was 436 m μ .

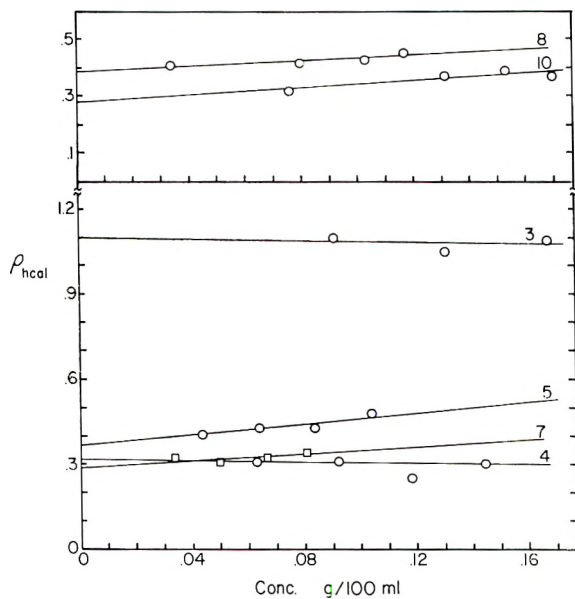


Fig. 9. Plots of ρ_h as a function of concentration. Numbering of curves is the same as in Fig. 1.

be small; hence the total anisotropy of the molecule as a whole increases. Thus amylopectin, by losing most of the side branches, becomes more isotropic. Similarly, limit dextrin, in spite of its high molecular weight, has essentially the same ρ_v value as amylose because of the side branches.

Values of ρ_h were obtained both from direct measurement and from Krishnan's equation. In most cases a difference of about 20% is observed. Graphs of the calculated values, $\rho_{h\text{ cal}}$, versus C are shown in Figures 9 and 10. Values of about 1.1 and 1.2 in water and 0.52 and 0.52 in KOH have

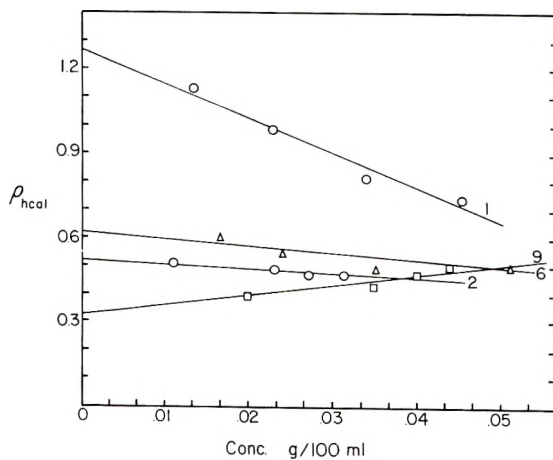


Fig. 10. Plots of ρ_h as a function of concentration. Numbering of curves is the same as in Fig. 1.

been obtained for low and high molecular weight dextran fractions. Similarly, values of about 0.37, 0.6, and 0.28 in KOH have been obtained for corn amylopectin, limit dextrin, and amylose, respectively. Values of about 0.39, 0.33, and 0.28 have been obtained in KOH for potato amylose fractions A, B, and C, respectively. Krishnan¹ and Doty⁵ point out that as the size of the particle increases, ρ_h should decrease and should always have values less than one. It is also pointed out by Doty that in the case of flexible molecules, the size of the molecule varies with solvent power; hence ρ_h should have a higher value in a poor solvent than in a good solvent. On the other hand, Gans¹³ and Neugebauer¹⁴ deduced theoretically that ρ_h should be greater than one for rodlike particles and less than one for disklike particles. For tobacco mosaic virus,¹⁵ a value of 1.04 for ρ_h has been observed. The values of ρ_h for both the dextran fractions are lower in KOH than in water, as expected by Doty. Both in the case of dextran fractions and potato amylose fractions in KOH ρ_h is found to increase with molecular weight. This result cannot be explained from Doty's theory. As is evident from theories of Gans and Neugebauer, ρ_h not only depends upon the size but also on the shape of the molecule. The flexible polymer molecule changes its size and shape with solvent power, hence the value of ρ_h changes. The authors feel it is difficult to interpret the value of ρ_h at the present.

The authors are indebted to Dr. F. R. Senti for supplying the two dextran samples employed. This research was supported by the Corn Industries Research Foundation, to whom we would like to express our thanks.

References

1. Krishnan, R. S., *Proc. Indian Acad. Sci.*, **1**, 211, 717 (1935); *ibid.*, **5**, 94 (1937); *ibid.*, **A7**, **21**, 91, 98 (1938).
2. Perrin, F., *J. Chem. Phys.*, **10**, 415 (1942).
3. Gehman, S. D., and J. E. Field, *Ind. Eng. Chem.*, **29**, 793 (1937).
4. Hoover, C. R., F. W. Putman, and E. G. Wittenberg, *J. Phys. Chem.*, **46**, 81 (1942).
5. Doty, P., *J. Polymer Sci.*, **3**, 750 (1948).
6. Doty, P., and H. S. Kaufman, *J. Phys. Chem.*, **49**, 583 (1945).
7. Doty, P., and S. J. Stein, *J. Polymer Sci.*, **3**, 763 (1948).
8. Bhatnagar, H. L., and A. B. Biswas, *J. Polymer Sci.*, **13**, 461 (1954).
9. Stacy, C. J., Ph.D. Thesis, Purdue University, 1956.
10. Stacy, C. J., and J. F. Foster, *J. Polymer Sci.*, **20**, 67 (1956).
11. Killion, P. J., and J. F. Foster, *J. Polymer Sci.*, **46**, 65 (1960).
12. Everett, W. W., and J. F. Foster, *J. Am. Chem. Soc.*, **81**, 3459 (1959).
13. Gans, R., *Physik. Z.*, **37**, 19 (1936).
14. Neugebauer, T., *Z. Physik.*, **122**, 471 (1944).
15. Horn, P., and H. Benoit, *J. Polymer Sci.*, **10**, 29 (1953).

Synopsis

The effect of branching on the depolarization of light scattered from polymer solutions has been investigated employing various branched and unbranched polysaccharides. Two dextran fractions of \bar{M}_w 71,000 and 131×10^6 were studied in a strong solvent (aqueous KOH) and an indifferent solvent (water). The other polymers, studied in

aqueous KOH only, included unfractionated corn amylopectin, the β -amylase limit dextrin of corn amylopectin, unfractionated corn amylose, and three subfractions of potato amylose ($\bar{M}_w = 2.4 \times 10^5$, 1.14×10^6 , and 0.27×10^6). Each polymer system was studied at several concentrations and all components of the scattered light, namely H_u , V_u , H_v , V_v , H_h , and V_h , were measured in each case. In general the results are in agreement with predictions of Krishnan and of Doty. However, certain important deviations from predicted behavior are noted and discussed.

Résumé

On a étudié l'influence de la ramification sur la dépolarisation de la lumière diffusée à partir de solutions de polymères au moyen de différents polysaccharides ramifiés et non ramifiés. Deux fractions de dextrane de \bar{M}_w 71.000 et 131×10^6 ont été étudiées dans un solvant fort (solution de KOH) et dans un solvant indifférent (eau). Les autres polymères, étudiés uniquement en solution aqueuse de KOH, comprenaient l'amylopectine de blé non fractionné, dextrine d'amylopectine de blé après action de β -amylase, l'amylose de blé non fractionné et trois fractions d'amylose de pommes de terre (M_w étant respectivement égal à 2.4×10^5 , 1.14×10^6 et 0.27×10^6). Chaque système polymérique a été étudié à différentes concentrations et toutes les composantes de la lumière diffusée, à savoir H_u , V_u , H_v , V_v , H_h et V_h , ont été mesurées dans chaque cas. En général, les résultats sont en accord avec les prédictions de Krishnan et de Doty. Cependant, on a relevé et discuté certaines déviations importantes au comportement prévu.

Zusammenfassung

Der Einfluss der Verzweigung auf die Depolarisation des Streulichtes von Polymerlösungen wurde an verschiedenen verzweigten und unverzweigten Polysacchariden untersucht. Zwei Dextranfraktionen mit $\bar{M}_w = 71.000$ und 131×10^6 wurden in einem starken (wässrige KOH) und einem indifferenten Lösungsmittel (Wasser) untersucht. Die anderen, nur in wässriger KOH untersuchten Polymeren waren; unfraktionierte Maisamylopektin, das β -Amylase-Grenz-dextrin des Maisamylopektins unfraktionierte Maisamylose und drei Subfraktionen von Kartoffelamylose (M_w $2,4 \times 10^5$, $1,14 \times 10^6$ bzw. $0,27 \times 10^6$). Jedes Polymersystem wurde bei mehreren Konzentrationen untersucht und in jedem Falle wurden alle Komponenten des Streulichtes, nämlich H_u , V_u , H_v , V_v , H_h , und V_h gemessen. In allgemeinen besteht Übereinstimmung mit den nach Krishnan und Doty zu erwartenden Werten. Gewisse, wichtige Abweichungen von den Erwartungswerten werden aber festgestellt und diskutiert.

Received October 6, 1961

Probability Matrices, Chain Dimensions and Statistical Thermodynamics for Semicrystalline Macromolecules

ARTHUR V. TOBOLSKY, *Frick Chemical Laboratory, Princeton
University, Princeton, New Jersey*

The successive n segments in an isolated polymer molecule which has randomly coiled regions and ordered helical regions can be written as a sequence $r r r h h h h r r h h h r h r r r r h h h r h r h h h h \dots$, where r represents a segment in a randomly coiled state and h represents a segment in an ordered crystalline region. The same representation can be used for a polymer chain which is part of a solid semicrystalline polymer, r representing a segment in an amorphous region and h representing a segment in a crystalline region.

Tobolsky and Gupta¹ have treated the sequence of r and h states as a Markoff chain, whose normalized probability matrix is:

$$P^{(1)} = \begin{matrix} & \begin{matrix} r & h \end{matrix} \\ \begin{matrix} r \\ h \end{matrix} & \begin{vmatrix} 1 - p & p \\ 1 - \alpha & \alpha \end{vmatrix} \end{matrix} \quad (1)$$

By this treatment we obtained expressions for: the expected value n_h of segments in the crystalline state; the expected value n_r of segments in the amorphous state, the average sequence length \bar{h} of segments in crystalline regions, the average sequence length \bar{r} of segments in amorphous regions, and expressions for the expected number of crystalline sequences $n_{\text{seq},h}$ and expected number of amorphous sequences $n_{\text{seq},r}$.

$$n_h = np/(1 - \alpha + p) \quad (2)$$

$$n_r = n(1 - \alpha)/(1 - \alpha + p) \quad (3)$$

$$\bar{h} = 1/(1 - \alpha) \quad (4)$$

$$\bar{r} = 1/p \quad (5)$$

$$n_{\text{seq},h} = np(1 - \alpha)/(1 - \alpha - p) \quad (6)$$

$$n_{\text{seq},r} = np(1 - \alpha)/(1 - \alpha + p) \quad (7)$$

We also derived an expression for the mean square length \bar{R}^2 of the polymer chain:^{1,6}

$$\bar{R}^2 = \left\{ \left[\frac{3 - 3\alpha + p}{3(1 - \alpha + p)} \right] \frac{3 + p}{3 - p} + \frac{2p(2 - \alpha)}{(1 - \alpha)(3 - p)(1 - \alpha + p)} \right\} nl_0^2 \quad (8)$$

where l_0 is the segment length. We also derived a more complicated formula which included as a parameter the pitch of the helix in the crystalline regions: in eq. (8) the helices of the crystalline region are assumed to have the minimum possible coiling. The problem of Keller-Till type folding has also been treated by one of us.⁷ A simplified form of equation (8) has also been presented.^{7,8}

The term segment as used here has the same multiple significance as it frequently does in polymer science. It may mean the link of the equivalent freely rotating chain, it may mean the chemically repeating unit of the polymer chain, or it may mean the atoms associated with an individual bond along the main polymer chain. One or the other use of the term may be more useful or appropriate for a particular problem.

The values of α and p that actually obtain for the r and h sequence may result from kinetic conditions (as in rapidly quenched specimens) or the values may in some cases be equilibrium values that can be determined by statistical thermodynamic considerations.

It is of interest in the latter case to relate the quantities α and p to appropriate segment partition functions.

We now consider the sequence of segments $rrrrh h h h r r \dots$ from the point of view of a linear Ising problem. This would appear to be valid for an isolated chain; for a chain which is a part of a solid semicrystalline polymer we assume that the partition functions of each chain can be computed independently of the others.

We first rewrite the sequence of segments given at the beginning of the paper as $rrrk h h h r r k h h r k r r r r k h h h r k n k h h h \dots$, where k now represents the first h segment in a sequence of h segments. This notation is used because we shall assign a special partition function to these segments.

By the matrix method,³ the basic matrix M for this problem is

$$\mathbf{M} = \begin{matrix} & \begin{matrix} r & k & h \end{matrix} \\ \begin{matrix} r \\ k \\ h \end{matrix} & \begin{bmatrix} f_r^{1/2} f_r^{1/2} & f_r^{1/2} f_k^{1/2} & 0 \\ f_k^{1/2} f_r^{1/2} & 0 & f_k^{1/2} f_h^{1/2} \\ f_h^{1/2} f_r^{1/2} & 0 & f_h^{1/2} f_h^{1/2} \end{bmatrix} \end{matrix} \quad (9)$$

The quantities f_r , f_h , and f_k which appear above are the partition functions for the r , h , and k segments.

The partition function Q for the chain is:

$$Q = \lambda_1^n \quad (10)$$

where λ_1 is the largest root of the matrix \mathbf{M} .

The largest root of the matrix \mathbf{M} is

$$\lambda_1 = 1/2 [(f_r + f_h) + \sqrt{(f_r - f_h)^2 + 4f_k f_r}] \quad (11)$$

When f_k/f_r and f_k/f_h are both smaller than unity it is easy to see that λ_1 is approximately f_r or f_h , depending on which is the larger. There is a region of transition between these two values whose sharpness depends on how small f_k/f_r and f_k/f_h are. If these quantities approach zero, the transition becomes perfectly sharp.

The number of r segments, k segments, and h segments (exclusive of k segments) will be denoted as n_r , n_k , and n_h^* , respectively. These values are given by:

$$\begin{aligned} n_r/n &= d \ln \lambda_1 / d \ln f_r \\ &= (f_r/R) (f_r - f_h + 2f_k + R) / (f_r + f_h + R) \end{aligned} \quad (12)$$

$$\begin{aligned} n_k/n &= d \ln \lambda_1 / d \ln f_k \\ &= (f_k/R) 2f_r / (f_r + f_h + R) \end{aligned} \quad (13)$$

$$\begin{aligned} n_h^*/n &= d \ln \lambda_1 / d \ln f_h \\ &= (f_h/R) (f_h - f_r + R) / (f_r + f_h + R) \end{aligned} \quad (14)$$

where R is defined as

$$R = +\sqrt{(f_r - f_h)^2 + 4f_k f_r} \quad (15)$$

The above statistical thermodynamic treatment of a chain with "amorphous segments" and "crystalline segments" is conceptually and mathematically very similar to the solution of the helix-coil transition in synthetic polypeptides proposed by Zimm and Bragg.² The matrix proposed by these authors is somewhat more complex than the matrix presented here because in the polypeptide problem it was necessary to exclude h states preceded by only one or two r states, i.e., the configurations $h r h$ or $h r r h$. Nevertheless the mathematical results are very similar whether or not one includes this restriction. Moreover, if the Ising model can be applied to a polymer chain which is a part of a solid semicrystalline polymer, there is no physical reason to include these restrictions inasmuch as a chain can touch a crystallite boundary and immediately return to the amorphous region.

We now turn to the problem of relating the partition functions f_r , f_h , and f_k to the quantities α and p which appear in the Markoffian matrix.

Inasmuch as the number of amorphous sequences is equal to the number of crystalline sequences, we have

$$\bar{r} = n_r/n_k = (f_r - f_h + 2f_k + R)/2f_k \quad (16)$$

and similarly,

$$\bar{h} = (n_h^* + n_k)/n_k = [f_h(f_h - f_r + R) + 2f_k f_r]/2f_k f_r \quad (17)$$

However, simple expressions for \bar{r} and \bar{h} in terms of α and p have previously been given in eqs. (4) and (5). Combining eq. (5) with eq. (16) and eq. (4) with eq. (17) we obtain

$$p = 2f_k/(f_r - f_h + 2f_k + R) \quad (18)$$

$$\alpha = [f_h(f_h - f_r + R)]/[f_h(f_h - f_r + R) + 2f_k f_r] \quad (19)$$

These relations are valid only if statistical thermodynamic equilibrium is reached. Under these conditions eq. (8) for the mean square length of the polymer chain can in principle be determined from the segment partition functions f_r , f_h , and f_k .

We shall now specialize to consider the segments of our chain to be the individual bonds along the main polymer chain. For many crystalline polymers the entropy of fusion S_f per mole of chain bonds is R ; the heat of fusion ΔH_f per mole of chain bonds ranges from 350 to 1500 cal. For explicit calculation we shall take $f_h = e^{\Delta H_f/RT}$ and $f_r = e$. This corresponds to a value of $\Delta S_f = R$ per mole of bonds. For $f_k f_r$ we shall take values of 0.1, 0.01, and 0.0001. In Table I we present values of n_r/n , n_k/n , n_h^*/n , p , and α as functions of the variable $x = RT/\Delta H_f$ for these three cases.

In eq. (8) is presented our result for the value of \bar{R}^2 for the molecules in an unoriented crystalline polymer. We have also calculated the value of \bar{R}_x^2 for the molecules of a semicrystalline polymer whose crystallites are

TABLE I

| | n_h^* | | | n_k | | | n_r | | |
|------|--------------------|---------------------|-----------------------|--------------------|---------------------|-----------------------|--------------------|---------------------|-----------------------|
| | $f_r f_k =$ 0.1 | $f_r f_k =$ 0.01 | $f_r f_k =$ 0.0001 | $f_r f_k =$ 0.1 | $f_r f_k =$ 0.01 | $f_r f_k =$ 0.0001 | $f_r f_k =$ 0.1 | $f_r f_k =$ 0.01 | $f_r f_k =$ 0.0001 |
| 0.10 | 1.000 | 1.000 | 1.000 | 0.000 | 0.000 | 0.000 | 0.000 | 0.000 | 0.000 |
| 0.50 | 0.999 | 1.000 | 1.000 | 0.000 | 0.000 | 0.000 | 0.000 | 0.000 | 0.000 |
| 0.75 | 0.989 | 1.000 | 1.000 | 0.002 | 0.000 | 0.000 | 0.008 | 0.000 | 0.000 |
| 0.90 | 0.915 | 0.999 | 1.000 | 0.009 | 0.000 | 0.000 | 0.077 | 0.001 | 0.000 |
| 0.95 | 0.781 | 0.995 | 1.000 | 0.014 | 0.000 | 0.000 | 0.205 | 0.005 | 0.000 |
| 1.00 | 0.482 | 0.498 | 0.503 | 0.018 | 0.002 | 0.000 | 0.500 | 0.501 | 0.540 |
| 1.05 | 0.217 | 0.059 | 0.000 | 0.015 | 0.000 | 0.000 | 0.768 | 0.994 | 1.000 |
| 1.10 | 0.106 | 0.002 | 0.000 | 0.012 | 0.000 | 0.000 | 0.882 | 0.998 | 1.000 |
| 1.50 | 0.011 | 0.000 | 0.000 | 0.005 | 0.000 | 0.000 | 0.989 | 1.000 | 1.000 |
| 2.00 | 0.001 | 0.000 | 0.000 | 0.003 | 0.000 | 0.000 | 0.996 | 1.000 | 1.000 |

| | α | | | p | | |
|------|--------------------|---------------------|-----------------------|--------------------|---------------------|-----------------------|
| | $f_r f_k =$ 0.1 | $f_r f_k =$ 0.01 | $f_r f_k =$ 0.0001 | $f_r f_k =$ 0.1 | $f_r f_k =$ 0.01 | $f_r f_k =$ 0.0001 |
| 0.10 | 1.000 | 1.000 | 1.000 | 1.000 | 1.000 | 1.000 |
| 0.50 | 1.000 | 1.000 | 1.000 | 0.78 | 0.78 | 0.78 |
| 0.75 | 0.998 | 1.000 | 1.000 | 0.290 | 0.45 | 0.45 |
| 0.90 | 0.991 | 1.000 | 1.000 | 0.114 | 0.196 | 0.196 |
| 0.95 | 0.983 | 1.000 | 1.000 | 0.068 | 0.050 | 0.100 |
| 1.00 | 0.965 | 0.996 | 1.000 | 0.036 | 0.004 | 0.000 |
| 1.05 | 0.934 | 0.954 | 0.95 | 0.020 | 0.000 | 0.000 |
| 1.10 | 0.901 | 0.918 | 0.92 | 0.013 | 0.000 | 0.000 |
| 1.50 | 0.711 | 0.75 | 0.71 | 0.005 | 0.000 | 0.000 |
| 2.00 | 0.61 | 0.61 | 0.61 | 0.003 | 0.000 | 0.000 |

completely oriented in the x direction.¹ \bar{R}_x^2 is the value of \bar{R}^2 projected in the x direction. $\bar{R}_{x,0}^2$ is the value of \bar{R}_x^2 for the same polymer chain when the polymer is brought into a completely amorphous condition. We showed that

$$\bar{R}_x^2/\bar{R}_{x,0}^2 = [2p(2 - \alpha)/(1 - \alpha)(1 - p)(1 - \alpha + p)] + [(1 + p)/(1 - p)] \quad (20)$$

We also made the tentative suggestion that $\bar{R}_x^2/\bar{R}_{x,0}^2$ could be related to the shrink ratio for a completely oriented fiber whose state before shrinking is defined by α and p and presented a simplified form of equation (20).⁸

In Table II we present values of \bar{R}^2 from eq. (8) and $\bar{R}_x^2/\bar{R}_{x,0}^2$ from eq. (20) for various values of $x = RT/\Delta H_f$, computed from the values of α and p listed in Table I. These values of α and p are, of course, values obtained from our statistical thermodynamic equilibrium theory.

TABLE II

| x | \bar{R}^2/nl_0^2 from eq. (8) | | | $\bar{R}_x^2/\bar{R}_{x,0}^2$ from eq. (20) | | |
|------|---------------------------------|---------------------|-----------------------|---|---------------------|-----------------------|
| | $f_r f_k =$ 0.1 | $f_r f_k =$ 0.01 | $f_r f_k =$ 0.0001 | $f_r f_k =$ 0.1 | $f_r f_k =$ 0.01 | $f_r f_k =$ 0.0001 |
| 0.10 | — | — | — | — | — | — |
| 0.50 | — | — | — | — | — | — |
| 0.75 | 215 | — | — | 832 | — | — |
| 0.90 | 72 | — | — | 238 | — | — |
| 0.95 | 34 | — | — | 107 | — | — |
| 1.00 | 10.8 | — | — | 32.1 | — | — |
| 1.05 | 3.38 | 1.02 | 1.00 | 8.64 | 1.00 | 1.00 |
| 1.10 | 1.80 | 1.02 | 1.00 | 3.63 | 1.00 | 1.00 |
| 1.15 | 1.50 | 1.00 | 1.00 | 1.16 | 1.00 | 1.00 |
| 2.00 | 1.18 | 1.00 | 1.00 | 1.06 | 1.00 | 1.00 |

The values of \bar{R}^2/nl_0^2 and $\bar{R}_x^2/\bar{R}_{x,0}^2$ approach infinity as α approaches unity. Inasmuch as α was calculated only to three places we do not tabulate \bar{R}^2/nl_0^2 and $\bar{R}_x^2/\bar{R}_{x,0}^2$ for $\alpha = 1.000$.

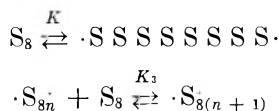
It should again be emphasized that eqs. (8) and (20) are the simplest forms of a more general equation¹ which accounts for short-range and long range folding of the molecules in the crystalline regions. Equations (8) and (20) are valid if there is no folding and if the unit cell of the crystallites is fully extended. The application of our results to more complex crystalline structures presents no difficulties in principle.

APPENDIX A

Application of the Ising Model to Equilibrium Polymerization

Tobolsky and Eisenberg^{4,5} have considered the problem of equilibrium polymerization by a straightforward application of the law of mass action, utilizing an equilibrium constant K for initiation and another equilibrium

constant K_3 for growth. In the case of sulfur, the equilibria considered were:



We call M_0 the initial monomer concentration, M the monomer concentration at equilibrium, and P the average degree of polymerization of the equilibrium polymer. The simple results obtained by applying the law of mass action were:

$$P = 1/(1 - K_3M) \quad (\text{A-1})$$

$$M_0/M = 1 + KP^2 \quad (\text{A-2})$$

We can also consider the problem of equilibrium polymerization as an Ising problem. Consider once again the sequence $r r r k h h h r r k h h r k r r r r k h h h r k r k h h h \dots$. In this instance we consider r to be an unreacted monomer, k to be the first monomeric segment of a polymer chain, and h to be any segment (exclusive of the first segment) of a polymer chain. The partition functions for r , k , and h segments are taken as f_r , f_k , and f_h . The matrix for this problem is identical with the matrix \mathbf{M} in the main section of this paper.

M_0/M can be immediately identified with n/n , given by eq. (12); P can be immediately identified with \bar{h} given by eq. (17).

By comparing eqs. (A-1) with (17) and (A-2) with (12) we can obtain explicit (but unwieldy) expressions for K and K_3 in terms of f_r , f_k , and f_h .

It is interesting to note that Tobolsky and Eisenberg⁵ were able to explain the extremely sharp transition in sulfur on the basis of two classical equilibrium constants K and K_3 . This Appendix shows that this sharp transition in sulfur (and all other floor and ceiling temperature phenomena in equilibrium polymerization), have exactly the same mathematical basis as the helix-coil transition in polypeptides.

APPENDIX B

It is possible to solve the statistical thermodynamic problem of the $r r r h h h h r r h h h r h r r r h h h r h h h h h \dots$ sequence by means of a simpler 2×2 matrix M' if we utilize segment pair partition functions

$$\mathbf{M}' = \begin{matrix} & \begin{matrix} r & h \end{matrix} \\ \begin{matrix} r \\ h \end{matrix} & \begin{vmatrix} f_{rr} & f_{rh} \\ f_{hr} & f_{hh} \end{vmatrix} \end{matrix} \quad (\text{B-1})$$

The quantities f_{rr} , f_{rh} , f_{hr} , and f_{hh} are the partition functions for an rr pair, an rh pair, an hr pair and an hh pair respectively, taking the pairs systematically from the left to the right. Although $f_{rh} = f_{hr}$ we prefer to preserve them as independent variables.

The partition function Q for the chain is

$$Q = \lambda_1^n \quad (\text{B-2})$$

where λ_1 is the largest root of the matrix M .

The roots of matrix M are

$$\lambda = 1/2 [(f_{hh} + f_{rr}) \pm \sqrt{(f_{hh} - f_{rr})^2 + 4f_{rh}f_{hr}}] \quad (\text{B-3})$$

When (f_{rh}/f_{rr}) and (f_{rh}/f_{hh}) are both smaller than unity it is easy to see that the largest root is approximately f_{hh} or f_{rr} , depending on which is larger. There is a region of transition between these two values whose sharpness depends on how small f_{rh}/f_{rr} and f_{rh}/f_{hh} are. If these quantities approach zero, the transition becomes perfectly sharp.

The number of hh pairs, hr pairs, rh pairs, and rr pairs will be denoted as n_{hh} , n_{hr} , n_{rh} , n_{rr} . These values are given by

$$\begin{aligned} n_{hh} &= n (d \ln \lambda_1 / d \ln f_{hh}) \\ &= (nf_{hh}/R) (f_{hh} - f_{rr} + R) / (f_{hh} + f_{rr} + R) \end{aligned} \quad (\text{B-4})$$

$$\begin{aligned} n_{hr} &= n (d \ln \lambda_1 / d \ln f_{hr}) \\ &= (nf_{hr}/R) 2f_{rh} / (f_{hh} + f_{rr} + R) \end{aligned} \quad (\text{B-5})$$

$$\begin{aligned} n_{rh} &= n (d \ln \lambda_1 / d \ln f_{rh}) \\ &= (nf_{rh}/R) 2f_{hr} / (f_{hh} + f_{rr} + R) \end{aligned} \quad (\text{B-6})$$

$$\begin{aligned} n_{rr} &= n (d \ln \lambda_1 / d \ln f_{rr}) \\ &= (nf_{rr}/R) (f_{rr} - f_{hh} + R) / (f_{hh} + f_{rr} + R) \end{aligned} \quad (\text{B-7})$$

where

$$R = \sqrt{(f_{hh} - f_{rr})^2 + 4f_{rh}f_{hr}}$$

In terms of the quantities previously used in the main portion of this paper

$$n_h^* = n_{hh} \quad (\text{B-8})$$

$$n_k = n_{hr} = n_{rh} \quad (\text{B-9})$$

$$n_r = n_{rr} + n_{hr} \quad (\text{B-10})$$

$$n_h = n_h^* + n_k = n_{hh} + n_{rh} \quad (\text{B-11})$$

The two statistical thermodynamic treatments are identical if:

$$f_{rr} = f_r \quad (\text{B-12})$$

$$f_{hh} = f_h \quad (\text{B-13})$$

$$f_{rh}f_{hr} = f_r f_k \quad (\text{B-14})$$

We present this alternate treatment because it is convenient for further theoretical advances being presently developed.

A grant from the California Research Institute is gratefully acknowledged. The aid of Dr. M. Takahashi in computing values for Tables I and II is greatly appreciated.

References

1. Tobolsky, A. V., and V. D. Gupta, *J. Chem. Phys.*, **36**, 430 (1962).
2. Zimm, B. H., and J. K. Bragg, *J. Chem. Phys.*, **28**, 1246 (1958); *ibid.*, **31**, 526 (1959).
3. Kramers, H. A., and G. Wannier, *Phys. Rev.*, **60**, 252 (1941); E. W. Montroll, *J. Chem. Phys.*, **9**, 706 (1941); E. N. Lassetre and J. P. Howe, *J. Chem. Phys.*, **9**, 747 (1941).
4. Tobolsky, A. V., *J. Polymer Sci.*, **25**, 220 (1957).
5. Tobolsky, A. V., and A. Eisenberg, *J. Am. Chem. Soc.*, **81**, 780 (1959).
6. Tobolsky, A. V. and V. D. Gupta, *Textile Research J.*, **32**, 85 (1962).
7. Tobolsky, A. V., *J. Chem. Phys.*, in press.
8. Tobolsky, A. V., *Textile Research J.*, **32**, 252 (1962).

Synopsis

In a previous paper the end-to-end dimensions of semicrystalline macromolecules were computed by the Markoff chain method, by use of a normalized probability matrix with two probability parameters α and p . The values of these parameters that actually obtain may result from kinetic conditions (as in rapidly quenched specimens) or the values may in some cases be equilibrium values that can be determined by statistical mechanical considerations. In this paper we calculate the overall partition function Q of a semicrystalline macromolecule by a method similar to that employed by Zimm and Bragg for polypeptide chains. Q is computed in terms of segment partition functions f_r , f_h , and f_k . By working out the consequences of this Ising-type model, we are able to relate α and p to f_r , f_h , and f_k . In an appendix we show that the phenomenon of ceiling and floor temperatures in equilibrium polymerization can be regarded from the same mathematical point of view as the helix-coil transition. Moreover, the mathematical results from this approach can be correlated with the results previously obtained by Tobolsky and Eisenberg by direct application of the law of mass action.

Résumé

Dans une étude antérieure, les distances entre extrémités des chaînes des macromolécules semi-cristallines ont été estimées par la méthode en chaînes de Markoff, en employant une matrice de probabilité normalisée avec deux paramètres de probabilité α et p . Les valeurs de ces paramètres, qui s'obtiennent effectivement, peuvent résulter des conditions cinétiques (comme dans des échantillons refroidis brutalement) ou les valeurs peuvent quelques fois être des valeurs d'équilibre pouvant être déterminées par des considérations de mécanique statistique. Dans cette étude nous calculons la fonction de partition globale Q d'une macromolécule semi-cristalline en employant une méthode semblable à celle employée par Zimm et Bragg pour les chaînes de polypeptide. Q est estimé sur la base de fonctions de partition des segments f_r , f_h , et f_k . En faisant ressortir les conséquences de ce modèle du type Ising, nous sommes capables de relier α et p à f_r , f_h et f_k . Dans un appendice nous montrons que le phénomène des températures limites supérieures et inférieures en polymérisation d'équilibre peut être considéré à partir du même point de vue mathématique que la transition de la forme hélicoïdale à la forme pelotte statistique. De plus les résultats mathématiques de ce traitement peuvent être mis en corrélation avec les résultats obtenus précédemment par Tobolsky et Eisenberg par application directe de la loi d'action des masses.

Zusammenfassung

In einer früheren Arbeit wurde der End-zu-Endabstand semikristalliner Makromoleküle mit der Methode der Markoffketten unter Benützung einer normalisierten Wahrscheinlichkeitsmatrix mit zwei Wahrscheinlichkeitsparametern α und p berechnet. Die

Werte für diese Parameter können kinetisch bedingt sein (wie bei rasch abgeschreckten Proben) oder sie können in gewissen Fällen Gleichgewichtswerte sein, die durch statistisch-mechanische Betrachtungen bestimmt werden können. In der vorliegenden Mitteilung wird die Gesamtzustandsfunktion Q eines semikristallinen Makromoleküls nach einer Methode berechnet, welche der von Zimm und Bragg für Polypeptidketten verwendeten ähnlich ist. Q wird aus den Segmentzustandsfunktionen f_r , f_h und f_k berechnet. Auf der Grundlage dieses Modells vom Ising-Typ lassen sich α und p zu f_r , f_h und f_k in Beziehung setzen. In einem Anhang wird gezeigt, dass die Erscheinung der oberen und unteren Grenztemperatur bei der Gleichgewichtspolymerisation vom gleichen mathematischen Gesichtspunkt aus betrachtet werden kann, wie die Helix-Knäuelumwandlung. Ausserdem können die mathematischen Ergebnisse einer solchen Betrachtung zu den früher von Tobolsky und Eisenberg durch eine direkte Anwendung des Massenwirkungsgesetzes erhaltenen Ergebnissen in Beziehung gebracht werden.

Received October 31, 1961

Solution Properties of Polysaccharides. IV. Molecular Weight and Aggregate Formation in Methylcellulose Solutions*

W. BROCK NEELY, *Biochemical Research Laboratory,
The Dow Chemical Company, Midland, Michigan*

INTRODUCTION

Water-soluble methylcellulose has achieved an important place in the list of industrial gums. For an extensive account of the practical applications of this polysaccharide ether, the review by Greminger and Savage is noteworthy.¹ The present investigation on methylcellulose was undertaken for two main reasons. First, previous reports from this laboratory^{2,3} indicated an aggregation of the polymer in solution. Secondly, a characterization of the hydrodynamic properties of this polysaccharide ether would help to extend our knowledge of cellulose derivatives. Molecular weight and radius measurements appeared to offer the best method for examining the solution behavior. In order to measure these parameters the light-scattering technique was employed, and these data will be reported on in detail.

Since this work was undertaken two reports have appeared on the hydrodynamic characteristics of methylcellulose in solution.^{4,5} The first⁴ substantiated our earlier findings on the ability of methylcellulose to aggregate in solution.² These authors⁴ used electrical double refraction to make their measurements, and, while our results are qualitatively identical, they differ by several orders of magnitude. The second report⁵ dealt with the molecular weight-intrinsic viscosity relationships as derived from sedimentation and diffusion measurements on the ultracentrifuge. Our work enlarges these earlier studies and, in addition presents a detailed account of the effect of ionic strength on the ability of methylcellulose and the hydroxypropyl derivatives of methylcellulose to form aggregates in solution.

EXPERIMENTAL

Material

The water-soluble methylcellulose was supplied by the Dow Chemical Company of Midland, Michigan. In addition two samples of a hydroxy-

* Presented in part at the 140th National Meeting of the American Chemical Society, Chicago, Ill., September 1961.

propoxyl derivative of methylcellulose were also supplied. The alkoxy analysis and the viscosity of the materials are shown in Table I. The polymers were solubilized by dispersing in boiling water and cooling in the refrigerator (0–5°C.) overnight. A 2% solution was prepared and the appropriate dilutions made for light-scattering studies.

TABLE I
Analysis of the Methylcellulose Samples

| Sample no. | Viscosity, c'poise ^a | Methoxyl, % | Hydroxypropoxyl, % |
|------------|---------------------------------|-------------|--------------------|
| 1 | 12 | 30.2 | — |
| 2 | 33 | 30.4 | — |
| 3 | 131 | 28.0 | — |
| 4 | 245 | 30.1 | — |
| 5 | 368 | 31.1 | — |
| 6 | 67 | 28.1 | 3.72 |
| 7 | 274 | 21.6 | 11.4 |

^a Viscosity measured on a 2% solution at 20°C.

Viscosity

Intrinsic viscosities were measured at 25°C. in Ubbelohde viscometer tubes. The flow time for water was 180 sec. The intrinsic viscosities were found by plotting η_{sp}/C against C (in g./100 ml.) and extrapolating to zero concentration.

Light Scattering

The light-scattering measurements were carried out in a Brice-Phoenix photometer with the use of the unpolarized blue light (436 m μ) of a mercury arc lamp. Scattering measurements were made as a function of angle between 30° and 135°. The specific refractive index increment, dn/dc , for methylcellulose was determined in a Brice-Phoenix differential refractometer. The value of dn/dc was found to be 0.154 at a wavelength of 436 m μ . This gives for the constant K in the light-scattering equation a value of 3.86×10^{-7} .

Clarification of the aqueous solutions of the polymer was carried out by centrifugation in the Spinco Model L ultracentrifuge for 1–2 hr. at 30,000 rpm. The middle layer was removed and used in the measurements. As a final aid in removing dust particles filtration through Millipore filters with a pore size of 0.45 μ was carried out directly into the light-scattering cell. Methylcellulose concentrations were determined by using the anthrone colorimetric procedure.⁶

Interpretation of Light-Scattering Data

The results were plotted in the form of the usual double reciprocal method of Zimm.⁷ It was found that the reciprocal envelope (K^c/R_θ) against $\sin^2(\theta/2)$ was curved. This type of curvature was assumed to be due to polydispersity in line with the reasoning given by Doty and his co-workers^{8,9} for cellulose nitrate and sodium carboxymethylcellulose. If this is the case,

the following method of evaluating the data is possible.⁸ Two limiting cases apply to the reciprocal envelope in Figure 1. At sufficiently low angles we have

$$K^c/R_{\theta, c=0} = (1/\bar{M}_w)[1 + N_z(u/3) + \dots] \quad (1)$$

where

$$u = [(4\pi/\lambda') \sin(\theta/2)]^2(b^2/6)$$

and λ' is the wavelength of light in the medium, θ is the scattering angle, \bar{M}_w is the weight-average molecular weight, b is the effective bond length,

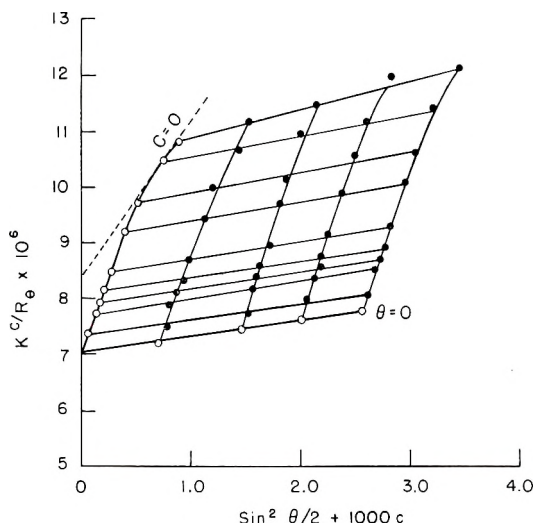


Fig. 1. Double reciprocal Zimm plot for methylcellulose sample (sample 2, Table I) in water after being refrigerated for 48 hr. The dashed line represents the approximate asymptote, since the true asymptote has not been reached at the available angles. The resultant number-average molecular weights and sizes are, accordingly, rough estimations.

and N_z is the Z -average degree of polymerization. The second limiting case is at the higher angles where the eq. (2) holds:

$$K^c/R_{\theta, c=0} = (1/\bar{M}_n)[1/2 + N_n(u/2) + \dots] \quad (2)$$

where \bar{M}_n is the number-average molecular weight. This defines an asymptote where the slope and intercept yield number averages of the dimension and molecular weight, respectively.

RESULTS

Characteristic Dimensions of the Methylcellulose Molecules

A freshly prepared aqueous solution of sample 1, Table I, that had not been refrigerated exhibited a M_w of 200,000. Refrigeration at 4°C. for 48 hr. caused the M_w to fall to 122,000; a longer time of cooling had no

detectable effect. With this in mind preliminary measurements on the polymer were made on solutions that had been previously refrigerated in order to rule out possibilities of aggregation.

Typical Zimm plots for samples 2 and 4 (Table I) are shown in Figures 1 and 2. The dotted line indicates the asymptote that the envelope reaches at the higher angles. The scattering diagrams for the other methylcelluloses listed in Table I were quite similar in shape. In Table II the relevant data have been collected in a summary form. The following remarks are pertinent in interpreting the information in this table. The number-average and weight-average molecular weights were calculated by use of

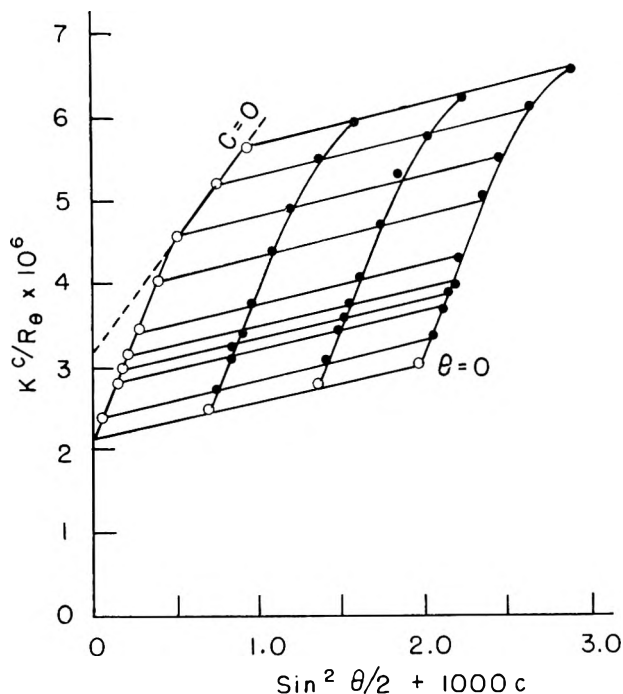


Fig. 2. Double reciprocal Zimm plot for methylcellulose sample (sample 4, Table I) in water after being refrigerated for 48 hr. Similar considerations apply to the dashed line as described for Fig. 1.

eqs. (1) and (2). The number-average and Z -average dimensions for the end-to-end distance of the random coil were determined from the appropriate slope in the plot of Kc/R_{θ} against $\sin^2 \theta/2$. The effective bond length b is $(r_n^2)^{1/2}/(N_n)^{1/2}$ where N_n and r_n represent the number-average degree of polymerization and the root-mean-square dimension, respectively. The constant Φ in the Flory-Fox viscosity equation is calculated from $[\eta]\bar{M}_n/(r_n^2)^{3/2}$.

The log-log plot of $[\eta]$ against \bar{M}_w is shown in Figure 3. From this graph the constants in the equation $[\eta] = KM_w^a$ may be calculated. The values for K and a turn out to be 3.16×10^{-3} and 0.55, respectively.

TABLE II
Summary of Data Obtained on a Series of Methylcellulose Samples^a

| Sam- ple | $[\eta]$ | \bar{M}_n | \bar{M}_w | N_n | $(r_n^2)^{1/2}$, A. | $(r_z^2)^{1/2}$, A. | b , A. | Φ \times 10^{-21} |
|-------------|----------|-------------|-------------|-------|-------------------------|-------------------------|----------|----------------------------------|
| 1 | 1.74 | 45,000 | 122,000 | 236 | 342 | 1030 | 21.2 | 1.96 |
| 2 | 2.04 | 59,500 | 143,000 | 313 | 366 | 1060 | 20.8 | 2.43 |
| 3 | 3.10 | 125,000 | 330,000 | 656 | 560 | 1430 | 21.8 | 2.20 |
| 4 | 3.50 | 159,000 | 465,000 | 840 | 680 | 1670 | 23.4 | 1.80 |
| 5 | 3.95 | 200,000 | 570,000 | 1050 | 715 | 1770 | 22.0 | 2.17 |
| 6 | 2.85 | 100,000 | 298,000 | 525 | 520 | 1550 | 22.8 | 2.02 |
| 7 | 4.25 | 275,000 | 690,000 | 1450 | 765 | 1800 | 20.0 | 2.50 |
| | | | | | | Avg. | 21.7 | 2.15 |

^a The number-average molecular weights and dimensions can only be considered as approximations. This follows from the difficulty of obtaining a true asymptote in the Zimm plot (see Figs. 1 and 2).

Aggregation Process

Ionic strength and time are important factors in the ability of these polymers to aggregate. This is demonstrated in Figure 4. Solution A represents sample 2 (Table I) prepared in 0.5M NaCl. Solution B is the same material in water. Both solutions were refrigerated for two days and then held at room temperature (approximately 24°C.) for the remainder of the experiment. After aggregation had occurred, solution A could be deaggregated by placing the solution in the refrigerator for a period of 48 hr. The effect of varying the ionic strength on the amount of aggregate formed is shown for two different samples of methylcellulose in Figure 5. The solid curve represents sample 3 (Table I), and the dashed curve represents the hydroxypropoxyl derivative (sample 6 in Table I). Sample 7,

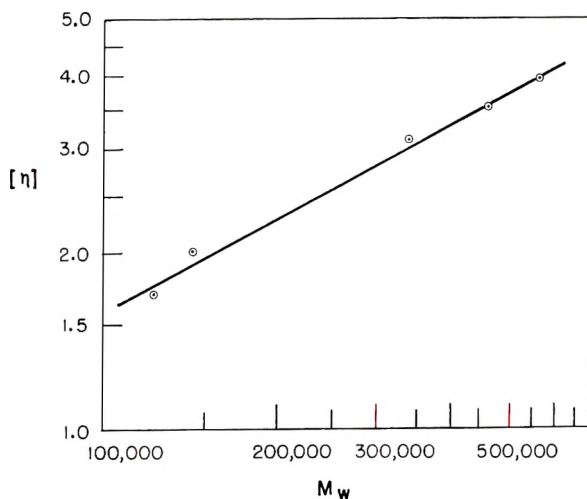


Fig. 3. Log-log plot of $[\eta]$ against \bar{M}_w for the various samples of methylcellulose.

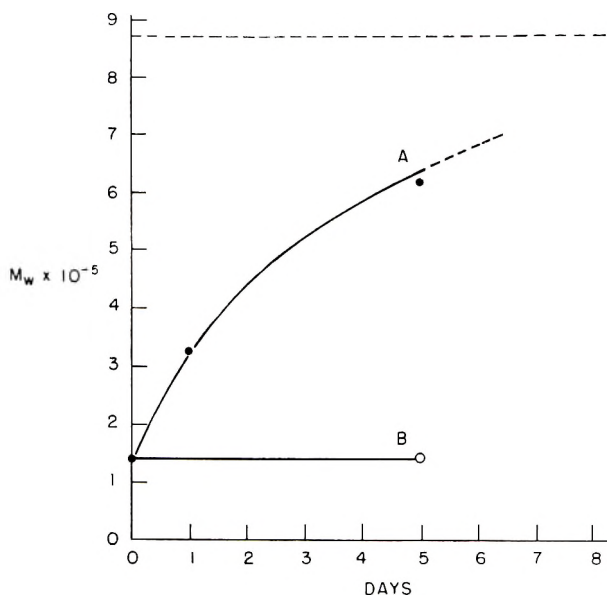


Fig. 4. Effect of time on the extent of aggregation on methylcellulose sample 2. The maximum aggregation is taken from Fig. 6, on the solution that had not been previously refrigerated. (The maximum should be 920,000 instead of 875,000 as indicated in the figure.) See text for description of curves A and B.

containing a higher content of hydroxypropoxyl, did not show any aggregation under the conditions of this experiment. The measurements were made on solutions that had been maintained at 24°C. for six days after the refrigeration treatment. The data for these various samples are summarized in Table III.

A few general remarks regarding the Zimm plots appear to be in order.

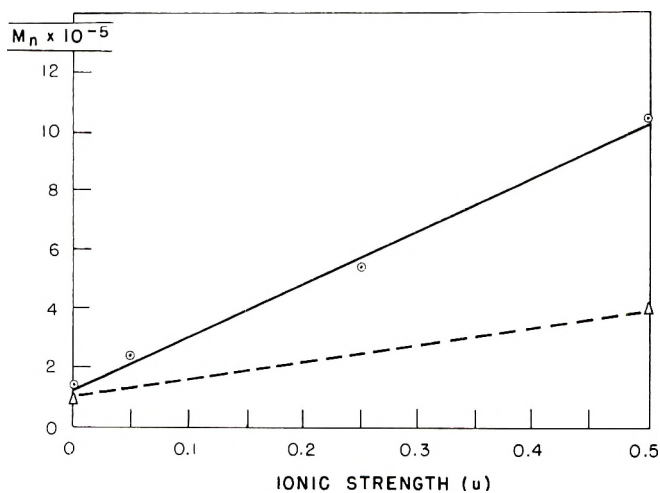


Fig. 5. Effect of ionic strength on the extent of aggregation. The top line represents data for sample 3; the bottom line represents data for sample 4.

TABLE III
Summary of Data for the Various Methylcellulose Samples in Water and 0.5M NaCl

| Sample | Solvent | $[\eta]$ | \bar{M}_w | $(r_z^2)^{1/2}$, A. ^a |
|--------|------------------------|----------|----------------------|--------------------------------------|
| 1 | H ₂ O | 1.74 | 122,000 | 420 |
| | 0.5M NaCl | | 740,000 ^c | 425 |
| 2 | H ₂ O | 2.04 | 143,000 | 430 |
| | 0.5M NaCl ^b | 2.20 | 675,000 | 480 |
| 3 | H ₂ O | 3.10 | 330,000 | 585 |
| | 0.5M NaCl ^b | | 2,080,000 | 480 |
| 6 | H ₂ O | 2.85 | 298,000 | 615 |
| | 0.5M NaCl ^b | 2.90 | 1,190,000 | 800 |
| 7 | H ₂ O | 4.25 | 690,000 | 730 |
| | 0.5M NaCl ^b | 4.30 | 695,000 | 735 |

^a Radius of gyration calculated from the initial slope in the Zimm plot by using the relation $(R_z^2)^{1/2} = (3/16\pi^2)\lambda^2(\text{slope}/\text{intercept})$.

^b Measurements in 0.5M NaCl were made on solutions that had been held at 24°C. for six days.

^c Measurement made on solution that had not been previously refrigerated.

The second virial coefficient may be calculated from the slope of $K^c/R_{\theta, \theta=0}$ against C . This coefficient is small in aqueous solution as shown in Figure 1 and approaches zero in the salt solution (Fig. 6). The curvature in the graph of $K^c/R_{\theta, c=0}$ against $\sin^2 \theta/2$ disappears as the methylcellulose becomes fully aggregated (Fig. 6). In the intermediate stages of aggregation, represented by the six-day-old solutions in Table II and Figures 4 and 5, the curvature is still present, and the number-average molecular weight and dimensions may be calculated. It is these number-average molecular weights that are used in Figure 5.

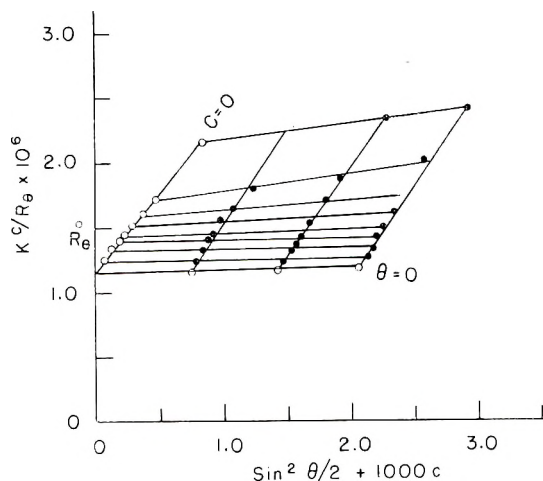


Figure 6. Double reciprocal Zimm plot for material in Fig. 1 dissolved in 0.5M NaCl and not refrigerated.

DISCUSSION

**Characteristics of the Deaggregated Methylcellulose
Molecule in Solution**

An examination of Table IV where the data for three different cellulose derivatives have been collected indicates that methylcellulose is more coiled than the other two polymers. This is demonstrated by the decrease in the effective bond length and intrinsic viscosity in going from sodium carboxymethylcellulose to methylcellulose. Cellulose trinitrate occupies an intermediate position in this series.

TABLE IV
Comparison of Various Cellulose Derivatives of Approximately
Similar Molecular Weight

| Material | \bar{M}_n | $(r_n^2)^{1/2}$, A. | b, A. | $[\eta]$ |
|--------------------|-------------|----------------------|-------|----------|
| NaCMC ^a | 170,000 | 1235 | 48.6 | 15.9 |
| CN ^b | 213,000 | 868 | 32.4 | 5.50 |
| MC ^c | 200,000 | 715 | 22.0 | 3.95 |

^a Data for sodium carboxymethylcellulose obtained from Schneider and Doty.⁹

^b Data for cellulose nitrate obtained from Holtzer, Benoit, and Doty.⁸

^c Data for methylcellulose obtained from this investigation.

The value of 0.55 for a in the modified Staudinger equation $[\eta] = K\bar{M}_w^a$ lends further support to the fact that methylcellulose is more coiled than either cellulose trinitrate or sodium carboxymethylcellulose. These latter two derivatives have a values¹⁰ of 0.8–1.0. The higher values indicate a more extended coil.

Upon comparing the number-average contour length ($N_n \times 5.15$ A., where 5.15 A. equals the length of the monomer unit) with $(r_n^2)^{1/2}$, it is seen that the ratio of the contour length to the mean dimension exceeds a value of three. This is usually taken as the criterion of chains whose mean configurations are Gaussian.¹¹

The Flory-Fox constant Φ continues to serve as a useful constant. It is seen from this investigation that the derived value of Φ for methylcellulose falls in line with the value calculated by other workers for other polymers, such as polystyrene, cellulose nitrate, etc.¹²

Characteristics of the Aggregation Process in Methylcellulose Solutions

As can be seen from the results, temperature and ionic strength play an important role in the solution behavior of methylcellulose. The second virial coefficient, as calculated from the slope of K^c/R_θ against c with $\theta = 0$ in Figure 1 and 2 is small and approaches zero with increasing salt concentration. This would imply that solute-solute interaction is favored over solute-solvent interaction. With this in mind we can picture the methylcellulose molecule becoming fully hydrated at the lower temperature due to the decreased mobility of the molecules, consequently lowering the probability for polymer-polymer contact. The solvated polymer is thus

shielded from contact with other polymers, and aggregation is impossible. As the temperature is raised, the water layer is disrupted, and the natural tendency for the methylcellulose molecules to interact with each other predominates and aggregation becomes possible. Salt competes with the polymer for the water molecules, and thus lowers the temperature at which aggregation occurs. This is partially supported by the lowering of the second virial coefficient in salt. The hydroxypropoxyl derivatives have a reduced tendency to aggregate under these conditions as witnessed by the results in Figure 5. The steric size of the hydroxypropyl group could conceivably prevent the intimate contact with the polymers which is so necessary for interaction. In addition the hydroxypropyl group will hydrate to a greater extent than the corresponding methyl group and thus prevent aggregation of the polymer.

The aggregate of methylcellulose appears to be built from molecules laid down side by side. Such association would give maximum contact and greater stability to the association. Partial support for this hypothesis comes from the negligible dependence of viscosity with ionic strength and the constant end-to-end distance of the polymer in the various salt solutions.

Kuhn, Moser, and Majer,⁴ using electrical double refraction, were also able to demonstrate that strong association of methylcellulose takes place in aqueous solution. Their calculations showed that in a 0.1% solution of the polymer of $\bar{M}_n = 23,000$, there were 4.2×10^3 molecules in each aggregate. As seen from our results the degree of aggregation obtained was in the order of 8. This difference might be explained by the difference in molecular weight of the materials used. Kuhn and his co-workers used a polymer of a low molecular weight; such material might have a greater tendency to aggregate. In fact, this was pointed out by these authors when they stated that the extent of aggregation decreased with increasing molecular weight.⁴

The behavior of this polysaccharide in solution is quite similar to that of the copolymer of polyvinyl alcohol and polyvinyl acetate reported by Nord and his co-workers.¹³ These workers demonstrated the ability of this copolymer to aggregate on raising the temperature and to disaggregate on lowering the temperature. The present investigation emphasizes the point made by Nord, namely, the physical properties of methylcellulose solutions depend on the previous thermal history. In addition, the ionic strength plays an important role in the state of aggregation of methylcellulose. Thus, a solution of the polymer in a salt solution at room temperature for several days will be more aggregated than the corresponding salt-free solution. This phenomenon might have important implications in certain industrial uses of this polysaccharide gum.

References

1. Greminger, G. K., Jr., and A. B. Savage, in *Industrial Gums*, R. L. Whistler, Ed., Academic Press, New York, 1959, Chap. 24.
2. Neely, W. B., *J. Am. Chem. Soc.*, **82**, 4354 (1960).
3. Neely, W. B., *J. Org. Chem.*, **26**, 3015 (1961).

4. Kuhn, W., P. Moser, and H. Majer, *Helv. Chim. Acta*, **44**, 770 (1961).
5. Uda, V. K., and G. Meyerhoff, *Makromol. Chem.*, **47**, 168 (1961).
6. Samsel, E. P., and R. H. DeLap, *Anal. Chem.*, **23**, 1795 (1951).
7. Zimm, B. H., *J. Chem. Phys.*, **16**, 1093, 1099 (1948).
8. Holtzer, A. M., H. Benoit, and P. Doty, *J. Phys. Chem.*, **58**, 624 (1954).
9. Schneider, N. S., and P. Doty, *J. Phys. Chem.*, **58**, 762 (1954).
10. Huggins, M. L., in *Cellulose and Cellulose Derivatives*, E. Ott, H. M. Spurlin, and M. W. Grafflin, Eds., Interscience, New York, 1955, p. 1196.
11. Benoit, H., and P. Doty, *J. Phys. Chem.*, **57**, 958 (1953).
12. Stacey, K. A., *Light Scattering in Physical Chemistry*, Butterworths, London, 1956.
13. Nord, F. F., M. Bier, and S. N. Timasheff, *J. Am. Chem. Soc.*, **73**, 289 (1951).

Synopsis

Light scattering has been employed to investigate the aqueous solution properties of partially methylated cellulose. The data indicate a random coil for the polymer with a stiffness characterized by a value of 21.8 Å for the effective bond length b . An increase in ionic strength in the methylcellulose solution causes aggregation which is temperature-dependent. Once the aggregates are formed in the salt solution, they may be dispersed by lowering the temperature of the solution. Within probable error the intrinsic viscosity-molecular weight relation is given by $[\eta] = 3.16 \times 10^{-3} \bar{M}_w^{0.55}$ throughout the region investigated.

Résumé

La diffusion lumineuse a été utilisée pour étudier les propriétés en solution aqueuse de la cellulose partiellement méthylée. Les résultats montrent que le polymère se présente sous la forme d'une pelote statistique possédant une rigidité caractérisée par une valeur de b , la longueur effective de liaison, égale à 21,8 Å. Une augmentation de la force ionique de la solution de méthylcellulose provoque une aggrégation qui est dépendante de la température. Une fois que les agrégats ont été formés dans la solution saline, ils peuvent être dispersés en abaissant la température de la solution. Dans la limite des erreurs probables, la relation entre la viscosité intrinsèque et le poids moléculaire est donnée par $(\eta) = 3,16 \times 10^{-3} \bar{M}_w^{0,55}$ dans toute la région étudiée.

Zusammenfassung

Zur Untersuchung der Eigenschaften partiell methylierter Cellulose in wässriger Lösung wurde die Lichtstreuung herangezogen. Die mitgeteilten Ergebnisse zeigen, dass das Polymere als statistisches Knäuel, mit einer durch den Wert 21,8 Å für b , die effektive Bindungslänge, charakterisierten Steifigkeit, vorliegt. Zunahme der Ionenstärke in der Methylcelluloselösung führt zu einer temperaturabhängigen Aggregation. Die einmal in der Salzlösung gebildeten Aggregate können durch Temperaturniedrigung der Lösung dispergiert werden. Innerhalb der Versuchsfehler gilt im untersuchten Bereich die Viskositätszahl-Molekulargewichtsbeziehung: $[\eta] = 3,16 \cdot 10^{-3} \bar{M}_w^{0,55}$.

Received October 6, 1961

Revised November 7, 1961

Effect of Crystallization on the Thermal Stability of Polyvinylphthalic Acid and Its Methyl Ester

EUGENE C. WINSLOW and JEAN A. MARRIOTT,* *Department of Chemistry, University of Rhode Island, Kingston, Rhode Island*

INTRODUCTION

In an earlier paper in this Journal¹ the preparation of polyvinylphthalic acid and the thermal stability of its salts was reported. The effect of crystallization on the thermal stability of the polyacid and its ester is a logical supplementary question.

DISCUSSION

Because many of the catalysts necessary for the preparation of crystalline polymers react with acid functional groups, the stereospecific acid cannot be synthesized directly. It was decided, therefore, to produce first a crystalline ester of poly(4-vinylphthalic acid) and then hydrolyze the ester to the free acid.

The synthesis of dimethyl 4-vinylphthalate was effected by the direct esterification of 4-vinylphthalic acid with diazomethane. This acid was polymerized stereospecifically with boron trifluoride etherate as a catalyst. Crystallization of poly(dimethyl 4-vinylphthalate) was realized by treatment with boiling *n*-octane. The hydrolysis of this ester gave crystalline poly(4-vinylphthalic acid). The presence of crystallinity was verified by x-ray diffraction and the polarizing microscope.

Thermogravimetry and differential thermal analysis was employed in the investigation of the thermal stability of the polymers. Analyses were carried out in air as well as in a nitrogen atmosphere, so that oxidative effects could be evaluated.

When boron trifluoride etherate was added to a solution of dimethyl 4-vinylphthalate, polymerization proceeded slowly. The polymer was isolated by destroying the catalyst with water and precipitating the mixture in petroleum ether. The material separated as an elastomer. Drying in air gave a brittle solid.

Polymerizations were carried out in the temperature range from -10 to -25°C . with toluene as solvent. The monomer: solvent ratio could be varied from 1:3 to 1:5. When this solvent was used, all polymers formed were found to be easily crystallized. In this temperature range, therefore,

* Present address: Electric Boat Company, New London, Connecticut.

temperature had no apparent effect on the crystallizability of the product. When dioxane was used as solvent, however, the polymers formed were difficult to crystallize. Perhaps the increased basicity of this solvent allowed sufficient separation of the propagating ion pair so that steric control is diminished. The conversion to the polymer over a period of three days was only 10%. The unreacted monomer, however, could be recovered and the yield therefore, was nearly 100%.

Williams et al.² found that polystyrene could be crystallized by refluxing in various organic solvents for periods of 16–18 hr. The methods of Williams were adopted and the polymers of dimethyl 4-vinylphthalate were crystallized by refluxing in *n*-octane for periods ranging from 16 to 32 hr.

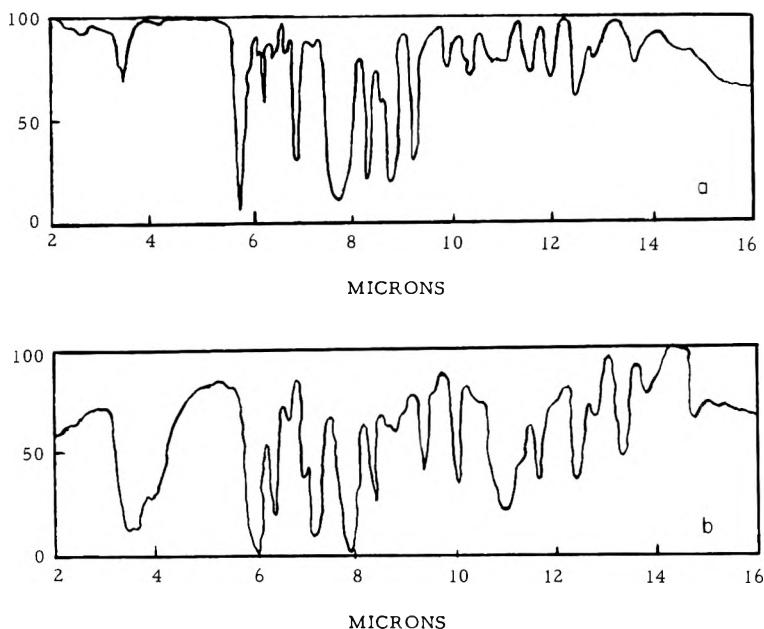


Fig. 1. Infrared spectra of: (a) dimethyl 4-vinylphthalate; (b) 4-vinylphthalic acid.

Dimethyl 4-vinylphthalate is a colorless, viscous liquid which rapidly becomes yellow in contact with air. It is very easily polymerized and solidifies on standing if left in an air atmosphere. A small amount of impurity such as water, however, will slow down the polymerization of the ester and, therefore, the liquid can be kept for longer periods of time in solution.

Polymeric dimethyl 4-vinylphthalic acid is a hard, brittle polymer which is insoluble in nearly all organic solvents with the exception of chloroform and methyl cellosolve. It is unusually clear and exhibits a remarkable adhesion to glass.

The infrared spectra of dimethyl 4-vinylphthalate and 4-vinylphthalic acid are given in Figure 1.

Viscosity measurements indicated a molecular weight range of crystalline methyl polyvinylphthalate in the vicinity of 60,000 if constants which have been determined for poly(methyl methacrylate) in chloroform were used.³ The vitreous benzoyl peroxide-initiated polymer from the same monomer gave a molecular weight in the vicinity of 30,000. Viscosity data for boron trifluoride etherate-catalyzed poly(dimethyl 4-vinylphthalate) with chloroform as a solvent are listed in Table I. The plot of these

TABLE I
Viscosity Data for Boron Trifluoride Etherate-Catalyzed Poly(dimethyl 4-Vinylphthalate) (Chloroform as Solvent)

| Concentration, g./100 cc. | Flow time, sec. | η_{red} | η_{sp} | η_{sp}/c |
|------------------------------|--------------------|--------------|-------------|---------------|
| 0.494 | 31.4 | 1.171 | 0.171 | 0.346 |
| 0.247 | 29.0 | 1.081 | 0.081 | 0.328 |
| 0.097 | 27.6 | 1.030 | 0.030 | 0.311 |
| 0.049 | 27.2 | 1.015 | 0.015 | 0.304 |
| 0.000 | 26.8 | — | — | — |

viscosity data is given in Figure 2. The viscosity data for benzoyl peroxide-catalyzed poly(dimethyl 4-vinylphthalate) with chloroform as a solvent are given in Table II. The plot of these data is presented in Figure 3.

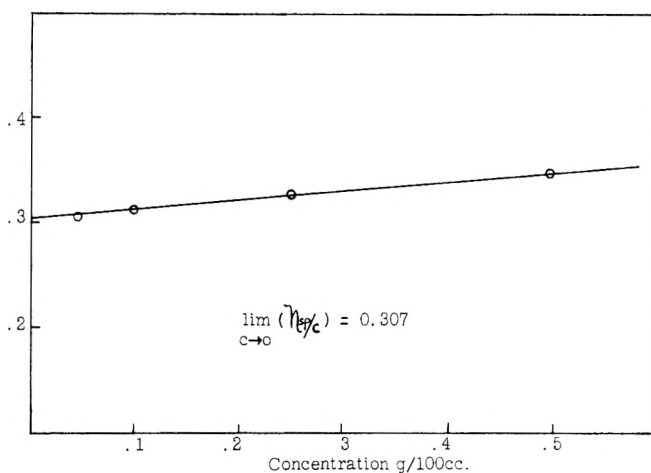


Fig. 2. Plot of viscosity data.

All thermogravimetric curves presented in this paper were determined at a heating rate of 2°C./min. in an air atmosphere. The thermogravimetric curve (Fig. 4) for crystalline poly(dimethyl 4-vinylphthalate) shows less weight loss initially than that of the noncrystalline polymer (Fig. 5). A larger amount of char as indicated by the inflection at the end

TABLE II
Viscosity Data for Benzoyl Peroxide-Catalyzed Poly(dimethyl 4-Vinylphthalate)
(Chloroform as Solvent)

| Concentration, g./100 cc. | Flow time, sec. | η_{red} | η_{sp} | η_{sp}/c |
|------------------------------|--------------------|--------------|-------------|---------------|
| 1.340 | 33.6 | 1.252 | 0.252 | 0.185 |
| 0.536 | 29.4 | 1.097 | 0.097 | 0.181 |
| 0.214 | 27.8 | 1.039 | 0.039 | 0.182 |
| 0.084 | 27.2 | 1.015 | 0.015 | 0.176 |
| 0.000 | 26.8 | — | — | — |

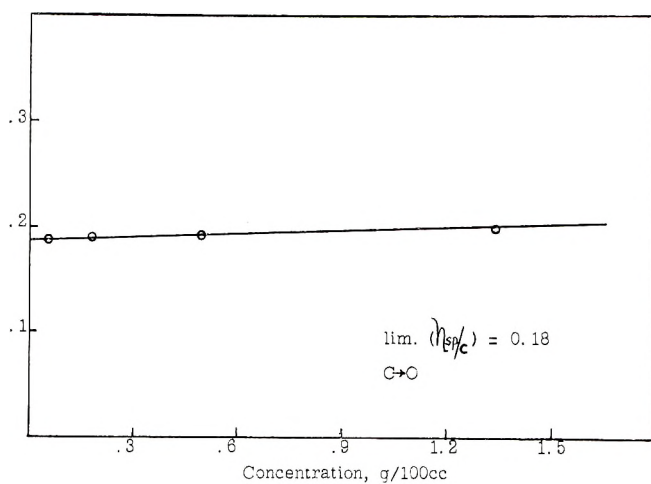


Fig. 3. Plot of viscosity data.

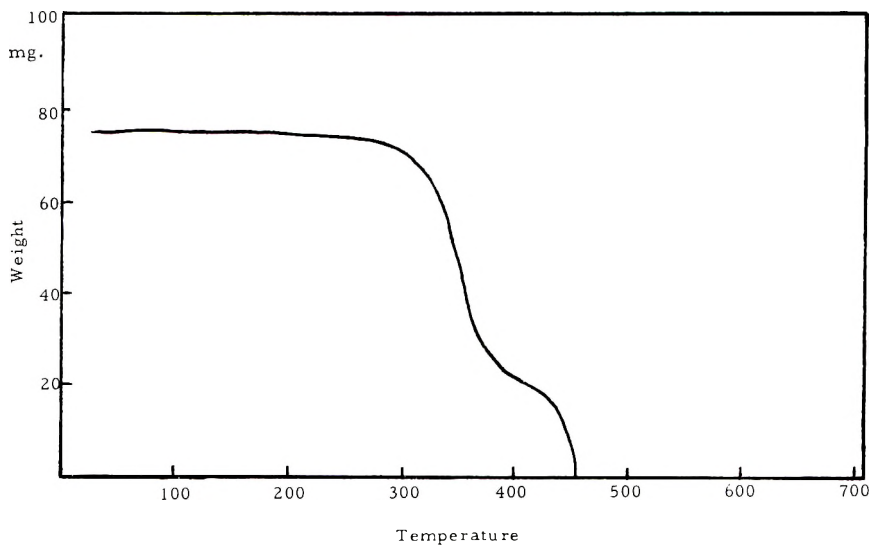


Fig. 4. TGA thermogram for crystalline poly(dimethyl 4-vinylphthalate).

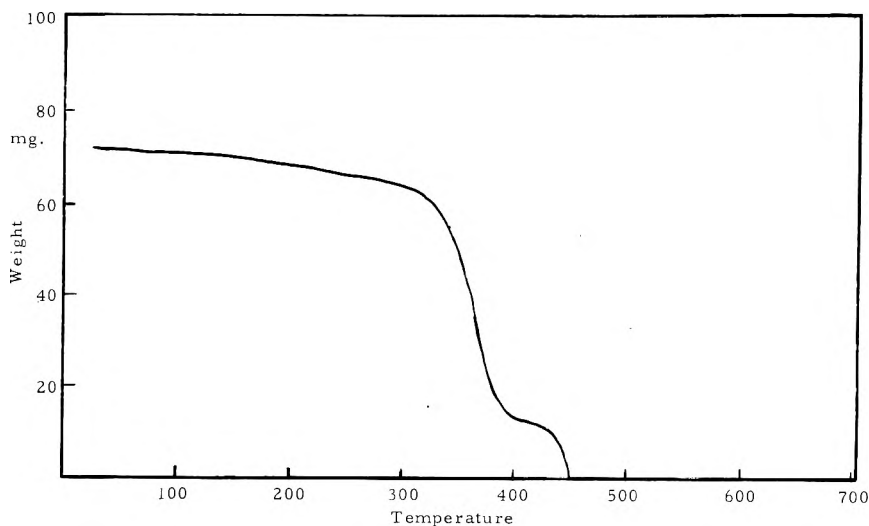


Fig. 5. TGA thermogram for noncrystalline poly(dimethyl 4-vinylphthalate).

of the curve is observed for the crystalline polymer. Apparently crystallization retards thermal breakdown to some extent. The major weight loss in both crystalline and noncrystalline material, however, occurs at about 300°C.

Figure 6 is the thermogravimetric curve for noncrystalline poly-(4-vinylphthalic acid). An inflection in the curve showing weight loss at about 200°C. can possibly be attributed to anhydride formation. After the major volatilization begins at 300°C., a second inflection occurs showing a retardation of the thermal breakdown at 400°C. No appreciable char remains at 500°C. The thermogravimetric curve for the crystalline

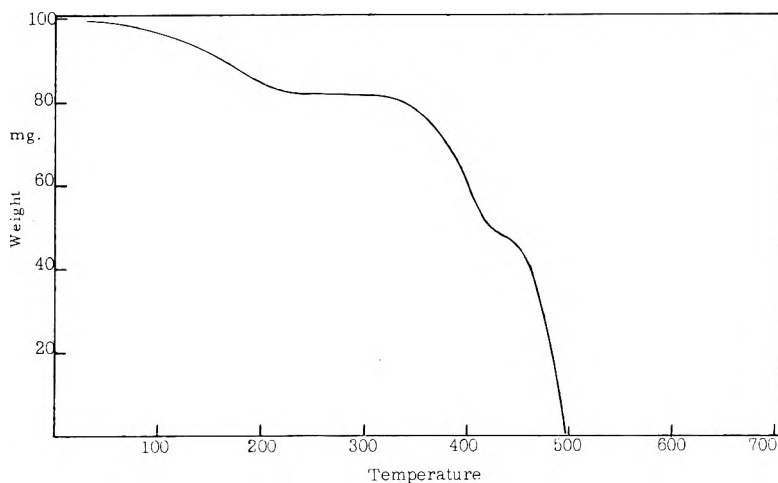


Fig. 6. TGA thermogram for noncrystalline poly(4-vinylphthalic acid).

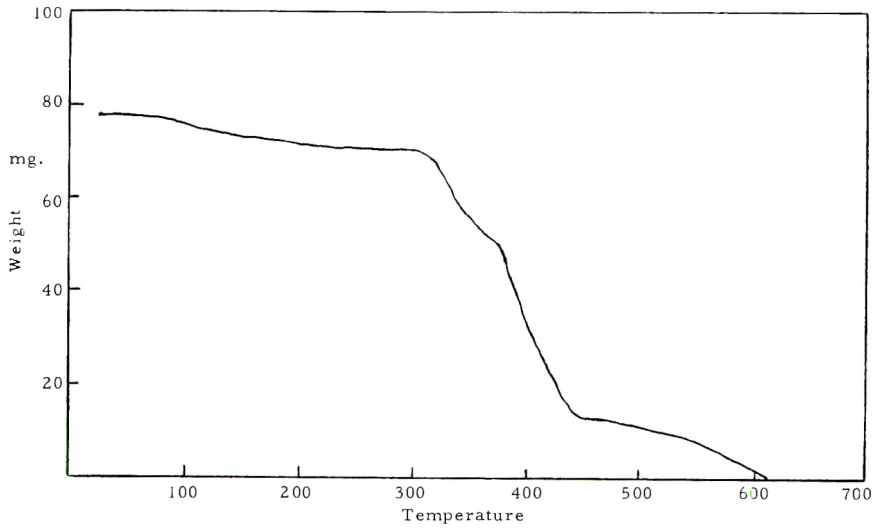


Fig. 7. TGA thermogram for crystalline poly(4-vinylphthalic acid).

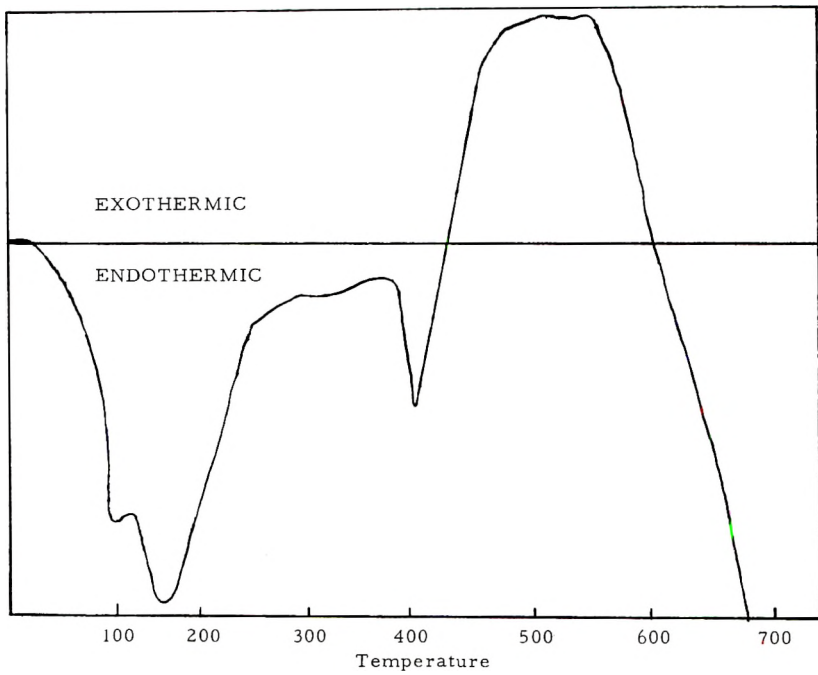


Fig. 8. DTA thermogram for noncrystalline poly(4-vinylphthalic acid), nitrogen atmosphere.

polymer (Fig. 7) shows no pronounced inflection at 200°C. corresponding to that of the noncrystalline polymer. The inflection in the curve during major thermal breakdown is less pronounced and occurs at a lower temperature than does that in the curve for the noncrystalline polymer. A marked difference in the two curves is the occurrence of an appreciable char residue, as evidence by the inflection at 450°C. in the crystalline polymer curve. The noncrystalline polymer does not show this char residue.

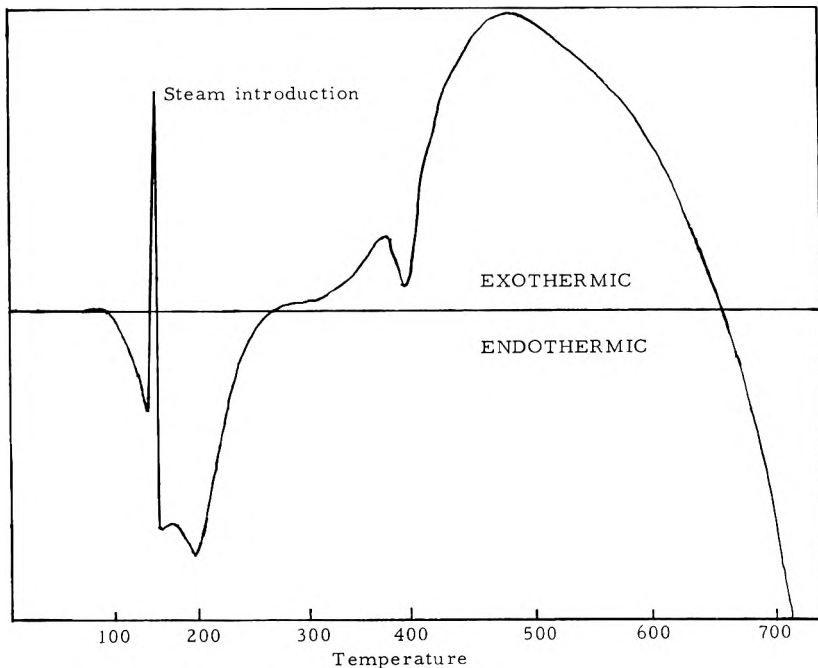


Fig. 9. DTA thermogram for noncrystalline poly(4-vinylphthalic acid), steam atmosphere.

As evidence for the possibility of anhydride formation in the noncrystalline polymeric acid, differential thermal analysis curves were run for the noncrystalline polymeric acid in nitrogen atmosphere (Fig. 8) and in steam atmosphere (Fig. 9). An endothermic trough can be observed in both curves in the vicinity of 200°C. A steam atmosphere displaces the trough to a higher temperature, indicating the probability of water evolution from the sample at that temperature. Anhydride formation is a reasonable explanation of this shift in the endothermic trough.

EXPERIMENTAL

Preparation of Dimethyl 4-Vinylphthalate

A suspension of 10 g. of 4-vinylphthalic acid¹ in 200 ml. of anhydrous ether was cooled to 0°C. in an ice bath. A calculated amount of stand-

ardized diazomethane was allowed to run in. The solution was dried over night with anhydrous magnesium sulfate and was filtered. Evaporation of ether gave 10.8 g. (95% of theoretical) of the pale yellow liquid, b.p. 176°C./1–2 mm.

ANAL. Calc.: C, 65.15%; H, 5.45%. Found: C, 65.09%; H, 5.40%.

Polymerization

Dimethyl 4-vinylphthalate (10 g.) and 30 ml. of toluene were placed in a gas pressure bottle and degassed by passing nitrogen through the solution. Boron trifluoride etherate (0.3 ml.) was added and the bottle was sealed. Precipitation occurred almost immediately upon addition of the catalyst. The mixture was stirred with a magnetic stirrer for two days. At the end of this time the catalyst was destroyed by the addition of 5 ml. of water. The organic layer was separated and poured into petroleum ether (b.p. 30–60°C.). A viscous liquid settled out. The petroleum ether was separated by decantation. To the viscous oil was added 25–50 ml. of dry toluene. The polymer separated as an elastomer and was removed. The remaining toluene was added to fresh petroleum ether and a second fraction of the polymer was precipitated. The conversion of monomer to polymer was low (approx. 10%). The unreacted monomer, however, could be recovered from the petroleum ether and the yield, therefore, was nearly 100%.

Polyvinylphthalic Acid (Crystalline)

A 1-g. portion of crystalline poly(dimethyl 4-vinylphthalate) was dissolved in concentrated sulfuric acid. The solution was poured on to chipped ice and poly(4-vinylphthalic acid) was separated. The solid was removed by suction filtration, washed with water, and dried in a vacuum desiccator.

A portion of this research was supported by a contract with the Quartermaster Corps of the United States Army.

References

1. Winslow, E. C., and A. L. Laferriere, *J. Polymer Sci.*, **60**, 65 (1962).
2. Williams, J. L. R., J. Van Den Berghe, K. R. Dunham, and W. J. Dulmage, *J. Am. Chem. Soc.*, **79**, 1719 (1957).
3. Walling, C., and K. B. Wolfstern, *J. Am. Chem. Soc.*, **69**, 852 (1947).

Synopsis

The synthesis of dimethyl 4-vinylphthalate was accomplished by direct esterification of 4-vinylphthalic acid with diazomethane. This monomer was polymerized stereospecifically by the use of boron trifluoride etherate. The polymer was crystallized by refluxing in *n*-octane. The preparation of crystalline poly(4-vinylphthalic acid) was realized by hydrolyzing crystalline poly(dimethyl 4-vinylphthalate) with concentrated sulfuric acid. The thermal behavior of the prepared polymers was studied by the techniques of differential thermal analysis and thermogravimetry. Crystallization apparently retards thermal breakdown somewhat but the temperature of major weight

loss by volatilization is essentially the same for the crystalline and the noncrystalline polymer. Differential thermal analysis indicates that anhydride formation occurs in the noncrystalline polymeric acid at 200°C. This transition is less pronounced in the case of the crystalline polymer.

Résumé

La synthèse du 4-vinylphthalate de diméthyle a été réalisée par estérification directe de l'acide 4-vinylphthalique par le diazométhane. Le monomère a été polymérisé stéréospécifiquement par l'emploi de trifluorure de bore éthéré. Le polymère était cristallisé dans l'octane-*n*. La préparation du polyacide 4 vinyl-phthalique cristallin a été réalisée en hydrolysant par l'acide sulfurique concentré le polydiméthyl-4-vinyl phthalate cristallisé. Le comportement thermique de ces polymères a été étudié en utilisant les techniques d'analyse thermique différentielle et par thermogravimétrie. La cristallisation retarde quelque peu la dégradation due à l'effet thermique mais la température à laquelle s'effectue la perte principale en poids par volatilisation est essentiellement le même pour un polymère cristallin et non-cristallin. L'analyse thermique différentielle montre que la formation d'anhydride apparaît à 200°C. pour le polyacide non-cristallin. Cette transition est moins prononcée pour le cas du polymère cristallin.

Zusammenfassung

Dimethyl-4-vinylphthalat wurde durch eine direkte Veresterung von 4-Vinylphthal-säure mit Diazomethen dargestellt. Dieses Monomere wurde mit Bortrifluoridätherat stereospezifisch polymerisiert. Das Polymere wurde durch Behandlung mit *n*-Oktan unter Rückfluß zur Kristallisation gebracht. Kristalline Poly-4-vinylphthalsäure wurde durch Hydrolyse von kristallinem Poly-dimethyl-4-vinylphthalat mit konzentrierter Schwefelsäure hergestellt. Das thermische Verhalten der hergestellten Polymeren wurde mit Differentialthermoanalyse und Thermogravimetrie untersucht. Kristallisation verzögert scheinbar die thermische Spaltung ein wenig, die Temperatur des Hauptgewichtsverlustes durch Verfluchtigung ist jedoch für kristalline und nichtkristalline Polymere gleich. Die Differentialthermoanalyse weist auf eine Anhydridbildung der nichtkristallinen polymeren Säure bei 200° hin. Diese Umwandlung tritt beim kristallinen Polymeren weniger hervor.

Received August 15, 1961

Revised October 23, 1961

Fundamental Studies on Cationic Polymerization. II. Mechanism and Theory of Inversion Temperature

J. P. KENNEDY, I. KIRSHENBAUM, R. M. THOMAS, and
D. C. MURRAY, *Chemicals Research Division Esso Research and
Engineering Company, Linden, New Jersey*

I. INTRODUCTION

In the first part of this series,¹ we described the discovery of inversion temperature. The inversion temperature T_i is the temperature level where the dependence of degree of polymerization on monomer concentration changes its sign, i.e., the temperature level where the molecular weight is independent of monomer concentration. Also, we presented evidence for the occurrence of this phenomenon in various chlorinated solvents. This remarkable observation interested us in a more thorough study to elucidate the fundamentals of cationic polymerization of isobutene. Although electrophilic polymerization is not a new area, and more specifically the isobutene-aluminum chloride system is one of the oldest known polymerization reactions, systematic kinetic investigation had not been carried out on this system. Progress in this area has been hampered by extreme reaction velocities and irreproducibility due to adventitious impurities.

In this paper we are reporting experiments carried out with the isobutene-aluminum chloride-methyl chloride system to study further the dependence of degree of polymerization (DP) on monomer concentration and temperature.

In another phase of our work, labeled materials proved to be valuable in mechanism studies. Isobutene polymerizations have been carried out in C¹⁴-methyl chloride and the amount of C¹⁴ incorporated into polymer determined. The fact that C¹⁴ from solvent enters the macromolecule had been reported earlier.² It has been established that the amount of C¹⁴ incorporation can be influenced in a characteristic manner by changing monomer concentration and temperature. In particular, C¹⁴ entry is favored by decreasing isobutene concentration and decreasing temperature.

Finally, experimental results obtained in this area are examined, and a theory which explains quantitatively the observed facts is proposed.

II. EXPERIMENTAL

The purity or purification of chemicals used, together with a description of apparatus and general material handling technique have been disclosed.³

a. Polymerization Technique in Methyl Chloride

A more detailed and somewhat larger scale experiment has been carried out to reconfirm the inversion temperature in the isobutene-aluminum chloride-methyl chloride system. Thus, 50 ml. of isobutene were diluted with 0, 15, 50, 75, 125, 150, 250, and 500 ml., respectively, of methyl chloride at -78°C . After thermoequilibration at the selected temperature level, catalyst was introduced through a 2-ml. capacity cooled hypodermic needle. The tip of the needle was adjusted so that slight pressure on the plunger produced a fine mist. About 0.5 ml. of precooled catalyst solution was sprayed into the vigorously stirred reaction mixtures. The catalyst was introduced in a series of short bursts, rather than in one continuous spray. The total time for catalyst introduction was about 10 sec. Isobutene concentrations (expressed in mole fractions) were: 1.0, 0.659, 0.368, 0.279, 0.189, 0.163, 0.104, and 0.065. The values correspond to 12.25, 9.42, 6.134, 4.89, 3.48, 3.07, 2.02, and 1.22 mole/l. at -55°C . Densities for isobutene and methyl chloride at -35 and -78°C . are: 0.664, 0.710, and 1.027, 1.104, respectively. Polymerization ensued instantly and, after 1 min. of stirring, an excess of precooled methanol was added to stop the reaction. After 5 min. more of stirring, the reaction flasks were allowed to come to room temperature and the unreacted gases were evaporated. The polymer product was washed with methanol, and dried *in vacuo* at 50°C . DP's represent the average of duplicate determinations. The determination of unfractionated polymer molecular weight has been described.³

b. Experiments with C^{14}

C^{14} -methyl chloride was purchased from New England Nuclear Corp., and was diluted with methyl chloride to yield a convenient specific activity of about 109 disintegrations/min. (DPM)/mole. The exact specific activity of methyl chloride used (S_{MeCl}) was determined in separate experiments. The catalyst solution was prepared by subliming small amounts of aluminum chloride (anhydrous, sublimed, certified reagent, Fisher Scientific Co.), and then extracting it with refluxing methyl chloride. The concentration of aluminum chloride in C^{14} methyl chloride used as catalyst in these studies was 1.88×10^{-2} mole/l.

Monomer solutions were prepared by mixing liquid isobutene and C^{14} -methyl chloride in desired proportions. The general polymerization technique was similar to that described above. A small amount of polymer was set apart for molecular weight determination, and the rest was used for radioactive assay. Molecular weight determinations were carried out in diisobutene solutions as reported previously.³ The number-average molecular weight (\bar{M}_n) was estimated from the viscosity-average molecular weight (\bar{M}_v) by use of the relation $\bar{M}_v = 1.832 \bar{M}_n$.⁵ Great care was taken to purify from adventitious C^{14} -methyl chloride contamination. Thus, known amounts of polymer were dissolved in 15 ml. phosphor solution

[4 g. of 2,5 diphenyloxazole and 0.05 g. *p*-bis (2,5-phenyloxazole) benzene in 1000 ml. toluene] and heated to 50–60°C. The boiling point of methyl chloride is -23.7°C . Heating was continued until constant specific activity was reached (usually 3–6 hr.). A liquid scintillation spectrometer (Packard tri-carb, Model 314X) was used for counting. Additional experimental details will be given in the text at appropriate places.

III. RESULTS

a. Influence of Temperature and Monomer Concentration on DP

As previously reported, the molecular weight of polyisobutene is independent of monomer concentration at the inversion temperature.¹ The phenomenon was reproduced in a number of cases. The results of a recent, more detailed experiment with methyl chloride are shown in Figures 1a and 1b. In Figure 1a, log DP is plotted against monomer concentration.

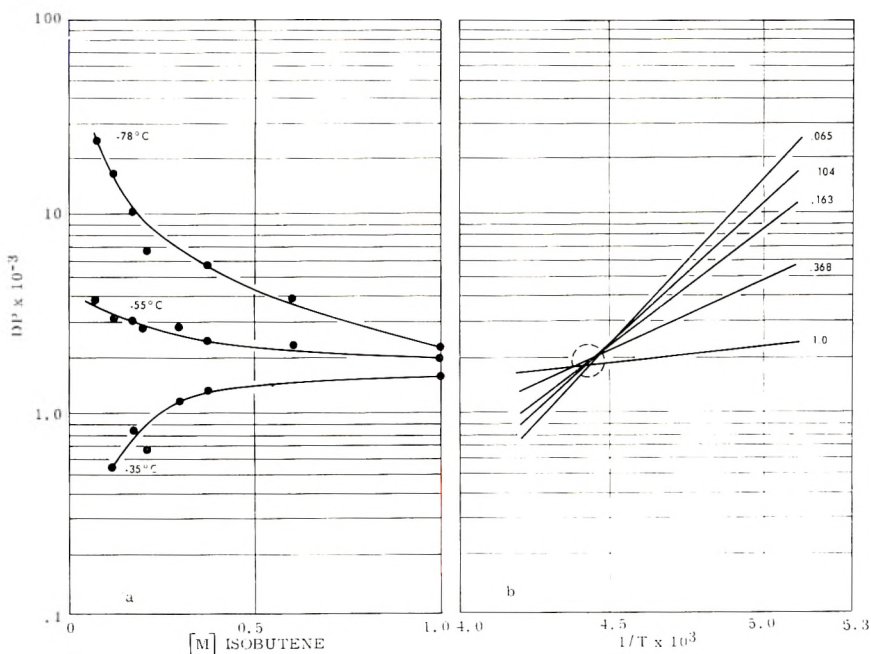


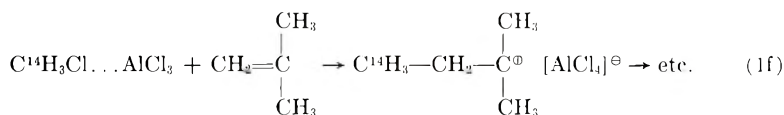
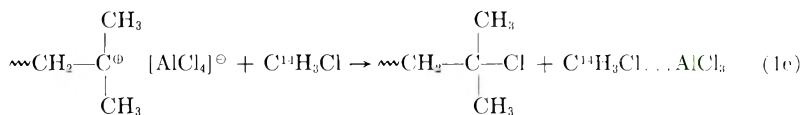
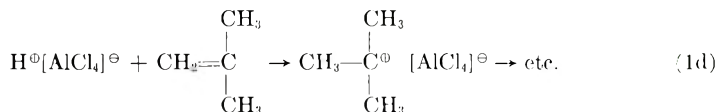
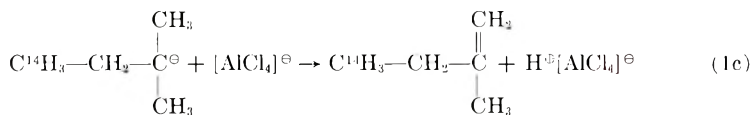
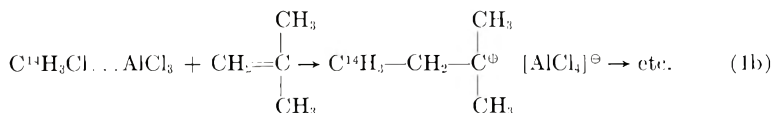
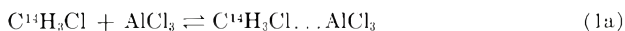
Fig. 1. (a) Dependence of DP of polyisobutene on monomer concentration at various temperatures. (b) Dependence of DP of polyisobutene on reciprocal temperatures at various monomer concentrations (constructed from Fig. 1a).

Figure 1b, which was constructed from Figure 1a, shows log DP versus $1/T$ at a few monomer concentration levels. One can regard this latter representation as vertical slices of Figure 1a. At -35°C ., increasing monomer concentrations result in higher molecular weights. The situation is just the reverse at -78°C ., where the molecular weight–monomer concentration dependence is a reciprocal one. These two areas are separated

by the inversion temperature, where the molecular weights obtained are independent of monomer concentration. The encircled area around -45°C . in the figure indicates the approximate location of the inversion temperature.

b. Experiments with C^{14} -Labeled Methyl Chloride

Previous experiments showed that when isobutene is polymerized in the presence of C^{14} -methyl chloride a considerable amount of C^{14} becomes incorporated in the product. A simplified concept of possible pathways leading to the incorporation of C^{14} into the polymer can be presented as follows in eqs. (1a)–(1f).



As indicated, C^{14} might enter by two processes: either by acting as a cocatalyst [reaction (1b)] or by participating in a chain-breaking process involving the solvent [reactions (1e) and (1f) or (1b)].

Experiments have been carried out to study the influence of monomer concentration and reaction temperature on C^{14} incorporation into polyisobutene. Thus, isobutene has been polymerized with AlCl_3 dissolved in refluxing $\text{C}^{14}\text{H}_3\text{Cl}$ at -35 , -60 , and -78°C ., the standardized technique of polymerization previously described being used. The monomer concentration was varied by admixing different amounts of $\text{C}^{14}\text{H}_3\text{Cl}$ with the isobutene. The initial monomer concentrations were 1.00, 0.38, and 0.28 mole fractions. Conversions were kept low. The molecular weight and radioactive incorporation (i.e., fraction of polymer molecules containing radioactivity) were determined for each monomer concentration at the different levels of temperature. Table I and Figure 2 show the results.

TABLE I
Effect of Monomer Concentration and Temperature on the Incorporation Ratio

| Expt. no. | Temp., °C. | [M] in mole fraction of <i>i</i> -C ₄ H ₈ | PIB formed, g. | Intrinsic viscosity × 10 ⁻³ | \bar{M}_w × 10 ⁻³ | \bar{M}_n × 10 ⁻³ | PIB counted, g. | PIB counted × 10 ⁵ | PIB activity, DPM | S_{PIB} × 10 ⁻⁸ , DPM/mole | $I = S_{PIB}/S_{Mec1}^a$ |
|-----------|------------|---|----------------|--|--------------------------------|--------------------------------|-----------------|-------------------------------|-------------------|---|--------------------------|
| 1 | -35 | 1.000 | 1.3007 | 0.430 | 70.2 | 38.3 | 1.0974 | 2.86 | 759 | 0.264 | 0.0266 |
| 2 | | | 1.5790 | 0.436 | 71.8 | 39.2 | 1.2018 | 3.06 | 950 | 0.309 | 0.0394 |
| 3 | | | 1.1104 | 0.411 | 65.7 | 35.9 | 0.9424 | 2.63 | 427 | 0.161 | 0.0162 |
| 4 | | | 1.3883 | 0.418 | 67.2 | 36.7 | 1.1131 | 3.08 | 646 | 0.213 | 0.0214 |
| 5 | -60 | | 1.2368 | 0.545 | 101.6 | 55.5 | 1.0617 | 1.91 | 700 | 0.366 | 0.0368 |
| 6 | | | 1.0249 | 0.545 | 101.6 | 55.5 | 0.8251 | 1.49 | 624 | 0.420 | 0.0422 |
| 7 | | | 0.7071 | 0.514 | 93.2 | 50.9 | 0.5224 | 1.03 | 600 | 0.585 | 0.0588 |
| 8 | | | 0.8669 | 0.568 | 108.4 | 59.3 | 0.6479 | 1.09 | 682 | 0.623 | 0.0627 |
| 9 | -78 | | 1.1282 | 0.621 | 124.8 | 68.1 | — | — | — | — | — |
| 10 | | | 1.4219 | 0.662 | 119.0 | 65.2 | 0.9902 | 1.15 | 1107 | 0.763 | 0.0767 |
| 11 | | | 1.4414 | 0.763 | 172.0 | 94.0 | 0.3426 | 0.36 | 363 | 0.995 | 0.1000 |
| 12 | | | 0.5234 | 0.775 | 176.0 | 96.2 | 0.4252 | 0.44 | 526 | 1.190 | 0.1195 |
| 13 | -35 | 0.38 | 1.4856 | 0.302 | 40.2 | 22.0 | 1.0330 | 4.70 | 2253 | 0.458 | 0.0487 |
| 14 | -60 | | 1.1332 | 0.808 | 211.0 | 115.4 | 0.9436 | 0.82 | 1220 | 1.490 | 0.1500 |
| 15 | -78 | | 1.5051 | 1.110 | 310.0 | 169.5 | 1.2646 | 0.75 | 1397 | 1.872 | 0.1880 |
| 16 | -35 | 0.28 | 0.8075 | 0.286 | 30.8 | 16.8 | 0.3645 | 0.22 | 1247 | 0.577 | 0.0580 |
| 17 | -60 | | 0.4998 | 0.972 | 251.2 | 137.5 | 0.3934 | 0.29 | 566 | 2.108 | 0.213 |
| 18 | -78 | | 0.9674 | 0.990 | 259.0 | 141.5 | 0.7626 | 0.54 | 1626 | 3.020 | 0.303 |

^a Specific activity of C₄H₈Cl used $S_{Mec1} = 0.995 \times 10^9$ DPM/mole; counting efficiency = 0.69; background = 36 DPM.

In the Table I, S_{PIB} is the specific activity of C^{14} incorporated into the polymer. It is equal to DMP/moles of polyisobutene (PIB) counted.

In Figure 2 the incorporation ratio I is plotted against the temperature at various monomer concentrations. I is obtained by taking the ratio of the specific activity (disintegrations per minute per mole) of the C^{14} incorporated into a polyisobutene molecule to specific activity of methyl chloride used, i.e., $I = S_{PIB}/S_{MeCl}$. According to Figure 2, both lowering the temperature and diluting the monomer result in increasing incorporation ratio.

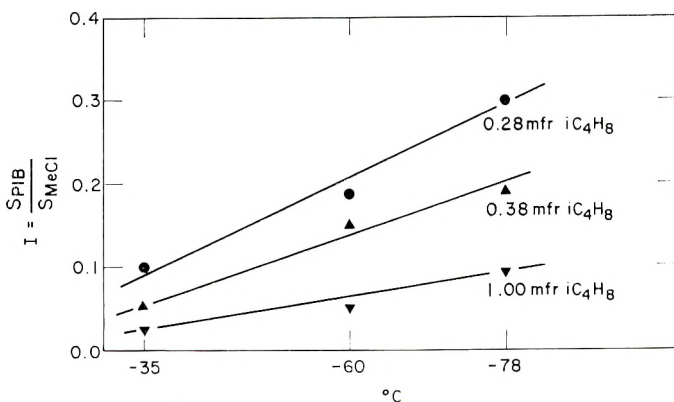


Fig. 2. C^{14} incorporation as a function of temperature of various monomer concentrations.

To explain such a straight-forward situation would not seem to be difficult, except that not only must the theory explain the facts presented in Figure 2 but at the same time it has to account for the occurrence of inversion temperature, which complicates the picture considerably. In other words, Figures 1 and 2 must be considered jointly and explained simultaneously. A kinetic theory which quantitatively accounts for the experimental facts has been developed as described below.

IV. DISCUSSION AND THEORY

Although the literature of cationic polymerization is quite extensive, no detailed studies have been published on the isobutene-aluminum chloride-alkyl chloride system. Houtman's investigations with this system (without alkyl chloride) were conducted under objectionable experimental conditions.⁶ Czech authors studied the polymerization of isobutene with dissolved aluminum chloride catalyst in the presence of various Lewis bases.^{7,8} They found that maximum electrical resistivity occurs at an $AlCl_3$: base ratio of = 1:1. A material of this general composition, when used as a catalyst for isobutene polymerization, yielded the highest molecular weight product. The authors assumed an equilibrium between Lewis

acid and base



and suggest that the "best" catalyst is the undissociated intermediate.⁹

Although a great number of experiments have been presented, the facts are hard to understand. According to older literature and the results obtained in these laboratories, the catalyst is very sensitive to impurities, and great care has to be taken to obtain reproducible results. Significantly, Lewis bases such as ethers, alcohols, aldehydes, etc. are potent catalyst "poisons," and small amounts suffice to destroy completely catalytic activity. Since the authors did not explain this apparent discrepancy, more research is needed to elucidate the phenomenon.

A substantially complete literature survey in the field of electrophilic polymerizations and other ionic systems did not result in finding a phenomenon similar to that of the inversion temperature. A few cases which might have a certain bearing on the phenomenon under study have been mentioned.¹

A quantitative kinetic theory of the low temperature aluminum chloride-catalyzed polymerization of isobutene must explain the following observations regarding the degree of polymerization (DP) data: (1) dependence of DP on monomer concentration: (a) at low temperatures, DP decreases with increasing monomer concentration; (b) at high temperatures, DP increases with increasing monomer concentration; (c) at the inversion temperature, DP is independent of monomer concentration; and (2) dependence of DP on temperature. The theory must simultaneously explain the C¹⁴ incorporation data obtained from experiments using C¹⁴-methyl chloride as solvent: (1) C¹⁴ incorporation increases with decreasing monomer concentration; (2) C¹⁴ incorporation decreases with increasing temperatures; (3) C¹⁴ is a function of monomer concentration even at inversion temperature. Also, a satisfactory mechanism should lead to a quantitative estimate of relative rate constants and activation energies.

Degree of Polymerization

The average length of a polymer chain (DP) is expressed as the ratio of the rate of chain propagation to the sum of the rates of all chain breaking and chain terminating processes. For simplicity, the propagation reaction is usually visualized as the addition of a monomer molecule to the growing polymer carbonium ion. Actually, however, the reaction is much more complicated since the growing cation involves an ion pair which, in solvents of high dielectric constant, is highly solvated. Consequently, activation (e.g., ion separation) of the growing polymer may be necessary before the monomer can react with the carbonium ion. This activation cannot require much energy but may, nevertheless, be the slow step in the propagation reaction. In this case, the rate of propagation becomes monomer-independent:



and



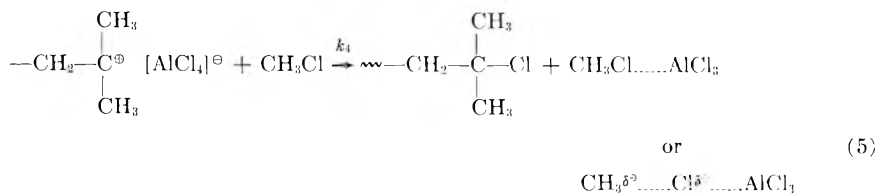
where R_n^\oplus is the polymer cation, A^\ominus is the gegenion (probably tetrachloroaluminate ion), M represents the monomer, and the k 's are the rate constants for the elemental steps. The process represented by eq. (3) is extremely fast and immediately consumes disassociated species; in other words $k_2 > k_1$. The reaction product of this step is an associated ion pair, which in turn has to be "activated" prior to the next propagating step. Thus, we may write:

$$- (d[M]/dt)_{prop} = k_1 [R_n^\oplus A^\ominus] \quad (4)$$

The assumption that the rate of propagation is monomer-independent was made earlier by Mayo and Walling¹⁰ to explain the $AlBr_3$ - HBr polymerization of propylene at $-80^\circ C$. Other mechanisms which consider propagation or initiation to be monomer concentration-independent have been described for cationic polymerization systems. About 10 years ago, to explain the various effects of hydrogen halides, Plesch¹¹ proposed that Friedel-Crafts polymerizations can be divided into two groups: (a) those in which the catalyst forms a complex with cocatalyst to form an ion pair, which in turn reacts with monomer, and (b) those in which the catalyst first reacts with the monomer and this complex reacts with the cocatalyst. Assuming that the rate-determining steps are not those involving reactions with monomer, monomer concentration-independent mechanisms are obtained. Another proposal along the same lines has been advanced for the promoted aluminum bromide catalyzed olefin polymerizations.¹² It is conceivable that in our case propagation involves a rapid, reversible addition of monomer to polymer ion pair, followed by a slower rearrangement. When the equilibrium constant is large for the first reaction, propagation would be monomer concentration independent.

Another monomer-consuming process is that of chain transfer to monomer which is an alternative to propagation at each encounter of growing polymer cation and monomer. However, in this chain-breaking process it is not necessary that the carbonium ion-gegenion pair be in an "activated" state; chain transfer can occur even with an undissociated ion pair. The reason for this was discussed earlier.¹³ The rate of monomer disappearance in this step can be written as $k_3 [R_n^\oplus A^\ominus][M]$. Obviously, this term is very much smaller than $k_1 [R_n^\oplus A^\ominus]$.

In addition to chain transfer to monomer, another chain-breaking process is that involving solvent. The latter can be visualized as follows:



and accordingly the rate expression is $k_4[R_n^{\oplus}A^{\ominus}][S]$, where S stands for solvent.

Studies conducted with CH_3Cl^{36} corroborated this concept. These experiments showed that Cl^{36} enters the polymer during low temperature polymerization. Details of these studies will be published later. The very reactive species $CH_3^{\delta\oplus} \cdots Cl^{\delta\ominus} \cdots AlCl_3$ can react rapidly either to initiate polymerization or can rearrange to regenerate methyl chloride and aluminum chloride:



Finally, accepting the concepts of cationic polymerizations, true chain termination is visualized as a unimolecular rearrangement with simultaneous loss of propagation ability. Other terminations e.g., with poisons, etc. are also monomer concentration-independent. The overall rate of termination cannot exceed the rate of initiation, and both are assumed to be small compared to the rate of monomer transfer or propagation. Summarizing these postulates, the DP equation may be written as:

$$DP = k_1/(k_3[M] + k_4[S]) \quad (7)$$

On conversion to mole fractions the DP equation becomes

$$DP = k_1/[(k_3 - k_4) N_m C + k_4 C] \quad (8)$$

where N_m is mole fraction of monomer and C is number of moles (solvent plus monomer) per liter. Thus, in order to maximize DP, C should be low, i.e. all things being equal, a solvent with high molecular weight and low density is preferred. This conclusion is borne out by the data. It is apparent from equation (8) that when $k_3 > k_4$, DP decreases with increasing monomer concentration; when $k_3 < k_4$, DP increases with increasing monomer concentration; when $k_3 = k_4$, DP becomes monomer-independent (inversion temperature).

Rearranging eq. (8) yields

$$1/DP = [(k_3 - k_4)/k_1] N_m C + (k_4 C/k_1) \quad (9)$$

It is evident that a plot of $1/DP$ versus N_m should give a straight line with a slope of $(k_3 - k_4)/k_1$, and with an intercept of $k_4 C/k_1$, provided C is comparatively constant. The agreement between theory and experiment can be seen from the typical plots in Figure 3 for the methyl chloride-isobutene and vinyl chloride-isobutene systems. Table II compiles the calculated rate constants obtained from these plots. The systems with methyl chloride and vinyl chloride show inversion temperatures at $-45^\circ C.$, whereas the ethyl chloride-isobutene inversion temperature is at $-48^\circ C.$ Since at the inversion temperature $k_3 = k_4$, eq. (8) permits a direct calculation of rate constants at the inversion temperature. These data are also shown in Table II. Within what is considered experimental error, the inversion temperatures and relative rate constants seem to be identical for the three solvents examined. This, of course, suggests great similarity

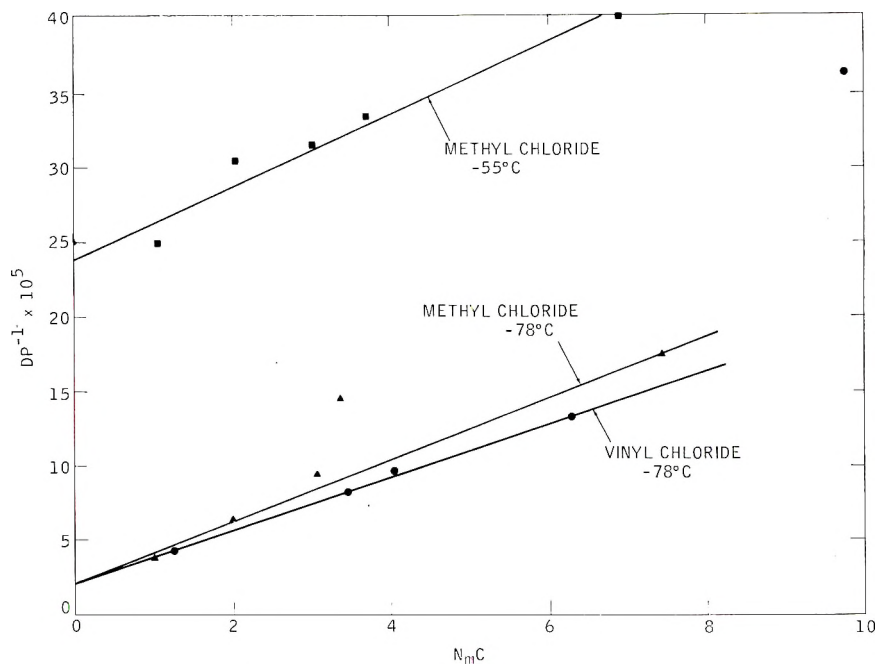


Fig. 3. Plot of reciprocal DP vs. monomer concentration.

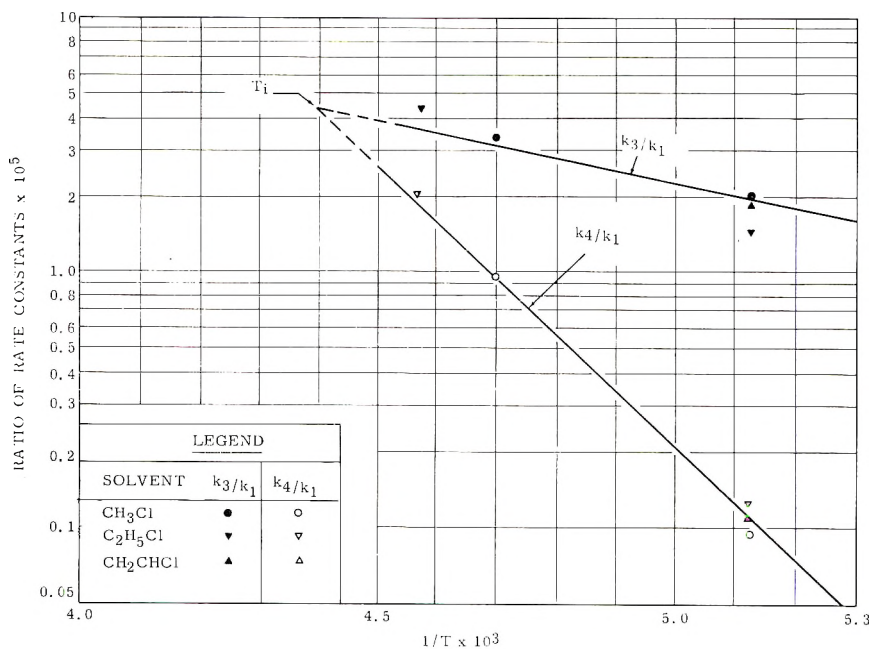


Fig. 4. Summary of relative rate constant data.

for the reaction mechanism in these particular solvents. Results obtained in nonpolar media will be reported in the next paper of this series. The ratios $\log k_3/k_1$ and $\log k_4/k_1$ obtained in three polar diluents have been plotted against $1/T$ (Fig. 4). On extrapolation of the lines toward higher temperatures, they are found to cross around -45°C ., very close to experimentally determined T_c . The similarity of the mechanism in the three solvents might seem surprising in light of the well known differences in chemical properties of methyl chloride, ethyl chloride, and vinyl chloride. However, all three solvents have about the same dielectric constant at -78°C . (i.e., 13-17). It would appear that properties such as this rather than apparent carbonium ion stability are important in the case of chain breaking involving the monomer or solvent.

TABLE II
Rate Constants for Isobutene Polymerizations

| Temperature, $^\circ\text{C}$. | $k_3/k_1 \times 10^5$ | | | $k_4/k_1 \times 10^5$ | | |
|---------------------------------|-----------------------|----------------|----------------|-----------------------|----------------|----------------|
| | Methyl chloride | Vinyl chloride | Ethyl chloride | Methyl chloride | Vinyl chloride | Ethyl chloride |
| -78 | 2.3 | 1.9 | 1.4 | 0.09 | 0.12 | 0.14 |
| -55 | 3.6 | — | 4.5 | 1.2 | — | 2 |
| Inversion temp. | 4.2 | 4.2 | 3.8 | 4.2 | 4.2 | 3.8 |
| -35 | — | 5.0 | — | — | 9.6 | — |

The theory was examined for internal consistency by the following process. Arrhenius plots were constructed for data obtained in vinyl chloride solvent at -78 and -45°C ., and the relative rate constant at -35°C . was calculated (Table II). From these values for the relative constants at -35°C ., DP's were calculated for the vinyl chloride system and compared with those found experimentally. These comparative data are shown in Table III.

The agreement between observed and calculated DP's is within experimental error. The calculated energies of activation are $E_3 - E_1 = 1$ kcal./mole, $E_4 - E_1 = 4$ kcal./mole, and $E_4 - E_3 = 3$ kcal./mole. A similar

TABLE III
Experimental and Calculated DP's Obtained in Vinyl Chloride Solvent at -35°C .

| Monomer concentration, mole fractions | DP | |
|---------------------------------------|--------------|------------|
| | Experimental | Calculated |
| 0.075 | 540 | 640 |
| 0.129 | 625 | 670 |
| 0.197 | 770 | 705 |
| 0.241 | 870 | 740 |
| 0.423 | 950 | 910 |
| 0.715 | 1195 | 1180 |

set of data for the methyl chloride system is shown graphically in Figure 5. The slope of this curve indicates $E_4 - E_3 = 4$ kcal./mole.

Thus the proposed mechanism explains the inversion temperature and predicts that DP increases with increasing monomer concentrations at reaction temperatures above the inversion temperature. It is conceivable, however, that the inversion temperature indicates a change in the reaction mechanism. As discussed previously, the rate of propagation is independent of monomer concentration. This, as we have seen, is probably a valid assumption for lower temperatures (-78°C .). However, as the temperature is raised, k_1 (activation of growing polymer cation) must become at least as large, if not larger than k_2 (reaction of monomer with grow-

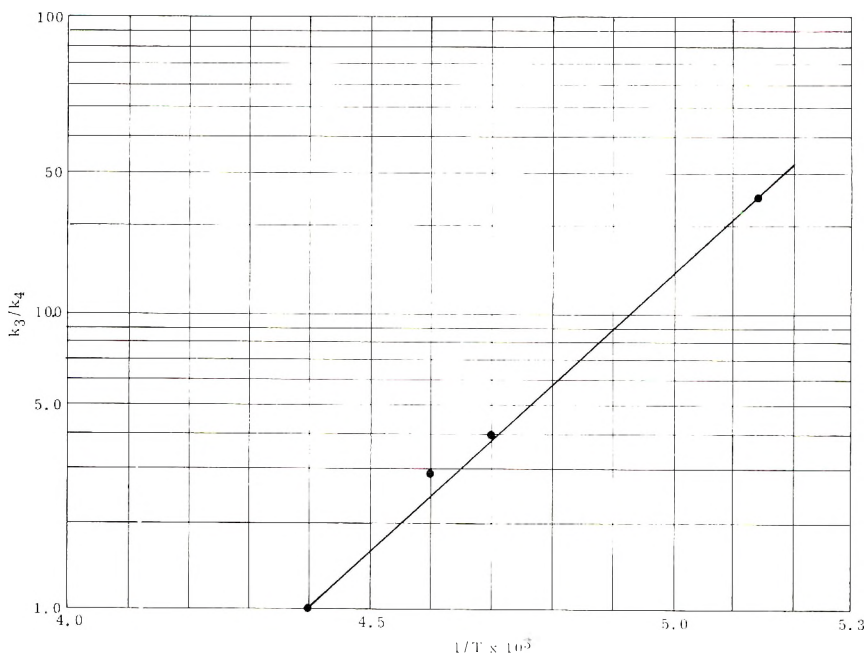


Fig. 5. Dependence of relative rate constants on reciprocal temperatures in the isobutene-methyl chloride system.

ing polymer). Therefore, the rate of propagation will no longer be monomer independent and

$$1/\text{DP} = [(k_3 - k_4)/k_1] + (k'/k_1)(1/N_m) \quad (10)$$

where k' includes k_4 as well as rate constants for other chain-terminating reactions which may have become important at higher temperatures. Thus, at temperatures lower than the inversion temperature the proposed mechanism I, as quantified by eq. (8), explains the data, whereas at temperatures above the inversion temperature either mechanism I or the alternate mechanism (II), expressed in eq. (10), or both may be applicable. Available experimental material does not permit us to choose unequivocally

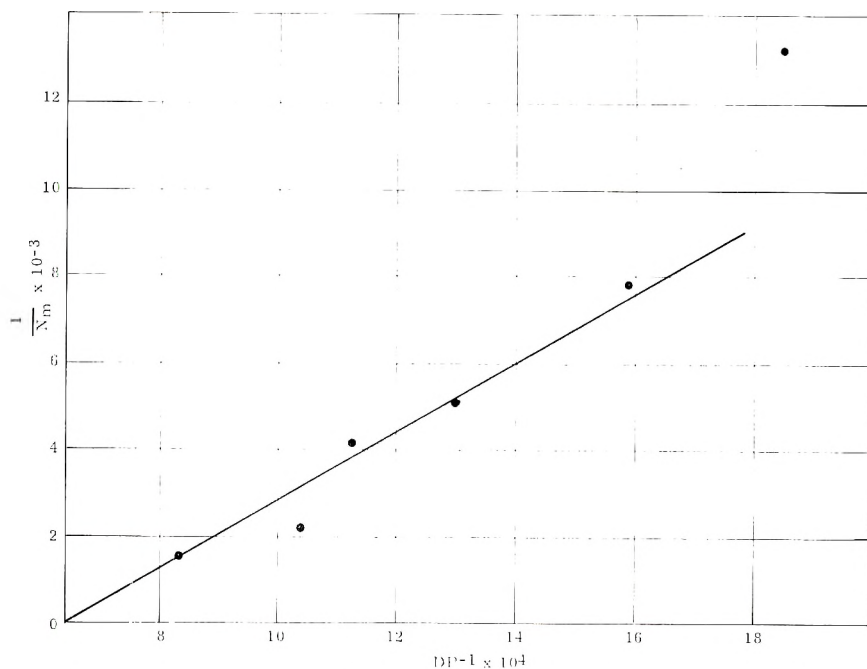


Fig. 6. Plot of eq. (10) for the isobutene-vinyl chloride system at -35°C .

between the two mechanisms at -35°C . As shown in Table III, mechanism I describes the data fairly well, but comparable agreement is shown for mechanism II in Figure 6.

When polar solvents are used, polymer precipitation occurs. If the precipitated polymer is kept in contact with the monomer solution for an extended period of time (16 hr.), the total weight of polymer increases steadily, whereas the average molecular weight remains constant or perhaps decreases slightly. The result of a representative experiment is shown in Table IV. In other experiments a larger decrease in DP was observed.

These results indicate that the polymer molecule probably precipitates after it has stopped growing, i.e., has undergone chain breaking or chain

TABLE IV^a
DP as a Function of Quenching Time

| | Quenching time | | | | | |
|--------------------|----------------|--------|---------|---------|---------|----------|
| | 0.5 min. | 2 min. | 10 min. | 30 min. | 60 min. | 930 min. |
| Polymer formed, g. | 2.016 | 2.740 | 5.670 | 6.510 | 6.921 | 7.584 |
| Conversion, % | 15.5 | 20.6 | 42.6 | 49.0 | 52.0 | 57.0 |
| DP | 4400 | 3110 | 3910 | — | 3730 | 3650 |

^a Experimental procedure was as follows. To a mixture of 13.13 g. (0.238 mole) isobutene and 6.85 g. (0.136 mole) methyl chloride, 1.0 ml. of 2.03×10^{-2} mole AlCl_3/l , methyl chloride was added at zero time at -78°C . The quenching time is the time of addition of quenching agent (methanol).

termination. The precipitated polymer apparently entraps active catalyst, and, therefore, to obtain reproducible results standardized quenching technique is mandatory. It is also not unreasonable to assume that not only DP but also molecular weight distribution might be a function of monomer concentration. Accordingly, molecular weight distribution data could cast further light on the mechanism of cationic isobutene polymerization.

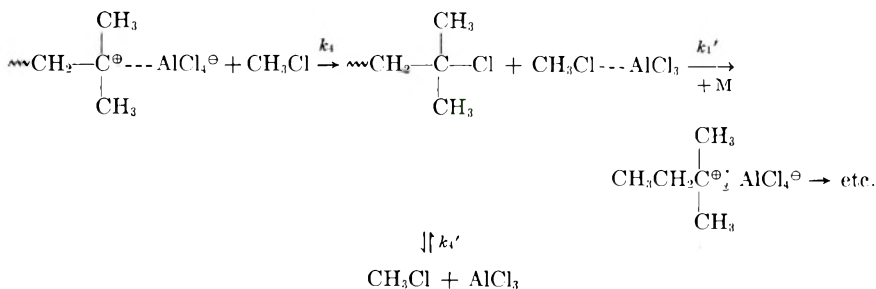
Experiments with C¹⁴-Labeled Methyl Chloride

The usefulness of tracer technique in cationic polymerization mechanism studies has been established earlier in these laboratories.² Thus, experiments conducted in the presence of C¹⁴ methyl chloride showed that conveniently measurable amounts of radioactivity become incorporated in the polyisobutene molecule by low temperature polymerization. This technique has been extended to study the effect of monomer concentration and temperature on the kinetics of C¹⁴ incorporation.

C¹⁴ entry from methyl chloride solvent can be visualized either by initiation or by chain breaking involving the solvent, as shown in eqs. (1b) and (1e). Therefore, in general terms, the measure of C¹⁴ entry, the incorporation ratio I , can be defined as the sum of the rates of the processes leading to incorporation to the sum of rates of those which do not. Thus,

$$I = F(V_1 + V_4)/[F(V_3 + V_4) + V_1] \quad (11)$$

where V_1 , V_3 , and V_4 are rates of initiation, transfer to monomer, and chain breaking involving the solvent respectively, and F is the fraction of the latter reaction with methyl chloride leading to new chains, against those processes which consume the reactive AlCl_4^\ominus specie:



Thus in first approximation $F \propto k_1'/k_4'$

Although it was previously indicated that radioactive methyl chloride might be introduced into the polymer by either primary initiation or by chain breaking involving the solvent, our data indicate that the latter is probably the more important. Other workers have also shown that alkyl chlorides, e.g., ethyl and propyl chloride, do not act as co-catalysts in low temperature cationic polymerization of isobutene and styrene with titanium tetrachloride.^{14,15} Accordingly, eq. (11) may be written as

$$I = F(1 - N_m)/[(k_3/k_4 - F)N_m + \phi(k_4)] \quad (12)$$

where $\phi(k_4)$ is a function of k_4 . This equation is in qualitative agreement with the experimental facts: namely, I increases as monomer concentration (N_m) decreases; it is a function of monomer concentration even at the inversion temperature; and it decreases with increasing temperature. This would mean that F decreases with increasing temperature.

Equation (11) may also be rewritten as

$$I = T_s F / (T_s F + T_m + 1) \quad (13)$$

where T_s and T_m are the number of solvent and monomer chain breaking reactions, respectively, per kinetic chain length (i.e., per bona fide initiation). Applying this equation to the C¹⁴ methyl chloride incorporation data, indicates an F value of about 0.1–0.15 at -45°C . and about 0.4–0.5 at -60°C . There are about five solvent transfers per kinetic chain length at -60°C . F is probably about 1.0 at -78°C . Unambiguous quantitative evaluation of C¹⁴ incorporation data requires the exact knowledge of number-average molecular weights (\bar{M}_n) and molecular weight distributions. Our \bar{M}_n values have been calculated from viscosity-average molecular weights with the use of 1.83 as conversion factor⁵ and with the assumption that the molecular weight distributions are substantially the same for every sample investigated. Thus the above numbers must be considered merely as semiquantitative indicators of trends.

References

1. Kennedy, J. P., and R. M. Thomas, *J. Polymer Sci.*, **55**, 311 (1961).
2. Kennedy, J. P., and R. M. Thomas, *J. Polymer Sci.*, **45**, 227 (1960).
3. Kennedy, J. P., and R. M. Thomas, *J. Polymer Sci.*, **46**, 481 (1960).
4. Flory, P. J., *J. Am. Chem. Soc.*, **65**, 372 (1943).
5. Rehner, J., *Ind. Eng. Chem.*, **36**, 124 (1944).
6. Houtman, J. P. W., *J. Soc. Chem. Ind.*, **66**, 102 (1947).
7. Ambroz, A., and Z. Zlamal, *J. Polymer Sci.*, **30**, 381 (1958).
8. Zlamal, Z., and A. Ambroz, *J. Polymer Sci.*, **29**, 595 (1958).
9. Vesely, K., *J. Polymer Sci.*, **30**, 357 (1958).
10. Mayo, R. M., and C. Walling, *J. Am. Chem. Soc.*, **71**, 3845 (1949).
11. Plesch, P. H., *J. Appl. Chem.*, **1**, 269 (1951).
12. Fontana, C. M., *J. Am. Chem. Soc.*, **70**, 3745 (1948).
13. Kennedy, J. P., and R. M. Thomas, *J. Polymer Sci.*, **46**, 233 (1960).
14. Biddulph, R. H., and P. H. Plesch, *J. Chem. Soc.*, **1960**, 3913.
15. Longworth, R. W., P. H. Plesch, and P. P. Rutherford, *Proc. Chem. Soc.*, **1960**, 68.

Synopsis

Further studies with the isobutene-aluminum chloride-methyl chloride system has led to a better understanding of the dependence of degree of polymerization on monomer concentration and on temperature. Polymerizations were also carried out in C¹⁴-labeled methyl chloride to determine solvent incorporation in the polymer. A quantitative kinetic theory has been developed which explains the behavior of the isobutene-aluminum chloride system in polar solvents such as methyl chloride, vinyl chloride, and ethyl chloride. The rate-determining step in propagation is polymer activation, presumably by ion separation. The DP of the polymer is determined principally by two competing chain-breaking processes; namely, chain transfer to monomer and/or chain breaking involving the solvent. The latter reaction becomes important in polar

solvents at higher temperatures. The influence of phase separation has also been studied. The results indicate that the polymer molecule precipitates after it has undergone either a chain breaking or a chain termination reaction.

Résumé

Des études ultérieures du système isobutène-chlorure d'aluminium-chlorure de méthyle ont permis de mieux comprendre la dépendance liant le degré de polymérisation (DP) à la concentration en monomère et à la température. On a également effectué des polymérisations dans du chlorure de méthyle marqué au C_{14} afin de déterminer l'incorporation du solvant dans le polymère. On a développé une théorie cinétique quantitative qui explique le comportement du système isobutène-chlorure d'aluminium dans des solvants polaires tels que le chlorure de méthyle, le chlorure de vinyle et le chlorure d'éthyle. L'étape déterminante de vitesse pour la propagation est l'activation du polymère, vraisemblablement par séparation de ion. Le DP du polymère est déterminé principalement par deux processus de rupture de chaîne en compétition, à savoir un transfert de chaîne sur le monomère et/ou une fracture de chaîne en réaction avec solvant. Cette réaction devient important dans des solvants polaires à des températures plus élevées. On a aussi étudié l'influence de la séparation de phase. Les résultats indiquent que la molécule de polymère précipite après avoir subi une réaction de transfert de chaîne ou de terminaison de chaîne.

Zusammenfassung

Die weitere Untersuchung des Isobuten-Aluminiumchlorid-Methylchlorid-Systems führte zu einem besseren Verständnis der Abhängigkeit des Polymerisationsgrades (DP) von der Monomerkonzentration und Temperatur. Die Polymerisation wurde, zur Bestimmung des Lösungsmiteleinbaus in das Polymere, auch in ^{14}C -markiertem Methylchlorid ausgeführt. Es wurde eine quantitative, kinetische Theorie entwickelt, die das Verhalten des Isobuten-Aluminiumchloridsystems in polaren Lösungsmitteln, wie Methylchlorid, Vinylchlorid und Äthylchlorid, erklären kann. Der geschwindigkeitsbestimmende Schritt beim Wachstum ist die Aktivierung des Polymeren, vermutlich durch Ionenstrennung. Das DP des Polymeren wird in der Hauptsache durch zwei Reaktionen bestimmt, nämlich Kettenübertragung zum Monomeren und/oder Kettenbruch in dem die Lösungsmittel irt verwickelt. Der Letzte gewinnt besonders in polaren Lösungsmitteln bei höherer Temperature Bedeutung. Der Einfluss der Phasentrennung wurde gleichfalls untersucht. Die Ergebnisse zeigen, dass das Polymermolekül nach Stattfinden einer Übertragungs- oder Abbruchsreaktion ausfällt.

Received August 9, 1961

Revised October 23, 1961

Unsaturation in High Impact Polystyrene Analytical Studies

T. R. CROMPTON and V. W. REID, *Carrington Research Laboratory,
Shell Chemical Co. Ltd., Urmston, Manchester, England*

INTRODUCTION

High impact polystyrene may be manufactured either by blending rubber with polystyrene by hot rolling or alternatively by the "inter-polymer" route, in which the rubber is copolymerized with the styrene during polymerization.

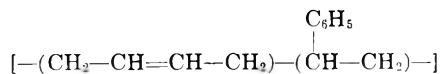
When manufactured by either method the final high impact product may consist of three types of material: free rubber, rubber which has grafted onto or copolymerized with the polystyrene, and a gel fraction. The gel fraction consists of a graft of rubber with the polystyrene, under such conditions that crosslinking of polymer chains takes place, with the result that the polymer becomes insoluble in solvents.

Free rubber and rubber-polystyrene graft polymer are difficult to determine in the presence of one another, as they are similar in molecular structure and do not show any wide differences in solubility in solvents. Crosslinked gel polymer, however, may be readily determined, as it is insoluble in aromatic solvents, such as toluene, in which the other polymer constituents are readily soluble.

Although it is not possible to distinguish between free rubber and soluble rubber-polystyrene graft polymer, we considered it desirable to determine the way in which added rubber distributes between the soluble and gel fractions of high impact polystyrene. This would provide additional information on interpolymerization reactions.

EXPERIMENTAL

When butadiene is copolymerized with styrene in the manufacture of a styrene-butadiene rubber, unsaturation due to the butadiene remains in the rubber. Butadiene-styrene units, of the type:



are formed, and Cheyney and Kelley¹ have developed procedures for the determination of this type of unsaturation in a variety of rubbers.

Each butadiene unit present in the rubber molecule, therefore, contains

an unsaturated ethylenic linkage. We considered it feasible, therefore, to follow rubber distribution between gel and soluble fractions by determination of unsaturation. Some loss of unsaturation was expected to occur through crosslinking of polymer chains, so our work was designed to determine any such loss of unsaturation during interpolymerization reactions.

Separation of Gel and Soluble Fractions

To separate a sample into gel and soluble fractions we first dissolve it in toluene. Only gel remains undissolved. Methanol is then added, which precipitates the polystyrene-rubber graft, ungrafted rubber, and polystyrene. Any styrene monomer, soap, or lubricant remain in the liquid phase, which is separated from the solids and rejected.

The addition of fresh toluene to the solids dissolves all the polymeric material with the exception of the gel. The toluene solubles are separated from the solid gel by centrifuging and made up to a standard volume with toluene. The gel is then dried *in vacuo* and weighed.

Both the gel and toluene soluble fractions are reserved for determination of unsaturation.

Determination of Unsaturation

Of the various halogenation methods employed for the determination of unsaturation a procedure employing iodine monochloride, developed by Cheyney and Kelley,¹ was considered most suitable. In this method, which is a modified iodine value procedure, a chloroform solution or suspension of the sample is first contacted with an excess of a standard solution of iodine monochloride in glacial acetic acid. Iodine monochloride is consumed which is equivalent to the bound butadiene present in the polymer. Unreacted iodine monochloride is then determined iodometrically by adding an excess of aqueous potassium iodide and titrating the liberated iodine.

We examined this procedure in detail, therefore, to evaluate its accuracy for the determination of unsaturation in styrene-butadiene rubbers and for the gel and toluene-soluble fractions separated from high impact polystyrene.

Unsaturation in Styrene-Butadiene Rubbers

To determine unsaturation in rubbers with good accuracy using the iodine monochloride procedure we found it necessary to contact the sample with chloroform for a considerable period before reaction with iodine monochloride. The chloroform softens or swells the rubber and allows the iodine monochloride reagent to permeate throughout the sample. A contact period with chloroform of 15 hr. was made standard procedure for all solid samples.

The influence of sample size and reaction time was then examined.

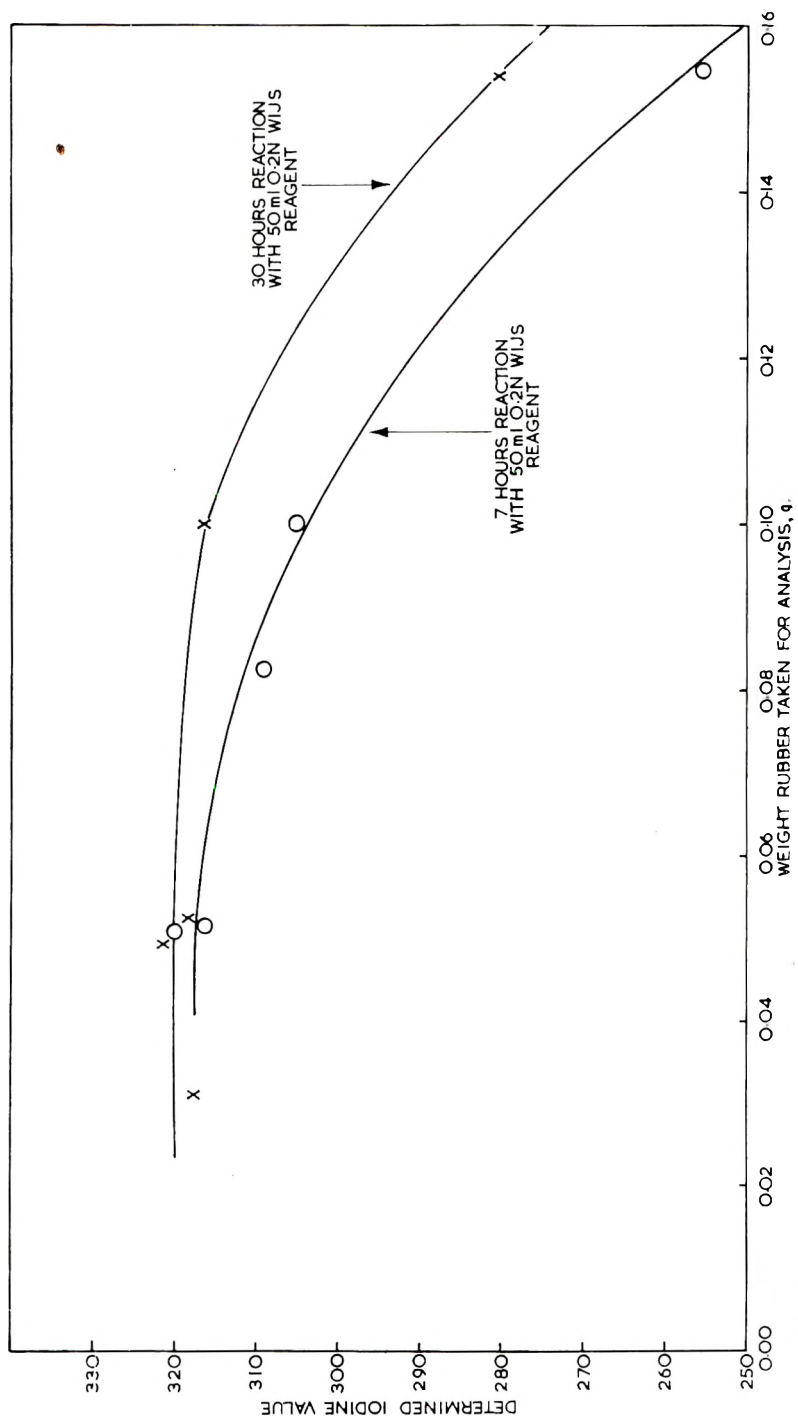


Fig. 1. Influence of excess iodine monochloride reagent and reaction time on the determination of the iodine value of rubber.

Various sample weights were contacted with chloroform and then a constant volume of iodine monochloride reagent (50 ml. 0.2*N* reagent) was added to each. Excess iodine monochloride was then determined in each case after 7 hr. reaction in the dark. This set of experiments was then repeated after the longer reaction time of 30 hr.

In Figure 1 a plot is made of sample size against the determined iodine value; it may be seen that, even with a 30-hr. reaction period, a constant iodine value (ca. 320) is obtained only when the sample size is 0.05 g. or less. This represents a fivefold excess of iodine monochloride reagent. A maximum sample weight of 0.05 g. together with a 30-hr. reaction period is employed, therefore, when rubbers with an iodine value in the 300 region are analyzed. With rubbers having a different order of iodine value, the sample size is adjusted accordingly, i.e., in analysis of polybutadiene (iodine value 470) a sample weight of about 0.03 g. is used.

Unsaturation in High Impact Polystyrene

Unfractionated high impact (HI) polystyrene may not dissolve completely in chloroform due to the presence of gel. It was considered possible, therefore, that a more prolonged period of contact with chloroform or with the iodine monochloride reagent would be required. For this reason we carried out a series of analysis on one sample of impact polystyrene, in which the contact time with chloroform and the reaction time with reagent were extended. As this sample contained some 5% of rubber, the sample size employed was some twenty times that used when analyzing the rubber itself. The sample size was varied in the 0.5–1.0 g. region, therefore, the same volume of reagent being employed as before.

The results obtained are shown in Table I, where it is seen that extension of the contact time with chloroform beyond 15 hr. or the reaction period with iodine monochloride reagent beyond 30 hr. is not required. Varying the sample size between 0.5 and 1.0 g. did not affect the result obtained.

TABLE I
Unfractionated HI Polystyrene

| Weight of sample taken, g. | Contact time | | Iodine value |
|----------------------------|----------------------|---------------------------------|--------------|
| | with chloroform, hr. | Reaction time with reagent, hr. | |
| 0.5 | 15 | 30 | 18.3 |
| 0.7 | 15 | 30 | 18.2 |
| 1.0 | 15 | 30 | 18.3, 18.1 |
| 1.0 | 30 | 65 | 18.1, 18.2 |
| 1.0 | 55 | 65 | 17.8, 18.2 |

Unsaturation in Gels

The solid gel, separated from a high impact polystyrene by solvent extraction procedures, is completely insoluble in chloroform and in the

iodine monochloride reagent solution. Furthermore, the gels obtained from a variety of samples showed considerable differences in their swelling properties with chloroform and in their rate of reaction with iodine monochloride reagent. We found, however, that if the period of contact with chloroform was extended to 90 hr. with a 75-hr. reaction period with reagent, then quantitative determination of unsaturation was obtained, even with the least reactive samples.

Unsaturation in Soluble Graft

After separation of soluble graft from the sample, as previously described, the graft is obtained as a solution in a known volume of toluene. It would be most convenient if determination of unsaturation could be made directly on this solution.

We checked to see whether the presence of toluene interfered in the determination of unsaturation by reacting different volumes of soluble graft solution with a fivefold excess of iodine monochloride solution. In a parallel series of tests the toluene was completely removed by drying under vacuum at 60°C. The residues were then dissolved in chloroform and similar volumes of reagent added, as in the previous tests, to give a fivefold excess of reagent.

The results obtained were expressed in terms of milligrams of iodine consumed per milliliter of graft solution and are shown in Table II. It is seen that, in the presence of toluene, high and inconsistent values for iodine consumption are obtained. Prior to analysis, therefore, it is necessary to remove toluene from these solutions and then dissolve the residue in chloroform.

TABLE II
Influence of Toluene on Determination of Unsaturation in Soluble Graft Solutions

| Volume of graft solution taken for analysis, ml. | Iodine consumed, mg./ml. sample | |
|---|---------------------------------|-----------------|
| | Toluene not removed | Toluene removed |
| 20 | 3.55 | 1.34 |
| 30 | 3.34 | 1.35 |
| 40 | 2.5 | 1.39 |

Distribution of Unsaturation

We used these procedures to study the distribution of rubber added in several laboratory preparations of high impact polystyrene. In these experiments 6 wt.-% of a styrene-butadiene rubber was added during interpolymerization with styrene. A range of polymers with varying gel contents was prepared, and these products were separated into gel and toluene solution fractions.

The iodine value of the rubber was determined and calculated as per cent butadiene. This calculated to an addition of butadiene unsaturation in the interpolymerization of 4.1%. The unsaturation present in the gel

and soluble fractions separated from each polymer was then determined and expressed in terms of per cent butadiene, calculated on the original sample before separation into fractions. The results obtained are given in Table III, which shows the way in which the added unsaturation of 4.1% butadiene distributes between the gel and soluble fractions. Values for the butadiene content of the isolated gel are also shown.

It is seen that the butadiene content of the separated gel remains fairly constant, in the 20–25% region, regardless of the quantity of gel present in the sample. As the gel content increases, therefore, so more of the rubber becomes incorporated into the gel and less remains as free rubber or soluble graft.

The fact that the butadiene content of the gel remains fairly constant suggests also that, for any given rubber addition, there will be a maximum gel content. For instance, a rubber addition equivalent to a butadiene content of 4.1% would result in a maximum gel content in the 16–20% region in the final polymer.

In Table III values are also shown for the total determined butadiene content in each sample, i.e., the total of the soluble graft and gel butadiene contents. These values are also expressed as a percentage of the butadiene originally added in the rubber addition (4.1%). It is seen that the recovered unsaturation lies mainly in the 90–95% region, indicating that loss of unsaturation due to grafting or crosslinking reactions occurs only to the extent of some 5–10%.

Although the butadiene content of gels did not vary widely, the precise level of butadiene in the gel obtained in an interpolymerization appeared to depend on the nature of the catalyst system employed.

Gel Formation During a Polymerization

We now studied gel formation during an interpolymerization reaction by removing samples from the reaction vessel at various times. Rubber (6%) was added, and the iodine value of the rubber was such that this was equivalent to the addition of 4.1% butadiene. The results obtained are shown in Table IV, where, as before, the results have been calculated as per cent butadiene on the original sample before fractionation.

It is seen that the butadiene content of the gels remains remarkably constant, regardless of the quantity of gel separated from the polymer. As the reaction proceeds, the quantity of butadiene present in the soluble graft fraction falls, while the butadiene that passes to the gel fraction increases. Rather less than 10% of the added unsaturation is consumed in grafting or crosslinking reactions.

Effect of Milling on Unsaturation

The effect of milling on the unsaturation characteristics of the gel and soluble graft fractions of a sample of high impact polystyrene was then examined. A sample of high impact polystyrene, prepared by the interpolymerization method, from a styrene–butadiene rubber (equivalent to

TABLE III
Distribution of Butadiene between Soluble and Gel Fractions Obtained from Polystyrenes Containing Different Amounts of Gel

| Gel content of sample, wt.-% | Butadiene content of isolated gel, wt.-% | Soluble graft buta- diene content <i>A</i> (calculated on original sample), wt.-% | Gel butadiene content <i>B</i> (calculated on original sample), wt.-% | Total butadiene content (<i>A</i> + <i>B</i>), (calculated on original sample), wt.-% | Amount of original rubber unsaturation in the sample, $C = \frac{(A + B)}{4.1} \times 100\%$ |
|---------------------------------|---|--|--|--|---|
| 0 | — | 3.5 | — | 3.5 | 85 |
| 4.7 | 19.5 | 2.8 | 0.9 | 3.7 | 90 |
| 5.3 | 18.6 | 2.8 | 1.0 | 3.8 | 93 |
| 5.6 | 16.2 | 2.9 | 0.9 | 3.8 | 93 |
| 8.6 | 19.7 | 2.0 | 1.7 | 3.7 | 90 |
| 8.9 | 23.3 | 1.5 | 2.1 | 3.6 | 88 |
| 9.4 | 25.8 | 1.4 | 2.4 | 3.8 | 93 |
| 11.8 | 20.0 | 1.5 | 2.4 | 3.9 | 95 |
| 11.8 | 21.4 | 1.3 | 2.6 | 3.9 | 95 |
| 11.8 | 20.0 | 1.5 | 2.4 | 3.9 | 95 |
| 12.5 | 20.0 | 1.4 | 2.5 | 3.9 | 95 |

TABLE IV. Distribution of Butadiene between Soluble and Gel Fractions during Interpolymerization

| Sample no. | Gel content, wt.-% | Butadiene content of isolated gel, wt.-% | Soluble graft butadiene content, A (calculated on original sample), wt.-% | Gel butadiene con- tent B (calculated on original sample), wt.-% | Total butadiene content (A + B) (calculated on original sample), wt.-% | Amount of original rubber unsaturation in the sample $C = \frac{C}{(A+B)} \times 100,$ wt.-% |
|------------|-----------------------|--|---|---|--|---|
| 1 | 6.2 | 24.8 | 2.5 | 1.5 | 4.0 | 97 |
| 2 | 6.5 | 23.3 | 2.2 | 1.5 | 3.7 | 90 |
| 3 | 7.5 | 24.1 | 2.0 | 1.8 | 3.8 | 93 |
| 4 | 9.2 | 25.0 | 1.5 | 2.3 | 3.8 | 93 |
| 5 | 8.7 | 25.6 | 1.6 | 2.2 | 3.8 | 93 |
| 6 | 9.4 | 25.8 | 1.4 | 2.4 | 3.8 | 93 |

TABLE V. Effect of Milling on Unsaturation

| Milling time, min. | Gel content of original polystyrene, wt.-% | Butadiene content of isolated gel, wt.-% | Soluble graft butadiene content A (calculated on original sample), wt.-% | Gel butadiene con- tent B (calculated on original sample), wt.-% | Total butadiene content (A + B) (calculated on original sample), wt.-% | Amount original rubber unsatura- tion in the sample $C = \frac{C}{(A+B)} \times 100,$ wt.-% |
|-----------------------|--|--|--|---|--|---|
| 5 | 8.1 | 23.0 | 1.7 | 1.9 | 3.6 | 88 |
| 10 | 6.8 | 24.9 | 2.0 | 1.7 | 3.7 | 90 |
| 15 | 6.2 | 26.3 | 2.1 | 1.6 | 3.7 | 90 |
| 30 | 5.8 | 27.7 | 2.3 | 1.6 | 3.9 | 95 |

the addition of 4.1% butadiene), was milled for various time intervals at a temperature of 160°C. The results obtained are shown in Table V.

It is seen that milling disrupts the gel fraction, so that as the period of milling increases the quantity of gel present decreases. This disruption would appear to occur by the breaking of chemical bonds in the high molecular weight gel fraction and this appears to lead to increased unsaturation in the gel fraction.

As the gel fraction decreases during milling so unsaturation increases in the soluble graft fraction. Milling, indeed, appears to result in a general increase of total unsaturation in the polymer.

The authors wish to express their thanks to the Directors of Shell Chemical Company Limited for permission to publish this work and also to Mr. B. Cope who carried out much of the experimental work.

Reference

1. Chcyney, La Verne E., and E. J. Kelley, *Ind. Eng. Chem., Ind. Ed.*, **34**, (1942).

Synopsis

A method for separating a pure gel and a soluble graft containing fraction from high impact polystyrene is described together with methods for determining the unsaturation of these two fractions and for the determination of unsaturation in polybutadiene rubber and unfractionated high impact polystyrene samples. The methods have been used to show how the rubber distributes between the gel and soluble fractions obtained from high impact polystyrenes prepared by the interpolymerization technique.

Résumé

On décrit une méthode de séparation d'un gel pur et d'un greffé soluble contenant des fractions provenant d'un polystyrène à haut impact, de même que des méthodes de détermination de l'insaturation de ces deux fractions et de celle du caoutchouc polybutadiène et d'échantillons de polystyrène à haut impact non fractionné. On s'est servi de ces méthodes pour montrer comment le caoutchouc se distribue entre le gel et les fractions solubles obtenues à partir de polystyrène à haut impact préparé par la technique d'interpolymérisation.

Zusammenfassung

Eine Methode zur Abtrennung einer reinen Gelfraktion und einer löslichen, aufgefropfte Anteile enthaltenden Fraktion aus schlagfestem Polystyrol wird zusammen mit Methoden zur Bestimmung der Doppelbindungen an diesen beiden Fraktionen sowie der Bestimmung von Doppelbindungen in Polybutadienkautschuk und in unfraktionierten, schlagfesten Polystyrolproben beschrieben. Die Methoden wurden zur Bestimmung der Verteilung des Kautschuks zwischen der Gelfraktion und der löslichen Fraktion aus schlagfestem, nach dem Interpolymerisationsverfahren hergestellten Polystyrol verwendet.

Received November 9, 1961

Thermodynamics of Crystalline Linear High Polymers. II. The Influence of Copolymer Units on the Thermodynamic Properties of Polyethylene*

BERNHARD WUNDERLICH and DOUGLAS POLAND, *Department
of Chemistry, Cornell University, Ithaca, New York*

INTRODUCTION

Any semicrystalline polymer can be characterized thermodynamically by three parameters. One is the mole fraction of crystallizable units in the amorphous phase X_A . (In this article random distribution is assumed throughout. For nonrandom distribution of the different repeating units additional information on the statistics may be required.) The second is the more complicated parameter σ , which accounts for the size and order of the crystalline phase. Ideally, this factor would be a surface free energy term; however, to account completely for the behavior of crystallites, separate values for surface free energies of different crystallographic planes must be known, as well as effects of defects in the crystal and on the surface. The third parameter is the weight fraction crystallinity c_w , a term which is calculated on the basis of the assumption that the semicrystalline polymer is made up of perfectly ordered and perfectly random (amorphous) parts only.

X_A determines the amount the chemical potential of the amorphous phase is lowered by copolymerized units. σ is the additional contribution of defects and surfaces to the chemical potential of the solid phase. Below the melting range c_w indicates how far the polymer is removed from thermodynamic equilibrium. For equilibrium below the melting range c_w would have a value corresponding to X_A in the completely amorphous phase above the melting range, and σ would be a small term for X_A close to 1.

The long-range goal of this laboratory is to gather information about the factors determining σ^{1-3} . One important step towards this goal is the knowledge of X_A and c_w . In this paper X_A and c_w will be discussed along with the maximum melting point, T_m , for copolymers containing besides the crystallizable unit $-\text{CH}_2-$, the foreign units $-\text{CHCH}_3-$ and $-\text{CO}-$.

* Presented in part at the 140th National Meeting of the American Chemical Society, Chicago, Ill., September 1961.

EXPERIMENTAL

Materials

Two series of copolymers were used for this investigation. A series of six ethylene-carbon monoxide copolymers of varying concentration (Table I), designated C₁ to C₆, were kindly supplied by the Polychemicals Department of the E. I. du Pont de Nemours Company. All polymers of this series were polymerized alike at pressures of 700–1100 atm. and temperatures of 200–250°C. The conversion in the continuous flow process was approximately 15%.

TABLE I
CO-CH₂ Copolymers

| Polymer | Density, g./cc. | Melt viscosity, poise | CO/ 100 C | Begin of melting, °C. | Extrap- olated m.p., °C. | X _{CH₂} |
|----------------|--------------------|-----------------------------|--------------|-----------------------------|--------------------------------|-----------------------------|
| Marlex 50 | 0.977 | — | 0.0 | 106.5 | 134.4 | (0.995) ^a |
| C ₁ | 0.913 | 170 | 0.0 | 28 64 | 104.5 | 0.909 0.91 ^b |
| C ₂ | 0.919 | 32 | 1.7 | 28 56 | 99.0 | 0.893 0.90 ^b |
| C ₃ | 0.942 | 16 | 5.2 | 31 46 | 91.7 | 0.872 0.89 ^b |
| C ₄ | 0.939 | 10,000 | 3.0 | 36 — | 103.2 | 0.906 0.91 ^b |
| C ₅ | 0.991 | 950 | 9.0 | 33 47 | 96.8 | 0.887 0.92 ^b |
| C ₆ | 1.022 | 55 | 13.2 | 30 50 | 90.8 | 0.869 0.92 ^b |

^a Data of Bryant.¹⁸

^b Recalculated values obtained from proportionally reduced heats of fusion.

A series of ten ethylene-propylene copolymers (Table II), designated P₁–P₁₀, was kindly supplied by the Research Department of the Hercules Powder Company. P₁ to P₉ were polymerized with a low pressure catalyst. P₁₀ is a predominantly atactic polypropylene.

The viscosity data on both sets of polymers were measured in the laboratories of the supplying companies.

Differential Thermal Analysis

Differential thermal analysis (DTA) was carried out by use of a brass cylinder with two symmetrical sample wells, one of which was filled with 0.50 g. of the polymer and the other with an Al₂O₃ reference. The cylinder was heated by an evenly wound heating tape. The power was supplied over a voltage stabilizer and a variable transformer. The heating assembly was contained in a Dewar vessel to allow cooling to low temperatures.

Fe-Constantan thermocouples with an ice bath reference were used as

TABLE II
 CHCH₃-CH₂ Copolymers

| Polymer | Density g./cc. | Viscos- ity number | CH ₃ / 100 C | Begin of melting, °C. | Extrap- olated m.p., °C. | X _{CH₂} |
|-----------------|-------------------|--------------------------|----------------------------|-----------------------------|--------------------------------|-----------------------------|
| Marlex 50 | 0.977 | — | 0 | 106.5 | 134.4 | (0.995) ^a |
| P ₁ | 0.964 | 3.4 | 0 | ~80 | 134.3 | 0.995 |
| P ₂ | 0.955 | 3.3 | 0.2 | ~80 | 132.8 | 0.990 |
| P ₃ | 0.942 | 3.0 | 0.7 | ~85 ^b | 129.6 | 0.982 |
| P ₄ | 0.948 | 10.3 | 2.5 | ~58 ^b | 129.3 | 0.980 |
| P ₅ | 0.912 | 1.8 | 5.0 | ~34 | 123.5 ^c | (0.976) |
| | | | | | 94.7 | 0.881 |
| P ₆ | 0.885 | 4.0 | 10.0 | 32 | 118.5 ^c | (0.950) |
| | | | | | 80.4 | 0.839 |
| P ₇ | 0.861 | 2.7 | 15.5 | — | — | — |
| P ₈ | 0.854 | 2.5 | 20.0 | — | — | — |
| P ₉ | 0.853 | 3.0 | 25.0 | — | — | — |
| P ₁₀ | 0.860 | 2.0 | 50.0 | — | — | — |

^a Data of Bryant.¹⁸

^b First weak deviation between 35 and 60°C.

^c Two distinct melting peaks.

detectors. For maximum reproducibility of the position within the sample, thermocouples enclosed in 1/16 in. diameter stainless steel tubing insulated with MgO were used (Aeropak, Aero Research Co.).

Quantities measured were the temperature of the sample and the difference between the sample and the reference. Continuous recording of the temperature was done with a millivolt recorder (2 mv. full-scale span with a precision potentiometer for range variation). The difference was recorded by the same instrument (two-point recorder, 2-sec. print cycle). Pre-amplification of the difference by a factor of 5 to 20 was necessary for high precision.

The sample thermocouple was calibrated by comparison with a Pt-resistance thermometer. The almost linear corrections to the values in the National Bureau of Standards tables⁴ ranged from -0.03 mv. to 0°C. to +0.09 mv. at 170°C. This deviation includes the constant zero point correction of the entire measuring set-up. The calibration accuracy was limited only by the readability of the recorder chart, or ±0.1°C. This is somewhat more precise than the location of the peaks and other temperatures on the recordings.

The heating rate employed was 2.7°C./min., a rate which is sufficiently fast to minimize recrystallization during the heating cycle and which is not too fast to shift the transition temperature recorded.³ Rates of 1.8°C./min. and 3.4°C./min. of identical samples gave variation of no more than ±0.1°C. for the peak position, which is well within the error limit. Peak areas varied linearly with heating rate over this limited range.

The purpose of the measurements is to get insight into the actual structure of the samples on hand at low temperature which is possible only if

any slow heating in the range where recrystallization is possible is avoided. To further this factor all samples were crystallized by cooling from at least 20°C. above their melting point down to room temperature at a rate between $1/10$ and $1/12$ the heating rate.

X-Ray Analysis

X-ray analyses were carried out on a General Electric XRD-5 recording instrument. The (200) and (110) peak areas were measured and crystallinities were estimated.⁵ The same peaks were used for the determination of the *a* and *b* unit cell dimensions. Internal calibration was achieved by using known data⁶ for the Marlex 50 *a* axis at the measuring temperature.

Copolymer Content

Microanalyses of the C₁-C₆ samples for C and H as well as ash content gave the amount of CO in the polymer. CH₃ data for samples P₁-P₁₀ were determined by the supplier. The composition was calculated as the number of sidegroups (carbonyl oxygen and —CH₃) per 100 carbons of the backbone chain (see Tables I and II).

Densities

Densities were determined by the flotation method. The density of the liquid kept the sample floating was determined in the same (25°C.) constant temperature bath with the use of a Westphal balance. The accuracy of the density determinations is estimated to be ± 0.001 from experiments on pure organic liquids.

Infrared Spectra

Infrared spectra were taken on films cut from bulk samples. They indicated that all CO was in form of keto groups.⁷ Crystallinity estimations⁵ from the C-H stretch in the amorphous and the CH₂-rocking mode in the crystalline correlated with the determination from the x-ray and DTA determinations.

RESULTS

The results are summarized in Tables I and II.

Densities

The densities in Tables I and II refer to the samples crystallized as described above at 25°C. Increasing CO content will increase the density, while the CH₃ content of amorphous polymers has little influence.

Molecular Weights

Comparison of the melt viscosity of C₁ with similarly prepared polyethylenes⁸ leads to an estimate of 12,000 for \bar{M}_n . The melt viscosities were measured at 125°C.

For the P series, a viscosity number of 3.0 which has been determined at a 0.1% concentration in decalin at 135°C. corresponds to a number-average molecular weight of about 20,000 for pure polyethylene (sample P₁). The uniformity of the samples containing increasing amounts of —CH₃ can be judged by their viscosity number relative to that of P₁.

Differential Thermal Analysis

Since only little work on the DTA of crystalline polymers has been done to date,⁹ the reliability of the DTA set-up was tested on a number of monomeric materials and on the well known Marlex 50^{1,3} linear polyethylene.

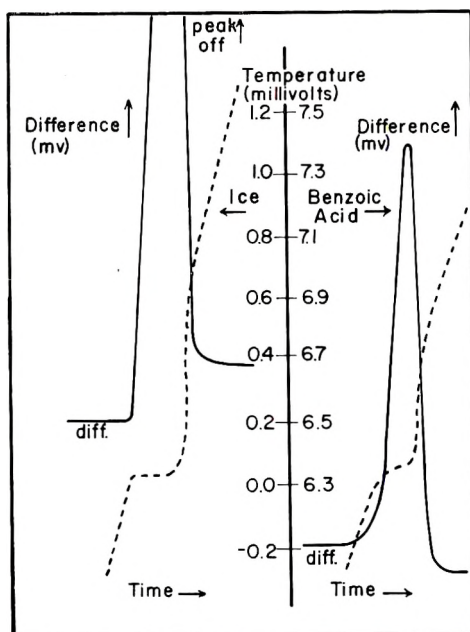


Fig. 1. Graph of (—) the difference in thermocouple potential between reference and sample and (--) the sample thermocouple potential for Ice and Benzoic Acid. The difference is preamplified by a factor of 5.

A series of measurements on 0.40–0.54 g. of ice showed a halt in the temperature recording at -0.002 mv. with a standard deviation of a single measurements of ± 0.005 mv. However ice was the only substance which showed an exact halt in the temperature recording. All other melting points had to be extrapolated from the difference recording peak, as is shown in Figure 1.

Two methods were employed: (a) the peak position was taken and (b) an extrapolation procedure was used. From the theory of DTA¹⁰ it can be seen, that, after the end of the heat-consuming process, the difference in temperature buildup during the melting will quickly be eliminated. This change in the temperature difference follows an exponential law.¹¹ This

drop, was determined experimentally by filling the sample chamber with a small heating coil and regulating the heat input, so that a constant difference recording was obtained. When the heater was turned off, the return to zero of the difference recording was observed. The curves obtained for different heat inputs were all superimposable, and a master curve was constructed for the return of the difference recording to zero (see Fig. 2). By comparing the tail of the melting peak with this master curve, it can be decided where the last trace of crystal melts, and the maximum melting point of the crystallite distribution present at room temperature can be evaluated.

For sharp melting materials this procedure is identical to a back-extrapolation of the sharp drop of the difference recording after the peak and

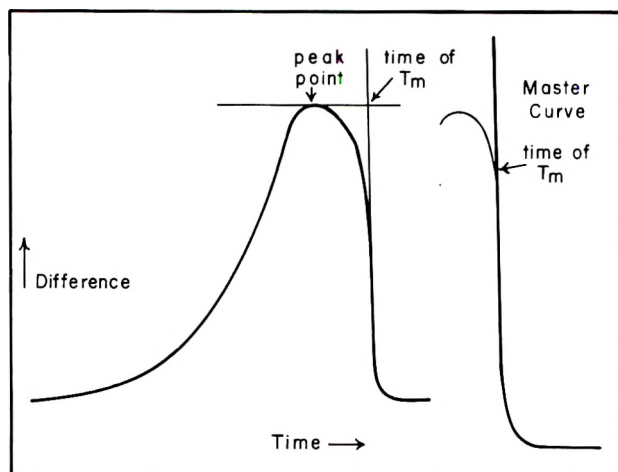


Fig. 2. Evaluation of the melting point tail. The time obtained from this plot is translated into temperature using the sample thermocouple time recording.

determination of the temperature of the point of intersection with the horizontal peak tangent.

For materials which show a sharp melting peak there is even little difference between the peak temperature (*a*) and the extrapolated value (*b*). For ice, 0.03 mv. or 0.6°C. is found. For less sharp melting organic solids, the extrapolated temperature (*b*) is closer to the recorded melting points and more reproducible. For acetamide (Baker Analyzed Reagent, reported m.p. 80.0°C.) the peak temperature was found at 77.5°C., while the extrapolation gives 79.1°C. The same was true for four measurements on recrystallized U.S.P. grade benzoic acid, which showed $121.2 \pm 0.2^\circ\text{C}$. for the extrapolated melting point, but $119.8 \pm 1.2^\circ\text{C}$. for the peak. For Marlex 50 linear polyethylene, the extrapolated temperature is $134.4 \pm 0.4^\circ\text{C}$., close to the maximum melting point of 134.8°C. found calorimetrically on similarly crystallized materials.¹

Eight separate samples of identically annealed Marlex 50 linear polyethylene were measured to check on the reproducibility. The weights varied between 0.48 and 0.54 g. (0.50 ± 0.03) with the exact weight of each sample known. All errors were calculated as the standard deviation of a single measurement.

The melting peak temperature (peak of the difference plot) was $133.5 \pm 0.3^\circ\text{C}$., in good accord with the flat peak of $133.01\text{--}133.60^\circ\text{C}$. of the calorimetric determination.¹ The first perceptible melting, taken as the temperature where DTA difference first deviated from an extrapolation from lower temperature, was $106.5 \pm 1.5^\circ\text{C}$. This value is dependent

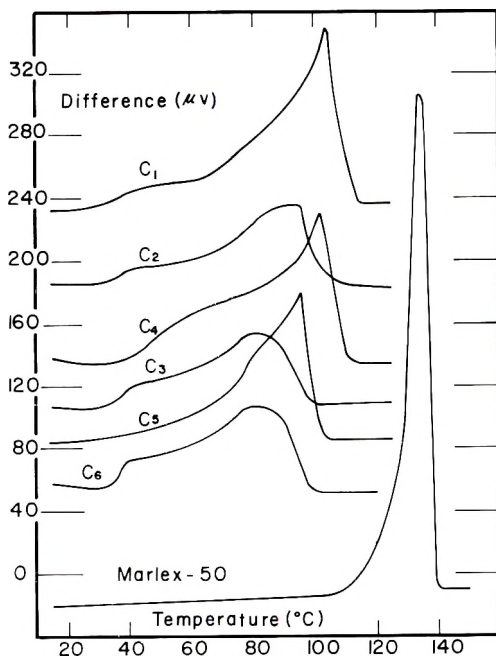


Fig. 3. Differential thermogram of Marlex 50 and CO copolymers. The successive ordinates are shifted.

upon the sensitivity of the measuring set-up and the heating rate. The area under the difference temperature curve in arbitrary units was 152 ± 4 . The heaviest samples have larger areas, but the area is not directly weight proportional. In the copolymer samples thus only equal weights have been compared. The peak height is less reproducible with $324 \pm 12 \mu\text{v}$.

A comparison between the peak half-width showed a 1:2 ratio between the monomeric materials (ice, acetamide, and benzoic acid) and Marlex 50.

DTA: Melting Points and Begin of Melting

The melting points recorded in Table I and II are extrapolated temperatures. The coincidence of these temperatures with the maximum melting

points of the crystal distribution present at low temperature can be estimated by comparison with the calorimetric values for Marlex 50.¹ Figures 3 and 4 give greatly reduced plots of the difference recordings to allow a comparison of the sharpness of the melting transitions.

The begin of melting in Table I is taken at the point where for the first time a deviation from low temperature values is clearly evident. If two values are given, the melting peak has a shoulder to the low temperature side.

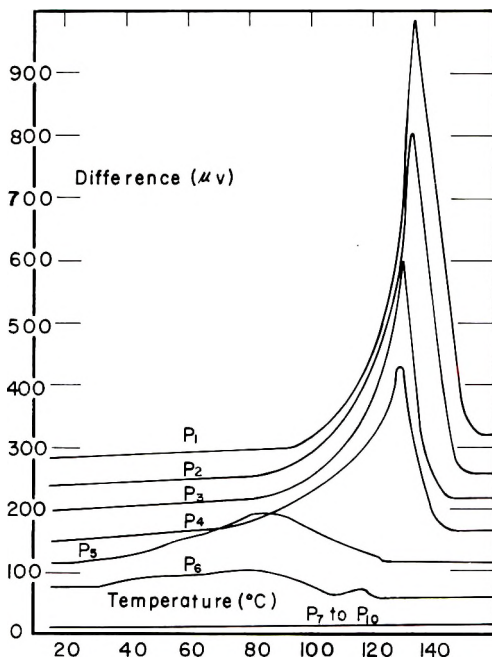


Fig. 4. Differential thermograms of CHCH_3 copolymers. The successive ordinates are shifted.

X-Ray Measurements

Figure 5 gives values for the a axis as a function of foreign groups. Figure 6 shows the x-ray crystallinities.

DISCUSSION

Maximum Melting Point

The melting point of any crystallite is determined by two factors: its surface free energy σ (including a term for crystal defects, which may be looked upon as an inner surface) and the mole fraction of A units X_A . An A unit² is a unit which by its nature could be accommodated in the crystalline lattice.

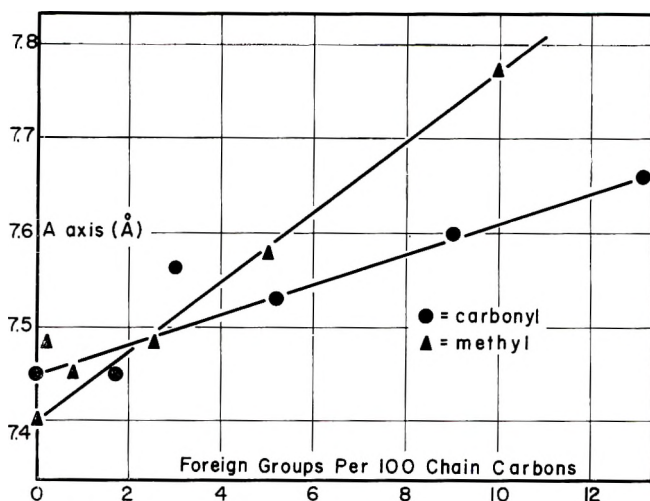


Fig. 5. A-axis dimension of the unit cells from x-ray analysis.

The usual definition of the maximum melting point, T_m , is the temperature where the effect of σ disappears, that means T_m is the melting point of practically perfect, large crystals. Experimentally T_m is closely approached¹² by the temperature where the last trace of crystallinity disappears in a heating experiment, but only if there are any perfect crystals present.

Recent results on solution-crystallized polyethylene¹³ point to the fact that the structure found in melt-crystallized polymers¹⁴ is little different from solution-grown polymer. This leads to the possibility that even the crystals present in a semicrystalline polymer are basically single crystalline or dendritic lamellae with a characteristic fold length in the chain direction.

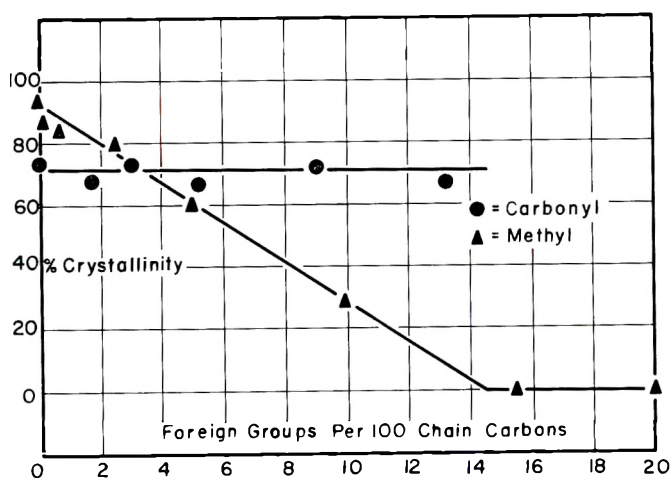


Fig. 6. X-ray crystallinities as a function of foreign groups. For a discussion of the absolute values see text.

This fold length f (crystal thickness in the crystallographic c direction) is largely independent of the occurrence of copolymer units, but depends critically on the crystallization temperature¹⁴ and pressure. The fold length f gives also a lower limit to the surface free energy, since even the largest crystal in a distribution will show the characteristic thickness f , determined by its crystallization temperature. The magnitude of the effect can be estimated by comparing melting temperatures of polyethylenes grown at different temperatures.¹⁵ At 90°C. solution-grown polyethylene has, for example, 8.5 cal./mole CH₂ more surface free energy than a bulk-annealed polyethylene crystallized at about 120–125°C.³

In the light of the above it is necessary to develop an expression for the maximum melting point T_m^f for lamella-type copolymer crystals present at low temperatures. These crystals are formed by a nonequilibrium process several degrees below their melting point. If during the melting of these crystals recrystallization can be avoided, as is the case in these experiments, the melting will occur at the temperature where those crystals formed at lower temperature are in equilibrium with the amorphous phase. In particular T_m^f corresponds to the temperature where the last trace of crystallinity vanishes. At this temperature equilibrium exists between the most perfect lamellae, the lamellae, with the smallest value of σ , and amorphous melt which has the composition specific by X_A . Crystals of larger thickness than f would still be stable at this temperature, but are not present in detectable quantity, and are not expected to form during the melting experiment to any extent if the heating cycle is much faster than the crystallization of the original sample had been.

The equilibrium condition for a large, B defect (amorphous defect, see below) free crystal lamella of fold length f in contact with a melt containing randomly spaced B units is

$$\Delta F_u + RT_m \ln X_A - \sigma_f = 0 \quad (1)$$

σ_f is the fold free energy calculated per mole of repeating units of the lamella of constant thickness f . ΔF_u represents the free energy of fusion per mole of bulk repeating unit. ΔF_u may be written

$$\Delta F_u = \Delta H_u - T\Delta S_u = \Delta H_u[1 - (T/T_m^\circ)] \quad (2)$$

where ΔH_u and ΔS_u are the enthalpy and entropy of fusion per mole of repeating unit, and $T_m^\circ = \Delta H_u/\Delta S_u$ is the melting point of infinitely thick lamellae in contact with a pure A melt. The change in $\Delta H_u/\Delta S_u$ with temperature is assumed to be negligible.

Substituting eq. (2) into eq. (1) yields

$$\ln X_A = (-\Delta H_u/RT_m^\circ) + (\Delta H_u/RT_m^\circ) + (\sigma_f/RT_m) \quad (3)$$

T_m° is the melting point for infinitely thick defect-free lamellae in equilibrium with a pure A unit melt, a temperature which is usually not available experimentally. To use eq. (3), to interpret experiments, it is useful to replace T_m° by T_m^f , the melting point for perfect lamellae of the thickness

present in the (isothermally crystallized) distribution in contact with pure A unit melt. At T_m^f the free energy of fusion of these perfect lamellae is zero, and from eqs. (1) and (2):

$$\Delta F_u^f = 0 = \Delta H_u [1 - (T_m^f/T_m^\circ)] - \sigma_f \quad (4)$$

from this equation one can calculate that

$$\Delta H_u/RT_m^\circ = (\Delta H_u/RT_m^f) - \sigma_f/RT_m^f \quad (5)$$

Substituting back into eq. (3) and neglecting the small term $(\sigma_f/R)[(1/T_m) - (1/T_m^f)]$ yields an equation amenable to experimental use:

$$\ln X_A = (-\Delta H_u/RT_m) + (\Delta H_u/RT_m^f) \quad (6)$$

This equation is identical in form to the Flory expression¹⁶ for the maximum melting point of copolymers without chain folding, but has T_m^f replacing T_m° . All previously published discussions^{1,12,17} should be looked upon as using this replacement. The seemingly perfect agreement usually reached is justified in the light of the identity of eq. (6) and Flory's expression. For the linear polyethylene (Marlex 50) this equation has been tested fully. Its B units are about 0.5/100C¹⁸ and $X_A = 0.995$. The t_m as found in this research and many others is 134.4°C. The calorimetrically found expression for the heat of fusion:¹

$$\Delta H_u = 54.6 + 0.176 t - 6.36 \cdot 10^{-4} t^2 \text{ (cal./g.)}$$

yields 136.2°C. for t_m^f . This value was found experimentally¹⁹ on similarly crystallized polymethylene which has practically no B units. Melting points for Marlex 50 as high as 137–139°C. have been reported^{15,20} by crystallization extremely close to the melting point, usually reached by very slow heating, so that recrystallization can occur, possibly making use of accidental double step nuclei from lower temperature crystallization. That these figures, which seem to push t_m^f up to 140°C. are reasonable can be seen from the ΔT_m^f of solution-crystallized and melt-annealed Marlex 50, which was of the order of magnitude 4°C.^{3,21}

All copolymers used in this research were crystallized in the same way, so that the fold characteristics should be similar for all samples; 136.2°C. was used for t_m^f as calculated from the known X_A of Marlex 50. X_A values have been calculated for all other copolymers from eq. (6) (Tables I and II).

The X_A values for the CO copolymers showed only a slight decrease from 0.91 to 0.84 for the additional inclusion of 20 keto oxygens/100C. This indicates that the keto oxygens are not actual B units, but fit into the lattice as could be predicted for their identical space requirement.²² If, however, keto groups are accommodated by the polyethylene lattice, its heat of fusion will be changed. To estimate this effect model compounds were used. A polyester of 15 acid CO/100 chain atoms has only half the heat of fusion of polyethylene.²³ Polyethers, in turn, have approximately the same heat of fusion as polyethylene.²⁴ With this information the X_A have been

recalculated on the basis of the assumption that for 15 keto oxygens/100 C ΔH_u is one half the value for polyethylene. The results are listed in Table I and show good constancy for all compositions.

For the CHCH_3 copolymers a different situation exists. The melting point T_m decreases with increasing CHCH_3 content. The X_A values drop from 0.995 for P_1 to 0.84 for P_6 , which has only 10 $\text{CH}_3/100$ C. An almost perfect correspondence of the number fraction of B units copolymerized and X_A calculated can be reached if one assumes that CH as well as CH_3 act as separate B units, as is illustrated in Figure 7. This points clearly to the fact that CHCH_3 acts thermodynamically as a noncrystallizable B unit and does not enter the polyethylene lattice.

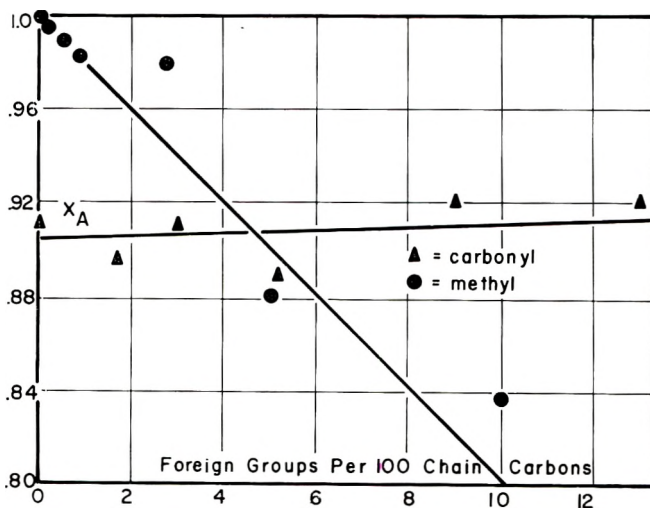


Fig. 7. X_A , the mole fraction of crystallizable units. Calculated from eq. (8). The values for the CO copolymer have been corrected for reduced heat of fusion.

The small shoulder on the melting peak of P_5 and P_6 (Fig. 4) indicates that perhaps the randomness of these samples was not complete.

Crystallinities

The densities, x-ray scattering intensities, and, to a lesser degree, the DTA areas are indicative of the crystallinity of the samples. Recently, doubts have been raised on the previously accepted values of specific volumes for amorphous and crystalline polyethylene.^{6,25-27} Also, the determination of the x-ray crystallinity by the method here employed⁶ has been found to give too high values of crystallinity because it neglects to include the coherent part of the amorphous scattering intensity contained in the background scattering.^{27,28}

In this research x-ray crystallinities are the most consistent, although they are too high by a factor of about 1.25, as can be seen from comparisons

with density crystallinities. Similar discrepancies have been found by Hendus and Schnell.²⁷

For the CO polymer series only x-ray crystallinities could be calculated. The density of the amorphous part increases with the CO content. The x-ray scattering of amorphous as well as crystalline polymer, however, contains the same amount of CO and cancels at least approximately. The important result to be derived from Figure 6 is the fact that for CO copolymers no decrease in crystallinity occurs. The absolute value is too high and probably more in the vicinity of 40–50% as can be seen from the density of C₁. A decrease in the DTA areas from C₁ to C₆ points to the fact that the heat of fusion decreases with increasing CO content. DTA areas are not accurate enough for samples of different nature to allow an improvement on the assumptions made in the discussion of the maximum melting points.

For the CHCH₃ copolymers, density as well as x-ray-crystallinities have been calculated. From the equation for the crystallinity c_w :

$$c_w = 100 (v_a - v)/(v_a - v_c) \quad (9)$$

where v_c is the specific volume (reciprocal of the density) of the x-ray crystalline part and v_a is the specific volume of the completely amorphous part. Any intermediate structures are by this method treated as contributing partially to the amorphous as well as partially to the crystalline phase, depending upon the degree of order. That much of the amorphous polymer in high percentage crystalline samples is partially ordered can be inferred from the increasing sharpness of the broad amorphous scattering centering around 4.5–4.6 Å. To get reliable data for v_c , the crystalline specific volume at the measuring temperature, the a unit cell dimension (see Fig. 5) for each sample was used to calculate the crystalline density. The b and c dimensions change only little and have been assumed constant at the values $c = 2.534$ Å. and $b = 4.93$ Å.²⁹

For v_a , the amorphous specific volume, the average of the four amorphous samples P₇–P₁₀ has been used ($v_a = 1.67$ cc./g.). This value is in good

TABLE III
Percentage Crystallinities

| Sample | Crystallinity, % | | |
|----------------|------------------|--------------|--------|
| | By x-ray | From density | Ratio |
| Marlex 50 | 93.8 | 82 | (1.14) |
| C ₁ | 74.0 | 43 | (1.72) |
| P ₁ | 93.5 | 74 | 1.26 |
| P ₂ | 87.8 | 73 | 1.20 |
| P ₃ | 84.9 | 62 | 1.37 |
| P ₄ | 80.0 | 68 | 1.18 |
| P ₅ | 61.2 | 47 | 1.30 |
| P ₆ | 29.7 | 24 | 1.24 |
| P ₇ | 0 | 0 | — |

accord with extrapolated values from the melt.^{15,20} The density and x-ray-crystallinities are compared in Table III. The average ratio between both values for the P series is 1.24.

The result of interest for the discussion is the fact that the crystallinity decreases for the P series linearly by 5 to 6% for each newly introduced $-\text{CH}_3$ per 100 chain atoms when the crystallization is carried out as described above.

X-Ray Dimensions

Figure 5 shows the a axis dimension as found on annealed samples as a function of the keto oxygen and CH_3 groups added. The data for the CH_3 groups would fit perfectly into the summary of measurements of a axis dimensions given by Cole and Holmes⁶ as a function of branching. This collection of data showed that the widening of the a dimension is independent of the length of branching up to C_4 . From thermodynamic reasoning it appears that the CHCH_3 groups do not enter the lattice; however, they reduce the crystallinity by 5–6 CH_2 per copolymerized CH_3 . This points to the conclusion that around the randomly occurring CH_3 , small amorphous defects of about 5–6 CH_2 are forming. These must occur as well inside the lamellae as at the surface, since they are randomly spaced. The occurrence of these amorphous defects would then account for the a axis widening. Another piece of evidence in accord with this picture is the fact that crystallization of polyethylene under elevated pressure (6,000 atm.) has a smaller a axis dimension even after removal of the hydrostatic pressure.

The CO copolymers show a smaller increase in a axis dimensions. The random occurrence of CO is contrary to the regularly spaced CO in polyesters, and the change in cohesive energy density would have to be discussed in this case. The b axis for the CO polymers shows a slight decrease from 4.98 Å. for C_1 to 4.86 Å. for C_6 .

Conclusions

The above results lead to a more precise picture of the crystalline state of polyethylene.

The influence of fold length can explain the change in maximum melting point with change in crystallization temperature. It is possible to derive an equation for the change in maximum melting point of copolymers to accommodate the case of constant fold length crystallization of copolymers.

CO copolymer units have no effect on the melting point. They enter into the crystalline lattice as a foreign group, occupying a lattice position otherwise occupied by CH_2 . CO can thus not be classified as a noncrystallizable B unit. The only changes on inclusion of CO in polyethylene is a reduction of the heat of fusion, a change of the cohesive energy density, an increase in the a direction of the unit cell, and a slight decrease in the b direction. A CHCH_3 copolymer unit (short-chain branches) is two B units thermodynamically. Each CHCH_3 reduces the crystallinity, as

was suggested earlier by Richards³⁰ and Bryant and Voter.³¹ The size of the amorphous defect caused by CHCH_3 is 4–5 CH_2 in addition to the B units. An a axis expansion goes parallel to the inclusion of amorphous defects.

In order to calculate exact structures and maximum crystallinities the behavior of all defects found in polyethylene must be known. Available is some information on long chain branches and folds. Work by Williams, Matsuo, and Dole³² indicates that long-chain branching (induced by γ -radiation) causes an increase of amorphous content of approximately 80 CH_2 per branch. This explains the intermediate values of Bryant and Voter³¹ ($\sim 13 \text{CH}_2$ per CH_3 -end) who did not separate short- and long-chain branching. The effect of folds, i.e., (001)-surfaces, can be estimated roughly from densities of "folds only" compounds like cyclododecane. The specific volume of cyclododecane is 1.059 cc./g.,³³ which corresponds to a crystallinity of about 65%.

DTA coupled with x-ray methods is shown to be a useful tool in the investigation of structure of solid high polymers.

This research has been supported in part by the Advanced Research Projects Agency. Their support is gratefully acknowledged.

References

1. Wunderlich, B., and M. Dole, *J. Polymer Sci.*, **24**, 201 (1957).
2. Wunderlich, B., *J. Chem. Phys.*, **29**, 1395 (1958).
3. Wunderlich, B., and W. H. Kashdan, *J. Polymer Sci.*, **50**, 71 (1961).
4. Shenker, H., J. I. Lauritzen, Jr., R. J. Corruccini, and S. T. Lonberger, *Natl. Bur. Standards Circ.* 561 (1955).
5. Nichols, J. B., *J. Appl. Phys.*, **25**, 840 (1954).
6. Cole, E. A., and D. R. Holmes, *J. Polymer Sci.*, **46**, 245 (1960).
7. Brubaker, M. M., D. D. Coffman, and H. H. Hoehn, *J. Am. Chem. Soc.*, **74**, 1510 (1952).
8. Ueberreiter, K., and H. J. Orthmann, *Kolloid-Z.*, **126**, 142 (1952).
9. Murphy, C. B., *Anal. Chem.*, **32**, 168R (1960); *ibid.*, **30**, 864 (1960); B. Ke *J. Polymer Sci.*, **42**, 15 (1960); N. D. Scott, *Polymer*, **1**, 114 (1960).
10. For a review see W. J. Smothers and Yao Chiang *DTA, Theory and Praxis* Chemical Publishing Co., New York, 1958.
11. Müller, F. H., and H. Martin, *Kolloid-Z.*, **172**, 97 (1960).
12. Dole, M., and B. Wunderlich, *Makromol. Chem.*, **34**, 29 (1959).
13. Wunderlich, B. and P. Sullivan, *J. Polymer Sci.* **56**, 19 (1962); *ibid.*, **61**, 195 (1962); *Polymer*, **3**, No. 2 (1962).
14. Price, F. P., and R. W. Kilb, *J. Polymer Sci.*, **57**, 395 (1961); for a review see A. Keller, *Makromol. Chem.*, **34**, 1 (1959).
15. Chiang, R., and P. J. Flory, *J. Am. Chem. Soc.*, **83**, 2857 (1961).
16. Flory, P. J., *Trans. Faraday Soc.*, **51**, 848 (1955).
17. Dole, M., *Advances in Polymer Sci.*, **2**, 221 (1960).
18. Bryant, W. M. D., *J. Polymer Sci.*, **34**, 569 (1959), discussion.
19. Mandelkern, L., M. Hellmann, D. W. Brown, D. E. Roberts, and F. A. Quinn, Jr., *J. Am. Chem. Soc.*, **75**, 4093 (1953).
20. Quinn, F. A., Jr., and L. Mandelkern, *J. Am. Chem. Soc.*, **80**, 3178 (1958).
21. Fischer, F. W., *Ann. N.Y. Acad. Sci.*, **89**, 620 (1961).
22. Fuller, C. S., *Chem. Revs.*, **26**, 143 (1940).
23. Wunderlich, B., and M. Dole, *J. Polymer Sci.*, **32**, 125 (1958).

24. Starkweather, H. W., and R. H. Boyd, *J. Phys. Chem.*, **64**, 410 (1960).
25. Charlesby, A., and L. Callaghan, *J. Phys. Chem. Solids*, **4**, 227 (1958).
26. Swan, P. R., *J. Polymer Sci.*, **42**, 525 (1960).
27. Hendus, H., and G. Schnell, *Kunststoffe*, **51**, 69 (1961).
28. Hermans, P. H., and A. Weidinger, *Makromol. Chem.*, **44**, 24 (1961).
29. Bunn, C. W., *Trans. Faraday Soc.*, **35**, 482 (1939).
30. Richards, R. B., *J. Appl. Chem.*, **1**, 370 (1951).
31. Bryant, W. M. D., and R. C. Voter, *J. Am. Chem. Soc.*, **75**, 6113 (1953).
32. Williams, T. F., M. Matsuo, and M. Dole, *J. Am. Chem. Soc.*, **80**, 2595 (1958).
33. Müller, A., *Helv. Chim. Acta*, **16**, 155 (1933).

Synopsis

CO and CHCH₃ copolymers with polyethylene have been investigated by means of DTA and X-ray methods. The reproducibility of DTA was investigated for monomeric and polymeric standard compounds and found usable for maximum melting point determinations. The maximum melting point is discussed for copolymers, and an equation is given which corrects the influence of chain folding. CO was found to be a crystallizable defect unit, while CHCH₃ causes a noncrystallizable amorphous defect.

Résumé

On a étudié les copolymères de CO et CHCH₃ avec le polyéthylène en se servant de la méthode DTA et de celle des rayons-X. La reproductibilité de la méthode DTA a été étudiée en utilisant des substances de références monomériques et polymériques et on a trouvé que cette méthode pouvait être utilisée pour les déterminations du point de fusion maximum. On discute ce point de fusion maximum dans le cas des copolymères et on donne une équation qui corrige l'influence du plissement des chaînes. On a trouvé que CO était une impureté cristallisable tandis que CHCH₃ constituait un élément amorphe non cristallisable.

Zusammenfassung

Copolymere von Polyäthylen mit CO und CHCH₃ wurden mit DTA- und Röntgenmethoden untersucht. Die Reproduzierbarkeit der DTA wurde an monomeren und polymeren Standardverbindungen überprüft und erwies sich brauchbar zur Bestimmung des Schmelzpunktsmaximums. Der maximale Schmelzpunkt für Copolymere wird diskutiert und eine Beziehung zur Korrektur des Einflusses der Kettenfaltung wird angegeben. CO erwies sich als eine kristallisierbare Defekteinheit, während CHCH₃ einen nichtkristallisierbaren "amorphen Defekt" bildet.

Received November 8, 1961

Separated Aluminum Alkyl-Titanium Tetrachloride Catalysts for Isoprene Polymerization

WILLIAM M. SALTMAN, *Research Division,
The Goodyear Tire and Rubber Company, Akron, Ohio*

INTRODUCTION

In the past few years several analyses of the liquid and solid portions of the trialkyl aluminum-TiCl₄ catalysts have been published.¹⁻⁴ In general, they indicate that the titanium is reduced and precipitated; the composition of this brown to black precipitate is complex and dependent on the conditions for its preparation but depends most importantly on the Al/Ti mol ratio. At 0.5 to 1.0 Al/Ti the brown solid is essentially β -TiCl₃, but at higher ratios it is further reduced, alkylated, and forms a more or less tenuous solid complex with aluminum. The solution portion of the catalyst meanwhile contains the aluminum alkyl halide formed by oxidation of the trialkyl, unreacted aluminum trialkyl, or small amounts of unreduced TiCl₄, depending on the Al/Ti ratio.

Little has been published on the polymerization activity of the separate components beyond the bare statement that neither solid nor liquid alone will polymerize olefinic monomers.⁵ Although the isolated solid from the 1.0 Al/Ti reaction will not polymerize isoprene alone, when it is recombined with the liquid portion, polymerization will occur.² There are patent examples describing the addition of fresh metal alkyl to the isolated solid⁶ and mention that isolated high ratio solids will polymerize butadiene,⁷ but there has been, to our knowledge, no previous publication which describes the formation of various of these "separated" catalysts, their use in polymerization and discussion of the results in a manner which may shed light on the reaction mechanism.

The results reported here refer to bottle polymerizations of isoprene in heptane with the use of catalysts prepared from TiCl₄ and triisobutylaluminum (to be referred to as AlR₃). The catalysts were all preformed, i.e., formed in solvent in the absence of monomer. After preforming, the suspensions were centrifuged and part or all of the supernatant liquor was removed and replaced with solvent. The solid was then resuspended and used in polymerization either alone or with the addition of fresh AlR₃ or diisobutylaluminum chloride (AlR₂Cl). The results obtained show that polymerization activity is markedly dependent on the ratio at which the components were originally mixed, the amount of supernatant removed, and the amount and type of organometallic added back.

EXPERIMENTAL

Triisobutyl aluminum (AlR_3) and TiCl_4 were the same grade as described before² and were used as received to prepare dilute solutions in heptane. The AlR_2Cl was prepared by dissolving the appropriate amount of aluminum chloride in an AlR_3 -heptane solution. Preformed catalysts were made by simple mixing of dilute AlR_3 and TiCl_4 solutions in 4 or 8 oz. screw-cap bottles to make a catalyst about 0.15M in titanium. After aging of the catalyst for at least 24 hr. at room temperature the bottles were centrifuged for 15 min. at 1700 rpm and portions of the supernatant liquid removed with a 50- or 100-ml. syringe whose needle was injected through the bottle cap. Up to about 70% of the original volume could be removed by one syringing of such a solution without disturbing the precipitate. To remove a larger amount, it was necessary to add more heptane, stir up the precipitate (usually by shaking overnight) and repeat the procedure. Generally the amounts removed were 33, 66, and 99% of the original total volume. To remove 99% at least five washes were required. In one test the last wash contained no weighable residue. For this operation and calculation the small volume of the solid was neglected, so that unless the organometallic was adsorbed on the solid it should have been at least 99% removed. The catalysts used and described below are designated by the original Al/Ti ratio used in mixing and the amount removed, e.g., 1.0 (66%). Catalysts were thus prepared at Al/Ti molar ratios of 0.5, 0.6, 1.0, 1.2, 2.0, 3.0, and higher and to the three degrees of separation. After the separation, sufficient heptane was added to reattain the original volume. Since at all these ratios this procedure of retaining the solid removes only or mainly aluminum compounds and leaves only or mainly titanium compounds, the separated or partially separated catalysts have been depleted mainly in the aluminum-bearing portion of the catalyst while retaining most of the titanium.

Polymerizations were then carried out in 4 oz. bottles with isoprene and heptane treated as has been described before.² The separated solids plus any organometallic addback were added to the monomer solution by a syringe. Throughout, the titanium was held constant at 0.45 phm calculated as original TiCl_4 . All polymerizations described here were made at 50°C. for 17 hr. with 20% isoprene in heptane solution. After tumbling of the reaction flask in the constant temperature bath for this time, the reaction was stopped by adding the contents of the bottle to a large excess of isopropanol. The solid polymer was then dried under vacuum and weighed. Infrared examination indicated all of these polymers to be high in *cis*-1,4 content with possibly up to 8-10% of vinylidene structure.

RESULTS

The effect of $\text{AlR}_3/\text{TiCl}_4$ molar ratio is well known for stereospecific polymerizations and has been previously reported for isoprene.^{2,8} Maximum yields occurred at 1.0 to 1.2 Al/Ti ratio; at higher ratios the yield of

solid polymer decreased, but small yields of low molecular weight oils were obtained. These oils are alcohol-soluble and are not normally recovered when the reaction mixtures are coagulated in isopropanol. If conditions are such that appreciable amounts of these oils form (e.g., at Al/Ti of 2 or more) then alcohol-coagulated polymer yields will appear to level off below 100% conversion, even though all the monomer has been consumed. These oils are dimers, trimers, and tetramers of isoprene which have been characterized by Zaharkin,⁹ who suggests their formation is catalyzed by the complex catalysts. They do not have infrared absorption bands characteristic of a high *cis* polymer.

1.0 and 1.2 Al/Ti Ratio Separated Catalysts

Figure 1 shows the yields obtained with separated catalysts prepared at 1.0 and 1.2 Al/Ti ratios. Since there appeared to be very little difference

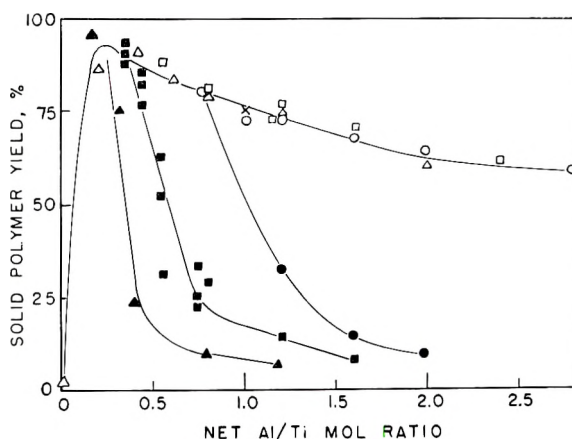


Fig. 1. Effect of separation and addback on the 1.0 and 1.2 Al/Ti separated catalysts; (Δ) 1.0(99%) with AlR_2Cl addback; (\blacktriangle) 1.0 (99%) AlR_3 addback; (\square) 1.0 (66%) AlR_2Cl addback; (\blacksquare) 1.0 (66%) AlR_3 addback; (\circ) 1.0 (33%) AlR_2Cl addback; (\bullet) 1.0 (33%) AlR_3 addback; (\times) conventional system, no separation.

between these two ratios they are plotted and will be considered together. Assuming all the titanium has remained in the solid and all the aluminum in the liquid, we have calculated the amounts of Al and Ti actually present in the polymerization mixture after removal and addback and plotted all yields versus the resultant net Al/Ti ratio. Thus, the results of polymerizations from the 1.0 (99%) solid begin at zero Al/Ti; those from the 1.0 (66%) catalyst begin at 0.33 Al/Ti, and those from the 1.0 (33%) solid at 0.67 Al/Ti. Addition of small amounts of either AlR_3 or AlR_2Cl to the 1.0 (99%) solid results in a marked improvement in yield; further additions diminish the yield. The upper curve shows the result of adding AlR_2Cl to the various solids while the lower curves show the effect of adding AlR_3 .

These results may be interpreted in terms of the activity of the aluminum

alkyls on TiCl_3 and the difference in activity of AlR_3 and AlR_2Cl . At 1.0 Al/Ti the catalyst reaction is mainly:¹⁰



Thus, the alkyl present in 1.0 Al/Ti catalysts is already AlR_2Cl and removal and addback of aluminum alkyl halide to the 33, 66, or 99% solids should all give polymer yields which fall on the same curve, since there is no change in the type of alkyl present but only in its amount. This is confirmed by the fact that when the net Al/Ti ratio is 1.0, the yield with AlR_2Cl corresponds to that obtained with a conventional, unseparated 1.0 Al/Ti catalyst. With lesser amounts of AlR_2Cl , higher yields of solid polymer are obtained, and conversely, if AlR_2Cl is present in excess, the solid polymer yield decreases. Some organometallic must still be present for initiation of polymerization to occur because the completely isolated solid, 1.0 (99%), gives only a small yield of resinous polymer until addition of either AlR_2Cl or AlR_3 .

Addition of AlR_3 to the 1.0 (33%) and 1.0 (66%) catalyst decreases the yield of polymer sharply, much more so than with addback of AlR_2Cl . Comparing the effect of the two organometallics, we see that in each case the higher yield occurs when (for a fixed total of Al) there is a greater proportion of dialkyl halide to trialkyl present. Addition of AlR_3 to the 1.0 (99%) solid forms very active catalysts if the AlR_3 is added in small amounts, but the yield of solid polymer decreases sharply on addition of further AlR_3 . In spite of these lower solid polymer yields, bottles containing isoprene soon become either warm or hot on addition of the catalysts, indicating a rapid reaction to very low molecular weight oils. This does not occur on adding back AlR_2Cl .

The sharply peaked activity of AlR_3 for formation of solid polymer is connected at least in part with the change in the chemical nature of the solid surface; on adding the trialkyl the surface turns darker and becomes black as do conventional catalysts formed at higher Al/Ti ratios.²

0.5 and 0.6 Al/Ti Ratio Separated Catalysts

Figure 2 shows the results obtained with the catalysts formed at 0.5 and 0.6 Al/Ti plotted together. When these catalysts are used without separation or addback they give rise to resinous polyisoprenes which have been reported to be high *trans* in structure.¹¹ With separation and addback, rubbery products are obtained which infrared analyses indicate to be high *cis*-polyisoprene.

The same interpretation as for the 1.0 catalysts may be made, except that here the dominant reaction is



Now, although the same solid is present as in the 1.0 catalysts, the organometallic present is the dichloride instead of the monochloride. The difference between Figure 1 and Figure 2 may be accounted for in terms of

this difference. It is obvious that AlRCl_2 is not a cocatalyst for the *cis*-polymerization, while AlR_3 and AlR_2Cl are. Thus addition of AlR_3 will initiate polymerization more readily (at lower net Al/Ti ratios) when less AlRCl_2 has been left behind in the separation of the catalyst components. Since the AlR_3 is involved in the equilibration



the first effect of adding AlR_3 is to form AlR_2Cl and only later would we expect much free AlR_3 to be present. When polymerization is initiated with these catalysts, maximum yield seems to occur at the point where the alkyl is stoichiometrically all AlR_2Cl . For example, for the 0.5–0.6 (66%) catalysts (with 0.17–0.2 net Al/Ti), very little yield is obtained; on addition

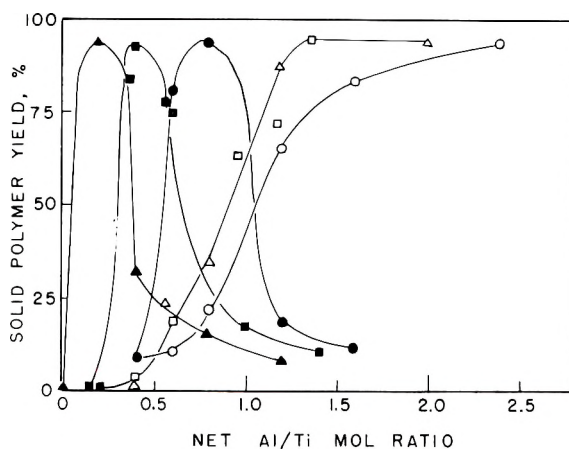


Fig. 2. Effect of separation and addback on 0.5 and 0.6 Al/Ti separated catalysts: (Δ) 0.5 (99%) AlR_2Cl addback; (\blacktriangle) 0.5 (99%) AlR_3 addback; (\square) 0.5 (66%) AlR_2Cl addback; (\blacksquare) 0.5 (66%) AlR_3 addback; (\circ) 0.5 (33%) AlR_3Cl addback; (\bullet) 0.5 (33%) AlR_3 addback.

of one equivalent of AlR_3 to a net Al/Ti ratio of 0.34–0.40, maximum yield is obtained. Similarly with the 33% removed catalysts, maximum yield occurs at about 0.8 net Al/Ti ratio. This would be even more apparent if we plotted the yields of Figure 2 against the millimoles of AlR_3 added (rather than the net Al/Ti ratio), as all three curves shown for AlR_3 addback then fall roughly on the same curve. Addition of further AlR_3 beyond one equivalent starts the downward trend in yield characteristic of the high ratio systems which give oils as well as solid polymer.

Addback of AlR_2Cl to these catalysts makes for a slow increase in rate leading eventually to high yields. In Figure 2 one line is drawn for the 66 and 99% plus AlR_2Cl addback data, since the results overlap. The addbacks were not carried far enough to show any drop in yield at high ratios as occurred with the 1.0 catalysts.

2.0 and Higher Al/Ti Ratio Separated Catalysts

Figure 3 shows the behavior of the 2.0 Al/Ti catalysts. The plotted results for the 3.0 ratio catalysts are quite similar to those shown in Figure 3, except that the maximum solid polymer yield obtained was 5% with the 3.0 (99%) catalyst without addback. Note that in Figure 3 we have plotted the "total" Al/Ti ratio (as though there had been no removal of the liquid component). This was done since there is some question¹⁻³ as to the amount of aluminum in the solid portion of the catalyst. If plotted on the same assumptions as Figures 1 and 2, the results with the partially separated catalysts would be displaced to the right relative to the results

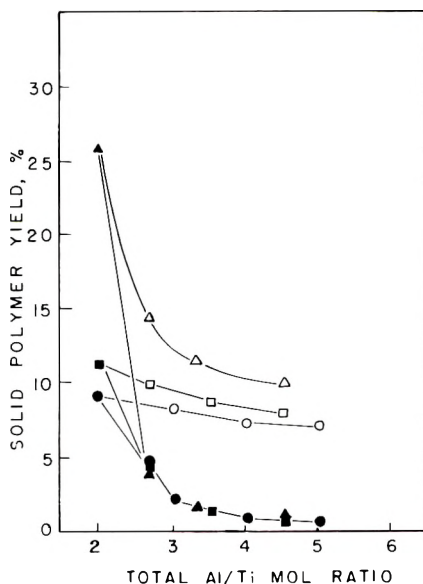


Fig. 3. Effect of separation and addback on 2.0 Al/Ti separated catalysts: (Δ) 2.0 (99%) AlR_2Cl addback; (\blacktriangle) 2.0 (99%) AlR_3 addback; (\square) 2.0 (66%) AlR_2Cl addback; (\blacksquare) 2.0 (66%) AlR_3 addback; (\circ) 2.0 (33%) AlR_2Cl addback; (\bullet) 2.0 (33%) AlR_3 addback.

for completely separated catalyst. For both ratios the catalyst solids themselves, 2.0 (99%) and 3.0 (99%), are the most effective polymerization catalysts, and the addition of either fresh AlR_3 or AlR_2Cl decreases the yield of solid polymer. The 2.0 (66%) catalysts are inferior to the 2.0 (99%), and the 2.0 (33%) are still poorer catalysts. The 3.0 Al/Ti catalysts shows the same trend. With no separation of catalyst liquid and solid, yields of solid polymer were less than 1%.

While addbacks of AlR_3 and AlR_2Cl both decrease the yield of polymer, the AlR_3 has a much more depressing effect. As before, on addition of AlR_3 to the isolated solids, bottles containing isoprene become warm or hot, indicating a very rapid reaction yielding low molecular weight oils.

DISCUSSION

One of the more complex aspects of the heterogeneous stereospecific catalysts has been the variety of kinetics reported and the changing Al/Ti ratios at which maximum polymerization rates occur for different monomers.^{2,12} These results are unexpected only if we are dealing with a single organometallic and a single surface. All indications have been that such is not the case and that a family of catalysts¹³ with a variety of surfaces are made available by the graduated reducing power of the aluminum trialkyls, dialkyl chlorides, and alkyl dichlorides, and by the ability of TiCl_4 to be alkylated and complexed as well as reduced. The simultaneous growth of random and high *cis*-polybutadiene chains on what must be different sites of the same catalyst⁷ is an example of this multiplicity.

We recently described the kinetics of propylene polymerization in a semiquantitative way in terms of two components: solid surface and adsorbed organometallic cocatalyst.¹⁴ With isoprene, this behavior is complicated by the variety of catalyst reactions mentioned above. Nevertheless, the low (0.5–1.2) ratio catalysts appear to behave predominantly so as to polymerize isoprene by means of the AlR_2Cl , while both alkyl and monomer are adsorbed on a $\beta\text{-TiCl}_3$ surface. AlR_3 will also serve as the alkyl as long as the TiCl_3 surface is not too greatly affected by the reaction between them; indeed, the active polymerization alkyl may be the AlR_2Cl formed in the initial stages of this reaction. In addition, there is the little-explored competing reaction which gives rise to oligomeric oils. In spite of these complicating factors the requirement for both insoluble surface and soluble metal-alkyl components is evident. One can hardly speak of propagation from a titanium center when removal of the other (supposedly inert) component prevents polymerization. That the surface has not been poisoned is proven by the revival of activity on reuniting the original liquid and solid portions² or by the addition of fresh organometallic as described in the experimental section above.

The behavior of high ratio catalysts differs⁷ and may indicate that an alkylated titanium solid can serve in place of the aluminum alkyls as the organometallic component. Until recently, the oligomerization reaction activity of the aluminum alkyl-high ratio solid has masked the polymerization catalyst activity of the high ratio separated solids. When originally made, high ratio catalysts contain AlR_2Cl and some excess AlR_3 in their solution phase. The solid portion has been reported to be essentially free of aluminum² or to contain an appreciable fraction of aluminum;^{1,3} all authors agree that the solids appear to contain organometallic linkages. In either case of C—Al or C—Ti bonds, the polymerization activity of the higher ratio separated solids still seems to demand an organometallic cocatalyst along with a properly oriented solid surface. With the high ratio catalysts, both of these components are combined in the solid rather than being part solid, part solution as in the low Al/Ti ratio systems. Whether organoaluminum or organotitanium is the active species is still a

moot point, but in conjunction with β -TiCl₃, either should be capable of producing high *cis*-polyisoprenes through complexes containing two metal atoms¹⁵ which may be alike or unlike. By analogy with the low ratio catalysts, we would expect that the two metal atoms are unlike.

These conclusions appear to be a consequence of the following argument. The alkylation of the titanium and its reduction to divalency by aluminum do not proceed completely^{2,3} due to the heterogeneous nature of the reaction. Until high Al/Ti ratios are attained there must still, therefore, be some β -TiCl₃ structure remaining in the catalyst solid. As long as this surface is available for directing the structure, *cis*-polyisoprene will form, provided an active organometallic is also present. In the 2.0 (99%) catalysts only part of the TiCl₃ has been reduced or alkylated, and the insoluble mixture contains the components needed for an active catalyst pair. The 3.0 (99%) solid is inferior to the 2.0 (99%) as a polymerization catalyst, even though its organic and aluminum contents are higher than for the 2.0 Al/Ti ratio catalysts. Thus, the 2.0 solid must contain a more nearly optimum mixture of metal alkyl and β -TiCl₃. Neither high ratio catalyst shows an initial rise in polymerization activity on adding AlR₃, as did the 1.0 (99%) catalysts, because of the already present solid organometallic component. The behavior shown in Figure 3 may be compared with the behavior on the right side only of Figure 1. In similar fashion, adback of AlR₂Cl depresses the yield only slowly, while addition of AlR₃ is strongly depressing. It is also pertinent that the 4.0 (99%) and 6.0 (99%) catalysts give only a trace of solid polymer. The 2.0 (99%) catalyst made with triethylaluminum behaves like the 3.0 (99%) catalyst made with AlR₃ in accordance with the greater reducing power of the triethyl. The behavior of these high ratio Al/Ti catalysts resembles that reported by Natta et al.¹⁶ for aluminumtriethyl with VCl₄ or VOCl₃. On separation of solid and liquid, the liquid was found to be inactive, while the solid still possesses catalytic activity. Analysis of the solid shows Al, V, Cl, and alkyl groups. VCl₃, to the contrary, shows little or no reaction with the aluminum alkyl and behaves like α -TiCl₃ according to these authors. In a similar vein, methyltitanium trichloride is an inactive catalyst until after partial thermal decomposition.¹⁷ Since the decomposition product itself (β -TiCl₃) is also inactive, both organometallic and solid surface must be required.

The imprint of the solid surface on the structure of the polymer has been shown by Natta¹⁸ for α - and β -TiCl₂, which form *trans*- or *cis*-polyisoprene, respectively. Carrick has also shown the structural similarities obtained with the same solid and a variety of metal alkyls in the ethylene-propylene copolymers.¹⁹ In our case, too, the various alkyls have given the same product on the same solid surface although the polymerization rates appear to be quite different. High ratio catalysts which depend solely on insoluble Ti-Ti or Al-Ti couples show a lower activity than the 1.0 ratio catalysts, which are based on a soluble aluminum compound, and the kinetics to be expected from completely insoluble catalysts are unknown.

With the $\text{AlR}_3\text{-TiCl}_3$ system or its analogs, the expected rates are of the types indicated before.^{2,14} In these cases it is only with low metal alkyl concentrations that the rates of polymerization of the same solid but with various alkyls should be expected to differ. At higher alkyl concentrations, identical polymerization rates are to be expected (see, e.g., the discussion of eq. V in reference 2). Thus work at high Al/Ti ratios obscures the role of the aluminum alkyl in the reaction mechanism. The independence of the rate on the metal alkyl cannot be used to imply propagation by a titanium species; indeed, this is just what is to be expected for growth on an aluminum moiety completely adsorbed in a solid surface complex.

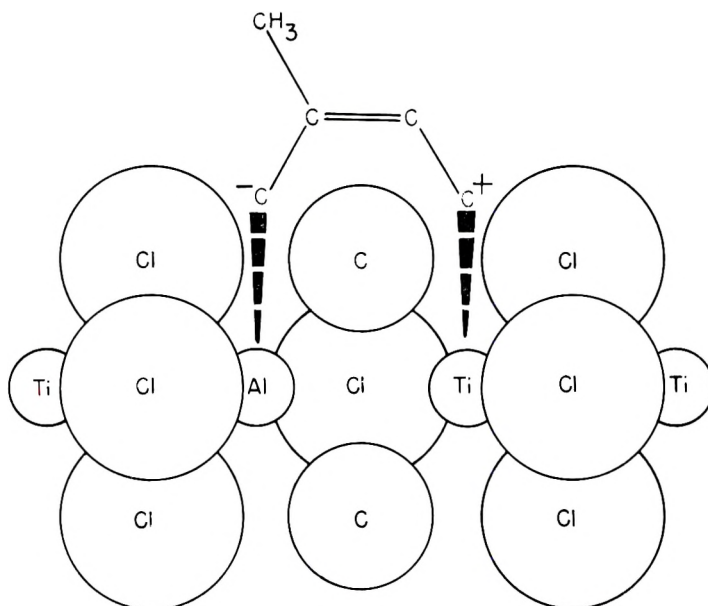


Fig. 4. Top view of the $\beta\text{-TiCl}_3$ lattice with an epitactically adsorbed AlR_2Cl molecule and showing the approach from above of a polarized *cis*-isoprene monomer unit.

A simple coordination^{1,20} mechanism seems adequate to describe isoprene propagation. Mechanisms based on transition metals alone are objectionable on the grounds given above. The mechanism of Gaylord and Mark²¹ seems more complicated than necessary. Fontana's mechanism²² requiring a six-point circular site cannot explain growth on a linear polymeric crystal²³ such as $\beta\text{-TiCl}_3$.

Consider a surface layer of a linear crystal such as $\beta\text{-TiCl}_3$ and assume that, due to a flaw in the lattice, one TiCl_3 unit is missing. Because of the similarity in atomic sizes, an organometallic, AlR_2Cl , can readily replace the TiCl_3 , i.e., be epitactically adsorbed on the surface. The top view of such a crystal surface might look like Figure 4 where we show only the first carbon of the alkyl groups and assume the remainder of the alkyl chains trail out into the solution phase. The lattice structure is that

reported²³ for β -TiCl₃. The metal to carbon bonds are of the well known "electron deficient" type, and we only note here that a Ti—C bond is much weaker than either an Al—C bond or a C—C bond, but that a C—C bond is stronger than an Al—C bond.²⁴

An isoprene unit approaching such an Al—Ti couple would be polarized, and the electron-releasing CH₃ group would be oriented toward the more electropositive Al atom as in Figure 4. In the *cis* configuration for isoprene, the 1-4 carbon-carbon distance is almost identical to the Ti—Ti distance (2.9 Å.) (no chemical bond is implied here) in β -TiCl₃ and therefore almost identical to the Al—Ti distance in the coordination complex, so that it may be considered a good fit for a two-point adsorption at the 1 and 4 carbon atoms.

Following this, the two weak C—Ti bonds break (C₄ from the adsorbed isoprene unit and the α -carbon from AlR₂Cl) and the two neighboring carbons bond with each other. The original Al—C bond must then break, and a new Al—C bond is formed with C₁ of the entering isoprene molecule. A rotation around the Al—C axis now moves this isoprene unit out into the solution and allows repetition of the process. Thus, the chain spirals out like a screw. Growth continues until the now polymeric AlR₂Cl is desorbed from the TiCl₃ lattice whereupon termination follows.

Results obtained with butadiene⁷ on the β -TiCl₃ surface indicate that the lattice flaws must occur with a (limited) range of sizes so that this monomer, lacking a side methyl group, may enter the complex either *cis* or on its side, as it were, in the *trans* configuration. The polymeric products thus range from high *cis* to random *cis* and *trans* mixtures, depending on whether the flaw is large enough to admit the longer *trans* unit.

With the violet α -TiCl₃ the longer *trans* structure is highly favored by the much longer Ti—Ti distance (3.54 Å.) in the layer lattice, and the only fruitful interaction between surface and monomer gives rise to high *trans* polymers.

The author wishes to express his thanks to Dr. H. J. Osterhof and The Goodyear Tire and Rubber Company for permission to publish this paper. This is contribution No. 275 from the Research Laboratory of the Goodyear Tire and Rubber Company.

References

1. Natta, G., paper presented at International Meeting on Chemistry of Coordination Compounds, Rome, September 15-21, 1957.
2. Saltman, W. M., W. E. Gibbs, and J. Lal, *J. Am. Chem. Soc.*, **80**, 5615 (1958).
3. Cooper, M. L., and J. B. Rose, *J. Chem. Soc.*, **1959**, 795.
4. Malatesta, A., *Can. J. Chem.*, **37**, 1176 (1959).
5. Ziegler, K., *Angew. Chem.*, **68**, 581 (1956).
6. Vanderberg, E. J., Belg. Pat. 546,846, to Hercules Powder Co., April 7, 1956.
7. Natta, G., L. Porri, A. Mazzei, and D. Morcro, *Chim. e ind. (Milan)*, **41**, 398 (1959).
8. Adams, H. E., R. S. Stearns, W. A. Smith, and J. L. Binder, *Ind. Eng. Chem.*, **50**, 1507 (1958).
9. Zakahrin, L. I., *Doklady Akad. Nauk S.S.S.R.*, **131**, 1069 (1960).

10. Feldman, C. F., L. C. Arnold, and D. W. McDonald, paper presented at 131st National Meeting of the American Chemical Society, Miami, Florida, April 1957.
11. Belg, Pat. 543,292, to Goodrich-Gulf Chemicals Co., December 2, 1955.
12. Gaylord, N. G., T. K. Kwei, and H. F. Mark, *J. Polymer Sci.*, **42**, 417 (1960); D. B. Ludlum, A. W. Anderson, and C. E. Ashly, *J. Am. Chem. Soc.*, **80**, 1380 (1958); A. I. Medalia, A. Orzechowski, J. A. Trichera, and J. P. Morley, *J. Polymer Sci.*, **41**, 241 (1959).
13. Breslow, D. S., W. P. Long, and N. R. Newburg, *Rubber and Plastics Age*, **41**, 155 (1960).
14. Saltman, W. M., *J. Polymer Sci.*, **46**, 375 (1960).
15. Natta, G., and G. Mazzanti, *Tetrahedron*, **8**, 86 (1960).
16. Natta, G., L. Porri, and A. Mazzei, *Chim. e ind. (Milan)*, **41**, 116 (1959); G. Natta, L. Porri, P. Corradini, and D. Moreno, *ibid.*, **40**, 362 (1958).
17. Beermann, C., and H. Bestian, *Angew. Chem.*, **71**, 618 (1959).
18. Natta, G., *J. Polymer Sci.*, **34**, 21 (1959).
19. Carrick, W. L., F. J. Karol, G. L. Karapinka, and J. J. Smith, *J. Am. Chem. Soc.*, **82**, 1502 (1960).
20. Natta, G., *Chim. e ind. (Milan)*, **42**, 1207 (1960).
21. Gaylord, N. G., and H. Mark, paper presented at the Symposium on Monomers and Polymers, 139th National Meeting of the American Chemical Society, St. Louis, April, 1961; *Petroleum Preprints* p. C-49.
22. Fontana, C. M., and R. J. Osborne, *J. Polymer Sci.*, **47**, 522 (1960).
23. Natta, G., P. Corradini, and G. Allegra, *J. Polymer Sci.*, **51**, 399 (1961).
24. Cottrell, T. L., *The Strength of Chemical Bonds*, Butterworth, London, 1954, pp. 275-277.

Synopsis

The liquid portions of triisobutyl-aluminum TiCl_4 catalysts were partially or completely removed from catalysts formed at Al/Ti ratios of 0.5, 0.6, 1.0, 1.2, 2.0, 3.0, and higher. The partially separated catalysts (0.5-1.2 Al/Ti) are still highly active for the polymerization of isoprene to a high *cis* polymer. The completely separated solid is inactive, but regains polymerization activity if triisobutyl aluminum or diisobutyl-aluminum chloride is added back. Polymer yield quickly reaches a maximum and then falls off sharply on addback of more trialkyl; the drop in yield is much slower on addback of excess dialkyl halide. The results indicate that trialkyl or dialkyl halide plus $\beta\text{-TiCl}_3$ make active catalyst systems for *cis*-polyisoprene; the alkyl dihalide is not satisfactory. Excess trialkyl changes the solid surface or mechanism and results in lowered solid polymer yield and increased oily oligomer formation. Completely separated high ratio (2.0 and 3.0 Al/Ti) catalysts are more active than those only partially separated but still much less active than catalysts formed at lower ratios. Addbacks of either aluminum trialkyl or dialkyl halide depress the solid *cis* polymer yield. Without any separation no solid polymer at all forms. The results suggest that the catalyst at these high ratios is a solid complex of $\beta\text{-TiCl}_3$ with an organometallic. A simple coordination mechanism is sufficient to correlate all the experimental results.

Résumé

Les fractions liquides des catalyseurs triisobutyl aluminium- TiCl_4 ont été partiellement retirées des catalyseurs formés dans le rapport Al/Ti de 0.5, 0.6, 1.0, 1.2, 2.0, 3.0, et plus élevés. Les catalyseurs partiellement séparés (0.5-1.2 Al/Ti) sont encore fortement actifs pour la polymérisation de l'isoprène en un haut polymère de forme *cis*. Le catalyseur solide complètement séparé est inactif, mais reprend l'activité de polymérisation si le chlorure de triisobutyl aluminium ou de diisobutyl est de nouveau ajouté. Le rendement en polymère atteint rapidement un maximum et diminue ensuite brusquement par addition ultérieure de plus de trialkyle; la chute du rendement est beaucoup

plus lente par addition ultérieure d'un excès d'halogénure de dialkyle. Les résultats indiquent que l'halogénure de trialkyle ou de dialkyle plus β -TiCl₃ font un système catalyseur actif pour le *cis*-polyisoprène; le dihalogénure d'alkyle n'est pas satisfaisant. Un excès de trialkyle change la surface solide ou le mécanisme et donne un rendement plus bas de polymère solide et augmente la formation d'oligomères huileux. Les catalyseurs à rapports élevés (2.0 et 3.0 Al/Ti) et complètement séparés sont plus actifs que ceux seulement partiellement séparés mais encore beaucoup moins actifs que des catalyseurs formés à des rapports plus faibles. Des additions ultérieures soit d'halogénure de dialkyle ou trialkyle diminuent le rendement en polymère *cis*-solide. Sans aucune séparation on n'obtient pas de polymère solide. Les résultats suggèrent que le catalyseur obtenue à rapports élevés est un complexe *solide* de β -TiCl₃ avec un organométallique. Un simple mécanisme de coordination est suffisant pour interpréter tous les résultats expérimentaux.

Zusammenfassung

Von Triisobutylaluminium-TiCl₃-Katalysatoren, die bei Al/Ti-Verhältnissen von 0,5, 0,6, 1,0, 1,2, 2,0, 3,0, und höher gebildet wurden, wurde der flüssige Anteil partiell oder vollständig entfernt. Die partiell getrennten Katalysatoren (0,5-1,2 Al/Ti) sind für die Polymerisation von Isopren zu einem hochgradig-*cis* Polymeren noch sehr wirksam. Der vollständig abgetrennte Festkörper ist inaktiv, erhält aber bei neuerlichem Zusatz von Triisobutylaluminium oder Diisobutylaluminiumchlorid seine Polymerisationswirksamkeit zurück. Bei weiterem Zusatz von Trialkyl erreicht die Polymerausbeute rasch ein Maximum und fällt dann scharf ab. Der Ausbeuteabfall ist bei Zusatz von überschüssigem Dialkylhalid viel langsamer. Die Ergebnisse zeigen, dass Trialkyl oder Dialkylhalid mit β -TiCl₃ wirksame Katalysatorsysteme für *cis*-Polyisopren bilden; das Alkyldihalid liefert keine befriedigenden Ergebnisse. Überschüssiges Trialkyl verändert die feste Oberfläche oder den Mechanismus und führt zu einer niedrigeren Ausbeute an festem Polymeren und erhöhter Bildung öligem Oligomeren. Vollständig getrennte Katalysatoren mit hohem Verhältnis (2,0 und 3,0 Al/Ti) besitzen eine höhere Aktivität als nur partiell getrennte, sind aber immer noch viel weniger aktiv als die bei niedrigerem Verhältnis gebildeten Katalysatoren. Neuerlicher Zusatz von Trialkylaluminium oder Dialkylaluminiumhalid setzt die Ausbeute an festem *cis*-Polymeren herab. Ohne Trennung bildet sich überhaupt kein festes Polymeres. Die Ergebnisse sprechen dafür, dass der Katalysator bei diesen hohen Verhältnissen ein fester Komplex von β -TiCl₃ und einer organometallischen Verbindung ist. Ein einfacher, koordinativer Mechanismus kann alle Versuchsergebnisse erklären.

Received September 27, 1961

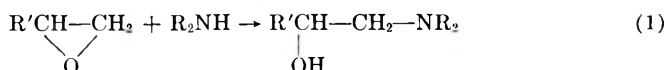
Hydrogen Bonding in Amine-Epoxy Adducts

J. F. HARROD, *General Electric Research Laboratory, Schenectady, New York*

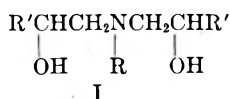
INTRODUCTION

The importance of hydrogen bonding in the structure and properties of polymers has long been recognized; indeed, in biological systems hydrogen-bonded structures are as common as polymers themselves. The phenomenon is somewhat less frequently encountered in synthetic systems, but some of the outstanding properties of synthetic polyamides and polyvinyl alcohol may be attributed to hydrogen bonding.^{1,2}

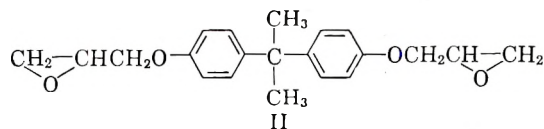
The present investigation concerns the study of hydrogen-bonding in amine-cured epoxides. The reaction of an amine, possessing active hydrogen, with an epoxide results in the formation of a 2-amino alcohol, according to eq. (1):³



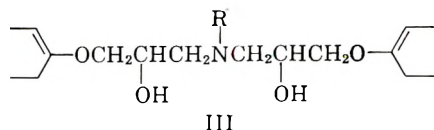
If the amine is primary, it will add to two epoxide groups to give a bis-(1-substituted ethanol)amine (I):



The most important epoxy resins used in practice are those based on the diglycidyl ether of bisphenol-A (II):



Cure of this type of resin by primary amines leads to a repeating unit of the type (III):



in which any hydroxyl may be involved in one of at least six types of

hydrogen bonding, three short-range and three long-range. The term short-range is used to describe bonds formed by groups within the same unit (III), and long-range describes bonds formed by groups in different units (III). The three possible types of hydrogen-bond: O—H...O (hydroxyl), O—H...O (ether), and O—H...N, may be present as both short-range and long-range bonds.

In order to obtain information on the nature of the hydrogen bonding in such systems, a study of the —OH stretching bands in the 3- μ region of the infrared⁴ has been made on a variety of model compounds and polymers.

EXPERIMENTAL

Model Compounds

To determine the relative importance of the various possible types of hydrogen bonding in amine-cured epoxy resins, the infrared spectra of the model compounds IV–VII were measured both in bulk and in dilute CCl₄ solution:

| | |
|------------------------------------|-----|
| $(C_6H_5OCH_2CHOHCH_2)_2NC_4H_9$ | IV |
| $(C_6H_5OCH_2CHOHCH_2)N(C_3H_7)_2$ | V |
| $C_6H_5OCH_2CHOHCH_3$ | VI |
| $HO-(CH_2)_3-OH$ | VII |

Compounds IV and V were prepared by reaction of phenyl glycidyl ether with the appropriate amine in stoichiometric amount. Compound VI was prepared by reaction of phenyl glycidyl ether with LiAlH₄.

Spectra of pure compounds were of thin films spread between rock-salt plates.

Spectra of solutions were of samples in 10 cm. quartz cells.

Solutions were initially $\sim 0.001M$ in carbon tetrachloride and were further diluted to establish the absence of intermolecular hydrogen bonding at these concentrations. Spectra were measured against a 10-cm. quartz cell filled with pure carbon tetrachloride, and a small cell correction was applied from a blank of pure CCl₄. All solution spectra were measured at 30°C.

Polymers

A sample of OH-free compound II was cured as a thin film between rock-salt plates with a stoichiometric amount of ethylene diamine. Cure was continued at room temperature until the resin had hardened and then at 150°C. until no further changes in the —OH band occurred.

A second sample of OH-free compound II was reacted with an equivalent of *n*-butylamine in toluene for several days at room temperature and was finally heated to 100°C. for several hours. The polymer produced was completely soluble in toluene and melted to a viscous liquid below 200°C. Reaction of butylamine with II under more vigorous conditions resulted in

gel formation due to base-catalyzed hydroxyl-epoxide reactions. A sample of the polymer solution was coated onto a rock-salt plate, and solvent was removed *in vacuo*. The film was covered by a second salt plate and the sandwich was hermetically sealed with a coating of thermosetting resin about its edge. This latter procedure was necessary to prevent molten polymer from oozing out at high temperature.

Spectra of both the three-dimensional and the linear epoxy-amine polymers were measured at a series of temperatures up to 200°C.

All spectra were measured on a Beckmann IR7 instrument with sodium chloride optics.

RESULTS AND DISCUSSION

Hydrogen Bonding in Aminoalcohols

Figure 1 shows spectra of model compounds IV to VII, for pure materials and for solutions. As expected, all of the bulk materials show intense, broad peaks around 3400 cm.^{-1} , typical of hydrogen-bonded OH groups.

The solution spectra fall into two distinct groups: those in which hydrogen bonding is virtually destroyed by dilution with CCl_4 and those in which a considerable amount remains, independent of dilution.

The first group includes compounds VI and VII, and it appears that intramolecular bonding is relatively unimportant in these compounds. Probably in VI the aryl ether is too weakly basic to form strong hydrogen bonds,⁵ while in VII the OH groups are too widely separated.⁶

In both of the aminoalcohols (IV and V), the persistence of a broad band in the 3450 cm.^{-1} region suggests a considerable amount of intramolecular bonding exists in dilute solution. In compound V, assuming bonding to the ether is negligible, the only possible intramolecular bond is of the O—H---N type, but in IV both O—H---O and O—H---N are possible.

The general similarity that exists between the dilute solution spectra of IV and V tempts the suggestion that the bonding is the same type in both compounds, namely O—H---N. On the other hand, consideration of available data on the relative strengths of O—H---O and O—H---N bonds does not clearly support this conclusion. It has recently been shown that for the case^{7,8} of structurally similar molecules, the O—H---N bond is somewhat stronger than the O—H---O bond, but in IV, the OH---O and O—H---N are in rings of different sizes and geometries. The various arguments may be summarized thus: although the five-membered ring containing O—H---N in IV will give rise to a stronger intramolecular hydrogen bond than is possible with an eight-membered ring, such as pentamethylene glycol would give, replacement of one of the carbons in the pentamethylene chain by nitrogen and substitution at the terminal carbon atoms will give rise to an increase in intramolecular hydrogen bond strength in the eight-membered ring system (in the first case because of the shorter C—N bond and in the second because of Thorpe-Ingold effects).⁹ It is

still doubtful if these effects are sufficiently large to allow O—H---O bonding to compete significantly with O—H---N.

The difference of 30 cm^{-1} (ca. 1 kcal. bond strength)¹⁰ between the absorption maxima for bonded OH in IV and V seems too large to be accounted for in terms of the IV peak being weighted to higher frequencies

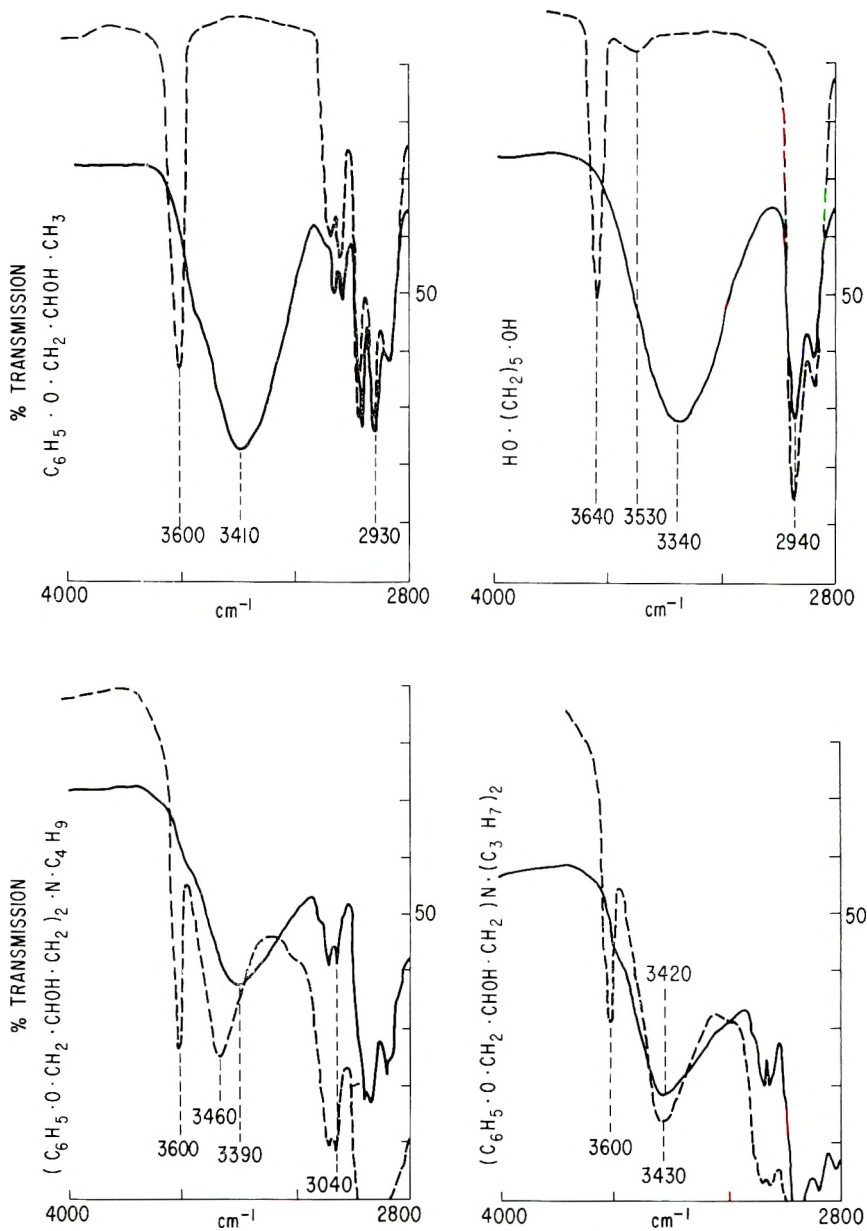


Fig. 1. Spectra of model compounds IV to VII: (—) bulk materials; (--) solutions in CCl_4 .

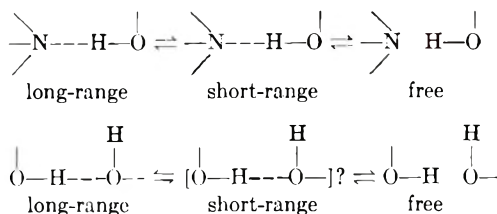
by a contribution from weaker O—H---O absorptions. It is possible that in IV, the second OH group can lower the effective charge of the nonbonding *p*-electrons on the nitrogen, thus reducing the electrostatic component of the hydrogen-bond strength.

Hydrogen Bonding in Amine-Epoxy Copolymers

Figure 2 shows a series of spectra of the epoxy resin II cured by reacting with ethylenediamine and with butylamine. The changes occurring were reversible, and the temperature could be cycled several times without causing permanent alteration to the room-temperature spectrum. The aliphatic CH bands at ~ 2900 cm^{-1} remained virtually unchanged throughout the cycle.

At room temperature the spectra of the polymers were essentially the same as those of compounds IV and V in the pure state. At higher temperature, systematic changes occurred which may be summarized as follows: (a) intensification of shoulder on the high frequency side of the bonded OH band; (b) decrease in integrated intensity of the bonded OH band; (c) shift of bonded OH absorption maximum to higher frequency.

All of these observations are consistent with the equilibria:



moving progressively to the right with increasing temperature.

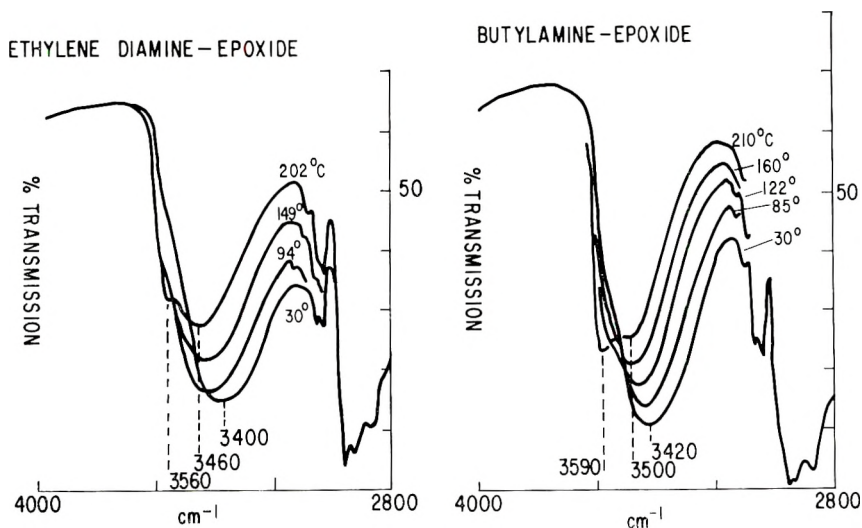
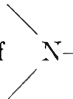


Fig. 2. Spectra of amine-cured epoxy resin at different temperatures.

The appearance of a peak attributable to free OH is more pronounced in the thermoplastic butylamine-epoxide copolymer than it is in the thermosetting ethylenediamine-cured resin. Such an effect may reflect the difference in free volume between the two polymers. When the thermoplastic material is heated, expansion is restricted only by primary valency forces along the axis of the chain; in the other dimensions thermal motions easily overcome weak, interchain forces, and strain is readily relieved. In the case of a three-dimensional network, motion is restricted in all directions by primary valency forces, and, as the temperature is raised, a situation will develop in the network tending to increase the mutual encroachment of groups in much the same way as pressure does. It is conceivable that such a situation will inhibit the rupture of hydrogen bonds, the vibrational instability being compensated for by the strain in the system, or by the larger repulsive forces existing in the space the proton would occupy if it were not hydrogen-bonded.

The almost complete lack of free —OH groups in the three-dimensional polymer at room temperature is surprising. It is reasonably certain that at least half of the available OH groups in the polymer will be involved in O—H---O bonding and that most of these bonds will be of the long range type. If all groups within the network were randomly oriented, the probability of all OH groups being able to form approximately colinear hydrogen bonds would be very small; on the other hand, there would be a relatively large fraction of OH groups whose orientation would exclude the possibility of long-range hydrogen bonds. The randomness of the network is probably restricted by the intimate involvement of hydrogen bonding in network growth. Apart from the simple hydrogen-bonded aggregation of OH-containing molecules with other N- and OH-containing molecules during network growth, it is well established¹¹ that hydrogen

bonding is intimately involved in the reaction of  N—H with the epoxide group. In such a situation, sufficient order may be imposed on the growing network to allow more or less complete hydrogen bonding of all available groups in the final product.

The author would like to thank Mr. R. Chrenko for assistance in measuring infrared spectra.

References

1. Huggins, M. L., *Physical Chemistry of High Polymers*, Wiley, New York, 1958 Chap. 12.
2. Maeda, H., T. Kawai, and S. Sekii, *J. Polymer Sci.*, **35**, 228 (1959).
3. Schechter, L., J. Wynstra, and R. P. Kurkijy, *Ind. Eng. Chem.*, **48**, 94 (1956).
4. Pimentel and McClellan, *The Hydrogen Bond*, Freeman, 1960, Chap. 3.
5. Gordy, W., and S. C. Stanford, *J. Chem. Phys.*, **8**, 170 (1940); *ibid.*, **9**, 204 (1941).
6. Kuhn, L. P., *J. Am. Chem. Soc.*, **74**, 2492 (1952).
7. Freedman, H. H., *J. Am. Chem. Soc.*, **83**, 2900 (1961).
8. Bergmann, E., E. Gil-Av, and S. Pinchas, *J. Am. Chem. Soc.*, **75**, 68 (1953).

9. Schleyer, P. v. R., *J. Am. Chem. Soc.*, **83**, 1368 (1961).
10. Badger, R. M., and S. H. Bauer, *J. Chem. Phys.*, **5**, 839 (1937).
11. Smith, I. T., *Polymer*, **2**, 95 (1961).

Synopsis

The infrared spectra of several alcohols and aminoalcohols were measured in bulk and in dilute solution in the 2800–4000 cm^{-1} region to determine the nature of hydrogen bonding in these compounds. An epoxy resin was cured with both an aliphatic monoamine and a diamine, and the OH-stretching bands of the polymers were studied in the temperature range 30–200°C. It is concluded that the hydroxyl groups in the polymers are extensively involved in long-range hydrogen bonding, particularly of the O—H—N type, at room temperature. The shift in the bonded OH band to lower frequency with increasing temperature is attributed to a shift from long range to short range bonds. Even at 200°C. there are relatively few free hydroxyl groups in these polymers.

Résumé

Les spectres infra-rouges de plusieurs alcools et amino-alcools à l'état pur et en solutions diluées, ont été mesurés dans la région de 4000 à 2800 cm^{-1} afin de déterminer la nature des ponts hydrogène dans ces produits. Ensuite, une résine époxy a été traitée avec une mono- et une diamine aliphatique, et les bandes d'absorption de valence OH de ces polymères ont été étudiées dans la gamme de température de 30 à 200°C. On en conclut que les groupes hydroxyles dans les polymères sont inclus pour la plupart dans des ponts hydrogène de longue portée, du type O—H—N, à température de chambre. Le glissement de la bande d'absorption OH ponté vers de plus basses fréquences par augmentation de la température est attribuée à un raccourcissement des ponts hydrogène. Même à 200°C il y a relativement peu de groupes hydroxyles libres dans ces polymères.

Zusammenfassung

Die Infrarotspektren einiger Alkohole und Aminoalkohole wurden in Substanz und in verdünnter Lösung im Bereich von 2.800 bis 4.000 cm^{-1} gemessen, um die Natur der Wasserstoffbindung in diesen Verbindungen zu bestimmen. Ein Epoxyharz wurde mit einem aliphatischen Mono- und Diamin behandelt und die OH-Bindungsbanden der Polymeren im Temperaturbereich von 30 bis 200° C untersucht. Daraus wird geschlossen, dass die Hydroxylgruppen in den Polymeren bei Zimmertemperatur in grossem Masse Wasserstoffbindungen, besonders vom Typ O—H—N, bilden. Die Verschiebung der Banden für OH-Brücken mit steigender Temperatur zu niedrigerer Frequenz wird einem Übergang von Bindungen mit grossem Abstand zu solchen mit kleinem Abstand zugeschrieben. Sogar bei 200°C sind in diesen Polymeren verhältnismässig wenig freie Hydroxylgruppen vorhanden.

Received November 13, 1961

On the Fractionation of Polypropylene by Coacervation

O. REDLICH, A. L. JACOBSON,* and W. H. McFADDEN,†
Shell Development Company, Emeryville, California

Various early investigations of polypropylene proceeding in these laboratories required the preparation of relatively large fractions (several grams) of fairly uniform molal weight. From results on polyethylene,¹⁻³ it was obvious that only distribution between two liquid phases would lead to a satisfactory fractionation. The same method has been used by other authors^{4,5} since that time. This report therefore can be restricted to the aspects not discussed by others.

Coacervation

The repetition of the same groups in a single molecule results in a high selectivity of the polymer toward solvents. Consequently two good solvents for a given polymer are in general so similar that they are miscible. The equilibrium between two phases, both containing appreciable amounts of the same polymer is a somewhat exceptional case, called coacervation.^{6,7} The thermodynamics of coacervation has been elucidated by Tompa.⁸

Coacervation may occur even with a single, fairly poor solvent below the critical solution temperature. According to solubility determinations (Fig. 1), two different liquid solutions of polypropylene in phenyl acetate are in equilibrium between 197°C. (critical solution temperature) and 154°C. at various weight fractions below 0.44. At higher polypropylene concentrations, equilibrium exists between a liquid phase and a solid phase between 150°C. and the melting point (170°C.). The solubility of polypropylene in the solvents of Figure 2 is too high for the occurrence of a critical solution point at an appreciable polypropylene concentration; no coacervation field exists here.

The use of phenyl acetate for coacervation would be inadvisable, because the high temperature required leads to more serious degradation than desirable. In general, one obtains sufficient freedom in the choice of conditions by using two solvents (Fig. 3). One of these is inevitably poor, since the solvents otherwise would be completely miscible. The low solubility of the polymer in one phase presents a considerable practical difficulty. Con-

* Present address: Department of Chemistry, University of Alberta, Calgary, Alberta.

† Present address: U. S. Department of Agriculture, Western Regional Research Laboratory, Albany, California.

sequently, one tries to work not too far from the plait point. Preferably two solvents are chosen which have a critical solution point not far above the temperature of operation.

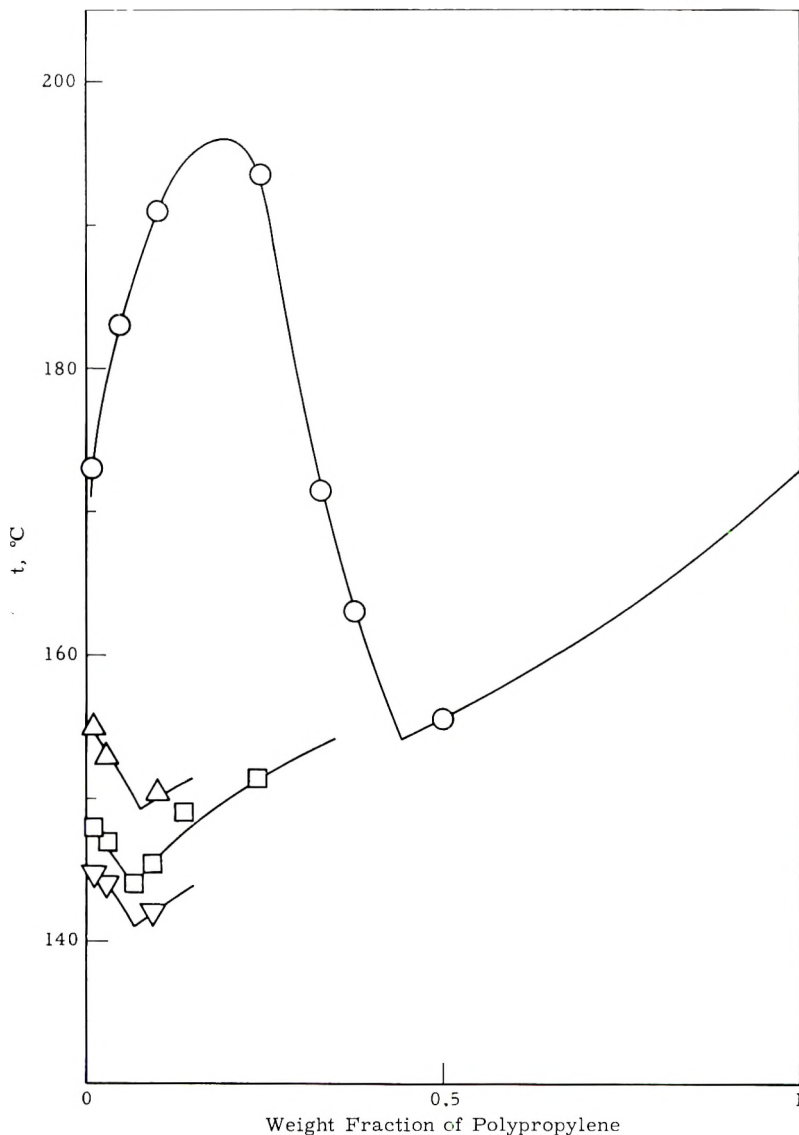


Fig. 1. Solubility of polypropylene in moderately poor solvents: (O) phenyl acetate-polypropylene mixture, intrinsic viscosity = 1.9; (Δ) diphenyl ether-polypropylene mixture, intrinsic viscosity = 6.1; (∇) diphenyl ether-polypropylene mixture, intrinsic viscosity = 1.07; (\square) diphenyl ether-polypropylene mixture, intrinsic viscosity = 1.9.

Approximate equilibrium data, obtained in a fractionation set for the purpose of general orientation, are shown in Figure 3. Polypropylene was determined by washing a weighed sample with ethanol and weighing the

dried polymer. Carbowax 200 was found in the coacervate (concentrated solution) by oxygen determination and in the (dilute) solution by the measurement of the density. The tetralin content was obtained by difference. While these analytical methods are not very accurate, the devia-

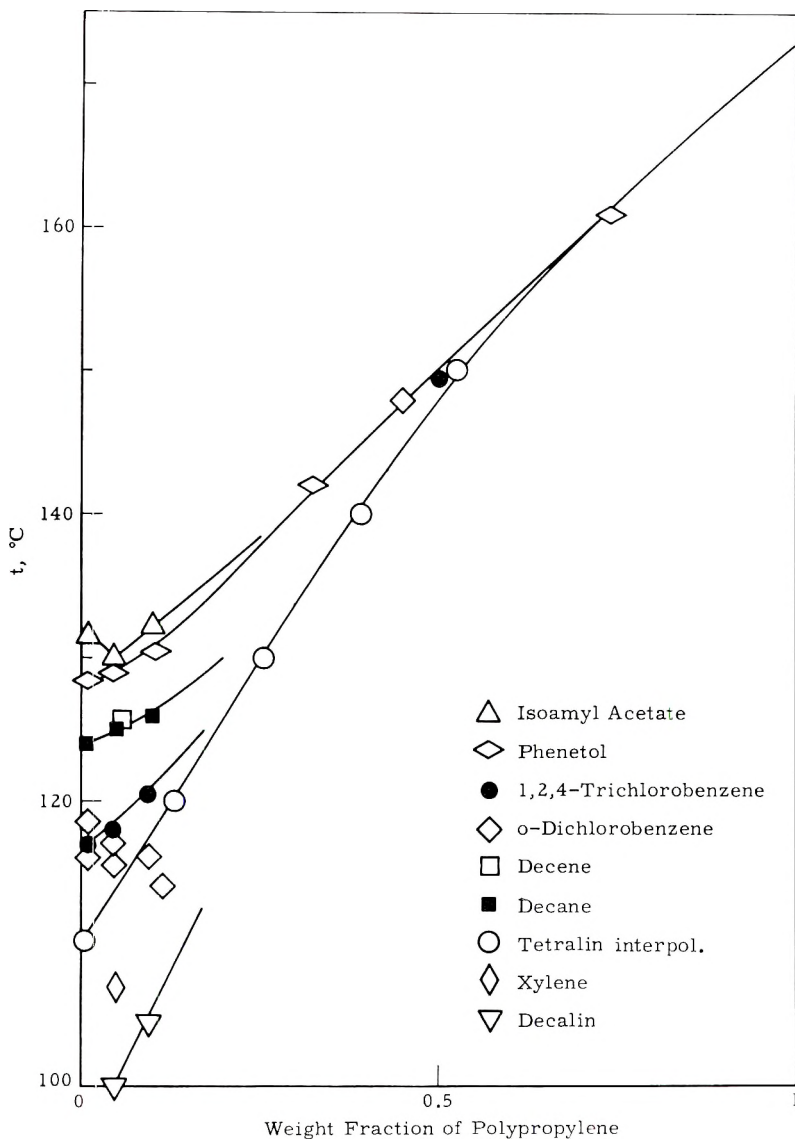


Fig. 2. Solubility of polypropylene (intrinsic viscosity = 1.9) in good solvents.

tions obtained for the first two fractionation equilibria (14.3 and 13.6 vol.-% Carbowax 200) are probably real and due to the influence of the heaviest polymer fractions.

The solubility of crystalline polymer, indicated in Figure 3, is important,

since the precipitation of a crystalline phase should be avoided in the fractionation, in view of experiences with polyethylene.¹⁻³

Fractionation

The slopes of the solubility curves of polypropylene fractions in tetralin (Fig. 4) show that fractionation efficiency decreases with increasing temperature. Nevertheless, one has to go near 140°C. in order to avoid precipitation of a crystalline phase.

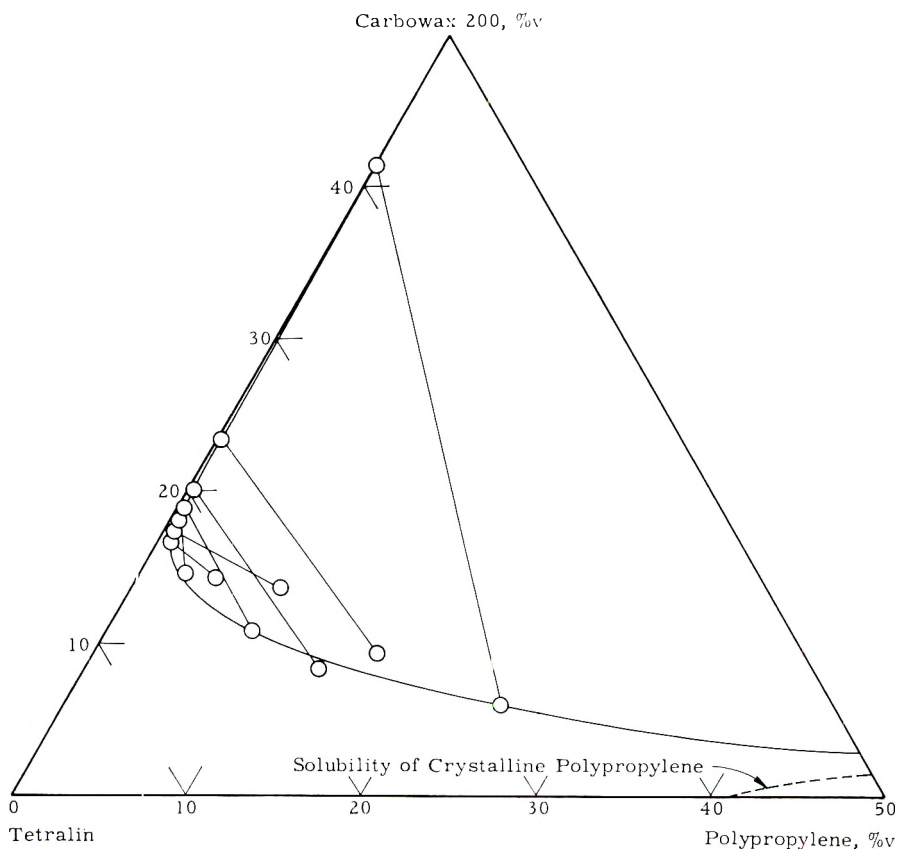


Fig. 3. Partial phase diagram for the system polypropylene-tetralin-Carbowax 200 at 140°C.

Tetralin and Carbowax 200 (polyethylene glycol of average molecular weight 200) have been found to be the best solvent combination. The use of a less poor solvent, namely, phenyl acetate instead of Carbowax did not lead to a coacervate at 140°C. but to a crystalline precipitate at 130°C. Tetralin cannot be replaced by the slightly poorer solvent diphenyl ether because the densities of the two liquid phases are too close for a separation. Phentol gives as good a fractionation as tetralin but there is a danger of crystalline precipitation of the lightest fractions. Moreover, the expense is not inconsiderable for a large fractionation.

The separations were carried out in an 8-liter bottle containing 38 g. of polypropylene and 3.8 liters of tetralin in an oil bath at $140 \pm 0.5^\circ\text{C}$. Coacervates were produced by addition of a heated mixture of Carbowax 200 alone or mixed with tetralin. After settling, the coacervate and some solution were transferred to a cylinder in the same oil bath. Then, after resettling, the coacervate was removed and the solution returned to the big bottle. Nitrogen was used for stirring and for transferring the liquids.

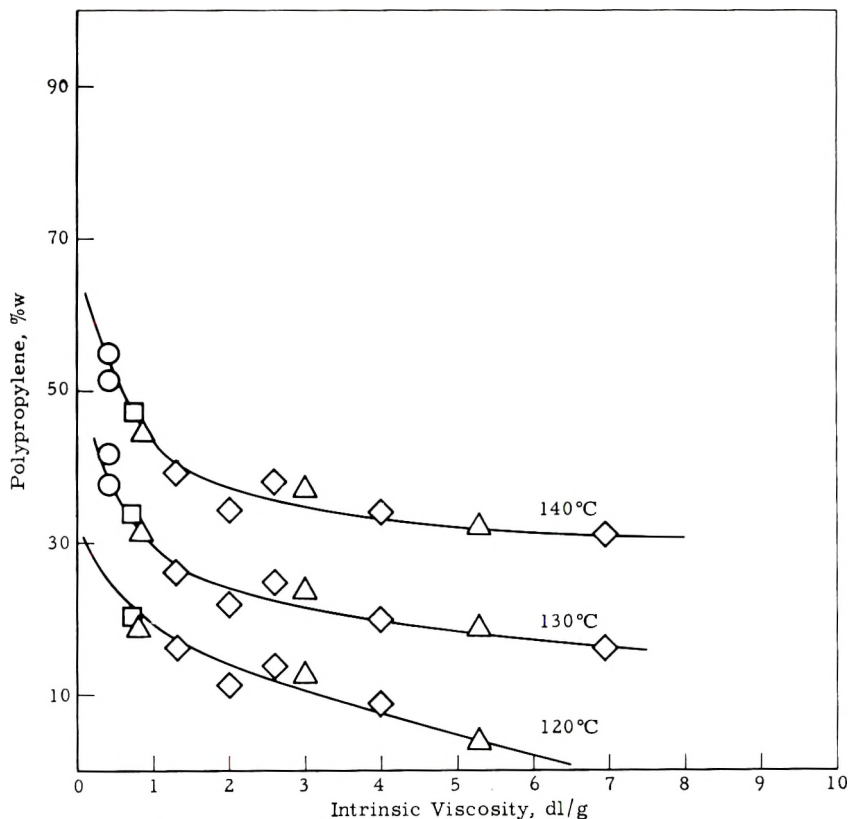


Fig. 4. Solubility of polypropylene in tetralin as a function of the intrinsic viscosity: (O), (Δ), (\diamond) fractions of laboratory preparations; (\square) commercial sample.

The cumbersome step of redissolution of the fractions could be eliminated by treating the raw polypropylene fractions with ethanol in an air-driven Waring Blendor (electric equipment should be avoided in view of danger of explosion).

Viscosity-average molecular weights have been calculated by the Mark-

$$[\eta] = 1.06 \times 10^{-4} M^{0.782}$$

Houwink relation derived from a large number of data by Mr. J. H. Badley in these laboratories.

Results

As an example of the fractionation, Figure 5 shows results for the early laboratory sample A, representing the logarithm of the molecular weight M as a function of cumulative weight per cent W on a probability scale. The first of the six primary fractions was split in a smaller apparatus into five subfractions; the last primary fraction was split into six subfractions. Although the technique was not fully developed at that time, the refractionations are in good accord with the primary fractionation. Results for two commercial samples are shown in Figure 6. These examples are not

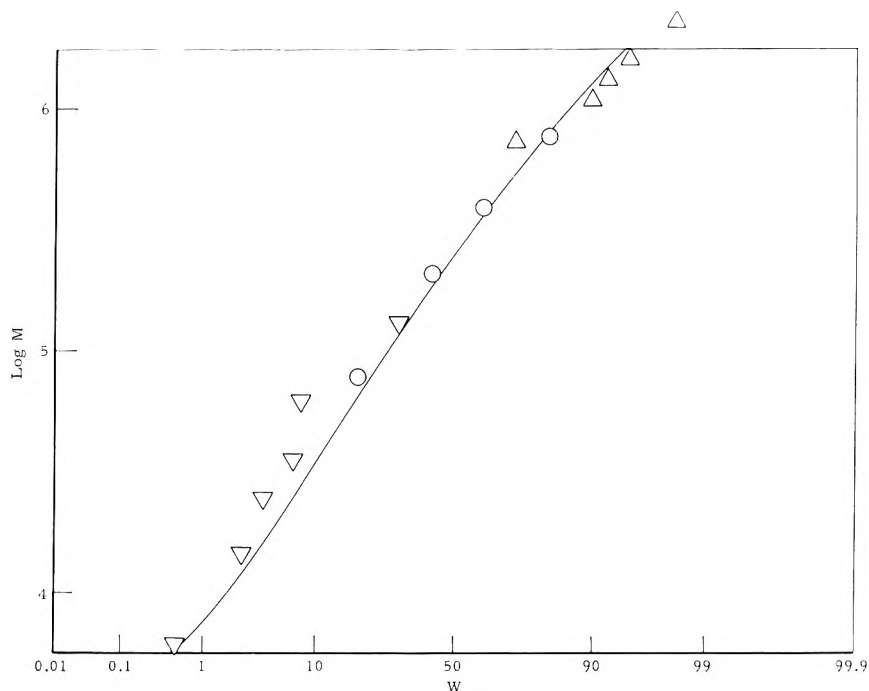


Fig. 5. Integral distribution of laboratory sample A: (O) primary fractions; (∇), (Δ) refractionated from the first and last fractions.

necessarily characteristic of present-day commercial polypropylene in average molecular weight or distribution.

Fractionation results were automatically computed by a procedure similar to that developed by Booth,⁹ but the fractions were assumed to be lognormally distributed. The final results were expressed by a "nearly lognormal" distribution function (curves in Figs. 5 and 6) previously¹⁰ found to be useful for oil mixtures.

As an example for the use of the fractions, Figure 7 shows the yield stress as a function of the molal weight. Although the test samples were small (below 2 g.) the decrease of the yield stress with increasing molecular weight is apparent. The variation of the yield stress in the molecular weight range

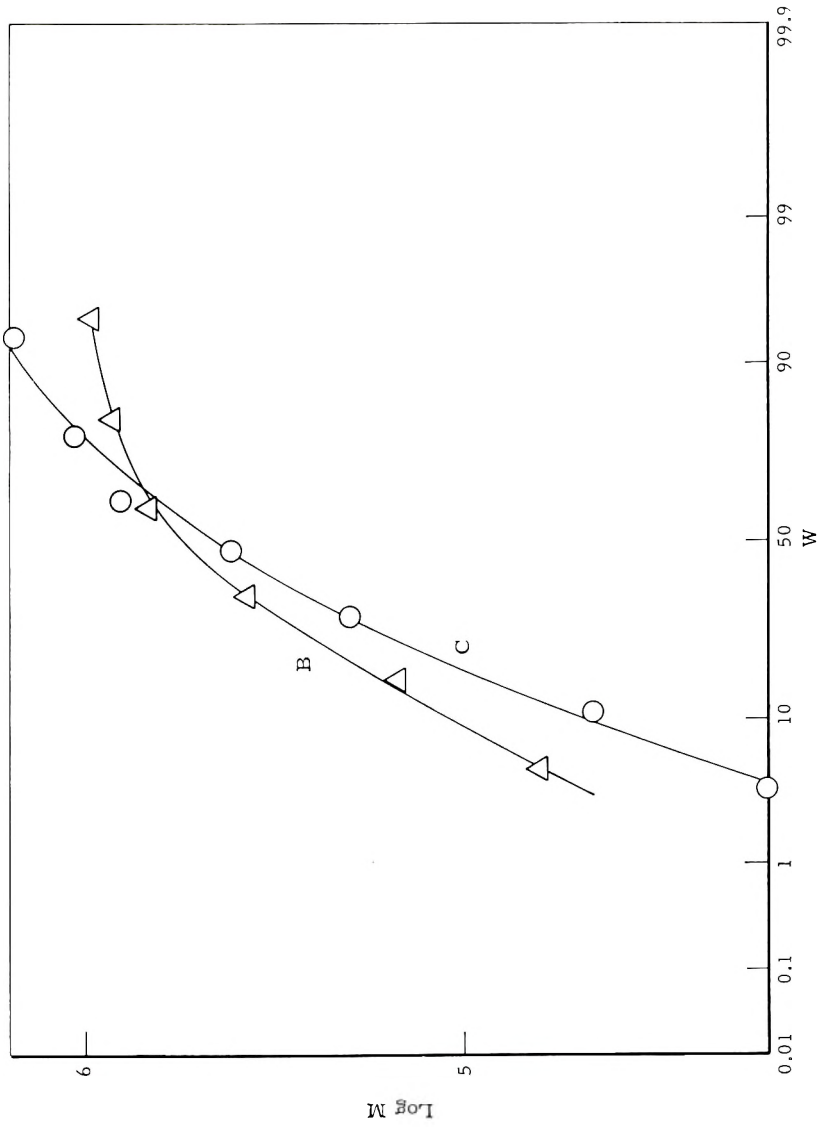


Fig. 6. Distributions of commercial samples: (Δ) sample B; (\circ) sample C.

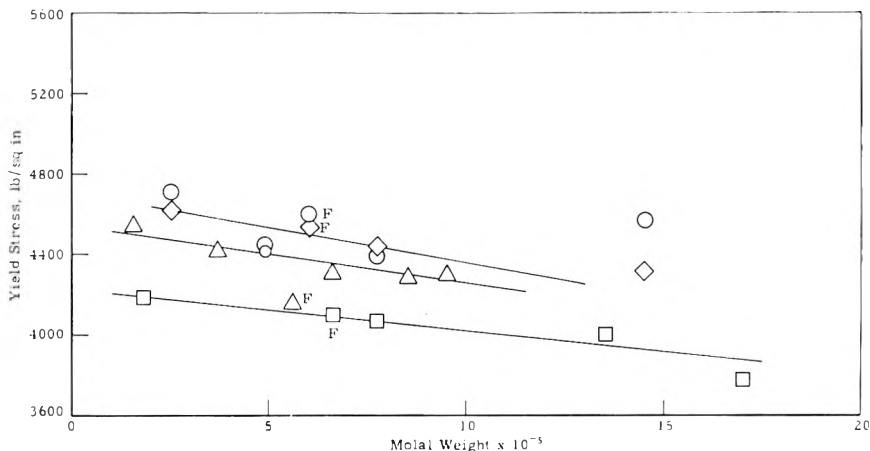


Fig. 7. Yield stress of fractionated polypropylenes: (O), (◇), (□) fractions of laboratory preparations; (△) commercial sample. F (feed) denotes original sample.

from 150,000 to 1,700,000 amounts to less than 10%, but it exceeds experimental errors.

We are indebted to Dr. F. H. Stross, Dr. D. E. Burge and Dr. D. B. Bruss for the molecular weight determinations and many helpful discussions. Most of the experimental work has been carried out by Mr. L. S. Kjelmeyr and Mr. E. R. Sevilla.

References

1. Nicholas, L., *Compt. rend.*, **236**, 809 (1953); see also *Makromol. Chem.*, **24**, 173 (1957).
2. Tung, L. H., *J. Polymer Sci.*, **20**, 495 (1956).
3. Nasini, A., and C. Mussa, *Makromol. Chem.*, **22**, 59 (1957).
4. Wijga, P. W. O., J. van Schooten, and J. Boerma, *Makromol. Chem.*, **36**, 115 (1960); J. van Schooten and P. W. O. Wijga, *ibid.*, **43**, 23 (1961); J. van Schooten, H. van Hoorn, and J. Boerma, *Polymer*, **2**, 161 (1961).
5. Davis, T. E., and R. L. Tobias, *J. Polymer Sci.*, **50**, 227 (1961).
6. Bungenberg de Jong, H. G., and H. R. Kruyt, *Kolloid-Z.*, **50**, 39 (1930); *ibid.*, **80**, 221, 350 (1937).
7. Dobry, A., *J. chim. phys.*, **35**, 387 (1938); *ibid.*, **36**, 102 (1939); *ibid.*, **42**, 92, 109 (1945); A. Dobry and Chou-Huin Ouang, *ibid.*, **36**, 296 (1939).
8. Tompa, H., *Trans. Faraday Soc.*, **45**, 1142 (1949); H. Tompa and C. H. Bamford, *ibid.*, **46**, 310 (1950).
9. Beason, L. R., and C. Booth, *Chem. & Ind. (London)*, **1959**, 993.
10. Redlich, O., *A.I.Ch.E. Journal*, **6**, 173 (1960).

Synopsis

In the development of a method for the molal weight fractionation of polypropylene some solubility data were collected. Consistent fractionation results were obtained. The size of the fractions (several grams) was sufficient for the investigation of the influence of the molal weight and its distribution on various properties.

Résumé

En développant une méthode pour le fractionnement du polypropylène en fonction du poids moléculaire, on a obtenu des données sur la solubilité de ce polymère. Des

fractionnements satisfaisants ont été réalisés et les poids des fractions (quelques grammes) ont permis d'étudier l'influence du poids moléculaire et de sa distribution sur différentes propriétés.

Zusammenfassung

Bei der Entwicklung einer Fraktionierungsmethode für Polypropylen wurden einige Löslichkeitsdaten gesammelt. Die Fraktionierungsergebnisse erwiesen sich als konsistent. Die Grösse der Fraktionen (einige Gramm) genügte zur Untersuchung des Einflusses des Molekulargewichts und seiner Verteilung auf verschiedene Eigenschaften.

Received November 17, 1961

The Nature of Active Components in Catalytic Systems Prepared from TiCl_3 , Monoalkylaluminum Dihalides, and Electron-Donor Substances, in the Polymerization of Propylene

A. ZAMBELLI, J. DIPIETRO,* and G. GATTI, *Istituto di Chimica Industriale del Politecnico, Milan, Italy*

The polymerization of propylene and of α -olefins in general to prevalingly isotactic polymers was first achieved by Natta and co-workers. Catalysts possessing a great stereospecificity in such polymerizations consisted of a crystalline halide of a transition metal, having a crystalline modification of a layer structure and an oxidation number lower than the possible maximum (such as violet TiCl_3 , TiCl_2 , VCl_3 , etc.), used with a metalloorganic compound, such as trialkylaluminum, dialkylaluminum halides,^{1,2} beryllium alkyls,³ etc. These catalytic systems could be placed in the same class as Ziegler catalysts, but they differ from the ones proposed by Ziegler for the polymerization of ethylene at low pressure⁴ in the degree of their stereospecificity; the latter ones, (based on TiCl_4), being less stereospecific for the polymerization of α -olefins than those mentioned above.

Various other catalytic systems for the polymerization of α -olefins to isotactic polymers have since been proposed in the literature. Recently the use as catalysts of a combination of crystalline TiCl_3 and monoalkylaluminum dihalides added to substances like hexamethylphosphoramide, triphenylphosphine, etc.,^{5,6} has been described. A crystalline, so-called "stereosymmetric" polymer of propylene having a melting point of 183°C. was reported as one of the products in one of these patents.⁵ According to these authors, such a polymer would represent a type of crystalline polypropylene different from the isotactic one obtained and described by Natta.

It appeared of some interest to establish whether a catalytic system prepared from TiCl_3 , monoalkylaluminum dihalides, and substances such as hexamethylphosphoramide differed in any way from catalysts prepared from TiCl_3 and dialkylaluminum halides, as previously described by Natta and co-workers.

Reaction Products of Monoalkylaluminum Dihalides with Electron-Donor Substances

In addition to hexamethylphosphoramide and triphenylphosphine, various other substances which can be employed with RAlX_2 to produce

* NATO Postdoctoral Fellow.

along with TiCl_3 stereospecific systems for the polymerization of α -olefins to isotactic polymer⁷ were investigated. Among these substances were amines, amides, ethers, alkali metal halides, and "onium" salts.

The ratio of the electron-donating substances to the monoalkylaluminum dihalide is important with respect to the activity and the stereospecificity of the resulting catalytic system. Such a ratio should always be below 1; the most satisfactory results in the polymerization are obtained when the ratio is equal to 0.5.

Jacober and Kraus⁸ have studied the reaction of methylaluminum dibromide with dimethyl ether, in which they found a maximum conductivity when 0.5 mole of $(\text{CH}_3)_2\text{O}$ was added to 1 mole of CH_3AlBr_2 . They have attributed such a phenomenon to the existence of a complex of the type $(\text{AlBr}_2(\text{CH}_3)_2 \cdot (\text{CH}_3)_2\text{O})$. Such a product, however, was not isolated. We asked ourselves, therefore, if the metalloorganic component, active in the polymerization, consisted of those hemicomplex compounds, formally analogous to those obtained from $2\text{AlR}_2 + \text{MX}$ (where M is an ion of an alkaline metal or an "onium" ion, and X is a halide) recently discovered by Ziegler.⁹

The products of the reaction between 2 moles of monoalkylaluminum dihalide and 1 mole of the donor substance were soluble in aromatic solvents. The addition of *n*-heptane to the prepared solution in aromatic solvents generally resulted in the formation of two phases, one consisting of the solvents used and their solutes, which in the presence of TiCl_3 can promote the polymerization of propylene to an isotactic polymer; the other, consisting of oils or semisolid substances, which in certain cases could be crystallized, was not able to promote, in the presence of TiCl_3 , the polymerization of propylene to an isotactic polymer. We were able to separate these two phases and determine the Al/Cl ratio for each one. In the case where the separation of the solid product was possible, we did the analysis on certain

TABLE I

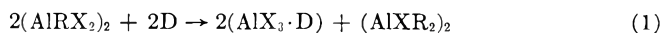
| Reagents | Cl/Al ratio (hydrocarbon phase) ^a | Analyses (solid or oily phase) | | | | Cl/Al ratio |
|---|--|--------------------------------|-------|----------------------------|-------------------|-------------|
| | | Al, % | Cl, % | C_2H_5 , % | D, % ^b | |
| $\text{C}_5\text{H}_5\text{N} + (\text{AlC}_2\text{H}_5\text{Cl}_2)_2$ | 1.30 | 13.7 | 48.21 | 5 | 33 | 2.6 |
| $(\text{CH}_3)_2\text{NCHO} + (\text{AlC}_2\text{H}_5\text{Cl}_2)_2$ | 21.25 | 13.99 | 45.68 | 7.5 | 22.8 | 2.5 |
| $[(\text{CH}_3)_2\text{N}]_3\text{PO} + (\text{AlC}_2\text{H}_5\text{Cl}_2)_2$ | 1.25 | — | — | — | — | 2.5 |
| $\text{KCl} + (\text{AlC}_2\text{H}_5\text{Cl}_2)_2$ | 1.06 | 12.71 | 64.2 | 1.5 | 21.59 | 3.8 |
| $(\text{CH}_3)_4\text{NCl} + (\text{AlC}_2\text{H}_5\text{Cl}_2)_2$ | 1.12 | 10.8 | 58.2 | — | 29.9 | 3.9 |
| $(\text{C}_6\text{H}_5)_3\text{P} + \text{Al}(i\text{-C}_4\text{H}_9)_2\text{Cl}_2$ | 1.6 | 7.4 | 26.9 | 1.9 | 63.8 | 2.76 |

^a In the hydrocarbon phase the donor substance is also present; its quantity increases with an increase in the Cl/Al ratio. This is due to the partial solubility of compounds of the type $\text{AlCl}_3 \cdot \text{D}$ or $\text{AlCl}_2\text{Et} \cdot \text{D}$.

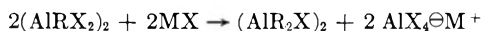
^b D denotes donor substance, or cation (K^+), or $\text{N}(\text{CH}_3)_4^+$. The percentage of the donor substance was calculated by difference, considering the ratio Cl/Al.

samples of a known weight. In these cases the amount of the donor substance was determined by difference. The results obtained in these such experiments are reported in Table I.

It can be observed that the Cl/Al ratio in the hydrocarbon phase is below 2, whereas that in the other phase is above 2. We assume that this is due to the fact that the donor substance causes conversion of the dihalide to the monoalkylaluminum halide, according to the reaction:



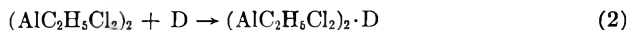
With the alkali halides, this reaction occurs in the following way:



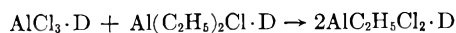
Some tests were carried out with the purpose of confirming this hypothesis, as for instance, the removal of AlR_2X compound from the reaction system as soon as it was formed (i.e., by distillation). These runs demonstrated that the distillate was actually the metalloorganic compound, AlR_2X . This type of reaction can also be employed as a method of preparation of dialkyl monohalides from dihalides or from sesquihalides of alkylaluminum, in analogy with what was observed for the preparation of AlR_3 from $\text{AlR}_2\text{-Cl}$.^{9,10}

We also studied reaction (1) in a homogeneous system using benzene as the solvent. Cryoscopic measurements were performed for this purpose.

In fact, if only the reaction (2) occurs:



the addition of the donor substance D in a $1/2$ molecular quantity (or less) with respect to the monoalkyl aluminum dichloride in benzene solution should not give rise to any cryoscopic decreases. On the contrary, if only reaction (1) takes place in a quantitative way, the value of ΔT , referred to the solution containing $(\text{AlC}_2\text{H}_5\text{Cl}_2)_2$, would be half the ΔT values obtained for benzene solutions containing the same amount of donor substance in the absence of monoalkyl aluminum dihalide. The cryoscopic data obtained with solutions containing either $(\text{AlC}_2\text{H}_5\text{Cl}_2)_2$ or $[\text{Al}(i\text{-C}_4\text{H}_9)\text{Cl}_2]_2$ in the presence of $(\text{C}_6\text{H}_5)_3\text{P}$, in a small molar quantity (less than $1/2$ that of the aluminum alkyl), agreed well with the theoretical values based on reaction (1). This suggests that in the reactions under consideration, the formation of hemicomplex compounds of monoalkyl aluminum dihalides as shown in eq. (2) does not take place. It is also possible to foresee for reaction (1) similar conductivity behavior as that obtained experimentally by Jacober and Kraus.⁸ A conductivity maximum for a Al/D ratio of $1/2$ could be due to the $\text{AlCl}_3 \cdot \text{D}$ formed, while successive additions of D could generate the reaction:



final product having a lower conductivity. The choice of triphenylphosphine was mostly favored because of its ability to provide a single reac-

tion center, and for the good solubility of its complex, $\text{AlCl}_3 \cdot \text{P}(\text{C}_6\text{H}_5)_3$, in benzene.

Polymerization Runs

In a recent study on the polymerization of propylene we demonstrated that the stereospecificity of catalytic systems prepared from TiCl_3 (violet), previously washed to eliminate traces of TiCl_4 , is dependent on the nature of the metalloorganic compound used.⁷ For instance, those systems prepared from $\text{Al}(\text{C}_2\text{H}_5)_2\text{I}$ are more stereospecific than those prepared from $\text{Al}(\text{C}_2\text{H}_5)_2\text{Cl}$ or from $\text{AlC}_2\text{H}_5\text{Cl}_2$ to which a donor substance had been added. They are also more stereospecific than those prepared from AlR_3 . The systems prepared from $\text{Al}(\text{C}_2\text{H}_5)_2\text{I}$ are indeed among the most stereospecific ones described up to now. (Per cent of material nonextractable with boiling *n*-heptane in the crude product obtained at 70°C. was 98–99%). From the crude polymers obtained with these systems, it was possible to separate a fraction of highly crystalline isotactic polypropylene having a melting point of 176–177°C. (determined by the polarizing microscope with heating at a rate of 10–12°C./hr.).

Catalytic systems prepared with BeR_2 , already described in 1957,³ also have a high stereospecificity, greater than that of those systems prepared from AlR_3 .

The results previously discussed and reported in Table I indicate that the metalloorganic component which is active in the polymerization of the α -olefins with the ternary catalytic systems here studied, is $\text{Al}(\text{C}_2\text{H}_5)_2\text{Cl}$. As the stereospecificity of those systems with TiCl_3 (violet) depends on the nature of the metalloorganic compounds, the stereospecificity of the ternary systems here studied should be the same as for systems prepared

TABLE II
Stereospecificity of Catalytic Systems in the Polymerization of Propylene to Isotactic Polymers Obtained by δ - TiCl_3 - (containing 4.5% Al as AlCl_3 in the Solid Solution), and from the Products of the Given Reaction^a

| Metalloorganic compound | Fractionation of the crude polymer | | | [η] ^b |
|--|------------------------------------|--------------------|--------------------|-------------------------|
| | Ether extract, % | Heptane extract, % | Heptane residue, % | |
| $(\text{C}_2\text{H}_5)_2\text{AlCl}$ | 4.3 | 2.7 | 93.0 | 4.0 |
| $[(\text{C}_2\text{H}_5)\text{AlCl}_2]_2 + \text{C}_5\text{H}_5\text{N}$ | 4.0 | 3.8 | 92.2 | 4.5 |
| $[(\text{C}_2\text{H}_5)\text{AlCl}_2]_2 + (\text{CH}_3)_2\text{NCHO}$ | 4.5 | 3.5 | 92.0 | 4.4 |
| $[(\text{C}_2\text{H}_5)\text{AlCl}_2]_2 + [(\text{CH}_3)_2\text{N}]_3\text{PO}$ | 4.0 | 3.0 | 93.0 | 4.3 |
| $[(\text{C}_2\text{H}_5)\text{AlCl}_2]_2 + \text{KCl}$ | 4.2 | 2.8 | 93.0 | 4.2 |
| $[(\text{C}_2\text{H}_5)\text{AlCl}_2]_2 + (\text{CH}_3)_4\text{NCl}$ | 4.0 | 2.0 | 94.0 | 3.2 |
| $[(\text{C}_2\text{H}_5)\text{AlCl}_2]_2 + (\text{C}_6\text{H}_5)_3\text{P}$ | 4.1 | 1.8 | 94.1 | 4.2 |
| $(\text{C}_2\text{H}_5)\text{AlI}$ | 1 | 1 | 98 | 3.5 |

^a Experimental conditions: $T = 70^\circ\text{C}$.; $p(\text{C}_3\text{H}_6) = 2,000$ mm. Hg.; solvent toluene; $\text{Al/Ti} = 1.5\text{--}2$; $\text{Al}(\text{C}_2\text{H}_5)_2\text{Cl}$ concentration = 3.0×10^{-2} mole/l.

^b Intrinsic viscosity of the polymer measured in Tetralin at 135°C .

starting from $\text{Al}(\text{C}_2\text{H}_5)_2\text{Cl}$. This is completely confirmed by the experimental data reported in Table II. It is obvious that the stereospecificity of the ternary systems containing violet TiCl_3 , alkyl aluminum dichloride and a Lewis base (or an alkali metal or "onium" chloride), practically coincides with the stereospecificity of those catalysts consisting of violet TiCl_3 and an alkyl aluminum monochloride. The differences noticed in the molecular weight of the polymers could be attributed to the fact that the numerical value of the molecular weight depends on the rate of the chain-transfer processes, which ultimately depend on the concentration of the metalloorganic compound.¹¹

The polymerization rate for the binary catalytic system is always equal to or higher than that obtained with the ternary systems. Probably this phenomenon can be attributed to physical surface phenomena occurring between TiCl_3 and $\text{AlX}_3 \cdot \text{D}$, which decrease the active surface of TiCl_3 . In fact, if one introduces $\text{AlCl}_3 \cdot \text{Py}$ to a hydrocarbon suspension of TiCl_3 , a conglomeration of particles of TiCl_3 occurs at once, and the catalytic activity of TiCl_3 decreases.

Experimental

Products Separated by Addition of n-Heptane. The reaction between alkyl aluminum dihalides and donor substances was carried out in the following way. To a previously dried vessel under nitrogen atmosphere there were introduced in the following order: 30 cc. of toluene, 10 mmoles of AlRX_2 , and 5 mmoles of donor substance. The reaction mixture was then heated to 60°C . for 30 min., at which time approximately 30 cc. of anhydrous *n*-heptane was added. Two phases were immediately obtained. The hydrocarbon (upper) phase was removed by a pipet and then reacted with a 15% aqueous solution of KOH. The Cl/Al ratio was determined. The lower phase was washed with 50 cc. of *n*-heptane, then also reacted with KOH in aqueous solution and later analyzed. In some cases, the lower phase was previously dried at room temperature under a vacuum of 0.1 mm. Hg and both Al and halogens determined on a weighed sample.

Distillation. The distillation was carried out with 2.1 cc. (20 mmoles) of EtAlCl_2 and 0.85 cc. (10 mmoles) of pyridine mixed in a previously dried vessel and under nitrogen atmosphere. Since the reaction was very exothermic, the flask was cooled down to -50°C .; after adding pyridine, the reagents were slowly heated up to room temperature, then distilled on a Vigreux column. The product obtained (b.p. $30\text{--}32^\circ\text{C}/0.5$ mm.), was diluted in heptane, reacted with a 15% solution of KOH and analyzed. The composition which was found was: Al, 22.4%; Cl, 29%; (calculated for AlEt_2Cl ; Al, 22.5%; Cl, 29.5%).

The distillation residue consisted of a crystalline substance which was essentially the $\text{AlCl}_3 \cdot \text{pyridine}$ complex.

Cryoscopy. The cryoscopic measurements were performed under nitrogen atmosphere in anhydrous benzene, with the use of a Beckman thermom-

eter in a closed vessel equipped with a magnetic stirrer. The quantitative data are reported in Table III.

TABLE III

| Run no. | Experimental conditions | Apparent freezing point, °C. | ΔT , °C. Found | Calculated for reaction (1) |
|---------|---|------------------------------|------------------------|-----------------------------|
| 1 | Benzene (11.439 g.) | 2.882 | — | — |
| | Benzene (11.43 g.) + [Al(<i>i</i> -C ₄ H ₉)Cl ₂] ₂ (2.5 × 10 ⁻³ M) | 1.705 | 1.177 | — |
| | Benzene (11.431 g.) + [Al(<i>i</i> -C ₄ H ₉)Cl ₂] ₂ (2.5 × 10 ⁻³ M) +(C ₆ H ₅) ₃ P (0.560 g.) | 1.274 | 0.431 ^a | 0.476 |
| 2 | Benzene (17.000 g.) | 4.295 | — | — |
| | Benzene (17.000 g.) + [Al(C ₂ H ₅)Cl ₂] ₂ (2.5 × 10 ⁻³ M) | 3.535 | 0.760 | — |
| | Benzene (17.000 g.) + [Al(C ₂ H ₅)Cl ₂] ₂ (2.5 × 10 ⁻³ M) +(C ₆ H ₅) ₃ P (0.396 g.) | 3.325 | 0.210 ^a | 0.227 |

^a Referred to the benzene solution containing (AlRCl₂)₂.

Conclusions

The results obtained indicate that in those systems containing one mole of an electron donor substance, (Lewis base, alkali metal halide, "onium" halide), and two moles of alkyl aluminum dihalide, a reaction takes place forming a coordinated aluminum trihalide complex and a free dialkyl aluminum halide.

The ternary catalytic systems consisting of TiCl₃ (violet), Al(C₂H₅)Cl₂, and an electron-donor substance, contain, therefore, free Al(C₂H₅)₂Cl responsible for promoting the polymerization of α -olefins.

The stereospecificity of these ternary catalytic systems in the polymerization of propylene is wholly identical to that of the binary systems prepared from TiCl₃ (violet) and Al(C₂H₅)₂Cl.

This confirms, therefore, the identity, in the two types of catalytic systems, of the nature of the metalloorganic compound active in the polymerization. In the binary system the dialkyl aluminum halide is added directly, while in the case of the ternary systems the dialkyl aluminum halide is generated from the reaction of alkyl aluminum dihalide and an electron-donor substance.

One must conclude therefore that the active catalysts derived from the here studied ternary mixtures are identical with the active catalyst previously obtained from TiCl₃-dialkyl aluminum monohalides by Natta et al.

It follows that the polypropylene obtained with those ternary mixtures and which has been called "stereosymmetric" is identical with the polypropylene previously prepared by Natta and collaborators.¹²

This is confirmed by the fact that the melting point is never higher and

is generally lower than the melting point of isotactic polypropylene (as determined with the aid of a polarizing microscope at a rate of temperature increase of 10–12°C./hr.).

In fact the maximum values for the melting point of isotactic polypropylene obtained with the catalysts of highest stereospecificity known up to now⁷ is 176–177°C., although some literature sources have given a value of 183°C., failing, however, to indicate the method used in the determination.

We wish to thank Prof. Natta and Prof. Pasquon for all their suggestions.

References

1. Natta, G., P. Pino, and G. Mazzanti, *Ital. Pat.* 526,101 (Dec. 3, 1954).
2. Natta, G., *Angew. Chem.*, **68**, 363 (1956); *Chim. Ind. (Paris)*, **77**, 1009 (1957); *Chem. Ind. (London)*, **1957**, 1520.
3. Natta, G., G. Mazzanti, and P. Longi, *Ital. Pat.* 586,441 (July 16, 1957).
4. Ziegler, K., E. Holzkamp, H. Breil, and H. Martin, *Angew. Chem.*, **67**, 426 (1955); *ibid.*, **67**, 547 (1955).
5. Coover, H. W., Jr., F. B. Joyner, and N. H. Shearer, Jr., *Belg. Pat.* 577,214 (March 28, 1959, USA priority March 31, 1958).
6. Eastman Kodak, *Austral. Pat. Appl.* 55135/59 (November 27, 1959).
7. Natta, G., I. Pasquon, A. Zambelli, and G. Gatti, *J. Polymer Sci.*, **51**, 387 (1961).
8. Jacober, G., and C. A. Kraus, *J. Am. Chem. Soc.*, **71**, 2409 (1949).
9. Ziegler, K., R. Köster, H. Lehmkuhl, and K. Reinert, *Ann.*, **629**, 33 (1960).
10. Köster, R., and W. R. Kroll, *Ann.*, **629**, 50 (1960).
11. Natta, G., I. Pasquon, and E. Giachetti, *Chim. Ind. (Milan)*, **40**, 97 (1958).
12. Natta, G., and I. Pasquon, *Rubber Plastics Age*, **42**, 1339 (1961).

Synopsis

The reaction of two molecules of AlRCl_2 with an electron donor molecule D, gives rise to the practically quantitative formation of AlR_2Cl and $\text{AlCl}_3 \cdot \text{D}$. This can explain the catalytic activity in the stereospecific polymerization of propylene to isotactic polymer of the systems prepared from violet TiCl_3 , AlRCl_2 , and an electron-donor substance. These systems have the same degree of stereospecificity as the systems consisting of $\text{AlR}_2\text{Cl-TiCl}_3$ (violet).

Résumé

La réaction entre deux molécules de AlRCl_2 et une molécule d'un donneur d'électron D donne lieu à la formation, pratiquement quantitative de AlR_2Cl et $\text{AlCl}_3 \cdot \text{D}$. Cela permet d'expliquer l'activité catalytique dans la polymérisation stéréospécifique du propylène à polymère isotactique, des systèmes préparés à partir de TiCl_3 (violette), AlRCl_2 et un donneur d'électrons. Ces systèmes ont la même stéréospécificité que les systèmes $\text{AlR}_2\text{Cl-TiCl}_3$ (violette).

Zusammenfassung

Die Reaktion zwischen zwei Molekülen AlRCl_2 und einem Elektronendonormolekül D führt zur praktisch quantitativen Bildung von AlR_2Cl und $\text{AlCl}_3 \cdot \text{D}$. Dadurch kann die katalytische Aktivität der aus violetterem TiCl_3 , AlRCl_2 und einer Elektronendonorsubstanz dargestellten System bei der stereospezifischen Propylenpolymerisation zu isotaktischen Polymeren erklärt werden. Diese Systeme besitzen den gleichen Grad an Stereospezifität wie $\text{AlR}_2\text{Cl-TiCl}_3$ (violette).

Received March 22, 1962

The Molecular Weight Distribution in Polypropylene

LOWELL WESTERMAN, *Research and Development Division,
Humble Oil and Refining Company, Baytown, Texas*

INTRODUCTION

Although numerous studies concerning the molecular weight and the molecular weight distribution in both Ziegler and high pressure polyethylenes may be found in the literature, little data are available describing the molecular weight distribution in polypropylene. Several papers have appeared reporting measurements of intrinsic viscosity and number-average molecular weight for both amorphous and crystalline polypropylene.¹⁻⁴ Intrinsic viscosity and weight-average molecular weight measurements for fractionated polypropylene samples have been reported by Chiang⁵ and by Kinsinger.⁶ Insufficient data are found in these papers to indicate the degree of polydispersity or the type of molecular weight distribution to be found in unfractionated or commercial polypropylene. Recently Davis and Tobias⁷ have shown from fractionation data on polypropylene that the molecular weight distribution is consistent with the log-normal distribution of Wesslau.⁸

In attempting to obtain data on the molecular weight distribution in commercial polypropylene samples we have chosen the combined measurements of weight, number, and viscosity-average molecular weights.

The samples selected for measurement were commercial and pilot unit samples which were unfractionated except for that small amount which may have occurred due to soluble polymer rejection in the polymerization diluent. Samples furthermore were selected to cover the molecular weight range normally encountered in commercial practice. Isotactic content, determined by the method of Natta,⁹ fell in the range of 80 to 95 wt.-%.

EXPERIMENTAL

Light Scattering Measurements

General Procedure

Light scattering measurements were conducted at a temperature of 140°C. on solution of polypropylene in α -chloronaphthalene. Intensity measurements relative to the intensity at 0° were made in angular increments of 10° from $\theta = 40^\circ$ to $\theta = 130^\circ$. For each sample the scattering measurements were made on a series of solutions having the approximate

concentrations of 0.2, 0.4, 0.6, 0.8, and 1.0 wt.-% polypropylene. The relative scattering intensity of pure α -chloronaphthalene was also measured at each angle, and these values were subtracted from the solution scattering intensity at the corresponding angle to yield the net scattering intensity used in the calculation of excess turbidity values. All measurements were made with mercury green light, 5460 Å.

The Light Scattering Instrument

A Brice-Phoenix light scattering photometer, series 1000, similar to the instrument described by Brice et al.,¹⁰ was employed for these measurements. The instrument was modified for elevated temperature measurement by providing a water-cooled housing for the photomultiplier tube to prevent loss in sensitivity due to excess heat transfer. A heated cell jacket and light scattering cell arrangement similar to that described by Moore¹¹ was installed for maintaining the sample solutions at 140°C. Temperature control was effected by means of a thermistor sensing element in conjunction with a Yellow Springs Instrument Co., model 63, temperature controller and a powerstat for controlling heater wattage. Solution temperatures were controlled to within $\pm 1^\circ\text{C}$. and were monitored with a copper-Constantan thermocouple.

Calibration and Correction Factors

Rayleigh ratios for pure benzene and carbon tetrachloride were measured using the original wide light beam geometry (1.2 cm.) in order to check the original calibration of the instrument by Phoenix Precision Instrument Co. The values obtained are shown in Table I and were found to be in good agreement with accepted literature values.¹²⁻¹⁵ Use of the heated cell jacket and the cell arrangement described above necessitated the use of a narrow light beam geometry and required an additional calibration, which was accomplished by measuring the scattering from solutions of Ludox, as recommended by Oster.¹⁶ The Rayleigh ratio obtained for benzene on the

TABLE I
Rayleigh Ratios for Benzene and Carbon Tetrachloride
(Rayleigh ratio, $R_{90} \times 10^6$ 546 m μ , 25°C.)

| Found | Literature | Ref. |
|-------------------|----------------------|------|
| | Benzene | |
| 17.1 ^a | 17.6 | 12 |
| 17.3 ^b | 17.2 | 13 |
| | 16.3 | 14 |
| | 16.4 | 15 |
| | Carbon Tetrachloride | |
| 6.10 | 5.88 | 13 |
| | 5.8 | 15 |

^a Original instrument calibration, "wide" beam.

^b Calibration for "narrow" light beam geometry.

completely modified instrument is shown in Table I and agrees with that found with the wide beam geometry.

Optical symmetry of the cells was checked by viewing the green fluorescence from sodium fluorescein solutions through a yellow filter, illuminating the solution with blue light. A constant intensity was obtained within $\pm 1\%$ for angles between 40° and 135° , after applying the $\sin \theta$ correction.

Since a sample of Cornell polystyrene standard was not available, cross-check measurements were made between our instrument and a similarly modified instrument in the laboratories of Esso Research and Engineering Co., which had been calibrated against the Cornell polystyrene sample. Using identical procedures on two selected polypropylene samples the \bar{M}_w values obtained on each instrument agreed to within 7%.

The specific refractive increment, dn/dc , for polypropylene in α -chloronaphthalene has been reported by Chiang⁵ as -0.188 cc./g. at 140°C . for mercury green light (5460 Å.), and has recently been supported by the measurements of Weston and Billmeyer.¹⁷ Chiang's value was used in the calculation of \bar{M}_w from scattering data together with a refractive index value of 1.594 for α -chloronaphthalene.

Preparation and Clarification of Solutions

All solutions were prepared using deoxygenated α -chloronaphthalene. Appropriate quantities of a 1 wt.-% sample solution were filtered into weighed Erlenmeyer cells followed by filtration of the necessary volume of solvent to produce solutions having the approximate concentrations of 0.2, 0.4, 0.6, 0.8, and 1.0 wt.-% polypropylene. True concentrations of each sample solution were determined gravimetrically, following scattering measurements, by quantitatively precipitating the polymer with a 20 volume excess of methanol.

Nitrogen pressure filtration through heated Sela porcelain filter candles, No. 03, was used in clarification of the solutions and solvent.

Solubilization of the sample in α -chloronaphthalene was effected by rapidly heating the sample, under nitrogen, to the boiling point of the solvent followed by cooling to 140°C . in a convection oven. Samples were maintained at elevated temperatures for the minimum time required to prepare true solutions and to make scattering measurements. No degradation of the sample was noted in the course of sample preparation and measurement.

Osmotic Pressure Measurements

Osmotic pressure measurements were conducted at a temperature of $130 \pm 0.01^\circ\text{C}$., using the latest modification of the osmometer described by Stabin and Immergut,¹⁸ which employs 6.5 cm. diam. membranes and was especially designed for elevated temperature measurements. Spurious changes in the hydrostatic head were noted in early runs. This was traced to movement of the membranes and was corrected by incorporating 100

mesh stainless steel wire screens between the membranes and the outer stainless steel flanges, providing increased membrane support.

For the purpose of observing temperature equilibrium conditions within the osmometer jacket, a micro-Beckman thermometer was attached to the osmometer assembly. Changes in the hydrostatic head were followed with a cathetometer, reading to 0.01 mm.

The solvent employed for this work was *o*-dichlorobenzene to which 0.001% 2,2'-methylenebis(4-methyl-6-*tert*-butylphenol) was added as an inhibitor. Sample solutions were prepared at the osmometer temperature and were transferred hot into the osmometer. Solubilization was effected in a manner similar to that described for light scattering solutions. Nitrogen blanketing was used for the preparation and in running the solutions.

Gel cellophane No. 450 membranes were used throughout this work. They were conditioned by immersion in each of the following solutions for at least 12 hr.: (1) water, (2) 50:50 water:ethanol, (3) ethanol, (4) absolute ethanol, (5) 75:25 ethanol:*o*-dichlorobenzene, (6) 50:50 ethanol:*o*-dichlorobenzene, (7) 25:50 ethanol:*o*-dichlorobenzene, (8) *o*-dichlorobenzene. The membranes were finally stored in fresh *o*-dichlorobenzene. After assembly into the osmometer the membranes were conditioned to polymer solutions by filling the instrument with a 1% solution of polypropylene. This solution was allowed to remain in contact with the membranes for at least 12 hr. Membranes conditioned in this way showed no tendency to adsorb solute from the solution being measured. Half-times for these membranes (the time necessary for the hydrostatic head to drop to one-half of the initial setting) were of the order of 15 min. for *o*-dichlorobenzene with an initial hydrostatic head of 3 cm.

Each determination of osmotic pressure was conducted in the following manner. The cell was filled with two successive portions of the solution to be measured, and each portion was allowed to wash the membranes for 30 min. before final filling. Thirty minutes were allowed after the final filling for temperature equilibration followed by readings on the ascending and descending hydrostatic heads. The point of convergence of these two branches was taken as the uncorrected osmotic pressure. Asymmetry pressure measurements were made before and after the completion of measurements on each series of polymer solutions. The average asymmetry pressure thus obtained was used to correct the observed osmotic pressures for each run of the series. Asymmetry pressure corrections normally were of the order of 0.1 to 0.2 cm. positive. The reduced osmotic pressure at infinite dilution, $(\pi/C)_6$, was calculated by the method of least squares.

Intrinsic Viscosity Measurements

Measurement of the intrinsic viscosity of these polypropylene samples was made at a temperature of 135°C. using decalin as the solvent and with modified Ubbelohde viscometers. The procedure was essentially the same as that described in ASTM D-1601-58T.¹⁹

RESULTS AND DISCUSSION

Weight-Average and Number-Average Molecular Weights

Using the technique described above, angular scattering measurements were conducted on ten commercial and pilot unit polypropylene samples designated *A* through *J*. Both the "dissymmetry" method²⁰ and the method of Zimm²¹ were used to evaluate the weight-average molecular weight of each sample. Typical plots of Hc/τ_{90° vs. c and Hc/τ_θ vs. $50c + \sin^2 \theta/2$, obtained for these samples are shown in Figures 1 and 2, respectively. All of the samples produced linear Zimm plots. A comparison of \bar{M}_w values obtained by each method is given in Table II, from which it may

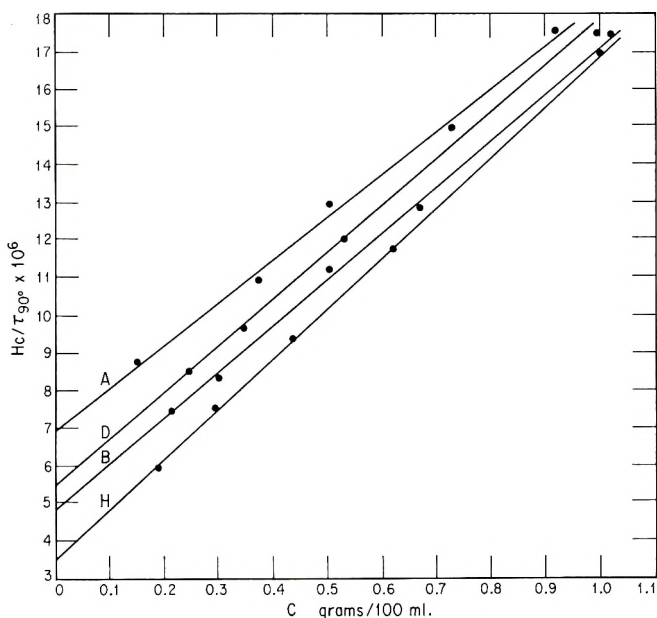


Fig. 1. Hc/τ_{90° versus concentration.

be seen that the weight-average molecular weights evaluated from angular scattering measurements by the method of Zimm agree closely with those obtained by the "dissymmetry" method, assuming the polydisperse random coil model. On this basis, it appears that the particle scattering factors, calculated on this assumption, are adequate for compensating for the effect of the dissymmetry of angular scattering in the case of samples in the \bar{M}_w range from 200,000 to 800,000 and $[z]$ from 1.49 to 2.37. Agreement shown between these two methods of evaluating \bar{M}_w was found to be extremely sensitive to proper clarification of solutions.

The second virial coefficient, B , calculated from the slope of the line $\theta = 0$, and the z -average dimension, $(\bar{R}_z^2)^{1/2}$, calculated by means of eq. (1) are given in Table II.

TABLE II
 Light Scattering Data

| Sample | $\bar{M}_w \times 10^{-3}$ | | [z] | $(\bar{R}_z^2)^{1/2} \text{A.}$ | $B \times 10^4$ |
|--------|----------------------------|-------------|---------|---------------------------------|-----------------|
| | Zimm | Dissymmetry | | | |
| A | 221 | 213 | 1.62 | 1170 | 5.2 |
| B | 296 | 287 | 1.49 | 0760 | 5.3 |
| D | 299 | 296 | 1.79 | 1250 | 5.7 |
| C | 377 | 367 | 1.82 | 1360 | 4.7 |
| E | 465 | 467 | 1.95 | 1410 | 5.4 |
| F | 462 | 457 | 2.10 | 1480 | 5.5 |
| H | 479 | 497 | 1.91 | 1290 | 5.6 |
| J | 562 | 593 | 1.72 | 1610 | 5.2 |
| I | 625 | 625 | 2.33 | 1840 | 4.9 |
| G | 720 | 718 | 2.37 | 1850 | 5.3 |

$$\bar{R}_z^2 = \frac{9\lambda'^2 (\text{slope of the line } c = 0)}{8\pi^2 (\text{intercept})} \quad (1)$$

where λ' the wavelength of light in α -chloronaphthalene = $5460/1.59 = 3434 \text{ A.}$

The $(\bar{R}_z^2)^{1/2}$ values obtained are larger than those reported by Chiang⁵ for comparable \bar{M}_w levels, as would be predicted on the basis of the greater polydispersity of the samples.

Reduced osmotic pressure measurements as well as $(\pi/c)_0$ and the second virial coefficient, A , calculated therefrom by the method of least squares are shown in Table III. Plots of π/c vs. c for this series of samples are shown in

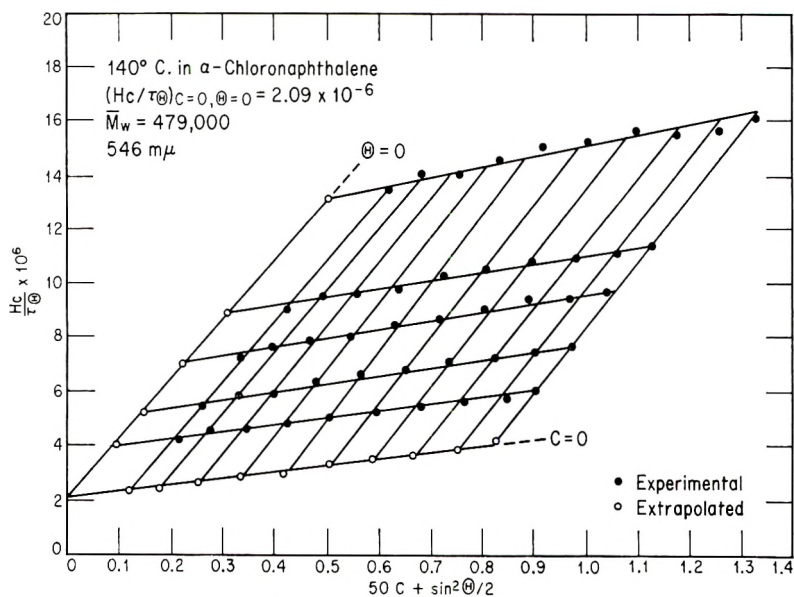


Fig. 2. Zimm plot for polypropylene sample H.

TABLE III
 Reduced Osmotic Pressures for Solutions of Various Polypropylene Samples in
o-Dichlorobenzene at 130°C., Using Gel Cellophane No. 450 Membranes

| Sam- ple | π/c in cm./gram/100 ml. | | | | | $(\pi/c)_0$ | $A \times 10^4$ | \bar{M}_n |
|-------------|-----------------------------|-------|-------|-------|-------|-------------|-----------------|-------------|
| | c in gram/100 ml. | | | | | | | |
| A | π/c | 10.07 | 9.61 | 8.89 | 8.04 | 7.47 | 8.3 | 38,600 |
| | c | 1.033 | 0.775 | 0.517 | 0.256 | | | |
| B | π/c | 8.72 | 7.91 | 7.33 | 6.47 | 5.77 | 8.5 | 50,000 |
| | c | 1.013 | 0.762 | 0.509 | 0.255 | | | |
| C | π/c | 8.56 | 7.75 | 7.22 | 6.28 | 5.59 | 9.1 | 51,600 |
| | c | 1.037 | 0.779 | 0.528 | 0.261 | | | |
| D | π/c | 8.44 | 7.64 | 6.85 | 6.15 | 5.36 | 9.5 | 53,900 |
| | c | 1.028 | 0.772 | 0.512 | 0.257 | | | |
| E | π/c | 8.13 | 7.38 | 6.50 | 5.73 | 4.93 | 9.9 | 58,500 |
| | c | 1.038 | 0.777 | 0.515 | 0.257 | | | |
| F | π/c | 7.98 | 7.20 | 6.39 | 5.64 | 4.85 | 9.0 | 59,400 |
| | c | 1.023 | 0.761 | 0.497 | 0.259 | | | |
| G | π/c | 7.94 | 7.16 | 6.20 | 5.68 | 4.76 | 9.1 | 60,600 |
| | c | 1.011 | 0.767 | 0.516 | 0.263 | | | |
| H | π/c | 7.75 | 6.90 | 6.26 | 5.36 | 4.63 | 9.6 | 62,300 |
| | c | 1.036 | 0.765 | 0.514 | 0.255 | | | |
| I | π/c | 7.78 | 6.95 | 6.16 | 5.34 | 4.53 | 10.1 | 63,700 |
| | c | 1.024 | 0.769 | 0.517 | 0.253 | | | |
| J | π/c | 7.65 | 6.86 | 5.95 | 5.20 | 4.35 | 9.3 | 66,400 |
| | c | 1.036 | 0.768 | 0.514 | 0.258 | | | |

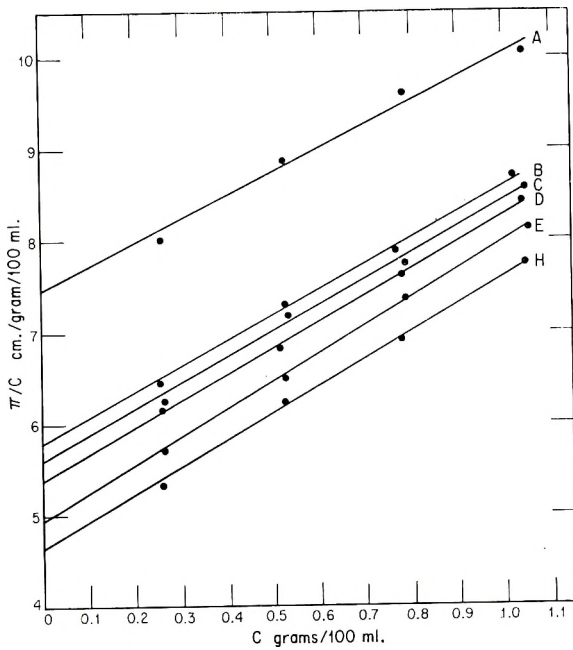


Fig. 3. Plot of π/c versus c for various polypropylene samples.

Figure 3. The weight-average molecular weight was calculated from these data according to the following equation:

$$\bar{M}_n = RT/d(\pi/c)_0$$

where R is the gas constant in grams · 100 ml./cm.²/deg./mole = 848, T is the absolute temperature, 403°K., d is the density of *o*-dichlorobenzene at 130°C. = 1.1842, π is the osmotic pressure in centimeter of solvent, c is concentration in grams per 100 ml.

The density of *o*-dichlorobenzene at 130°C. was calculated from its density at 25°C. and from an experimentally determined value for the temperature coefficient of density; $\Delta d/\Delta t = -0.001097$ between 25 and 130°C.

Replicate determinations of \bar{M}_n , made on two of the samples, indicated an average deviation of the order of $\pm 3\%$. Cross-check measurements conducted between this laboratory and that of the Chemicals Research Division, Esso Research and Engineering Co., on samples *C* and *I* yielded \bar{M}_n values which were in agreement to within 7 and 1%, respectively.

Molecular Weight Distribution

A summary of the results of \bar{M}_w , \bar{M}_n , and \bar{M}_v measurements are given in Table IV, arranged in order of increasing intrinsic viscosity. From these data a general trend in the polydispersity of the samples may be noted. The breadth of molecular weight distribution, denoted by \bar{M}_w/\bar{M}_n , decreases as the average molecular weight of the sample decreases, approaching the limiting value of $\bar{M}_w/\bar{M}_n = 1$, as the molecular weight approaches that of the monomer propylene.

TABLE IV
Intrinsic Viscosity-Molecular Weight Data for Polypropylene Samples

| Sample | [η] 135°C. decalin deciliters/g. | $\bar{M}_v \times 10^3$ [Chiang equation, eq. (2)] | $\bar{M}_n \times 10^{-3}$ | $\bar{M}_w \times 10^{-3}$ | \bar{M}_w/\bar{M}_n |
|--------|---|---|----------------------------|----------------------------|-----------------------|
| | | | | | |
| A | 1.60 | 180 | 38.6 | 217 | 5.62 |
| B | 2.12 | 256 | 50.0 | 292 | 5.84 |
| D | 2.23 | 272 | 53.9 | 298 | 5.53 |
| C | 2.46 | 308 | 51.6 | 372 | 7.21 |
| F | 2.49 | 313 | 59.4 | 460 | 7.74 |
| E | 2.63 | 335 | 58.5 | 466 | 7.97 |
| H | 2.83 | 367 | 62.3 | 488 | 7.83 |
| J | 2.89 | 377 | 66.4 | 578 | 8.70 |
| I | 3.52 | 482 | 63.7 | 625 | 9.81 |
| G | 3.59 | 494 | 60.6 | 720 | 11.9 |

A conventional plot of $\log [\eta] 135^\circ\text{C./decalin}$ vs. $\log \bar{M}_w$ for this series of unfractionated samples is shown in Figure 4, together with the data reported by Chiang⁵ for fractionated polypropylene. The relationship

between intrinsic viscosity and \bar{M}_w for these *unfractionated* samples may be expressed by the equation:

$$[\eta]_{\text{decalin}}^{135^\circ\text{C.}} = 5.43 \times 10^{-4} \bar{M}_w^{0.65}$$

compared with the equation of Chiang for fractionated samples:

$$[\eta]_{\text{decalin}}^{135^\circ\text{C.}} = 1.00 \times 10^{-3} \bar{M}_w^{0.80} \quad (2)$$

The divergence of these lines with increasing \bar{M}_w is also indicative of the trend toward increasing polydispersity with increasing average molecular weight.

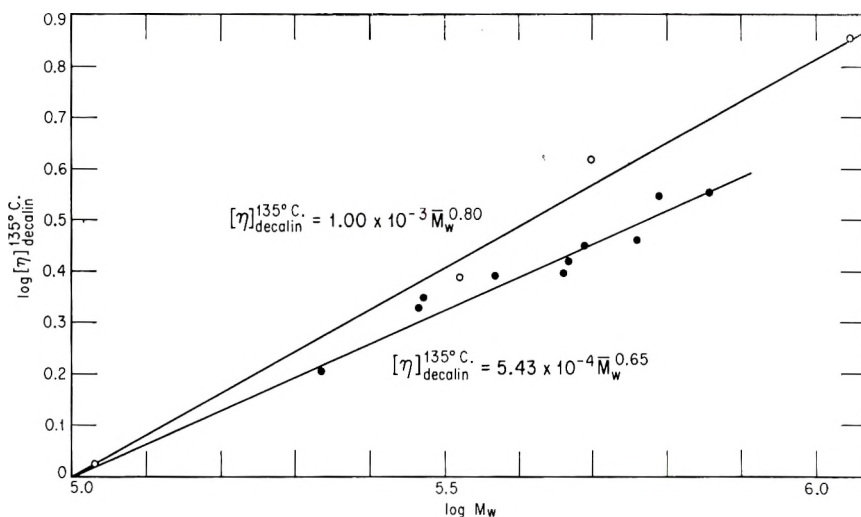


Fig. 4. Intrinsic viscosity-weight-average molecular weight relationships: (O) data of Chiang⁸ for fractionated samples; (●) data for unfractionated samples.

According to Wesslau,⁸ the molecular weight distribution in Ziegler type *polyethylene* can best be expressed by a log-normal distribution function as follows:

$$f(M) = \frac{1}{\beta\sqrt{\pi}} \left(\frac{1}{M}\right) \exp \left\{ - \left(\frac{1}{\beta} \ln \frac{M}{M_0} \right)^2 \right\} \quad (3)$$

where $f(M)$ is the normalized distribution function and

$$\int_0^\infty f(M) dM = 1$$

This type of distribution has been supported by the fractionation studies of Francis et al.²² and by Chiang,²³ who has discussed the log-normal distribution in relation to viscosity-weight average molecular weight relationships for polyethylene. Chiang shows the development of the equations given below.

The weight-average, number-average, and viscosity-average molecular

weights may be defined in terms of the log-normal distribution function or Wesslau, eq. (3) as follows:

$$\bar{M}_w = \int_0^\infty Mf(M)dM = M_0 \exp \{\beta^2/4\} \quad (4)$$

$$\bar{M}_n = 1/\int_0^\infty f(M)/M dM = M_0 \exp \{-\beta^2/4\} \quad (5)$$

$$\bar{M}_v = [\int_0^\infty M^\alpha f(M)dM]^{1/\alpha} = M_0 \exp \{\alpha\beta^2/4\} \quad (6)$$

where α is the exponent in the intrinsic viscosity-molecular weight relationship,

$$[\eta] = KM^\alpha$$

Combination of eqs. (4), (5), and (6) yields the expressions:

$$\left(\frac{\bar{M}_w}{\bar{M}_n}\right) = \left(\frac{\bar{M}_v}{\bar{M}_n}\right)^{(1+\alpha)/2} \quad (7)$$

$$\left(\frac{\bar{M}_v}{\bar{M}_n}\right) = \left(\frac{\bar{M}_w}{\bar{M}_n}\right)^{(1-\alpha)/2} \quad (8)$$

Chiang⁵ has given an equation for the intrinsic viscosity-weight-average molecular weight relationship for fractionated polypropylene, expressed in the usual form by eq. (2) above. If this equation is used to calculate molecular weight of an unfractionated polypropylene sample from its intrinsic viscosity, the result is the viscosity-average molecular weight \bar{M}_v referred to in eqs. (6), (7), and (8) above. Assuming Chiang's polypropylene fractions to be nearly monodisperse and applying eq. (7) to experimentally determined values of \bar{M}_v and \bar{M}_n given in Table IV, the values shown in Table V are obtained. The calculated ratio, \bar{M}_w/\bar{M}_n ,

TABLE V
Comparison of Experimental and Calculated Values of \bar{M}_w/\bar{M}_n , Assuming Log-Normal Distribution

| Sample | \bar{M}_v/\bar{M}_n , measured | \bar{M}_w/\bar{M}_n calc., eq. (7) | \bar{M}_w/\bar{M}_n , measured |
|--------|----------------------------------|--------------------------------------|----------------------------------|
| A | 4.66 | 5.5 | 5.6 |
| D | 5.05 | 6.0 | 5.5 |
| B | 5.12 | 6.1 | 5.8 |
| F | 5.27 | 6.4 | 7.7 |
| J | 5.69 | 6.9 | 8.7 |
| E | 5.73 | 7.0 | 8.0 |
| H | 5.89 | 7.2 | 7.7 |
| C | 5.97 | 7.3 | 7.2 |
| I | 7.57 | 9.5 | 9.8 |
| G | 8.15 | 12.6 | 11.9 |

from eq. (7), agrees quite closely with the experimentally determined ratio, suggesting that the molecular weight distribution in polypropylene approaches a log-normal distribution of the type attributed to Ziegler polyethylene.

A similar comparison may be made using eq. (8); however, the ratio \bar{M}_w/\bar{M}_v is so small that a 10% error in the experimentally determined value of \bar{M}_w can change the value of \bar{M}_w/\bar{M}_n as calculated from this equation by 100%.

On the basis of the agreement between \bar{M}_w/\bar{M}_n values calculated for a log-normal distribution, and the experimentally determined ratios \bar{M}_w/\bar{M}_n , it is not unreasonable to conclude that the molecular weight distribution in unfractionated commercial Ziegler polypropylene samples, having \bar{M}_w values between 2×10^5 and 7.5×10^5 , approaches the log-normal distribution expressed by eq. (3). Davis and Tobias⁷ have arrived at this same conclusion from fractionation data on several polypropylene samples. The \bar{M}_w/\bar{M}_n values calculated by these authors from their fractionation data are somewhat larger than the values which we have found at a comparable molecular weight level. This may be due to a greater degree of soluble polymer rejection in the preparation of the commercial and pilot unit samples than in the laboratory polymerized samples which were fractionated by Davis and Tobias.

Appreciation is expressed to Mr. J. O. Brewer and Mr. G. A. Reidland who conducted much of the experimental measurements reported herein; to Dr. P. L. Mercier and the late Dr. D. M. Stern for cross-check measurements on several samples; and to the Humble Oil and Refining Co. for permission to publish these data.

References

1. Ciampa, G., *Chim. e ind. (Milan)*, **38**, 298 (1956).
2. Danusso, F., G. Moraglio, and V. Giannella, *Atti Accad. Naz. Lincei Rend. Classe Sci. Fis. Mat. Nat.*, **25**, 498 (1958).
3. Danusso, F., and G. Moraglio, *Makromol. Chem.*, **28**, 250 (1958).
4. Moraglio, G., *Chim. e ind. (Milan)*, **41**, 879 (1959).
5. Chiang, R., *J. Polymer Sci.*, **28**, 235 (1958).
6. Kinsinger, J. B., Ph.D. thesis, Univ. of Pennsylvania, 1958.
7. Davis, T. E., and R. L. Tobias, *J. Polymer Sci.*, **50**, 227 (1961).
8. Wesslau, H., *Makromol. Chem.*, **20**, 111 (1956).
9. Natta, G., G. Mazzanti, G. Crespi, and G. Moraglio, *Chim. e ind. (Milan)*, **39**, 275 (1957).
10. Brice, B. A., M. Halwer, and R. Speiser, *J. Opt. Soc. Am.*, **40**, 768 (1950).
11. Moore, L. D., Jr., *J. Polymer Sci.*, **20**, 137 (1956).
12. Maron, S. H., and R. H. L. Lou, *J. Polymer Sci.*, **14**, 29 (1954).
13. Carr, C. I., and B. H. Zimm, *J. Chem. Phys.*, **18**, 1616 (1950).
14. Doty, P., and R. F. Steiner, *J. Chem. Phys.*, **18**, 1211 (1950).
15. Stam, R. F., and P. A. Button, *J. Chem. Phys.*, **23**, 2456 (1955).
16. Oster, G., *J. Polymer Sci.*, **9**, 525 (1952).
17. Weston, N. E., and F. W. Billmeyer, Jr., *J. Phys. Chem.*, **65**, 576 (1961).
18. Stabin, J. V., and E. H. Immergut, *J. Polymer Sci.*, **14**, 209 (1954).
19. *Tentative Method of Test for Dilute Solution Viscosity of Ethylene Polymers*, ASTM D1601-58T, *ASTM Standards on Plastics*, Sept. 1958.
20. Debye, P., *J. Phys. & Colloid. Chem.*, **51**, 18 (1947).
21. Zimm, B. H., *J. Chem. Phys.*, **16**, 1093 (1948).
22. Francis, P. S., R. C. Cooke, Jr., and J. H. Elliott, *J. Polymer Sci.*, **31**, 453 (1958).
23. Chiang, R., *J. Polymer Sci.*, **36**, 91 (1959).

Synopsis

Light scattering, osmotic pressure, and dilute solution viscosity measurements were utilized to determine the weight-average, number-average, and viscosity-average molecular weights of 10 unfractionated commercial and pilot unit polypropylene samples. Weight-average molecular weights evaluated from angular scattering data by the method of Zimm were found to agree with those determined by means of the "dissymmetry" method when proper solution clarification procedures were employed. As would be predicted, the z -average dimension, \bar{R}_z^2 , for these polydisperse samples was found to be larger than those reported by Chiang for fractionated samples of comparable weight-average molecular weight. A general trend toward increased breadth of molecular weight distribution with increasing average molecular weight was detected from the variation of \bar{M}_w/\bar{M}_n values with average molecular weight, and is supported by the $[\eta]-\bar{M}_w$ relationship found for these unfractionated samples as compared with the relationship established by Chiang for fractionated samples. The log-normal distribution function of Wesslau was applied to data on \bar{M}_w , \bar{M}_n , and \bar{M}_v , demonstrating that commercial Ziegler-type polypropylene displays this type of molecular weight distribution within the molecular weight range studied.

Résumé

Des mesures de diffusion lumineuse, de pression osmotique et de viscosité en solution diluée ont été effectuées pour déterminer les poids moléculaires moyens en poids, en nombre et viscosimétrique de dix échantillons de polypropylène commercial non fractionné et de polypropylène provenant d'unité pilote. Les poids moléculaires moyens en poids évalués à partir des données de la diffusion angulaire d'après la méthode de Zimm sont en parfait accord avec ceux déterminés par la méthode de "dissymétrie" lorsque des procédés spéciaux de clarification des solutions sont employés. Comme on pouvait le prévoir, la dimension moyenne, \bar{R}_z^2 pour ces échantillons polydispersés est plus grande que celle rapportée par Chiang pour des échantillons fractionnés de poids moléculaire moyen en poids comparable. Une tendance générale vers un élargissement de la distribution du poids moléculaire lorsque le poids moléculaire moyen augmente a été détectée à partir de la variation des valeurs de \bar{M}_w/\bar{M}_n avec le poids moléculaire moyen. Cela a été confirmé par la relation $[\eta] - \bar{M}_w$ trouvée pour ces échantillons non fractionnés si on la compare avec la relation établie par Chiang pour des échantillons fractionnés. Le logarithme normal de la fonction de distribution de Wesslau appliqué aux données obtenues pour \bar{M}_w , \bar{M}_n et \bar{M}_v , montre que le polypropylène commercial du type Ziegler appartient à ce type de distribution du poids moléculaire dans le domaine de poids moléculaire étudié.

Zusammenfassung

Die Messung der Lichtstreuung, des osmotischen Drucks und der Viskosität verdünnter Lösungen wurden zur Bestimmung des Gewichts-, Zahlen- und Viskositätsmittels des Molekulargewichts von zehn unfractionierten, handelsüblichen und Versuchs-Polypropylenproben herangezogen. Die aus der Winkelabhängigkeit der Streuintensität nach der Methode von Zimm erhaltenen Gewichtsmittelwerte des Molekulargewichts stimmen bei Verwendung geeigneter Verfahren zur Klärung der Lösungen mit nach der "Dissymetrie"-Methode bestimmten überein. Wie vorauszusehen, ergab sich für diese polydispersen Proben ein grösserer Dimensions- z -Mittelwert, \bar{R}_z^2 , als er von Chiang für fraktionierte Proben mit vergleichbarem Gewichtsmittel des Molekulargewichts erhalten wurde. Eine allgemeine Zunahme der Breite der Molekulargewichtsverteilung mit zunehmendem mittleren Molekulargewicht wurde aus der Abhängigkeit des \bar{M}_w/\bar{M}_n -Wertes vom mittleren Molekulargewicht festgestellt und findet eine Stütze durch den Vergleich der für diese unfractionierten Proben gefundenen $[\eta]-\bar{M}_w$ -Beziehung mit der von Chiang für fraktionierte Proben aufgestellten. Die

log-normal-Verteilungsfunktion von Wesslau wurde auf die \bar{M}_w , \bar{M}_n und \bar{M}_v -Werte angewendet und es wurde so gezeigt, dass handelsübliches Polypropylen vom Ziegler-Typ innerhalb des untersuchten Molekulargewichtsbereiches diese Molekulargewichtsverteilung aufweist.

Received September 21, 1961

Kinetics of Propylene Polymerization Catalyzed by α -Titanium Trichloride–Diethylaluminum Chloride

JAMES C. W. CHIEN, *Hercules Research Center, Wilmington, Delaware*

INTRODUCTION

Gaylord and Mark,¹ in a recent review, summarized the results of mechanistic and kinetic studies on the polymerization of ethylene at low pressure with organometallic catalysts. While heterogeneous catalysts were used by most investigators, detailed information on the kinetics² and the mechanism³⁻⁵ of ethylene polymerization was obtained by use of soluble catalyst systems.

The low pressure polymerization of propylene to crystalline polymers with organometallic catalysts is of great commercial and scientific interest. The properties⁶ and the structure⁷ of stereoregular polypropylene have been described in detail elsewhere. The most often studied catalyst systems⁸⁻¹⁰ for the polymerization of propylene to stereoregular polymers are the α -TiCl₃-(C₂H₅)₃Al and α -TiCl₃-(C₂H₅)₂AlCl systems. Bier, Gumbolt, and Lehmann¹¹ described polymerizations initiated by halogen-containing organoaluminum compounds and TiCl₃. Both α -TiCl₃ and TiCl₃ prepared from TiCl₄ by treatment with aluminum or organoaluminum compounds were used in their work. Other monomers can also be polymerized to stereoregular polymers with similar organometallic catalysts. Thus, Burnett and Tait¹² used α -TiCl₃ with (C₂H₅)₃Al, (C₂H₅)₂-AlCl, and (C₂H₅)₂AlBr to initiate stereospecific polymerization of styrene.

The object of this investigation was to determine the kinetic rate constants and to understand the mechanism of the various processes in a stereospecific polymerization of propylene and to obtain information about the polymerization process which gives amorphous polymers. The catalyst system used in this work was α -TiCl₃-(C₂H₅)₂AlCl.

EXPERIMENTAL

Materials

Inorganic titanium trichloride, α -TiCl₃, and titanium dichloride were treated with diethylaluminum chloride, to eliminate the reported⁸ induction period, and then washed with purified heptane. In the tracer experiments, C¹⁴-labeled diethylaluminum chloride was used in this pretreatment. Diethylaluminum chloride labeled with C¹⁴ was prepared from C₂¹⁴ H₅Cl

(Tracerlab, Houston, Texas) in a vacuum system according to the method of Grosse and Mavity.¹³ Phillips Petroleum pure grade (99.5%) heptane was further purified by shaking with concentrated sulfuric acid and then with acid permanganate solution. This treatment was followed by separation, neutralization, washing, drying over anhydrous magnesium sulfate, and filtration. The treated heptane was passed through a 20-in. silica gel column directly into the reaction vessel under an atmosphere of nitrogen. Phillips Petroleum research grade propylene (99.5% pure) was used without further purification.

Procedures

Polymerization and sampling procedures have been described previously.² The reproducibility of the sampling procedure was demonstrated at several polymer concentrations. For example, in a typical, quenched polymerization mixture, eighteen 10-ml. samples averaged 56.2 g. of polypropylene per liter of diluent with a standard deviation of 1.82%.

The amorphous and the crystalline polypropylene were separated as follows. The polymer in a reaction mixture was completely precipitated by the addition of a 10% solution of HCl in methanol and washed repeatedly with methanol until the washings were neutral to litmus. The amorphous fraction was repeatedly extracted with hot heptane. The heptane extracts were combined and the solvent was evaporated at room temperature. Both the crystalline and the amorphous polymers were dried at 90°.

Determination of Radioactivity. The polymer was weighed and suspended in a toluene solution of diphenyloxazole, a primary scintillator, and POPOP, a wavelength shifter. A gelling agent, Thixin, was also added. The scintillation counter had a sensitivity higher than 50%. The total counts were always in excess of 10,000. The number of labeled ethyl groups was calculated from the C¹⁴ activity of polymer samples with a factor determined as follows: aliquots of a stock solution of (C₂¹⁴H₅)₂AlCl were hydrolyzed and converted to BaCO₃ by standard technique,¹⁴ and the BaC¹⁴O₃ was counted in the aforementioned counting mixture.

Determination of Number-Average Molecular Weights. Number-average molecular weights, \bar{M}_n , of several polymer samples were determined by fractionation. The fractionation procedure developed by Shyluk for polypropylene and the calculation of \bar{M}_n from the fractionation data has been described in detail.¹¹

Determination of Ethyl Groups Complexed to TiCl₃. The apparatus used in these experiments was H-shaped and consisted of two 30-mm o.d. tubes connected by an arm containing a sintered-glass disk. The tops of the tubes were 29/42 tapered joints. Stainless steel tubes (29/42 taper), inserted in the glass joints, made it possible to crimp metal caps on the ends of the tubes. These caps have a self-sealing neoprene liner and a small hole for insertion of a hypodermic needle. A neoprene cap was wrapped over the metal cap and nitrogen was continually bled into this

cap through a hypodermic needle. A 20-g. portion of aluminum chloride and 10 g. of sodium chloride were added to one section of the apparatus. Then the whole apparatus was evacuated thoroughly and filled with nitrogen. Into the other section was introduced 24 ml. of α - TiCl_3 slurry (1.23*M* in heptane) and 14 ml. of $(\text{C}_2\text{H}_5)_2\text{AlCl}$ (2.85*M* in heptane). Radioactive $(\text{C}_2\text{H}_5)_2\text{AlCl}$ was not used because of the prohibitive cost. After overnight reaction, the supernatant liquid was transferred to the other section where unreacted $(\text{C}_2\text{H}_5)_2\text{AlCl}$ was converted to $(\text{C}_2\text{H}_5)_2\text{AlCl}$ which was strongly complexed by NaCl. The TiCl_3 slurry was washed three times with 40-ml. portions of purified heptane. A 2-ml. sample of the supernatant liquid and a 2-ml. sample of the slurry were taken. Washing and sampling were repeated until six samples of each were obtained. These samples were added to 40 ml. of a radioactive iodine solution (0.1*N* in heptane). After overnight reaction in the absence of air, the unreacted iodine was removed by thiosulfate and 5 ml. of ethyl iodide was added as carrier. The I^{131} activity in the organic layer was counted. The difference between the counting rate of the slurry sample and that of the supernatant liquid sample was converted to the number of complexed ethyl groups. All six sets of samples agreed within 10%, giving an average value of 0.091 mole of ethyl groups per mole of TiCl_3 present. A duplicate experiment gave 0.11 mole of ethyl groups complexed per mole of TiCl_3 .

Determination of Solubility of Propylene in Heptane. The solubility of propylene in heptane was determined by pressure-volume measurements at 0, 15, 30, 45, 60, 70, and 90°C. and 79, 110, 155, and 245 cm. Solubility depends linearly on pressure at all temperatures. The solubility at 0°C. and 76 cm. was 1.62 moles l^{-1} . The heat of solution was found to be 4.73 kcal. mole $^{-1}$.

RESULTS

Unless otherwise specified, the results pertain to measurements made on crystalline polymers.

Chain Initiation

Chain initiation is defined as the formation of an active ethyl-metal bond, on which growth subsequently takes place. Since the titanium trichloride used in this work had been pretreated with diethylaluminum chloride, within experimental accuracy, propagation on most of the available active sites took place as soon as the catalyst was introduced. The rate of polymerization was found to remain relatively constant throughout the reaction. Therefore, it is assumed that the total number of propagating sites remains unchanged during the polymerization. Consequently, the initial C^{14} activity in the polymer may be equated to the number of reactive ethyl groups, $[\text{C}]$, initially on the surface.

The total C^{14} activity increases with time because of chain-transfer processes which will be discussed below. The value of $[\text{C}]$ was determined

TABLE I
 Kinetic Results

| [Ti] ^a mmole l. ⁻¹ | [Al] ^b mmole l. ⁻¹ | Temp., °C. | ρ _{C₂H₆} , cm. | [C ¹⁴] ₀ mmole | k _p , l. mole ⁻¹ sec. ⁻¹ | (R _r) × 10 ³ , mole l. ⁻¹ sec. ⁻¹ | | (M _n) × 10 ^{-5d} | | Fraction- ation |
|--|---|---------------|--|--|--|---|--------|---------------------------------------|--------|--------------------|
| | | | | | | Obsd. | Calcd. | Obsd. | Calcd. | |
| 2.5 | 5 | 30 | 100 | 0.24 | 0.90 | | | | | |
| 5 | 10 | 30 | 100 | 0.51 | 1.10 | | | | | |
| 1.25 | 10 | 50 | 100 | 0.14 | 0.442 | 1.08 | 1.08 | 4.52 | 4.35 | |
| 2.5 | 5 | 50 | 100 | 0.215 | 0.400 | 1.50 | 1.50 | 4.08 | 4.12 | |
| 5 | 1.3 | 50 | 100 | 0.12 | 0.406 | 1.56 | 1.00 | 2.74 | 2.87 | |
| 5 | 7.25 | 50 | 100 | 0.41 | 0.438 | 3.34 | 4.22 | 3.83 | 4.06 | |
| 5 | 40 | 50 | 100 | 0.53 | 0.443 | 9.0 | 9.87 | 3.05 | 2.50 | |
| 10 | 5 | 50 | 100 | 0.34 | 0.442 | 6.83 | 4.78 | 2.74 | 2.43 | |
| 10 | 20 | 50 | 100 | 0.54 | 0.442 | 11.7 | 10.1 | 2.23 | 2.17 | 1.80 |
| 2.5 | 5 | 50 | 175 | 0.20 | 0.426 | 1.65 | 1.4 | 6.80 | 6.72 | |
| 2.5 | 10 | 50 | 175 | 0.27 | 0.411 | 2.32 | 2.4 | 6.63 | 6.78 | |
| 1.25 | 5 | 50 | 255 | 0.12 | 0.435 | | | | | |
| 2.5 | 5 | 50 | 255 | 0.23 | 0.402 | | | | | |
| 5 | 40 | 70 | 100 | 0.18 | 1.05 | 11.6 | 14.3 | 1.51 | 1.62 | |
| 10 | 20 | 70 | 100 | 0.285 | 1.38 | 20.2 | 19.5 | 1.03 | | 0.679 |
| 40 | 10 | 70 | 100 | 0.50 | 1.02 | 4.17 | 4.17 | 2.96 | 2.84 | |
| 1.25 | 2.5 | 90 | 100 | 0.05 | 3.52 | | | | | |
| 2.5 | 2.5 | 90 | 100 | 0.095 | 3.49 | | | | | |
| 2.5 | 2.5 | 90 | 100 | 0.09 | 3.63 | | | | | |
| 2.5 | 5 | 90 | 100 | 0.08 | 3.70 | 10.7 | 9.63 | 1.79 | 1.73 | 1.65 |
| 2.5 | 10 | 90 | 100 | 0.09 | 3.56 | 19.3 | 15.0 | 1.14 | 1.07 | |
| 2.5 | 20 | 90 | 100 | 0.11 | 3.62 | 25.5 | 25.5 | 1.17 | 1.01 | |
| 5 | 15 | 95 | 100 | | | | | 0.34 | | 0.28 |

^a Denotes [TiCl₃]₀.^b Denotes [(C₂H₅)₂AlCl]₀.^c Specific viscosity measured at 0.1% in Decalin at 135°C.^d Values of M_n for samples taken at t ≈ 2400 min. for experiments at 50°C. and at t ≈ 1200 min. for experiments at 70 and 90°C.

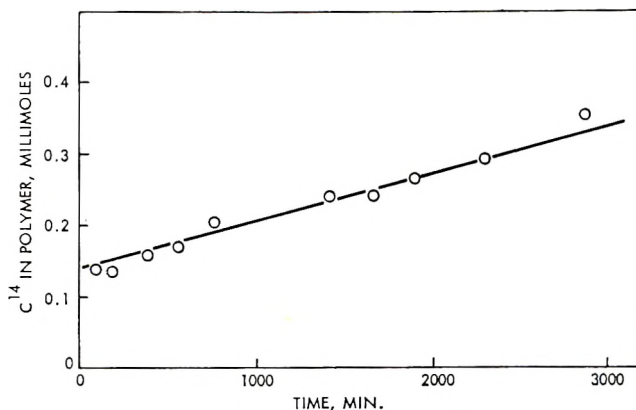


Fig. 1. C^{14} activity in polymer samples as a function of time. Experimental conditions: $[TiCl_3]_0$, 1.25 mmole l^{-1} ; $[Al(C_2H_5)_2Cl]_0$, 10 mmole l^{-1} ; $P_{C_3H_6}$, 100 cm.; temp., $50^\circ C$.

graphically by extrapolating the C^{14} activity in polymer samples to zero time (Fig. 1). The values of $[C]$ are summarized in Table I, column 5.

At 30 and $50^\circ C$., $[C]$ decreases with increase of $[\alpha-TiCl_3]$ at constant $[(C_2H_5)_2AlCl]$. At the same $[\alpha-TiCl_3]$, the values of $[C]$ increase with increase of $[(C_2H_5)_2AlCl]$. These variations at $50^\circ C$. are illustrated in Figure 2. Furthermore, $[C]$ decreases rapidly with increase of temperature, but its value is no longer sensitive to the ratios of $[\alpha-TiCl_3]$ and $[(C_2H_5)_2AlCl]$.

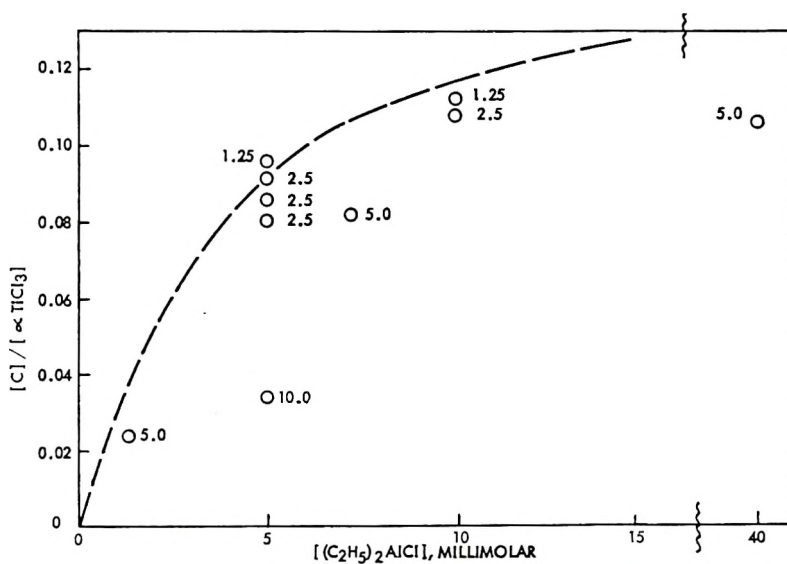


Fig. 2. Variation of $[C]$ with $[\alpha-TiCl_3]_0$ and $[(C_2H_5)_2AlCl]_0$, the numbers shown next to the points in the figure are the concentrations of $\alpha-TiCl_3$.

Chain Propagation

Preliminary results indicated a relationship

$$R_p = dP/dt = k_p[C][m] \quad (1)$$

where P is the amount of polymer formed in moles of monomer, k_p is the rate constant of propagation, and $[m]$ is the concentration of monomer. Since the rate of polymerization, R_p , was constant throughout the reaction, values of R_p were obtained readily from the slope of the plot of polymer weight versus time (Fig. 3). Values of k_p calculated according to eq. (1) by use of experimentally determined monomer concentrations are given in Table I, column 6.

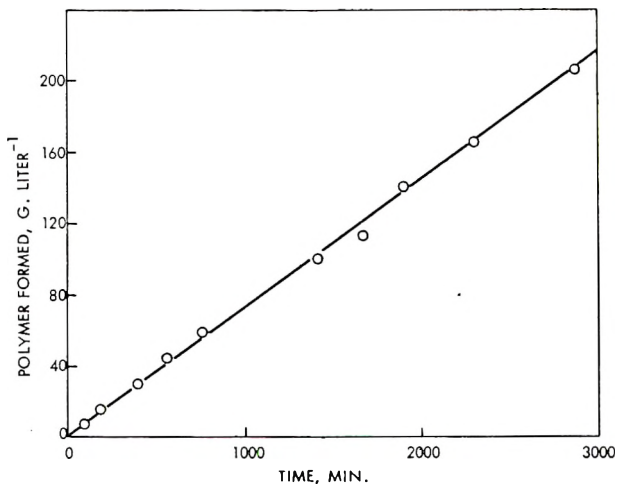


Fig. 3. Increase of polymer yields with time. Experimental conditions same as in Fig. 1.

Chain Termination

The absence of any important chain termination process is inferred from the observed invariance of R_p with time. In confirmation of this inference, when the monomer in a reaction was replaced by nitrogen at $t = 66$ min. and was readmitted at $t = 1463$ min., the polymerization rates before and after the interruption were identical. It will be shown later that the observed dependence of polymer molecular weight upon reaction time, temperature, and catalyst concentration in a given polymerization can be accounted for by kinetics which include no termination processes. Occasionally, decreases of R_p were observed at very long reaction times, for reasons which are not understood. Possibly, air leaked into the reaction vessel, or the reaction became diffusion limited because of a thick layer of polymer on the active sites, or the catalyst was somehow modified.

Chain Transfer

The C¹⁴ activity in polymer samples was found to increase linearly with time. In two experiments where polymerizations were stopped by replacing the monomer with nitrogen, the polymer samples taken subsequently, up to 4000 min., showed no increase in total C¹⁴ activity. Therefore, the observed increase in C¹⁴ activity during a polymerization was not due to secondary reactions. Furthermore, the rise in C¹⁴ activity is not accompanied by an increase in the rate of polymerization.

The increase of C¹⁴ activity during a polymerization is attributed to two chain transfer processes whose combined rate has the following concentration dependence:

$$R_{tr} = k_{tr_1}[C][(C_2H_5)_2AlCl]^{1/2} + k_{tr_2}[C][\alpha-TiCl_3] \quad (2)$$

where R_{tr} is the rate of increase of C¹⁴ activity, and k_{tr_1} and k_{tr_2} are the rate constants of the chain transfer reactions. The values of the observed and the calculated R_{tr} are given in Table I, columns 7 and 8, respectively.

Activation Energies

The average values of k_p , k_{tr_1} , and k_{tr_2} are given in Table II. The energy of activation for the propagation step, E_p , is 13.0 kcal. mole⁻¹. The energies of activation for the transfer reactions are: $E_{tr_1} = 18.6$ kcal. mole⁻¹, and $E_{tr_2} = 7.6$ kcal. mole⁻¹.

TABLE II
Values of the Rate Constants

| Temp., °C. | k_p l. mole ⁻¹ sec. ⁻¹ | k_{tr_1} mole ^{-1/2} l. ^{1/2} sec. ⁻¹ | k_{tr_2} l. mole ⁻¹ sec. ⁻¹ |
|---------------|---|---|--|
| 30 | 0.100 ± 0.20 | — | — |
| 50 | 0.426 ± 0.018 | 6.54×10^{-5} | 9.54×10^{-4} |
| 70 | 1.15 ± 0.20 | 3.50×10^{-4} | 1.90×10^{-3} |
| 90 | 3.50 ± 0.12 | 1.58×10^{-3} | 3.60×10^{-3} |

Number-Average Molecular Weights

The kinetic data obtained in this work enabled calculation of number-average molecular weights for comparison with those determined from fractionation of polypropylenes and with the values obtained from the C¹⁴-tracer results directly (total weight of the polymer sample)/(moles of C¹⁴ activity in the polymer sample). The validity of the last method is confirmed by the agreement between the \bar{M}_n values obtained by this method and those values obtained by fractionation of the polymers.

The C¹⁴ specific activity decreased, and therefore the \bar{M}_n increased, with the time of polymerization, t . The observed value of \bar{M}_n and its variation with t agreed with those values calculated from the kinetic data.

To calculate \bar{M}_n from the kinetic data, the following eqs. (3)–(5) were derived:

$$\begin{aligned} d[P_0]/dt &= -k_p[m][P_0] + k_{tr_1}[Al]^{1/2} \sum_{i=1}^{\infty} [P_i] + k_{tr_2}[Ti] \sum_{i=1}^{\infty} [P_i] \\ &= -k_p[m][P_0] + B_{tr} \sum_{i=1}^{\infty} [P_i] \end{aligned} \quad (3)$$

$$d[P_i]/dt = k_p[m][P_{i-1} - P_i] - B_{tr}[P_i] \quad (4)$$

$$d[R_i]/dt = B_{tr}[P_i] \quad (5)$$

where

$$B_{tr} = k_{tr_1}[Al]^{1/2} + k_{tr_2}[Ti]$$

$[P_i]$ and $[R_i]$ are the concentrations of the growing and the nongrowing i -mers, respectively, and $\sum_{i=0}^{\infty} [P_i] = [C]$; $[Al]$ and $[Ti]$ are the concen-

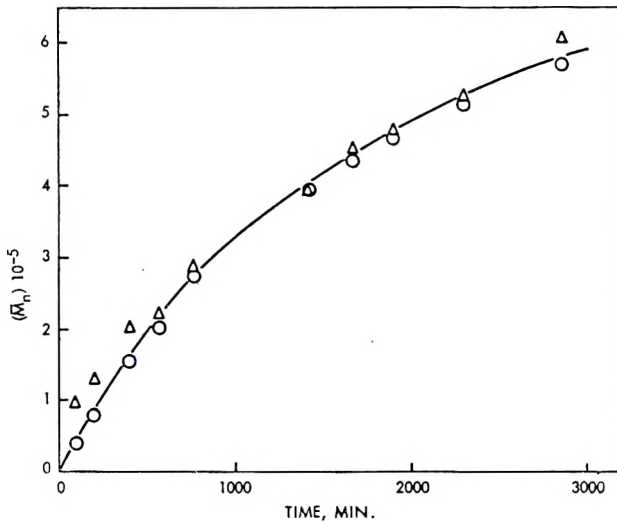


Fig. 4. Variation of \bar{M}_n with time: (O) calculated; (Δ) observed. Experimental conditions same as in Fig. 1.

trations of $(C_2H_5)_2AlCl$ and $\alpha-TiCl_3$, respectively. The j -th moment is then

$$M_j = \sum_{i=1}^{\infty} i^j ([P_i] + [R_i]) \quad (6)$$

The number-average molecular weight in moles of monomer is

$$\begin{aligned} \bar{M}_n &= \frac{M_1}{\bar{M}_0} = (k_p[m]t + B_{tr}t) \times \\ &\quad \left(B_{tr}t + \frac{k_p[m]}{k_p[m] + B_{tr}} [1 - \exp \{ -k_p[m]t - B_{tr}t \}] \right)^{-1} \end{aligned} \quad (7)$$

The weight-average molecular weight, M_w , in moles of monomer is

$$\bar{M}_w = \frac{M_2}{M_1} = 1 + \frac{2 k_p [m]}{B_{tr}} \left[1 - \left(\frac{1 - \exp \{-B_{tr}t\}}{B_{tr}t} \right) \right] \quad (8)$$

For $t > 25$ sec., equation (7) can be simplified to

$$\bar{M}_n = \frac{k_p [m] t}{1 + (k_{tr1} [Al]^{1/2} + k_{tr2} [Ti])t} \quad (9)$$

The calculated values of \bar{M}_n are summarized in Table I, column 11, along with the values obtained directly from C^{14} activity (column 10) and from fractionation of the polymer samples (column 12). Variation of \bar{M}_n with time is illustrated in Figure 4.

Other Catalyst Systems

A number of polymerizations were carried out under identical conditions with $TiCl_3-(C_2H_5)_2AlCl$ and $TiCl_3-(C_2H_5)AlCl_2$ as catalysts. The average values of R_p , total yields, and the yields of crystalline polymers are given in Table III.

TABLE III
Results of Polymerization with Other Catalyst Systems^a

| Catalyst | $R_p \times 10^{-6}$, mole l. ⁻¹ sec. ⁻¹ | Yield of polymer, g. l. ⁻¹ |
|-------------------------|--|--|
| $TiCl_3-(C_2H_5)_2AlCl$ | 3.14 | 138 |
| $TiCl_3-(C_2H_5)AlCl_2$ | 0.36 | 15.0 |

^a Experimental conditions $[Ti]_0$, 20 mmole l.⁻¹ $[Al]_0$, 5, 20, 80, and 120 mmole l.⁻¹ temp., 30°C.; $p_{C_3H_6}$, 279 mm.

^b Each value is the average of four experiments.

Polymerization to Amorphous Polymers

Polymerizations carried out at 50°C. or lower yielded amounts of amorphous polymers insufficient for various physicochemical determinations. At higher temperatures only the samples taken after 1000 min. contained enough amorphous polymers for such determinations. Therefore, it was not possible to determine the initial number of active sites or the rate of the chain transfer reaction. The approximate rates of polymerization, which were assumed to be constant throughout a reaction, are given in Table IV column 4.

The total C^{14} activities found in the amorphous polymer samples are given in Table IV, column 6. The values of \bar{M}_n are found in column 8. For the purpose of comparing the processes which yielded amorphous polymer with those which gave crystalline products, the corresponding values of R_p , $[C^{14}]$, and \bar{M}_n for the crystalline polypropylenes obtained in the same polymerizations are given in columns 5, 7, and 9, respectively.

While the total C^{14} activities increased with time of polymerization, the

TABLE IV
 Polymerization to Amorphous Polypropylenes^a

| [Ti], ^b mmole l. ⁻¹ | [Al], ^c mmole l. ⁻¹ | Temp., °C. | $R_p \times 10^6$, l. mole ⁻¹ sec. ⁻¹ | | Total C ¹⁴ , mmole | | $\bar{M}_n \times 10^{-5}$ | |
|--|--|---------------|--|-------------------------|-------------------------------|-------------------------|----------------------------|-------------------------|
| | | | Amorphous polymers | Crystalline polymers | Amorphous polymers | Crystalline polymers | Amorphous polymers | Crystalline polymers |
| 5 | 40 | 70 | 0.71 | 5.17 | 2.37 | 1.25 | 0.10 | 1.15 |
| 10 | 20 | 70 | 0.54 | 10.7 | 2.41 | 2.40 | 0.17 | 0.82 |
| 40 | 10 | 70 | 0.48 | 13.9 | 1.90 | 2.20 | 0.11 | 0.87 |
| 2.5 | 5 | 90 | 0.95 | 4.85 | 1.85 | 1.05 | 0.22 | 1.48 |
| 2.5 | 10 | 90 | 1.43 | 5.22 | 3.45 | 1.90 | 0.17 | 1.25 |
| 2.5 | 20 | 90 | 2.30 | 6.50 | 3.88 | 1.76 | 0.18 | 1.35 |
| 20 | 2.5 | 90 | 1.17 | | 0.79 | 0.37 | 0.59 | 4.14 |

^a All polymerizations were carried out at 100 cm. of monomer pressure.

^b Denotes [TiCl₄]₀.

^c Denotes [(C₂H₅)₂AlCl]₀.

C^{14} specific activities were invariant with the time of polymerization. To demonstrate this invariance, a large-scale polymerization was carried out at 95°C. The results on the C^{14} specific activities are given in Table V.

TABLE V
 C^{14} Specific Activities in Amorphous Polymers^a

| Time, min. | Amorphous polymers, g. | $[C^{14}] \times 10^{-4}$, counts min. ⁻¹ g. ⁻¹ |
|------------|------------------------|---|
| 118.3 | 6.5 | 5.17 |
| 170.5 | 7.5 | 5.67 |
| 256.2 | 9.3 | 5.44 |
| 1238 | 12.6 | 4.28 |
| 1314 | 14.3 | 4.9 |
| 1444 | 15.0 | 4.86 |
| 1596 | 18.0 | 5.2 |
| 2658 | 28.4 | 4.8 |
| 2776 | 28.45 | 5.6 |

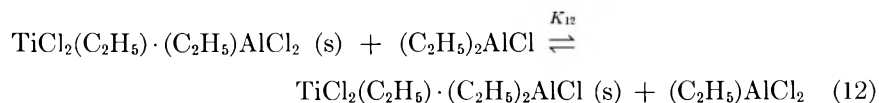
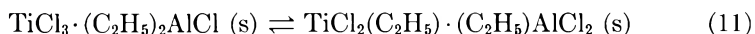
^a Polymerization conditions: $[\alpha\text{-TiCl}_3]_0$, 5 mmole l.⁻¹; $[(C_2H_5)_2AlCl]_0$, 15 mmole. l.⁻¹; temp., 95°C.; $p_{C_3H_6}$, 100 cm.

DISCUSSION OF RESULTS

Chain Initiation

Upon addition of $(C_2H_5)_2AlCl$ to $\alpha\text{-TiCl}_3$, presumably a complex was formed at the surface and then alkylation occurred. Several alkyltitanium compounds have been isolated recently. Long⁴ obtained $(C_5H_5)_2Ti(CH_3)Cl$ by reaction of $(C_5H_5)_2TiCl_2$ with CH_3MgCl . Beermann and Bestian¹⁶ prepared $RTiCl_3$, where R was methyl, ethyl, and isobutyl, from the reactions of $TiCl_4$ and the respective dialkylaluminum chlorides. By reacting $(CH_3)_2TiCl_3$ with $(CH_3)_3Al$, they also prepared $(CH_3)_2TiCl_2$. Long et al.^{4,5} deduced from spectroscopic evidence that both alkylation and complex formation took place upon mixing $(C_5H_5)_2TiCl_2$ with alkylaluminum chlorides. They assigned certain absorption maxima to $(C_5H_5)_2(CH_3)TiCl \cdot AlCl_3$ and $(C_5H_5)_2(C_2H_5)TiCl \cdot (C_2H_5)AlCl_2$ and were able to correlate the spectral intensities of these complexes with their catalytic activities in ethylene polymerization.

By analogy, the following reactions are written to give the postulated initiating species $TiCl_2(C_2H_5) \cdot (C_2H_5)_2AlCl$ (I) and $TiCl_2(C_2H_5) \cdot (C_2H_5)AlCl_2$ (II):



where (s) denotes surface sites. Of the two postulated species, I is much

more active than II (Table III). The Ti and the Al in these complexes are believed to be bridged by the chlorine atoms. Bridging via the alkyl group is unlikely. Proton magnetic resonance study¹⁷ of the $(C_2H_5)_2TiCl_2-(CH_3)_2AlCl$ and the $(C_2H_5)_2TiCl_2-(C_2H_5)_2AlCl$ systems showed that there were no bridging methyl and ethyl groups.

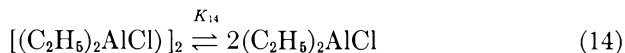
Complexes I and II are probably not the only possible active species. For example, $TiCl_2(C_2H_5) \cdot TiCl_3$ could be another one. Beermann and Bestian¹⁶ showed conclusively that systems containing Ti only, such as $(CH_3)TiCl_3-TiCl_3$, are catalytically active.

Dependence of [C] on the Al/Ti Ratios

In Figure 2, it was shown that [C] is sensitive to the Al/Ti ratios. This dependence can be explained on the basis of an equilibrium between complexes I and II where I has much higher polymerization activity

$$K_{12} = \frac{[TiCl_2(C_2H_5) \cdot (C_2H_5)_2AlCl][(C_2H_5)AlCl_2]}{[TiCl_2(C_2H_5) \cdot (C_2H_5)AlCl_2][(C_2H_5)_2AlCl]} \quad (13)$$

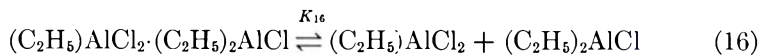
Since dialkylaluminum chlorides and monoalkylaluminum dichlorides are dimeric both as vapor and in solution,¹⁸ the dissociation equilibrium for $(C_2H_5)_2AlCl$ is



It will be shown later that only monomeric alkylaluminum halides are effective in transfer processes. The concentration of the monomeric diethylaluminum chloride is

$$[(C_2H_5)_2AlCl] = K_{14}^{1/2} [(C_2H_5)_2AlCl]_2^{1/2} = (K_{14}/2)^{1/2} [(C_2H_5)_2AlCl]_0^{1/2} \quad (15)$$

where $[(C_2H_5)_2AlCl]_2$ is the concentration of the dimeric diethylaluminum chloride. A similar equilibrium exists for the ethylaluminum dichloride in the presence of excess diethylaluminum chloride,



and

$$[(C_2H_5)AlCl_2] = K_{16} [(C_2H_5)AlCl_2 \cdot (C_2H_5)_2AlCl] / [(C_2H_5)_2AlCl] \quad (17)$$

From Figure 2, the number of initiating ethyl groups at low $[\alpha-TiCl_3]$ and high $[(C_2H_5)_2AlCl]$ is about 0.14 $[\alpha-TiCl_3]$. Under this condition of high Al/Ti ratio, most of the active complex is in the form of I according to the law of mass action. Since there are three ethyl groups on I, the concentration of I is equal to $1/3$ [C] or $(0.14/3) [\alpha-TiCl_3]$. At other Al/Ti ratios,

$$\begin{aligned} [TiCl_2(C_2H_5) \cdot (C_2H_5)_2AlCl] &= 1/3 [C] \\ [TiCl_2(C_2H_5) \cdot (C_2H_5)AlCl_2] &= 1/3 \{0.14 [\alpha-TiCl_3] - [C]\} \end{aligned}$$

$$[(C_2H_5)_2AlCl] = (K_{14}/2)^{1/2} [(C_2H_5)_2AlCl]_0^{1/2},$$

and

$$[(C_2H_5)AlCl_2] \approx 1/3 K_{16} 0.14 [\alpha-TiCl_3]/(K_{14}/2)^{1/2} [(C_2H_5)_2AlCl]_0^{1/2}$$

Substitution into eq. (13) gives

$$\frac{3K_{12}K_{14}}{2K_{16}} \approx \frac{0.14 [\alpha-TiCl_3] [C]}{\{0.14 [\alpha-TiCl_3] - [C]\} [(C_2H_5)_2AlCl]_0} \quad (18)$$

The constancy of the values of $3K_{12}K_{14}/2K_{16}$ calculated for polymerizations at 50°C. (Table VI) renders support to the above discussions.

TABLE VI
Values of $3K_{12}K_{14}/2K_{16}$ at 50°C.

| $[\alpha-TiCl_3]_0$, mmole l. ⁻¹ | $[(C_2H_5)_2AlCl]_0$, mmole l. ⁻¹ | $3K_{12}K_{14}/2K_{16}$ |
|--|---|-------------------------|
| 1.25 | 10 | 0.070 |
| 2.5 | 5 | 0.110 |
| 5 | 1.3 | 0.110 |
| 5 | 7.25 | 0.14 |
| 5 | 40 | 0.054 |
| 10 | 5 | 0.090 |
| 10 | 20 | 0.044 |
| 2.5 | 5 | 0.093 |
| 2.5 | 10 | 0.12 |
| 1.25 | 5 | 0.076 |
| 2.5 | 5 | 0.13 |
| | | Avg. 0.094 |
| | | S.D. 0.033 |

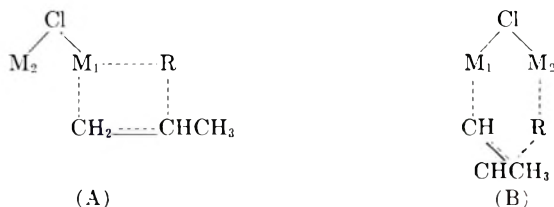
Therefore, at low $[\alpha-TiCl_3]$ and high $[(C_2H_5)_2AlCl]$, each mole of $TiCl_3$ has initially 0.14 mole of reactive ethyl groups, or 0.05 mole of complex I. At other concentrations, the combined concentration of complexes I and II is 0.05 mole per mole of $\alpha-TiCl_3$. Earlier, the treatment of one mole of $\alpha-TiCl_3$ with two moles of $(C_2H_5)_2AlCl$ resulted in the incorporation of 0.1 mole of ethyl groups not removable by repeated washing. This result is consistent with those derived from the polymerization experiments.

At 70 and 90°C., $[C]$ is relatively insensitive to Al/Ti ratios. The values of $[C]/[TiCl_3]_0$ remain at about 0.04 for Al/Ti ratios from 1 to 8. Furthermore, at comparable concentrations of $\alpha-TiCl_3$ and $(C_2H_5)_2AlCl$, $[C]$ at 50°C. was five times that at 90°C. It is possible that changes in surface characteristics and surface area take place at a higher temperature reducing the amount of stereospecifically active sites. The apparent increase of nonstereospecific active sites with temperature supports this view. However, full understanding of the results obtained at elevated temperature is not possible at this time.

Chain Propagation

The mechanism of the propagation postulated earlier for a soluble system² is applicable to this heterogeneous system. The systems differ kinetically, however, in that all the active centers can be considered nearly identical in the soluble catalyst system, but the same may not be true in the heterogeneous system. Therefore, the values of k_p for various active sites which differ geometrically, i.e., edge, corner, crevice, sterically hindered, etc., are probably different. Furthermore, the k_p for the various possible active species which differ chemically are probably also different.

Two types of transition state complexes are possible in the propagation step depending upon whether only one metal is directly involved, A, or two metals are involved, B. It is interesting to note that



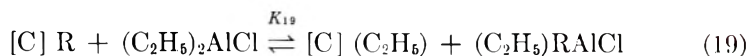
B has two modes of propagation. In one, the growing chain transfers from M_1 to M_2 after each addition; in the other, incoming monomers attack M_1 and M_2 alternatively. In the latter mode, M_1 and M_2 must impose the same restriction on the orientation of the incoming monomer if isotactic polymers are to be formed.

Chain Termination

Earlier the author found² that, in the soluble catalyst system for ethylene polymerization, the only important termination process is the bimolecular disproportionation. Such a process is unimportant in a heterogeneous system for obvious reasons. Dissociation to active hydride as postulated in the literature^{9,11} is inconsistent with the \bar{M}_n data obtained in this work. The observed and the fractionated values of \bar{M}_n agree well with the calculated values, whereas the calculated values would have been lower if there were an appreciable incidence of dissociation.

Chain Transfer

Two chain transfer processes were observed. The rate of the first process is proportional to $[C]$ and $[(C_2H_5)_2AlCl]^{1/2}$. The square-root dependence on the diethylaluminum chloride concentration is attributed to the assumption that only the monomeric $(C_2H_5)_2AlCl$ is effective in the chain transfer reaction



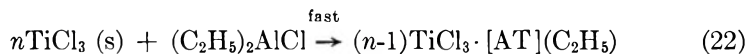
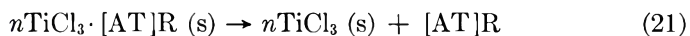
The rate of transfer is

$$R_{tr_1} = k_{tr_1} [C] [(C_2H_5)_2AlCl]_0^{1/2} \quad (20)$$

where

$$k_{tr_1} = k_{19}(K_{14}/2)^{1/2}$$

The second chain transfer process has a rate which is dependent upon [C] and $[\alpha\text{-TiCl}_3]$. Electron microscopy studies showed that during a polymerization TiCl_3 became intimately dispersed in the polymer in the form of fine needles. It is possible that the following interactions are important.



where [AT]R is the Ti-Al complex. [AT]R becomes inactive when it is separated from the main $\alpha\text{-TiCl}_3$ surface. When reaction (22) is fast, the rate of reaction (20) is proportional to $[\alpha\text{-TiCl}_3]$ and [C].

In the absence of any termination process, the life of a growing chain is determined by the chain transfer reactions. To illustrate the unusually long chain life time in this heterogeneous catalyst system, the average life before chain transfer for the experiment shown in Figure 1 is about 410 min. Bier et al.¹¹ also concluded that the growing chains have very long lives.

Number-Average Molecular Weights

The agreement between calculated and observed values of \bar{M}_n is good everywhere except at the beginning of the polymerization, where the agreement is only fair. The observed values of \bar{M}_n at short reaction times were higher, possibly because the low molecular weight fractions were partially extracted by the hot heptane along with the amorphous products.

On the other hand, correlation of the experimental and the calculated weight-average molecular weights, \bar{M}_w was poor. Values of \bar{M}_w obtained by either fractionation of polypropylene or by the viscosity- \bar{M}_w relationship developed by Chiang¹⁹ were higher than those calculated from the kinetic data because average values of k_p , k_{tr_1} and k_{tr_2} were used in these calculations. A spread of any or all of these rate constants results in higher values of \bar{M}_w . It should be noticed that the values of \bar{M}_n are independent of nonuniformity in the rate constants. The polymer molecular weight distribution, \bar{M}_w/\bar{M}_n , was found to change with time. The results will be presented in another communication.

Polymerization to Amorphous Polymers

The kinetic results in the formation of amorphous polymers are only qualitative. However, several interesting points were uncovered and compared with the corresponding data for the formation of crystalline polymers. In the following discussion, subscripts c and a are used to designate the crystalline and the amorphous products, respectively.

The polymerization rates appeared to be proportional to the square root of the diethylaluminum chloride concentration but almost independent of the α -TiCl₃ concentration. The polymerization rates at 90° are about four times that at 70°. Therefore, the sites which polymerize propylene to amorphous polymers seem to be formed by a process relatively insensitive to the initial α -TiCl₃ concentration, but dependent upon the concentration of monomeric diethylaluminum chloride and temperature. The nature of these sites is unknown to us.

In comparison with $(R_p)_c$, $(R_p)_a$ was smaller by a factor of 3-5 at 90°C., 7-30 at 70°C. Insignificant amounts of amorphous polymers were separated at 50 and 30°C. The possibility that $(k_p)_a$ has a higher temperature dependence than $(k_p)_c$ can be discounted because $(\bar{M}_n)_c$ is about seven times $(\bar{M}_n)_a$ at both 70 and 90°C. Sites giving amorphous polymers were therefore formed in increasing amounts at elevated temperatures and their increase was accompanied by a decrease in the number of sites giving crystalline polymers (Table I, column 5).

Several additional observations offer some clue to the mechanism of polymerization to amorphous products. The comparisons made on polymerizations leading to crystalline and to amorphous polymers at 70°C. revealed that: $(R_p)_c \approx (7 \text{ to } 30)(R_p)_a$ and $(\bar{M}_n)_c \approx 7(\bar{M}_n)_a$; the C¹⁴ specific activity in crystalline polymers decreased rapidly with time of polymerization, but the C¹⁴ specific activity in amorphous polymers remained unchanged; and the total C¹⁴ activity in the crystalline polymers was about the same as that in the amorphous polymers.

The low values of $(R_p)_a$ must mean that $[C]_a$, the concentration of active species which gives amorphous polymers, is much smaller than $[C]_c$. It is assumed that $(k_p)_a$ is not appreciably different from $(k_p)_c$. The invariance of C¹⁴ specific activity in amorphous polymers indicates that chain transfer processes play a very important role here. The low values of $(\bar{M}_n)_a$ and high value of total C¹⁴ activity in amorphous polymers support the argument. It remains possible that the active species which yield amorphous polymers are soluble in heptane. Then chain termination is probably also important. Therefore, the active sites, which do not stereospecifically orient the incoming monomer, are more susceptible to chain transfer and possibly chain termination reactions.

The values of $(\bar{M}_n)_a$ shown in Table IV and used in the above discussion were calculated from the C¹⁴ specific activity. However, these polymers have not yet been fractionated.

The author is indebted to Drs. H. M. Spurlin and H. G. Tennent for discussions and assistance in the preparation of this paper. He is grateful to Dr. W. E. Davis for his aid with the mathematical analysis. The radioactivity measurements were supervised by Dr. A. K. Wiebe. Fractionation of polymer samples was done by Mrs. S. K. Shyluk. Mrs. M. Korden's assistance in the experimental work is also appreciated.

References

1. Gaylord, N. G., and H. F. Mark, *Linear and Stereoregular Addition Polymers*, Interscience, New York, 1959.
2. Chien, J. C. W., *J. Am. Chem. Soc.*, **81**, 86 (1959).

3. Breslow, D. S., and N. R. Newburg, *J. Am. Chem. Soc.*, **79**, 5079 (1957); *ibid.*, **81**, 81 (1959).
4. Long, W. P., *J. Am. Chem. Soc.*, **81**, 5312 (1959).
5. Long, W. P., and D. S. Breslow, *J. Am. Chem. Soc.*, **82**, 1953 (1960).
6. Repka, B. C., Jr., and E. A. Harris, in *The Encyclopedia of Chemical Technology*, 2nd Suppl., Interscience Encyclopedia, New York, 1960, p. 661.
7. Natta, G., *Makromol. Chem.*, **35**, 94 (1960).
8. Natta, G., I. Pasquon, and E. Giachetti, *Angew. Chem.*, **69**, 213 (1957); *Makromol. Chem.*, **24**, 258 (1957); *Chim. e ind. (Milan)*, **39**, 993 (1957).
9. Natta, G., I. Pasquon, E. Giachetti, and G. Pajaro, *Chim. e ind. (Milan)*, **40**, 267 (1958).
10. Natta, G., *J. Polymer Sci.*, **34**, 21 (1959).
11. Bier, G., A. Gumbolt, and G. Lehman, *Plastics Inst. (London) Trans. and J.*, **28**, 98 (1960).
12. Burnett, G. M., and P. J. T. Tait, *Polymer*, **1**, 151 (1960).
13. Grosse, A. V., and J. N. Mavity, *J. Org. Chem.*, **5**, 106 (1940).
14. Calvin, M., et al., *Isotopic Carbon*, Wiley, New York, 1949.
15. Shyluk, S. K., *J. Polymer Sci.*, in press.
16. Beermann, C., and Bestian, H., *Angew. Chem.*, **71**, 618 (1959).
17. Chien, J. C. W., to be published.
18. Coates, G. E., *Organometallic Compounds*, Wiley, New York, 1956, p. 81.
19. Chiang, R., *J. Polymer Sci.*, **28**, 235 (1958).

Synopsis

The kinetics of propylene polymerization catalyzed by α -titanium trichloride-diethylaluminum chloride in heptane diluent were studied. Initiation and transfer processes were followed by using C^{14} -labeled $(C_2H_5)_2AlCl$. There was no important termination process in this system. The initial C^{14} activity found in the polymers gave the concentration of active ethyl groups on the surface, $[C]$. The propagation step was first order in $[monomer]$ and $[C]$, with an activation energy of 13.0 kcal. mole $^{-1}$; k_p at 50°C. was 0.426 ± 0.018 l. mole $^{-1}$ sec. $^{-1}$. There were two transfer processes: (1) $R_{tr1} = k_{tr1}[C] - [(C_2H_5)_2AlCl]^{1/2}$, with an activation energy of 18.6 kcal. mole $^{-1}$, and a value of k_{tr1} at 50°C. of 6.54×10^{-5} mole $^{-1/2}$ sec. $^{-1}$; and (2) $R_{tr2} = k_{tr2}[C][\alpha-TiCl_3]$, with an activation energy of 7.6 kcal. mole $^{-1}$, and a value of k_{tr2} at 50°C. of 9.45×10^{-4} l. mole $^{-1}$ sec. $^{-1}$. These kinetic data were used to calculate number-average molecular weights \bar{M}_n , which agreed well with the ones obtained directly from the C^{14} specific activity in the polymer. Furthermore, fractionation of four polypropylene samples gave values of \bar{M}_n in agreement with those obtained above. At low temperatures, $[C]$ is sensitive to the Al/Ti ratios. This dependence was interpreted as the result of an equilibrium between an active complex containing $(C_2H_5)_2AlCl$ and a much less active complex containing $(C_2H_5)AlCl_2$. At higher temperatures, $[C]$ is insensitive to the Al/Ti ratios, and polymerization to give amorphous polymers becomes important. Qualitative information was obtained about the processes which give amorphous polymers.

Résumé

On a étudié la cinétique de la polymérisation du propylène catalysée par le trichlorure de titane α -diéthylaluminium dilué dans l'heptane. On suit les processus d'initiation et de transfert et utilisant du $(C_2H_5)_2AlCl$ contenant du C^{14} marqué. Il n'y a pas, dans ce système, de processus de terminaison important. L'activité C^{14} initiale trouvée dans le polymère, donne la concentration des groupes éthyle actifs à la surface, $[C]$. L'étape de propagation est caractérisée par un ordre un par rapport à la concentration et par rapport à $[C]$, par une énergie d'activation de 13.0 kcal/mole $^{-1}$, k_p à 50° était de 0.426 ± 0.018 l. mole $^{-1}$ sec. $^{-1}$. Il existe deux processus de transfert: (1) $R_{tr2} = k_{tr2}[C][\alpha-TiCl_3]$

$\text{AlCl}]^{1/2}$, avec une énergie d'activation de 18,6 kcal. mole⁻¹ et une valeur de k_{tr1} à 50° de $6,54 \times 10^{-5}$ mole^{-1/2} sec.⁻¹; et (2) $R_{tr2} = k_{tr2}[\text{C}][\alpha\text{-TiCl}_3]$, avec une énergie d'activation de 7,6 kcal. mole⁻¹ et une valeur de k_{tr2} à 50° de $9,45 \times 10^{-4}$ l. mole⁻¹sec.⁻¹. Ces données cinétiques ont servi à calculer les poids moléculaires moyens en nombre, qui concordent bien avec ceux obtenus directement à partir de l'activité spécifique du C¹⁴ dans le polymère. De plus, le fractionnement de quatre échantillons de polypropylène donne des valeurs de \bar{M}_n en accord avec ceux obtenus ci-dessus. A basse température, [C] est sensible au rapport Al/Ti. Cette dépendance a été interprétée comme le résultat d'un équilibre entre un complexe actif contenant $(\text{C}_2\text{H}_5)_2\text{AlCl}$ et un complexe beaucoup moins actif qui contient $(\text{C}_2\text{H}_5)\text{AlCl}_2$. À des températures plus élevées, [C] est insensible au rapport Al/Ti et la polymérisation qui donne des polymères amorphes devient importante. On obtient des informations qualitatives concernant les processus qui fournissent des polymères amorphes.

Zusammenfassung

Die Kinetik der durch α -Titantrichlorid-Diäthylaluminiumchlorid in Heptan als Lösungsmittel katalysierten Propylenpolymerisation wurde untersucht. Start und Übertragungsprozesse wurden unter Verwendung von C¹⁴-markiertem $(\text{C}_2\text{H}_5)_2\text{AlCl}$ verfolgt. Die Abbruchsreaktion hatte in diesem System keine grössere Bedeutung. Die an den Polymeren gefundene Anfangs-C¹⁴-aktivität ergab die Konzentration der aktiven Äthylgruppen an der Oberfläche, [C]. Die Wachstumsreaktion war erster Ordnung in bezug auf [Monomeres] und [C], mit einer Aktivierungsenergie von 13,0 kcal.Mol⁻¹ und einem k_p bei 50° von $0,426 \pm 0,018$ l.Mol⁻¹sec.⁻¹. Es bestanden zwei Übertragungsreaktionen: (1) $R_{tr1} = k_{tr1}[\text{C}][(\text{C}_2\text{H}_5)_2\text{AlCl}]^{1/2}$ mit einer Aktivierungsenergie von 18,6 kcal.Mol⁻¹ und einem k_{tr1} -Wert bei 50° von $6,54 \cdot 10^{-5}$ Mol^{-1/2}.sec⁻¹; und (2) $R_{tr2} = k_{tr2}[\text{C}][\alpha\text{-TiCl}_3]$ mit einer Aktivierungsenergie von 7,6 kcal.-Mol⁻¹ und einem k_{tr2} -Wert bei 50° von $9,45 \cdot 10^{-4}$ l.Mol⁻¹ sec.⁻¹. Diese kinetischen Daten wurden zur Berechnung von Zahlenmittelwerten des Molekulargewichtes \bar{M}_n verwendet, die mit den direkt aus der spezifischen ¹⁴C-Aktivität im Polymeren erhaltenen Werten recht gut übereinstimmten. Weiters ergab die Fraktionierung von vier Polypropylenproben \bar{M}_n -Werte, die mit den oben erhaltenen übereinstimmten. Bei tiefen Temperaturen hängt [C] vom Al/Ti-Verhältnis ab. Diese Abhängigkeit wird als des Ergebnis eines Gleichgewichts zwischen einem aktiven Komplex mit $(\text{C}_2\text{H}_5)_2\text{AlCl}$ und einem wesentlich weniger aktivem Komplex mit $(\text{C}_2\text{H}_5)\text{AlCl}_2$ angesehen. Bei höheren Temperaturen ist [C] vom Al/Ti-Verhältnis unabhängig und die Polymerisation unter Bildung amorpher Polymerer gewinnt an Bedeutung. Über die Vorgänge, die zu amorphen Polymeren führen, wurden qualitative Aufschlüsse erhalten.

Received July 26, 1961

Homogeneous Anionic Polymerization. I. Molecular Weights of Polystyrene Initiated by Sodium Naphthalene*

MAURICE MORTON and RALPH MILKOVICH,† *Institute of Rubber Research, University of Akron, Akron, Ohio*, and D. B. McINTYRE and L. J. BRADLEY, *National Bureau of Standards, Washington, D. C.*

INTRODUCTION

It has only recently¹ been demonstrated that certain polymerization reactions involving carbanions as active species exhibit a complete absence of chain termination. These systems are therefore unique, in that each growing chain continues to add monomer units as long as any monomer is present, and hence the chain length is determined by the ratio between the total number of monomer units polymerized and the number of active chains present. Of course, the above condition will apply only in the absence of any component which can react with these carbanions, e.g., water, acids, alcohols, etc.

Actually this type of system has been known for some time, at least in theory, in the case of the polymerization of cyclic oxides, such as ethylene oxide² and the cyclic siloxanes.^{3,4} The general case of a polymerization having no termination step and where all the growing chains can compete equally for available monomer has been treated by Flory,² who showed that these conditions should lead to an extremely narrow molecular weight distribution, i.e., the Poisson distribution, approaching monodispersity.

However, such distributions had not, in fact, been achieved, or even approached, until very recently, when homogeneous anionic polymerizations of unsaturated monomers began to be studied more carefully. This was due to various factors which obscured the true possibilities of these systems, such as the presence of impurities or solvents which could terminate or transfer with the growing chains, or the presence of a reversible propagation step (equilibrium polymerization) or of interchange reactions between polymer chains. The two latter phenomena, for instance are both present in the anionic polymerization of cyclosiloxanes.

Furthermore, although polymerization by alkali metals, e.g., sodium polymerization of butadiene, has been well known for many years, it has

* Presented in part at the 136th National Meeting, American Chemical Society, Division of Polymer Chemistry, Atlantic City, N. J.

† Present address: Shell Chemical Company, Torrance, California.

been noted as a process leading to narrow chain length distribution. This has been due to an additional factor which can destroy any approach toward monodispersity, i.e., the heterogeneous nature of the initiation step. Thus, in this case, new polymer chains are being continually initiated by reaction of the monomer with the metal surface at the same time as other chains are growing in the homogeneous liquid phase.

Hence, in view of the above, it is obvious that the following conditions are generally required if an approach to the Poisson distribution is to succeed: (a) absence of equilibrium polymerization or bond interchange, (b) rigorous exclusion of substances capable of terminating chains, and (c) a high ratio of initiation to propagation rates.

The monomers used in this investigation, e.g. styrene, isoprene, butadiene, are known to show only little depropagation at the moderate temperatures used. The detailed description of the techniques used, which follows, will indicate the steps taken to exclude reactive compounds. As for the initiation/propagation rate ratio, it should be remembered that initiation is a one-step reaction while the growth of a chain involves a large number of consecutive propagation steps. Hence, even if the individual initiation step is considerable slower than the individual propagation step, the actual formation of a chain may take considerably longer than its initiation. However, if the initiation step is two or three orders of magnitude slower than propagation, then the two processes may become competitive.

The above considerations must, therefore, be taken into account in considering the best method for mixing the monomer and initiator, and several alternative procedures have been used in this work. Thus, where initiation and propagation are both very fast, the technique was used of adding the monomer, in dropwise fashion, to the initiator solution, with rapid stirring. On the other hand, where the initiation was rapid but propagation slow, monomer and initiator could be thoroughly mixed and allowed to polymerize. Finally, where initiation and propagation were competitive, the special technique of "seeding" was used, i.e., a two-stage process where the initiator was premixed with a small amount of monomer to form a "seed" of low molecular weight, which was then used for polymerization of the bulk of the monomer.

This first paper of the series is intended to show the type of molecular weight distributions which can be obtained by the sodium naphthalene polymerization of styrene, under the given conditions, as described.

Since the start of this work, a publication by McCormick⁵ has appeared which showed that this system can lead to the experimental attainment of a narrow molecular weight distribution, as shown by sedimentation analysis. Subsequently, other workers⁶⁻¹⁰ have shown similar data to indicate how closely the Poisson distribution may be approached. It is obvious that the degree of attainment of such a narrow distribution is completely dependent on the rigorousness of the techniques used. Hence this paper contains as detailed a description as possible of these techniques.

EXPERIMENTAL TECHNIQUES

High Vacuum Apparatus

It was noted in a previous investigation in which a sodium-naphthalene-tetrahydrofuran complex was employed as a polymerization initiator, that this type of initiating system and the resulting anionic propagation reaction were quite sensitive to traces of air or water. Therefore, very rigorous experimental conditions must be maintained in order to obtain quantitative data. An apparatus is required with which it is possible to remove all impurities that can react with either the complex employed as the initiator or the growing anionic polymers produced. Some impurities, i.e., water or peroxides, can be removed by conventional means. However, for the reaction studied here, even traces of carbon dioxide, water, and oxygen from

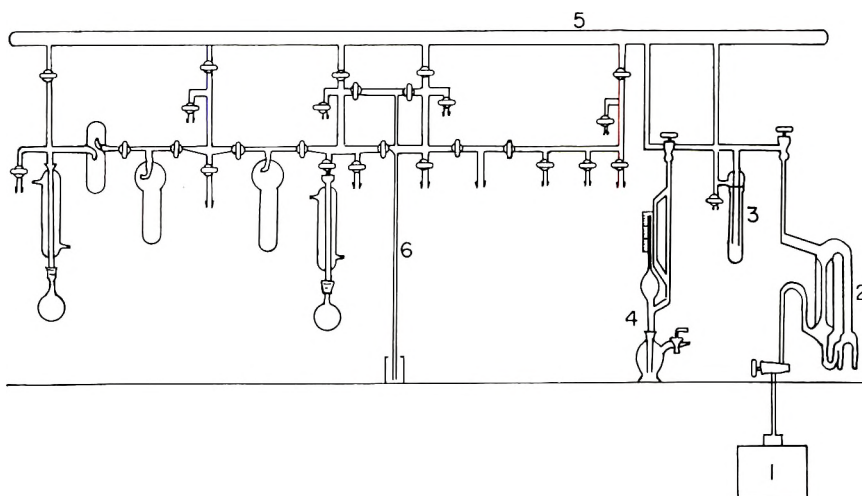


Fig. 1. High vacuum apparatus.

air must be excluded. A high-vacuum apparatus permits such rigorous experimental conditions. The type employed in this research work is shown in Figure 1. It is primarily composed of an oil pump (1) capable of producing a vacuum of the order of magnitude of 10^{-1} to 10^{-2} mm Hg. This pump acts as a fore pump for the mercury diffusion pump (2) which reduces the pressure in the system to 10^{-6} mm. Hg. A liquid nitrogen trap (3) is used to condense any condensable gases so that the pressure measured by the McLeod gage (4) is that of the noncondensable gases, such as oxygen and nitrogen. A second purpose of the liquid nitrogen trap is to prevent the mercury in the diffusion pump from entering the main manifold (5) of the vacuum system.

The first four items identified in Figure 1 are commercially available and will not be discussed further. The remaining portion of the high-vacuum system was handmade in place on a metal supporting frame. A

brief discussion of the latter component parts, i.e., the main manifold and the pressure release system, will serve to point out their functions and limitations more clearly.

The Main Manifold. At low pressures, the mean free path of the molecules of a gas is large, i.e., 10^{-6} mm. Hg corresponds to a mean free path of 5000 cm. Therefore, as the vacuum approaches 10^{-6} mm. Hg, the diameters of the glass tubing in the vacuum apparatus should be about 3 cm. to permit efficient evacuation of a vessel. In the apparatus used here, only the main manifold was of this size, i.e., 35 mm. The remaining connecting tubes were of 12 mm. diameter, since this is about the largest size of glass tubing that is practical in constructing a large and rigid piece of apparatus where proper annealing is impractical.

Pressure Release. This device is simply a tube over 760 mm. in length, connected at one end to the vacuum apparatus, the other end being submerged in mercury. When gases are used in vacuum systems there is always the danger of pressure building up to the point of fracturing the apparatus. Gases were normally collected in a cooled container in the vacuum apparatus, then purified by drying, degassing, etc. prior to use. A slight pressure difference is sometimes required to facilitate diffusion of a gas into another medium or, sometimes, in the distillation of a gas from one portion of the vacuum apparatus to another, pressures exceeding 760 mm. Hg may develop. The purpose of the pressure release is to relieve such pressure in the apparatus and still maintain an air-tight system.

The remaining portions of this apparatus will be discussed in the following sections on high vacuum techniques.

General High Vacuum Techniques.

Treatment of Glassware. Flasks, reactors, etc. were first cleaned with hydrofluoric acid, cleaning solution, or concentrated nitric acid to which a few drops of ethanol were added. They were then rinsed with distilled water, followed by acetone, and dried in an oven set at 110°C . For the purpose of the work involved here, the clean glassware, after removal from the drying oven, was immediately connected to the vacuum line and evacuated. When a pressure reading of 10^{-3} mm. Hg or less was obtained, as indicated by the McLeod gage, the glassware was heated with a hand torch adjusted to give a white to blue flame until the yellow sodium flame was given off from the glass surface. This corresponds to a temperature of approximately 300°C . The heating was continued for 15–30 min., depending on the size of the glassware. The glassware during this heating period was continuously being evacuated. When a pressure of 10^{-6} mm. Hg was reached during the heating cycle, the heat was removed and the glassware was allowed to cool to room temperature while still under evacuation. The purpose of this treatment was to remove the adsorbed gas and water film on the surface of the glassware. On checking the pressure, via the McLeod gage, often during the heat treatment of the glassware, it was possible to observe an increase in pressure when the glass was heated

to 150°C. This was due to the release of the greater part of the absorbed water vapor and gases from the glass surface. At 300°C., a unimolecular gas film which invariably adheres to glass surfaces can be expected to be released and can be noted via the McLeod gage. In a few cases, the glassware used in an experiment was so large that the heat treatment might have aggravated the strains which may be present in homemade glass equipment. Such a vessel was then not heat treated, but evacuated at 10^{-6} mm. Hg for 16–24 hr. prior to use.

Removal of Air from Liquids. All materials employed in this work were degassed prior to any subsequent operation, such as drying or distillation. The degassing procedure for liquids was carried out as follows. The flask containing the liquid to be degassed was connected to the vacuum line and then cooled until it was frozen. Cooling baths, such as liquid nitrogen, a freezing mixture of alcohol and Dry Ice, or a brine solution may be used, depending on the freezing point of the liquid being degassed.

Once the liquid contained in the flask was in a syrupy or frozen state, it was evacuated by opening the stopcock between it and the vacuum line. After approximately 5 min., the stopcock was closed and the frozen material thawed to a liquid state by warming to room temperature by means of an alcohol bath. The freezing and thawing procedure was repeated until at least two initial readings on the McLeod gage of 10^{-6} mm. were obtained with the material in a frozen state. The material was then considered degassed, and was ready for subsequent use.

Distillation of Liquids in a Vacuum System. The technique of handling volatile materials in a high vacuum system depends upon the fact that gases diffuse rapidly throughout a vacuum. This makes it possible to transfer volatile materials to any desired part of the system merely by cooling that part to a temperature at which the materials have a low vapor pressure. In the absence of appreciable amounts of noncondensable gases, this transfer of volatile materials to a cooled zone takes place rapidly. However, in the presence of even small concentrations of noncondensable gases, the diffusion of the condensable molecules is hindered. It is necessary to keep the partial pressure of noncondensables below 10^{-3} mm. Hg, in order to effect quantitative transfer of condensable materials at a practical rate. Therefore, it is quite important to properly degas the liquids prior to distillation. A second factor influencing the rate of distillation of condensable vapors is the temperature of the cooling bath in relation to the freezing point of the condensed material. An alcohol bath was usually sufficient to keep the temperature of the still pot near room temperature. However, it was noted that if too cold a bath was used for the receiver, the condensate froze and coated the walls of the receiver. When this occurred, at least in the case of styrene, the distillation rate slowed down considerably. Hence, it was usually arranged that the temperature of the cooling bath was just above the freezing temperature of the condensate.

Preparation of Metallic Mirrors. Sodium metal was extensively used throughout this research work as a reagent in preparation of the sodium-

naphthalene-tetrahydrofuran complex employed as the initiator, and also as a drying agent. For use as a drying agent for traces of moisture, a thin sodium mirror was found advantageous. Such mirrors are easily prepared with a high vacuum apparatus as follows. The sodium mirror was prepared directly in the flask used in the drying operation. Pieces of dry sodium metal (not kept under mineral oil) were placed in the flask to be used in the drying operation and connected to the vacuum line. The stop-cock between the flask and the vacuum was opened and the flask evacuated until a pressure of approximately 10^{-3} mm. Hg or less was obtained. While still being evacuated, a small area at the bottom of the flask was intermittently and gently heated with a small, soft yellow flame of a hand torch until the sodium metal just began to melt. If this was done carefully, and not heated too strongly, the sodium metal vaporized and deposited on the walls of the flask, to form a mirror. When large quantities, e.g., 10 g. of sodium were used, the latter would tend to form a pool of solidified metal at the bottom of the flask; hence care was taken to avoid careless reheating which could cause the flask to crack. The scum present in or on the sodium sank to the bottom of the flask when the sodium metal was in a liquid state. Thus, after the desired mirror was formed, all surfaces with which the liquid to be dried would come in contact were active pure sodium. Once the mirror was formed, evacuation was continued until the flask had cooled to room temperature. Then the liquid to be dried was distilled into the flask containing the sodium mirror. It was found advisable to perform preliminary drying operations on the liquid before it was introduced into the high-vacuum system, so that the subsequent drying procedure was used to remove only trace quantities of water. Once the liquid was in contact with the sodium mirror, it was degassed again to remove any hydrogen formed by the reaction of moisture with sodium metal. If large amounts of peroxide or any other impurity which would quickly coat the sodium surface are present, it was often found necessary to use two or three such sodium mirrors to ensure dryness.

A second method of preparation of sodium mirrors was that principally employed in the formation of the naphthalene-sodium-tetrahydrofuran complex. Here the sodium metal was placed in a small glass bulb, which had been sealed to the bottom of the flask in which the mirror was to be formed. After evacuation of the flask, the sodium in the bulb was heated and distilled up into the flask, where it condensed and formed a mirror. Any residue or hydroxide remained in the bulb, which was sealed off at a constriction between the bulb and the flask, and removed, thus leaving a slightly cleaner and more uniform mirror.

Materials

Solvent Purification. *Tetrahydrofuran*, Eastman Organic Chemicals, b.p. 64–66°C, was purified by first distilling it over sodium metal through a 40-in. distillation column. The ether was collected in a flask into which small lumps of sodium, potassium and naphthalene were added. This flask

was then connected to a reflux condenser on the high-vacuum rack, and the mixture was refluxed until the dark green-black color of the sodium or potassium naphthalene complex was formed. The ether was then degassed by high vacuum and distilled into ampoules fitted with break-seals.

Styrene Purification. *Styrene*, Dow Chemical Company, stabilized with *tert*-butylpyrocatechol, was first vacuum-distilled in the usual manner to remove the inhibitor. Then it was degassed, dried over calcium hydride, and collected in weighed ampoules equipped with break-seals.

Preparation of Naphthalene Sodium–Tetrahydrofuran Complex

The reactor used in the preparation of the naphthalene-sodium-tetrahydrofuran complex is shown in Figure 2. This reactor, having an ampoule

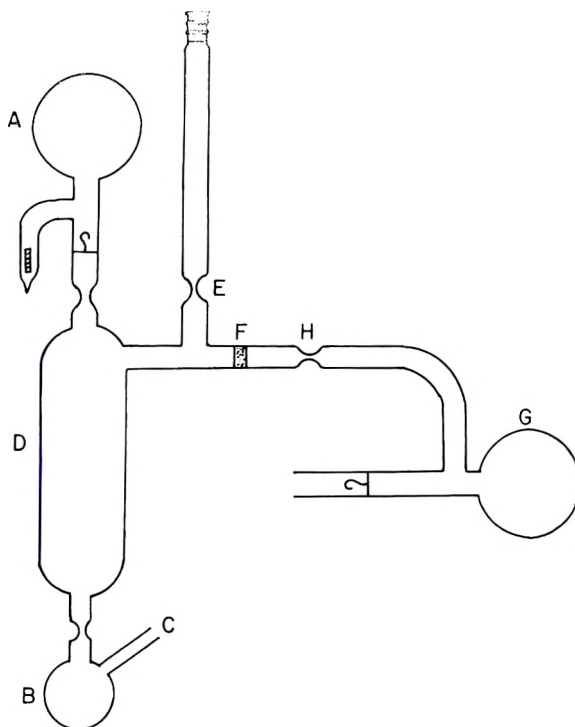


Fig. 2. Reactor for the preparation of naphthalenesodium-THF complex.

of naphthalene-tetrahydrofuran solution (A), was assembled as shown and connected to the vacuum line and tested for leaks. Small pieces of sodium metal were placed in a bulb (B) through the open side tube (C), after which this tube was sealed and the reactor was evacuated and flamed. After the reactor had cooled to room temperature, bulb (B) containing the sodium metal was heated with a hand torch until a sodium mirror was formed in the reaction chamber (D). Bulb (B) was then sealed off at the constriction, and the reactor was allowed to cool while being evacuated. When cooled

to room temperature, and brought to a vacuum of 10^{-6} mm. Hg, the reactor was sealed off from the high-vacuum line at the constriction (E).

The break-seal between (A) and (D) was broken by means of a magnetic hammer, thus permitting the tetrahydrofuran-naphthalene solution to flow into contact with the sodium mirror. The immediate appearance of a dark green color which is characteristic of the complex was noted. Since this is a reversible reaction, it was left for about 16 hr. to establish equilibrium. The amount of sodium present was in excess of that required for complete consumption of the weighed amount of naphthalene.

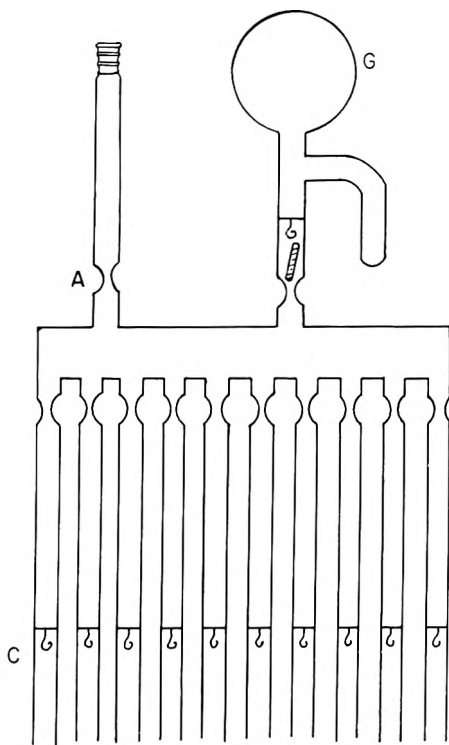


Fig. 3. Apparatus for subdivision of initiator solution.

After equilibrium had been reached, the solution was poured through a coarse sintered filter (F) into a flask (G) fitted with a break-seal. Flask (G) was then cooled in an alcohol-Dry Ice bath and sealed at the constriction (H).

The flask containing the initiator solution was sealed onto a manifold containing 10 ampoules as shown in Figure 3. This manifold was connected to the high-vacuum apparatus, evacuated, leak-tested, and flamed in the manner previously described. After removal from the high vacuum apparatus by sealing the manifold off at the constriction (A), the break-seal of the initiator solution was broken thus permitting the solution (G) to

flow into the break-seal ampules (C). Flask (G) was removed by sealing it off at the constriction, after the ampules had been cooled in an alcohol-Dry Ice mixture. The manifold was then inverted so that mixing of the initiator solution in all of the ampules was achieved, in order to obtain a uniform solution. If the concentration of initiator solution is high, the low temperature of the cooling bath will cause some of it to come out of solution. Therefore, care was always taken to keep the solution homogeneous prior to dividing it into ampules. It was also found that if large differences in volume of liquid are obtained in the ampules, there will occur some distillation of solvent from the ampules having the larger volumes to the ampules having smaller volumes of solution, when they are cooled prior to sealing off at the constrictions. This is due to the slower rate of cooling of the larger ampules. This distillation of solvent among the ampules may cause errors in the determination of the initiator concentration.

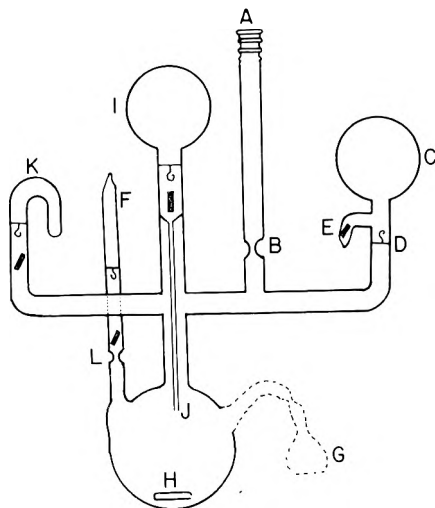


Fig. 4. Styrene polymerization reactor.

Polymerization Procedure

To perform an experiment, the various ampules were sealed onto the reactor in such a manner that the separate components could be conveniently added to the reaction mixture while maintaining a closed system. A vacuum line consisting of a standard-taper ground-glass joint at one end and a constriction at the other was also sealed onto the reactor in a position that would evenly support the weight of the reactor. The vacuum line was the only connection and, many times, the only support holding the reactor to the high vacuum apparatus. Therefore, it was important that the weight of the reactor and its components was balanced. A typical reactor, equipped for the polymerization of styrene, is shown in Figure 4

to help illustrate this point. Two sizes of reactors were used for the polystyrene experiments, having a capacity of 500 ml. and 1000 ml.

Once the reactor was assembled as shown in Figure 4, it was connected to the high-vacuum apparatus by means of the ground-glass joint on the vacuum tube (A) and evacuated. After several minutes, the reactor was tested with a Tesla coil for pinholes or cracks, especially in the area where the component parts were sealed on. If no pinholes were found, or after those that were found were sealed, the reactor was evacuated until a pressure of 10^{-6} mm. was obtained. All of the glass surfaces, except the ampules containing the reaction ingredients, were flamed strongly with a hot yellow-white flame of a hand-torch. The reactor was continuously under evacuation until it cooled to room temperature. At this time the vacuum was again checked, and when a pressure of 10^{-6} mm. Hg was obtained, the reactor was sealed off from the high vacuum line at the constriction (B). Tetrahydrofuran (C) was admitted into the reactor by breaking the break-seal (D) by means of a hammer (iron nail enclosed in glass) (E) and a magnet. The dark-green colored initiator (F) was then added to the solvent in the same manner. A quantitative transfer of the initiator was effected by refluxing solvent up into the initiator ampule. It was found, after several experiments, that some of the catalyst was being destroyed when it was diluted with excess solvent. This may be due to the small amounts of water and carbon dioxide adsorbed on the glass walls of the reactor that was not removed during the flaming operation. In later experiments, a small ampule (G), shown by the dotted lines in Figure 4, was used to take a sample of the initiator solution just prior to monomer addition, for analysis. Once the initiator was completely transferred into the reactor, the solution was then cooled to either 0°C . by an ice bath, or to -78°C . by a freezing mixture of alcohol and Dry Ice, and stirred by means of a magnetic stirrer (H). After allowing sufficient time for thermal equilibrium to be attained, the monomer (I) was then added dropwise by means of a capillary (J) into the cooled, stirred initiator solution. In earlier experiments, the monomer was added as a solvent-monomer solution, but in later experiments, the monomer was added undiluted. Upon addition of the monomer, or monomer solution, an immediate color change for green-black to orange-red occurred. The polymerization was completed when the last drop of monomer was added. Termination of the polystyrene dianions was accomplished by the addition of a few drops of water (K) and the orange-red color immediately disappeared. The reactor was then opened to the atmosphere at (L) by breaking off the initiator ampule. The polymer solution was poured into an excess of methanol, and the coagulated polystyrene separated by filtration. The polymer was dried at 80°C . in an oven. The yields of polymers obtained were always 100%.

Determination of Active Initiator Content

The naphthalenesodium-tetrahydrofuran complex, after preparation, was kept in 12 mm. diameter sealed tubes which had a break-seal at one

end. The volume of solution in these tubes was determined by comparison with a similar tube which had been calibrated in 1-ml. increments. The accuracy of the volume reading was ± 0.1 ml. Since the preparation of the initiator solution was adjusted so that the average volume obtained in the ampules was 8–9 ml. whenever possible, this represents an error of 1.1–1.2%. After the volume of the sample was determined, the ampule was opened under water, and the aqueous solution titrated with 0.01*N* hydrochloric acid to a phenolphthalein endpoint. Two ampules from each batch of initiator preparation were titrated in this manner, to determine the concentration of active initiator per ml of solution.

Based on the amount of naphthalene used in the preparation of the complex, yields were found to vary from 79 to 90% for approximately 16 hr. of contact time with the sodium.

As mentioned previously under the polymerization procedure, it was found that some of the initiator was destroyed upon being mixed with the tetrahydrofuran, prior to the addition of the styrene. Hence, in later work, it was thought advisable to analyze the initiator solution after mixing with solvent and just prior to styrene addition in order to determine more accurately the actual content of active species. However, some of the polymers whose molecular weight data are presented here were prepared before this procedure was instituted, so that there are no reliable data on their active initiator content. This renders impossible any stoichiometric predictions of molecular weight, but should not affect the molecular weight distribution, since such destruction of the initiator occurred prior to the polymerization.

To determine the type of initiator losses experienced during mixing with the solvent, it was necessary to measure the actual content of active initiator prior to monomer addition. This could not be done by a simple alkalinity titration, which would include both active and hydrolyzed initiator. Hence the active species was actually determined by colorimetric titration of the green naphthalene complex by standard *n*-butanol in tetrahydrofuran with the use of a vacuum buret, as described in a forthcoming publication. In this way, it was possible to titrate an aliquot sample of the naphthalene initiator, prior to polymerization, as well as red styrene anion at the conclusion of the polymerization.

Table I contains the results, showing the losses incurred on mixing the naphthalene complex with the additional THF solvent, as well as the losses

TABLE I
Initiator Losses in Na-Naphthalene Systems

| System | Temp., °C. | Moles active anion $\times 10^3$ | | Loss, % |
|-------------|------------|----------------------------------|--------|---------|
| | | Initial | Final | |
| THF | 27 | 0.0804 | 0.0511 | 37.4 |
| THF-styrene | -80 | 0.0923 | 0.0419 | 54.7 |
| " | -80 | 0.0906 | 0.0467 | 48.4 |
| " | -80 | 0.1060 | 0.0517 | 51.3 |

caused by mixing of this initiator solution with the styrene. It can be seen that, at these initiator levels, about one-third of the initiator may be destroyed by the system even before adding the monomer. Furthermore, addition of the styrene may account for an additional 10–15% loss of original initiator.

Molecular Weight Determinations (NBS)

Polymer Purification. The samples were dissolved in benzene and precipitated in 10× the volume of methanol. Thereafter all samples were recovered by freeze drying, after redissolving in benzene and filtering.

Solvents. Reagent grade cyclohexane (Fisher) was used throughout the work. The cyclohexane was distilled before use, and all of the solvent used had a refractive index of 1.4205 ± 0001 .

Solution Viscometry. All samples were filtered before use. Ubbelohde viscometers were used, and kinetic energy corrections were applied.

Osmometry. Block osmometers¹¹ as well as Stabin osmometers were used for equilibrium osmotic pressure measurements. All the osmometric measurements were carried out with cyclohexane solutions. Gel cellophane No. 600 (never-dried) was conditioned and used as membranes.

Light Scattering. The measurements were made with a new absolute light scattering photometer¹² on cyclohexane solutions of polystyrene. The refractive index increment for 546 m μ wavelength light used was 0.1708 at 35°C.¹³

Equilibrium Ultracentrifuge. A Svedberg equilibrium ultracentrifuge manufactured by LKB Produkter was used as described elsewhere.¹⁴ Measurements were made at 37°C. in cyclohexane solutions.

Fractionation. Sample No. 31 was fractionated from a 0.3 g./dl. solution of polymer in a mixed acetone–methyl ethyl ketone (3:2) solvent by the addition of methanol. The molecular weights of the fractions were determined by viscosity measurements.

RESULTS AND DISCUSSION

Table II summarizes all of the molecular weight data obtained at the National Bureau of Standards from the study of the whole polymers and fraction 31-D. Column 3 lists the number-average molecular weight calculated from eq. (1) for the kinetic scheme proposed by Szwarc,¹ i.e.,

$$\bar{M}_n = [\text{Monomer}]^{1/2} [\text{Catalyst}] \quad (1)$$

Column 2 reports the number-average molecular weight obtained from osmometry, and column 4 lists the intrinsic viscosities of the samples in cyclohexane at 35°C. Column 5 reports the weight-average molecular weight calculated from the intrinsic viscosity relation,

$$[\eta] = 6.53 \times 10^{-4} M^{0.52} \quad (2)$$

for polystyrene in cyclohexane at 35°C. Column 6 lists the weight-average molecular weights calculated from the intrinsic viscosity relation

TABLE II
Molecular Weights of Polystyrene Samples

| | \bar{M}_n (O.P.) | \bar{M}_n (kin.) | $[\eta]$ (C ₆ H ₁₂), dl./g. | \bar{M}_w (L.S.) | \bar{M}_w (U.C.) | $\frac{\bar{M}_n \text{ (kin.)}}{\bar{M}_n \text{ (O.P.)}}$ | $\frac{\bar{M}_w \text{ (L.S.)}}{\bar{M}_n \text{ (O.P.)}}$ | $\frac{\bar{M}_w \text{ (U.C.)}}{\bar{M}_n \text{ (O.P.)}}$ | $\frac{\bar{M}_w \text{ (ave.)}}{\bar{M}_n \text{ (O.P.)}}$ |
|------------------|--------------------|--------------------|---|--------------------|--------------------|---|---|---|---|
| 42 | 47,800 | 32,500 | 0.185 | 52,000 | 59,000 | 0.68 | 1.09 | 1.23 | 1.16 |
| 41 | 41,400 | 29,500 | 0.192 | 55,000 | 61,700 | 0.71 | 1.33 | 1.49 | 1.41 |
| 37 | 88,600 | 86,800 | 0.258 | 98,000 | 114,000 | 0.98 | 1.11 | 1.29 | 1.20 |
| 38 | 166,000 | 151,200 | 0.350 | 175,000 | 204,000 | 0.91 | 1.05 | 1.23 | 1.14 |
| 39 | 297,600 | 447,100 | 0.510 | 360,000 | 420,000 | 1.50 | 1.21 | 1.41 | 1.31 |
| 40 | 341,100 | 504,600 | 0.598 | 489,000 | 575,000 | 1.48 | 1.43 | 1.69 | 1.56 |
| 31 | 80,200 | ^a | 0.245 | 88,000 | 102,000 | | 1.10 | 1.27 | 1.18 |
| 31D ^b | 88,800 | ^a | 0.245 | 89,000 | 102,000 | | 0.991 | 1.15 | 1.07 |
| 2 | 116,200 | ^a | 0.33 | 155,000 | 186,000 | | 1.33 | 1.60 | 1.47 |
| 28 | 148,000 | ^a | 0.378 | 203,000 | 235,000 | | 1.37 | 1.59 | 1.48 |
| 30 ^c | 547,200 | ^a | 0.720 | 700,000 | 820,000 | | 1.28 | 1.50 | 1.39 |

^a Values not available due to unknown initiator or loss prior to polymerization.

^b Main fraction from Sample 31.

^c Polymerized at -78°C .

$$[\eta] = 6.10 \times 10^{-4} M^{0.52} \quad (3)$$

The remaining columns list the ratios of these various quantities. Relations (2) and (3) were derived from work at the NBS on polymer fractions of conventional free radical-initiated polystyrenes. This work has not been completed. At the present time it is felt that the difference is larger than the expected experimental error although the reason is not obvious. However, an average value of columns 5 and 6 can be used for the purposes of this paper if it is realized that this value may be in error by $\pm 8\%$. Eventually the difference may be resolved so that the moments of the distribution can be quantitatively applied to the details of kinetics of polymerization.

Since the polystyrene fractions used to establish relations (2) and (3) were prepared by a different mechanism from the polystyrene samples used in this work, the actual weight averages were determined in two cases. Sample 42 was examined by light scattering and found to have the same weight-average molecular weight, within experimental error, as that found in Table II, column 5. Sample 38 was examined by the equilibrium ultracentrifuge and found to have the same molecular weight, within experimental error, as that reported in Table II, column 6.

The fractionation results are shown in Table III, where W_i is the dry weight fraction of the original sample and M_i is the molecular weight from

TABLE III
Fractionation of Sample 31

| Fraction | M_i | W_i |
|----------|---------|--------|
| A | 140,000 | 0.0154 |
| B | 138,000 | 0.0286 |
| C | 112,500 | 0.245 |
| D | 89,000 | 0.330 |
| E | 71,000 | 0.028 |
| F | 68,000 | 0.203 |
| G | 49,000 | 0.066 |
| H | 22,500 | 0.0195 |

viscosity measurements and eq. (2). Figure 5 shows the integral weight distribution when the data are rationalized to 100% recovery. The molecular weights as determined from this integral curve are $\bar{M}_n = 81,000$, $\bar{M}_w = 88,000$, confirming the values shown for the whole polymer in Table II.

The molecular weight data of Sample 42 and 41 (Table II) indicate that, even in the same laboratory, the procedure may yield vastly different results in molecular weight distributions. For this reason any arbitrary assumption that a given sample is "monodisperse" because it was prepared by the described technique can be most erroneous.

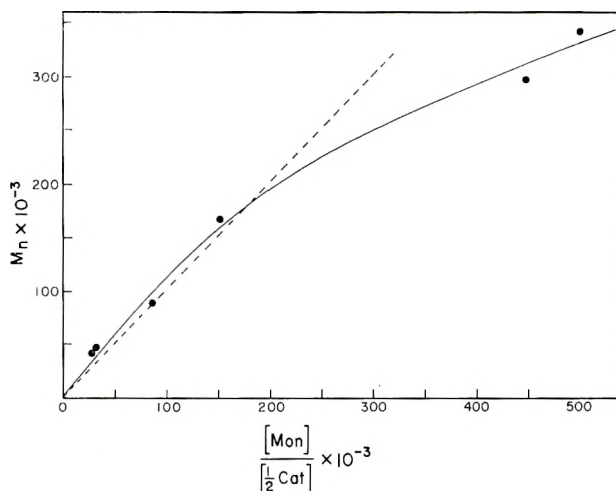


Fig. 5. Integral weight distribution curve for polystyrene.

Also it is apparent from Table I that the successful preparation of a "monodisperse" polymer of a very high molecular weight is difficult to achieve. No doubt both the variation in the polydispersity at any molecular weight "monodisperse" polymer are due to the impurities in the styrene monomer which is added to the growing chains. Szwarc¹⁵ has calculated that more than 70% of the growing chains would have to be killed by the impurities in the system in order to achieve the broad distributions of \bar{M}_w/\bar{M}_n reported. In the low molecular weight polymers reported here, this would require close to 0.5 mmole of reactive impurities. The higher molecular weight samples would only need 0.1 mmole of impurity, which no doubt can exist.

It is interesting to note that, upon a direct fractionation of a good sample, a fraction may be obtained which has become, from an experimental point of view, monodisperse. With samples such as these future experimental techniques may be examined much more critically without the fear of polydispersity corrections. With such samples in hand it is hoped that the earlier weight-average molecular weight difference may be resolved.

A rather surprising result is that the plot of the kinetic number-average molecular weights, in Figure 6, derived from the eq. (1), against the osmotic

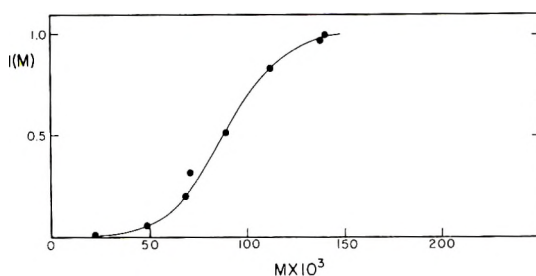


Fig. 6. Comparison of number-average and kinetic molecular weights.

pressure number-average molecular weight is not a line with a slope of unity as was to be expected. A systematic error in the analysis of the catalyst, or an increase in the osmotic pressure molecular weight above the true molecular weight could shift the intercept to zero. However, the similarity of samples 42 and 41 on the plot, and the absence of any detectable permeating species in the osmometry do not seem to support such a conclusion. Also, any systematic analytical error would affect sample 38 as well as the higher points and consequently not improve the overall fit.

The most likely explanation for the unexpectedly low values of osmotic \bar{M}_n (and broader distributions) of the higher molecular weight polymers (samples 39 and 40) would be the occurrence of chain transfer reactions. These would obviously not be as noticeable at the lower as at the higher molecular weights. One possibility that suggested itself along this line was that, at these low initiator concentrations, the mutual termination of the styrene radical-ions may be sufficiently slow to permit some polymerization and radical transfer reactions to occur before termination. An attempt was, therefore, made to investigate this possibility by allowing the initiation reaction (electron transfer) to occur in small versus large volumes of solvent, and then allowing the chains to grow to the same high molecular weights (ca. 500,000) in both cases. However, no difference could be observed between the two results, the osmotic \bar{M}_n values being much lower than predicted (and the distributions much broader) in both cases, confirming the results shown for samples 39 and 40. Hence, if any chain transfer occurs, it must presumably be on the part of the anionic polymer itself.

The assistance of J. H. O'Mara and L. Williams of the National Bureau of Standards is gratefully acknowledged. This work was supported at the University of Akron by a National Science Foundation grant.

References

1. Milkovich, R., M. Szwarc, and M. Levy, *J. Am. Chem. Soc.*, **78**, 2656 (1956).
2. Flory, P. J., *J. Am. Chem. Soc.*, **62**, 1561 (1940).
3. Grubb, W. T., and R. C. Osthoff, *J. Am. Chem. Soc.*, **77**, 1405 (1955).
4. Bostick, E. E., Ph.D. Dissertation, University of Akron, 1959.
5. McCormick, H., *J. Polymer Sci.*, **36**, 341 (1959); *ibid.*, **39**, 91 (1959).
6. Lyssy, T., *Helv. Chim. Acta*, **42**, 2245 (1959).
7. Cantow, H. J., *Makromol. Chem.*, **30**, 169 (1959).
8. Meyerhoff, G., *Z. physik. Chem.*, (Frankfurt), **23**, 100 (1960).
9. Figini, R. V., and G. V. Schulz, *Z. physik. Chem.* (Frankfurt), **23**, 233 (1960).
10. Wenger, F., *Makromol. Chem.*, **36**, 200 (1960); *ibid.*, **37**, 143, 153 (1960).
11. McIntyre, D., J. H. O'Mara, and G. C. Doderer, *J. Research Natl. Bur. Standards*, **62**, 63 (1959).
12. McIntyre, D., and G. C. Doderer, *J. Research Natl. Bur. Standards*, **62**, 153 (1959).
13. McIntyre, D., J. H. O'Mara, and B. C. Konnoek, *J. Am. Chem. Soc.*, **81**, 3498 (1959).
14. Mandelkern, L., L. C. Williams, and S. G. Weissberg, *J. Phys. Chem.*, **61**, 271 (1957).
15. Szwarc, M., and M. Litt, *J. Phys. Chem.*, **62**, 568 (1958).

Synopsis

A study has been carried out on the molecular weight distributions of polystyrene initiated by sodium naphthalene in tetrahydrofuran solution. Stringent high-vacuum techniques were used in order to minimize initiator destruction or chain termination. Molecular weights were measured by osmotic pressure, dilute solution viscosity, light scattering and sedimentation equilibrium. In general, the molecular weight distributions found were quite narrow, as predicted, and corresponded to a stoichiometry of one polymer chain for two initiator molecules. However, the breadth of the distribution was very sensitive to experimental conditions, the \bar{M}_w/\bar{M}_n values found ranging from 1.1 to 1.5. At the higher molecular weights, there was some indication of a chain transfer reaction, leading to a lower molecular weight than expected, as well as a broadening of the distribution. This transfer reaction did not appear to be due to any transfer step between the short-lived radical-anions and the solvent.

Résumé

On présente une étude de la distribution des poids moléculaires du polystyrène initié par du naphthalène-sodium en solution dans le tétrahydrofuranne. On utilise la technique du vide poussé afin de réduire au maximum la destruction de l'initiateur ou la terminaison de chaîne. Les poids moléculaires sont mesurés par pression osmotique, par viscosimétrie en solution diluée, par diffusion lumineuse et par équilibre de sédimentation. En général, la distribution des poids moléculaires est très étroite, comme prévu, et correspond à une stœchiométrie d'une chaîne polymérique par molécule d'initiateur. Bien que la largeur de la distribution soit très sensible aux conditions expérimentales, les valeurs de \bar{M}_w/\bar{M}_n se répartissent entre 1.1 et 1.5. À des poids moléculaires plus élevés, certaines indications sont en faveur d'une réaction de transfert de chaîne, conduisant à des poids moléculaires plus bas que prévus, de même qu'à un élargissement de la distribution. Cette réaction de transfert ne semble pas être due à une étape de transfert entre les petits radicaux-anions et le solvant.

Zusammenfassung

Eine Untersuchung der Molekulargewichtsverteilung von naphthalinnatrium-(in-Tetrachlorkohlenstofflösung)-gestarteten Polystyrolen wurde durchgeführt. Zur möglichen Herabdrückung von Starterzerstörung und Kettenabbruch wurde vollkommen unter Hochvakuum gearbeitet. Molekulargewichte wurden osmotisch, viskosimetrisch, durch Lichtstreuung und Sedimentationsgleichgewicht bestimmt. Im allgemeinen erwiesen sich die erhaltenen Molekulargewichtsverteilungen erwartungsgemäss als ziemlich eng und entsprachen dem stöchiometrischen Verhältnis von einer Polymerkette auf zwei Startermolekel. Die Verteilungsbreite war aber sehr von den experimentellen Bedingungen abhängig und die gefundenen \bar{M}_w/\bar{M}_n -Werte lagen im Bereich von 1,1 bis 1,5. Bei den höheren Molekulargewichten bestanden gewisse Hinweise auf eine Übertragungsreaktion, die zu einem niedrigeren als dem erwarteten Molekulargewicht und einer Verbreiterung der Verteilung führte. Diese Übertragungsreaktion scheint nicht auf einer Übertragung zwischen den kurzlebigen Radikalanionen und dem Lösungsmittel zu beruhen.

Received November 20, 1961

Homogeneous Anionic Polymerization. II. Molecular Weight of Polystyrene Initiated by Lithium Alkyls*

MAURICE MORTON, A. A. REMBAUM,† and J. L. HALL, *Institute of Rubber Research, University of Akron, Akron, Ohio*

INTRODUCTION

In the previous paper¹ of this series, some data were shown on the type of molecular weight distribution which can be expected from the polymerization of styrene by sodium naphthalene. In the latter system, the polymeric chains grow at both ends, subsequent to initiation by electron transfer from the naphthalene complex to the styrene. Hence these dianionic chains have two possibilities of fortuitous termination by reaction with impurities. This should result in a narrower molecular weight distribution than would be the case for a monoanionic chain under similar reaction conditions.

The alkyllithiums are known to be soluble, monofunctional compounds capable of polymerizing unsaturated monomers, presumably by direct addition to the double bonds. Such systems should, therefore, lead to monoanionic growing chains and should also lead, under the right conditions, to a very narrow molecular weight distribution. Preliminary indications² had shown that this system generally obeys the stoichiometry corresponding to one polymer chain formed from each initiator molecule. The work reported herein shows both the stoichiometry of the reaction and the molecular weight distribution which can be expected under varying conditions with butyllithium and ethyllithium as initiators and benzene and tetrahydrofuran as solvents.

EXPERIMENTAL TECHNIQUES

Apparatus

The general apparatus has already been described.¹ The particular sections of vacuum line used for various purposes will be described under the appropriate procedures.

† Present address, Frick Chemical Laboratory, Princeton University, Princeton, New Jersey.

* Presented in part at the 136th National Meeting, American Chemical Society, Division of Polymer Chemistry, Atlantic City, N. J., September 1959.

Purification of Tetrahydrofuran

For this work, the THF was purified somewhat differently than previously described.¹ It was felt that this procedure was an improvement over the original one. The special solvent purification manifold is shown in Figure 1.

Tetrahydrofuran (Merck) was refluxed over sodium for several hours and distilled into a flask containing lumps of sodium and potassium. To this was added 10–20 mg. of naphthalene (Eastman Recrystallized), and the flask (R) was fitted to the reflux condenser (C) of the vacuum system.

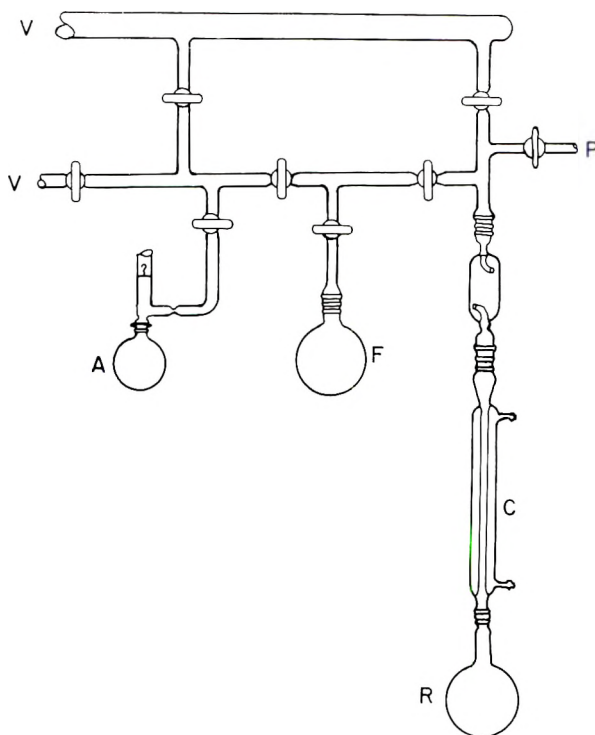


Fig. 1. Solvent purification.

The pressure release (P) was left open, and refluxing was continued until sodium and potassium naphthalene complexes were formed, characterized by the appearance of a dark green color. The tetrahydrofuran solution of sodium and potassium naphthalene complexes was then thoroughly degassed by closing (P), freezing, and pumping to (V), the main vacuum line at 10^{-6} mm. Hg pressure. Isolation from (V) and thawing was done in order to remove dissolved and occluded air from the solution. Measured quantities of tetrahydrofuran were flash-distilled to a sodium-coated flask (F) and finally to a sodium-coated ampule (A) as needed. Shielding tetrahydrofuran from sunlight or any ultraviolet light source was practiced

as a precaution against peroxide formation and other deleterious side reactions.

Benzene Purification

The apparatus used for the purification of benzene was similar to that illustrated in Figure 1, and the following description of the procedure used refers thereto.

Benzene (Merck Analyzed Reagent Grade) was thoroughly degassed and flash-distilled to (R) which contained either sodium-potassium alloy or finely ground lithium hydride. Stirring was continued for several hours in flask (R). Then, portions were flashed to a sodium-coated flask (F')

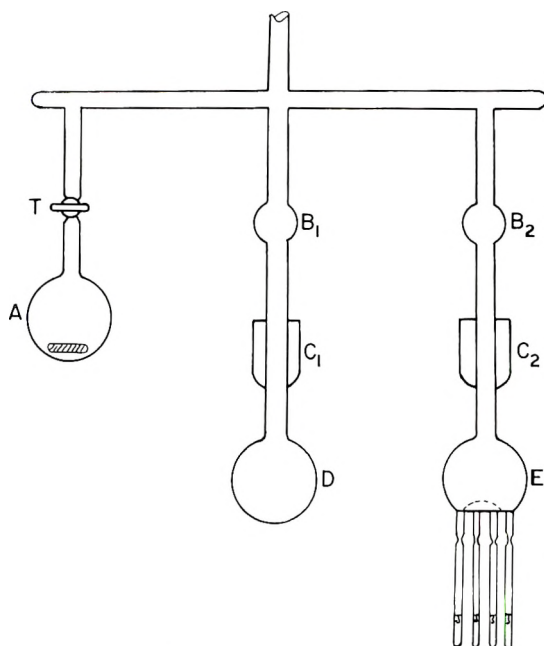


Fig. 2. Styrene monomer purification.

and to (A) as needed. Ampule (A) was coated on the inside with freshly distilled sodium and pumped to 10^{-6} mm. Hg pressure before being used as a receiver.

Styrene Purification

Styrene (Dow Chemical Company) was purified in a high vacuum apparatus as follows. A flask (A), Figure 2, was prepared, containing a slurry of finely ground lithium hydride, with traces of lithium metal, in styrene, and was degassed by flashing to a vacuum line (10^{-6} mm. Hg). The contents was then agitated by means of a magnetic stirrer until a stable threshold concentration of styrene/lithium adduct was formed, as evidenced by the appearance of a faint pink color. The stopcock (T) was then opened

and styrene was flash-distilled through the manifold past a sodium-coated bulb (B_1), condensed by a Dry Ice-alcohol mixture at (C_1), collected in flask (D), and thoroughly pumped to 10^{-6} mm. Hg pressure by alternately freezing and thawing. The degassed styrene was then flash-distilled past another sodium mirror (B_2), condensed at C_2 , and collected in a manifold receiver (E) where as many as 8-10 ampules of styrene were collected in tubes fitted with breakable seals (Eck and Krieb). The ampules were removed by sealing off with a fine-point flame under continuous pumping. Storage was at $-20-0^\circ\text{C}$.

Preparation of Butyllithium

The special apparatus used to prepare the *n*-butyl-lithium is shown in Figure 3. Di-*n*-butylmercury (Eastman Reagent) was placed in a clean, dry flask fitted with a standard-taper joint vacuum connection and a breakable seal (Eck and Krieb). After the flask and contents were thoroughly degassed, *n*-hexane was distilled in (ca. 50-75 ml.), degassed, and the flask was sealed off. This di-*n*-butyl mercury-hexane solution was then sealed

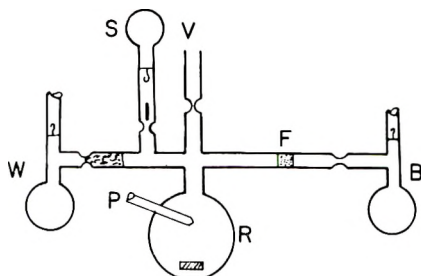


Fig. 3. *n*-Butyllithium preparation.

to the apparatus (S) as illustrated in Figure 3. This apparatus was then attached to a vacuum line through (V). Lithium ribbon or wire with petrolatum coating intact was then charged into (R), a reaction flask, through (P), an open side arm, and (P) was sealed off. After pumping to a high vacuum (ca. 10^{-5} mm. Hg), 50 ml. of anhydrous hexane was distilled into (R) and degassed. In some cases, adding a few drops of *n*-butanol, which etched the lithium surface, was found to be beneficial. After degassing, the apparatus was removed from the vacuum line and the contents of flask (R) was stirred for several hours. The resultant solution of petrolatum in hexane was decanted to (W). Clean hexane was flashed back to (R) from (W), and the cycle repeated. When the lithium surface had been properly cleaned, (W) was removed by sealing off. The di-*n*-butylmercury in hexane was then added to the lithium in (R) and stirring was continued for 120 hr. at room temperature. Reaction was indicated by lithium amalgam formation. At the end of 120 hr. reaction time, the *n*-butyllithium produced was transferred to (B) through a fine porosity fritted glass disk, (F). (R) was rinsed by back-distillation in order to

insure a clean transfer. The contents of (B) was then divided into several ampules having breakable seals. Analysis was according to the method of Gilman and Haubein.³

Preparation of Ethyllithium

Synthesis. A vacuum modification of the method reported by Telalaeva and Kocheskov⁴ was used for the preparation of ethyllithium. Hexane, treated as described previously, was distilled into a clean, dry evacuated ampule containing ethyl bromide. After degassing and isolating from the vacuum line, the resulting solution, in flask (E), was sealed to the apparatus illustrated in Figure 4. Lithium ribbon, coated with petrolatum, was placed in reaction flask (R) of this apparatus which was then fitted to a high vacuum line by means of a 14/35 standard-taper joint at (V). After evacuation, hexane (50–75 ml.) was distilled into (R), and the apparatus

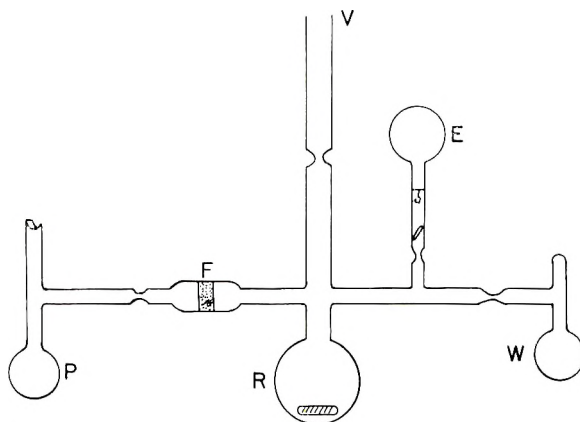


Fig. 4. Preparation of ethyllithium.

was sealed off from the vacuum line. Then the lithium ribbon was degreased by stirring, followed by decanting contaminated hexane to (W) and backflashing pure hexane to (R) for further cycles. After satisfactory cleaning of the wire had been accomplished, (W) was removed and ethyl bromide transferred from (E) to (R) by snapping the breakable seal on (E). Vigorous stirring was continued throughout the reaction time which was allowed to reach 40 hr. in order to achieve maximum extent of reaction. Reaction progress was accompanied by the formation of lithium bromide and the appearance of a violet color in the slurry. After 40 hr. at room temperature (ca. 25–27°C.), the reaction mixture was filtered through (F), a medium porosity Pyrex fritted disk, into (P). After complete transfer, (P) was sealed off with a fine point flame and attached to a manifold apparatus illustrated in Figure 5 for the purpose of purifying the ethyllithium by recrystallization.

Recrystallization. The crude ethyllithium was sealed to the apparatus

illustrated in Figure 5, where (E) represents the ethyllithium ampule. An ampule of anhydrous, degassed benzene, (B), was included as a replacement solvent for the hexane used as reaction medium. The assembled apparatus was evacuated, flamed, and pumped to a pressure of 10^{-6} mm. Hg. The apparatus was then allowed to remain connected to the vacuum manifold but was isolated from the pump by closing an appropriate stopcock. The solution in (E) was then transferred to (R) and the line reopened in order to distill off hexane solvent. The apparatus was then removed from the vacuum line, and the benzene in (B) added to the crude ethyllithium in (R), after which the top cross-tube of the apparatus was removed at the constriction. Next, the entire apparatus was rotated so as to filter the ethyllithium solution through glass wool (G) into one of the product ampules (P). Benzene was then distilled back to (R) until crystal formation began. After maximum crystal formation had occurred,

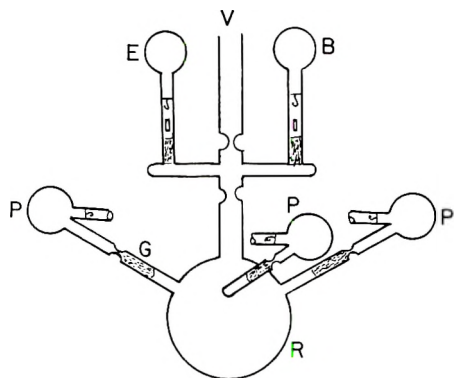


Fig. 5. Recrystallization of ethyllithium.

the mother liquor was decanted to (R) and just enough fresh benzene to effect solution was back-distilled to (P). The constriction was rinsed thoroughly and (P) was sealed off to be divided into smaller ampules for analysis and use. The process was then repeated on the residual mother liquor. With this apparatus design, several crystal crops could be obtained without breaking the vacuum. Care was exercised to completely rinse all ethyllithium away from an intended seal-off since ethyllithium pyrrolyzes to lithium, lithium hydride, and gaseous hydrocarbon by-products. Analysis was according to a vacuum-modification of the method reported by Gilman and Haubein.³

A single recrystallization of ethyllithium could be accomplished by simply sealing the ampule of crude solution to a tube containing a filter plug of glass wool or fritted Pyrex, a clean product flask, and an ampule of benzene. However, for maximum yield of pure crystals, the apparatus described previously is considered better.

Polymerization Procedure

Styrene was polymerized for purposes of characterization and stoichiometric investigation in the apparatus illustrated in Figure 6. This apparatus was so constructed as to enable an accurate analysis of the initiator concentration immediately before mixing with the monomer, as well as an analysis of the actual concentration of active anion species immediately after the polymerization. The latter was accomplished by titration of the red styryl anion *in vacuo* to a colorless endpoint by *n*-butanol.

Styrene monomer was sealed to the neck (M) which contained an inner-sealed capillary. A solvent ampule (S) and an initiator ampule (I) were sealed to a cross-bar tube as shown. A sampling ampule (T) and a vacuum buret were sealed to the reaction flask (R), which was either 500 ml. or

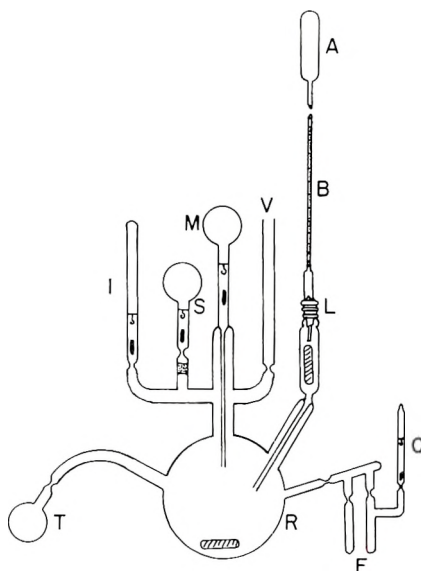


Fig. 6. Styrene polymerization apparatus.

1000 ml. capacity. The vacuum buret consisted of a 12/30 standard-taper outer joint with a 12/30 standard taper inner joint enclosing a magnet which allowed a slow permanent leak to the drip tube shown. The leak valve (L) supported a 10-ml. microburet closed at the top with an ampule of standardized *n*-butanol-benzene solution. The butanol solution was prepared with anhydrous benzene and butanol, which had been dried over calcium hydride and thoroughly degassed. This solution was standardized by reacting with CH_3MgI and measuring evolved methane.

Once assembled, the apparatus was evacuated through (V), flamed thoroughly, and pumped to 10^{-6} mm. Hg. The apparatus was then removed by sealing off and was placed on a magnetic stirrer. Now, two different approaches were used for polymerization. One involved adding

solvent (S) and initiator (I) only. The other involved adding an extra ampule of catalyst first, thus purging the system, and draining this catalyst to (T) where it was sealed off. The first method was followed in the initial stages of the research.

The initiator was introduced into the main reaction vessel by breaking the seal with the glass-covered nail provided. The solvent was then added in a similar manner. A glass wool plug had been placed above the constriction in flask (S) to filter any sodium particles which might be carried from the mirror on which the solvent was stored. The solvent and initiator were mixed in the reactor and samples removed for determination of the initiator concentration at this stage, by means of a Gilman double titration. This mixing and removal was done at room temperature when benzene was used as the solvent. However in the case of ethers evidence that reaction between the initiator and the ether was taking place caused a change in procedure. Gilman⁵ found that ethers are cleaved by organometallics above -35°C ., so all mixing and removal was done in a Dry Ice-methanol bath at -80°C .

The reactors were placed in the appropriate constant temperature baths, i.e., benzene at 0°C . and THF at -80°C . The solution was agitated by means of a magnetic stirrer. A few drops of styrene were introduced from flask (M) through the 1-mm. capillary. When the development of maximum color indicated the conversion of alkyl lithium into styryl anions (instantaneous for the THF but 15-30 min. for benzene) the remainder of the styrene was allowed to enter the reactor dropwise. The slow addition of monomer with constant stirring gave all growing anions equal opportunity to react with the monomer. The monomer generally comprised about 10 vol.-% of the polymerization mixture, depending on the molecular weight of the polymer, and 5-20 g. of monomer was usually charged.

At the conclusion of the polymerization (almost instantaneous in THF but at least several hours in benzene), the concentration of active centers was determined by *n*-butanol titration in situ. The microburet (B) was filled by breaking the seal on ampule (A). The permanent leak at (L) allowed the standard solution to be mixed with the stirred polymer solution in (R). Titration was carried to a colorless endpoint. The reaction flask (R) was then opened, and the polymer was recovered by precipitating in methanol, collecting, and drying in a vacuum oven at $40-60^{\circ}\text{C}$. Polymers were stored in a cool, dark place.

The above titration of styryl red anions was not carried out in all cases, but was used from time to time to check on the purity of the polymerization system. Typical results of such titrations are shown in Table I, where a comparison is made of the initial concentration of ethyllithium and the final concentration of styryl anion. A total loss of active centers of 10-15% is indicated, and this indicates the extent of deviation from a monodisperse distribution that may be expected in the molecular weights.

In those cases where the above titration was not performed, the active

TABLE I

| Wt. styrene, g. | C ₂ H ₅ Li concn., moles/l. × 10 ⁴ | Final anion concn., moles/l. × 10 ⁴ | Loss, % |
|-----------------|--|---|---------|
| 20.7 | 3.15 | 2.83 | 10.2 |
| 17.2 | 2.70 | 2.28 | 15.6 |
| 20.0 | 4.56 | 3.85 | 15.6 |

polymer was terminated instead by direct addition of water or *n*-butanol, followed by coagulation and drying of the polymer.

Molecular Weight Determination

Viscometry. Dilute solution viscosities were determined as previously described,¹ with thiophene-free benzene as solvent. The equation of Flory⁶ was used for the calculation of the molecular weights from intrinsic viscosities.

Osmometry. Osmotic pressure measurements were made with a Stabin-type osmometer⁷ with Avisco No. 300 cellulose membranes. These membranes were conditioned by the procedure of Wagner⁸ with the noted changes. The membranes were washed in water to remove the formaldehyde, and then transferred through a progression of 25, 50, 75, and 100% acetone-in-water mixtures. Then instead of a direct transfer from acetone to the desired solvent, the membranes were transferred through a progression of 25, 50, 75, and 100% desired solvent-in-acetone mixtures. Care was taken to keep the membranes submerged in solvent while they were being placed in the osmometers. Either benzene or cyclohexane was used as solvent for these osmotic pressures. The osmometers were kept in a constant temperature bath with the following temperatures used: benzene 30°C. and cyclohexane 35°C. Four concentrations of each polymer were used: approximately 2, 1, 0.5, and 0.25 wt.-% polymer, as determined by solids content of an aliquot portion of the 2% solution.

Light-Scattering Determination. Weight-average molecular weight measurements were made with a Brice-Phoenix Universal light scattering photometer, Series 1999-32. The scattering cell was a cylindrical cell with dimensions of 75 × 26 mm. The instrument was calibrated against a calibrated opal reference standard as well as Zimm's value⁹ for the turbidity of benzene. Both methods gave essentially the same calibration constant. The scattering of benzene was symmetric within approximately 1% between 45° and 135°. All solutions were filtered directly into the cell, through sintered glass filters. The experimental data were treated by a Zimm plot. The intercept of the Zimm plot was treated by the usual light scattering equation to give the molecular weight.

RESULTS AND DISCUSSION

The stoichiometry of the reaction and the molecular weight distribution of the polystyrene are shown in the data contained in Tables II-IV.

TABLE II
 Butyllithium Polymerization of Styrene in Benzene at 0°C.

| Polymer | Styrene, g. | <i>n</i> -C ₄ H ₉ Li, mmole | [η] _{C₆H₆} ³⁰ dl./g. | Molecular weight $\times 10^{-3}$ | |
|-----------------|-------------|--|---|-----------------------------------|-----------|
| | | | | Kinetic | Viscosity |
| 41 | 15.6 | 0.660 | 0.178 | 23.6 | 25.1 |
| 42 | 10.4 | 0.510 | 0.175 | 20.4 | 24.3 |
| 43 | 9.8 | 0.151 | 0.333 | 64.9 | 69.8 |
| 45 ^a | 11.4 | 0.080 | 0.655 | 142.5 | 147.7 |
| 48A | 5.7 | 0.037 | 0.700 | 154.0 | 157.2 |
| 47 | 11.0 | 0.030 | 1.345 | 366.7 | 378.1 |

^a Osmotic pressure, light-scattering and ultracentrifuge measurements (see ref. 1 for description) on this polymer by D. B. McIntyre, National Bureau of Standards, yielded the following values: $\bar{M}_n = 136,000$; \bar{M}_w (LS) = 144,000; \bar{M}_w (UC) = 160,000; Hence \bar{M}_w (ave)/ $\bar{M}_n = 1.12$.

Tables II and III show molecular weights obtained in the polymerization of styrene in benzene solution by butyllithium and ethyllithium, respectively. As explained previously, in these cases, the competition between initiation and propagation was avoided by using the "seeding" technique. In other words, the initiator solution was first mixed with a few drops of styrene at 25°C. and allowed to stand 15–30 min. to allow complete reaction between initiator and monomer (full development of orange-red color). Then the solution was cooled to 0°C. and the remaining monomer added slowly with rapid stirring. It can be seen that, under these conditions, a very narrow molecular weight distribution was obtained, as shown by the agreement between viscometric and osmotic or kinetic molecular weights. Furthermore, the stoichiometry corresponds very closely to the predicted one of one polymer chain per initiator molecule.

It is important, however, to consider the factors which may enter in a comparison between the predicted and measured molecular weights. Viscometric methods are, of course, the most convenient to use and have been used in most cases, except for several osmotic pressure measurements included to check the results. However, it should be remembered that the viscosity-molecular weight equation, whereby the molecular weights are actually calculated, is based on a calibration against osmotic molecular weights of a series of fractions, which themselves can be expected to have a distribution corresponding to a \bar{M}_w/\bar{M}_n ratio of about 1.1. In other words,

 TABLE III
 Ethyllithium Polymerization of Styrene in Benzene at 0°C.

| Polymer | Styrene, g. | C ₂ H ₅ Li, mmole | [η] _{C₆H₆} ³⁰ dl./g. | Molecular weight $\times 10^{-3}$ | |
|---------|-------------|--|---|-----------------------------------|-----------|
| | | | | Kinetic | Viscosity |
| E1 | 12.5 | 0.400 | 0.235 | 31.2 | 36.1 |
| E2 | 12.8 | 0.373 | 0.238 | 34.2 | 36.8 |
| E3 | 15.2 | 0.180 | 0.445 | 84.6 | 85.5 |

such fractions would have about the same type of distribution as would be expected for the whole polymers described here. Hence the molecular weight values deduced from such viscometric data should yield the \bar{M}_n values (number-average) obtainable by osmometry, if the polymers have the expected narrow molecular weight distribution.

The stoichiometry of the reaction is related to the molecular weight distribution of the polymer as follows. The main factor causing experimental deviation from the expected stoichiometry would be the reactions between active anionic species and impurities. This could occur in two ways, i.e., before the monomer is added to the initiator or after monomer addition. In the former case, the result would be essentially loss of initiator, so that the actual molecular weight would be higher than predicted but it would still have a narrow distribution, i.e., agreement between viscometric and osmometric values but deviation from predicted

TABLE IV
Butyllithium Polymerization of Styrene in THF

| Polymer | Temp., °C. | Styrene, g. | <i>n</i> -C ₄ H ₉ Li, mmole | [η] _{C₆H₆} ³⁰ , dl./g. | Molecular weight × 10 ⁻³ | |
|------------------|---------------|----------------|--|--|--|-----------|
| | | | | | Kinetic | Viscosity |
| T5 | 25 | 9.07 | 0.400 | 0.246 | 22.7 | 38.6 |
| T16 | 25 | 9.07 | 0.177 | 0.407 | 51.2 | 75.9 |
| T14 | 25 | 9.07 | 0.040 | 1.334 | 227.4 | 373.3 |
| T20 ^a | 25 | 9.98 | 0.307 | 0.586 | 32.5 | 123.5 |
| T21 ^b | 25 | 9.07 | 0.334 | 2.86 | 27.2 | 1041 |
| T23 | -80 | 16.6 | 0.515 | 0.225 | 32.2 | 34.2 |
| T24 | -80 | 11.7 | 0.426 | 0.190 | 27.5 | 27.3 |
| T25 | -80 | 20.0 | 0.380 | 0.319 | 52.5 | 54.8 |
| T26 | -80 | 13.4 | 0.170 | 0.423 | 78.8 | 82.0 |
| T27 | -80 | 16.5 | 0.141 | 0.565 | 117.1 | 117.8 |

^a 5 min. delay before addition of monomer to initiator solution.

^b 30 min. delay before addition of monomer to initiator solution.

(kinetic values). In the second case, where active chain ends are being destroyed during polymerization, there should be agreement between osmometric and kinetic values but higher viscometric values, indicating a broadening of the molecular weight distribution. Hence, in the absence of any osmometric data, it is obvious that an agreement between the kinetic and viscometric molecular weights must indicate both good stoichiometry and a narrow distribution.

However, there is one additional factor which may vitiate any conclusions that are drawn from a comparison of kinetic and viscometric molecular weights. It has been shown previously¹ that, at sufficiently low initiator concentrations (high molecular weights), there is evidence of chain transfer between the growing chains and some impurity. This would then lead to a polymer having a lower number-average molecular weight than predicted. However, such a random chain-transfer reaction would also

destroy the monodispersity of the polymer, leading to a broader molecular weight distribution. Hence the \bar{M}_v values obtained from viscosity measurements would be considerably higher than the \bar{M}_n values. In this way, the occurrence of chain transfer (with or without concomitant chain termination) may lead to an apparent agreement between the kinetic and viscometric molecular weights. In that case, only osmometry can lead to a true value of \bar{M}_n for comparison with the other methods.

From the data in Tables II and III, it can be seen that there is good agreement between all three values of molecular weight, thus indicating the absence of transfer and termination reactions, and the presence of narrow molecular weight distributions.

The results obtained in the polymerization of styrene with butyllithium in THF are shown in Table IV. It can be seen at once that, at 25°C., there appeared a noticeable discrepancy between the predicted and measured molecular weights, the latter always being higher. In this connection, it is important to remember that, for purposes of molecular monodispersity, the technique used in all cases involved first adding the butyl lithium to

TABLE V
Molecular Weights of Polystyrene

| Polymer | $\bar{M}_n \times 10^{-3}$ | | $[\eta]_{\text{C}_6\text{H}_6}^{30}$ | $\bar{M}_r \times 10^{-3}$ | $\bar{M}_w \times 10^{-3}$ | \bar{M}_w/\bar{M}_n (O.P.) |
|------------------|----------------------------|---------|--------------------------------------|----------------------------|----------------------------|---------------------------------|
| | Kinetic | Osmotic | | | | |
| T34 ^a | 279.2 | 294.9 | 1.16 | 309.9 | 310.0 | 1.051 |
| 125 | 319.6 | 324.0 | 1.25 | 342.5 | 355.0 | 1.096 |
| 127 | 253.8 | 320.9 | 1.18 | 321.0 | — | — |
| 128 | 458.4 | 530.9 | 1.75 | 538.7 | 595.0 | 1.121 |

^a Prepared in THF at -80°C. All others prepared in benzene at 0°C.

the THF, followed by slow addition of styrene, with good mixing. However it is known⁵ that alkyl lithium compounds can cleave ethers, especially at temperature above -35°C. Hence, during the few minutes before the addition of the styrene, such a reaction may actually occur. Once the styrene is added, all the alkyl lithium would be instantaneously converted to an aryllithium type, which is relatively stable in ether solvents. To check the possible loss of initiator by this side reaction, some experiments were carried out in which the butyllithium was deliberately allowed to have a longer "contact time" with the THF, before styrene was added. The results are also shown in Table IV, where it can be seen that, after 30 min. reaction time, only 2-3% of the original initiator remains.

Since this polymerization is almost instantaneous at room temperature, it is possible to carry it out very rapidly even at Dry Ice temperature (ca. -80°C.). The results in Table IV show that, at this low temperature, the side-reaction between the butyllithium and the THF is suppressed, and there is good agreement between the predicted and measured molecular weights.

In order to further characterize the molecular weight distribution of these polymers, four different samples of polystyrene, polymerized both in THF and in benzene, were subjected to osmotic pressure and light scattering measurements. The results are shown in Table V. Again it can be seen that there is quite good agreement between the predicted and measured molecular weights, although there is some indication of initiator losses in some cases (127 and 128). Furthermore, the molecular weight distributions are quite narrow, as expected, ranging from \bar{M}_w/\bar{M}_n ratios of 1.05 to 1.1.

This work was supported by National Science Foundation Grant G-5919. Light-scattering measurement data were kindly supplied by T. E. Helminiak.

References

1. Morton, M., R. Milkovich, D. B. McIntyre, and J. L. Bradley, *J. Polymer Sci.* **1**, 439 (1963).
2. Morton, M., A. Rembaum, and J. L. Hall, paper presented at 132nd Meeting, American Chemical Society, New York, September 1957.
3. Gilman, H., and A. H. Haubein, *J. Am. Chem. Soc.*, **66**, 1515 (1944).
4. Talalaeva, T. V., and K. A. Kocheskov, *Zhur. Obshchei Khim.*, **23**, 392 (1953).
5. Gilman, H., and B. J. Gaj, *J. Org. Chem.*, **22**, 1165 (1957).
6. Krigbaum, W. R., and P. J. Flory, *J. Polymer Sci.*, **11**, 37 (1953).
7. Stabin, V. J., and E. H. Immergut, *J. Polymer Sci.*, **14**, 209 (1954).
8. Wagner, R. H., *Ind. Eng. Chem., Anal. Ed.*, **16**, 520 (1944).
9. Carr, C. I., and B. H. Zimm, *J. Chem. Phys.*, **18**, 1616 (1950).

Synopsis

A study has been carried out on the molecular weights and their distribution for polystyrene prepared by means of ethyl and butyl lithium initiators, using benzene and tetrahydrofuran as solvents. Stringent high vacuum techniques were employed in order to minimize any destruction of initiator or termination of growing chains in these anionic polymerizations. Under these conditions, it was found that the stoichiometry corresponded to the formation of one chain from each initiator molecule. Furthermore, the molecular weight distribution could be made very narrow ($\bar{M}_w/\bar{M}_n = 1.05 - 1.1$) in these cases, where the initiation reaction was very rapid compared to the propagation step. In the case of the benzene systems, the initiation reaction was too slow, leading to a broadening of the molecular weight distribution, and this could be circumvented by a "seeding" technique whereby all the chain anions were pre-initiated before the main polymerization took place. The alkyl lithium initiators were found to react rapidly with THF at room temperature, but the styryl lithium apparently did not.

Résumé

On étudie les poids moléculaires et leur distribution pour le polystyrène préparé à l'aide d'initiateurs d'éthyl-et de butyl-lithium en utilisant comme solvants le benzène et le tétrahydrofurane. On emploie des techniques de haut vide poussé afin de diminuer toute destruction de l'initiateur ou la terminaison de chaîne en croissance dans les polymérisation anioniques. Dans ces conditions on trouve que la stoechiométrie correspond à la formation d'une chaîne pour chaque molécule d'initiateur. De plus, on peut déterminer très précisément la distribution des poids moléculaires ($\bar{M}_w/\bar{M}_n = 1.05 - 1.1$) dans ces cas, où la réaction d'initiation est trop rapide comparée à l'étape de

propagation. Dans le cas des systèmes benzéniques, la réaction d'initiation est trop lente, ce qui mène à un élargissement de la distribution des poids moléculaires, et ceci peut être circonvenu par une technique "d'ensemencement" par laquelle toutes les chaînes anioniques sont pré-initiées avant que la polymérisation principale ne prenne place. On trouve que les initiateurs alcoyl-lithium réagissent rapidement avec le THF à température de chambre, mais le styryle-lithium n'agit apparemment pas.

Zusammenfassung

Eine Untersuchung des Molekulargewichts und der Molekulargewichtsverteilung wurde an Polystyrol durchgeführt, das mit Äthyl- und Butyllithium als Starter in Benzol- und Tetrahydrofuranlösung dargestellt worden war. Zur Vermeidung einer Zerstörung des Starters oder eines Kettenabbruchs bei dieser anionischen Polymerisation wurde ausschliesslich unter Hochvakuum gearbeitet. Unter diesen Bedingungen wurde stöchiometrisch auf jede Startermolekel eine Kette gebildet. Ausserdem konnte die Molekulargewichtsverteilung in den Fällen, wo die Startreaktion sehr rasch im Vergleich zum Kettenwachstum verlief sehr eng ($\bar{M}_w/\bar{M}_n = 1,05 - 1,1$) gemacht werden. In Benzol war die Startreaktion zu langsam, was zu einer Verbreiterung der Molekulargewichtsverteilung führte. Das konnte durch ein "Keimungs"-verfahren umgangen werden, bei welchem alle Anionenkette vor Stattfinden der Hauptpolymerisation vorgestartet wurden. Alkylolithiumstarter zeigten bei Raumtemperatur eine rasche Reaktion mit THF, Styryllithium offenbar jedoch nicht.

Received November 20, 1961

Homogeneous Anionic Polymerization. III. Molecular Weight of Polyisoprene Initiated by Butyllithium*

MAURICE MORTON, E. E. BOSTICK,† and R. G. CLARKE,‡ *Institute of Rubber Research, University of Akron, Akron, Ohio*

INTRODUCTION

As is well known, in the polymerization of the dienes there is an additional feature over and above the question of chain length, i.e. chain microstructure. Although it has been known for some years that the different alkali metals, e.g., sodium or potassium, can lead to differences in such chain structure, it is only recently that the revolutionary discovery¹ has been made that the use of lithium can lead to the formations of polyisoprene having over 90% *cis*-1,4 structure, i.e., virtually duplicating the structure of Hevea rubber.

Further work² has since shown that this chain structure is not dependent upon the use of the lithium metal but can be obtained as well in homogeneous systems with the use of lithium alkyls. However, it was also found^{2,3} that the chain structure of the polyisoprene was very markedly affected by the solvent present. Thus the high *cis*-1,4 structure was obtained in bulk polymerization with lithium or lithium alkyls or in the presence of hydrocarbon solvents, but even the presence of small amounts of solvents such as ethers, amines, etc. led to a drastic decrease in *cis*-1,4 content. Temperature also affected the chain structure, but to a much lesser extent. The polymerization of isoprene in homogeneous solution with lithium alkyls therefore offers an interesting study, not only because of the presumed absence of any termination step, but also because of the additional factor of chain structure control. Such studies could be important in helping to elucidate the mechanism whereby such structure control is achieved. It was considered advisable to study two aspects of this polymerization, i.e., stoichiometry (and molecular weight distribution) and kinetics. Two typical solvents were used, i.e., *n*-hexane and tetrahydrofuran, since these were known to yield markedly different chain structures, as stated previously. The *n*-hexane yields a very high propor-

* Presented in part at the 136th National Meeting, American Chemical Society, Division of Polymer Chemistry, Atlantic City, N. J., September 1959.

† Present address, Research Laboratory, General Electric Co., Schenectady, N. Y.

‡ Present address: Goodyear Tire and Rubber Co., Akron, Ohio.

tion of *cis*-1,4 units, whereas use of the THF results in a polymer of mixed structure, predominantly of the 3,4-structure. This paper deals with the first aspect mentioned above, i.e., stoichiometry and molecular weight distribution.

EXPERIMENTAL TECHNIQUES

The general apparatus⁴ and the techniques used in the purification of the tetrahydrofuran and the preparation of butyllithium⁵ have already been described previously.

Purification of *n*-Hexane

The apparatus used for the purification of *n*-hexane was similar to that illustrated in Figure 1 of the previous paper,⁵ and the following description of the procedure used refers thereto.

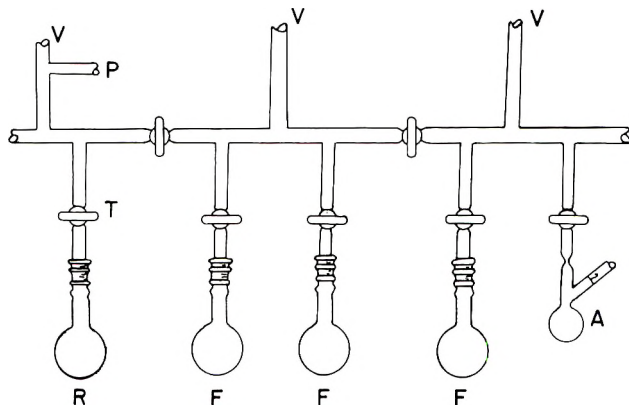


Fig. 1. Apparatus for purification of isoprene.

n-Hexane (Merck) was treated with concentrated sulfuric acid by rapid stirring and shaking. The hexane layer was then removed by distillation into flask (R) which contained freshly prepared sodium-potassium alloy. The hexane was stored in flask (R) until needed. Then, portions were flashed to (F) which contained a freshly prepared sodium mirror. Required amounts of solvent were next flash-distilled to (A), degassed to 10^{-6} mm. Hg pressure, and sealed off under continuous pumping.

Purification of Isoprene

Isoprene (Phillips, 99 mole-% purity) was purified in a high vacuum manifold illustrated in Figure 1. The monomer was degassed over lump sodium in flask (R). Then the isoprene was flash-distilled three times to flasks (F) which were coated with freshly sublimed sodium metal. The first distillation removed the inhibitor, *tert*-butyl pyrocatechol. Top cuts were taken from each distillation. Finally, designated quantities of mono-

mer were collected in ampule (A), where degassing was completed by pumping to 10^{-6} mm. Hg pressure. The ampules (A) fitted with Eck and Krieb breakable seals were sealed off with a fine point flame under continuous pumping and stored at 0°C . until ready for use ($n_{\text{D}}^{20} = 1.4216$).

Polymerization Procedure

The polymerization apparatus used was essentially the same as that used in the polymerization of styrene⁵ by alkyllithium initiators, except for the fact that no vacuum buret was incorporated in this apparatus, since the absence of color, in hexane, made such titrations impossible. The active chain anions were therefore terminated at the end of the polymerization by introducing *n*-butanol from an ampule attached to the manifold of the apparatus in the usual way.

The polymerizations were also carried out more or less as previously described for styrene,⁵ about 10 vol. % of monomer being used. Since the initiation step appeared to be somewhat slow in *n*-hexane solvent, the "seeding" technique previously described for styrene was used. This was done by mixing all of the butyllithium with about 1 g. of isoprene in the *n*-hexane solvent and allowing this to react at 50°C . for several hours. The resulting low molecular weight polyisoprene seed (6,000–10,000 M.W.) was then titrated for active anion concentration by the Gilman double titration method, as previously described,⁵ and was used as the initiator for further polymerization. The polymerizations were generally allowed to go on overnight to ensure completion.

In the case of THF solvent, since the polymerization was considerably slower than for styrene, it could not be conducted at -80°C . but was done at 0°C . In order to minimize the well known reaction between the butyllithium and THF, care was always taken to add the isoprene first, followed by addition of the butyllithium, with good mixing. In this way, direct contact of the initiator with the THF was avoided. Furthermore, since the initiation reaction appeared to be almost instantaneous at this temperature, no recourse to seeding techniques was needed. The polymerizations were usually complete in a few hours, at most.

The polymer was coagulated and dried *in vacuo*, as in the case of styrene,⁵ except for the presence of an antioxidant (phenyl β -naphthylamine) to protect the polymer (ca. 2% based on polymer).

Molecular Weight Determination

The method used for osmometric determination of molecular weight has been previously described.⁵ The only difference in technique used for the polyisoprene was the presence of 0.006% of phenyl- β -naphthylamine in the benzene solutions to protect the polymer.

The viscometry techniques have also been previously described.⁴ For the polyisoprene, toluene was used as solvent, and it contained 0.006% of phenyl- β -naphthylamine as antioxidant. Since these polymers were of high *cis*-1,4 content, approaching the molecular structure of Hevea rubber,

it was possible to use the well-known equation, determined by Carter, Scott, and Magat,⁶ which relates intrinsic viscosity to molecular weight:

$$[\eta]_{\text{C}_6\text{H}_6}^{25} = 5 \times 10^{-4} \bar{M}_v^{0.667} \quad (1)$$

It has since been shown⁷ that the above equation is quite accurately applicable to these synthetic *cis*-1,4-polyisoprenes.

In the case of the polyisoprene prepared in THF solution, it has been shown³ that the chain structure is of the "mixed" type, containing a relatively high proportion of 3,4-units. No viscosity equation has been available for this polymer, and such an equation was therefore determined in this laboratory⁸ only very recently to be as follows:

$$[\eta]_{\text{C}_6\text{H}_6}^{30} = 1.11 \times 10^{-4} \bar{M}_v^{0.74} \quad (2)$$

The light scattering method used has been previously described.⁵ The only modification used was to perform this determination on the polymer in the *n*-hexane solvent in which it was polymerized without any prior isolation of the polymer. In this way the polymer was protected from such drastic procedures as coagulation and drying, which could possibly induce some crosslinking and distort the light-scattering measurements. Hence it was sufficient, at the end of the polymerization, merely to add a few drops of *n*-butanol for termination, after which the hexane solution of the polyisoprene was diluted to the desired concentration for light-scattering determination.

RESULTS AND DISCUSSION

Butyllithium Polymerization of Isoprene in *n*-Hexane

As described in the previous section, the polymerization of isoprene in *n*-hexane was carried out in two ways, (a) by mixing all of the monomer directly with the initiator, and (b) by premixing all of the initiator with a very small amount of the monomer to form a polymer "seed." The latter method (seeded polymerization) was used in those cases where the initiation reaction was slow enough to persist during a substantial period of the polymerization process, thus leading to broader chain length distributions.

The results obtained with isoprene in *n*-hexane by direct polymerization at 50 and 29°C., as described above, are shown in Table I. As in the previous work,⁵ the kinetic molecular weights were the calculated values based on the assumption of one chain for each initiator molecule charged, while the viscometric molecular weights were calculated from the intrinsic viscosities by means of eq. (1). It can be seen at once that the molecular weights show indications of some distribution. Although this is not too serious at 50°C., there is certainly no doubt about the presence of a considerable spread in the molecular weights of the polymer prepared at 29°C. Evidence will be presented later that this discrepancy between the viscometric molecular weights and the predicted kinetic values cannot be due

TABLE I
 Direct Polymerization of Isoprene in *n*-Hexane

| Temp., °C. | <i>n</i> -C ₄ H ₉ Li, moles/g. mono- mer × 10 ⁸ | [η] _{C₇H₈} ²⁵ dl./g. | Molecular weight × 10 ⁻³ | |
|---------------|--|--|-------------------------------------|-------------|
| | | | Kinetic | Viscometric |
| 50 | 16.5 | 0.99 | 60.0 | 79.0 |
| 50 | 7.45 | 1.45 | 134.5 | 146.0 |
| 50 | 5.65 | 1.52 | 177.0 | 158.5 |
| 29 | 52.6 | 0.48 | 19.0 | 27.9 |
| 29 | 28.7 | 0.60 | 34.9 | 39.9 |
| 29 | 25.6 | 0.83 | 39.1 | 64.0 |
| 29 | 12.5 | 1.29 | 79.7 | 123.0 |
| 29 | 6.6 | 2.62 | 151.0 | 353.0 |

to any destruction of initiator by impurities, but is due to the simultaneous existence of initiation and propagation reactions during a considerable period of the polymerization.

In order to eliminate this effect introduced by a relatively slow initiation step, a seeded polymerization technique was used, as described above, and the results are shown in Table II. It can be seen that these results

 TABLE II
 Seeded Polymerization of Isoprene in *n*-Hexane at 29°C.

| <i>n</i> -C ₄ H ₉ Li, moles/g. monomer × 10 ⁵ | [η] _{C₇H₈} ²⁵ dl./g. | Molecular weight × 10 ⁻³ | | |
|---|--|-------------------------------------|---------|-------------|
| | | Kinetic | Osmotic | Viscometric |
| 3.62 | 0.49 | 27.6 | — | 28.7 |
| 2.30 | 0.64 | 43.4 | — | 42.4 |
| 1.72 | 0.83 | 58.0 | — | 63.3 |
| 3.23 | 0.59 | 30.6 | 38.2 | 38.9 |
| 1.86 | 0.81 | 53.8 | 53.2 | 61.2 |
| 0.65 | 1.76 | 154.0 | 191.0 | 197.0 |

show a much better agreement between the predicted and measured molecular weights, both osmometric and viscometric. A comparison of the kinetic and osmotic values shows good general agreement, with some initiator loss indicated at the lower initiator levels (higher molecular weights), as might be expected. However, the viscometric values agree very well with the osmotic, indicating a negligible amount of chain termination during the polymerization itself.

As a further check on the molecular weight distribution of polyisoprene prepared by this seeded technique, additional samples were prepared and characterized not only by solution viscosity but by light scattering as well, in order to obtain weight-average molecular weight (\bar{M}_w) values. The results are shown in Table III, and confirm the type of narrow distribution previously indicated by the data in Table II.

As was mentioned in a previous section, the light-scattering measurements were carried out on the polyisoprene solutions in *n*-hexane, taken directly from the high vacuum apparatus, without any coagulation or drying. This was done because it had been found that such treatment of the polymer led to spurious results in the light scattering determination. Thus two polymers, which had been so treated, had predicted \bar{M}_k (kinetic) values of 174,600 and 247,300 whereas the \bar{M}_w values were 4,550,000 and 2,750,000, respectively. Furthermore, the Zimm plots for these polymers showed marked curvature, indicating the presence of a very high molecular weight species.

TABLE III
Seeded Polymerization of Isoprene in *n*-Hexane at 29°C.

| <i>n</i> -C ₄ H ₉ Li, moles/g. monomer × 10 ⁵ | [η] _{C₇H₈} ²⁵ dl./g. | Molecular weight × 10 ⁻³ | | | \bar{M}_w/\bar{M}_n |
|---|--|-------------------------------------|-------------|---------------------|-----------------------|
| | | Kinetic | Viscometric | Light scattering | |
| 1.80 | 0.86 | 55.8 | 67.0 | 77.0 | 1.15 |
| 0.53 | 1.80 | 189.6 | 200.0 | 216.0 | 1.08 |

The fact that the uncoagulated polymer solutions used for the data in Table III showed no such "microgel" species indicates that this is not formed during the polymerization, but is a direct result of the coagulation and drying process. It can be assumed that such small amounts of microgel may be present in all the coagulated polymers examined in the course of this work. However, solution viscosity measurements are known to be largely unaffected by such microgel, so that small amounts would not affect the molecular weight found from viscosity, but would, of course, greatly affect light-scattering measurements.

Butyllithium Polymerization of Isoprene in Tetrahydrofuran

In view of the rapid initiation reaction between the butyl lithium and the isoprene in tetrahydrofuran (THF), as evidenced by the almost instantaneous formation of a yellow color, it was not necessary to resort to seeded polymerization techniques in this case. The speed of the initiation reaction has also been confirmed by kinetic data, hence there should be no broadening in the molecular weight distribution in this case due to simultaneous occurrence of initiation and propagation.

The results obtained are shown in Table IV, which includes the predicted and measured molecular weights, both viscometric and osmometric. A comparison of the three molecular weights for each polymer shows that the actual number-average molecular weight (\bar{M}_n) is definitely higher than predicted from the stoichiometry. This can be taken to indicate destruction of some initiator prior to initiation, and is similar to the phenomenon observed in the case of styrene polymerization,⁵ where a competitive

TABLE IV
 Polymerization of Isoprene in THF at 0°C.

| <i>n</i> -C ₄ H ₉ Li, moles/g. × 10 ⁵ | [η] _{C₆H₆} ³⁰ dl./g. | Molecular weight × 10 ⁻³ | | | |
|--|---|-------------------------------------|----------------------------|--------------------------------|-----------------------|
| | | Kinetic | Osmotic (\bar{M}_n) | Viscometric (\bar{M}_v) | \bar{M}_v/\bar{M}_n |
| 2.25 | 0.45 | 44.2 | — | 74.8 | |
| 2.13 | 0.42 | 46.0 | 52.0 | 69.0 | 1.32 |
| 1.74 | 0.57 | 57.4 | 75.1 | 103.0 | 1.37 |
| 1.55 | 0.60 | 64.4 | — | 110.0 | |
| 1.00 | 0.82 | 100.0 | — | 168.0 | |
| 0.76 | 0.98 | 130.0 | 172.0 | 217.0 | 1.26 |

reaction between butyl lithium and THF was shown to be very rapid at room temperature. In addition, however, the viscometric molecular weights \bar{M}_v also are considerably higher than the osmotic \bar{M}_n , indicating a spread in the molecular weight distribution. This can be taken as a sign of an additional reaction between the growing anionic chains and the THF, leading to some early termination of chains.

It is not likely that this partial termination is caused by the presence of impurities in the THF, since this solvent was subjected to very rigorous purification procedures, similar to those used for the hexane solvent. Hence it is much more likely that there is an actual, but slow, reaction between the isoprene anions and the THF itself. Although no information is available concerning such a possible reaction, it is quite logical to assume that an alkenyllithium group would show some reactivity toward THF, obviously less than the more reactive alkyl lithium, but more than the relatively unreactive aromatic lithium obtained in styrene polymerization.

This work was supported by National Science Foundation Grant G-5919.

References

1. Stavelly, F. W., et al., *Ind. Eng. Chem.*, **48**, 778 (1956).
2. Diem, H. E., H. Tucker, and C. F. Gibbs, paper presented at 132nd Meeting, American Chemical Society, September 1957.
3. Morita, H., and A. V. Tobolsky, *J. Am. Chem. Soc.*, **79**, 5853 (1957).
4. Morton, M., R. Milkovich, D. B. McIntyre, and J. L. Bradley, *J. Polymer Sci.*, **1**, 439 (1963).
5. Morton, M., A. A. Rembaum, and J. L. Hall, *J. Polymer Sci.*, **1**, 457 (1963).
6. Carter, H. C., R. L. Scott, and M. Magat, *J. Am. Chem. Soc.*, **68**, 1480 (1946).
7. Brantley, H., M. S. Thesis, University of Akron, 1960.
8. Clarke, R. G., M. S. Thesis, University of Akron, 1959.

Synopsis

A study has been carried out on the molecular weights and their distribution for polyisoprene prepared with butyl lithium as initiator in *n*-hexane and tetrahydrofuran solvents. A stoichiometry of one chain per initiator molecule was found to apply. As in the case of styrene, the initiation reaction in the hydrocarbon solvent was relatively

slow compared to propagation, thus leading to a broadening of the molecular weight distribution. However, narrow distributions were obtained by using a preinitiation technique, whereby all chains had an opportunity of growing simultaneously. In the THF solvent, the molecular weight distribution was somewhat broader ($\bar{M}_v/\bar{M}_n \sim 1.3$) presumably due to a slow competitive chain termination reaction between the growing anionic chains and the solvent, at room temperature.

Résumé

On a entrepris une étude sur la valeur et la distribution des poids moléculaires de polyisoprènes préparés avec du butyl-lithium comme initiateur en solution dans l'hexane et le tétrahydrofurane. On a trouvé une stoechiométrie d'une chaîne par molécule d'initiateur. Comme avec le styrène, la réaction d'initiation dans le solvant hydrocarboné est lente comparée à la propagation, ce qui conduit à un élargissement de la distribution des poids moléculaires. Toutefois on a pu obtenir des distributions étroites grâce à la technique de pré-initiation par laquelle toutes les chaînes ont l'occasion de croître en même temps. Dans le tétrahydrofurane, la distribution des poids moléculaires était plus large ($\bar{M}_v/\bar{M}_n \sim 1.3$) probablement à cause d'une réaction compétitive de terminaison entre les chaînes croissantes anioniques et le solvant, à température de chambre.

Zusammenfassung

Eine Untersuchung des Molekulargewichts und der Molekulargewichtsverteilung wurde an Polyisopren ausgeführt, das mit Butyllithium als Starter in *n*-Hexan- und Tetrahydrofuranlösung hergestellt worden war. Die Stöchiometrie entsprach der Bildung einer Kette auf eine Startermolekel. Wie im Falle des Styrols verlief die Startreaktion in Kohlenwasserstofflösung verhältnismässig langsam im Vergleich zum Wachstum, was zu einer Verbreiterung der Molekulargewichtsverteilung führte. Mit Hilfe eines Vorstartverfahrens, wodurch alle Ketten gleichzeitig wachsen konnten, war es aber möglich enge Verteilungen zu erhalten. In THF-Lösung trat eine etwas breitere Molekulargewichtsverteilung auf ($\bar{M}_v/\bar{M}_n \sim 1,3$), was wahrscheinlich auf eine langsame, kompetitive Kettenabbruchsreaktion zwischen den wachsenden Anionenketten und dem Lösungsmittel bei Raumtemperatur zurückzuführen ist.

Received November 20, 1961

Rheology of Polytetrafluoroethylene

A. V. TOBOLSKY, D. KATZ, and M. TAKAHASHI, *Frick Chemical Laboratory, Princeton University, Princeton, New Jersey*

Introduction

The correlation between the viscoelastic behavior of samples of polytetrafluoroethylene in their rubbery flow region and their molecular weights was described previously.¹

The aim of this work was to continue the investigation of the viscoelastic properties of polytetrafluoroethylene above the melting temperature and one of the polymers used in the previous work was chosen for the study. The points of interest were: (1) the influence of the degree of crystallinity of the polymer on its maximum relaxation time; (2) the relation between the maximum relaxation time and temperature, in particular, the possibility of using the Williams-Landel-Ferry equation² for the case of polytetrafluoroethylene; (3) the application of procedure X for finding some of the characteristic parameters for Teflon and to estimate its polydispersity; (4) the degradation of the polymer.

Materials

The two Teflon samples used for this work were kindly supplied by the Research and Development Division of E. I. du Pont de Nemours & Co. and they were designated B6043-3 and B6043-4. The difference between them is only in their degree of crystallinity at room temperature, the first one being 78% and the second 49% crystalline. These differences were produced by different quenching procedures.

Experimental Procedure

The experiments were carried out by use of a stress relaxation balance box and the values of $\log E_r(t)$ were plotted against time for the different temperatures. From the linear parts of the plots E_m and τ_m were obtained by use of the equation:

$$\log E_r(t) = \log E_m - (t/2.303 \tau_m)$$

In the above equation $E_r(t)$ is the relaxation modulus, τ_m the maximum relaxation and E_m the modulus corresponding to the maximum relaxation time. The time of each experiment was considerably longer than the maximum relaxation time, and the linearity of the plot persisted for long

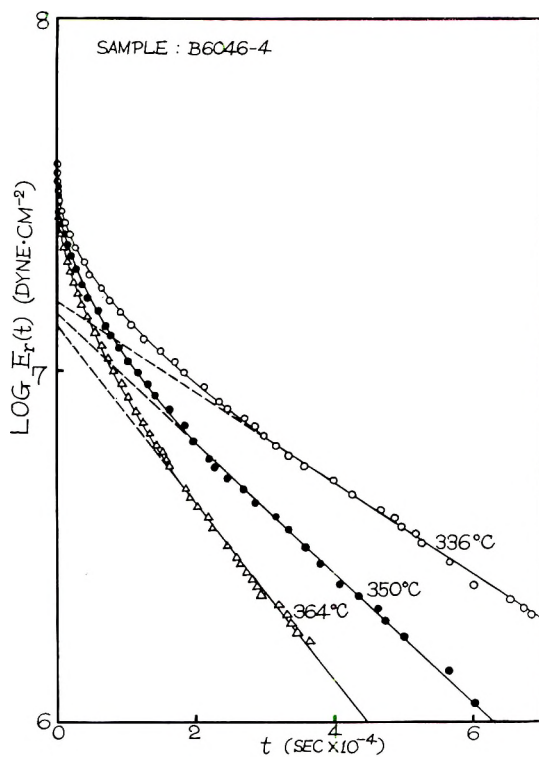


Figure 1.

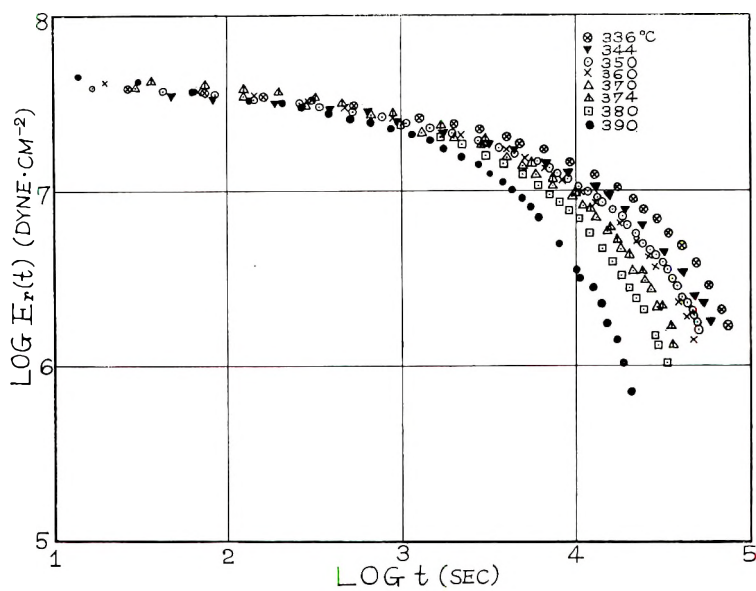


Figure 2.

TABLE I

| Sample | Temperature, °C. | Maximum relaxation time τ_m , sec. | E_m , dyne/cm. ⁻² | $K(T)$ |
|---------|------------------|---|--------------------------------|--------|
| B6046-4 | 336 | 33,900 | 1.57×10^7 | 1.55 |
| | 344 | 28,200 | 1.45 | 1.26 |
| | 350 | 23,500 | 1.47 | 1.00 |
| | 360 | 20,400 | 1.50 | 0.89 |
| | 364 | 17,300 | 1.34 | 0.78 |
| | 370 | 15,100 | 1.60 | 0.72 |
| | 374 | 14,200 | 1.73 | 0.71 |
| | 380 | 12,600 | 1.40 | — |
| | 390 | 6,140 | 1.91 | — |
| B6046-3 | 400 | 4,260 | 1.70 | — |
| | 346 | 31,000 | 1.50 | — |
| | 370 | 17,200 | 1.50 | — |
| | 370 ^a | 16,600 | 1.80 | — |
| | 386 | 10,600 | 1.62 | — |
| | 386 ^a | 6,500 | 0.79 | — |
| | 390 | 8,200 | 1.55 | — |

^a Rerun.

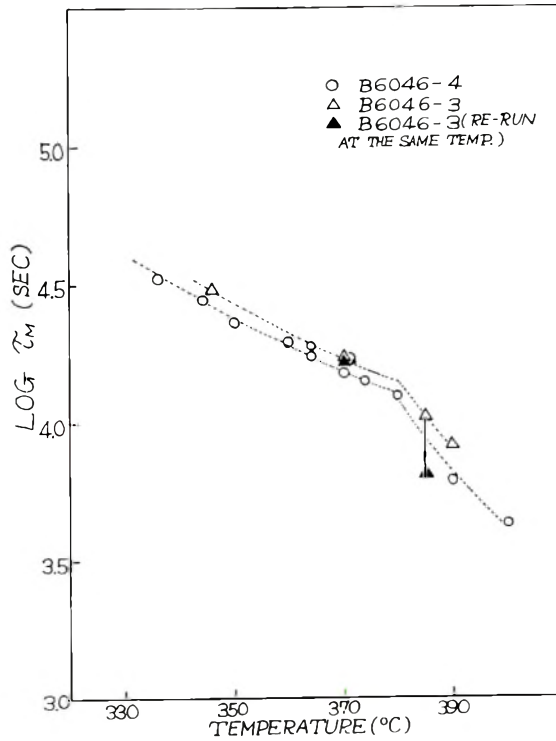


Figure 3.

periods (Fig. 1). The results are listed in Table I and represented in Figures 2 and 3.

Discussion

It may be expected that the Williams-Landel-Ferry equation should be applicable to the relation between $\log \tau_m$ and temperature also in the case of polytetrafluoroethylene. In other words, the equation

$$\log \tau_m = \log A - [17.44(T - T_g)/51.6 + (T - T_g)] + 3.4 \log \bar{n}_w$$

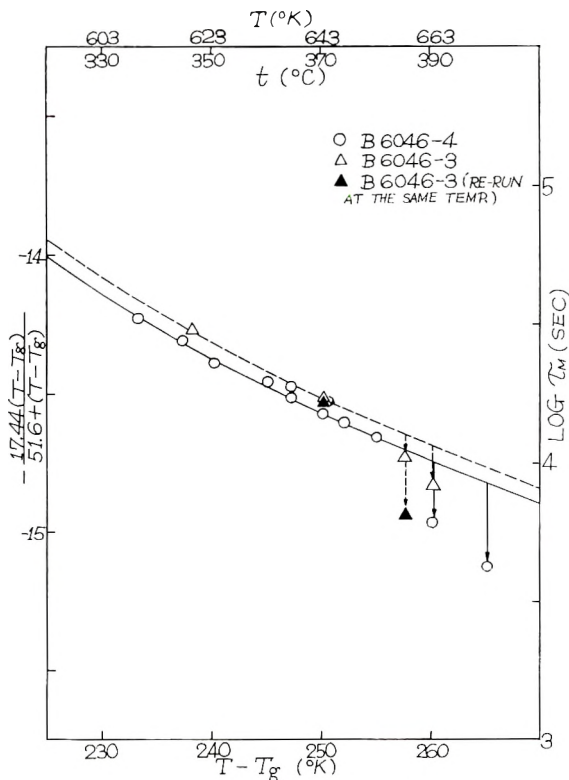


Figure 4.

which was found to be a general one for some other amorphous polymers³⁻⁵ may give the correlation between T_g and relaxation times for Teflon too. In the above equation \bar{n}_w is the weight-average number of links in the chain. A plot of $\log \tau_m$ versus temperature should fall on the calculated line of $-17.44(T - T_g)/[51.6 + (T - T_g)]$ versus $T - T_g$ when $(T - T_g)$ and $(\log \tau_m - \log A - 3.4 \log \bar{n}_w)$ are taken as new horizontal and vertical coordinates, respectively. In a case where there are no data for T_g , A , and \bar{n}_w , T_g can be found by horizontal and vertical sliding of the graph showing the relation between $\log \tau_m$ on the calculated curve of $-[17.44(T - T_g)/51.6 + (T - T_g)]$ versus $T - T_g$. The results

obtained by this procedure are shown in Figure 4, and it can be seen that those points obtained in the experiments below 380°C. show good agreement with the WLF equation, but the data above 380°C. deviate from the mentioned relation. This deviation from the WLF equation above 380°C. seems to be due to the decrease of \bar{n}_w caused by decomposition of the sample at these high temperatures. We found that after repeating the experiment at 370°C. with a previously run sample, the values of the maximum relaxation times agreed within experimental error, but in the case of repetition of the experiment at 386°C. with the sample used once before at that temperature, the maximum relaxation time decreased considerably. The data are shown in Table I and Figures 3 and 4, and they prove that the decomposition of polytetrafluoroethylene becomes appreciable above 380°C.

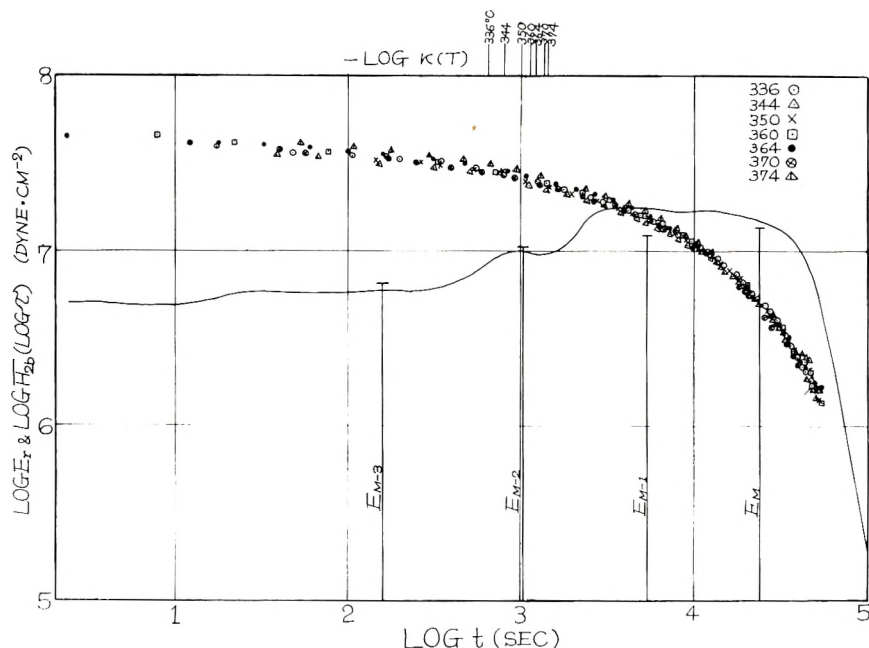


Figure 5.

The good agreement of experimental data below 380°C. with the WLF equation enabled us to obtain the value of 110°C. as the T_0 for polytetrafluoroethylene. This result is fairly close to the value of 127°C. obtained from the measurement of the dynamic modulus.⁶ By application of a method similar to the one used for determination of T_0 , the value of 155°C. was found for the T_s of Teflon.

The fact that the values of τ_m for B6046-3 are almost the same as those of B6046-4 for the same temperatures shows that the viscoelastic behavior of polytetrafluoroethylene in the region of rubbery flow is not affected by the room temperature degree of crystallinity of the sample.

The master curve $E_r(t)$, reduced to 350°C. was computed from the data

shown in Figure 2. The time-temperature superposition principle was applied to the data, and the master curve $\log E_r(t)$ versus $\log t$ is shown in Figure 5. The time factors $K(T)$ obtained are given in Table I. Assuming a continuous distribution of relaxation times, the second approximation of the distribution function $\overline{H}_{2b}(\log \tau)$ was computed at 350°C. and is also shown in Figure 5.

As a maximum relaxation time for polytetrafluoroethylene truly exists, as seen from the linearity of the plot of $\log E_r(t)$ versus t for long times, procedure X was applied, and other characteristic parameters for Teflon were calculated. The values of the E_i and τ_i obtained for sample B6046-4 by procedure X³ are shown in Table II and in Figure 5.

TABLE II
Discrete Relaxation-Time Spectra for Polytetrafluoroethylene

| | $E_i \times 10^7$ | i |
|---------|-------------------|--------|
| m | 1.37 | 24,000 |
| $m - 1$ | 1.22 | 5,400 |
| $m - 2$ | 1.05 | 1,010 |
| $m - 3$ | 0.65 | 158 |

The distribution \overline{H}_{2b} seems to be fairly close to the box distribution function for the region of rubbery flow.

The flow viscosity in shear for this sample at 350°C. was computed from \overline{H}_{2b} by the equations

$$\eta = [1/(3 \times 2.303)] \int_0^\infty \overline{H}_{2b}(\tau) \cdot d\tau = 1.18 \times 10^{11} \text{ dyne sec./cm.}^2$$

$$\eta' = \sum \tau_m E_m / 3 = 1.36 \times 10^{11} \text{ dyne sec./cm.}^2$$

These two values are in satisfactory agreement.

The contribution to the shear viscosity of the maximum relaxation time is

$$\eta'' = \tau_m E_m / 3 = 1.09 \times 10^{11} \text{ dyne sec./cm.}^2$$

Our previous results with polystyrene show that the quantity $\alpha = \eta''/\eta'$ can be used as an indicator for the polydispersity of the sample. For this sample of Teflon $\alpha = 0.81$, which is indicative of a quite sharp molecular weight distribution.

Summary and Conclusions

(1) There seems to be no influence of the degree of crystallinity at room temperature on the viscoelastic behavior of polytetrafluoroethylene above the melting point of the polymer.

(2) The correlation between the maximum relaxation time and temperature is the same as that defined by the Williams-Landel-Ferry equation for other polymers and by its use we obtain a value of $T_g = 110^\circ\text{C.}$ for Teflon.

(3) The degradation of the polymer is appreciable at temperatures above 380°C.

- (4) Procedure X was successfully applied to Teflon.
(5) The molecular weight distribution of the sample we used appeared to be sharp.

References

1. Tobolsky, A. V., D. Katz, and A. Eisenberg, ONR Technical Report RLT-36, *J. Appl. Polymer Sci.*, in press.
2. Williams, M. L., R. F. Landel, and J. D. Ferry, *J. Am. Chem. Soc.*, **77**, 3701 (1955).
3. Tobolsky, A. V., and K. Murakami, *J. Polymer Sci.*, **47**, 55 (1960).
4. Andrews, R. D., and A. V. Tobolsky, *J. Polymer Sci.*, **7**, 221 (1951).
5. Ninomiya, K., *J. Colloid Sci.*, **14**, 49 (1959).
6. McCrum, N. G., *J. Polymer Sci.*, **34**, 355 (1959).
7. Tobolsky, A. V., and K. Murakami, *J. Polymer Sci.*, **40**, 443 (1959).

Synopsis

The rheology of polytetrafluoroethylene above its melting point was studied by the technique of stress relaxation. The temperature shift for the maximum relaxation time at various temperatures fits the WLF equation, if the value of T_g is taken to be 110°C. Degradation of the polymer becomes appreciable above 380°C. Master stress relaxation curves were constructed from the data between 336 and 380°C. The continuous distribution of relaxation times was obtained, and also the discrete distribution of relaxation times by procedure X. The contribution of the maximum relaxation time to the total flow viscosity indicates that the molecular weight distribution of the sample used was narrow.

Résumé

On étudie l'écoulement du polytétrafluoroéthylène au-dessus de son point de fusion, par la technique de relaxation de tension. La variation de température pour le temps de relaxation maximum à diverses températures, s'adapte à l'équation WLF, si la valeur de T_g est prise à 110°C. La dégradation du polymère devient importante au-dessus de 380°C. On construit les principales courbes de relaxation de tension à partir des résultats entre 336 et 380°C. On obtient la distribution continue des temps de relaxation et aussi la distribution discontinue des temps de relaxation par la méthode X. La contribution des temps de relaxation maximum à la viscosité d'écoulement total indique que la distribution de poids moléculaires de l'échantillon est étroite.

Zusammenfassung

Die Rheologie von Polytetrafluoräthylen oberhalb seines Schmelzpunktes wurde mit dem Verfahren der Spannungsrelaxation untersucht. Die Temperaturverschiebung der maximalen Relaxationszeit entspricht bei verschiedenen Temperaturen der WLF-Gleichung, wenn der Wert für T_g mit 110°C angenommen wird. Abbau des Polymeren wird oberhalb 380°C merklich. Verallgemeinerte Spannungsrelaxationskurven wurden aus Daten zwischen 336°C und 380°C konstruiert. Man erhielt die kontinuierliche Verteilung der Relaxationszeiten und ebenso die diskrete Verteilung der Relaxationszeiten durch das Verfahren X. Der Beitrag der maximalen Relaxationszeit zur Gesamtflussviskosität spricht für eine enge Molekulargewichtsverteilung der verwendeten Probe.

Received November 27, 1961

Behavior of Polymer Solutions in a Velocity Field with Parallel Gradient. I. Orientation of Rigid Ellipsoids in a Dilute Solution

RACHELA TAKSERMAN-KROZER and ANDRZEJ ZIABICKI,
*Institute of General Chemistry, Department of Technical Physics,
Warsaw, Poland*

Introduction

There have been numerous theoretical and experimental studies devoted to the problems of molecular orientation, anisotropy of various physical properties, and rheological behavior of solutions and polymer melts flowing in a velocity field with perpendicular gradient, i.e. with a deformation rate tensor:

$$\mathbf{V}_{i,j} = \begin{pmatrix} 0 & q & 0 \\ q & 0 & 0 \\ 0 & 0 & 0 \end{pmatrix}$$

The deformation involved was shearing; such a field occurs always when the flowing liquid is bound within a wall (e.g., in a capillary or couette apparatus). Peterlin and Stuart¹ analyzed theoretically the orientation and intrinsic viscosity of dilute solutions containing rigid particles. Analogous studies for dilute solutions containing flexible, chain macromolecules were carried out by Kuhn and Kuhn,² J. J. Hermans,³ Kirkwood and Riseman,⁴ Ikeda,⁵ Cerf,⁶ Peterlin and Čopić⁷ and others. Several theories concerning the streaming birefringence and viscosity of concentrated solutions and polymer melts flowing in a field with perpendicular velocity gradient have also been published.⁸⁻¹⁰

There is also another velocity field of considerable importance, viz, that with a parallel velocity gradient, characterized by a deformation rate tensor typical for uniaxial elongation:

$$\mathbf{V}_{i,j} = \begin{pmatrix} q & 0 & 0 \\ 0 & -\sigma q & 0 \\ 0 & 0 & -\sigma q \end{pmatrix}$$

where $q = \partial V_x / \partial x$ is the parallel velocity gradient and σ is the Poisson ratio.

The latter field occurs, among others, in free-running vertical jets and in synthetical fibers spun from liquid polymers. The behavior of polymer

liquids in such a field has not been intensively investigated. Recently, a number of experimental works concerning the molecular orientation¹¹ and mechanical aspects of the melt-spinning process,¹² published by one of us with Kędzierska, indicated a great need of systematic theoretical approach.

Since there are no theories of behavior of macromolecular liquids subjected to uniaxial drawing, we have started with investigations involving various simple molecular models. The first two papers in this series deal with the orientation and dissipation of energy in dilute suspensions or solutions containing rigid, ellipsoidal particles.

Definition of the Model

A monodisperse system containing rigid ellipsoids of revolution suspended in an incompressible liquid will be considered. The concentration of ellipsoids is assumed small enough to permit the effects of interaction to be neglected. The deformation rate tensor for a constant velocity gradient q and Poisson ratio $\sigma = 0.5$ may be written as:

$$\mathbf{V}_{i,j} = \begin{pmatrix} q & 0 & 0 \\ 0 & -q/2 & 0 \\ 0 & 0 & -q/2 \end{pmatrix} \quad (1)$$

Equations of Motion of Single Ellipsoid

We will consider the motion of a single ellipsoid. According to Jeffery,¹³ an ellipsoid in a velocity field with deformation rate tensor $\mathbf{V}_{i,j}$ and rotation (ξ, η, ζ) , rotates with an angular velocity, the components of which expressed in a coordinate system $x_1x_2x_3$ directed along the ellipsoid axes a, b, c amount to:

$$\begin{aligned} (b^2 + c^2)\omega_1 &= b^2(\xi + V_{23}) + c^2(\xi - V_{23}) \\ (c^2 + a^2)\omega_2 &= c^2(\eta + V_{13}) + a^2(\eta - V_{13}) \\ (a^2 + b^2)\omega_3 &= a^2(\zeta + V_{12}) + b^2(\zeta - V_{12}) \end{aligned} \quad (2)$$

We shall introduce now a coordinate system $x'_1x'_2x'_3$ fixed in space. Let the directional cosines of the axes with respect to the axes of the new system $x'_1x'_2x'_3$ be $l_1m_1n_1$; $l_2m_2n_2$; $l_3m_3n_3$, respectively, and the components of the deformation rate tensor expressed in coordinates $x'_1x'_2x'_3$ be $\mathbf{V}_{i',j'}$.

The velocity field in the fixed coordinate system is described by the equations:

$$\begin{aligned} V_{x'_1} &= qx'_1 \\ V_{x'_2} &= -1/2qx'_2 \\ V_{x'_3} &= -1/2qx'_3 \end{aligned} \quad (3)$$

The deformation rate tensor:

$$\mathbf{V}_{i',j'} = \begin{pmatrix} q & 0 & 0 \\ 0 & -q/2 & 0 \\ 0 & 0 & -q/2 \end{pmatrix} \quad (4)$$

expressed in the system $x_1x_2x_3$ bounded by the particle will become

$$\mathbf{V}_{ij} = 3q/2 \begin{pmatrix} l_1^2 - 1/3 & l_1l_2 & l_1l_3 \\ \cdot & l_2^2 - 1/3 & l_2l_3 \\ \cdot & \cdot & l_3^2 - 1/2 \end{pmatrix} \tag{5}$$

It may be shown that the rotation components for the considered velocity field are zero:

$$\xi = \eta = \zeta = 0 \tag{6}$$

In view of eqs. 5 and 6, eq. (2) takes the form:

$$\begin{aligned} (b^2 + c^2)\omega_1 &= q(b^2 - c^2)(l_2l_3 - 1/2m_2m_3 - 1/2n_2n_3) \\ (c^2 + a^2)\omega_2 &= q(c^2 - a^2)(l_1l_3 - 1/2m_1m_3 - 1/2n_1n_3) \\ (a^2 + b^2)\omega_3 &= q(a^2 - b^2)(l_1l_2 - 1/2m_1m_2 - 1/2n_1n_2) \end{aligned} \tag{7}$$

For an ellipsoid of revolution ($a \neq b = c$), making use of the general properties of directional cosines, we obtain:

$$\begin{aligned} \omega_1 &= 0 \\ \omega_2 &= -3/2qRl_1l_3 \\ \omega_3 &= -3/2qRl_1l_2 \end{aligned} \tag{8}$$

where

$$R = (a^2 - b^2)/(a^2 + b^2)$$

When the coefficient R lies between 0 and +1, the ellipsoids are elongated (rods). Flattened disks are characterized by R values between 0 and -1. $R = 0$ corresponds to a sphere, and $R = \pm 1$ to infinitely elongated or infinitely flattened particles respectively.

We will introduce the Euler angles φ, ψ, θ , to describe the motion of the coordinate system $x_1x_2x_3$ with reference to the fixed system $x'_1x'_2x'_3$ (Fig. 1).

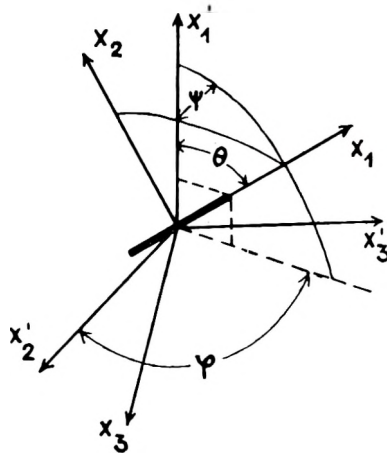


Figure 1.

Here, φ is an angle between the planes $x'_1x'_2$ and $x_1x'_1$; ψ is that between $x_1x'_1$ and x_1x_2 , and θ is the angle between axes x_1 and x'_1 . The directional cosines $l_1l_2l_3$ may then be written as follows:

$$\begin{aligned} l_1 &= -\cos \theta \\ l_2 &= \cos \psi \sin \theta \\ l_3 &= -\sin \psi \sin \theta \end{aligned} \quad (9)$$

Therefore, from eq. 8:

$$\begin{aligned} \omega_1 &= 0 \\ \omega_2 &= -3/2qR \sin \psi \sin \theta \cos \theta \\ \omega_3 &= -3/2qR \cos \psi \sin \theta \cos \theta \end{aligned} \quad (10)$$

It is known, that angular velocity components are related to the Euler angles:

$$\begin{aligned} \omega_1 &= \dot{\varphi} \cos \theta + \dot{\psi} \\ \omega_2 &= -\dot{\varphi} \cos \psi \sin \theta + \dot{\theta} \sin \psi \\ \omega_3 &= \dot{\varphi} \sin \psi \sin \theta + \dot{\theta} \cos \psi \end{aligned} \quad (11)$$

From the equation systems 10 and 11 we obtain ultimately eqs. (12):*

$$\begin{aligned} \dot{\varphi} &= 0 \\ \dot{\psi} &= 0 \\ \dot{\theta} &= -3/2qR \sin \theta \cos \theta \\ &= -3/4qR \sin 2\theta \end{aligned} \quad (12)$$

The angular velocity of an ellipsoid has only the θ component different from zero, i.e., the rotation proceeds exclusively in the direction of changing the angle between the axis of symmetry of the ellipsoid and the direction of tension. The velocity $\dot{\theta}$ depends in an equal manner on velocity gradient and shape coefficient R .

An integration of eq. (12) gives the trajectory:

$$\tan \theta = \exp \{ -3/2qR(t - t_0) \} \quad (13)$$

It is apparent from eqs. (12) that the rotation velocity is different from zero only for nonspherical particles ($R \neq 0$). In Figure 2 there are given the relations $\dot{\theta}$ versus θ . It is apparent that $\dot{\theta}$ is zero for θ equal to $\pi/2$ and zero and reaches its extreme values at $\theta = \pi/4$. The positions $\theta = 0$ and $\theta = \pi/2$, however, are not equivalent from the viewpoint of equilibrium

* A similar formula, $\dot{\theta} = -1/2qR \sin 2\theta$ was given by Peterlin¹⁴ for the ultrasonic field. This result corresponds to the velocity field with deformation rate tensor:

$$\mathbf{v}_{i,j} = \begin{pmatrix} q & 0 & 0 \\ 0 & 0 & 0 \\ 0 & 0 & 0 \end{pmatrix}$$

In an early paper by one of us¹¹ a similar problem has also been discussed. However the equation of orientation given there (p. 26, eq. 8) is not valid for the case considered here. It was derived for a two-dimensional problem with $\mathbf{V} = (qx, 0)$ and $R = 1$.

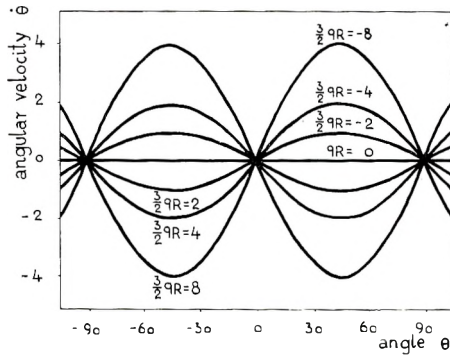


Fig. 2. Angular velocity $\dot{\theta}$ vs. orientation angle θ .

stability. Let us consider an elongated ellipsoid with its axis of symmetry placed originally at $\theta = \pi/2$ (Fig. 3). The velocity field does not cause any rotation as long as θ remains $\pi/2$. The slightest deviation from this position of $d\theta$ however, brings about an angular velocity:

$$\begin{aligned} \dot{\theta} &= -3/4qR \sin(\pi + 2d\theta) \\ &= 3/4qR \sin 2d\theta \end{aligned}$$

It is quite evident, that in the case of elongated ellipsoids (R positive) the direction of further rotation will be consistent with that of the original deviation; for disks (R negative) it will be opposite. Therefore the position $\theta = \pi/2$ is connected with a stable equilibrium for disks, an unstable one for rods. Analogous considerations with respect to the position $\theta = 0$ lead to the conclusion that the latter determines a stable equilibrium for rods, and an unstable one for disks.

In other words, a velocity field with parallel velocity gradient causes such a rotation of ellipsoids that an elongated particle tends to occupy a position with its axis of symmetry parallel to the direction of tension; a

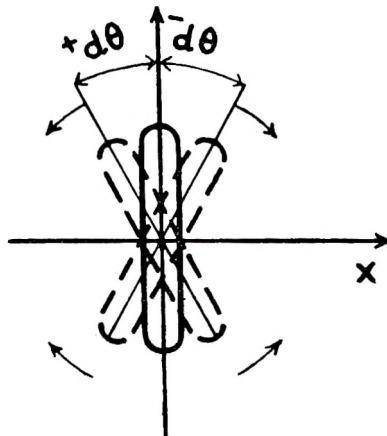


Figure 3.

flattened disk tends to a position with its symmetry plane parallel to that direction.

Tan θ , describing the trajectory [eq. (3)] is an exponential, aperiodic function of time, decreasing to zero for $R > 0$ and increasing to infinity for $R < 0$.

It should be noted that the character of ellipsoid motion in a velocity field with perpendicular gradient (cf. introduction) is quite different. According to Jeffery,¹³ there are three different from zero velocity components:

$$\begin{aligned}\dot{\varphi} &= q/2(1 + R \cos 2\varphi) \\ \dot{\psi} &= qR/2(\cos 2\varphi \cos \theta) \\ \dot{\theta} &= qR/4(\sin 2\varphi \sin 2\theta)\end{aligned}$$

In the latter case, ellipsoids rotate periodically, and there are no equilibrium positions for particles with finite dimensions ($R^2 < 1$). The rotation does not vanish even for spherical particles.

The eqs. (12) describe with high accuracy the hydrodynamic behavior of large particles (above 10^{-4} cm.). In the case of macromolecules, the dimensions of which are of the order 10^{-6} cm., Brownian motion should be taken into account, and the orientation treated statistically.

Spatial Distribution of Ellipsoid Axes

A rigid macromolecule in a liquid medium will undergo the action of: (a) the velocity field and (b) diffusion (Brownian motion). In order to describe the spatial orientation of macromolecules, a distribution function $\rho(t, \varphi, \theta)$ was introduced which determines the density of probability of finding an axis of symmetry of the ellipsoid within an elementary solid angle in time t .

The distribution function must satisfy an equation of continuity:

$$\partial\rho/\partial t + \text{div } \vec{J} = 0 \quad (14)$$

The intensity of stream \vec{J} is a sum of two components:

$$\vec{J}_q = \rho \vec{\omega} = \rho(\dot{\varphi} \sin \theta, \dot{\theta}) \quad (15a)$$

and

$$\vec{J}_D = -D \text{grad } \rho = -D[(1/\sin \theta)(\partial\rho/\partial\varphi), (\partial\rho/\partial\theta)] \quad (15b)$$

arising from the hydrodynamic action of velocity field with gradient q and the rotational diffusion with diffusion constant D , respectively.

Considering the equations of motion [eqs. (12)] and substituting eqs. (15a) and (15b) into eq. (14) we obtain a differential equation for the distribution function:

$$\begin{aligned}\partial\rho/\partial t = \partial^2\rho/\partial\theta^2 + \\ (\cot \theta + 3/4\alpha R \sin 2\theta)\partial\rho/\partial\theta + 3/2\alpha R(3 \cos^2 \theta - 1)\rho\end{aligned} \quad (16)$$

where the parameters are

$$\begin{aligned} \beta &= 1/D \\ \alpha &= q/D \end{aligned}$$

It was attempted to find the solution of eq. (16) in the form:

$$\rho(t, \theta) = \sum_{k=0}^{\infty} T_k(t)F_k(\theta) \tag{17}$$

Separation of variables gives:

$$\beta(1/T_k)dT_k/dt = -\lambda_k \tag{18}$$

$$\begin{aligned} d^2F_k/d\theta^2 + (\cot \theta + {}^3/4\alpha R \sin 2\theta) dF_k/d\theta \\ + [{}^3/2\alpha R(3 \cos^2 \theta - 1) + \lambda_k]F_k = 0 \end{aligned} \tag{19}$$

where λ_k are eigenvalues.

For the determination of the eigenvalues λ the function F_k was developed in a series of Legendre polynomials:

$$F_k(\theta) = \sum_{n=0}^{\infty} b_n^k P_{2n} \tag{20}$$

On substituting eq. (20) into eq. (19) and making use of the properties of Legendre polynomials, a recurrence formula for coefficients b_n^k results:

$$\begin{aligned} \frac{(2n - 1)(2n)(2n + 1)}{(4n - 3)(4n - 1)} \alpha R b_{n-1}^k \\ + \left[\frac{(2n + 1)^2 (2n + 3)}{(4n + 1)(4n + 3)} \alpha R - \frac{(2n - 2)(2n)^2}{(4n - 1)(4n + 1)} \alpha R \right. \\ \left. - \alpha R - {}^4/3 n(2n + 1) + {}^2/3\lambda_k \right] b_n^k - \frac{2n(2n + 1)(2n + 2)}{(4n + 3)(4n + 5)} \alpha R b_{n+1}^k = 0 \end{aligned} \tag{21}$$

A characteristic equation of the infinite system of eqs. (21) is:

$$\begin{bmatrix} -\lambda & 0 & 0 & 0 & \dots \\ -3\alpha R & (6 - {}^3/7\alpha R - \lambda) & {}^4/7\alpha R & 0 & \dots \\ 0 & -{}^{18}/7\alpha R & (-{}^{30}/77\alpha R + 20 - \lambda) & {}^{180}/143\alpha R & \dots \\ 0 & 0 & -{}^{35}/11\alpha R & (42 - {}^{21}/55\alpha R - \lambda) & \dots \\ \dots & \dots & \dots & \dots & \dots \end{bmatrix} = 0 \tag{22}$$

The application of the theory of perturbations¹⁵ gives in the second approximation:

$$\lambda_k = C_{kk} - \sum_{l \neq k} \frac{C_{kl}C_{lk}}{C_{ll} - C_{kk}} \tag{23}$$

where C_{lk} are elements of the determinant in eq. (22).

Integration of eq. (18) gives the time dependence of the distribution function:

$$T_k(t) = \exp \{ -\lambda_k t D \} \quad (24)$$

Since all the λ_k values are real, $T_k(t)$ is an aperiodic function of time, tending to unity.

$\lambda_0 = 0$ is the eigenvalue of function F_0 describing the distribution of ellipsoids axes in the steady state.

$$\lambda_1 = \frac{783(\alpha R)^2 - 3108\alpha R + 45276}{21\alpha R + 7546}$$

Time $t_u = -1/(d \ln T_1/dt) = \frac{1}{D\lambda_1}$ is a measure of the rate of settlement of the equilibrium. When the velocity gradient is zero we obtain a relaxation time τ a constant characteristic of the system:

$$\lim_{q \rightarrow 0} t_u = \tau = 1/6D$$

Peterlin and Stuart¹ obtained the same value for τ when they analyzed the orientation of ellipsoids in the perpendicular-gradient velocity field.

For finite values of q and D , t_u depends on the relaxation time and the parameter αR :

$$t_u = \tau f(\alpha R)$$

With increasing q , t_u increases.

In other words, the smaller the relaxation time of the system and the smaller the velocity gradient q , the sooner the steady state will be reached.

The distribution function $\rho(t, \theta)$ according to eq. (17) with a normalization condition:

$$\int_0^{2\pi} \int_0^\pi \rho(t, \theta) \sin \theta d\varphi d\theta = 1 \quad (25)$$

may be in the first approximation written as:

$$\rho(t, \theta) = F_0 - [F_0 - (1/4\pi)] \exp \{ -\lambda_1 t D \} \quad (26)$$

where F_0 is the steady-state distribution function.

Steady-State Distribution

The steady-state distribution function F_0 satisfies the equation:

$$d^2 F_0 / d\theta^2 + (\cot \theta + 3/4 \alpha R \sin 2\theta) dF_0 / d\theta + 3/2 \alpha R (3 \cos^2 \theta - 1) F_0 = 0 \quad (27)$$

The solution of this equation will be obtained by means of the double series:

$$F_0(\theta) = \sum_{n=0}^{\infty} \sum_{i=0}^{\infty} a_{ni} (\alpha R)^i P_{2n} \quad (28)$$

where the coefficients a_{ni} are determined by the recurrence formula:

$$3n(2n + 1)a_{ni} = \frac{(2n - 1)(2n)(2n + 1)}{(4n - 3)(4n - 1)} \bar{a}_{n-1,i-1} + \left[\frac{(2n + 1)^2(2n + 3)}{(4n + 1)(4n + 3)} - \frac{(2n - 2)(2n)^2}{(4n - 1)(4n + 1)} - 1 \right] a_{n,i-1} - \frac{2n(2n + 1)(2n + 2)}{(4n + 3)(4n + 5)} a_{n+1,i-1} \quad (29)$$

Hence ultimately:

$$F_0(\theta) = \frac{1}{4\pi} \left\{ 1 + \frac{1}{4}(\alpha R)(3 \cos^2 \theta - 1) + \frac{9}{4}(\alpha R)^2 \left[\frac{1}{126}(3 \cos^2 \theta - 1) + \frac{1}{280}(35 \cos^4 \theta - 30 \cos^2 \theta + 3) \right] + (\alpha R)^3 [\dots] + \dots \right\} \quad (30)$$

For $\alpha R \rightarrow \pm \infty$ we obtain an asymptotic form of eq. (27):

$$\frac{1}{2} \sin 2\theta \frac{dF_0}{d\theta} + (3 \cos^2 \theta - 1)F_0 = 0 \quad (31)$$

Then, for elongated ellipsoids ($R > 0$):

$$\begin{aligned} F_0 &= 0 \text{ at } \theta \neq 0 \\ F_0 &= \infty \text{ at } \theta = 0 \end{aligned} \quad (32a)$$

and for flattened ellipsoids ($R < 0$):

$$\begin{aligned} F_0 &= 0 \text{ at } \theta \neq \pi/2 \\ F_0 &= \infty \text{ at } \theta = \pi/2 \end{aligned} \quad (32b)$$

The asymptotical distribution is entirely consistent with the positions of stable equilibrium as follows from hydrodynamic considerations.

In Figure 4 there are shown the steady-state distribution functions $F_0(\theta)$

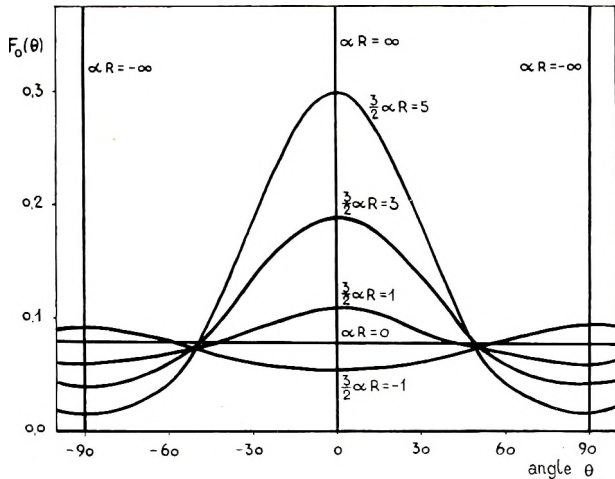


Fig. 4. Steady-state distribution function $F_0(\theta)$ of axes of symmetry of ellipsoids

for a number values of αR . The distribution functions have extremes at $\theta = 0$ and $\theta = \pi/2$, the heights of these extremes increasing with absolute values of αR .

In the case $R = 0$ (velocity gradient $q = 0$ or diffusion constant $D = \infty$; or involved particles are spherical, $R = 0$), the distribution of axes of symmetry is random: $F_0 = \text{constant} = 1/4\pi$. A uniform distribution is connected with infinitely large R values.

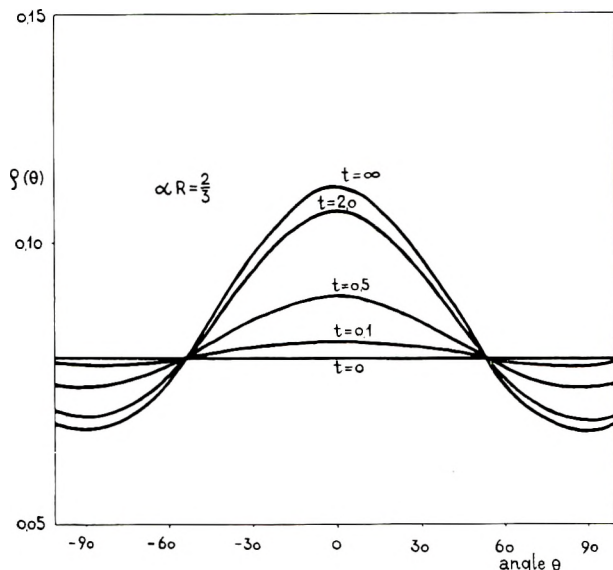


Fig. 5. Time-dependent distribution function $\rho(t, \theta)$

In Figure 5 there is presented the time-dependent distribution function for rods ($p = a/b = 8$; $R = 2/3$). It is apparent that the original distribution ($t = 0$) is random, then becomes more and more bell-shaped, tending asymptotically to the steady-state distribution with increasing time.

Axial Orientation Factor

For the characterization of the mean degree of orientation we considered a factor of orientation, defined as the ratio of polarization anisotropy of the given system to that of a system containing the same number of particles, ideally extended and parallelized along the one direction (axis of orientation)

$$f = (\sigma_{\parallel} - \sigma_{\perp}) / (\sigma_{\parallel} - \sigma_{\perp})_t \quad (33)$$

It is required that interaction and internal field effects¹¹ be neglected in the summation of polarization components.

The orientation factor f is approximately proportional to the birefringence. For a system of rigid particles it amounts to:¹⁶

$$f = 1 - \frac{3}{2} \overline{\sin^2 \theta} \tag{34}$$

According to the distribution function [eq. (30)] the mean square of $\sin \theta$ is:

$$\begin{aligned} \overline{\sin^2 \theta} &= (4\pi/3) \sum_0^\infty \sum_0^\infty (\alpha R)^i a_{ni} \int_0^\pi P_{2n}(P_0 - P_2) \sin \theta d\theta \\ &= (4\pi/3) [2a_\infty - (2/5) \sum_1^\infty (\alpha R)^i a_{1i}] \end{aligned} \tag{35}$$

and the axial orientation factor for the steady state is:

$$\begin{aligned} f_0 &= (7/5) [(\alpha R/14) + (\alpha R/14)^2 \\ &\quad - (7/5)(\alpha R/14)^3 + (\alpha R/14)^4(\dots) + \dots] \end{aligned} \tag{36}$$

The relation between f_0 and α for various ellipsoids is shown in Figure 6. At $\alpha = 0$ (velocity gradient $q = 0$ or diffusion constant $D = \infty$) the orien-

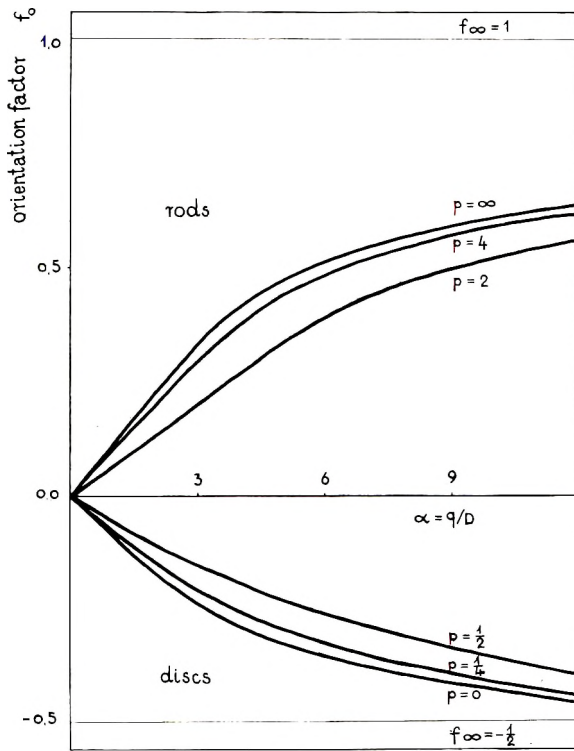


Fig. 6 Steady-state axial orientation factor f_0 vs. velocity gradient/diffusion constant ratio α .

tation factor is zero and the system does not exhibit any anisotropy of physical properties. At $\alpha = \infty$ (infinite velocity gradient $q = \infty$ or zero diffusion constant $D = 0$), the orientation factor for nonspherical par-

ticles ($R \neq 0$) according to asymptotical distribution [eqs. (32a) and (32b)] is:

$$\begin{aligned} f_0 &= 1 \text{ for rods } (R > 0) \\ f_0 &= -1/2 \text{ for disks } (R < 0) \end{aligned}$$

The negative values of f_0 for disks (Fig. 6.) arise from the fact that the axes of symmetry of disks tend to the perpendicular positions with respect of orientation.

The time dependence of orientation factor as resulting from the distribution function [eq. (26)] is given by:

$$f = f_0(1 - \exp \{-tD\lambda_1\}) \quad (37)$$

The latter relation for $\alpha R = 2/3$ and $D = 1/6$ is plotted in Figure 7.

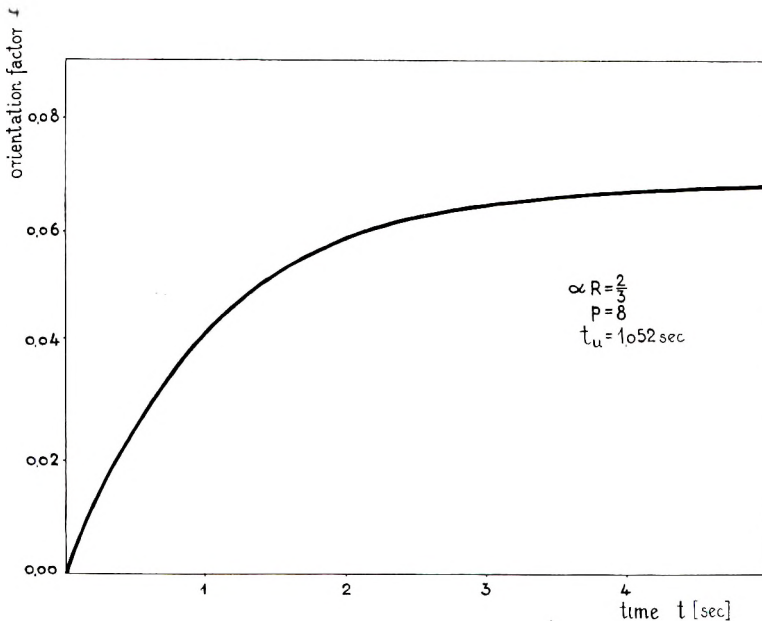


Fig. 7. Time-dependent orientation factor f vs. time t .

It is evident from Figure 6 that the absolute values of f_0 for the same values of α are less for disks than for rods. These differences may be explained in terms of the symmetry of the velocity field. The parallel-gradient velocity field exhibits uniaxial symmetry. In such a field orientation of rods, the longer axes of which tend to occupy positions parallel to the direction of tension, is complete; in the case of disks, the angles between their short axes (axes of symmetry) and the direction of tension do not define completely their orientations. There remains a freedom with respect to the orientation in the plane normal to the axis of orientation (see Fig. 8). For complete orientation of disks a field with biaxial sym-

metry would be needed. This condition is fulfilled in the velocity field with perpendicular gradient, where actually the absolute values of f_0 are equal for disks and rods.¹

On comparing our results with those obtained by Peterlin and Stuart for the perpendicular-gradient field¹ some further differences become evident. Asymptotic values of the orientation factor obtained by Peterlin

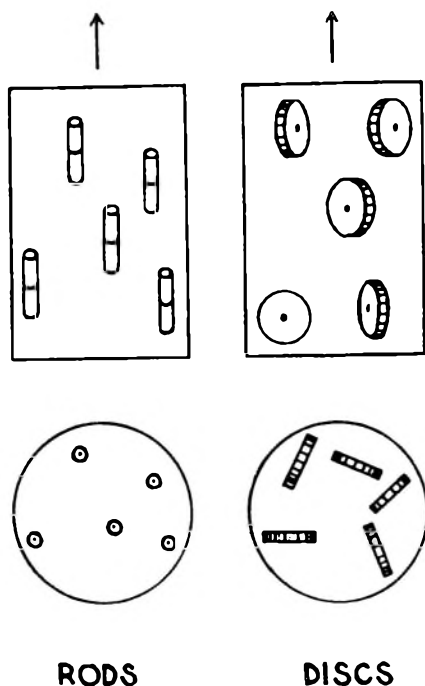


Fig. 8. Scheme of orientation of rods and disks in a field with uniaxial symmetry.

and Stuart depend on the shape of ellipsoids; even in a velocity field with an infinite q/D ratio not all ellipsoids may be fully oriented. The maximal degree of orientation ($f = 1$) may be reached only by infinitely elongated or infinitely flattened ellipsoids at $\alpha = \infty$.

Discussion

It has been shown that the action of a velocity field with a velocity gradient parallel to the direction of tension together with Brownian motion brings about such an orientation of rigid ellipsoidal particles that the maximum distribution density corresponds to the position of the axes of symmetry or symmetry planes parallel to the direction of tension for rods and disks, respectively.

The factor of axial orientation f characterizing the width of the distribution curve, monotonically increases with αR from $-1/2$ for $\alpha R = -\infty$ (disks in a field with infinite q/D ratio) to $+1$ for $\alpha R = +\infty$ (rods in the same field).

The distribution function and orientation factor are aperiodic exponential functions of time, tending to a definite steady state. The rate of settlement of equilibrium depends on the relaxation time of the system $\tau = 1/6D$ as well as on the parameter αR .

The orientation of rigid particles in a field with parallel velocity gradient evidently differs from that found when common shear flow is involved (velocity field with perpendicular gradient).

References

1. Peterlin, A., *Z. Physik.*, **111**, 232 (1938); A. Peterlin and H. A. Stuart, *ibid.*, **112**, 1 (1939).
2. Kuhn, W., and H. Kuhn, *Helv. Chim. Acta*, **26**, 1394 (1943).
3. Hermans, J. J., *Physica*, **10**, 777 (1942).
4. Kirkwood, J. G., and J. Riseman, *J. Chem. Phys.*, **16**, 6 (1948).
5. Ikeda, Y., *J. Phys. Soc. Japan*, **12**, 378 (1957).
6. Cerf, R., *J. phys. radium*, **19**, 122 (1958).
7. Peterlin, A., and M. Čopič, *J. Appl. Phys.*, **27**, 434 (1956).
8. Bueche, F., *J. Chem. Phys.*, **25**, 599 (1956); *J. Polymer Sci.*, **43**, 527 (1960).
9. Lodge, A. S., *Trans. Faraday Soc.*, **52**, 120 (1956).
10. Gillespie, T., *J. Polymer Sci.*, **46**, 383 (1960).
11. Ziabicki, A., and K. Kędzierska, *J. Appl. Polymer Sci.*, **2**, 14, 24 (1959); *ibid.*, **6**, 111, 361 (1962).
12. Ziabicki, A., and K. Kędzierska, *Kolloid Z.*, **171**, 51, 111 (1960); *ibid.*, **175**, 14 (1961).
13. Jeffery, G. B., *Proc. Roy. Soc. (London)*, **A102**, 161 (1922).
14. Peterlin, A., *J. phys. radium*, **11**, 45 (1948).
15. Zimm, B., G. Roe, and L. Epstein, *J. Chem. Phys.*, **24**, 279 (1956).
16. Hermans, J. J., in *Contribution to the Physics of Cellulose Fibres*, Elsevier, Amsterdam, 1946, p. 195.

Synopsis

The spatial orientation of rigid ellipsoidal particles was analyzed as proceeding in a dilute solution flowing in a velocity field with parallel gradient, i.e., in a field characterized by the deformation rate tensor:

$$\mathbf{V}_{ij} = \begin{pmatrix} q & 0 & 0 \\ 0 & -1/2q & 0 \\ 0 & 0 & -1/2q \end{pmatrix}$$

On the basis of general relations given by Jeffery, the hydrodynamic equations of motion for a single ellipsoid were obtained as $\dot{\psi} = 0$, $\dot{\varphi} = 0$, $\dot{\theta} = -2/3qR \sin 2\theta$, where $q = \partial V_x / \partial x$ is the parallel velocity gradient and $R = (a^2 - b^2)/(a^2 + b^2)$ is the shape coefficient of ellipsoids. Considering the action of velocity field and that of Brownian motion (rotational diffusion), a distribution density function $\rho(t, \theta)$ was derived, which describes the spatial orientation of the axes of symmetry of the ellipsoids:

$$\rho(t, \theta) = F_0 - [F_0 - (1/4\pi)] \exp \{-\lambda_1 tD\}$$

where

$$F_0(\theta) = (1/4\pi) \{ 1 + (\alpha R/4)(3 \cos^2 \theta - 1) + (9/4)(\alpha R)^2 [\dots] + \dots \}$$

is the steady-state distribution. In a similar way, the axial orientation factor $f_0 = 1 - 3/2 \sin^2 \theta$ was obtained:

$$f_0 = (7/5) [(\alpha R/14) + (\alpha R/14)^2 - (7/5)(\alpha R/14)^3 + (\alpha R/14)^4 (\dots) + \dots]$$

where $\alpha = q/D$ is the velocity gradient/diffusion constant ratio. The effects of ellipsoid shape, velocity gradient, and diffusion rate were discussed. The results were compared with those obtained by other authors, studying the orientation in a shear flow (velocity field with perpendicular gradient).

Résumé

L'orientation spatiale de particules ellipsoïdales rigides a été analysée sur la base d'une solution diluée s'écoulant dans un champ de vitesse à gradient parallèle c.à.d. dans un champ caractérisé par le tenseur de vitesse de déformation:

$$\mathbf{v}_{ij} = \begin{pmatrix} q & 0 & 0 \\ 0 & -1/2q & 0 \\ 0 & 0 & -1/2q \end{pmatrix}$$

Sur la base de relations générales de Jeffery on peut obtenir les équations hydrodynamique du mouvement pour un ellipsoïde isolé: $\dot{\psi} = 0$; $\dot{\varphi} = 0$; $\dot{\theta} = -3/4 qR \sin 2\theta$ où $q = \partial V_x / \partial x$ est le gradient parallèle de vitesse et $R = (a^2 - b^2)/(a^2 + b^2)$ est le coefficient de configuration des ellipsoïdes. En considérant l'action d'un champ de vitesse et des mouvements Browniens (diffusion rotationnelle) on peut dériver une fonction de distribution de densité $\rho(t, \theta)$ qui décrit l'orientation spatiale des axes de symétrie des ellipsoïdes:

$$\rho(t, \theta) = F_0 - [F_0 - (1/4\pi)] \exp \{-\lambda_1 tD\}$$

où $F_0(\theta) = 1/4\pi \{1 + (\alpha R/4)(3 \cos^2 \theta - 1) + (9/4)(\alpha R)^2[\dots] + \dots\}$ est la distribution Stationnaire. Le facteur d'orientation axiale $f_0 = 1 - 3/2 \overline{\sin^2 \theta}$ a été obtenu de façon analogue:

$$f_0 = 7/5[\alpha R/14 + (\alpha R/14)^2 - 7/5(\alpha R/14)^3 + (\alpha R/14)^4(\dots) + \dots]$$

où $\alpha = q/D$ est le rapport gradient de vitesse versus constante de diffusion. L'influence de la forme des ellipsoïdes du gradient de vitesse et de la vitesse de diffusion a été discutée. Les résultats sont comparés à ceux obtenus par d'autres auteurs lors de l'étude de l'orientation lors d'un écoulement dans un champ de vitesse à gradient perpendiculaire.

Zusammenfassung

Eine Analyse der räumlichen Orientierung von starren, ellipsoidförmigen Teilchen in verdünnter Lösung bei Strömung in einem Geschwindigkeitsfeld mit parallelem Gradienten, d.h. in einem durch den Deformationsgeschwindigkeitstensor:

$$\mathbf{v}_{ij} = \begin{pmatrix} q & 0 & 0 \\ 0 & -1/2q & 0 \\ 0 & 0 & -1/2q \end{pmatrix}$$

charakterisierten Feld, wurde durchgeführt. Auf Grundlage der allgemeinen, von Jeffery angegebenen Beziehungen, wurden die hydrodynamischen Bewegungsgleichungen für ein einzelnes Ellipsoid erhalten: $\dot{\psi} = 0$; $\dot{\varphi} = 0$; $\dot{\theta} = -3/4 qR \sin 2\theta$; wo $q = \partial V_x / \partial x$ der Parallelgeschwindigkeitsgradient und $R = (a^2 - b^2)/(a^2 + b^2)$ der Gestaltsfaktor der Ellipsoide ist. Unter Berücksichtigung der Wirkung des Geschwindigkeitsfeldes und der Brownschen Bewegung (Rotationsdiffusion) wurde eine Verteilungsdichtefunktion $\rho(t, \theta)$ abgeleitet, welche die räumliche Orientierung der Symmetrieachsen der Ellipsoide angibt.

$$\rho(t, \theta) = F_0 - [F_0 - (1/4)\pi] \exp \{-\lambda_1 tD\}$$

$$\text{wo } F_0(\theta) = \{1 + \alpha R/4(3 \cos^2 \theta - 1) + 9/4(\alpha R)^2[\dots] + \dots\}$$

die Verteilung im stationären Zustand ist. In ähnlicher Weise wurde der axiale Orientierungsfaktor $f_0 = 1 - \frac{3}{2} \overline{\sin^2 \theta}$ erhalten:

$$f_0 = \frac{7}{5} [\alpha R/14 + (\alpha R/14)^2 - 7/5 (\alpha R/14)^3 + (\alpha R/14)^4 (\dots) + \dots]$$

wo $\alpha = q/D$ das Verhältnis Geschwindigkeitsgradient zu Diffusionskonstante ist. Der Einfluss der Form der Ellipsoide, des Geschwindigkeitsgradienten und der Diffusionsgeschwindigkeit wurde diskutiert. Die Ergebnisse wurden mit den von anderen Autoren bei der Untersuchung der Orientierung bei Strömung unter Scherung (Geschwindigkeitsfeld mit senkrechten Gradienten) erhaltenen verglichen.

Received October 11, 1961

Behavior of Polymer Solutions in a Velocity Field with Parallel Gradient. II. Viscosity of Dilute Solutions Containing Rigid Ellipsoids

RACHELA TAKSERMAN-KROZER and ANDRZEJ ZIABICKI,
*Institute of General Chemistry, Department of Technical Physics,
Warsaw, Poland*

Introduction

In the previous paper¹ there was derived the distribution function of ellipsoids axes and axial orientation factor, as occurring when a dilute solution flows in a velocity field with parallel gradient. It is the purpose of the present paper to give the relations of specific viscosity of solutions, and to discuss the effects of velocity gradient, diffusion constant, and shape of ellipsoids.

Rate of Energy Dissipation in a Liquid Due to the Motion of a Rigid Ellipsoid

The rate of energy dissipation dW/dt in a liquid of viscosity η_0 due to the motion of a single ellipsoid with half-axes $a \neq b = c$ (rotational ellipsoid) amounts to:²

$$\frac{dW}{dt} = \frac{16}{3} \pi \eta_0 \left[\frac{\alpha_0'' V_{11}^2}{2b^2 \alpha_0' \beta_0''} + \frac{V_{22}^2 + V_{33}^2 + 2V_{23}^2}{2b^2 \alpha_0'} + \frac{2(V_{13}^2 + V_{12}^2)}{\beta_0'(a^2 + b^2)} \right] \quad (1)$$

where the V_{ij} are components of the deformation rate tensor. In a velocity field with parallel gradient, the deformation rate tensor expressed in the spatially fixed system of coordinates $x'_1 x'_2 x'_3$ is given by:¹

$$V_{i'j'} = \begin{pmatrix} q & 0 & 0 \\ 0 & -q/2 & 0 \\ 0 & 0 & -q/2 \end{pmatrix} \quad (2)$$

Considering the coordinate system $x_1 x_2 x_3$ bounded by an ellipsoid, and introducing the Euler angles φ, ψ, θ , to describe the relative motion of the latter system with reference to the first one, we obtain:

$$V_{ij} = \frac{3}{2} q \begin{pmatrix} \cos^2 \theta - (1/3) & -(q/2) \cos \psi \sin 2\theta & (q/2) \sin \psi \sin 2\theta \\ \cdot & \cos^2 \psi \sin^2 \theta - (1/3) & -(q/2) \sin 2\psi \sin^2 \theta \\ \cdot & \cdot & \sin^2 \psi \sin^2 \theta - (1/3) \end{pmatrix} \quad (3)$$

The parameters in eq. (1) are integrals:

$$\begin{aligned}\alpha_0' &= \int_0^\infty dx / [(a^2 + x)^{1/2}(b^2 + x)^3] \\ \alpha_0'' &= \int_0^\infty x dx / [(a^2 + x)^{1/2}(b^2 + x)^3] \\ \beta_0' &= \int_0^\infty dx / [(a^2 + x)^{3/2}(b^2 + x)^2] \\ \beta_0'' &= \int_0^\infty x dx / [(a^2 + x)^{3/2}(b^2 + x)^2]\end{aligned}$$

For longated ellipsoids (rods) with an axial ratio $p = a/b > 1$ the integrals amount to:

$$\begin{aligned}\overline{\alpha_0'} &= ab^4\alpha_0' = \frac{1}{4} \mu \left(2p^2 - 5 + \frac{3}{2} \gamma \right) \\ \overline{\alpha_0''} &= ab^2\alpha_0'' = \mu \left(\frac{1}{2} p^2 + \frac{1}{4} + \frac{4p^2 - 1}{8} \gamma \right) \\ \overline{\beta_0'} &= ab^4\beta_0' = \mu \left(\frac{2}{p^2} + 1 - \frac{3}{2} \gamma \right) \\ \overline{\beta_0''} &= ab^2\beta_0'' = \mu \left(-3 + \frac{2p^2 + 1}{2} \gamma \right)\end{aligned}\tag{4}$$

for spheres ($p = 1$), the integrals are:

$$\begin{aligned}\alpha_0' = \beta_0' &= \int_0^\infty dx / (a^2 + x)^{3/2} = 2/5a^5 \\ \alpha_0'' = \beta_0'' &= \int_0^\infty x dx / (a^2 + x)^{3/2} = 4/15a^3\end{aligned}\tag{5}$$

and for oblate ellipsoids (disks), $p < 1$:

$$\begin{aligned}\overline{\alpha_0'} &= ab^4\alpha_0' = (1/4) \mu(2p^2 - 5 + 3\delta) \\ \overline{\alpha_0''} &= ab^2\alpha_0'' = \mu \left(\frac{1}{2} p^2 + \frac{1}{4} + \frac{1 - 4p^2}{4} \delta \right) \\ \overline{\beta_0'} &= ab^4\beta_0' = \mu[(2/p^2) + 1 - 3\delta] \\ \overline{\beta_0''} &= ab^2\beta_0'' = \mu[-3 + (2p^2 + 1)\delta]\end{aligned}\tag{6}$$

where

$$\begin{aligned}\gamma &= (1/p\sqrt{p^2 - 1}) \ln [(p + \sqrt{p^2 - 1}) / (p - \sqrt{p^2 - 1})] \\ \delta &= (1/p\sqrt{1 - p^2}) \arctan (\sqrt{1 - p^2}/p) \\ \mu &= p^2 / (p^2 - 1)^2\end{aligned}$$

Substitution of the components of the tensor, eq. 3, in eq. 1 yields the expression for the energy dissipation rate:

$$\begin{aligned}dW/dt &= 6\pi q^2 \eta_0 ab^2 [K \cos^4 \theta + M \sin^4 \theta + N \sin^2 2\theta + \\ &\quad (2/3)(K - M) \sin^2 \theta + (2M - 5K)/9]\end{aligned}\tag{7}$$

where

$$\begin{aligned} K &= \overline{\alpha_0''/\alpha_0'} \overline{\beta_0''} \\ M &= 1/\overline{\alpha_0'} \\ N &= 1/\overline{\beta_0'}(p^2 + 1) \end{aligned}$$

Specific Viscosity of Solutions

The specific viscosity of a solution:

$$\eta_{sp} = (\eta - \eta_0)/\eta_0$$

is related to an average rate of dissipation of energy (dW/dt) as follows:

$$\eta_{sp} = (c/q^2\eta_0v\overline{dW/dt}) \tag{8}$$

where η is the viscosity of the solution, η_0 is the viscosity of the solvent, c is the volume concentration of solute, and v is the volume of a single dissolved particle.

The average value of dW/dt may be obtained by substitution into eq. (7) the values $\overline{\cos^4 \theta}$, $\overline{\sin^4 \theta}$, etc., averaged by use of the previously derived distribution function $F_0(\theta)$ for the steady state:¹

$$F_0(\theta) = \sum_{n=0}^{\infty} \sum_{i=0}^{\infty} a_{ni}(\alpha R)^i P_{2n} \tag{9}$$

with coefficients a_{ni} calculated from the recurrence formula:

$$\begin{aligned} 3n(2n + 1) a_{ni} &= \frac{(2n - 1)(2n)(2n + 1)}{(4n - 3)(4n - 1)} a_{n-1, i-1} \\ &+ \left[\frac{(2n + 1)^2(2n + 3)}{(4n + 1)(4n + 3)} - \frac{(2n - 2)(2n)^2}{(4n - 1)(4n + 1)} - 1 \right] a_{n, i-1} \\ &- \frac{2n(2n + 1)(2n + 2)}{(4n + 3)(4n + 5)} a_{n+1, i-1} \end{aligned} \tag{10}$$

where $\alpha = q/D$ is the velocity gradient diffusion constant ratio, R is the shape coefficient given by

$$R = (a^2 - b^2)/(a^2 + b^2) = (p^2 - 1)/(p^2 + 1)$$

and P_{2n} are even Legendre polynomials.

The averaged trigonometric functions amount to:

$$\begin{aligned} \overline{\cos^4 \theta} &= \frac{4\pi}{5} \left[a_{00} + \frac{4}{7} \sum_{i=1}^{\infty} (\alpha R)^i a_{1i} + \frac{8}{63} \sum_{i=2}^{\infty} (\alpha R)^i a_{2i} \right] \\ \overline{\sin^4 \theta} &= \frac{32\pi}{15} \left[a_{00} - \frac{2}{7} \sum_{i=1}^{\infty} (\alpha R)^i a_{1i} + \frac{1}{21} \sum_{i=2}^{\infty} (\alpha R)^i a_{2i} \right] \\ \overline{\sin^2 2\theta} &= \frac{32\pi}{15} \left[a_{00} - \frac{1}{7} \sum_{i=1}^{\infty} (\alpha R)^i a_{1i} - \frac{4}{21} \sum_{i=2}^{\infty} (\alpha R)^i a_{2i} \right] \\ \overline{\sin^2 \theta} &= \frac{8\pi}{3} \left[a_{00} - \frac{1}{5} \sum_{i=1}^{\infty} (\alpha R)^i a_{1i} \right] \end{aligned} \tag{11}$$

Taking into consideration eqs. (7) and (11) we obtain from eq. (8):

$$\eta_{sp} = c \frac{2\pi}{5} \left[a_{00}(29K + 4M + 24N) + \frac{4}{7}(2K - 5M + 6N) \sum_{i=1}^{\infty} (\alpha R)^i a_{1i} + \frac{8}{7}(K + M - 4N) \sum_{i=2}^{\infty} (\alpha R)^i a_{2i} + \frac{5}{4\pi}(2M - 5K) \right] \quad (12)$$

In Figure 1 the intrinsic viscosity $\nu = [\eta_{sp}/c]_{c=0}$ is plotted versus the velocity gradient/diffusion constant ratio α for various ellipsoids. It is

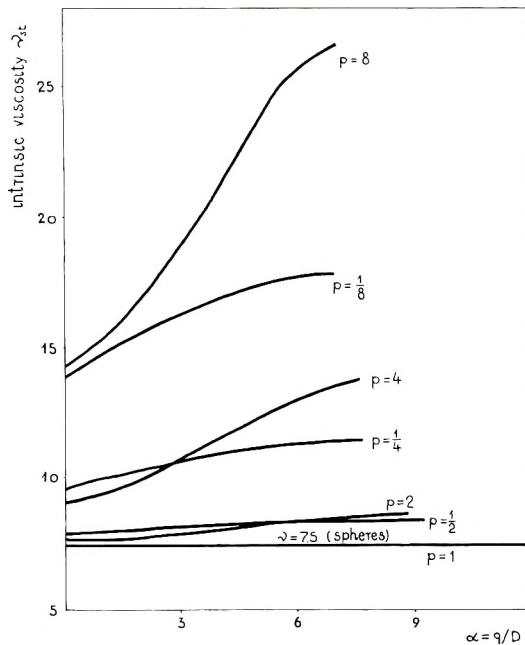


Fig. 1. Intrinsic viscosity in a steady state ν_{st} vs. velocity gradient/diffusion constant ratio α .

evident that intrinsic viscosity increases monotonically with α from an original value ν_0 to a saturation value ν_∞ . These limiting ν values are given by eqs. (13):

$$\begin{aligned} \nu_0 &= (1/5)(2K + 7M + 12N) \\ \nu_\infty &= \begin{cases} (2K + M) & \text{at } p > 1 \text{ (rods)} \\ 1/2(K + 5M) & \text{at } p < 1 \text{ (disks)} \end{cases} \end{aligned} \quad (13)$$

The dependence of ν_0 , ν_∞ , and ν_6 , on the axial ratio p is demonstrated in Figure 2.

We will now introduce the "structural factor" s , defined as a relative,

maximal increase of intrinsic viscosity due to the change of ratio $\alpha = q/D$:

$$s = (\eta_{\alpha=\infty} - \eta_{\alpha=0}) / (\eta_{\alpha=0} - \eta_0) = (\nu_\infty - \nu_0) / \nu_0 \quad (14)$$

For rods, this factor amounts to:

$$s = (8K - 2M - 12N) / (2K + 8M + 12N)$$

and for disks,

$$s = (K + 11M - 24N) / (4K + 14M + 24N) \quad (15)$$

The structural factor s is always positive in considered field and increases with the degree of asymmetry of the ellipsoid $|\log p|$ (cf. Fig. 3) with the

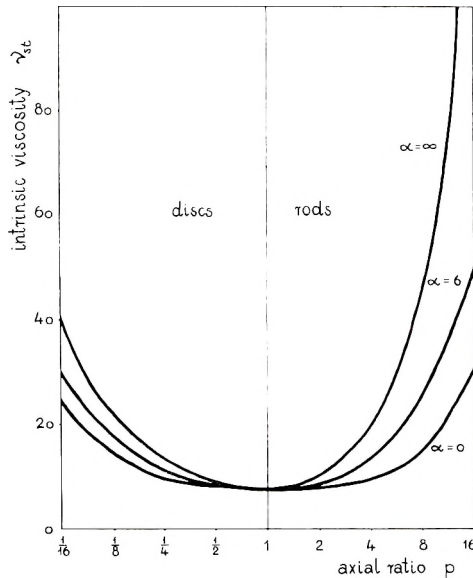


Fig 2. Intrinsic viscosity in a steady state ν_{st} vs. axial ratio of ellipsoids $p = a/b$

limiting values:

$$s_{p=\infty} = 4 \quad (\text{rods})$$

$$s_{p=0} = 3/4 \quad (\text{discs})$$

Solutions containing spherical particles ($p = 1$) do not show any change of viscosity: $s = 0$. The intrinsic viscosity of such solutions is constant:

$$\nu_{sph} = 7.5$$

The value 7.5 for the considered velocity field is entirely consistent with the value of 2.5 given by Einstein³ for shear flow, since the assumed Poisson ratio is 0.5.

Time Dependence

When the averaging of trigonometric functions in eq. (7) is accomplished by use of the time-dependent distribution function:¹

$$\rho(t, \theta) = F_0(1 - \exp\{-\lambda_1 Dt\}) + (1/4\pi) \exp\{-\lambda_1 Dt\} \quad (16)$$

the time-dependent intrinsic viscosity is obtained:

$$\nu(t) = \nu_{st}(1 - \exp\{-\lambda_1 Dt\}) + \nu_0 \exp\{-\lambda_1 Dt\} \quad (17)$$

where ν_{st} is the intrinsic viscosity for a given steady state and ν_0 is the intrinsic viscosity for $t = 0$.

The function $\nu(t)$ for $\alpha = 2/3$ and $\lambda_1 D = 0.9598 \text{ sec.}^{-1}$ is demonstrated in Figure 4. It is apparent both from eq. (17) and Figure 4 that intrinsic viscosity increases monotonically with time. The original value $\nu(t = 0)$ is equal to that which is possessed by the same solution at $\alpha = 0$, i.e., at random distribution of ellipsoid axes.

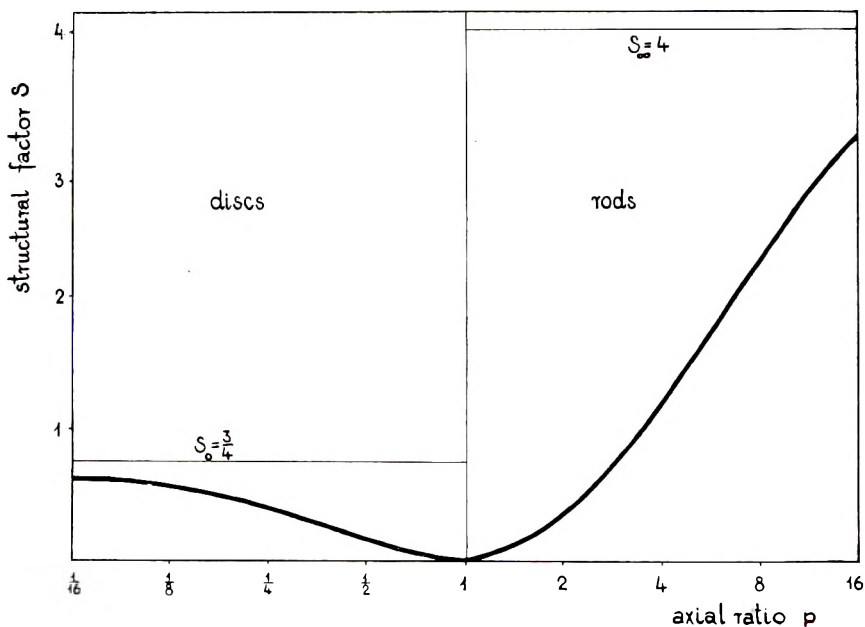


Fig. 3. Structural factor $s = (\nu_\infty - \nu_0)/\nu_0$ vs. axial ratio of ellipsoids $p = a/b$.

An increase of viscosity with time as well as that with parameter α arises from corresponding changes of orientation. In order to explain the mechanism responsible for this increase we will consider an individual ellipsoid in the velocity field. The velocity of liquid (solvent) is different in various points of the ellipsoid's surrounding. Since the ellipsoid itself is rigid, any of its points moves with equal velocity. As a consequence of this, an additional energy is dissipated, which is the greater, the greater is velocity difference on both ends of ellipsoid. In other words, the rate of dissipation of additional energy, hence viscosity of solution, should increase with degree of parallelization (orientation factor) and asymmetry of the particle ($|\log p|$), as was just shown in the derived formulae.

Conclusions

In the two papers dealing with the behavior of macromolecular liquids in a velocity field with parallel gradient, a general analysis of orientation and viscosity in dilute solutions containing rigid ellipsoids was given.

According to this theory, rigid ellipsoids in the considered field undergo orientation with a maximum of distribution density at angle $\theta = 0$ or $\theta = \pi/2$ for rods and disks, respectively. The average degree of orientation (axial orientation factor f) determining the anisotropy of a flowing system depends on the shape coefficient R and the velocity gradient/diffusion constant ratio α . The ellipsoids move aperiodically in time, tending to a

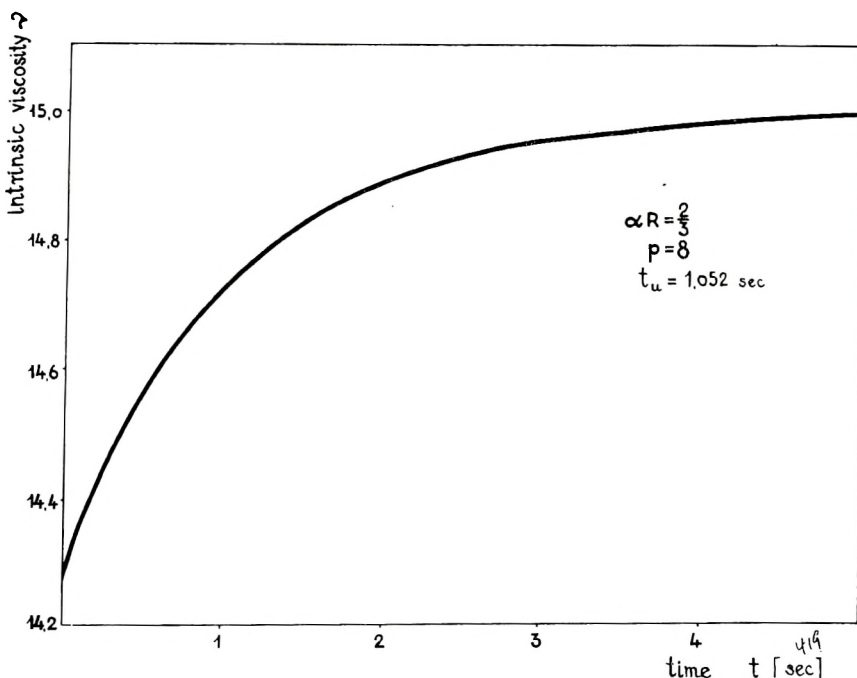


Fig. 4. Intrinsic viscosity vs. time.

definite equilibrium. The orientation factor increases exponentially with time to a saturation value in the steady state.

An intrinsic viscosity of dilute solutions containing such particles increases with product αR , from an original value ν_0 corresponding to the random distribution of ellipsoid directions, to an asymptotic value ν_∞ , characteristic for uniform orientation (all ellipsoids oriented with their axes of symmetry along the direction of tension). Intrinsic viscosity also increases with time from ν_0 at $t = 0$ to ν_{st} at $t = \infty$. The relative, maximal increase of intrinsic viscosity (structural factor s) increases with $|\log p|$ from 0 to 4, and from 0 to $3/4$, for rods and disks, respectively.

The increase of viscosity with velocity gradient q and with time t , are

formal reminders of the known effects of dilation and antithixotropy, respectively. It is significant, that the same rheological system as analyzed in our works (dilute solution or rigid ellipsoids) behaves quite differently in the conditions of shear flow (velocity field with perpendicular gradient). Peterlin and Stuart⁴ have shown that in the latter case ellipsoids rotate periodically and there is no position of equilibrium for particles of finite dimensions. Orientation factor and anisotropy of a system depend not only on the product αR but also on the shape coefficient R alone. Intrinsic viscosity in the field with perpendicular velocity gradient decreases with gradient, and probably also with time.

Most of the apparatus used for investigation of dynamic behavior of macromolecular liquids is based on the principle of shear flow, e.g., capillary, rotational, or falling body viscometers, instruments for measuring the flow birefringence, etc. Our results doubtless proved, that any conclusions drawn out of experiments made in one velocity field may not be necessarily valid for another field. This explains, among others, the difficulties met by investigators, who tried to interpret the so-called spinnability of polymer liquids in terms of structural viscosity found in capillary or rotational viscometers.

Our theory applies to all phenomena involving uniaxial drawing of liquids; in particular it concerns the polymer jets and process of fiber formation.

References

1. Takserman-Krozer, R., and A. Ziabicki, *J. Polymer Sci.*, **1**, 487 (1963).
2. Jeffery, G. B., *Proc. Roy. Soc. (London)*, **A102**, 161 (1922).
3. Einstein, A., *Ann. Physik*, **19**, 289 (1906).
4. Peterlin, A., *Z. Physik*, **111**, 232 (1938); A. Peterlin and H. A. Stuart, *ibid.*, **112**, 1 (1939).

Synopsis

On the basis of Jeffery's general relations, formulas for the rate of dissipation of energy due to the motion of a rigid rotational ellipsoid in a liquid, uniaxially drawn, were derived. By use of the previously found distribution function, intrinsic viscosity ν , was calculated and effects of ellipsoid shape, velocity gradient, diffusion rate constant and time were discussed. The intrinsic viscosity monotonically increases with velocity gradient and with time t . This behavior is quite different from that observed in shear flow. It was stated that phenomena connected with a velocity field with parallel gradient (i.e., flow with uniaxial deformation):

$$\mathbf{V}_{ij} = \begin{pmatrix} q & 0 & 0 \\ 0 & -\sigma q & 0 \\ 0 & 0 & -\sigma q \end{pmatrix}$$

such as liquid jets, fiber spinning etc., cannot be explained in terms of experiments or theories concerning the shear flow (velocity field with perpendicular gradient):

$$\mathbf{V}_{ij} = \begin{pmatrix} 0 & q & 0 \\ q & 0 & 0 \\ 0 & 0 & 0 \end{pmatrix}$$

as obtained in viscosity measurements in common types of viscometers (capillary, rotational, falling body), or investigations of flow birefringence in coaxial apparatus.

Résumé

Les expressions de la vitesse de dissipation de l'énergie due au mouvement dans un liquide d'un ellipsoïde de rotation rigide, étiré uniaxialement, ont été dérivées à partir des relations générales de Jeffery. La viscosité intrinsèque ν a été calculée à l'aide de la fonction de distribution trouvée précédemment et l'influence de la forme de l'ellipsoïde, du gradient de vitesse, de la constante de vitesse de diffusion et du temps a été discutée. La viscosité intrinsèque croît de façon monotone avec le gradient de vitesse et avec le temps t . Ce comportement est tout différent de celui qui a été observé lors de l'écoulement par cisaillement. On a établi que les phénomènes reliés à l'existence d'un champ de vitesse à gradient parallèle, c.à.d. d'un écoulement avec déformation uniaxiale:

$$v_{ij} = \begin{pmatrix} q & 0 & 0 \\ 0 & -\sigma q & 0 \\ 0 & 0 & -\sigma q \end{pmatrix}$$

tels que l'extrusion de liquides, la filature de fibres etc. ne peuvent être expliqués sur la base des expériences ou théories concernant l'écoulement dans un champ de vitesse à gradient perpendiculaire.

$$v_{ij} = \begin{pmatrix} 0 & q & 0 \\ q & 0 & 0 \\ 0 & 0 & 0 \end{pmatrix}$$

C'est à dire celui qui se présente au cours des mesures de vitesse à l'aide de viscosimètres ordinaires (capillaire, rotatin, corps tombant) au cours des études de biréfringence dans un appareil coaxial.

Zusammenfassung

Auf Grundlage der allgemeinen Beziehungen von Jeffery wurden Formeln für die Geschwindigkeit der Energiedissipation durch die Bewegung eines starren Rotationsellipsoïds in einer Flüssigkeit bei uniaxialer Bewegung abgeleitet. Mit der früher erhaltenen Verteilungsfunktion wurde die Viskositätszahl berechnet und der Einfluss der Form des Ellipsoïds, des Geschwindigkeitsgradienten, der Diffusionsgeschwindigkeitskonstanten und der Zeit diskutiert. Die Viskositätszahl nimmt mit dem Geschwindigkeitsgradienten und mit der Zeit t monoton zu. Dieses Verhalten unterscheidet sich völlig von dem bei Strömung unter Scherung beobachteten. Es wurde festgestellt, dass die Erscheinungen in einem Geschwindigkeitsfeld mit parallelem Gradienten (d.h. Strömung mit uniaxialer Deformation):

$$V_{ij} = \begin{pmatrix} q & 0 & 0 \\ 0 & -\sigma q & 0 \\ 0 & 0 & -\sigma q \end{pmatrix}$$

wie in einem Flüssigkeitsstrahl, beim Faserspinnen etc., nicht durch Versuche oder Theorien, die sich auf die Strömung unter Scherung (Geschwindigkeitsfeld mit senkrechten Gradienten):

$$V_{ij} = \begin{pmatrix} 0 & q & 0 \\ q & 0 & 0 \\ 0 & 0 & 0 \end{pmatrix}$$

beziehen, z.B. Viskositätsmessungen in Viskosimetern vom üblichen Typ (Kapillar-, Rotations-, Fallkörperviskosimeter), Strömungsdoppelbrechungsuntersuchungen im koaxialen Apparat, erklärt werden können.

Received October 11, 1961

Depolarization Measurements of Polymer Solutions in High Dilutions. Part I

V. KALPAGAM and M. RAMAKRISHNA RAO, *Department of Inorganic and Physical Chemistry, Indian Institute of Science, Bangalore, India*

INTRODUCTION

The size, shape, and optical anisotropy of polymer molecules have a pronounced influence on the physicochemical properties of these substances. The relationship between the physical structure and the complex behavior of these molecules in solution have been investigated by a number of methods like viscosity, light scattering, flow birefringence, sedimentation and diffusion, etc. In order to have a clear understanding of the geometry and structure of these molecules it is necessary to have as much information as possible from different techniques. Hence the depolarization studies on light scattered from polymer solutions have been carried out.

An extensive study in colloidal solutions¹⁻⁴ has been carried out in measuring the depolarization ratios of unpolarized light (ρ_u), vertically polarized light (ρ_v) and horizontally polarized light (ρ_h). An attempt was made by Doty^{5,6} et al. to extend these studies of depolarization measurements to macromolecular solutions and to correlate the data with the expected behavior.

The determination of ρ_u alone does not give us any specific information about the dimensions or anisotropy of the molecule, since the finite value of ρ_u may be either a function of particle diameter or a measure of optical anisotropy of the particle. Hence ρ_u and ρ_v measurements are necessary before an attempt is made to interpret the depolarization measurements.

According to Doty,⁷ ρ_v varies inversely as the turbidity of the solution and reflects the optical anisotropy of the flexible and rigid polymer molecules. The values of ρ_h will generally diminish from a value of unity as the size of the scattering particle increases. Studies by Gans⁸ and Neugebauer,⁹ however, show that small rodlike particles are exception to this behavior, the values of ρ_h for such particles being greater than unity. Doty⁷ has put forward a postulate that ρ_h can be greater than unity when the dimensions of the particles are not small. The value of ρ_h increases to a maximum when the particle dimensions are such that the first-order interference clearly dominates and then decreases, passing through unity when the length is equal to 0.25λ , and then decreases further to successively lower values.

The depolarization measurements in polymer solutions have been so far

carried out by the Cornu apparatus which is not very sensitive in the dilution range where anomalous behavior has been observed in the viscosity measurements. Secondly, the values of ρ_h have so far been computed from Krishnan's reciprocity theorem,¹⁰ but could not be determined directly as the conventional experimental apparatus could not record the feeble components of the horizontally polarized light.

The present investigation was undertaken to study the depolarization ratios of polymer solutions in order (1) to correlate these ratios to the intrinsic properties of the molecules, (2) to determine the effect of polymer-solvent interactions and the effect of high dilutions on the size and geometry of the molecules, and (3) to evaluate the ρ_h values experimentally by constructing a differential amplifier in order to test the validity of Doty's theory.

EXPERIMENTAL

For the depolarization measurements a Brice-Phoenix Universal light-scattering photometer, type 1000D,¹¹ was used. In order to obtain reliable measurements the sensitivity of the instrument had to be increased. For this a differential amplifier was designed in order to amplify the photomultiplier current.

Construction and Operation of the Differential Amplifier

The requirements for a d.c. amplifier are that (a) it should amplify the d.c. output of the photomultiplier tube, (b) it should give a full-scale deflection in the galvanometer for an input of about 1 mv. developed across 10,000 ohms, which is the anode load of the photomultiplier tube, and (c) it should be highly stable and independent of variations in supply voltage and tube constants. All these requirements are adequately met by a balanced difference amplifier. This circuit consists essentially of two cathode followers as shown in Figure 1, with the galvanometer connected between the two cathodes through a variable series resistance of the value 100K. A variable resistance has been used in this case in order to obtain a certain amount of control of the gain. Higher amplification has been achieved in this case by using two pentodes (6SJ7) instead of the triodes.

The differences in the constants of the two tubes will result in a certain initial current in the galvanometer, even without any input voltage. This has to be balanced out to bring the initial reading of the galvanometer to zero. The method of zero adjustment followed here is to insert a variable resistance in one of the cathodes and vary the cathode bias of the valve until it equals that of the other one.

Materials Employed

The fractions of poly(vinyl acetate) used in this investigation were prepared in this laboratory. The monomer vinyl acetate was first subjected to vacuum distillation to remove the inhibitor and then polymerized by

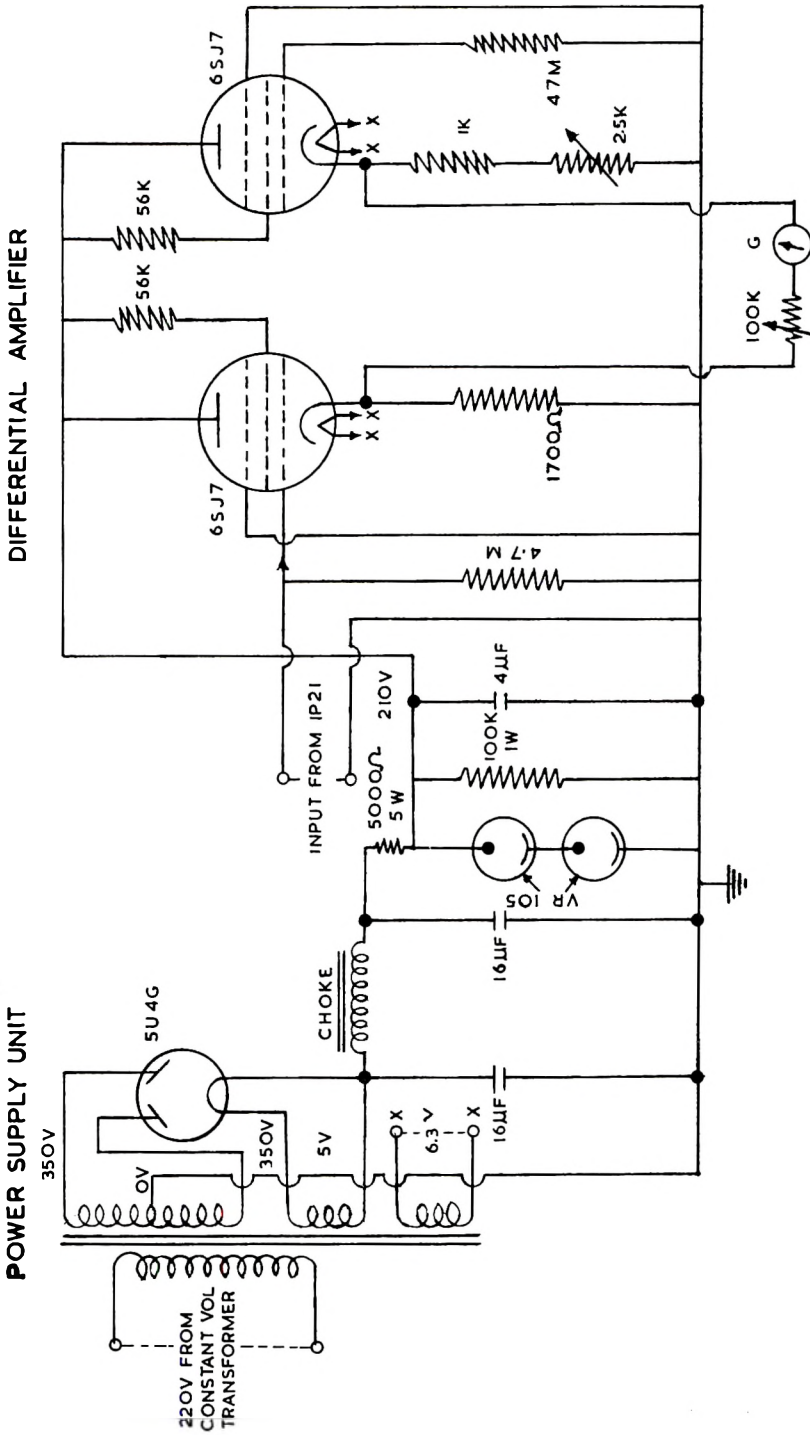


Fig. 1. Electronic circuit for differential amplifier.

the bulk method at a temperature of $40 \pm 0.25^\circ\text{C}$. in the presence of various concentrations of the catalyst benzoyl peroxide. The conversion of the monomer to polymer allowed was below 20%.¹² The polymers thus obtained were subjected to a number of fractionations to obtain narrow, homogeneous fractions.

All the solvents employed were purified by the standard methods and freshly distilled. Usually a stock solution of about 1% was prepared in freshly distilled solvents and about six different concentrations were obtained from this by pipetting out various volumes and diluting them.

To render the solutions of macromolecules dust-free for light-scattering measurements is a great problem.¹³⁻¹⁵ In the present investigation the solvents and solutions were rendered dust-free by filtering them successfully through two sintered glass filters, directly into the cell.

Depolarization Measurements

With the differential amplifier described above the depolarization measurements were taken at 90° for unpolarized, vertically polarized, and horizontally polarized light. For each polymer fraction these measurements were recorded for five or six different concentrations ranging from 0.03% to 0.2%. The mercury blue line (4360 Å.) was used for these measurements. When ρ_u or ρ_v is measured, a part of the scattered light may be rescattered and enter into the observation chamber. This effect has been minimized by working at high dilutions and using a very narrow beam of incident light.

RESULTS AND DISCUSSION

Figures 2 and 3 show the graphs of ρ_u , ρ_v , and ρ_h plotted against concentration C for the systems poly(vinyl acetate) (PVA)-ethyl acetate (EA) and PVA-methyl ethyl ketone (MEK), respectively, while Tables I and II give the corresponding data obtained in the present investigation for two fractions of the polymer. An inspection of the tables shows that the values

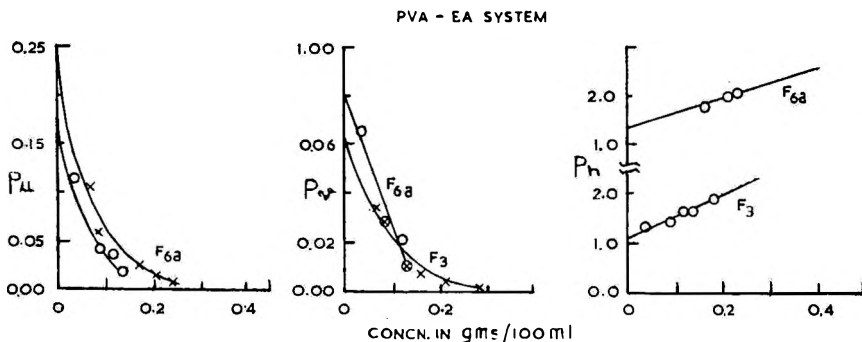


Fig. 2. Plots of depolarization ratios ρ_u , ρ_v , and ρ_h of PVA fractions in ethyl acetate as functions of concentration.

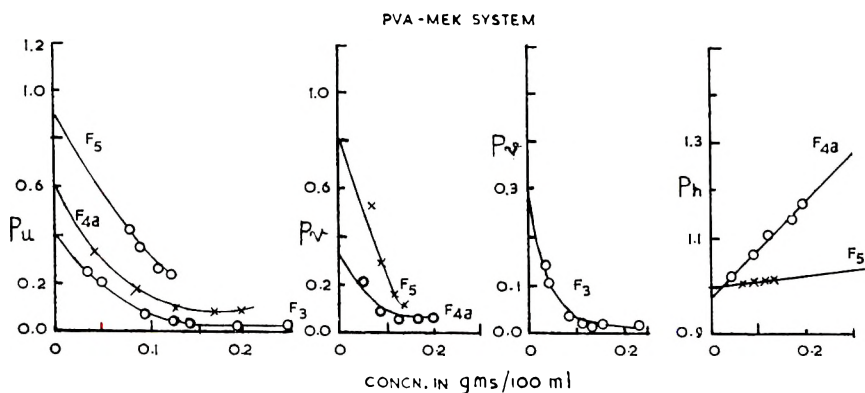


Fig. 3. Plots of depolarization ratios ρ_u , ρ_v , and ρ_h of PVA fractions in methyl ethyl ketone as functions of concentration.

of these depolarization ratios are dependent on three factors, namely, concentration, molecular weight, and nature of the solvent.

From Figures 2 and 3 it is observed that both ρ_u and ρ_v values decrease with increasing concentrations in both the solvents. The slopes of the ρ_v versus C plots also give us some information regarding the effect of the solvent on the anisotropy of the molecule. Over the concentration range (0.01% to 0.25%) studied, the plots show that the ρ_v values decrease sharply with increasing concentrations up to a concentration of about 0.1% and then the curves flatten, thereby showing that the slopes tend towards zero at about a concentration of 0.1% and above. For example, in the case of fraction F_3 both in butanone and ethyl acetate, the slopes of the ρ_u versus C and ρ_v versus C curves tend to zero above a concentration of 0.1%.

TABLE I
Poly(vinyl Acetate)-Ethyl Acetate System

| Fraction | Concn., g./ml. | ρ_u | ρ_v | ρ_h | | $\rho_{h_{r \rightarrow 0}}$ |
|--------------------------------------|-------------------|----------|----------|--|--|------------------------------|
| | | | | Experi- men- tally deter- mined value | Calcu- lated from Krish- nan's relation | |
| F_{6a} $M_w = 0.92 \times 10^6$ | 0.00060 | 0.104 | 0.033 | — | — | |
| | 0.00082 | 0.055 | 0.027 | — | — | |
| | 0.00159 | 0.019 | 0.007 | 1.83 | 0.60 | |
| | 0.00209 | 0.009 | 0.002 | 2.00 | 1.40 | |
| | 0.00210 | 0.009 | 0.003 | 2.00 | 0.65 | |
| F_3 $M_w = 1.53 \times 10^6$ | 0.00233 | 0.007 | 0.001 | 2.00 | 1.42 | 1.40 |
| | 0.00030 | 0.120 | 0.067 | 1.37 | 1.09 | |
| | 0.00079 | 0.042 | 0.027 | 1.44 | 1.72 | |
| | 0.00114 | 0.034 | 0.021 | 1.66 | 1.58 | |
| | 0.00132 | 0.020 | 0.010 | 1.59 | 0.98 | |
| | 0.00182 | — | — | 1.86 | — | 1.10 |

TABLE II
 Poly(vinyl Acetate)-Methyl Ethyl Ketone System

| Fraction | Concn., g./ml. | ρ_u | ρ_v | ρ_h | | $\rho_{h_{c \rightarrow 0}}$ |
|--------------------------|-------------------|----------|----------|--|--|------------------------------|
| | | | | Experi- men- tally deter- mined value | Calcu- lated from Krish- nan's relation | |
| F ₃ | 0.00065 | — | 0.535 | 1.00 | — | |
| | 0.00083 | 0.436 | 0.283 | 1.01 | 1.02 | |
| $M_w = 1.06 \times 10^6$ | 0.00098 | 0.357 | 0.161 | 1.02 | 0.63 | |
| | 0.00112 | 0.271 | 0.151 | 1.02 | 0.93 | |
| F _{4a} | 0.00119 | 0.245 | 0.133 | 1.02 | 0.93 | 1.0 |
| | 0.00040 | 0.316 | 0.204 | 1.02 | 1.15 | |
| $M_u = 1.49 \times 10^6$ | 0.00080 | 0.164 | 0.086 | 1.07 | 0.94 | |
| | 0.00122 | 0.093 | 0.051 | 1.11 | 1.08 | |
| F ₃ | 0.00166 | 0.092 | 0.060 | 1.14 | 1.59 | 0.98 |
| | 0.00193 | 0.095 | 0.061 | 1.17 | 1.53 | |
| $M_w = 1.53 \times 10^6$ | 0.00033 | 0.238 | 0.140 | — | — | |
| | 0.00046 | 0.189 | 0.106 | — | — | |
| | 0.00085 | 0.062 | — | — | — | |
| | 0.00092 | 0.074 | 0.037 | — | — | |
| | 0.00121 | 0.037 | 0.020 | — | — | |
| | 0.00126 | 0.028 | — | — | — | |
| | 0.00140 | 0.034 | 0.017 | — | — | |
| | 0.00244 | 0.035 | 0.016 | — | — | |

This can be explained as follows. At high dilutions there are more of solvent-solute interactions rather than solute-solute interactions. As a result of this the polymer molecules try to uncoil themselves, thereby altering the size and shape of the segments of the molecule. Of course the extent of uncoiling depends on the nature of the solvent; it is more in the case of a good solvent than a poor solvent. This is confirmed from the results obtained, as it is seen that for fraction F₃ the value of ρ_v at about a concentration of 0.03% is 0.14 in the good solvent (methyl ethyl ketone) while in the relatively poor solvent (ethyl acetate) it is only 0.067. Similar results are obtained in the case of ρ_u also.

At low dilutions the number of polymer-polymer contacts become predominant, as a result of which the molecules try to coil up and become more and more isotropic. The flattening of the curves both in good and a relatively poor solvent shows that the anisotropy of the segments of the molecules is not changing further with increasing concentration. Hence it can be concluded that, depending upon the nature of the solvent, there exists for each polymer-solvent system a critical concentration range above which the anisotropy of the molecules does not alter further.

The values of both ρ_u and ρ_v decrease with increasing molecular weight. In the poor solvent (ethyl acetate) these values are less than the corresponding values in the good solvent (butanone). This is in accordance with the

theory that the anisotropy of the polymer molecule decreases as the dimensions of the chain increase and the solvent power decreases.

ρ_h values

The values of ρ_h reported so far in the literature are all calculated from Krishnan's relation. A value less than unity has been observed for ρ_h in all the colloidal solutions. Lotmar² obtained a value of one for ρ_h for a low molecular weight nitrocellulose fraction.

The ρ_h values obtained in this investigation are shown in Tables I and II. From the tables, it is seen that the values of ρ_h are higher than unity in both the solvents and for all the fractions studied. In many cases the experimental and calculated values vary to the extent of 70%.

In general, ρ_h increases with increasing concentration for both the systems studied, but the rate of increase with concentration is less in the case of the poor solvent (ethyl acetate). This can be explained by the fact that the optical anisotropy and the physical dimensions of the segments have decreased upon diminishing the solvent power of the medium. A decrease in the value of ρ_h indicates that the particle size has increased. The limiting values of ρ_h are larger in the case of the poor solvent (ethyl acetate) than in the good solvent (methyl ethyl ketone). This shows that the molecules are more extended in a good solvent, which is in conformity with the light-scattering and viscosity data. Gans⁸ and Neugebauer's⁹ expressions indicate that ρ_h should be less than unity for disk-like particles and greater than unity for rodlike particles. In this investigation the ρ_h values at various concentrations are greater than unity and become one or less at infinite dilution. This suggests that the overall phenomena at higher concentrations are such that the polymer molecules tend to resemble more a rodlike formation. As the concentration decreases, the intramolecular interactions become less and less and the polymer molecules assume a disklike shape.

An inspection of the tables shows that the agreement between the calculated and experimental values of ρ_h is within experimental error when this value is close to unity. In the case of ρ_h values, however, where values are much higher than unity, the disagreement is as much as 70%. The precision of these measurements is $\pm 5\%$ which shows that the observed disagreement is not due to experimental error. From this it can be concluded that the reciprocity theorem holds only for such polymer solutions where ρ_h is one or less than one. This conclusion has been confirmed in other polymer solutions; these results will be published shortly.

The author's sincere thanks are due to Dr. S. Bhagavantam and Prof. M. R. A. Rao for suggesting this problem and for their helpful discussion during the course of this work.

References

1. Gehman, S. D., and J. E. Field, *Ind. Eng. Chem.*, **29**, 793 (1937).
2. Lotmar, W., *Helv. Chim. Acta*, **21**, 953 (1938).
3. Krishnan, R. S., *Proc. Indian Acad. Sci.*, **1A** 212 (1934); *ibid.*, **1A**, 782 (1935).

4. Krishnan, R. S., *Proc. Indian Acad. Sci.*, **3A** 211 (1936); *ibid.*, **5A**, 94, 305, 407, 409, 551 (1937); *ibid.*, **7A**, 21, 91, 98 (1938).
5. Doty, P., and H. S. Kaufman, *J. Phys. Chem.*, **59**, 583 (1945).
6. Doty, P., and H. J. Stein, *J. Polymer Sci.*, **3**, 763 (1948).
7. Doty, P., *J. Polymer Sci.*, **3**, 750 (1948).
8. Gans, R., *Physik. Z.*, **37**, 19 (1936).
9. Neugebauer, T., *Z. Physik*, **122**, 471 (1944).
10. Krishnan, R. S., *Proc. Indian Acad. Sci.*, **1A**, 717 (1935).
11. Brice, B. A., M. Halwer, and R. Speiser, *J. Opt. Soc. Am.*, **40**, 768 (1950).
12. Wheeler, O. L., S. L. Ernest, and R. N. Orozier, *J. Polymer Sci.*, **8**, 409 (1952).
13. Alexander, P., and K. A. Stacey, *Trans. Faraday Soc.*, **51**, 299 (1955).
14. Alexander, P., and K. A. Stacey, *Proc. Roy. Soc. (London)*, **A212**, 274 (1952).
15. Thurmond, C. D., *J. Polymer Sci.*, **8**, 607 (1952).

Synopsis

The depolarization ratios of unpolarized light, vertically polarized light, and horizontally polarized light at 90° have been measured for polyvinyl acetate solutions at high dilutions with the help of a specially designed differential amplifier. Over the concentration range (0.01–0.25%) studied, the values of ρ_u and ρ_v decrease sharply with increasing concentrations up to a concentration of about 0.1% and then the curves flatten out. Depending upon the nature of the solvent, there exists for each polymer-solvent system a critical concentration range above which the anisotropy of the molecules does not alter further. This behavior is the same both in the good solvent (methyl ethyl ketone) and the relatively poor solvent (ethyl acetate). The experimentally determined ρ_h values generally are in agreement with the values calculated from the reciprocity theorem, except where ρ_h values are greater than one. In the case of ρ_h values which are greater than unity the difference between the experimentally determined and the calculated values is as high as 70%.

Résumé

Les rapports de dépolarisation de la lumière non polarisée, de la lumière polarisée verticalement et de la lumière polarisée horizontalement à 90° ont été mesurés pour des solutions très diluées d'acétate de polyvinyle au moyen d'un amplificateur différentiel spécialement construit. Dans le domaine des concentrations étudiées (0.01 à 0.25%), les valeurs de ρ_u et de ρ_v diminuent fortement lorsque les concentrations augmentent et cela jusqu'à une valeur d'environ 0.1%. Ensuite les courbes s'aplatissent. D'après la nature du solvant, il existe pour chaque système polymère-solvant un domaine de concentration critique au dessus duquel l'anisotropie des molécules ne change plus. Ce comportement est le même pour un bon solvant comme la méthyl-éthyl-cétone que pour un solvant relativement mauvais comme l'acétate d'éthyle. Les valeurs de ρ_h déterminées expérimentalement sont généralement en accord avec les valeurs calculées à partir du théorème de réciprocity excepté lorsque les valeurs de ρ_h sont plus grandes que l'unité. Dans le cas où les valeurs de ρ_h sont plus grandes que l'unité, la différence entre les valeurs déterminées expérimentalement et les valeurs calculées atteint 70%.

Zusammenfassung

Das Depolarisationsverhältnis von unpolarisiertem, vertikal polarisiertem und horizontal polarisiertem Licht bei 90° wurde für Polyvinylacetatlösungen bei hoher Verdünnung mit Hilfe eines speziell konstruierten Differentialverstärkers gemessen. Im untersuchten Konzentrationsbereich (0,01 bis 0,25%) nehmen die Werte von ρ_u und ρ_v mit steigender Konzentration bis zu einer Konzentration von etwa 0,1% scharf ab; dann nehmen die Kurven einen flachen Verlauf. In Abhängigkeit von der Natur des Lösungsmittels besteht für jedes Polymer-Lösungsmittelsystem ein kritischer Kon-

zentrationsbereich, oberhalb dessen sich die Anisotropie der Moleküle nicht mehr ändert. Dieses Verhalten trifft sowohl für das gute Lösungsmittel Methyläthylketon als auch das verhältnismässig schlechte Lösungsmittel Äthylacetat zu. Die experimentell bestimmten ρ_h -Werte stimmen im allgemeinen, ausser für ρ_h -Werte grösser als eins, mit den aus dem Reziprozitätstheorem berechneten Werten überein. In Falle grösserer ρ_h -Werte als eins erreicht der Unterschied zwischen experimentell bestimmten und berechneten Werten bis zu 70%.

Received September 13, 1961

Effect of Solid Polymer Interaction on Transition Temperature and Diffusion Coefficients

CHARLES A. KUMINS and JEROME ROTEMAN, *Interchemical Corporation, Central Research Laboratories, New York, New York*

INTRODUCTION

A considerable body of literature exists on polymer-solid interaction, particularly in regard to rubber systems containing reinforcing fillers.¹

Despite unmistakable evidence of crosslinking due to pigmentation little information is available on the relationship between pigmentation and the glass transition temperature.

Landel² studied the temperature dependence of the dynamic mechanical properties of a polyisobutylene-glass bead system. He calculated from the Williams, Landel, and Ferry equation (WLF) an increase in transition temperature of 2, 6, and 7°C. for systems filled with 8.68, 20.3, and 36.7 vol.-% beads. Since the glass beads were nonreinforcing, Landel considered these increases to be reasonable and related to the small amount of crosslinking caused by polymer adsorption.

On the other hand, Mason³ found no change in the transition temperature of rubber loaded with 18 vol.-% of a reinforcing carbon black. His measurements were made dilatometrically. Since the transition temperature increases with molecular weight only in the lower range, it is possible that Mason's rubber was already too highly crosslinked to exhibit changes in the glass transition.

It would certainly appear reasonable to expect changes in the mobility of macromolecular segments due to the restriction of their motion caused by their adsorption on the surface of solids with which they are in contact. It is also conceivable that if sufficient surface were present to immobilize enough of the polymer, changes in the glass transition temperature should be observed.

It was the objective of our investigation to determine whether changes in the glass transition could be brought about by the addition of a nonreinforcing solid. In the event that such was the case, a further objective was to determine whether such changes affected the water vapor transport process which has been shown⁴ to be sensitive to the glass transition state.

MATERIALS

The copolymer used was poly(vinyl chloride-vinyl acetate). Its composition was 87% vinyl chloride and 13% vinyl acetate. The average

molecular weight was found to be 10,500 when calculated from viscosity data.⁵ This material was obtained from Union Carbide Chemicals Company, and is designated as VYHH.

The crystalline solid employed in this investigation was a rutile-type titanium dioxide that is approximately 97% pure. The particle size range is 0.070–0.400 microns with a mean diameter of 0.220 micron. The surface of the pigment was covered by 2% aluminum oxide (hydrated), 1% titanium dioxide (hydrated), and 0.75% silicon dioxide (hydrated). The pigment was heated to 500°C. and cooled in a vacuum desiccator before use. This material was supplied by E. I. du Pont de Nemours and Company.

PROCEDURE

Film Preparation

A concentrated dispersion was made by intimately mixing on a two-roll mill 75 parts titanium dioxide with 25 parts of the copolymer and 10 parts of methyl isobutyl ketone. The latter was added to facilitate dispersion.

The resulting solid was broken into small pieces and placed in a vacuum desiccator for two weeks at room temperature followed by a further conditioning at 60°C. for 24 hr.

Six different solutions were made which contained the solid in increasing amounts. The titanium dioxide-polymer solutions were made with a solvent composition of 40 parts methyl ethyl ketone, 40 parts methyl isobutyl ketone, and 20 parts xylene by volume.

The films were prepared as described previously.⁶ The titanium dioxide content was determined by analysis and is shown in Table I. From the weight per cent of titanium dioxide, the volume percentages were calculated at 25 and 47°C. on the basis of the following density values; titanium dioxide = 4.193 g./cc. at 25°C. and 4.191 g./cc. at 47°C. and VYHH = 1.349 g./cc. at 25°C. and 1.334 g./cc. at 47°C.

TABLE I

| Film | Titanium dioxide, wt.-% | Titanium dioxide, vol.-% | |
|------|-------------------------|--------------------------|-------|
| | | 25°C. | 47°C. |
| A | 3.38 | 1.11 | 1.10 |
| B | 8.86 | 3.03 | 3.00 |
| C | 13.77 | 4.89 | 4.83 |
| D | 17.90 | 6.55 | 6.49 |
| E | 31.56 | 12.92 | 12.79 |
| F | 42.56 | 19.25 | 19.08 |

Transition Temperature

Transition temperatures were obtained dilatometrically by the same technique described in the previous paper.⁷

Diffusion Coefficients

Two methods were employed to determine the diffusion coefficients. Where the solubility of the diffusant into the film was sufficiently great, a McBain-Bakr sorption balance patterned after Prager and Long⁸ was used. A film was suspended from a sensitive quartz spiral spring fixed in a thermostatted chamber. The gas or vapor under study was allowed to enter this chamber at any specified pressure. As the film absorbed gas, the spring elongated in proportion to the increased mass, and its extension was observed with a traveling microscope, or cathetometer. Thus, rates of sorption and desorption were studied, and the amounts of gas or vapor dissolved in a film were determined.

In instances where the solubility of the penetrant was too low to weigh accurately, as for carbon dioxide and water at low vapor pressure as is the case at low temperatures, a permeability apparatus was constructed to permit the necessary transport data to be obtained.

The film supported on the low pressure side by a flat nickel screen is used to separate two sections of a chamber, usually made of glass. The system is evacuated while the cell portion is immersed in mercury to insure an airtight seal, and the gas or vapor is admitted at a specific pressure at one side of the cell. As it permeates the film the pressure increases on the other side. The increased pressure is measured by a Pirani gage previously sealed into the wall. The pressure change is plotted against time. During the initial stages of the experiment, little or no gas appears on the other side of the coating. Gradually a steady state is reached where, if the diffusion process is Fickian, the data fall on a straight line. Extrapolation of this line to the time axis yields a point θ which corresponds to the commencement of the steady state of permeation. The intercept is called the time lag.

In the first method, a plot of $\log(Q_e - Q)$ versus time (where Q_e is the equilibrium amount of vapor sorbed and Q is the amount of vapor sorbed at time t) should produce a straight line if the process is Fickian and the diffusion coefficient does not change as the penetrant dissolves in the film. The slope of the curve is equal to

$$-\pi^2 D / 2.3 l^2 \quad (1)$$

where D is the diffusion coefficient and l is the film thickness.

In the permeability method, the diffusion coefficient is calculated from

$$\theta = l^2 / 6D \quad (2)$$

where θ is the time lag.

However the above equations presuppose no sitewise sorption of the penetrant. This may not be the case here since there is a good possibility (as will be shown later) that water may actually be sorbed on the titanium oxide surface even though it is completely surrounded by polymer.

Crank⁹ has considered several cases in which Fick's Law

$$dc/dt = D d^2c/dx^2 \quad (3)$$

may be modified to take care of just such contingencies. In the simplest case, where

$$S = R P/P_0 \quad (4)$$

S being solubility in grams/gram and P/P_0 being relative pressure, Fick's Law becomes

$$dc/dt = D'/(R + l)(d^2c/dx^2) \quad (5)$$

Therefore the D obtained from eqs. (1) and (2) may be written as

$$D = D'/(R + l) \quad (6)$$

and D' is the real coefficient of diffusion.

All diffusion data were obtained at a relative pressure of 0.525.

Sorption Data

The McBain-Bakr balance was also used to determine the equilibrium sorption of water on the titanium dioxide.

RESULTS

Table II indicates that incorporation of even as little as titanium dioxide in volume fraction of 0.01 causes a measurable lowering of the upper transition temperature of 4°C. A 15°C. decrease in the upper transition temperature occurs as the solid content is increased to a volume fraction of 0.03. In sample C the original point at 77°C. disappears. In samples A

TABLE II

| Film | TiO ₂ , wt.-% | Coefficient cm. ³ /g./°C. × 10 ⁴ (experimental) | Coefficient of expansion, cm. ³ /g./°C. × 10 ⁴ (corrected) | Tran- sition temper- ature, °C. |
|-------------|--------------------------|---|--|---|
| Unpigmented | — | 1.95 below 30°C. | — | 30 |
| | | 4.31 30-77°C. | — | 77 |
| | | 4.72 above 77°C. | — | |
| A | 3.38 | 1.76 below 32°C. | 1.82 | 32 |
| | | 4.48 32-73°C. | 4.64 | 73 |
| | | 4.78 above 73°C. | 4.95 | |
| B | 8.86 | 1.75 below 27°C. | 1.92 | 27 |
| | | 4.17 27-62°C. | 4.58 | 62 |
| | | 4.75 above 62°C. | 5.20 | |
| C | 13.77 | 1.61 below 28°C. | 1.87 | 28 |
| | | 4.14 above 28°C. | 4.80 | |
| D | 17.90 | 1.30 below 48°C. | 1.58 | 48 |
| | | 3.62 above 48°C. | 4.41 | |
| E | 31.56 | 1.12 below 51°C. | 1.64 | 51 |
| | | 3.05 above 51°C. | 4.46 | |
| F | 42.56 | 0.86 below 51°C. | 1.50 | 51 |
| | | 2.49 above 51°C. | 4.33 | |

to C the lower transition temperature remains essentially the same, being in the range of 27–30°C. However, on further addition of solid, both upper and lower transition temperatures disappear, and a new one in the region of 48–51°C. is manifested. Figures 1 and 2 illustrate typical specific volume versus temperature plots for films containing 0.03 and 0.128 volume fractions of solids. Column 3 of Table II lists the cubical coefficients of expansion per gram of pigmented and unpigmented film in each region.

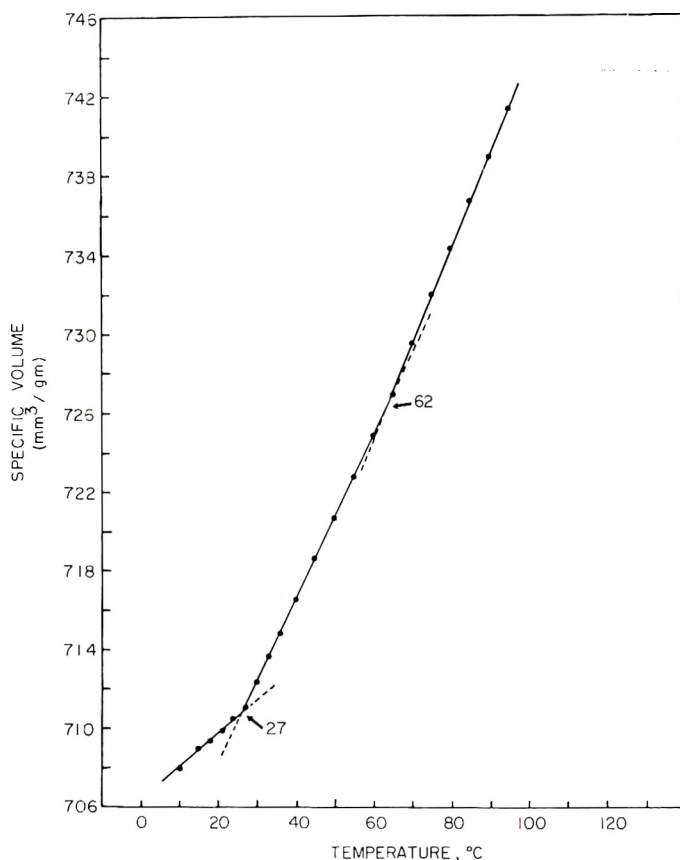


Fig. 1. Plot of specific volume vs. temperature for VYHH with 8.86 wt.-% TiO_2 (sample B).

Column 4 was calculated by assuming that the total volume increase was caused solely by the expansion of the polymer. Since the volume coefficient of expansion of titanium dioxide is $8 \times 10^{-6}/^\circ\text{C}$. and the maximum volume fraction is only 0.1925, it was felt that such an approximation was justified within the temperature region studied. It should be noted that just as in the case of the clear copolymer the greatest volume change occurs at the lower transition temperature.

Table III lists the diffusion coefficient for water vapor obtained for each

TABLE III

| | Diffusion coefficient $\times 10^6$, cm. ² /min. | | | |
|-------------|--|-------|-------|-------|
| | 32°C. | 47°C. | 55°C. | 60°C. |
| Unpigmented | 3.87 | 7.98 | 11.53 | 14.36 |
| A | 5.73 | 15.48 | 25.07 | 34.04 |
| B | 6.98 | 18.73 | 30.33 | 41.35 |
| C | 4.26 | 11.55 | 19.55 | 28.42 |
| D | 3.31 | 8.82 | 16.80 | 27.04 |
| E | 1.91 | 4.86 | 8.54 | 14.56 |
| F | 1.64 | 4.13 | 7.43 | 12.79 |

of the pigmented films obtained in the temperature region above and below their respective transition temperatures.

Diffusion data for carbon dioxide are also listed in Table IV.

Since the water vapor pick-up at low temperature was not sufficient to be weighed accurately, sample C was run in the Daynes' permeability

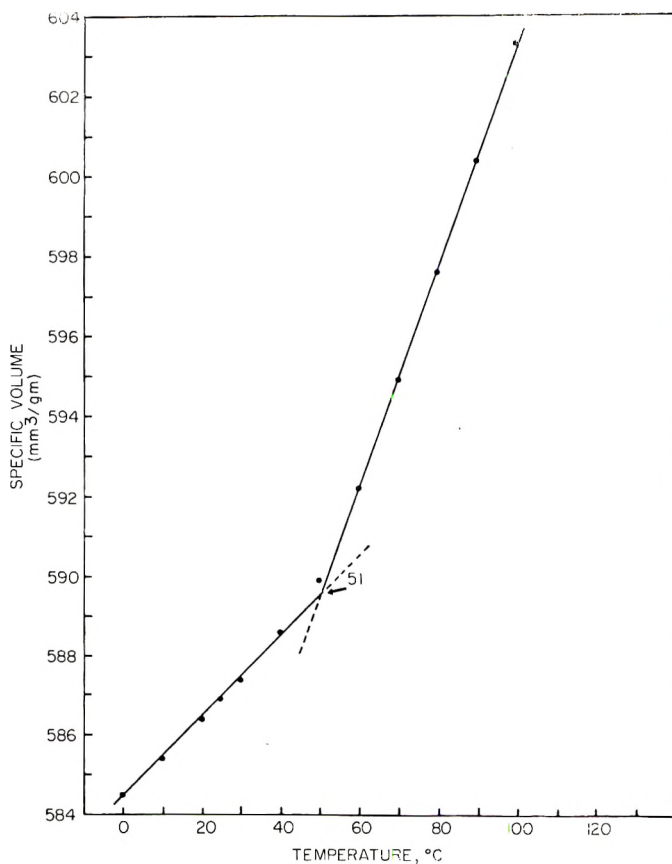


Fig. 2. Plot of specific volume vs. temperature for VYHH with 31.56 wt.-% TiO_2 (sample E).

TABLE IV

| Sample | Temp., °C. | $D \times 10^3$, cm ² /sec. |
|--------|------------|---|
| D | 0.5 | 0.91 |
| | 10.0 | 1.50 |
| | 22.0 | 2.60 |
| | 37.0 | 5.79 |
| | 37.0 | 6.02 |
| | 47.5 | 8.30 |
| | 54.0 | 14.2 |
| | 54.5 | 16.0 |
| | 59.0 | 18.4 |
| | 65.0 | 28.0 |
| | 68.0 | 29.9 |
| | 70.0 | 41.5 |
| | E | 29.0 |
| 42.1 | | 4.79 |
| 52.0 | | 8.08 |
| 65.0 | | 22.4 |

apparatus below 32°C. The carbon dioxide data were obtained in the same manner due to its low solubility within the polymer.

DISCUSSION

The data point to two quite surprising results. The first is the change in the transition temperature of the polymer brought about by as small an addition of solid as 0.01 volume fraction. The second is the trend of the transition temperature, the upper dropping till it coincides with the lower and then increasing with further addition of solid. It is not difficult to imagine that where a large surface area is available, as in high solid mixtures, sufficient adsorption and immobilization of the polymer could take place and cause the glass temperature to increase. This is not the case here.

However, on further reflection, it is possible to suggest a reasonable mechanism to explain the results.

In a previous publication⁴ it was shown that the transport rate of many gases through the polymer varied inversely with their van der Waals' diameter. Water was the exception, in that it diffused at a considerably faster rate than would be predicted from its large size. This phenomenon was ascribed to its ability to form hydrogen bonds with the acetate groups.

By so doing, any interchain bonding brought about by acetate interaction would be broken, thus producing a more flexible backbone capable of oscillation with less restriction thus increasing the probability of "hole" formation. In this case, the polar titanium dioxide could adsorb some of the acetate groups which originally contributed to the stiffening of not only the chain to which they were attached but also the adjacent ones with which they interact. This has the effect of freeing the latter for oscillation and rotation. This should cause a lowering of the upper transition temperature

which has been attributed to the motion of the vinyl backbone since its value of 77°C. is so close to that of polyvinyl chloride reported at 78–81°C.¹⁰

As is noted in Table II, gradually increasing the percentage of titanium dioxide causes the upper transition temperature to fall from 77°C. till in sample C it coincides with the lower one which has remained approximately constant as the solid content of the polymer was increased from 0.011 to 0.049 volume fraction. In the latter sample, sufficient inter-chain breakage has occurred, so that the backbone is now as flexible as that of the acetate group which corresponds to the lower transition temperature.

That acetate groups may be adsorbed on a titanium dioxide appears reasonable in the light of the rather large heat of immersion of 850 cal./g. of titanium dioxide reported by Boyd and Harkins¹¹ in ethyl acetate. (This compound was probably anatase in crystal habit, whereas the rutile variety has been used here. Correction for different densities would bring the heat of wetting down to about 800 cal./g. of rutile which is still quite high.)

As more solid is mixed with the polymer, more and more acetate groups are sorbed, and both their mobility and the chains to which they belong are restricted. This accounts for the increase of the lower transition temperature from 30 to 51°C.

The data in Table V may serve to make the above picture clearer.

Column 2 lists the total surface area of solid in the pigmented films. This was calculated from the mean diameter of titanium dioxide which was given as 0.22 or 6.5 μ^2 /g. Column 3 was obtained by assuming that the acetate groups, occupying 25 A.², cover the entire surface.

Column 3 was obtained from the weight per cent of polymer in each film. The number of base moles of copolymer which correspond to the data of column 4 are listed in column 5. This was calculated in the following manner.

The polymer contains 87% vinyl chloride (molecular weight 63) and 13% vinyl acetate (molecular weight 86). This corresponds to 9 moles of vinyl chloride to one of vinyl acetate or $(9 \times 63) + 86 = 653 =$ the base molecular weight. The excess unbound polymer is the ratio of column 6 over column 3. A glance at the figures listed in column 7 indicates that, even at the lower solid contents and even on a base mole estimate, the excess unbound polymer is only several hundred times that of the bound material. At higher concentrations, the excess is less by an order of magnitude dropping to 48 times at the highest solid levels. However, it is unreasonable to expect that all of the acetate groups in contact with the surface of the titanium dioxide come from the same macromolecule. Rather, it has been suggested^{12,13} that only very few of the adsorbed acetate radicals come from the same macromolecule.

Consequently, if, as a first approximation, it is assumed that only one acetate group per macromolecule is on the surface of the solid, this would more or less affect the motion of 16 base moles of vinyl acetate vinyl chloride. This latter figure is determined by dividing the molecular weight

TABLE V

| Film | Surface area of pigment in film, $A^2 \times 10^{-20}$ /100 g. of film | Maximum number of acetate groups possible on pigment $\times 10^{-20}$ | Polymer in film, wt.-% | Base moles of copolymer/100g. of film | Number of base molecules $\times 10^{-23}$ /100 g. of film | Column 6 Column 3 | Column 7 16 ^a |
|------|--|--|------------------------|---------------------------------------|--|----------------------|-----------------------------|
| A | 22 | 0.87 | 96.6 | 0.148 | 0.90 | 1034 | 65 |
| B | 57 | 2.29 | 91.1 | 0.140 | 0.85 | 371 | 23 |
| C | 89 | 3.56 | 86.2 | 0.132 | 0.81 | 228 | 14 |
| D | 116 | 4.65 | 82.1 | 0.126 | 0.77 | 166 | 10 |
| E | 204 | 8.15 | 68.4 | 0.105 | 0.64 | 79 | 5 |
| F | 276 | 11.0 | 57.4 | 0.088 | 0.53 | 48 | 3 |

^a Average molecular weight of copolymer divided by the base molecular weight.

(10,500) of the poly(vinyl acetate-vinyl chloride) copolymer by 653 which is, as pointed out earlier, the molecular weight of 9 moles of vinyl chloride and one of the acetate. If the amount of unbound base polymer in column 7 is divided by 16 one obtains the quantity of macromolecule which does not have at least one point of attachment to the titanium dioxide. Column 8 therefore shows that there is really not quite as great an excess of unbound polymer as would be supposed at a first and cursory consideration. In

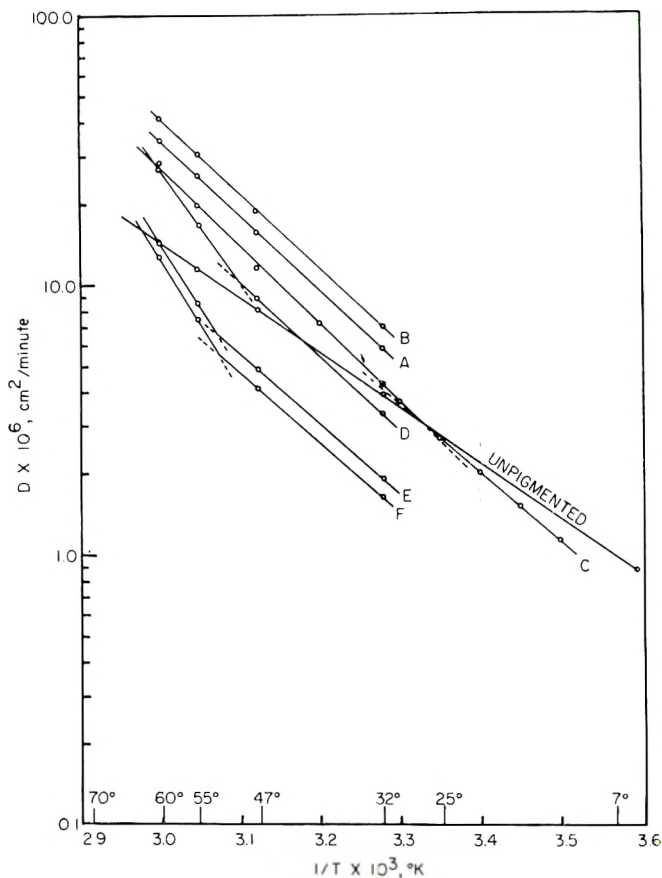


Fig. 3. Plot of log diffusion coefficient vs. $1/T$ for water vapor. Broken lines indicate direction data would have gone had no T_g existed.

fact, in the films containing larger amounts of solid the unbound macromolecule is only 3 to 5 times in excess of that in touch with the surface.

In summary, at low titanium dioxide content some of the acetate groups involved in intersegmental bonding and hence chain stiffening are removed by sorption on the solid surface. This loosens the segments of the polymer permitting it greater freedom of motion. Hence, that transition temperature characteristic of the backbone, i.e., the one at 77°C . drops until at a solid content of 13.77 wt.-% or 0.0489 volume fraction, backbone mobility

is equal to that of the acetate radicals' motion, and the two transition temperatures coincide at 30°C. At the higher concentration of titanium dioxide, so many acetate groups are sorbed and their freedom of motion is so restricted that the transition temperature of the polymer is now raised to about 51°C.

So far, the discussion has proposed a mechanism to explain the change in transition temperature on the basis of changes in the mobility of the poly-

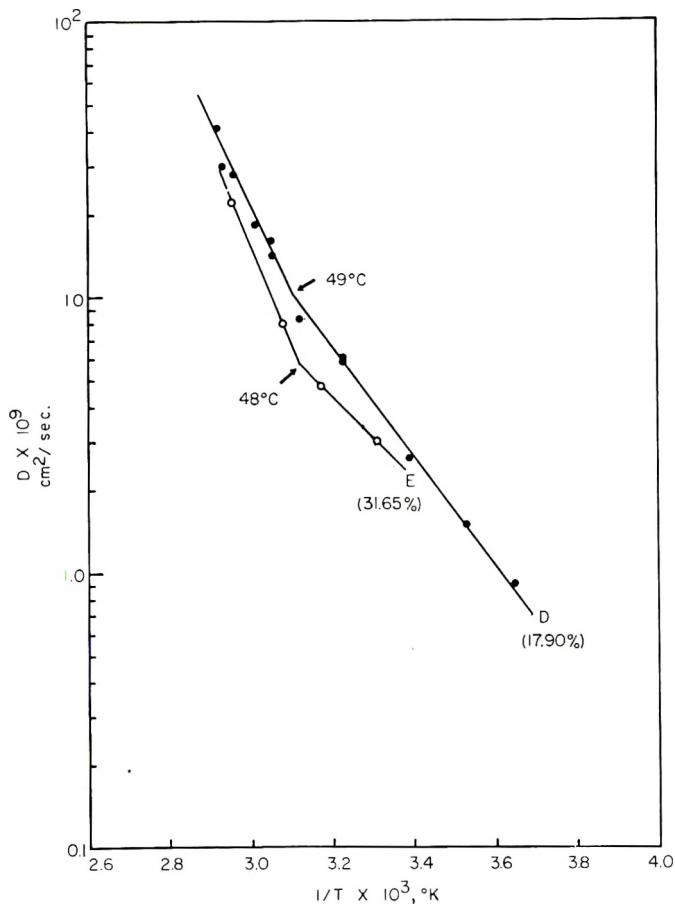


Fig. 4. Plot of log diffusion coefficients vs. $1/T$ for carbon dioxide gas.

mer segments. It is reasonable to ask whether there is an independent method which would indicate that such changes are possibly taking place. Such a method is, in fact, available in the form of a study on the diffusion of a gas or vapor through the polymer-solid film. It will be recalled that diffusion takes place as a result of density fluctuation or through "holes" formed by the motion of polymer segments.¹⁴ At the glass transition increased segmental mobility occurs, and the transport process increases accordingly.

It has been shown that water moving through the same copolymer exhibits an increase in the diffusion coefficient at higher T_g but not at the lower one.⁴ In the case of carbon dioxide, the transport process speeds up at the lower transition temperature but not at the higher. This is explained on the basis of the molecular size. The increased amplitude of oscillation occurring at 30°C. (the lower transition temperature) is sufficient to speed up the passage of the smaller carbon dioxide molecule (diameter = 3.23 Å.), whereas water (diameter = 3.48 Å.) requires a larger "hole," a greater number of which occur upon additional motion of the backbone, which occurs at the higher transition temperature (77°C.).

It would therefore be expected that an abrupt increase in the diffusion coefficient should take place at the transition temperature of the titanium dioxide, polymer films.

Plots of data in Tables III and IV in the form of $\log D$ versus $1/T$ show that this is indeed the case. Samples C, D, E, and F show the expected breaks for water at about 50 and 28°C. as indicated in Figure 3. Figure 4 shows the same thing for carbon dioxide for samples D and E.

The fact that sample C (transition temperature = 28°C.) shows a change in slope, which, of course, means a sharp increase in the diffusion coefficient in the liquidlike region, is significant when it is recalled that there is not sufficient segmental mobility in the clear film at the lower transition temperature to accommodate the large water molecule.⁴ However, as was conjectured earlier, if the 28°C. transition temperature in the filled polymer corresponds to the increased mobility of both the backbone and the acetate groups a "hole" of sufficient size could be formed to accommodate the water vapor.

The plot of Figure 3 shows that this takes place.

It is of interest to note that the adsorption of polymer on even a relatively large particle size solid (surface area = 6 m.²/g.) compared to a reinforcing solid like a carbon black (surface area = 120 m.²/g.) can produce long-range effects on the mobility and consequently the properties of the unadsorbed macromolecule.

The authors wish to express their appreciation to Interchemical Corporation for their encouragement and permission to publish this paper and to Dr. T. K. Kwei for many stimulating discussions of the subject matter.

Addendum

If it were assumed that the crystallite particles existed as completely separated individuals the distance between them, s , may be calculated by $\langle s = d \{ [(0.74)^{1/3}/V] - 1 \} \rangle$ where d is the mean particle diameter (2200 Å. in this case) and V is the volume fraction of powder.

Table VI lists these values. It would of course be naive to expect 100% dispersion of the solid and therefore the actual distances between particles will be even greater than the values tabulated here. Since the glass transition temperature and the diffusion process are related to the segmental mobility of the macromolecular species present between particles it

follows that the changes in the former must be a reflection of corresponding alterations in the latter.

Sorption of the polymer molecule on a surface decreases the number of degrees of freedom for oscillatory motion which then interferes with the movement of adjacent molecules or portions thereof. They in turn exert a similar effect on their nearest neighbors until like the ripples caused by a stone thrown into a pond, the results are felt a long distance from the point of origin; in the examples cited here, the range is 3350A. for the lowest volume fraction to 625A. for the highest loading (one half the distance between two particles).

TABLE VI
Interparticle Distance

| Vol. fraction of TiO ₂ at 25°C. | Distance between particles, A. |
|--|--------------------------------|
| 1.11 | 6700 |
| 3.03 | 4180 |
| 4.89 | 3230 |
| 6.55 | 2730 |
| 12.92 | 1740 |
| 19.25 | 1250 |

Gibbs and DiMarzio¹⁵ have developed from statistical mechanical considerations equations which relate the second order transition temperature (which has been assumed to be identified with the glass transition temperature) to the flex energy or the difference between the polymer chain conformational energies in different orientations ($E_1 - E_2$) and the energy of interaction between a pair of chemically non bonded but nearest neighboring segments and the molecular weight or degree of polymerization. They state that the values of ($E_2 - E_1$) must be "greater for chains which are known to be stiff, than for chains which are known to be flexible from independent experiments such as light scattering investigations of mean square (end to end) length in solution." They cite for example values of ($E_1 - E_2$) of 1.44 Kcal./mole of segments for polymethyl methacrylate, and 1.15 Kcal./mole of segments for polymethyl acetate etc.

Similar calculations were made using the data obtained with the pure copolymer film and with the one containing 31.56% TiO₂. For the former, the lower or 30° T_g was used since this corresponded to the 50° T_g for the pigmented polymers.

Substitutions into the appropriate equations of Gibbs and DiMarzio gives a ($E_1 - E_2$) value of 1.38 Kcal./mole of segments for pure poly (vinyl chloride-vinyl acetate) whereas the pigmented polymer has a value of 1.54.

Increased chain stiffness is expected in the latter and the higher value of the flex energy ($E_1 - E_2$) reflects the situation in accordance with one of the criteria of Gibbs and DiMarzio.

References

1. Bachmann, J. H., J. W. Sellers, M. P. Wagner, and R. F. Wolf, *Rubber Chem. and Technol.*, **32**, 1286 (1959).
2. Landel, R. F., *Trans. Soc. Rheology*, **2**, 53 (1958).
3. Mason, P., *J. Appl. Polymer Sci.*, **4**, 212 (1960).
4. Kumins, C. A., and J. Roteman, *J. Polymer Sci.*, **55**, 699 (1961).
5. Schildnecht, C. E., *Vinyl and Related Polymers*, Wiley, New York, 1952, p. 400.
6. Kumins, C. A., C. J. Rolle, and J. Roteman, *J. Phys. Chem.*, **61**, 1290 (1957).
7. Kumins, C. A., and J. Roteman, *J. Polymer Sci.*, **55**, 683 (1961).
8. Prager, S., and F. A. Long, *J. Am. Chem. Soc.*, **73**, 407 (1951).
9. Crank, J., *Mathematics of Diffusion*, Oxford Univ. Press, London, (1956), p. 123.
10. Spencer, R. S., and R. F. Boyer, *J. Polymer Sci.*, **2**, 155 (1947).
11. Boyd, G. E., and W. D. Harkins, *J. Am. Chem. Soc.*, **64**, 1190 (1942).
12. Frisch, H. L., and R. Simha, *J. Chem. Phys.*, **27**, 702 (1955).
13. Koral, J., R. Ullman, and F. R. Eirich, *J. Phys. Chem.*, **62**, 541 (1958).
14. Barrer, R. M., *Diffusion In and Through Solids*, Cambridge Univ. Press, 1951.
15. Gibbs, J. H. and J. H. DiMarzio, *J. Chem. Phys.*, **28**, 373 (1958).

Synopsis

It has been shown that a nonreinforcing solid such as titanium dioxide can radically alter the glass transition temperature of the model polymer, poly(vinyl chloride-vinyl acetate) copolymer after being mechanically incorporated within it. The T_g values were either higher or lower than that of the original unfilled polymer, depending on the volume fraction of the solid. The magnitude of these changes is in some cases as great as 49°C. This phenomenon was explained on the basis of adsorption of the acetate radicals on the surface of the solid and the breaking of interchain hydrogen bonds. The changes in segmental mobility of the polymer as indicated by the variation in T_g were also verified by gaseous diffusion studies.

Résumé

On montre qu'un solide non-reforçant comme le dioxyde de titane peut changer radicalement la température de transition vitreuse de l'échantillon de polymère, en l'occurrence le copolymère de chlorure de vinyle et d'acétate de vinyle, après avoir été incorporé mécaniquement à l'intérieur de celui-ci. Les valeurs de T_g indiquées sont soit plus élevées soit plus faibles que celles du polymère original non-traité, et elles dépendent de la fraction de volume du solide. La grandeur de ces variations est dans certains cas de l'ordre de 49°C. On explique ce phénomène sur la base d'une adsorption des radicaux acétates sur la surface du solide et de la rupture des liaisons hydrogène entre les chaînes. Les changements dans la mobilité des segments du polymère, mise en évidence par la variation des valeurs de T_g sont également vérifiés par des études de diffusion gazeuse.

Zusammenfassung

Es wurde gezeigt, dass ein nichtverstärkender Festkörper, wie Titandioxyd, die Glasumwandlungstemperatur des Modellpolymeren, Polyvinylchlorid-Vinylacetat-Copolymer, in das er mechanisch eingebracht wurde, radikal ändern kann. Die ermittelten T_g -Werte waren je nach dem Volumbruchteil des Festkörpers höher oder tiefer als die für das ursprüngliche, ungefüllte Polymere. Die Veränderung betrug in manchen Fällen bis zu 49°C. Diese Erscheinung wurde auf Grund einer Adsorption der Acetatradikale an der Oberfläche des Festkörpers und des Aufbrechens von Wasserstoffbindungen zwischen den Ketten erklärt. Die Änderung in der Beweglichkeit der Polymersegmente, wie sie sich in der Variation von T_g zu erkennen gibt, wurde auch durch Gasdiffusionsuntersuchungen bestätigt.

Received October 26, 1961

Water Sorption of Titanium Dioxide–Poly(Vinyl Acetate–Vinyl Chloride) Copolymer Films

CHARLES A. KUMINS, JEROME ROTEMAN, and
CLIFFORD J. ROLLE, *Interchemical Corporation, Central Research
Laboratories, New York, New York*

INTRODUCTION

In the preceding paper¹ the effects of solid–polymer interaction on the transition temperature for the system titanium dioxide–poly(vinyl acetate–vinyl chloride) have been described.

To gain a further insight into the relationship existing between a crystalline material and polymer in the solid phase a study was made of the transport process of water through films into which varying amounts of titanium dioxide had been dispersed. Data were also obtained on the equilibrium sorption of water in the titanium dioxide–polymer films.

Water was the penetrant of choice because it is readily adsorbed by titanium dioxide, and consequently it was hoped that indications of interaction between it and the solid surrounded by polymer as it is in the films studied could be more easily observed.

EXPERIMENTAL

Materials and Films Preparations

The materials and the method of film preparation are the same as described in the previous paper.¹

Measurements

All data were collected at 25 and 47°C. However, since the former indicated identical trends only the higher temperature figures will be discussed here.

Sorption Isotherms

These were obtained by employment of the same McBain-Bakr balance described previously.² Water vapor sorptions were determined at various relative pressures, at 47°C., for the titanium dioxide, the unpigmented, solvent-free polymer film, and the pigmented polymer films. The thicknesses of the various films were approximately 0.25 mm.

Density Determinations

Glass transition temperature measurements were made in the dilatometer as described in the previous paper.¹ In these measurements, the specific volumes of the films were obtained at a given temperature and the reciprocals are the densities.

Results

The isotherms for the rutile, unpigmented, and pigmented films D, E, and F obtained at 47°C. are illustrated in Figure 1. They are, as expected, Brunauer Type II isotherms³ such as have been obtained by numerous investigators.

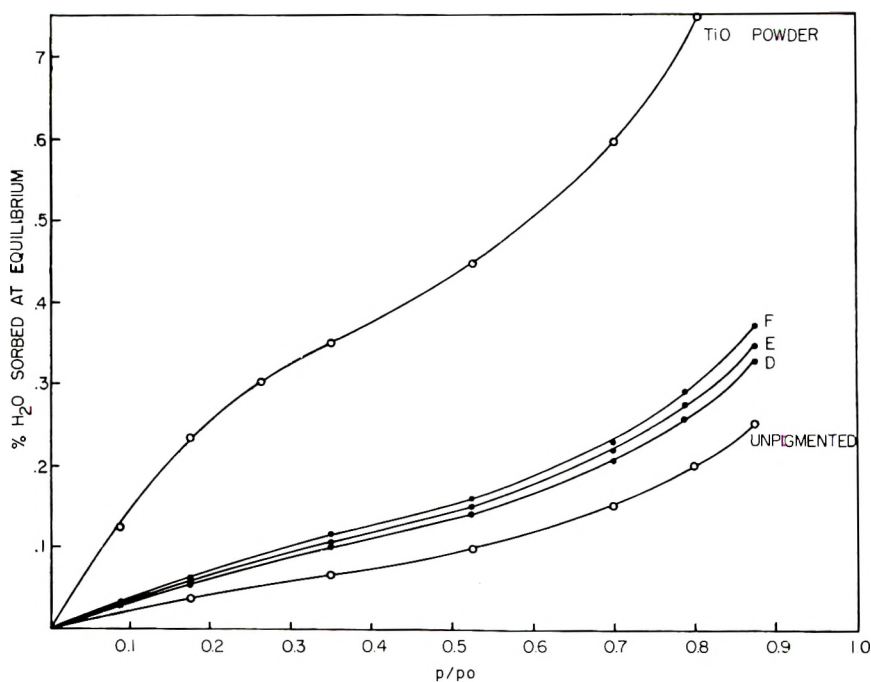


Fig. 1. VYHH-TiO₂/water vapor isotherms at 47°C.

The isotherm for the clear polymer is a solution-type curve with some very slight indication of a sigmoid shape. The latter is more pronounced in the curves of the pigmented polymers.

Table I lists the experimentally determined densities at 47°C. of the different films containing varying volume fractions of titanium dioxide.

Included also are the calculated densities (taking a value of 4.191 g./cc. at 47°C. for the rutile and 1.334 g./cc. at 47°C. for the copolymer) assuming volume additivity. The fourth column lists the decrease in density or expansion of the polymer-solid combination as a percentage of the calculated values. It is noted that in all cases the actual densities are less than that would be expected if a simple addition of components was all that was taking place,

TABLE I
Density Comparisons

| | Temp., °C. | Density, g./cc. | | Expansion, % |
|-------------|------------|-----------------|--------------|-----------------|
| | | Theory | Experimental | |
| Unpigmented | 25 | — | 1.349 | — |
| A | | 1.381 | 1.377 | 0.27 |
| B | | 1.435 | 1.407 | 2.07 |
| C | | 1.488 | 1.474 | 1.00 |
| D | | 1.535 | 1.525 | 0.90 |
| E | | 1.716 | 1.704 | 0.84 |
| F | | 1.896 | 1.880 | 1.08 |
| Unpigmented | 47 | — | 1.334 | — |
| A | | 1.366 | 1.357 | 0.63 |
| B | | 1.420 | 1.390 | 2.11 |
| C | | 1.472 | 1.463 | 0.66 |
| D | | 1.519 | 1.511 | 0.59 |
| E | | 1.700 | 1.690 | 0.66 |
| F | | 1.879 | 1.868 | 0.74 |

the maximum expansion (if one were to refer to this as such) taking place with the film containing 0.03 volume fraction of solid.

DISCUSSION

Since the densities of the polymer–solid combinations are lower than the calculated values, it would appear that the films are not as closely knit together as those obtained by the use of the clear poly(vinyl chloride–vinyl acetate) alone. This more porous structure may originate within the pigment region if the approximately spherical titanium dioxide particles are sufficiently flocculated to form a loose aggregate, with the interstitial spaces small enough to exclude polymer.

The expanded structure of the pigmented film is also corroborated by the values of the water vapor diffusion coefficients. Comparison of these with the densities (Table I) indicates that the maximum transport rate occurs through film B, which also exhibits the greatest negative deviation from the calculated density. This is brought out graphically in Figure 2, where it is observed that the curves for diffusion coefficients through the various pigmented films have the same general shape as that for the differences in densities between the calculated and the experimentally determined values. In both cases the maximum is exhibited at the same point. Based on the above, it would certainly be reasonable to conclude that the oxide exists in a more or less flocculated condition within the solid–polymer matrix.

The fact that the water vapor diffusion coefficients of the more highly pigmented films vary inversely with the volume fraction of titanium dioxide (Table II) in the film is not astonishing in view of the longer path length that must be traveled by a water molecule in order to pass around the impervious solid. Another factor in this relationship is the crosslinking effect of those polymer segments which are adsorbed on the titanium dioxide,

TABLE II
Water Vapor Diffusion Coefficients at 47°C.

| Film | Diffusion coefficient, cm. ² /min. × 10 ⁶ | Volume fraction of TiO ₂ |
|-------------|--|-------------------------------------|
| Unpigmented | 7.98 | — |
| A | 15.48 | 0.0110 |
| B | 18.73 | 0.0300 |
| C | 11.55 | 0.0483 |
| D | 8.82 | 0.0649 |
| E | 4.86 | 0.1297 |
| F | 4.13 | 0.1908 |

since it has been shown¹ that this will cause a decrease in the rate of transport through macromolecular films. The changes in the T_g discussed in the previous paper are cited as evidences for polymer adsorption.

In light of the above, it is now of interest to consider the water sorption data recorded in Table III. Here the quantities of water sorbed by each component, considered separately in each 100 g. of film, are listed in columns 2 and 3. These were obtained from the sorption isotherms for the titanium dioxide and the unfilled poly(vinyl chloride-vinyl acetate). For purposes of simplification the data refer to $P/P^0 = 0.525$ at a temperature of 47°C. Their sums are recorded in column 4. The amounts of water actually

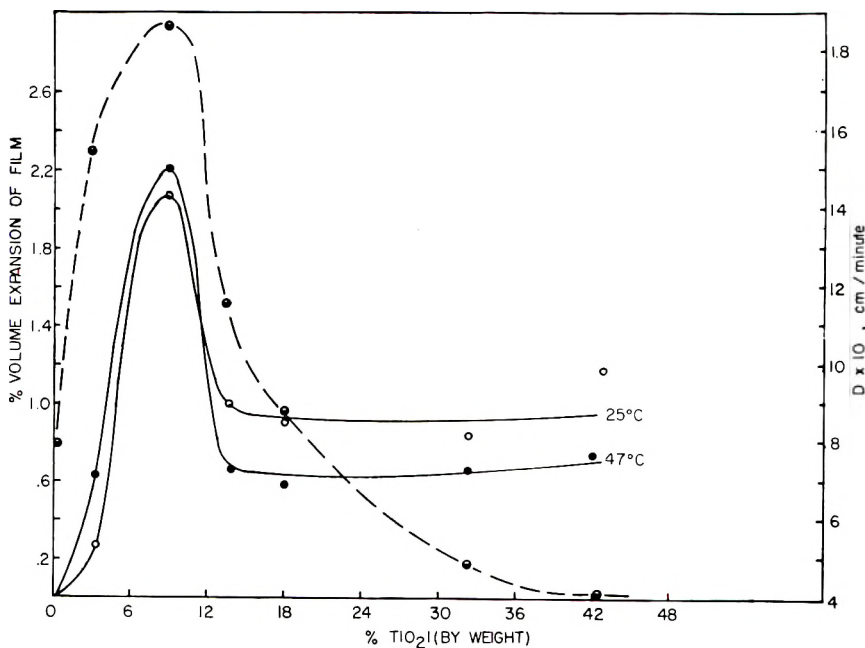


Fig. 2. Per cent volume expansion vs. wt.-% TiO₂ at 25 and 47°C. in comparison with water vapor diffusion coefficients vs. wt.-% TiO₂ at 47°C.: (—) volume expansion; (---) diffusion coefficients.

sorbed by the pigmented films are in column 5. Column 6 represents the difference between column 4 and 5. It is seen that in films A to D the water pick-up is greater than the amounts each component is capable of sorbing if each were in the completely separated state. In films E and F, where the oxide content is high, there is a reverse trend. However, in no case is the water pick-up just equal to the amount of polymer present, which would indicate an oxide surface completely covered by undisplaceable polymer.

All the data indicate that the solid surface is capable of sorbing water even though completely surrounded by polymer. It is believed that actually two phenomena occur.

TABLE III

| Film | Ratio copolymer: TiO ₂ | Theoret- ical wt. H ₂ O ab- sorbed on copoly- mer, g. | Theoret- ical wt. H ₂ O ab- sorbed on TiO ₂ , g. | Theoret- ical total wt. H ₂ O absorbed, g. | Actual wt. H ₂ O absorbed, g. | Difference H ₂ O absorbed, g. |
|------|---|---|--|---|---|--|
| A | 96.62: 3.38 | 0.0928 | 0.0152 | 0.1080 | 0.1600 | +0.0520 |
| B | 91.14: 8.86 | 0.0875 | 0.0410 | 0.1285 | 0.1560 | +0.0275 |
| C | 82.23: 13.77 | 0.0828 | 0.0620 | 0.1448 | 0.1511 | +0.0063 |
| D | 82.10: 17.90 | 0.0788 | 0.0806 | 0.1594 | 0.1684 | +0.0090 |
| E | 68.44: 31.56 | 0.0657 | 0.1420 | 0.2077 | 0.2013 | -0.0064 |
| F | 57.44: 42.56 | 0.0551 | 0.1915 | 0.2466 | 0.1861 | -0.0605 |

Since the changes in the transition temperature indicate that some polymer sorption is actually taking place, the solid particles must at least be partially dispersed. To account, therefore, for the complete availability of the titanium dioxide surface for water sorption as indicated by the data in films A to D, it must be concluded that the water can displace the polymer. This is energetically possible if we were to consider ethyl acetate as a mode for the polyvinyl acetate portion of the copolymer. The heat of immersion of rutile titanium dioxide in ethyl acetate has been determined by Chessick⁴ to be 215 ergs/cm.². Since corresponding value for water is 550 ergs/cm.², the process is at least thermodynamically possible.

Certainly, if the solid is partially flocculated (and it is believed that this is indicated by the lower densities of the filled film), it would indicate that a displacement reaction is not required for the water to reach the surface. The larger amounts of water sorbed by films A to D which are in excess of the sum of each of the components taken separately may be accounted for by capillary condensation in the interstitial spaces existing between flocculated pigment particles.

As noted above, films E and F (volume fractions 0.1279 and 0.1908, respectively) sorb water in lesser amounts than the sum of each component considered separately. Here again two explanations are suggested. One is related to the flocculated state of the oxide: the oxide is present in such high concentration and the particles are in such close contact, that the water molecules can not penetrate between them. However, this suggestion leaves something to be desired, since the water isotherms for the solid are obtained in the powdered state where it is expected that even closer particle-to-particle contact is made.

The other, and what seems to be a more plausible approach, is that the displacement of the sorbed polymer segments by water is actually an equilibrium process having a characteristic constant. Since at a $P/P_0 = 0.525$ at 47°C . the water content of the copolymer is only about 0.10% and since the volume fraction of the copolymer is only 0.8721 in film D and 0.8092 for film F, it is reasonable to assume that there is not sufficient water concentration at the pigment-polymer interface to cause the displacement reaction to go to completion.

If the further work which is continuing in our laboratory on other solid-polymer systems indicates little or no flocculation, it should be possible to use this experimental approach to obtain the differential heat of wetting between a powder and solid high molecular weight material. Determination of sorption isotherms at different temperatures which in the case discussed here is water (but it need not necessarily be) should give:

$$\Delta H_{\text{expt'l}} = \Delta H_{\text{water/solid}} - \Delta H_{\text{polymer/solid}} + \Delta H_{\text{water/polymer}}$$

Since $\Delta H_{\text{water/solid}}$ and $\Delta H_{\text{water/polymer}}$ may be determined separately or taken from the literature it should in principle be easy to calculate $\Delta H_{\text{solid/polymer}}$.

It is obvious, of course, that studies such as described here may also give an insight into the degree of dispersion of one solid in another as well.

The authors wish to express their appreciation to Interchemical Corporation for their encouragement and permission to publish this paper.

References

1. Kumins, C. A., and J. Roteman, *J. Polymer Sci.*, **A1**, 527 (1963).
2. Kumins, C. A., C. J. Rolle, and J. Roteman, *J. Phys. Chem.*, **61**, 1290 (1957).
3. Brunauer, S., *The Adsorption of Vapors and Gases*, Princeton Univ. Press, Princeton, N. J., 1943, p. 150.
4. Chessick, J. J., Lehigh University, private communication.

Synopsis

Crystalline solids, as exemplified by TiO_2 , incorporated within a film of a model polymer, poly(vinyl chloride-vinyl acetate) copolymer, have been shown to absorb relatively large amounts of water vapor on the surface. In some cases all of the crystal surface may participate in the sorption process, despite evidence that the polymer has been initially present on the surface of the former. This, coupled with anomalous density changes in the film, suggests the possibility of measuring crystal flocculation within the membranes as well as the displacement of adsorbed polymer segments by means of water

vapor. The anomalous density determinations were correlated with water transport measurements, and an equation for calculation of the heat of wetting of a crystal with a solid polymer is presented.

Résumé

On a montré que des solides cristallins, comme c'est le cas du TiO_2 , incorporé dans un film de structure polymérique (le copolymère de chlorure de vinyle et acétate de vinyle), absorbent une quantité relativement élevée de vapeur d'eau en surface. Dans plusieurs cas toute la surface cristalline peut participer au processus de sorption, bien que le polymère soit initialement présent à la surface du cristal. Ceci, accompagné des variations de densités anormales dans le film, suggère la possibilité de mesurer la flocculation du cristal dans la membrane aussi bien que le déplacement de segments de polymère adsorbés au moyen de vapeur d'eau. Les valeurs de densités anormales furent expliquées par des mesures de transport d'eau et une équation pour le calcul de la chaleur de mouillage d'un cristal avec un polymère solide est décrit.

Zusammenfassung

Kristalline Festkörper, wie zum Beispiel TiO_2 , in einen Film eines Polyvinylchlorid-Vinylacetatcopolymeren als Modellpolymeres eingebaut, absorbieren an ihrer Oberfläche relativ grosse Mengen von Wasserdampf. In manchen Fällen kann die ganze Kristalloberfläche am Sorptionsprozess teilnehmen, obwohl sich das Polymere anfänglich an der Oberfläche befindet. Diese Tatsache im Verein mit den anomalen Dichteänderungen im Film weist auf die Möglichkeit hin, die Kristallflockung in den Membranen und auch die Verschiebung der adsorbierten Polymersegmente mit Hilfe von Wasserdampf zu messen. Die Bestimmung der anomalen Dichte wurde mit der Messung des Wassertransports in Beziehung gebracht und eine Gleichung zur Berechnung der Benetzungswärme eines Kristalls mit einem festen Polymeren wird angegeben.

Received October 26, 1961

Polymerization of Acrylonitrile by Electron Transfer Catalysts

ALBERT ZILKHA and YAIR AVNY, *Department of Organic Chemistry, The Hebrew University, Jerusalem, Israel*

INTRODUCTION

The polymerization of several vinyl monomers, especially styrene, by electron transfer catalysts such as sodium naphthalene has been extensively studied.¹ The mechanism of the polymerization consisted of electron transfer to the monomer to yield a radical anion which on dimerization gave a dianion which initiated polymerization from both ends. "Living" polymers were obtained whose molecular weight was given by $[M]^{1/2}[C]$.²

As is known acrylonitrile is much more reactive than styrene in anionic, but less in free radical, polymerizations. In the present work the polymerization of acrylonitrile by alkali metal naphthalene and anthracene was investigated, to determine whether the polymerization takes place absolutely by an anionic mechanism, and if not, the extent of the contribution of the free radical formed by the electron transfer reaction to the polymerization.

The mechanism of the polymerization was studied from the effect of the changes in monomer and catalyst concentrations, of polymerization temperature, polycyclic aromatic radical and the alkali metal positive counterion on the molecular weight of the polymers obtained, and from copolymerization studies with styrene.

EXPERIMENTAL

Materials

Acrylonitrile (B.D.H., British Drug Houses) was purified according to the method of Bamford and Jenkins.³ Tetrahydrofuran previously dried over sodium hydroxide pellets was refluxed over sodium wire for several hours. Benzophenone (about 5 g./l.) was added and the reflux continued until the tetrahydrofuran became deeply blue or violet from the sodium benzophenone formed and then distilled under nitrogen. Anthracene (B.D.H.), m.p. 214-216°C., having a blue fluorescence, and naphthalene (B.D.H.), recrystallized, m.p. 80°C., were used.

Catalysts

The following procedure was used for the preparation of monosodium anthracene, disodium anthracene, sodium naphthalene, lithium anthracene and lithium naphthalene.

The polycyclic hydrocarbon was dissolved in the appropriate amount of tetrahydrofuran to obtain the catalyst concentration required, and the equivalent amount of alkali metal in the form of wire was added. In the case of the disodium anthracene, excess sodium metal was used. The reaction started immediately, and the deep color of the catalysts appeared at once. The reaction mixture was shaken for several hours until the catalyst concentration reached the theoretical value within $\pm 3\%$, as seen from titration of the catalyst solution with standard acid. The color of the anthracene catalysts was blue, and that of the naphthalene was green.

It was possible to prepare the anthracene catalysts up to a concentration of about 0.4*N*, and those of naphthalene, due to its greater solubility in tetrahydrofuran, to about 1*N*.

Polymerization Procedure

The addition of reagents and the polymerization were carried out under oxygen-free nitrogen. Into a three-necked flask fitted with a high speed stirrer, a gas adapter for introducing nitrogen, a thermometer, and an outlet fitted with a self-sealing rubber cap, freshly distilled solvent was transferred with a syringe; the flask was cooled to and kept at the required temperature of polymerization. The required amount of catalyst solution was then added, followed by monomer. The polymerization started immediately with precipitation of polymer. It was stopped after the required time by adding methanolic hydrochloric acid (50 ml.). The polymer was filtered off, washed with water, tetrahydrofuran to remove monomer or aromatic hydrocarbons, and methanol, and sucked dry on the water pump. It was further purified by trituration with tetrahydrofuran, water, tetrahydrofuran, and methanol and dried to constant weight in an oven at 60°C.

All polymerizations were carried out with the use of a constant volume of monomer, catalyst, and tetrahydrofuran (50 ml.).

Viscosities of polymer solutions were measured in dimethylformamide in an Ostwald viscometer. The weight-average molecular weights were determined from intrinsic viscosities by use of the equation of Cleland and Stockmayer:⁴

$$[\eta] = 2.33 \times 10^{-4} \bar{M}_w^{0.75}$$

Preparation of Block Polymers

Essentially the above polymerization procedure was followed. Monomers were added to the tetrahydrofuran followed by catalyst. The polymers were worked out as before, except that more methanol was added to insure the complete precipitation of any polystyrene formed. They were filtered and washed with water and methanol. After drying they were extracted several times with boiling benzene to remove any homopolystyrene formed. The residual polymer was washed with methanol and dried. It consisted of homopolyacrylonitrile together with block copolymer.

RESULTS

Dependence of Molecular Weight on Catalyst Concentration

It was found that for relatively high catalyst concentrations, the molecular weight was independent of catalyst concentration, while at relatively low catalyst concentrations, the molecular weight increased with decrease in catalyst concentration (Fig. 1). This behavior was the same for all

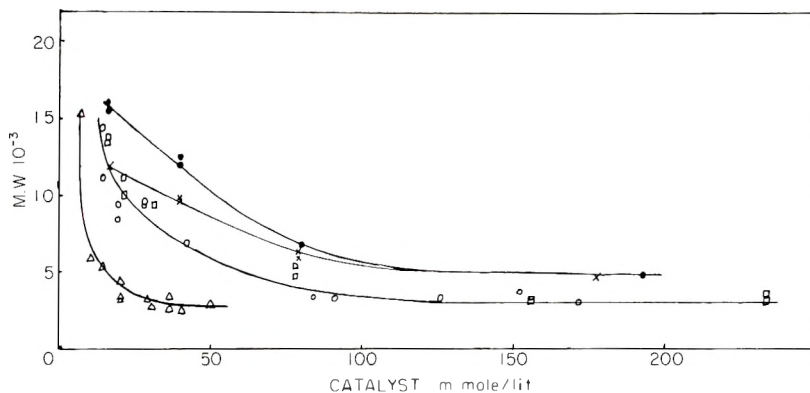


Fig. 1. Dependence of molecular weight on catalyst concentration: (O) monosodium anthracene; (Δ) disodium anthracene; (\square) sodium naphthalene; (\times) monolithium anthracene; (\bullet) lithium naphthalene.

the catalysts investigated: monosodium anthracene (Table I), disodium anthracene (Table II), sodium naphthalene (Table III), monolithium anthracene (Table IV), and lithium naphthalene (Table V). The yield increased with catalyst concentration.

TABLE I
Dependence of Molecular Weight on Catalyst Concentration in Polymerization with Monosodium Anthracene^a

| Run no. | [Catalyst], mmole/l. | Conversion, % | $[\eta]$, dl./g. | M |
|---------|-------------------------|------------------|-------------------|--------|
| 73 | 172 | 90 | 0.094 | 2,980 |
| 74 | 152 | 92 | 0.110 | 3,680 |
| 16 | 126 | 75 | 0.102 | 3,330 |
| 75 | 91 | 80 | 0.098 | 3,150 |
| 15 | 84 | 70 | 0.102 | 3,330 |
| 17 | 42 | 50 | 0.177 | 6,960 |
| 58 | 28 | 45 | 0.222 | 9,390 |
| 57 | 28 | 40 | 0.227 | 9,690 |
| 67 | 19 | 40 | 0.222 | 9,390 |
| 55 | 14 | 30 | 0.251 | 11,100 |
| 56 | 14 | 30 | 0.306 | 14,400 |

^a Experimental conditions: monomer concentration, 1.51 mole/l.; polymerization temp., 0°C.; time, 30 min.

TABLE II
Dependence of Molecular Weight on Catalyst Concentration in Polymerization with Disodium Anthracene^a

| Run no. | [Catalyst], mmole/l. | Conversion, % | $[\eta]$, dl./g. | M |
|---------|-------------------------|------------------|-------------------|--------|
| 8 | 50 | 75 | 0.091 | 2,990 |
| 7 | 40 | 70 | 0.082 | 2,500 |
| 46 | 36 | 70 | 0.085 | 2,610 |
| 45 | 36 | 75 | 0.107 | 2,540 |
| 6 | 30 | 60 | 0.087 | 2,690 |
| 44 | 29 | 65 | 0.100 | 3,240 |
| 5 | 20 | 40 | 0.100 | 3,240 |
| 10 | 20 | 45 | 0.102 | 3,330 |
| 12 | 20 | 50 | 0.128 | 4,370 |
| 42 | 14 | 45 | 0.145 | 5,320 |
| 76 | 10 | 35 | 0.158 | 5,970 |
| 41 | 7 | 25 | 0.320 | 15,300 |

^a Experimental conditions: monomer concentration, 1.51 mole/l.; polymerization temp., 0°C.; time, 30 min.

TABLE III
Dependence of Molecular Weight on Catalyst Concentration in Polymerization with Sodium Naphthalene^a

| Run no. | [Catalyst], mmole/l. | Conversion, % | $[\eta]$, dl./g. | M |
|---------|-------------------------|------------------|-------------------|--------|
| 99 | 234 | 90 | 0.097 | 3,110 |
| 100 | 234 | 85 | 0.108 | 3,590 |
| 101 | 156 | 80 | 0.098 | 3,150 |
| 102 | 156 | 85 | 0.097 | 3,110 |
| 103 | 78 | 80 | 0.146 | 5,370 |
| 104 | 78 | 75 | 0.133 | 4,740 |
| 105 | 31 | 55 | 0.222 | 9,390 |
| 118 | 21 | 45 | 0.233 | 10,000 |
| 119 | 21 | 45 | 0.253 | 11,200 |
| 107 | 15.5 | 40 | 0.290 | 13,400 |
| 108 | 15.5 | 45 | 0.297 | 13,800 |

^a Experimental conditions: monomer concentration, 1.51 mole/l.; polymerization temp., 0°C.; time, 30 min.

TABLE IV
Dependence of Molecular Weight on Catalyst Concentration in Polymerization with Lithium Anthracene^a

| Run no. | [Catalyst], mmole/l. | Conversion, % | $[\eta]$, dl./g. | M |
|---------|-------------------------|------------------|-------------------|--------|
| 128 | 178 | 90 | 0.133 | 4,730 |
| 130 | 79 | 75 | 0.162 | 6,160 |
| 131 | 79 | 80 | 0.157 | 5,920 |
| 132 | 40 | 55 | 0.228 | 9,730 |
| 133 | 40 | 60 | 0.230 | 9,840 |
| 134 | 16 | 34 | 0.263 | 11,770 |

^a Experimental conditions: monomer concentration, 1.51 mole/l.; polymerization temp., 0°C.; time, 30 min.

TABLE V
Dependence of Molecular Weight on Catalyst Concentration in Polymerization with Lithium Naphthalene^a

| Run no. | [Catalyst], mmole/l. | Conversion, % | $[\eta]$, dl./g. | M |
|---------|-------------------------|------------------|-------------------|--------|
| 140 | 193 | 90 | 0.134 | 4,790 |
| 141 | 80 | 70 | 0.154 | 5,760 |
| 142 | 80 | 80 | 0.172 | 6,680 |
| 143 | 40 | 60 | 0.275 | 12,470 |
| 144 | 40 | 65 | 0.266 | 12,000 |
| 145 | 16 | 50 | 0.326 | 15,700 |
| 146 | 16 | 40 | 0.332 | 16,100 |

^a Experimental conditions: monomer concentration, 1.51 mole/l.; polymerization temp., 0°C.; time, 30 min.

Dependence of Molecular Weight on Monomer Concentration

It was found that for relatively high catalyst concentrations, the molecular weight was independent of monomer concentration, while at relatively low catalyst concentrations, the molecular weight increased with increase in monomer concentration. This behavior was the same for all the catalysts investigated (Tables VI–VIII). From these tables it is also seen that the molecular weight depends on the ratios of the monomer to the catalyst concentrations, and that with the use of a sufficiently large monomer concentration the molecular weight increases even at the high catalyst concentrations.

TABLE VI
Dependence of Molecular Weight on Monomer Concentration in Polymerization with Monosodium Anthracene

| Run no. | [Monomer], mole/l. | Conversion, % | $[\eta]$, dl./g. | M |
|-----------------------|-----------------------|------------------|-------------------|--------|
| Series A ^a | | | | |
| 65 | 0.604 | 50 | 0.089 | 2,760 |
| 67 | 1.51 | 40 | 0.222 | 9,390 |
| 69 | 3.02 | 50 | 0.254 | 11,200 |
| 70 | 4.53 | 65 | 0.379 | 19,100 |
| 72 | 4.53 | 65 | 0.365 | 18,200 |
| Series B ^b | | | | |
| 19 | 0.604 | 75 | 0.102 | 3,330 |
| 15 | 1.51 | 70 | 0.102 | 3,330 |
| 20 | 3.02 | 60 | 0.157 | 5,920 |
| 21 | 4.53 | 60 | 0.307 | 14,500 |
| 22 | 6.04 | 55 | 0.386 | 19,600 |

^a Experimental conditions: catalyst concentration, 19 mmole/l.; polymerization temp., 0°C.; time, 30 min.

^b Experimental conditions: catalyst concentration, 84 mmole/l.; polymerization temp., 0°C.; time, 30 min.

TABLE VII
Dependence of Molecular Weight on Monomer Concentration in Polymerization with Disodium Anthracene

| Run no. | [Monomer], mole/l. | Conversion, % | $[\eta]$, dl./g. | M |
|-----------------------|-----------------------|------------------|-------------------|--------|
| Series A ^a | | | | |
| 39 | 1.208 | 85 | 0.095 | 3,030 |
| 46 | 1.51 | 70 | 0.085 | 2,610 |
| 45 | 1.51 | 75 | 0.107 | 3,540 |
| 38 | 2.11 | 65 | 0.124 | 4,320 |
| 37 | 3.04 | 60 | 0.219 | 9,220 |
| Series B ^b | | | | |
| 11 | 0.604 | 80 | 0.095 | 3,030 |
| 10 | 1.51 | 45 | 0.102 | 3,330 |
| 12 | 1.51 | 50 | 0.128 | 4,400 |
| 5 | 1.51 | 40 | 0.100 | 3,240 |
| 13 | 3.02 | 35 | 0.335 | 16,300 |
| 14 | 4.53 | 35 | 0.395 | 20,200 |

^a Experimental conditions: catalyst concentration 36 mmole/l.; polymerization temp., 0°C.; time, 30 min.

^b Experimental conditions: catalyst concentration 20 mmole/l.; polymerization temp., 0°C.; time, 30 min.

TABLE VIII
Dependence of Molecular Weight on Monomer Concentration in Polymerization with Sodium Naphthalene

| Run no. | [Monomer], mole/l. | Conversion, % | $[\eta]$, dl./g. | M |
|-----------------------|-----------------------|------------------|-------------------|--------|
| Series A ^a | | | | |
| 116 | 0.302 | 85 | 0.105 | 3,460 |
| 109 | 0.604 | 80 | 0.101 | 3,280 |
| 115 | 1.21 | 80 | 0.091 | 2,360 |
| 102 | 1.51 | 85 | 0.097 | 3,110 |
| 101 | 1.51 | 80 | 0.098 | 3,150 |
| 113 | 2.11 | 80 | 0.125 | 4,350 |
| 114 | 2.11 | 90 | 0.119 | 4,090 |
| 111 | 3.02 | 85 | 0.183 | 7,260 |
| 112 | 3.02 | 80 | 0.175 | 6,830 |
| Series B ^b | | | | |
| 117 | 0.604 | 60 | 0.157 | 5,910 |
| 118 | 1.51 | 45 | 0.233 | 10,000 |
| 119 | 1.51 | 45 | 0.253 | 11,200 |
| 120 | 3.02 | 40 | 0.584 | 34,100 |
| 121 | 4.53 | 45 | 0.740 | 46,700 |
| 122 | 4.53 | 58 | 0.800 | 51,860 |

^a Experimental conditions: catalyst concentration, 156 mmole/l.; polymerization temp., 0°C.; time, 30 min.

^b Experimental conditions: catalyst concentration, 21 mmole/l.; polymerization temp., 0°C.; time, 30 min.

Most of the experiments carried out at low catalyst concentrations and high $[M]/[C]$ values, to investigate the dependence of molecular weight on monomer concentration, had approximately the same conversion, and the conclusions arrived at concerning the increase in molecular weight with monomer concentration are mostly based on these experiments. Other experiments in which the conversion varied also support the general conclusions.

Dependence of Molecular Weight on $[M]/[C]$

It was found that for the same ratio of concentrations of monomer to catalyst, the molecular weight increased with increasing monomer concentrations at relatively low catalyst concentrations. This shows that the monomer concentration is more effective than that of the catalyst in increasing the molecular weight. This dependence was investigated with monosodium anthracene (Table IX) and with disodium anthracene (Table X).

TABLE IX
Dependence of Molecular Weight on Monomer and Catalyst Concentrations at Constant $[M]/[C]$ in Polymerization with Monosodium Anthracene^a

| Run no. | [Catalyst], mmole/l. | [Monomer], mole/l. | Conversion, % | $[\eta]$, dl./g. | M |
|---------|-------------------------|-----------------------|------------------|-------------------|--------|
| 61 | 2.04 | 0.302 | 25 | 0.141 | 5,120 |
| 62 | 6.12 | 0.906 | 30 | 0.181 | 7,150 |
| 63 | 12.24 | 1.812 | 30 | 0.357 | 17,700 |

^a Experimental conditions: the ratio of monomer to catalyst concentrations was kept constant ($[M]/[C] = 148$); polymerization temp., 0°C.; time, 30 min.

TABLE X
Dependence of Molecular Weight on Monomer and Catalyst Concentrations at Constant $[M]/[C]$ in Polymerization with Disodium Anthracene^a

| Run no. | [Catalyst], mmole/l. | [Monomer], mole/l. | Conversion, % | $[\eta]$, dl./g. | M |
|---------|-------------------------|-----------------------|------------------|-------------------|--------|
| 47 | 2.0 | 0.302 | 65 | 0.150 | 5,560 |
| 48 | 2.0 | 0.302 | 60 | 0.137 | 4,930 |
| 49 | 8.0 | 1.208 | 50 | 0.190 | 7,630 |
| 50 | 12.0 | 1.812 | 75 | 0.216 | 9,050 |
| 52 | 12.0 | 1.812 | 70 | 0.244 | 10,600 |
| 53 | 18.0 | 2.718 | 60 | 0.266 | 12,000 |
| 54 | 18.0 | 2.718 | 60 | 0.250 | 11,000 |

^a Experimental conditions: the ratio of monomer to catalyst concentrations was kept constant ($[M]/[C] = 151$); polymerization temp., 0°C.; time, 30 min.

Dependence of Molecular Weight on Polymerization Temperature

Under otherwise constant conditions, the molecular weight increased with lowering in temperature, as seen from the experiments carried out

TABLE XI
Dependence of Molecular Weight on Temperature^a

| Run no. | Temp., °C. | [Catalyst], mmole/l. | [Monomer], mole/l. | Conversion, % | [η], dl./g. | <i>M</i> |
|---------|------------|----------------------|--------------------|---------------|--------------------|----------|
| 20 | 0 | 84 | 3.02 | 60 | 0.157 | 5,920 |
| 28 | -50 | 84 | 3.02 | 95 | 0.412 | 21,400 |
| 29 | -50 | 84 | 3.02 | 90 | 0.426 | 22,400 |
| 30 | -50 | 42 | 0.604 | 100 | 0.262 | 11,700 |
| 17 | 0 | 42 | 1.51 | 50 | 0.177 | 6,960 |
| 31 | -50 | 42 | 1.51 | 85 | 0.457 | 24,600 |
| 32 | -50 | 42 | 2.416 | 80 | 0.591 | 34,600 |
| 34 | -50 | 9 | 1.51 | 60 | 2.03 | 179,000 |

^a Experimental conditions: catalyst used, monosodium anthracene; polymerization time, 30 min.

with monosodium anthracene at 0 and at -50°C . (Table XI). The yield increased with lowering in temperature.

Dependence of Molecular Weight on Anthracene Concentration

With monosodium anthracene as catalyst and with addition of anthracene to the polymerization mixture, it was found that the molecular weight was independent of anthracene concentration both at high and low catalyst concentrations (Table XII).

Block Copolymerization of Acrylonitrile with Styrene

Block copolymerization experiments of acrylonitrile with styrene were carried out with the use of the following catalysts: monosodium anthracene, monolithium anthracene, sodium naphthalene, and lithium naph-

TABLE XII
Polymerization in the Presence of Added Anthracene^a

| Run no. | [Catalyst], mmole/l. | [Anthracene] added, mmole/l. | [Anthracene] total, mmole/l. ^b | Conversion, % | [η], dl./g. | <i>M</i> |
|---------|----------------------|------------------------------|---|---------------|--------------------|----------|
| 55 | 14 | — | 14 | 30 | 0.251 | 11,100 |
| 56 | 14 | — | 14 | 30 | 0.306 | 14,400 |
| 57 | 28 | — | 28 | 40 | 0.227 | 9,690 |
| 58 | 28 | — | 28 | 45 | 0.222 | 9,389 |
| 59 | 14 | 14 | 28 | 32 | 0.269 | 12,100 |
| 60 | 14 | 14 | 28 | 30 | 0.312 | 14,800 |
| 23 | 84 | 22.4 | 106.4 | 70 | 0.105 | 3,410 |
| 25 | 84 | 170 | 254 | 60 | 0.110 | 3,680 |
| 15 | 84 | — | 84 | 70 | 0.102 | 3,330 |

^a Experimental conditions: monosodium anthracene catalyst was used; monomer concentration, 1.51 mole/l.; polymerization temp., 0°C .; time, 30 min.

^b This is the total concentration of anthracene that can be present in the polymerization mixture assuming that all the catalyst has reacted to liberate free anthracene.

TABLE XIII
Block Copolymerization of Acrylonitrile with Styrene

| Run no. | Catalyst | [Catalyst], mmole/l. | [Acryloni- trile], mole/l. | [Styrene], mole/l. | Polymeriza- tion time, min. | Temp., °C. | Polymer obtained, g. ^a | Infra- red absorp- tion ^b | Nitrogen in polymer, % |
|---------|---------------------------|-------------------------|----------------------------------|-----------------------|--------------------------------|------------|---|---|---------------------------------|
| 86 | Monosodium anthracene | 39 | 1.21 | 1.04 | 2 | 0 | 1.9 | — | 25.0 ^c |
| 87 | " | 39 | 1.21 | 1.04 | 2 | 0 | 1.8 | — | — |
| 88 | " | 39 | 0.6 | 2.62 | 10 | 0 | 1.4 | — | 23.8 ^e |
| 89 | " | 39 | 1.21 | 1.04 | 10 | 0 | 1.8 | — | — |
| 90 | " | 39 | 1.21 | 1.04 | 15 | -50 | 2.6 | — | — |
| 91 | " | 19.6 | 0.6 | 2.62 | 17 | -50 | 1.6 | — | 24.4 ^c |
| 123 | Sodium naphthalene | 21 | 1.21 | 1.04 | 2 | 0 | 1.3 | — | — |
| 124 | " | 21 | 1.6 | 1.04 | 15 | 0 | 1.4 | — | 23.8 ^e |
| 126 | " | 42 | 1.21 | 1.04 | 16 | 0 | 1.6 | — | — |
| 147 | Lithium naphthalene | 48.4 | 1.21 | 1.04 | 15 | 0 | 2.9 | + | 19.4 ^d |
| 148 | " | 16.1 | 1.21 | 1.04 | 15 | 0 | 1.2 | + | 20.3 ^d |
| 149 | " | 16.1 | 1.21 | 1.04 | 15 | 0 | 1.1 | + | 19.0 ^d |
| 136 | Monolithium anthracene | 40 | 1.21 | 1.04 | 10 | 0 | 1.5 | — | — |
| 137 | " | 61 | 1.21 | 1.04 | 15 | 0 | 2.5 | — | 25.0 ^c |
| 138 | " | 61 | 1.21 | 1.04 | 15 | 0 | 2.6 | — | — |

^a Extraction with benzene gave no solute, indicating the absence of homopolystyrene.

^b Positive absorption at 14.3 μ is indicative of styrene incorporated in the polymer.

^c The nitrogen content of polyacrylonitrile is 26.4%. Pure polyacrylonitriles tend to give low nitrogen analyses (about 25%).

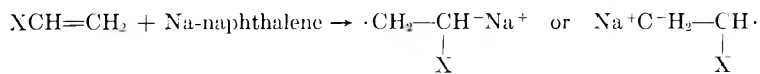
^d The low nitrogen analyses is due to the styrene incorporated in the polymer.

thalene (Table XIII). It was found that only lithium naphthalene led to the formation of a polymer containing styrene-acrylonitrile. This polymer is probably made up of a block of styrene-acrylonitrile random copolymer attached to a block of homopolyacrylonitrile, the former block being initiated by the free radical end and the latter by the anion. With all the catalysts no homopolystyrene was formed as seen from the benzene extraction. The distinguishing feature of the infrared spectra of the block polymers was the absorption band at 14.3μ (monosubstituted benzene), which was also present in an authentic block polymer of styrene and acrylonitrile prepared by polymerizing acrylonitrile on "living" polystyrene (prepared with sodium naphthalene) and extracting the homopolystyrene with benzene. This absorption band is absent in homopolyacrylonitrile.

DISCUSSION

Initiation

Electron transfer catalysts were found to initiate the polymerization of styrene and other vinyl monomers by the transfer of an electron to the double bond of the monomer, thus forming a radical anion which can propagate polymerization.¹



In the case of acrylonitrile, a similar electron transfer to the monomer probably takes place. This is seen from the absence of absorptions in the infrared spectra of the polymers for dihydro derivatives of anthracene and naphthalene. These should have been incorporated in the polymer had the catalyst initiated the polymerization by attachment to the polymer. Dihydronaphthalene was found to be present in polysiloxanes obtained by initiation with potassium naphthalene.⁵

Propagation

Theoretically, polymerization can be propagated through both the anion and the free radical of the anion-radical preliminarily formed. In the case of styrene, propagation was found to occur through the dianion formed after dimerization of the radical anions primarily formed, for that reason the molecular weights were given by $[\text{M}]/^{1/2}[\text{C}]$.² No polymerization of styrene by the free radicals occurred, due to the relatively low polymerization temperature used and the high rate of anionic polymerization as compared with that of free radical polymerization.

In the case of acrylonitrile, which is much more reactive than styrene in anionic polymerization but less so in free radical polymerization, no free radical polymerization probably occurs, and there is only the possibility of dimerization of the free radicals primarily formed.

However, consideration of the following points tends strongly to rule out

the possibility of dimerization for all the catalysts studied except lithium naphthalene.

(1) Extensive studies of the free radical heterogeneous polymerization of acrylonitrile have shown that there is occlusion of free radicals which is much more pronounced than in other monomers.^{6,7} The percentage of trapped radicals increases with the velocity of the polymerization, with decrease in temperature and other physical factors.⁷ In our heterogeneous polymerization, the very high rate of anionic polymerization as compared with the free radical one and the relatively low temperature of polymerization will cause the occlusion of a high percentage of the free radicals formed in the initiation and thus depress the dimerization of the free radical ends of the growing polymers.

(2) Initiation of the polymerization by electron transfer catalysts leads to the liberation of the polycyclic aromatic hydrocarbon, in the vicinity of the free radical formed. It is known that anthracene is used as inhibitor of the free radical polymerization of acrylonitrile.⁸ Batten⁹ has demonstrated that radical chain decomposition of benzoyl peroxide is almost completely inhibited by anthracene. Marvel and Wilson¹⁰ have found that solution copolymerization experiments with styrene and anthracene produced no polymer. Therefore, it is quite possible that the anthracene liberated can cause inhibition of the dimerization of the free radicals originally formed.

It may be mentioned that the inhibition mechanism of free radical polymerization by anthracene is not quite understood. Conclusive evidence that the inhibitory effect of the anthracene is due to its interaction with the growing free radical, and its incorporation in the polymer chain is lacking.¹¹ Also, in the study of the retardation of the chain decomposition of benzoyl peroxide, no evidence was found of a direct reaction between anthracene and the peroxide such as occurs with phenol inhibitors.⁹

(3) Figure 1 shows that at high catalyst concentrations, the molecular weights of the polymers obtained by monosodium anthracene, disodium anthracene, and sodium naphthalene were of the same order (about 3000). For the lithium catalysts of naphthalene and anthracene, also, the same order of molecular weights was obtained (about 5000). Since naphthalene does not inhibit free radical polymerization as does anthracene, this identity in the molecular weights shows that the main factor governing the possibility of the free radical dimerization is the high rate of the anionic polymerization. Thus the phenomenon of trapped radicals seems to dominate, and no dimerization occurs also with the naphthalene catalysts.

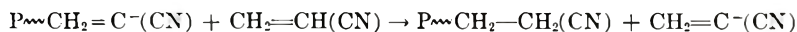
(4) The results of the block copolymerization experiments with acrylonitrile and styrene (Table XIII) show that only with lithium naphthalene acrylonitrile-styrene block copolymers were formed. This is probably due to the following. (a) Naphthalene is not a free radical inhibitor as anthracene. (b) The rate of polymerization with the sodium catalysts is probably greater than that with the lithium catalysts, as was found by Kelley and Tobolsky¹² in the copolymerization of styrene and isoprene.

This smaller velocity will reduce the difference between the rates of the anionic and the free radical polymerizations, so that some free radical polymerization with the lithium naphthalene can occur. O'Driscoll and Tobolsky¹³ have suggested that, although initiation of polymerization by lithium or sodium metal is probably by electron transfer mechanism, nevertheless, the greater rate of anionic polymerization of the sodium catalyst (which is many orders of magnitude greater than free radical growth) leads to the fact that polymerization by sodium, contrary to that by lithium, is purely anionic. (c) The smaller rate of anionic polymerization with the lithium catalysts will also lead to a smaller degree of occlusion of the free radicals formed, thus enabling free radical polymerization of styrene, which is more reactive than acrylonitrile in free radical polymerization, so that more of it can be incorporated in the polymer.

(5) It may be mentioned that in the polymerization of acrylonitrile by sodium benzophenone¹⁴ where most probably polymerization is initiated largely by the dianion of the dimeric structure, the molecular weights obtained were of about twice the order of those obtained by sodium naphthalene or anthracene at the high catalyst concentrations. This indicates the possibility that no significant combination of chains of polyacrylonitrile through dimerization of the free radicals has occurred.

Termination

At high catalyst concentrations and at relatively low $[M]/[C]$ values, it is seen (Tables I-X) that the molecular weights are independent of both catalyst and monomer concentrations as is consistent with the assumption that termination is by chain transfer to monomer (abstraction of the acidic α -hydrogen atom of the monomer):



In accordance with this, the polymers contain terminal double bonds ($\text{CH}_2=$) shown by infrared absorption bands at 6.1–6.2 μ as well as absorptions at 4.55–4.6 μ due to conjugation between the triple bond of the cyano groups and the terminal double bonds.¹⁵ The absorption band at 6.1–6.2 μ can be also due to $-(\text{C}=\text{N})_x$ units which were found to occur in colored methacrylonitrile polymers obtained by anionic polymerization.¹⁶ But the presence of the absorption bands at 4.55–4.6 μ and the fact that the polymers were generally not colored show that these absorption bands are mostly due to the ($\text{CH}_2=$) double bonds.

The alternative possibility of chain transfer by hydride transfer to monomer:



does not seem to be favored on energy grounds. It is improbable that a hydride transfer occurs from a position which is α to a very strong electron withdrawing group, such as the cyano group. Furthermore, in the anionic polymerization of styrene living polymers were obtained whose molecular

weight was given by $[M]^{1/2}[C]^2$, i.e., no termination by hydride transfer was energetically possible, even with a weak electronegative group. Also, in the anionic polymerization of methacrylonitrile (which has no acidic α H-atom) with lithium in liquid ammonia¹⁶ and with quaternary ammonium hydroxide¹⁷ no chain transfer to monomer occurred, showing that this possibility of hydride transfer is ruled out.

At relatively low catalyst concentrations it is seen (Fig. 1, Tables I–X) that the molecular weights decrease with increasing catalyst concentration, i.e., the principle of termination by chain transfer is not being followed. Since these catalysts are able to initiate polymerization either anionically or radically, the cause for the increase in molecular weight at low catalyst concentrations may be due theoretically either to the radical or to the anionic mechanism. However, we have shown that the possibility of free radical polymerization, especially with the anthracene catalysts and the sodium derivatives, is ruled out.

O'Driscoll, Boudreau, and Tobolsky¹⁸ have shown that in the copolymerization of styrene and methyl methacrylate with lithium metal as initiator (which initiates polymerization through the formation of a radical-anion) the percentage of styrene in the copolymer goes over to zero at low temperature (about -50°C). Our results at -50°C . (Table XI) at low catalyst concentrations (which show increase in molecular weight with decrease in catalyst concentration and increase in monomer concentration) also indicate that this behavior is due to anionic polymerization and the increase in molecular weight is not due to free radical polymerization.

Study of the anionic polymerization of acrylonitrile by the classical anionic catalyst, butyllithium,¹⁹ at a wide range of catalyst concentrations has shown that the termination of the polymerization at high catalyst concentrations was by chain transfer to monomer, while at low catalyst concentrations, where the molecular weight increased with increase in monomer concentration, monomolecular termination was found to occur. In our present polymerization, the increase in molecular weight with monomer concentration at low catalyst concentrations seems to be due to the same reason.

Effect of the Polycyclic Aromatic Component of the Catalyst

In addition to the inhibitory effect of anthracene on free radical polymerization, it was found that with sodium and lithium naphthalenes the molecular weights obtained at low catalyst concentrations and relatively high monomer concentrations were higher than those for the corresponding anthracene derivatives (Compare Tables VI and VIII) with (Tables IV and V). In the case of lithium naphthalene this may be partially due to dimerization of free radical ends. The smaller catalyst concentration lowers the rate of initiation and the total rate of the polymerization, so that the amount of trapped radicals is decreased and dimerization is possible. As mentioned before, dimerization was not found to occur at the high catalyst concentrations.

Effect of the Positive Alkali Metal Counterions

In addition to the differences found between the lithium and the sodium catalysts as regards the influence of the free radicals formed on the polymerization, the lithium catalysts, in the chain transfer region, gave polymers having greater molecular weights than those obtained by the sodium catalysts. Such differences in the molecular weights due to the counterion have been found in other anionic polymerizations.^{17,20,21} The smaller molecular weights with the sodium catalyst were attributed²¹ to the greater size and electropositivity of the sodium as compared to lithium, which increases the ionic character of the growing ion-pair leading to a greater attraction of protons by the carbanion of the growing chain.

References

1. Szwarc, M., M. Levy, and R. Milkovich, *J. Am. Chem. Soc.*, **78**, 2656 (1956).
2. Waack, R., A. Rembaum, J. D. Coombes, and M. Szwarc, *J. Am. Chem. Soc.*, **79**, 2026 (1957).
3. Bamford, C. H., and A. D. Jenkins, *Proc. Roy. Soc. (London)*, **A216**, 515 (1953).
4. Cleland, R. L., and W. H. Stockmayer, *J. Polymer Sci.*, **17**, 473 (1955).
5. Morton, M., A. Rembaum, and E. E. Bostick, *J. Polymer Sci.*, **32**, 530 (1958).
6. Thomas, W. M., *Fortschr. Hochpolymer Forsch.*, **2**, 401 (1961).
7. Bamford, C. H., and A. D. Jenkins, *Proc. Roy. Soc. (London)*, **A228**, 220 (1955); C. H. Bamford, A. D. Jenkins, M. C. R. Symons, and M. G. Townsend, *J. Polymer Sci.*, **34**, 181 (1959).
8. Blout, E. R., H. F. Mark, and W. P. Hohenstein, *Monomers*, Interscience, New York, 1949, p. 14.
9. Batten, J. J., *J. Chem. Soc.*, **1956**, 4687.
10. Marvel, C. S., and B. D. Wilson, *J. Org. Chem.*, **23**, 1479 (1958).
11. Magat, M., and R. Bonème, *Compt. rend.*, **232**, 1657 (1951).
12. Kelley, D. J., and A. V. Tobolsky, *J. Am. Chem. Soc.*, **81**, 1597 (1959).
13. O'Driscoll, K. F., and A. V. Tobolsky, *J. Polymer Sci.*, **37**, 363 (1959).
14. Zilkha, A., P. Neta, and M. Frankel, *J. Chem. Soc.*, **1960**, 3357.
15. Bellamy, L. J., *The Infrared Spectra of Complex Molecules*, 2nd Ed., Methuen, London, 1958, p. 264.
16. Overberger, C. G., E. M. Pearce, and N. Mayes, *J. Polymer Sci.*, **34**, 109 (1959).
17. Zilkha, A., B. A. Feit, and M. Frankel, *J. Polymer Sci.*, **49**, 231 (1961).
18. O'Driscoll, K. F., R. J. Boudreau, and A. V. Tobolsky, *J. Polymer Sci.*, **31**, 115 (1958).
19. Ottolenghi, A., and A. Zilkha, *J. Polymer Sci.*, in press.
20. Goode, W. E., W. H. Snyder, and R. C. Fettes, *J. Polymer Sci.*, **42**, 367 (1960).
21. Feit, B. A., and A. Zilkha, *J. Appl. Polymer Sci.*, in press

Synopsis

The heterogeneous polymerization of acrylonitrile in tetrahydrofuran by chain transfer catalysts: monosodium anthracene, disodium anthracene, sodium naphthalene, monolithium anthracene, and lithium naphthalene was investigated. The free radical formed in the initiation was found to participate in the polymerization process only in the case of lithium naphthalene at low catalyst concentrations. Also, block copolymerization with styrene, which is more reactive in free radical polymerization than acrylonitrile and less in anionic, succeeded only with lithium naphthalene. The absence

of dimerization of the free radicals is mainly due to their occlusion caused by the high rate of the anionic polymerization of acrylonitrile and the low polymerization temperature, and in the case of the anthracene catalysts also due to inhibition of the free radical dimerization by the liberated anthracene. The mechanism of the termination of the polymerization was found to depend on the catalyst concentration and the ratio $[M]/[C]$. At high catalyst concentrations and relatively low $[M]/[C]$ values, termination was by chain transfer to the monomer, as can be seen from the independence of the molecular weights on both monomer and catalyst concentrations. At low catalyst concentrations and relatively high $[M]/[C]$ values, the molecular weights were found to increase with monomer concentration and decrease with catalyst concentration. This was found to be due to the anionic mechanism of the polymerization, and the results are similar to those obtained in a typical anionic polymerization of acrylonitrile with butyllithium.

Résumé

On a étudié la polymérisation hétérogène d'acrylonitrile dans le tétrahydrofurane par des catalyseurs de transfert de chaîne: monosodium-anthracène, disodium-anthracène, sodium-naphthalène, monolithium-anthracène et lithium-naphthalène. On a trouvé que le radical libre formé au cours de l'initiation participe au processus de polymérisation uniquement dans le cas du lithium-naphthalène à des basses concentrations en catalyseur. La copolymérisation à séquences avec le styrène, qui est plus réactif que l'acrylonitrile dans la polymérisation anionique, n'a réussi qu'avec du lithium-naphthalène. L'absence de dimérisation des radicaux libres est principalement due à leur occlusion causée par la grande vitesse de la polymérisation anionique de l'acrylonitrile et la basse température de polymérisation, et dans les cas des catalyseurs à anthracène, elle est aussi due à l'inhibition de la dimérisation des radicaux libres par l'antracène libéré. On a trouvé que le mécanisme de la terminaison de la polymérisation dépend de la concentration en catalyseur et du rapport $[M]/[C]$. Aux fortes concentrations en catalyseur et valeurs relativement basses de $[M]/[C]$ la terminaison se fait par transfert de chaîne sur le monomère, comme il ressort de l'indépendance des poids moléculaires à la fois par rapport aux concentrations en monomère et catalyseur. Aux faibles concentrations en catalyseur et valeurs relativement élevées de $[M]/[C]$ on a trouvé que les poids moléculaires augmentaient avec la concentration en monomère et diminuaient avec la concentration en catalyseur. On a trouvé que ceci est dû au mécanisme anionique de la polymérisation et les résultats sont semblables à ceux obtenus dans la polymérisation anionique typique de l'acrylonitrile avec du butyllithium.

Zusammenfassung

Die heterogene Polymerisation von Acrylnitril in Tetrahydrofuran mit Mononatrium-anthracen, Dinatriumanthracen, Natriumnaphthalin, Monolithiumanthracen und Lithiumnaphthalin als Kettenübertragungskatalysatoren wurde untersucht. Es wurde gefunden, dass die beim Start gebildeten freien Radikale nur im Fall des Lithiumnaphthalins bei kleinen Katalysatorkonzentrationen am Polymerisationsprozess teilnehmen. Auch Blockcopolymerisation mit Styrol, das bei radikalischer Polymerisation reaktionsfähiger und bei anionischer weniger reaktionsfähig als Acrylnitril ist, gelang nur mit Lithiumnaphthalin. Das Fehlen einer Dimerisation der Radikale ist hauptsächlich auf die durch die hohe Geschwindigkeit der anionischen Polymerisation von Acrylnitril und die niedrige Polymerisationstemperatur verursachte Okklusion und im Falle des Anthracens als Katalysator auch auf die Verhinderung der Radikaldimerisation durch in Freiheit gesetztes Anthracen zurückzuführen. Der Mechanismus des Abbruchs der Polymerketten hängt von der Katalysatorkonzentration und vom Verhältnis $[M]/[C]$ ab. Bei hohen Katalysatorkonzentrationen und relativ kleinen $[M]/[C]$ -Werten findet Kettenübertragung zum Monomeren statt, wie aus der Unab-

hängigkeit des Molekulargewichts sowohl von der Monomer- als auch von der Katalysatorkonzentration ersichtlich ist.—Bei niedrigen Katalysatorkonzentrationen und relativ hohen $[M]/[C]$ -Werten stiegen die Molekulargewichte mit zunehmender Monomerkonzentration und fallender Katalysatorkonzentration an. Dies erwies sich als Folge des anionischen Mechanismus der Polymerisation und die Ergebnisse gleichen denen, die bei einer typischen anionischen Polymerisation von Acrylnitril mit Butyllithium erhalten wurden.

Received September 11, 1961

Revised November 20, 1961

Nitroso Fluorocarbon Elastomers. Polymerization Mechanism

G. H. CRAWFORD, D. E. RICE, and B. F. LANDRUM, *Central Research Department, Minnesota Mining & Manufacturing Company, St. Paul, Minnesota*

Introduction

Since the discovery that the addition reaction of CF_3NO to C_2F_4 can be made to propagate successfully to a high polymer,¹ the unique polymerization reaction of the $\text{N}=\text{O}$ double bond and the unusual characteristics of the copolymers deriving therefrom have been the subject of much interest. This presentation will cover experiments aimed at elucidating the various steps in the polymerization reaction and relating the properties of the copolymers to the chemical structure whose essential feature is the $\text{N}-\text{O}$ linkage in the backbone.

This work was initiated as part of a U. S. Army Quartermaster sponsored project which has been under way for the past several years. The objectives reflect a continuing need of the armed services for rubbers serviceable under the extreme environmental conditions likely to be encountered in modern warfare. Specifically, the project seeks to discover and develop elastomeric polymers containing fluorine which resist chemical or solvent attack and are serviceable at -70°F . or below. This is part of a coordinated effort in which groups under Paul Tarrant (University of Florida) and J. D. Park (University of Colorado) carry out monomer synthesis research and J. C. Montermoso (Quartermaster Research and Engineering Center) has been responsible for evaluation and curing studies.

A considerable backlog of research in this area had led to the conclusion that conventional approaches, e.g., vinyl polymerizations of olefinically unsaturated fluorocarbons, could produce only incremental improvements over existing materials. Hence, the approach adopted has been to try to discover and utilize for the preparation of high polymers, functionalities and reactions which were either totally new or previously unapplied to polymer chemistry. The fluorocarbon field provides fertile ground for novel approaches, since fluorocarbons undergo many reactions which have no counterpart in conventional organic chemistry. Conversely, many classical organic reactions either do not occur, or produce unstable products when applied to fluorocarbon materials.

Perhaps the most interesting outgrowth of this approach has been the family of nitroso fluorocarbon elastomers. The parent copolymer CF_3-

NO/C₂F₄ has been developed from an experimental raw gum elastomer to a rubber for which the technology from monomer synthesis and polymerization through vulcanization has been established. Other nitroso fluorocarbon elastomers have been or are now undergoing similar development. These have been called the first true fluorocarbon elastomers since, unlike other fluorine-containing rubbers, they do not depend upon the presence of CH₂ linkages for elastomeric character or chemical stability. The whole spectrum of their physical properties, including their solubility characteristics and reactivities (or lack of reactivity) toward chemical reagents, puts them in the class of fluorocarbon rather than hydrocarbon derivatives.

The structure of the repeating unit of CF₃NO/C₂F₄ copolymer has been shown to be —N(CF₃)—O—CF₂CF₂—.

Regardless of detailed reaction mechanisms, this structure is the *prima facie* consequence of a process in which the —N=O linkage behaves like a —C=C— linkage in an addition polymerization reaction.

Polymerization Mechanism

The reaction of trifluoronitrosomethane with tetrafluoroethylene to give $\overline{\text{CF}_3-\text{N}-\text{O}-\text{CF}_2-\text{CF}_2}$ and a polymeric oil having the structure $+\text{N}-(\text{CF}_3)-\text{O}-\text{CF}_2-\text{CF}_2+_n$ was first reported in 1955.³ An ionic mechanism was proposed for the reaction. Later, the same workers² suggested the alternative possibility of a gas-phase, radical-type mechanism for the formation of polymer, oxazetidine, or both, and presented arguments in support of and against both types of mechanism.

Crawford, Rice, and Montermoso, on the other hand, presented experimental data¹ which appear both to preclude an ionic mechanism and heavily support a free-radical mechanism, concluding on the basis of these data that the polymerization was indeed of the free-radical type. Preliminary kinetic data in support of this type of mechanism were later presented.⁴

The evidence obtained to date is summarized as follows.

(1) The fact that the polymerization takes place in systems containing water (Table I) is strong evidence against an ionic mechanism. Polymerizations have been carried out in aqueous suspension and emulsion systems as well as in the presence of water alone. In no case does there appear to be inhibition of polymerization due to water. In fact, the presence of

TABLE I
Copolymerizations of CF₃NO/C₂F₄ in Aqueous Media

| Medium | Temp., °C. | $\langle \eta \rangle$ |
|--|------------|------------------------|
| Bulk (control) | 23 | 0.18 |
| 40% monomers in water | 23 | 0.32 |
| 40% monomers in 3% C ₇ F ₁₅ COOK, pH 12 | 23 | 0.34 |
| 40% monomers in 3% C ₇ F ₁₅ COOH, pH 1 | 23 | 0.28 |